ESA-WPP-344
February 2016

Proceedings of the

29th European Space Thermal Analysis Workshop

ESA/ESTEC, Noordwijk, The Netherlands

3–4 November 2015

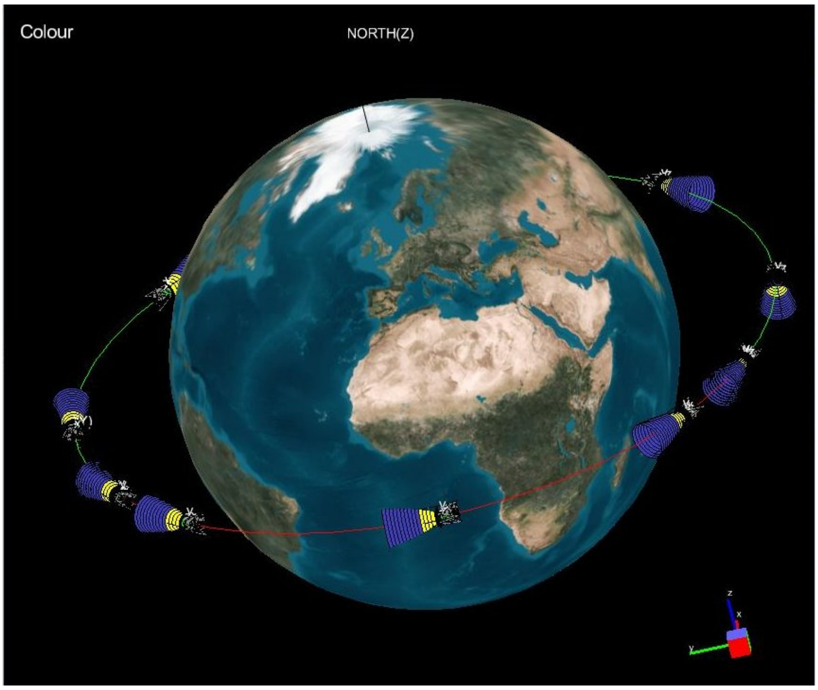

courtesy: ITP Engines U.K. Ltd.

European Space Agency
Agence spatiale européenne

Abstract

This document contains the presentations of the 29th European Space Thermal Analysis Workshop held at ESA/ESTEC, Noordwijk, The Netherlands on 3–4 November 2015. The final schedule for the Workshop can be found after the table of contents. The list of participants appears as the final appendix. The other appendices consist of copies of the viewgraphs used in each presentation and any related documents.
Proceedings of previous workshops can be found at http://www.esa.int/TEC/Thermal_control under 'Workshops'.

⇒ Please note that text like this are clickable hyperlinks in the document.

⇒ This document contains video material. By (double) clicking on picture of a video the movie file is copied to disk and then played with an external viewer. This has been tested with Adobe Reader 9 in Windows and Linux using vlc as external viewer. Other pdf readers may not work automatically. As a last resort the user can manually extract the movie attachment from the file and play it separately.

Contents

Appendices

Programme Day 1

9:00 Registration

9:45 **Welcome and introduction**

Harrie Rooijackers (ESA/ESTEC, The Netherlands)

10:00 **OrbEnv** — A tool for Albedo/Earth Infra-Red environment parameter determination

Alex Green (University College London, United Kingdom)
Romain Peyrou-Lauga (ESA-ESTEC, The Netherlands)

10:25 **Mercury Retro-Reflection** — Modelling and Effects on MPO Solar Array

Anja Frey & Giulio Tonellotto (ESA/ESTEC, The Netherlands)

10:50 **On the thermal design and modelling of calibration blackbodies for the FCI and IRS instruments on MTG**

Nicole Melzack (RAL Space, United Kingdom)

11:15 Coffee break in the Foyer

11:45 **Development of methodologies for Brightness Temperature evaluation for the MetOp-SG MWI radiometer**

Alberto Franzoso (CGS, Italy)
Sylvain Vey (ESA/ESTEC, The Netherlands)

12:10 **MASCOT thermal design** — how to deal with late and critical changes

Luca Celotti & Małgorzata Sołyga (Active Space Technologies GmbH, Germany)
Volodymyr Baturkin & Kaname Sasaki & Christian Ziach (DLR, Germany)

12:35 **Solar Orbiter SPICE** — Thermal Design, Analysis and Testing

Samuel Tustain (RAL Space, United Kingdom)

13:00 Lunch in the ESTEC Restaurant

14:00 **Spatial Temperature Extrapolation Case Study** — Gaia in-flight

Matthew Vaughan (ESA/ESTEC, The Netherlands, Airbus Defence and Space, France)

14:25 **Accelerating ESATAN-TMS Thermal Convergence for Strongly Coupled Problems**

Christian Wendt & Sébastien Girard (Airbus Defence and Space, Germany)

14:50 **OHB System** — Thermal Result Viewer

Markus Czupalla & S. Rockstein & C. Scharl & M. Matz (OHB System, Germany)

15:15 **Overview of ECSS Activities for Space Thermal Analysis**

James Etchells (ESA/ESTEC, The Netherlands)

15:45 Coffee break in the Foyer

16:15 **Improve thermal analysis process with Systema V4 and Python**

Alexandre Darrau (Airbus Defence and Space, France)

16:40 **Finite element model reduction for spacecraft thermal analysis**

Lionel Jacques & Luc Masset & Gaetan Kerschen
(Space Structures and Systems Laboratory, University of Liège, Belgium)

17:05 **The Thermal Design of the KONTUR-2 Force Feedback Joystick**

Ralph Bayer (DLR, Germany)

17:30 Social Gathering in the Foyer

19:30 Dinner in *La Galleria*

Programme Day 2

9:15 **ESATAN Thermal Modelling Suite** — Product Developments and Demonstration
Chris Kirtley & Nicolas Bures (ITP Engines UK Ltd, United Kingdom)

10:00 **SYSTEMA — THERMICA**
Timothée Soriano & Rose Nerriere (Airbus Defense and Space SAS, France)

10:45 **Thermal Spacecraft Simulator Based on TMM Nodal Model** — Return of Experience
Sandrine Leroy & François Brunetti (DOREA, France)

11:10 Coffee break in the Foyer

11:40 **Correlation of two thermal models**
Marije Bakker & Roel van Benthem (NLR, The Netherlands)

12:05 **Experience of Co-simulation for Space Thermal Analysis**
François Brunetti (DOREA, France)

12:30 **GENETIK+** — Introducing genetic algorithm into thermal control development process
Guillaume Mas (CNES, France)

12:55 Closure

13:00 Lunch in the ESTEC Restaurant

14:00 Lab visits

15:30

Appendix A

Welcome and introduction

Harrie Rooijackers
(ESA/ESTEC, The Netherlands)

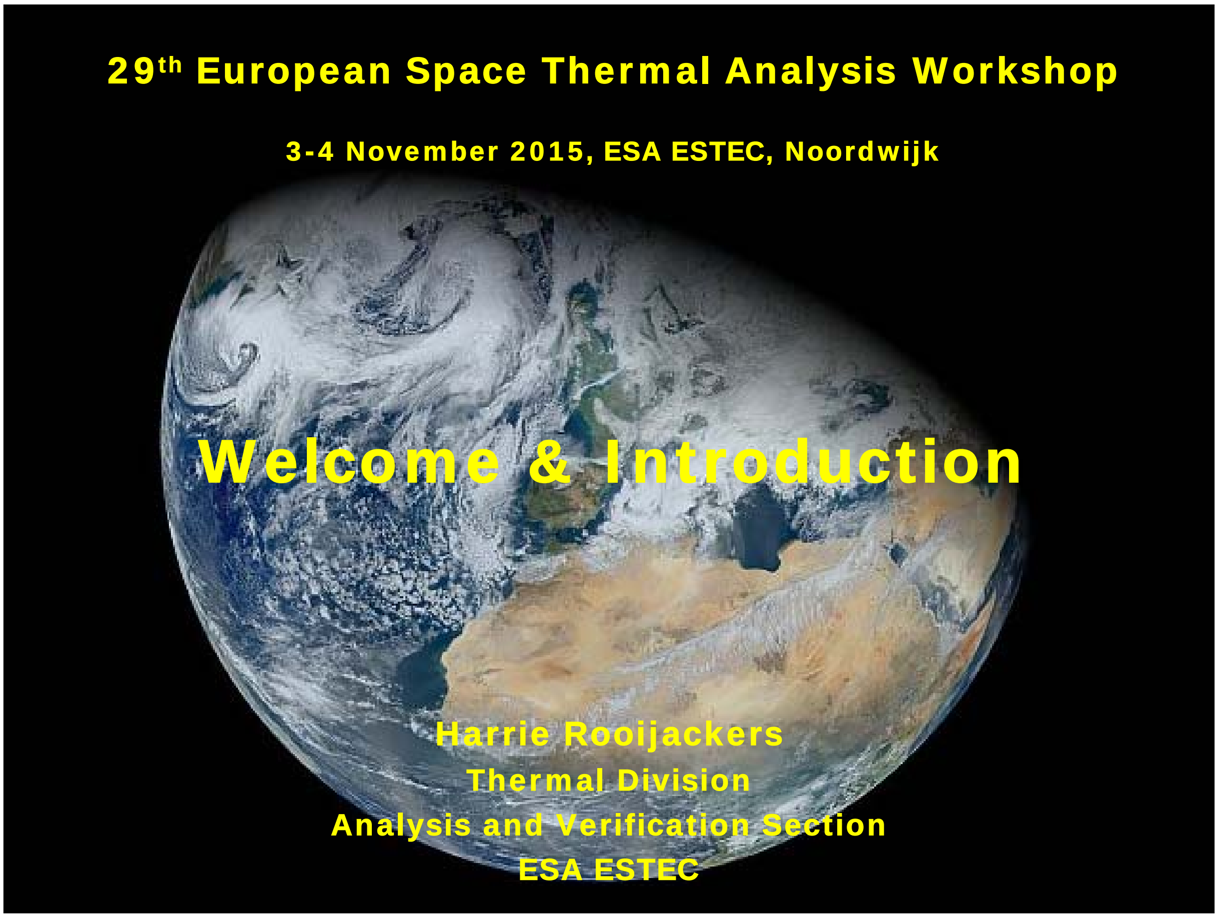

Workshop objectives

- To promote the exchange of views and experiences amongst the users of European thermal engineering analysis tools and related methodologies
- To provide a forum for contact between end users and software developers
- To present developments on thermal engineering analysis tools and to solicit feedback
- To present new methodologies, standardisation activities, etc.

European Space Agency

29th European Space Thermal Analysis Workshop 2

ESA Team

esa

Benoit Laine Head of Section
James Etchells
Duncan Gibson
Harrie Rooijackers

Workshop organised by the Thermal Analysis and Verification Section TEC-MTV with help from the ESA Conference Bureau

European Space Agency

29th European Space Thermal Analysis Workshop 3

Programme

esa

- Two-day programme
- Presentations of 25 min, including 5 minutes for questions and discussions
- Presenters:
  If not done already please leave your presentation (PowerPoint or Impress and PDF file) with Harrie before the end of Workshop.
- No copyrights, please!
- Workshop Proceedings will be supplied to participants afterwards, on the Web.

European Space Agency

29th European Space Thermal Analysis Workshop 4

Practical information

esa

- Lunch: 13:00 - 14:00
- Cocktail today around 17:30 in the Foyer
- Check your details on the list of participants and inform the Conference Bureau of any modifications.
  Leave your email address!
- Taxi service and Shuttle service to Schiphol Airport
  contact ESTEC Reception ☎ ext. 54000, ESTEC.Reception@esa.int
  or Taxi Brouwer ☎ +31(0)71 361 1000, info@brouwers-tours.nl
- Optional workshop dinner tonight!

European Space Agency

29th European Space Thermal Analysis Workshop 5

Workshop dinner

esa

- in "La Galleria", Kon. Wilhemina Boulevard 18,
  2202 GT Noordwijk, ☎ +31(0)71 19 17196
- fixed menu with choice of main course (fish, meat or vegetarian) for €29,50 excl. drinks
  drinks are charged individually.
- Restaurant booked today for 19:30
- Please arrange your own transport
- "Dutch" dinner == to be paid by yourself
- If you would like to join, then fill in the form on the last page of your hand-outs and drop it at the registration desk today **before 13:00**, to let the restaurant know what to expect

European Space Agency

29th European Space Thermal Analysis Workshop 6

Restaurant “La Galleria”

ICES

- The 46th International Conference on Environmental Systems (ICES) will be held 10-14 July, 2016, Vienna, Austria.
- Deadline for submitting abstracts: 16 November, 2015
- Abstracts must include paper title, author(s) name(s), mailing and e-mail addresses, phone and fax numbers
- Abstracts may be submitted online at www.depts.ttu.edu/ceweb/ices

European Space Agency

29th European Space Thermal Analysis Workshop 9

Workshop

Next year: 30th workshop, 5-6 October 2016

Wed – Thu !!!

Why not Tue as usual?

European Space Agency

29th European Space Thermal Analysis Workshop 10

On 3 October 1574 the siege of Leiden ended. This is still annually celebrated in Leiden with festivities in the centre with herring and white bread and "hutspot" (carrot and onion stew), the available liberation food at that time.
Public transport is a mess and even road tansport in the area suffers.
On 4 October they can clean up the mess.
On 5 October everything is back to normal again.

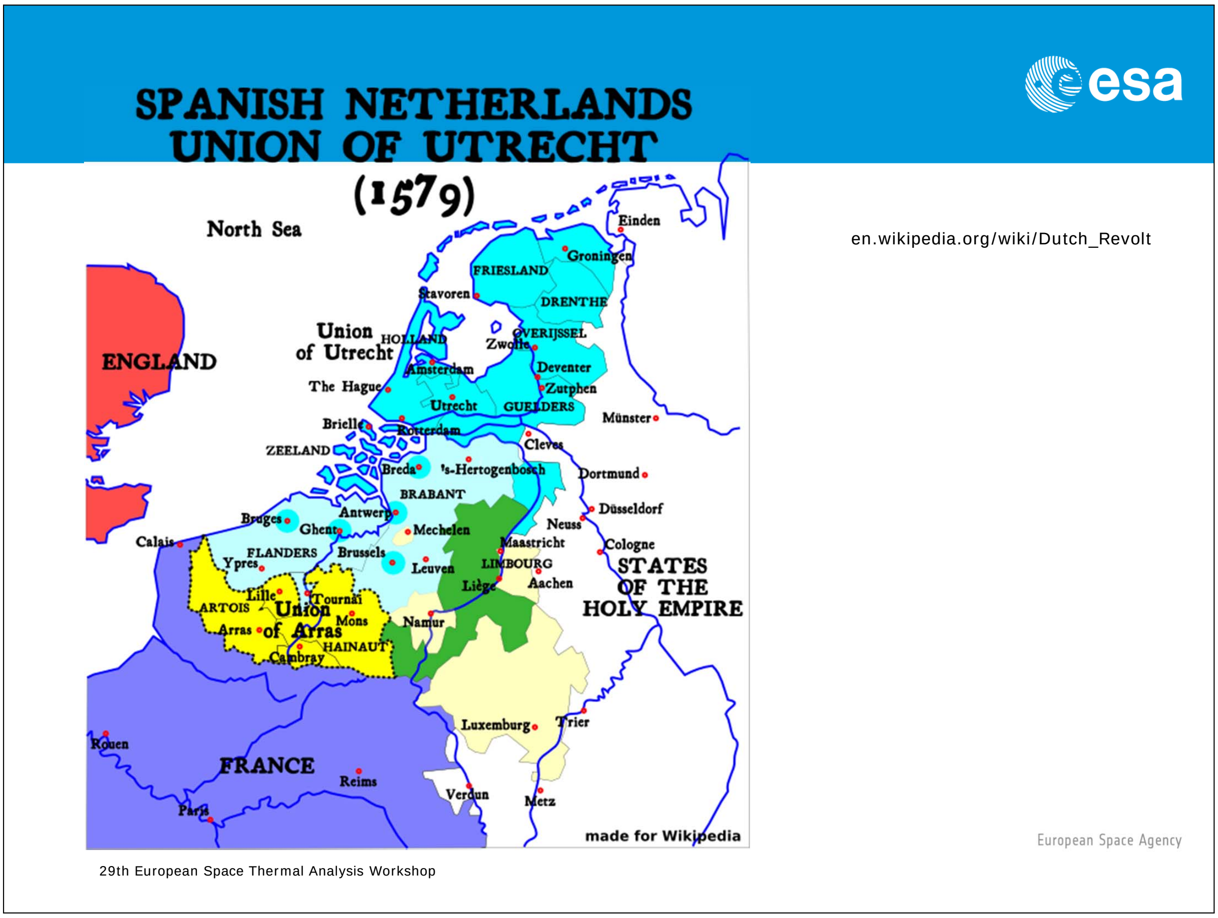

In the war (eventually called the Eighty Years' War) that had broken out, Dutch rebels took up arms against the king of Spain, whose family had inherited the Seventeen Provinces of the Netherlands. Most of the counties of Holland and Zeeland were occupied by rebels in 1572, who sought to end the harsh rule of the Spanish Duke of Alba, governor-general of the Netherlands.
See also:

- en.wikipedia.org/wiki/Siege_of_Leiden
- en.wikipedia.org/wiki/Dutch_Revolt

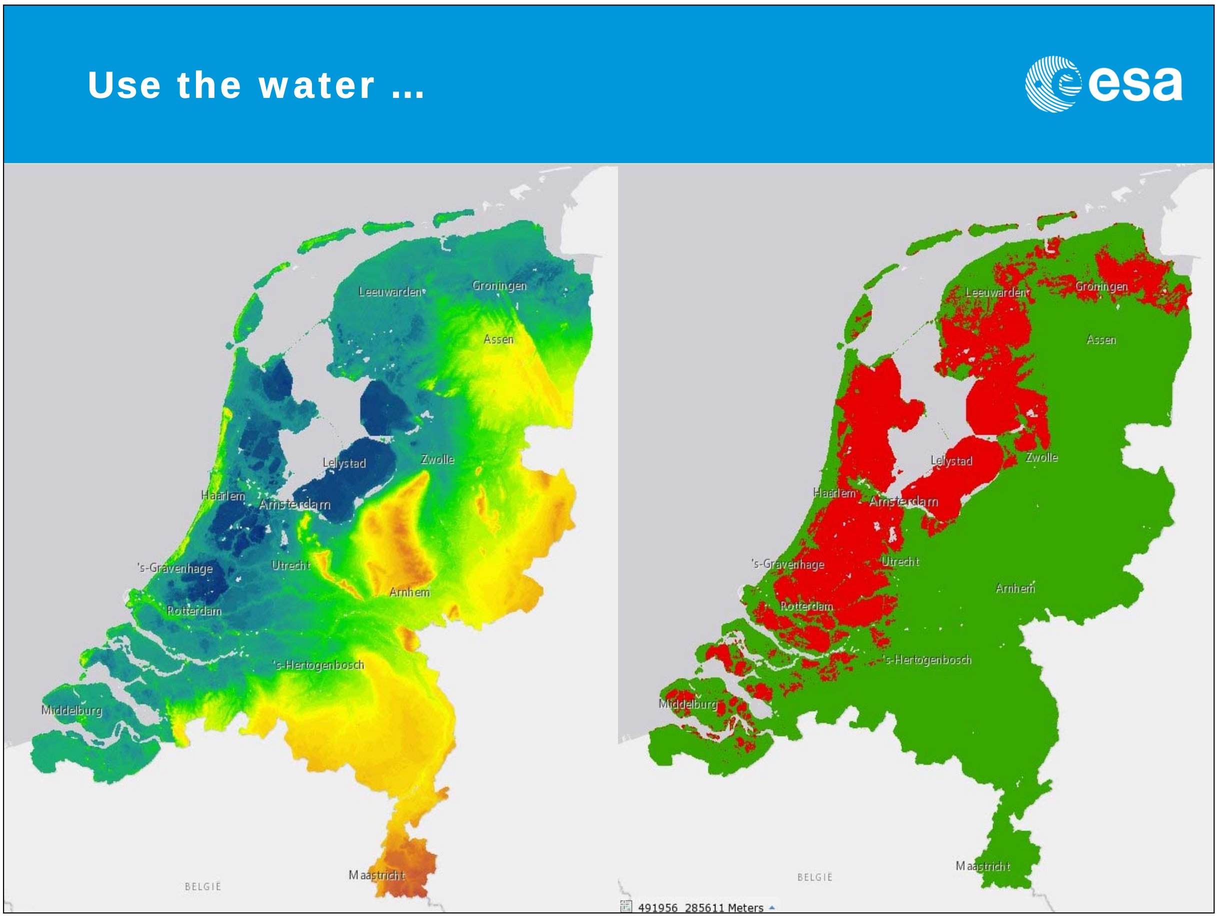

The territory had a very high density of cities, which were protected by huge defense works and by the low-lying boglands, which could easily be flooded by opening the dykes and letting in the sea.
The picture on the left shows a current altitude map of the Netherlands.
The picture on the right shows the part of the country above sealevel in green and the part below in red.

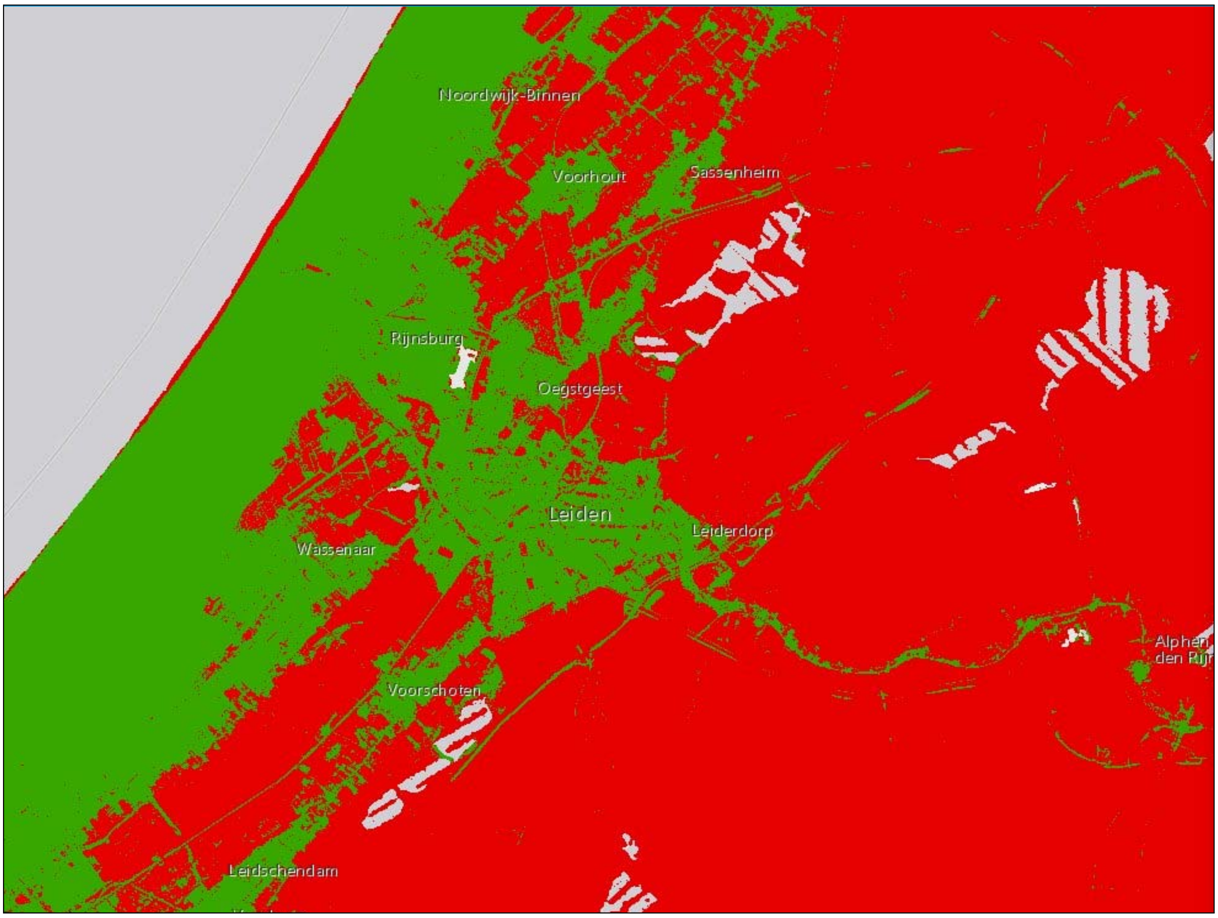

Here is a zoom in on the current area of Leiden showing the sealevel.

Workshop

Current workshop:

19 very interesting presentations covering:

- Range of general applications
- New tools
- Existing thermal tools
  - Enhancements
  - Applications
  - User experiences

European Space Agency

Workshop

Listen, Ask, Discuss

most of all: Enjoy

European Space Agency

Appendix B

OrbEnv
A tool for Albedo/Earth Infra-Red environment parameter determination

Alex Green
(University College London, United Kingdom)

Romain Peyrou-Lauga
(ESA-ESTEC, The Netherlands)

Abstract

OrbEnv is a tool developed for ESA missions to provide realistic and less enveloping albedo coefficient and Earth temperature range for an orbit using data measured by satellites. The tool is able to treat the most common orbit types (LEO, SSO, HEO, MEO...) and is able to calculate impinging albedo and Earth fluxes for several basic geometries and several time steps. Data comes from the CERES instrument on NASA's Terra satellite and covers more than 6 years of measurement.

OrbEnv: A tool for Albedo / Earth Infra-Red environment parameter determination

Alex Green (University College London)
Romain Peyrou-Lauga (ESA - ESTEC)

ESTEC Thermal Analysis Workshop
03/11/2015

Why develop such a tool ?

OrbEnv tool development was initiated by several facts:

1. Thermal analyses of spacecraft in low Earth orbit rely on thermal environment parameters coming from various standards, not always in accordance

2. Such environmental parameters are generally expected to cover the worst hot/ cold cases for thermal analysis and design.

3. Environmental parameters are sometimes assumed regardless
- the orbit definition,
- the season,
- the time constant of the spacecraft (or of local parts exposed to the external environment…

4. For more than a decade, extensive and continuous measurements of Earth radiated and reflected flux have been performed by spaceborne instruments (CERES) and data are available.

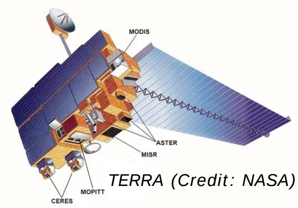

TERRA (Credit: NASA)

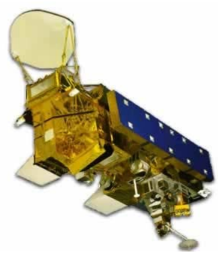

AQUA (Credit: NASA)

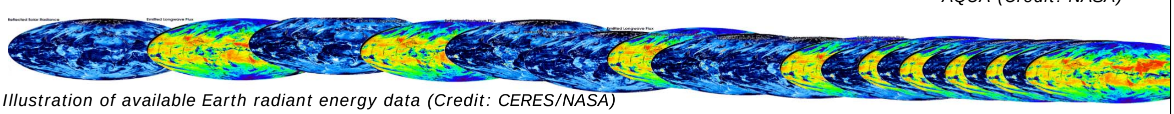

Illustration of available Earth radiant energy data (Credit: CERES/NASA)

Objectives of OrbEnv tool

OrbEnv activity and tool development objectives:

1. Understanding CERES data (albedo, IR flux) and compare them with existing standards

2. Find a method to use CERES data and determine albedo / IR flux depending on:
- the orbit definition,
- the season,
- the time constant of the spacecraft

(or of local parts exposed to the external environment.

3. Develop a tool to determine albedo / IR flux for any Earth orbit with several options:
- basic geometry of the spacecraft (plane, sphere, cube)
- time step

OrbEnv | 03/11/15 | Slide 3/31

ESA UNCLASSIFIED – For Internal Use

European Space Agency

Earth Infra-Red equivalent temperature depending on season and latitude (NASA CERES measured data)

Earth Infra-Red equivalent temperature depending on season and latitude (NASA CERES measured data)

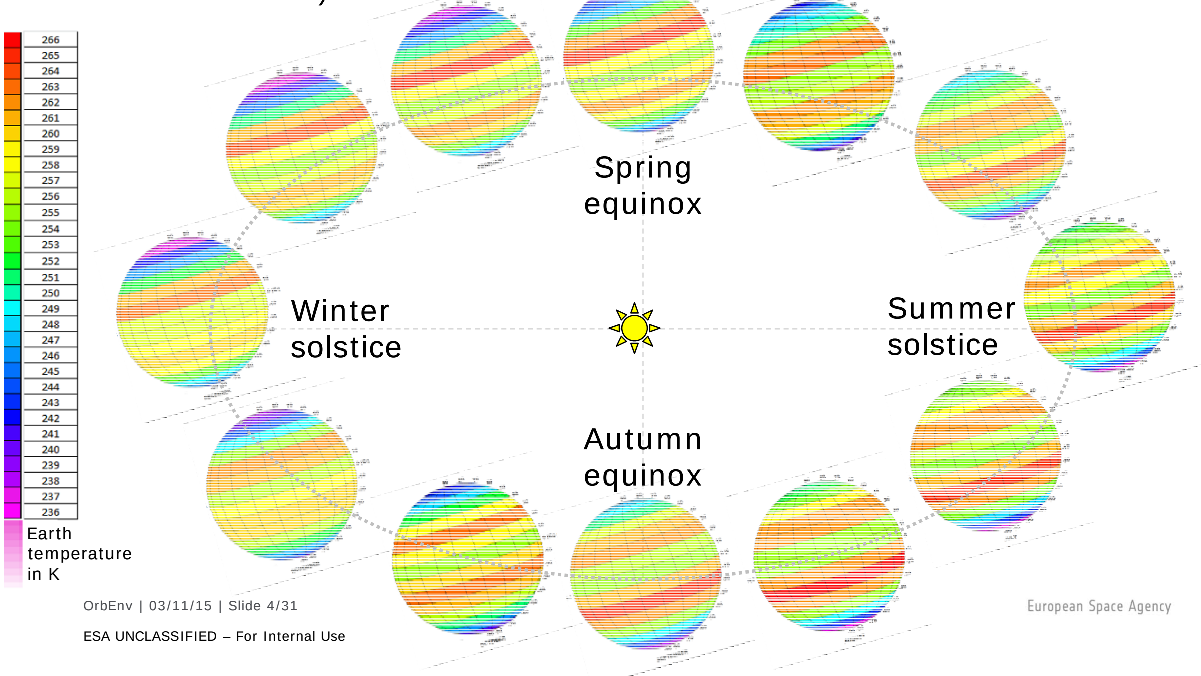

OrbEnv | 03/11/15 | Slide 4/31

ESA UNCLASSIFIED – For Internal Use

European Space Agency

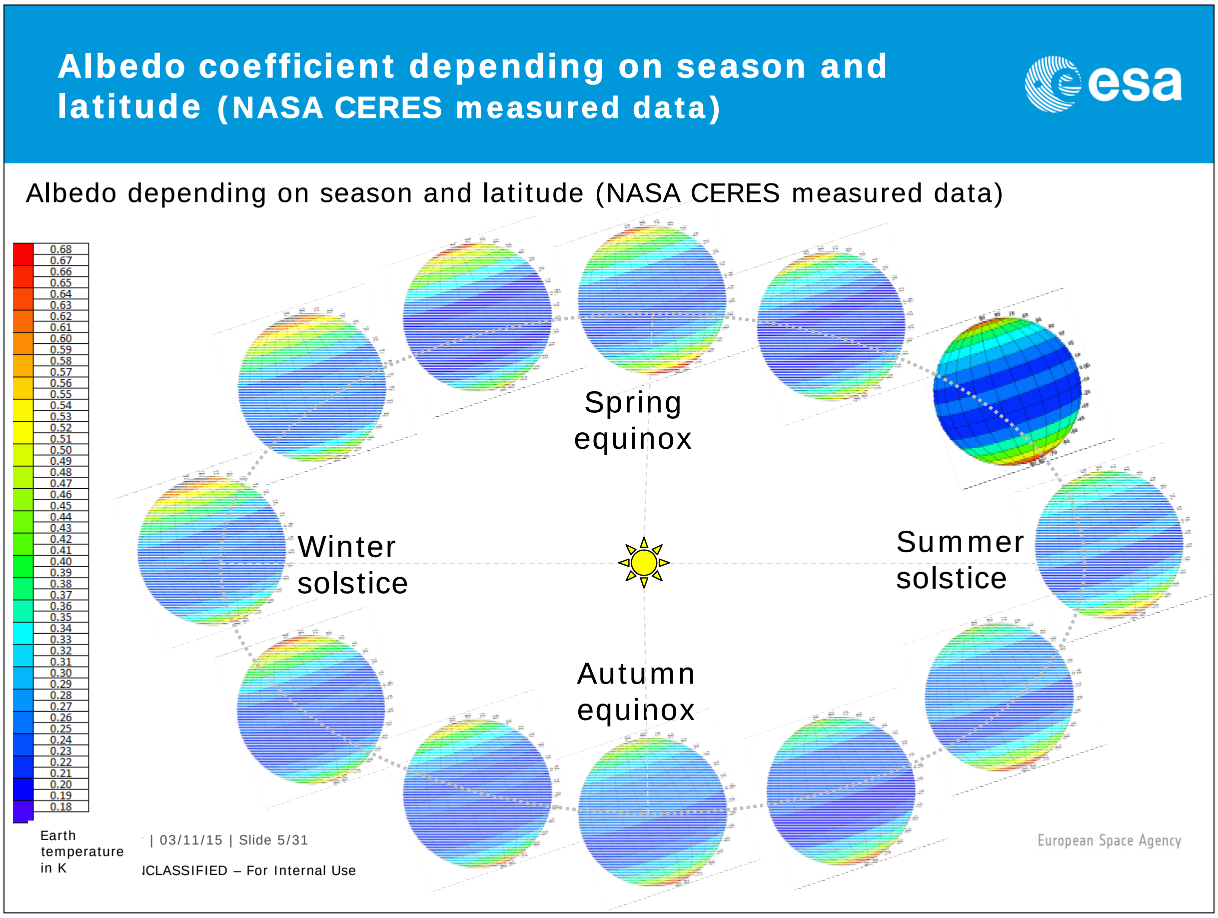
Albedo coefficient depending on season and latitude (NASA CERES measured data)
esa
Albedo depending on season and latitude (NASA CERES measured data)
Spring equinox
Winter solstice
Summer solstice
Autumn equinox
0.68
0.67
0.66
0.65
0.64
0.63
0.62
0.61
0.60
0.59
0.58
0.57
0.56
0.55
0.54
0.53
0.52
0.51
0.50
0.49
0.48
0.47
0.46
0.45
0.44
0.43
0.42
0.41
0.40
0.39
0.38
0.37
0.36
0.35
0.34
0.33
0.32
0.31
0.30
0.29
0.28
0.27
0.26
0.25
0.24
0.23
0.22
0.21
0.20
0.19
0.18
Earth temperature in K
| 03/11/15 | Slide 5/31
ICLASSIFIED – For Internal Use
European Space Agency

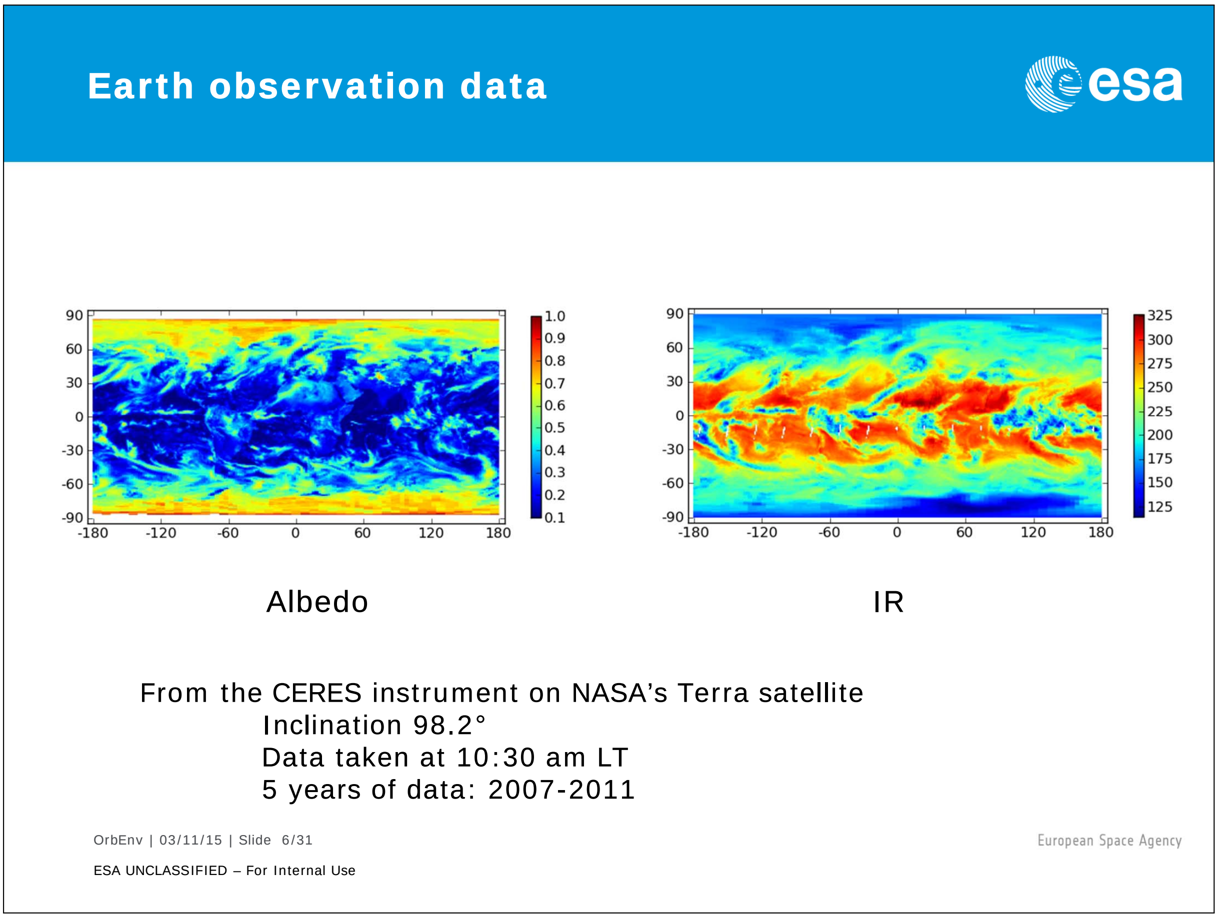

Real data was obtained for every day during the period of interest. Given as a map with 1 degree by 1 degree grid points. The planetary IR emission is given in W/m^2. The same features can be seen in both maps, for example clouds tend to be more reflective than land so have a higher albedo, but are colder so have lower thermal IR emission.

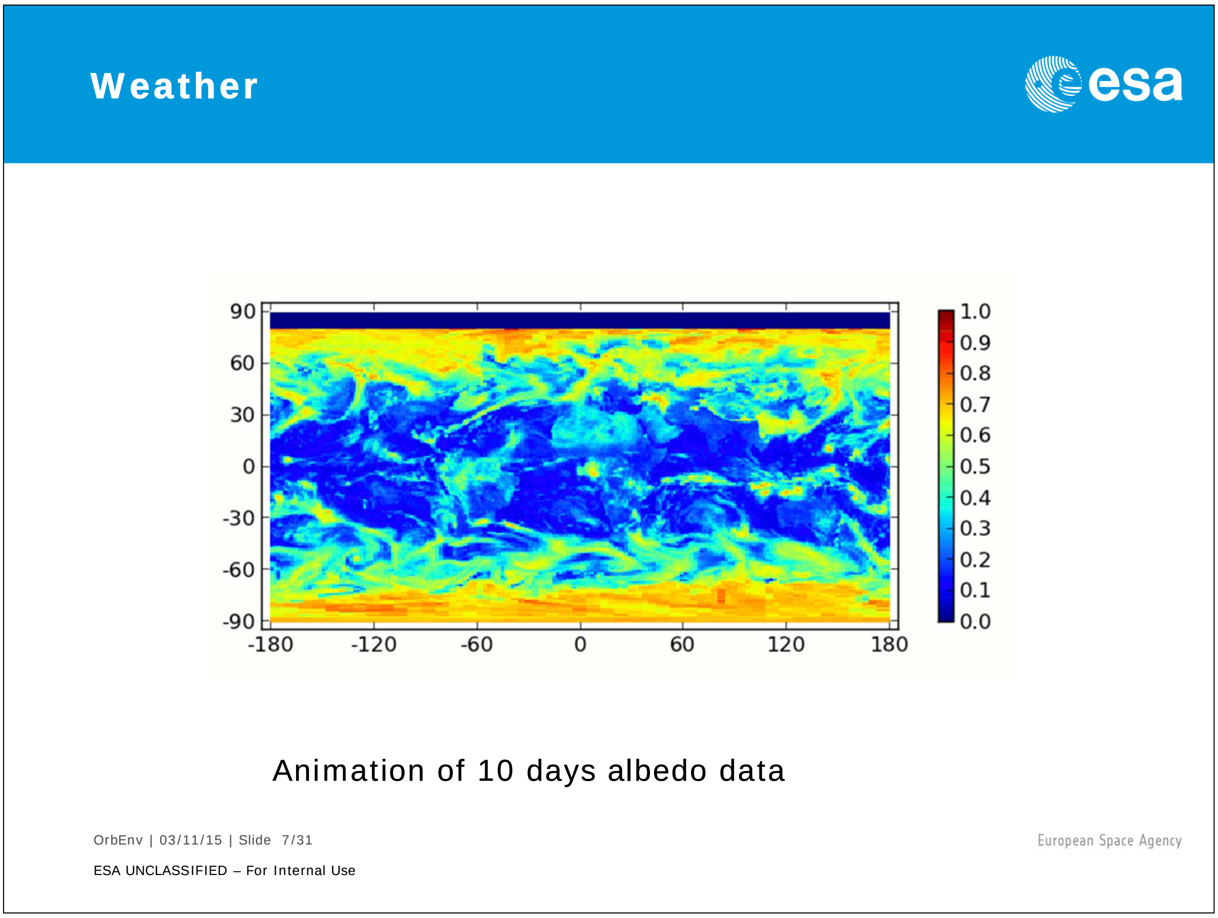

The movement of cloud features can be seen in this 10 day period. The lack of sunlight at the pole due to the northern hemisphere winter can be also be seen.

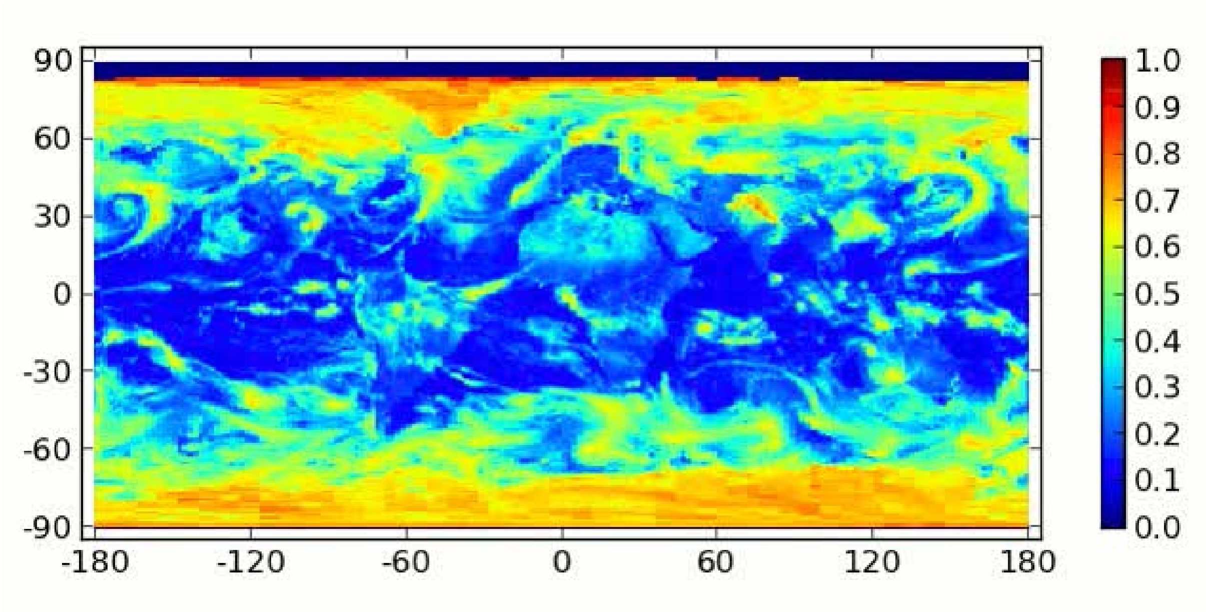

Save the attachment to disk or (double) click on the picture to run the movie.

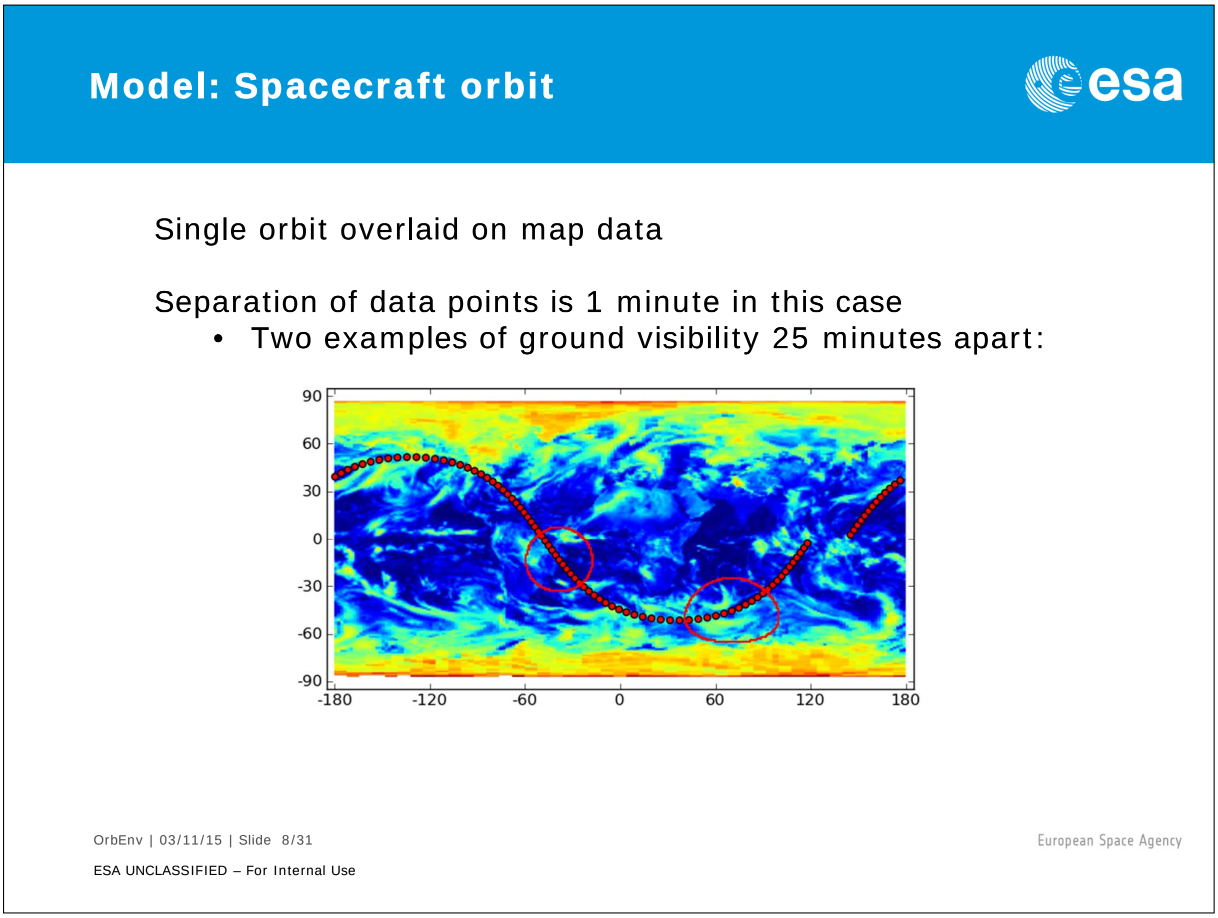

The flux received at each point of the orbit varies according the features visible at each instant. In one of these two examples the spacecraft is over the coast of Brazil and sees mainly low albedo ocean and forest, but later is over ocean with lots of cloud cover and thus a much higher average albedo.

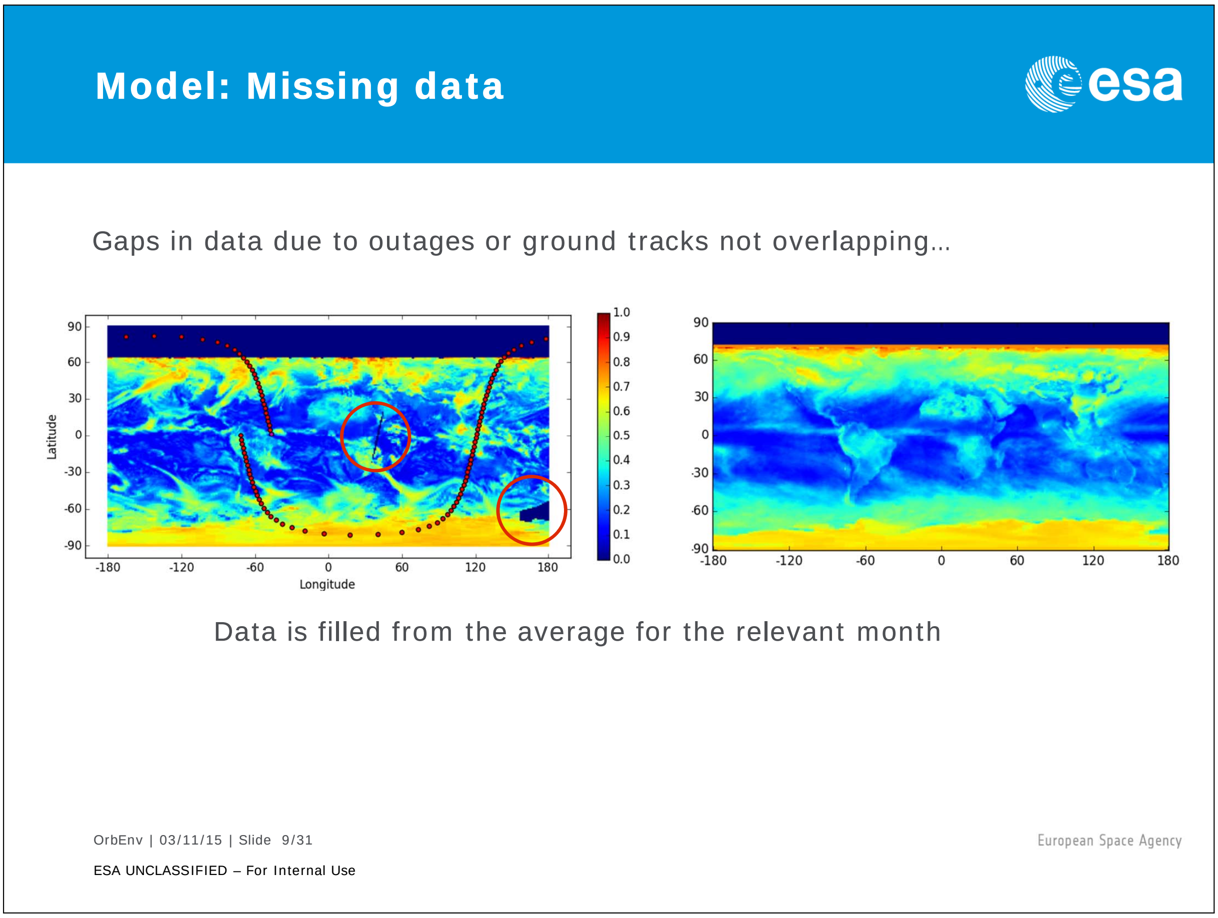

Where there is missing data the average value for the month is used. If a time period outside the data range is requested then the date can be be mapped around into the range, or average values can also be used.

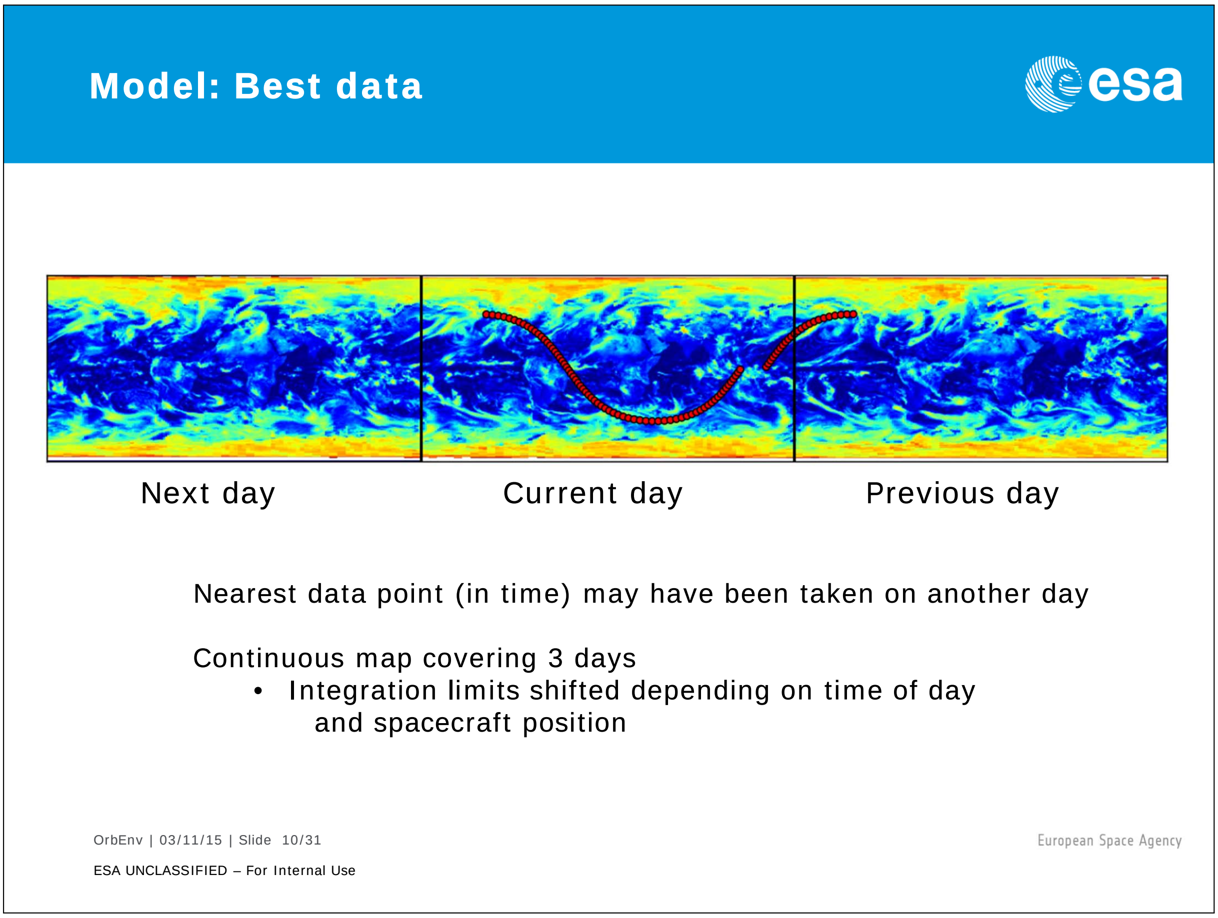

The data is taken by the satellite in a sun-synchronous orbit by building up ground tracks that have an equator crossing at 10:30 am local time. When integrating over the area visible to the satellite the data for the grid point should therefore be the one taken closest to 10:30 am local time even if it was taken on the previous or next calendar day according to UTC.

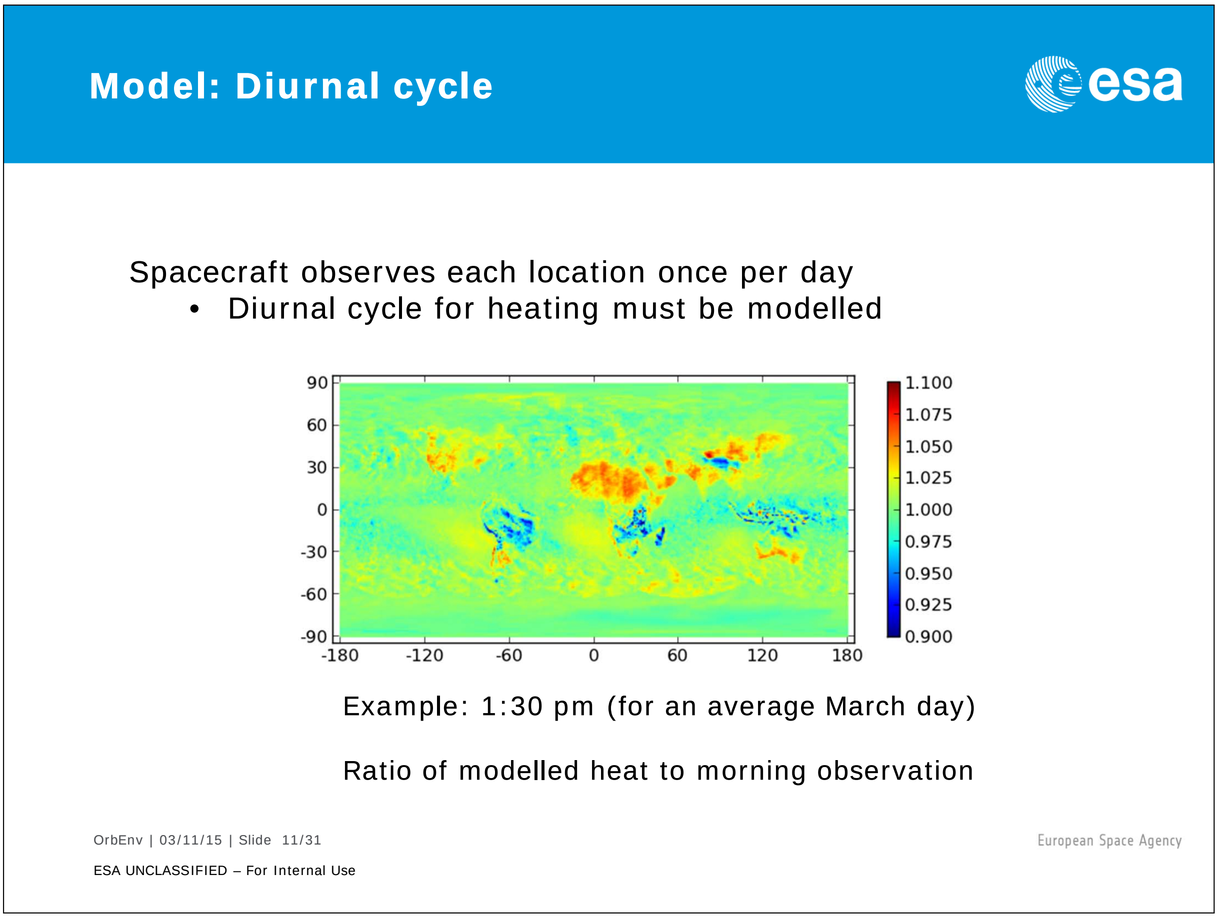

The data is provided as a single value for each day, but thermal IR emission has a strong variation during the day which must be allowed for. This also depends on location; ocean sees little variation due to the large thermal inertia of water, while desert sees a much bigger cycle. Also some areas experience different cycles due to cloud cover changes, e.g. clouds tend to form over rainforests in the afternoon, reducing IR emission. To estimate this cycle, data was processed that shows how IR emission varies during the day for each grid point, by each month of the year. So for example we can say that on a typical March day the IR emission from a grid point in the Sahara is 5% greater at 1:30 pm than at 11:30 am when the satellite data was taken. This is combined with the satellite data for that day to provide an estimate of the emission at any time during the day in question.

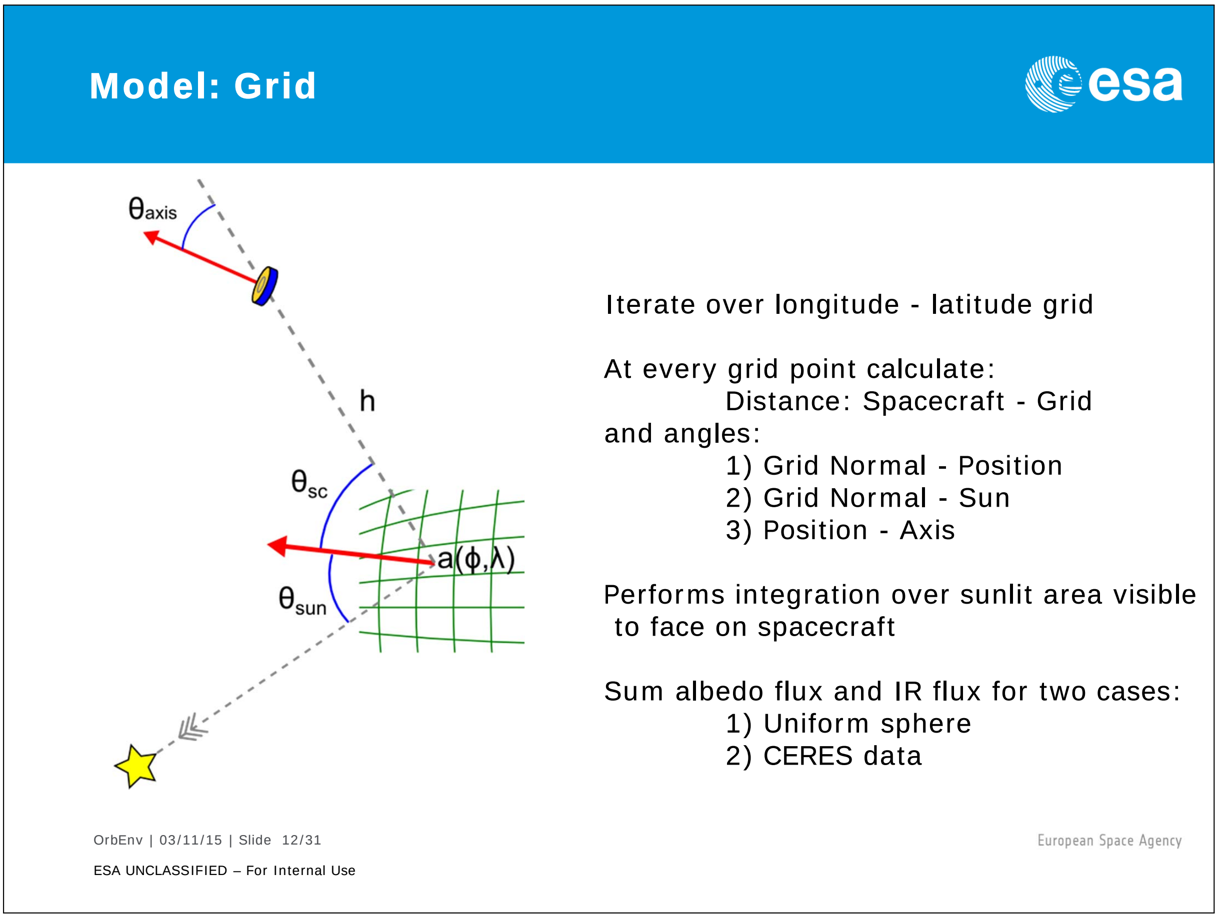

At every grid square on the map the contribution to the flux received at the spacecraft location is calculated if the spacecraft is visible (the angle between the grid point normal and the grid-to-spacecraft vector is < 90 deg). Both albedo and IR fluxes are calculated for each face on the spacecraft. In addition the flux is calculated for two cases:

1. If the Earth had a uniform value for albedo/IR
2. With the real, varying albedo/IR values measured by satellite.

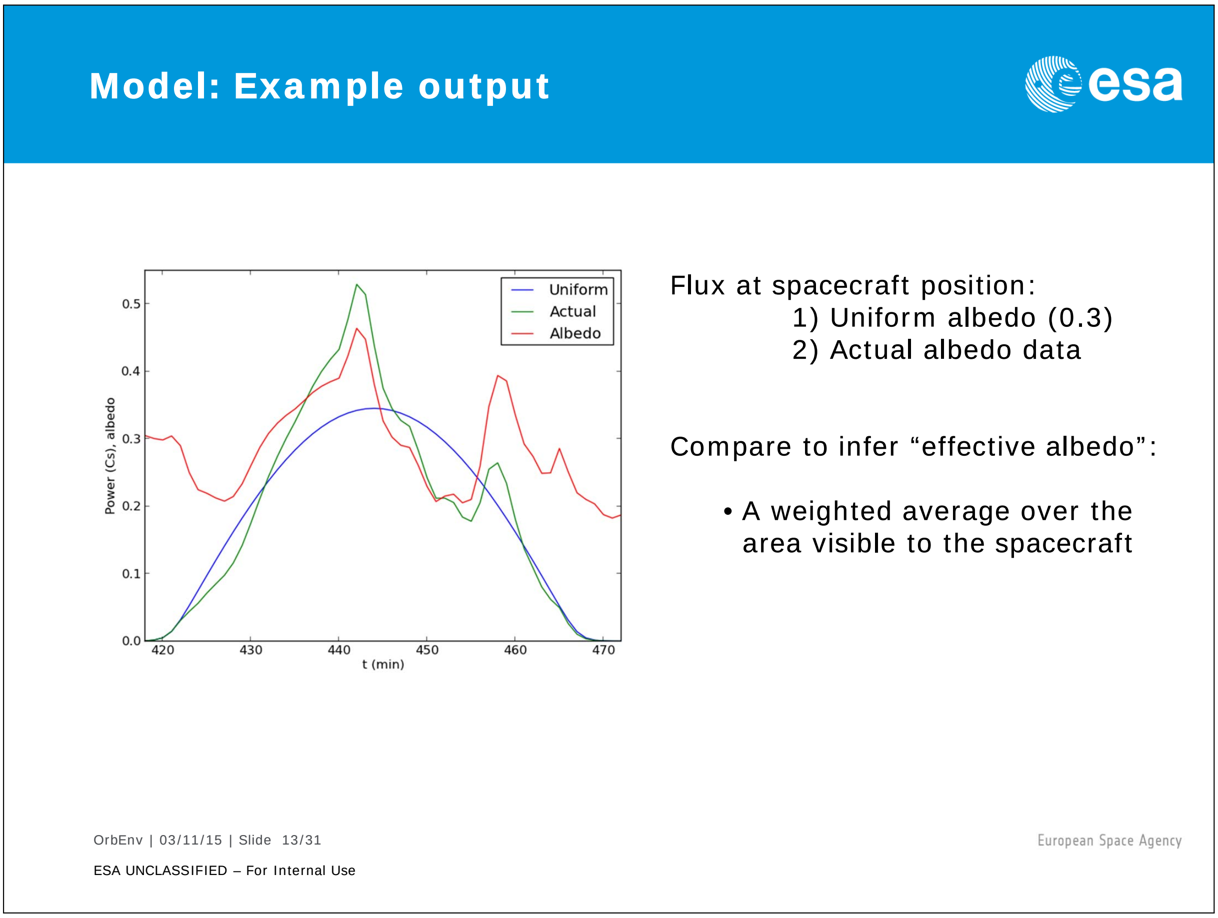

The sunlit portion of one orbit is shown. The albedo flux (in units of the solar constant) at the spacecraft position is shown for two cases:

1. Earth has a uniform albedo value of 0.3
2. An actual flux with albedo varying according to satellite measurements for the relevant day.

By comparing the two we can calculate an effective albedo value at each point - a uniform value for the earth that would produce the same heating as predicted using the varying albedo data. For example if the predicted (actual) flux at the spacecraft position is higher than the calculation for the uniform (0.3) case then we can infer that the effective albedo at that moment must have been proportionally greater than 0.3. It can be seen that on this orbit the effective albedo during the orbit is around 0.3 on average, with some variation between 0.2 and 0.4 due to the features the spacecraft passes over.

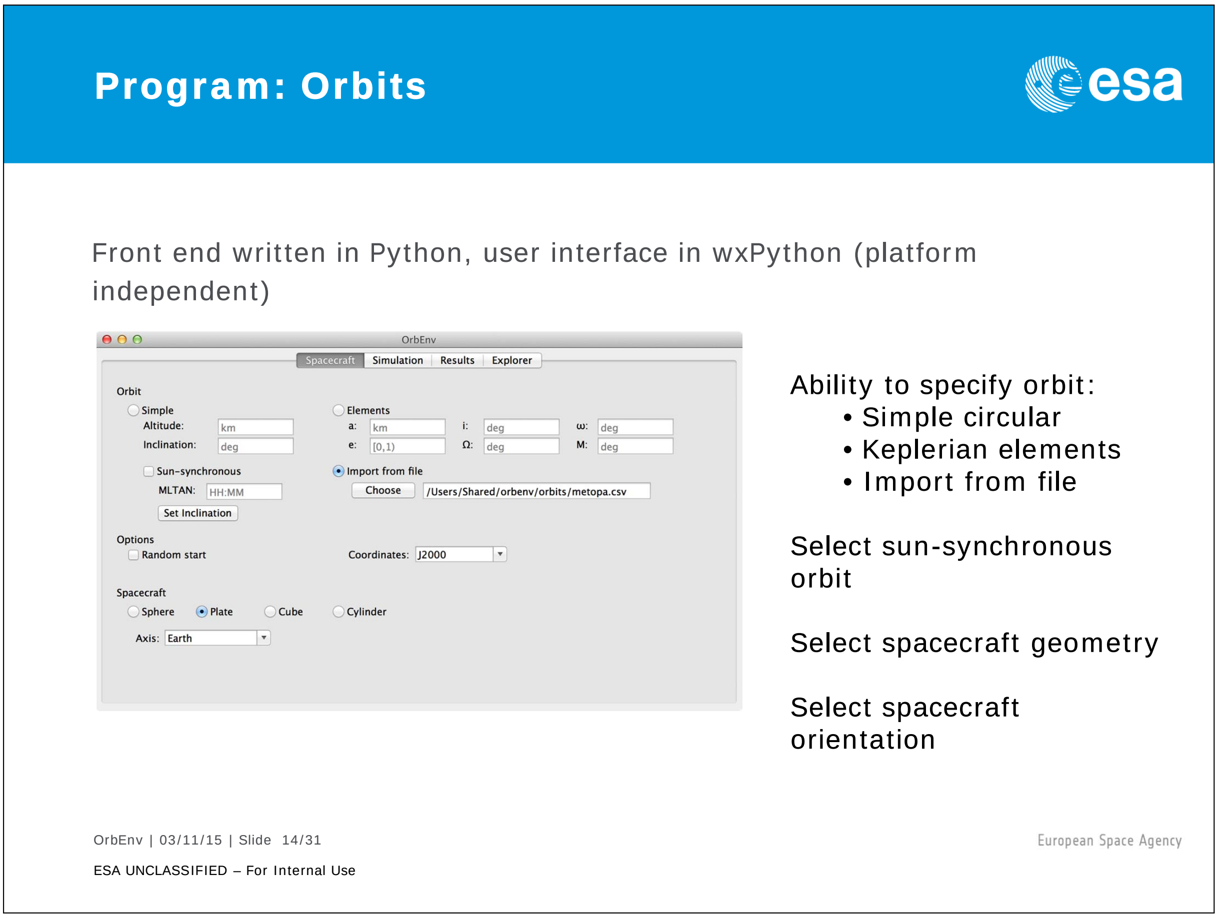

A front end for the model has been written to make it easy for engineers to set up and study cases of interest. The orbit can be specified in several ways, or imported from a file (e.g. output from STK). The spacecraft geometry and orientation (earth/velocity/sun/polar/ecliptic) can also be specified.

Program: Simulation

Back end calculations performed in Fortran

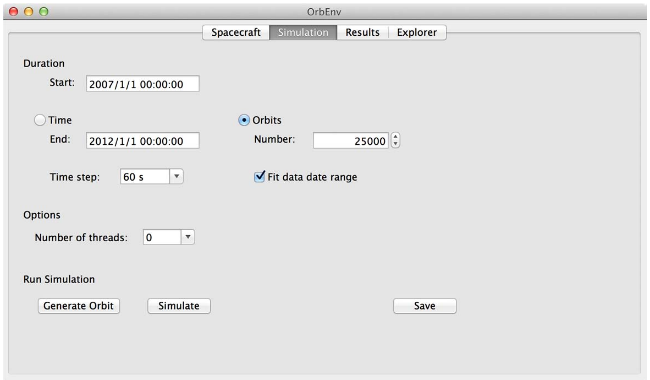

Specify duration of interest:
- By time
- By number of orbits

Simulation time step

Fully multi-threaded:
~300 orbits / min

OrbEnv | 03/11/15 | Slide 15/31

European Space Agency

ESA UNCLASSIFIED – For Internal Use

The model calculations are implemented in Fortran for speed. The simulation can be completed in under an hour on a reasonably powerful computer, so does not have a significant impact on workflow.

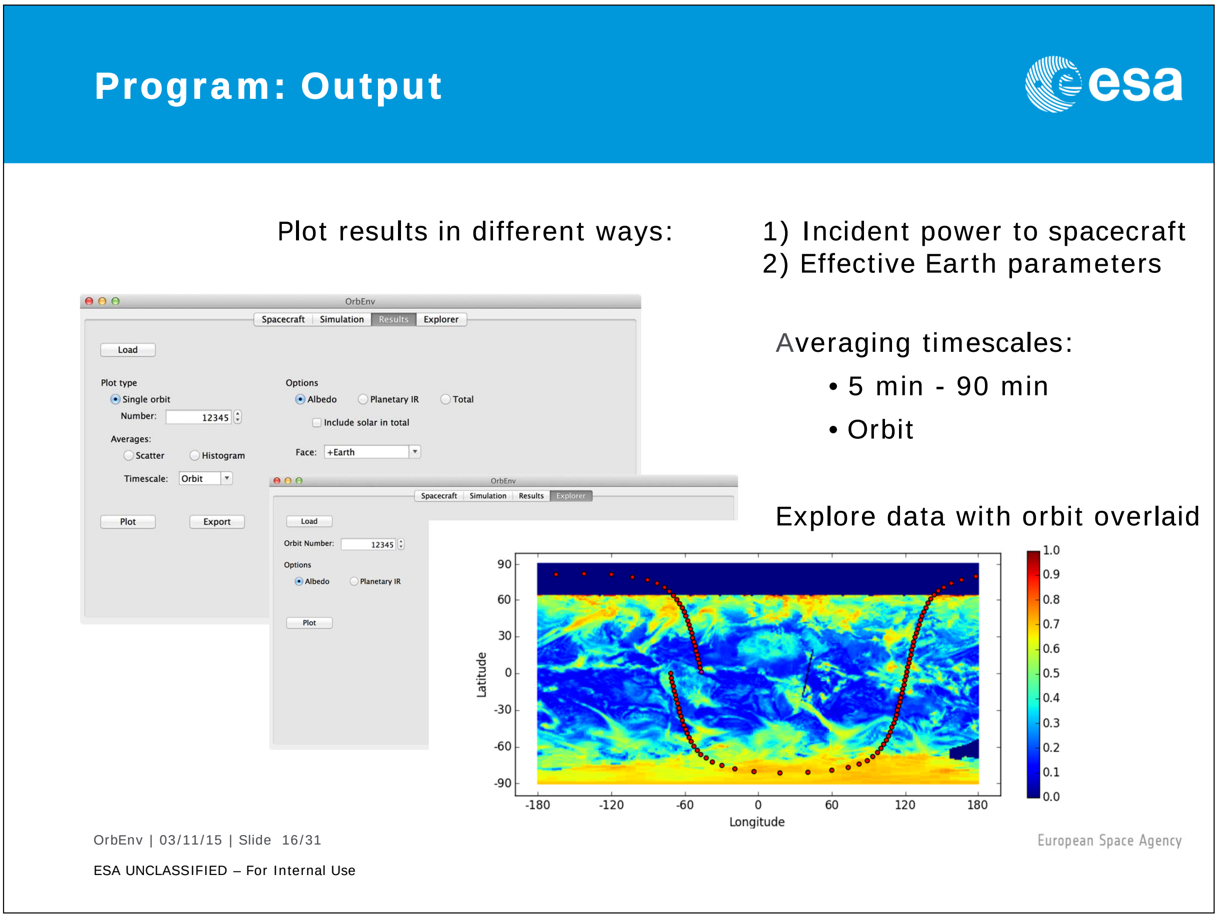

The results can be explored graphically or exported to file for further study.

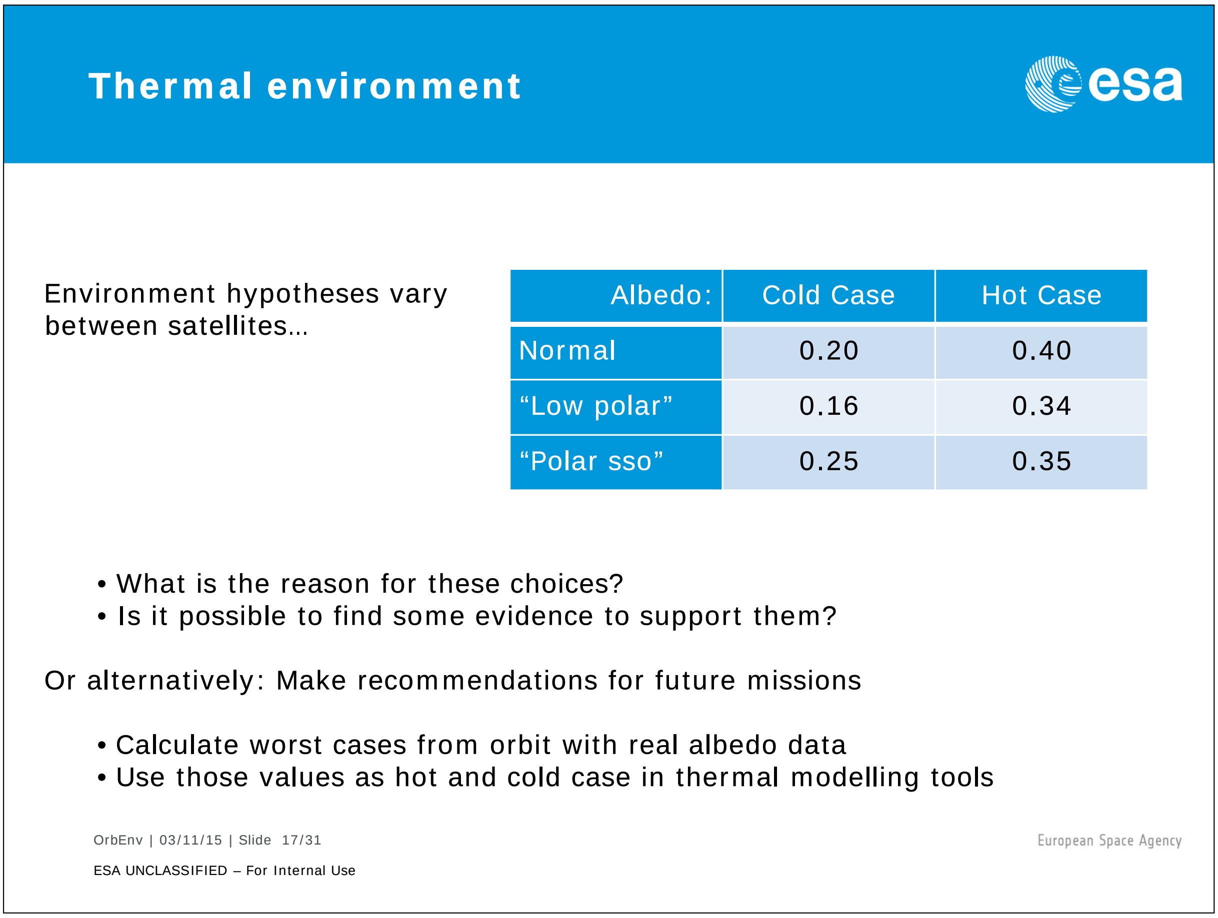

The issue has been raised lately of why certain values for Earth's thermal environment are used; why the chosen values are not consistent, and what justifies the choices. Earth's albedo is approximately 0.3 when averaged over the entire globe, so values of 0.2 - 0.4 are common choices for the cold and hot cases. But for example, in the case of some polar spacecraft, flying over areas with greater albedo on average, we see lower values are chosen, why?

Instead the model that has been developed can be used to combine spacecraft orbits with real Earth observation data to estimate the range of environment variables that would have been experienced in reality. This can provide evidence to support the choice of values for thermal modelling.

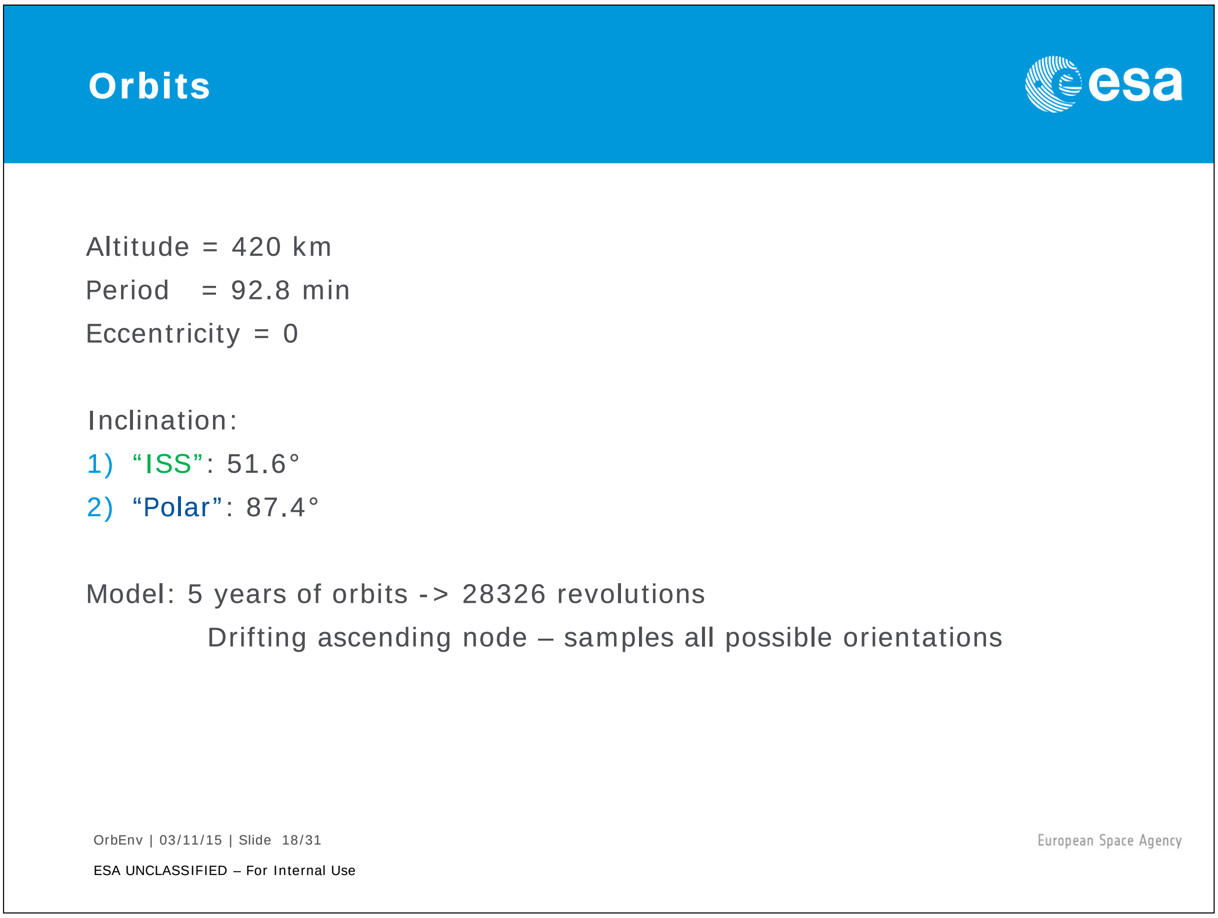

Two orbits have been chosen for comparative purposes; one orbit similar to the ISS, and one with the same altitude but in a polar orbit. Five years are modelled, providing a large number of revolutions to give a large statistical sample.

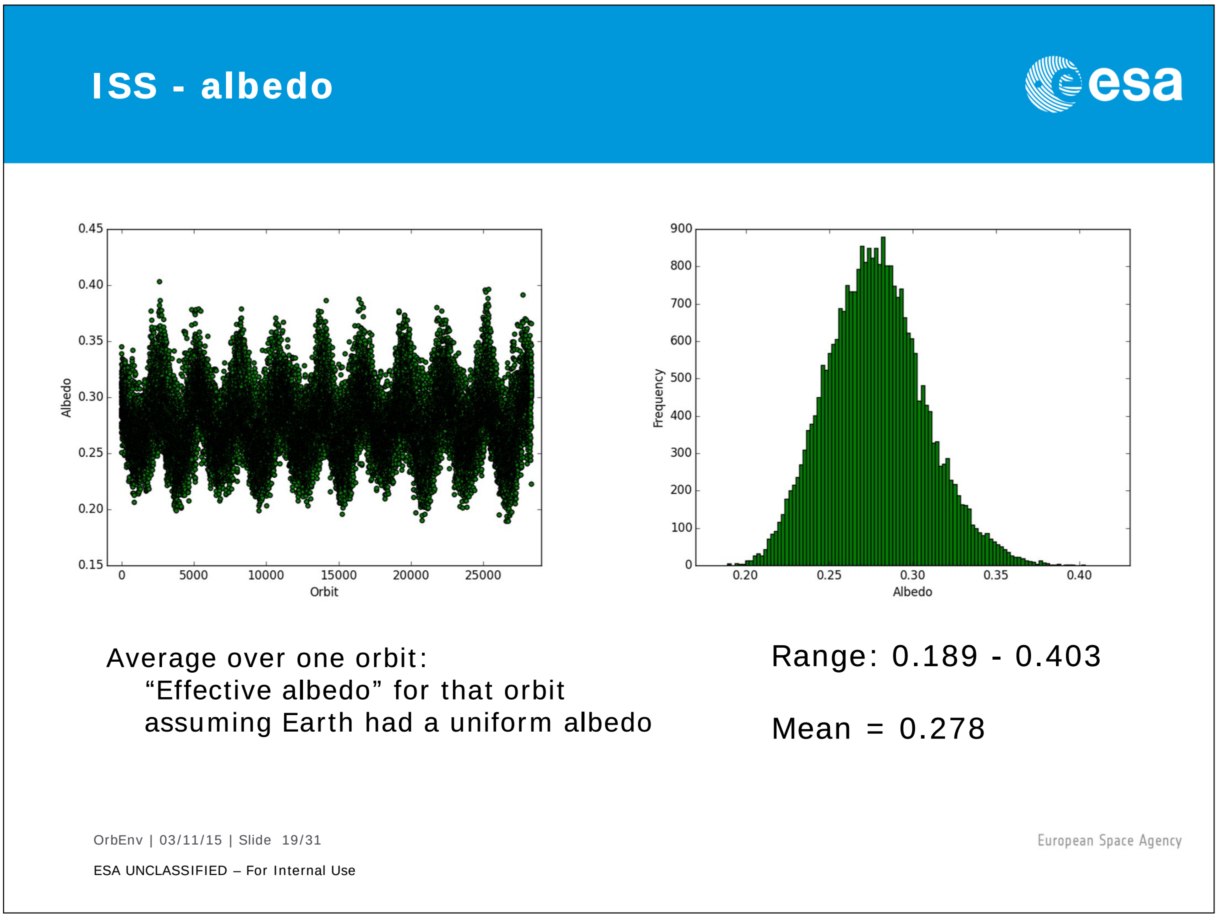

The data can be averaged over different timescales, here an average over one orbit is calculated. This shows what uniform value of albedo the earth would have needed for the spacecraft to receive the same energy over one orbit as it does in the case when actual albedo data is used. For the ISS orbit a range of 0.2 - 0.4 appears sensible for the extreme cases. There are appear to be two peaks of albedo per year.

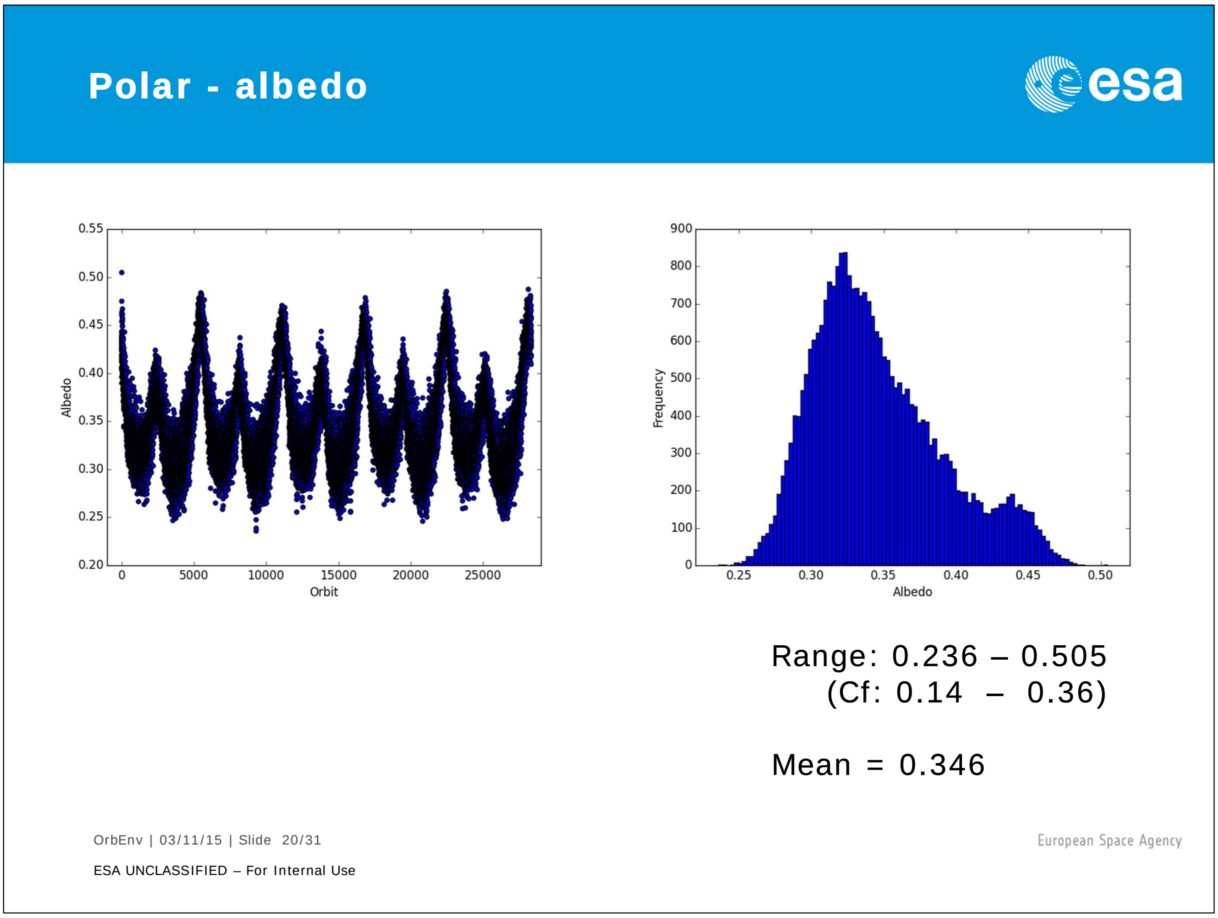

In the polar case the effective albedo range observed is much higher, the ranges assumed for polar spacecraft earlier does not appear to be appropriate. The distribution also appears to be somewhat bimodal.

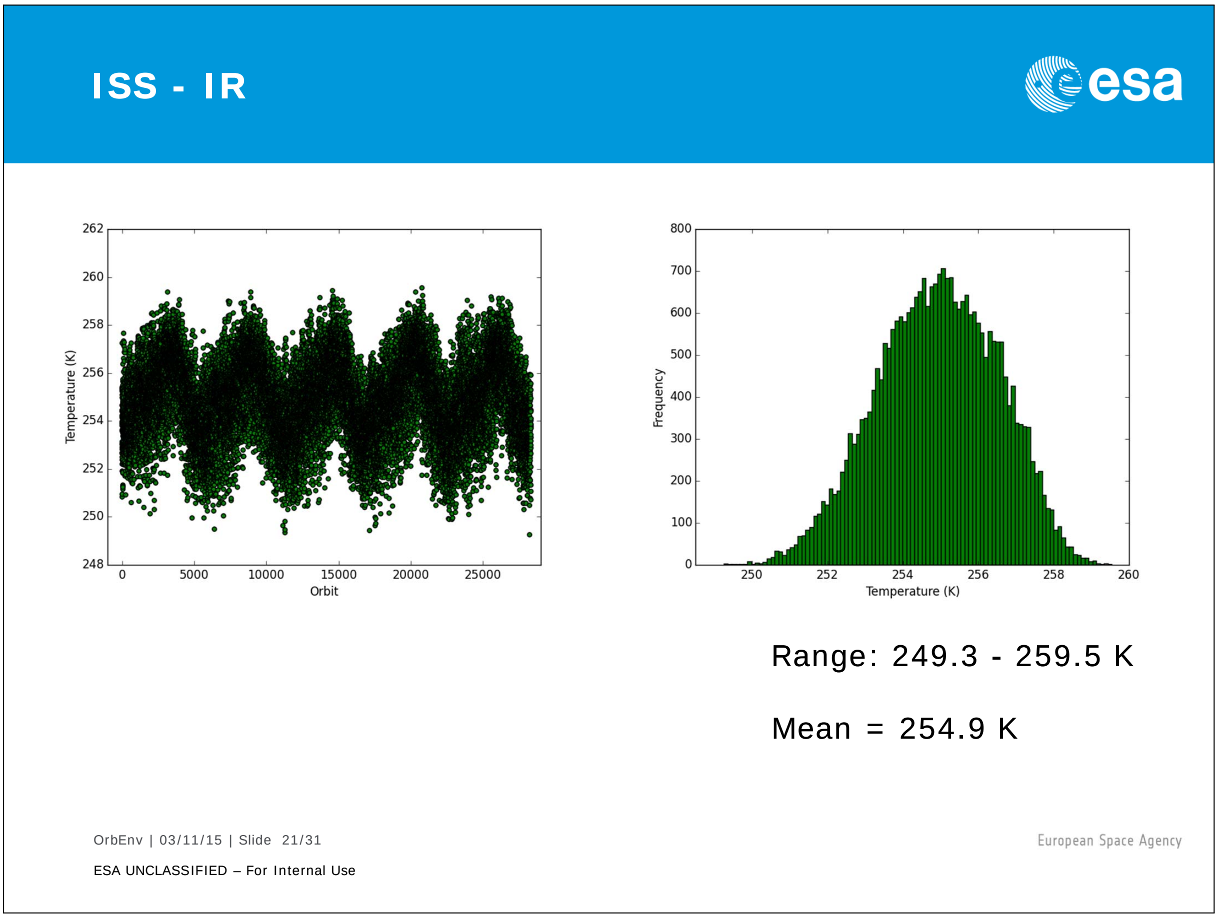

The same calculations can be done for thermal IR emission in the ISS case. There is only one peak per year.

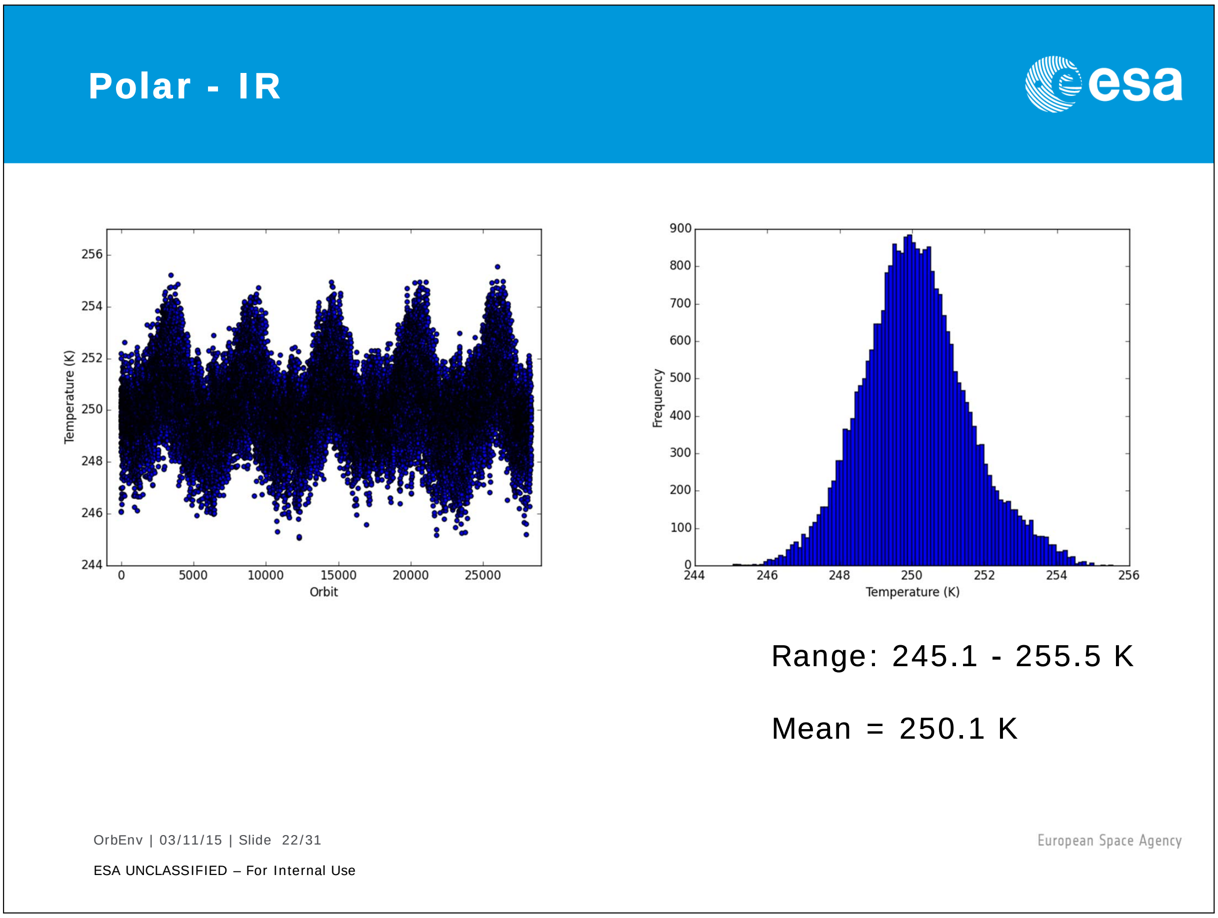

Polar orbit, IR.

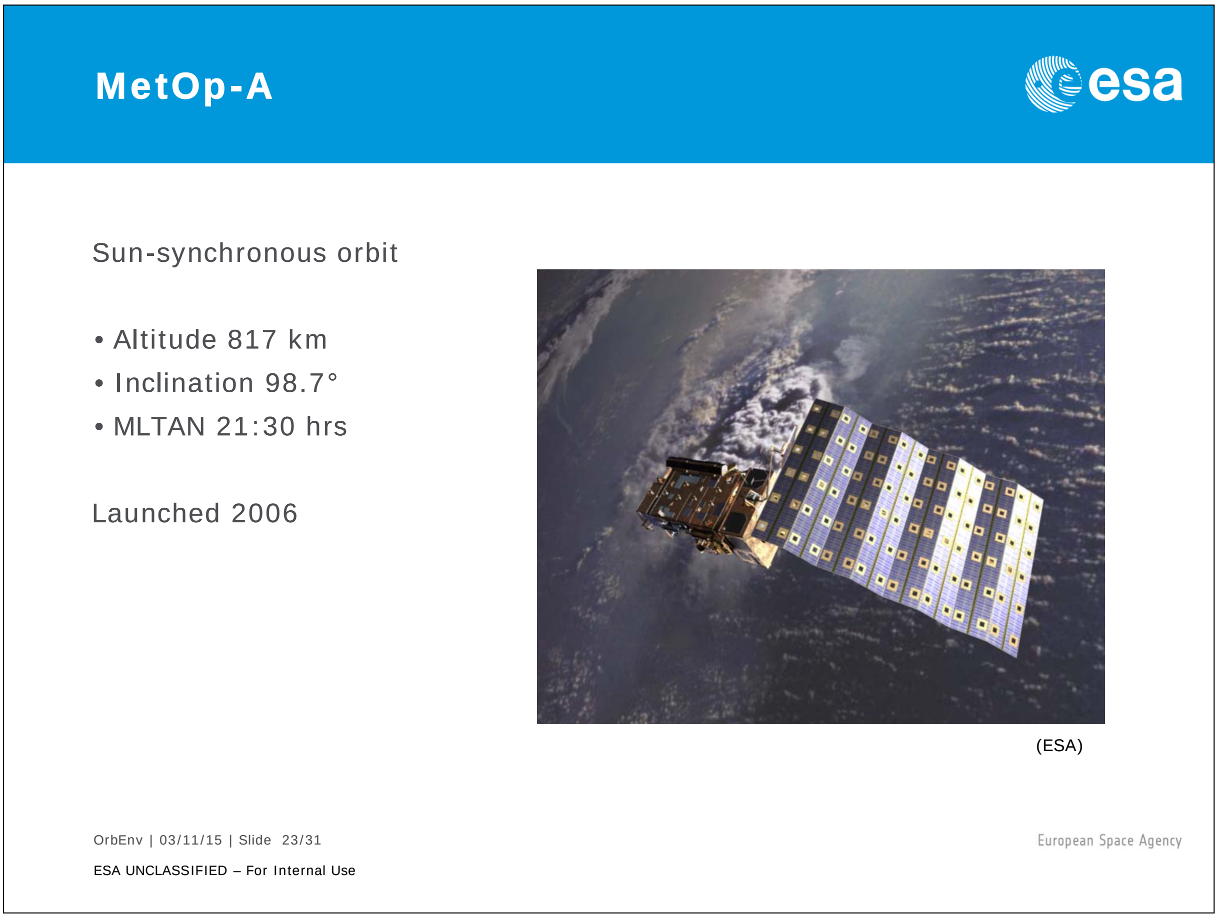

MetOp-A has an orbit typical of sun-synchronous earth observation satellites. It was launched in 2006 so here the real spacecraft position data for the period 2007-2011 could be imported into the simulation. This allows us to observe the actual features/weather the spacecraft flew over.

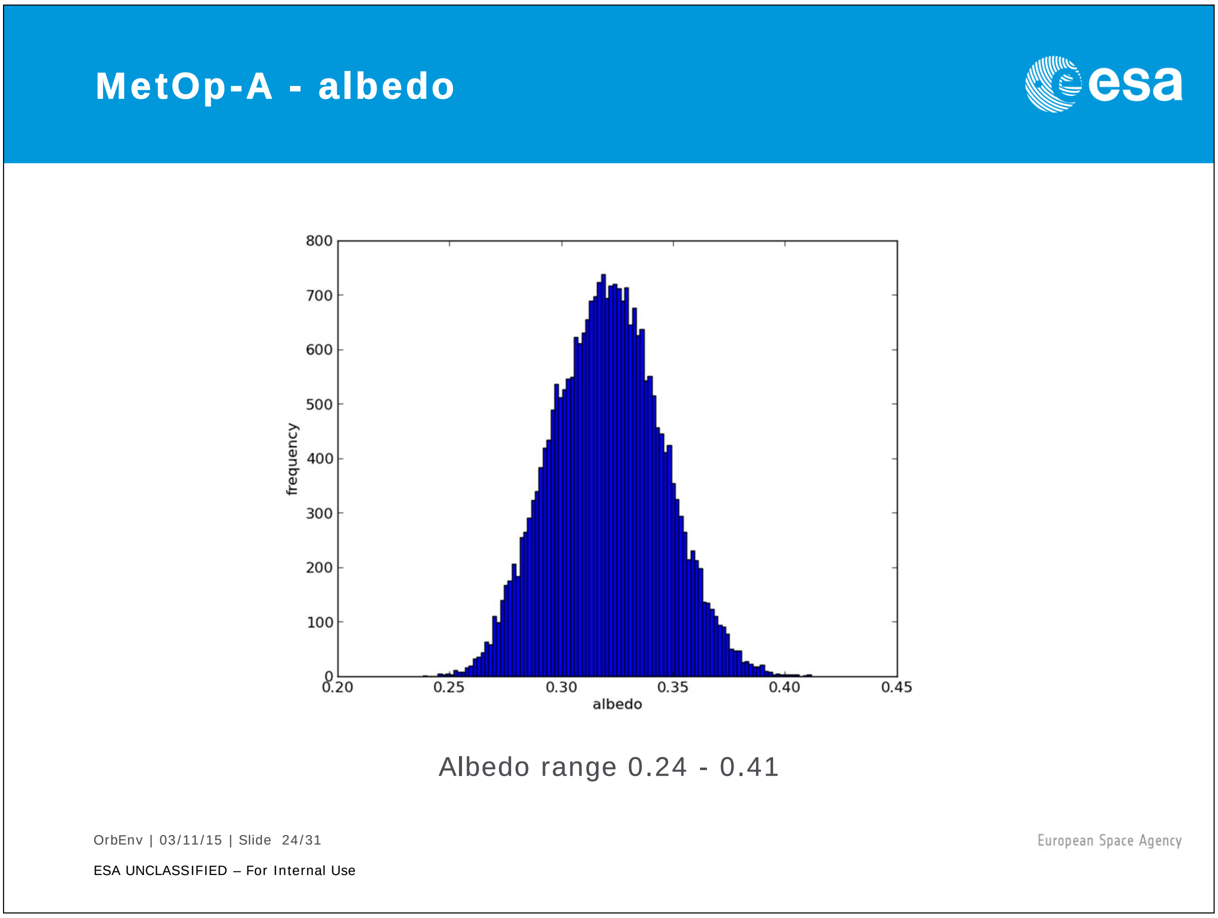

The range of effective albedo averaged over one orbit is observed to vary between 0.24 and 0.41. We can see that the normal range of 0.2 - 0.4 would perhaps be a little too conservative in the cold case.

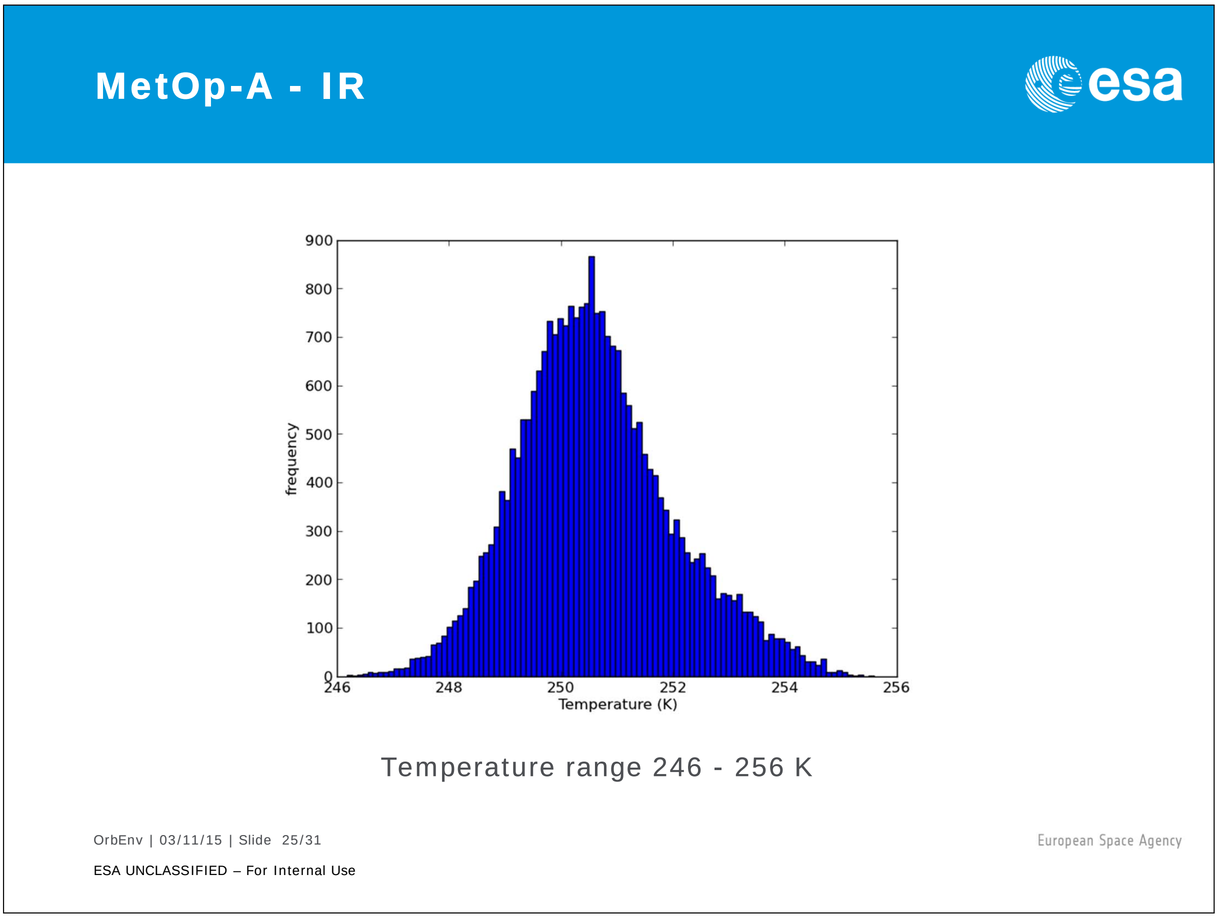

For IR emission the effective surface temperature varies between 246 and 256 K.

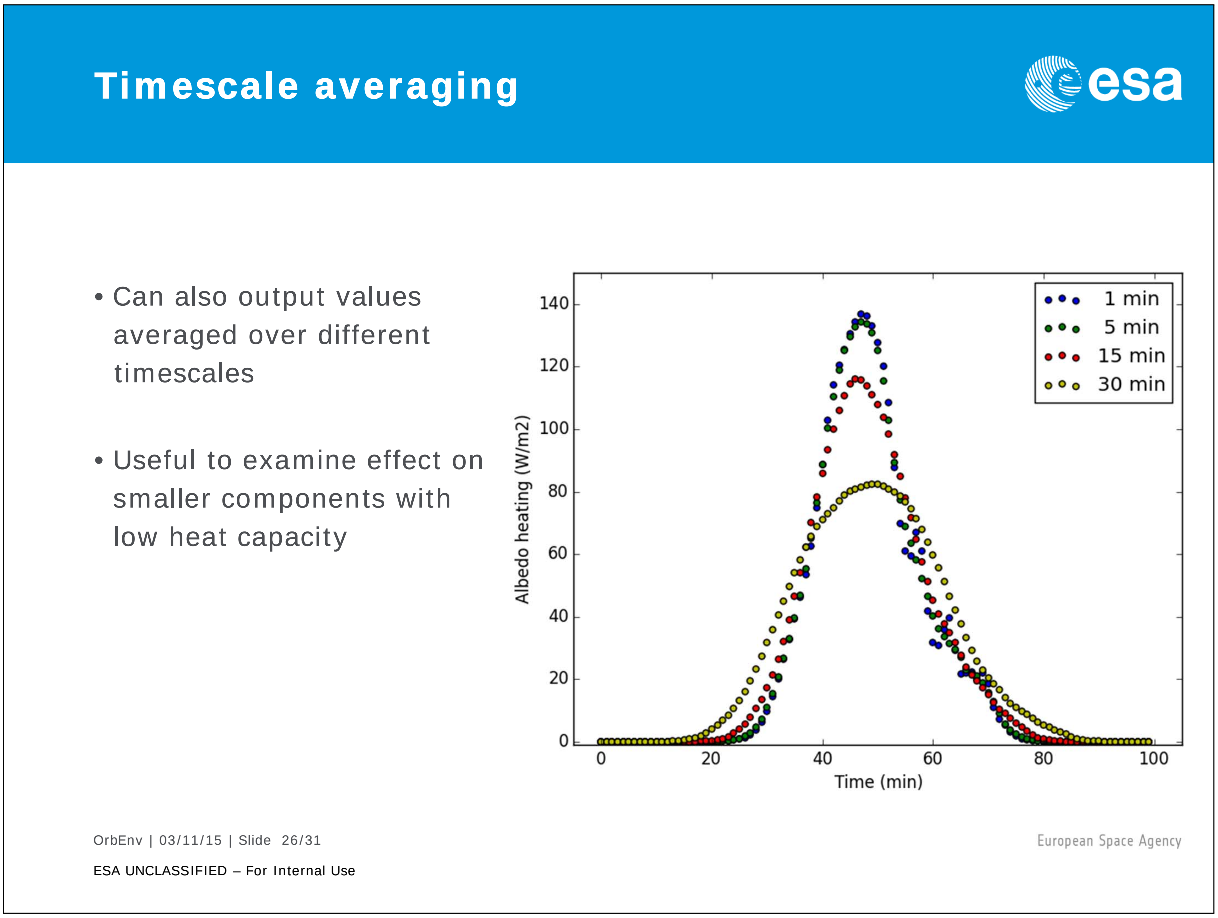

The results so far have shown effective surface parameters when averaged over a single orbit. The model can also output the instantaneous albedo/IR heating received by the spacecraft, and perform averaging over different timescales.

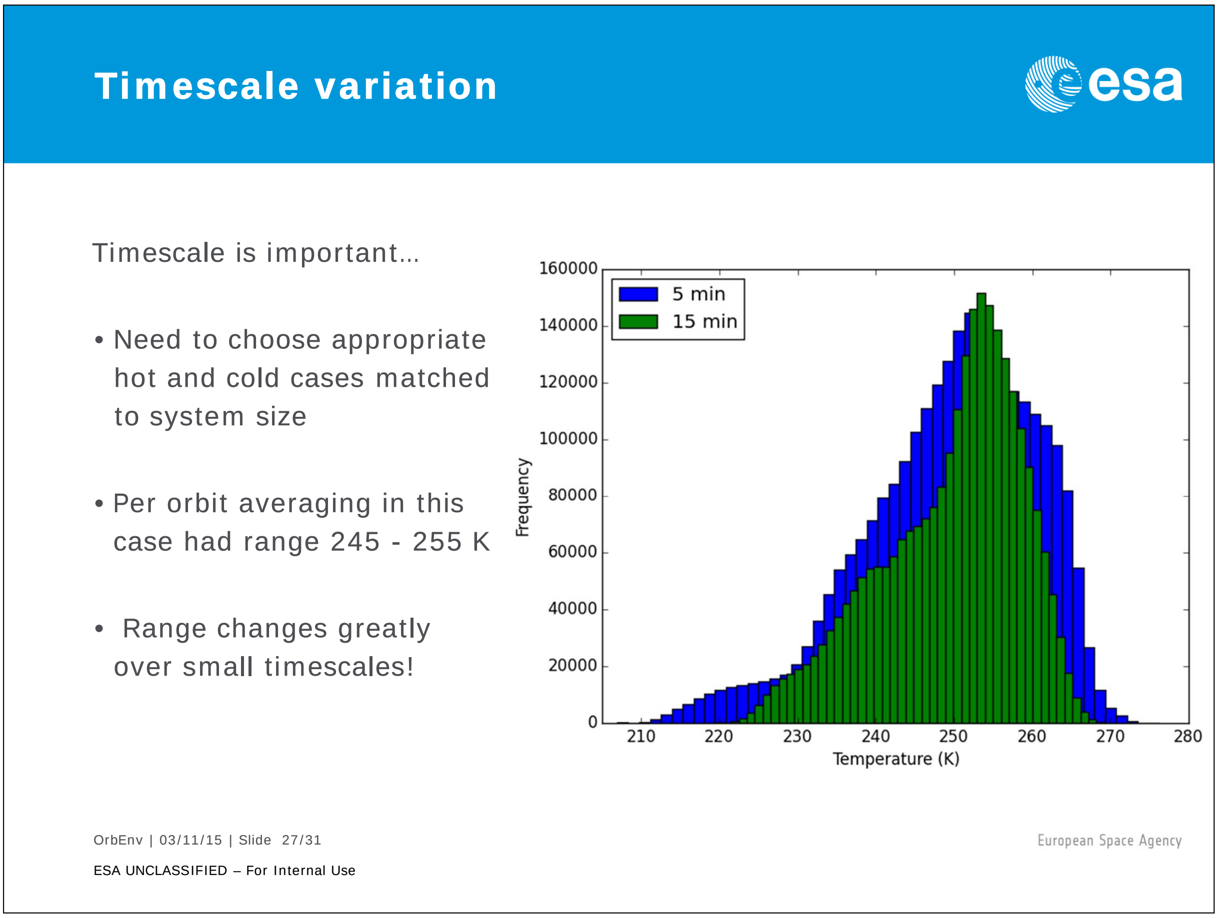

It can be seen that the variations are much greater when averaged over smaller timescales.

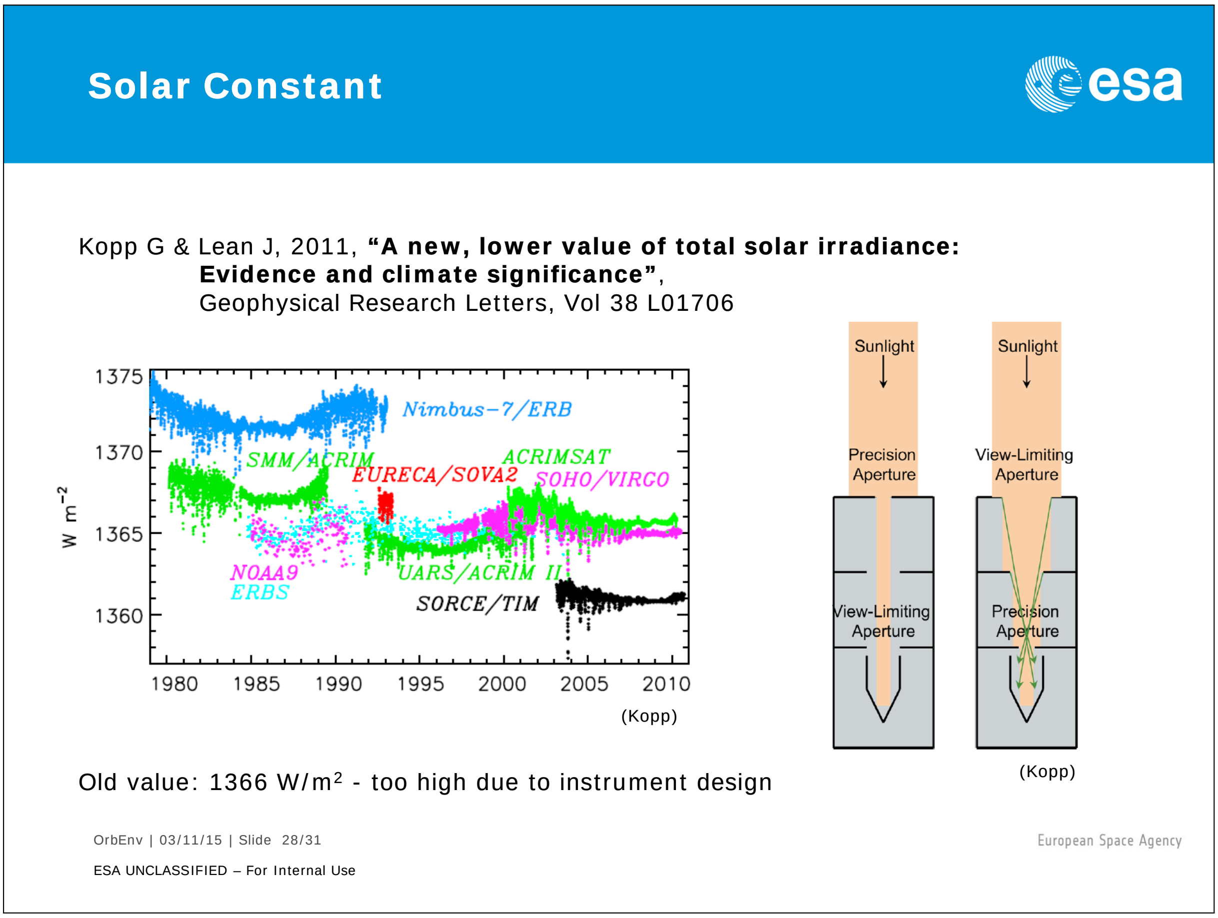

In addition to albedo and planetary IR, the other major parameter of the orbital thermal environment is direct solar heating. In recent years the value of solar ”constant” has been questioned due to new measurements. The commonly employed, old values of solar irradiance appear to be in error due to scattering and diffraction internal to the instruments used.

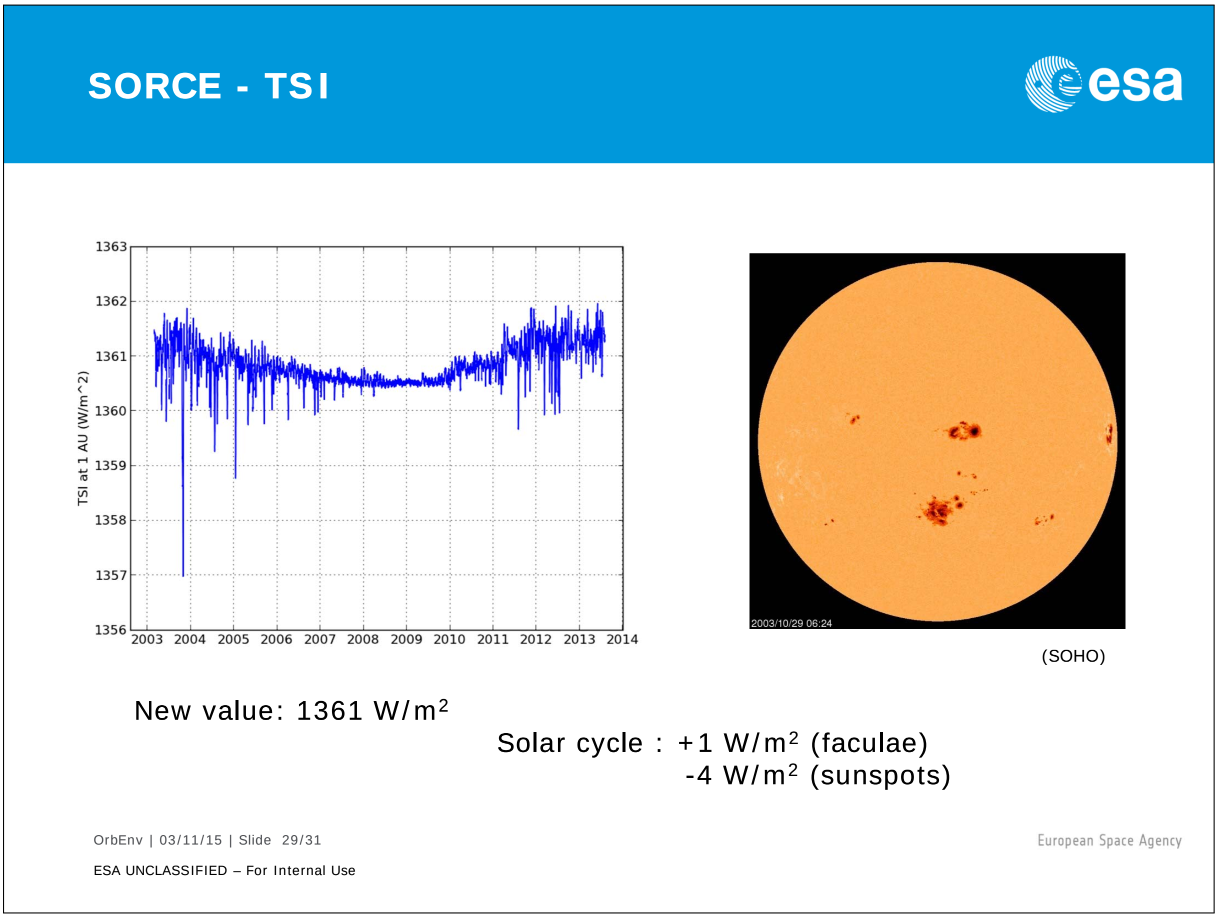

The Total Irradiance Monitor on NASA's SOlar Radiation and Climate Experiment satellite measures the Total Solar Irradiance much more accurately and gives a new lower figure. This value is now accepted by climate scientists and is recommended in the latest report from the United Nations Intergovernmental Panel on Climate Change.

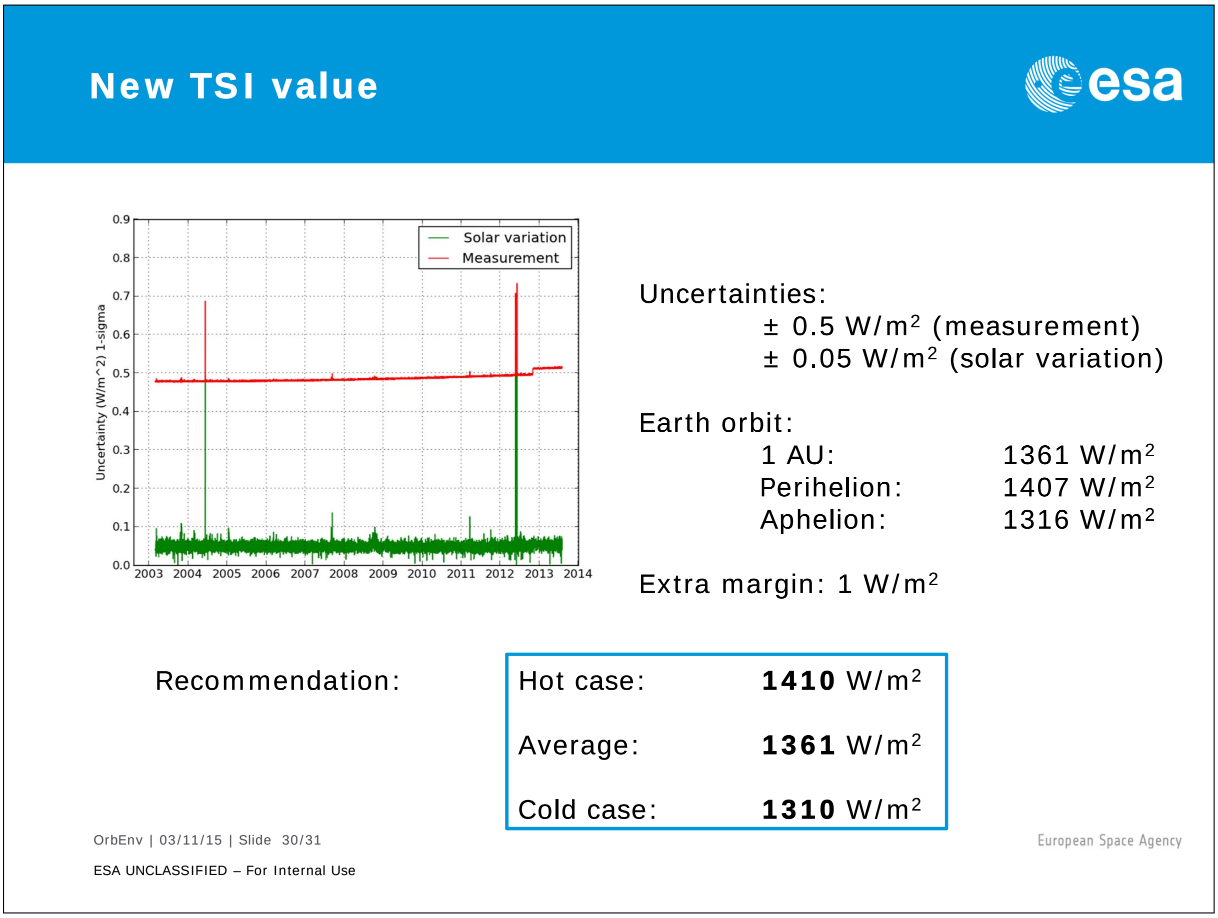

When taking into account Earth's orbit, the solar cycle, and the uncertainties, then new values of solar heating for hot and cold cases are recommended for a spacecraft in orbit around the Earth.

End

Thank you!

Questions?

OrbEnv | 03/11/15 | Slide 31/31

ESA UNCLASSIFIED – For Internal Use

European Space Agency

http://www.kuu.org.uk/orbenv/

Appendix C

Mercury Retro-Reflection
Modelling and Effects on MPO Solar Array

Anja Frey Giulio Tonellotto
(ESA/ESTEC, The Netherlands)

Abstract

Mercury's regolith might reflect the incident sun light preferably in the direction of the Sun, causing a retro-reflection effect. In the case of the BepiColombo Mercury Planetary Orbiter solar array this deviation from the bond albedo, which is implemented in most thermal analysis software, may cause significant temperature differences. This causes power losses since the solar array is continuously steered throughout the orbit in order to optimize its sun aspect angle (maximum sun power) without exceeded the design temperatures.

To estimate the influence of this albedo variation the mathCAD sheet Mercury Orbital Heat Fluxes Assessment (Merflux), developed by ESTEC's D. Stramaccioni, was adapted to calculate the heat fluxes that a spacecraft experiences in orbit around Mercury when considering the retro-reflection. Different albedo modelling options were implemented and finally the diffusive reflection modelling was compared with a directional reflection case, where sunlight is reflected back into the direction of the Sun more than into the other directions. The directional reflection modelling was considered the most realistic, based on findings in literature.

The peak albedo flux, impinging on a nadir-pointing cube, calculated with this directional model, was found to be more than twice the flux calculated with the diffusive approach, while the integral remains the same (energy balance of the planet). An extensive parametric study, with different solar panel models and attitudes, concluded that the influence of the albedo modelling has a non-negligible influence on the solar array temperature. For a fixed solar aspect angle throughout the whole orbit, the biggest difference in temperature between the two albedo models was found to be +14°C/ -10°C. A more realistic approach used a steering profile provided by ESOC and found maximum ΔT of +8°C/ -5°C. These worst ΔT are local peaks, not applicable to the whole orbit, nor applicable to the most critical panel wing of the solar array, whose ΔT is only +4°C/ -4°C. Around the sub-solar point the directional albedo provides the highest temperatures, while they are lower at the poles.

This information will permit preparing the best approach for solar array in orbit steering functions definition and calibration.

esa

Mercury Retro-Reflection:
Modelling and Effects on MPO Solar Array

Anja Frey
Giulio Tonellotto
ESTEC
03/11/2015

European Space Agency

BepiColombo (spacecraft/mission)

- Europe's first mission to the planet Mercury, planned launch 2017
- Three modules:
  - Mercury Planetary Orbiter (MPO, ESA): studies surface and internal composition
  - Mercury Magnetospheric Orbiter (MMO, JAXA) surrounded by the Sunshield (ESA): studies magnetosphere
  - Mercury Transfer Module (MTM, ESA): carries the whole SC to Mercury
- Journey to Mercury takes 7.5 years with eight gravity-assist manovers at Earth, Venus, and Mercury
- Planned mission duration in orbit around Mercury is minimum one year

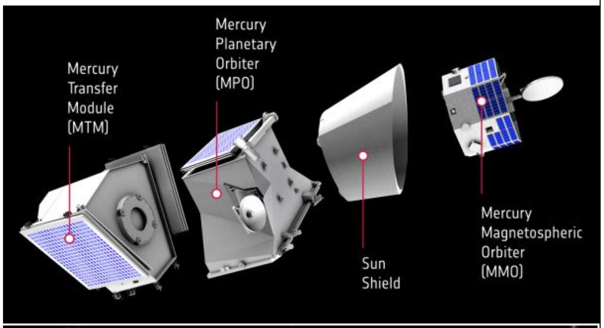

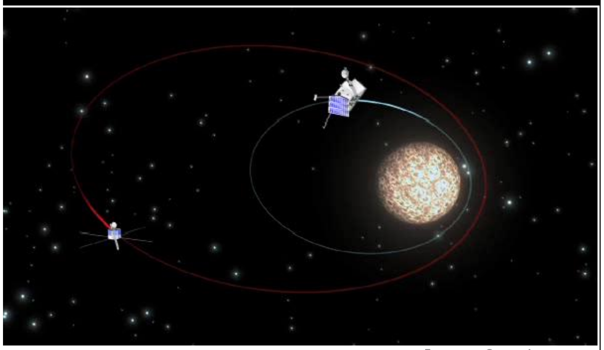

European Space Agency

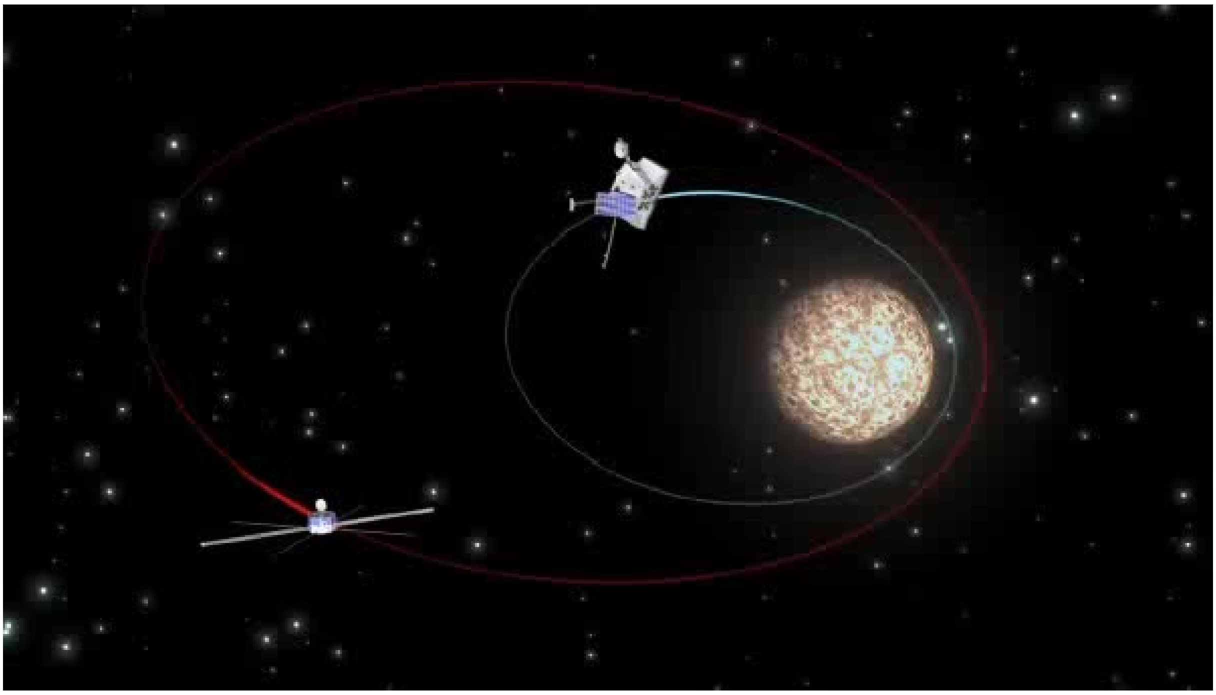

Save the attachment to disk or (double) click on the picture to run the movie.

Scope of the Activity

1. **Modelling of Mercury retro-reflection effects**: this was obtained by adapting the Merflux Worksheet (*) to account for retro-reflection in the albedo calculation
2. **Estimation of retro-reflection effects on MPO Solar Array**: a simplified two nodes model of the SA was analyzed in order to determine the change in the predicted solar panel temperatures

(*) Merflux Worksheet is a MathCAD tool created by D.Stramaccioni for in orbit heat fluxes calculation. This tool was validated against Esatan-TMS by J. Etchells, "MathCAD Heat Flux Calculator Verification Report" [2006, TEC-MCV/2006/3176/ln/JE]

European Space Agency

Environmental Specification: BC-EST-TN-00112

- *Bond albedo:* 0.119
  - Bond albedo is the fraction of incident solar energy that is reflected back to space by a spherical body over all wavelengths. [...] Origin of this value and its derivation can be found in reference [3.1] below.
- *Visual geometric albedo:* 0.138
  - Geometric albedo (or head-on reflectance) is the fraction of incident solar energy that is reflected back by a planet into the direction of the Sun (phase angle equal to 0). It can be also thought as the amount of radiation reflected from a planet relative to that from a flat Lambertian surface, which is a diffuse perfect reflector at all wavelength. The reported value is taken from reference [3.1].

[3.1] Vilas F., Chapman C. R. and Matthews M. S. (Eds.), *'Mercury'*, The University of Arizona Press, Tucson, 1988.

European Space Agency

Mercury Albedo

TABLE III
Estimates of Bond Albedo

	p_v	q_v	A_B
Moon[a]	0.113	0.611	0.123 ± 0.002
Mercury[b]	0.138	0.486	0.119

[a]Values from Lane and Irvine 1973.
[b]This work.

p_v	geometric albedo in the V filter of the UBV system
q_v	phase integral in the V filter of the UBV system
$A_v = p_v q_v$	spherical albedo in the V filter of the UBV system
A_B	bond albedo

$$\left(\frac{A_B}{A_V}\right)_{☿} \simeq \left(\frac{A_B}{A_V}\right)_{☾}$$

UBV: a wide band photometric system for classifying stars according to their colors.
U: ultraviolet
B: blue
V: visual

Vilas F., Chapman C. R. and Matthews M. S. (Eds.), '*Mercury*', The University of Arizona Press, Tucson, 1988.

European Space Agency

UBV photometric system, also called the Johnson system (or Johnson-Morgan system), is a wide band photometric system for classifying stars according to their colors. It is the first known standardized photoelectric photometric system. The letters U, B, and V stand for ultraviolet, blue, and visual magnitudes.

Lane and Irvine (1973), who determined p and q as a function of wavelength, between 350 and 1000 nm, and used these values to calculate the radiometric Bond albedo shown in Table 111. In the case of Mercury, we lack sufficient information to derive the wavelength dependence of q, and as far as p is concerned, an adequate first approximation is that the wavelength behavior is similar to that of the Moon.

Mercury Orbital Heat Fluxes Assessment (Merflux)

1. Solar flux: $QS_{k,j} = SC \cdot \alpha_k \cdot A_k \cdot F_{ss\,k,j}\left(1 - \delta_{ecl\,j}\right)$
2. Planet IR flux: $QIR_{k,j} = \sum_{grid} \sigma \cdot T_{grid}^4 \cdot S_{grid} \cdot \varepsilon_k \cdot A_k \cdot \frac{C1 \cdot C2}{\pi \cdot d^2}$
3. Directional emissivity: $\frac{\varepsilon(\varphi)}{\varepsilon_H} = 0.9(\cos(\varphi))^{\varepsilon n} / \varepsilon_H$
4. Albedo flux: $QA_{k,j} = \sum_{grid,sunlit} SC \cdot a \cdot C3 \cdot S_{grid} \cdot \alpha_k \cdot A_k \cdot \frac{C1 \cdot C2}{\pi \cdot d^2}$

total solar irradiance at the actual distance from the sun *SC*, visible hemispherical absorptance α, and area of the surface *A*, sun illumination factor F_{ss} , shadow terminator function δ_{ecl}

Stefan–Boltzmann constant *σ*, Area of the facet S_{grid}, infrared hemispherical emittance ε_k of the spacecraft surface, distance of the spacecraft from the grid element *d*, angle between the facet and the location of the spacecraft C1, angle between the spacecraft surface and the location of the facet C2

hemispherical emissivity ε_H, emission angle *φ, εn* is a number that was found by Mariner 10 to vary between 0.19 ±0.07

angle between the sun incident flux and the grid facets C3, albedo coefficient *a*

J. Etchells, "MathCAD Heat Flux Calculator Verification Report" 2006, TEC-MCV/2006/3176/In/JE

European Space Agency

Albedo Models alternatives

1. Diffusive Model:
   a. Incident flux is reflected diffusively in all directions
   b. The spatial distribution is even in all directions
2. Retro-reflection Model:
   a. The solar flux is reflected back into the direction of the Sun
   b. The reflection resembles that of a flat mirror
3. Directional Reflection Model:
   a. Compromise between diffusive and retro-reflection
   b. Light is primarily reflected into one direction while some of it is still reflected diffusively

European Space Agency

Directional Emissivity

"Radiation: Processes and Properties
Surface Radiative Properties",
http://me.queensu.ca/Courses/346/

- The spectral, directional emissivity:

$$\varepsilon_{\lambda,\theta}(\lambda,\theta,\phi,T) \equiv \frac{I_{\lambda,e}(\lambda,\theta,\phi,T)}{I_{\lambda,b}(\lambda,T)}$$

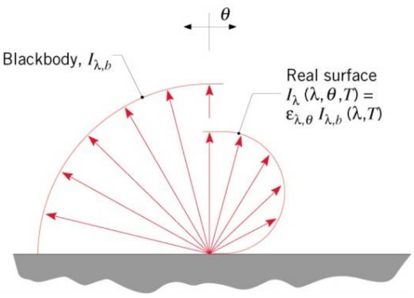

- The spectral, hemispherical emissivity (a directional average):

$$\varepsilon_\lambda(\lambda,T) \equiv \frac{E_\lambda(\lambda,T)}{E_{\lambda,b}(\lambda,T)} = \frac{\int_0^{2\pi}\int_0^{\pi/2} I_{\lambda,e}(\lambda,\theta,\phi,T)\cos\theta\sin\theta\, d\theta\, d\phi}{\int_0^{2\pi}\int_0^{\pi/2} I_{\lambda,b}(\lambda,T)\cos\theta\sin\theta\, d\theta\, d\phi}$$

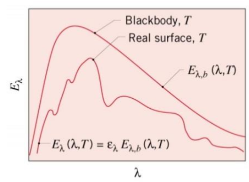

F. P. Incropera, Fundamentals of heat and mass transfer, John Wiley & Sons , 2011.

European Space Agency

Directional reflection

```
QA_k,j :=  qη ← 0·watt
           C0 ← cos(Δη/2)
           for η ∈ 1..Nη
               qξ ← 0·watt
               for ξ ∈ 1..Nξ_η
                   D ← OS_o^<j> − R_p·C0·NP_η,ξ
                   d ← |D|
                   D1 ← D/d
                   C1 ← sun_o·D1  if (sun_o·D1) > 0
                   C1 ← 0  otherwise
                   C2 ← n_o_k,j·(−D1)  if [n_o_k,j·(−D1)] > 0
                   C2 ← 0  otherwise
                   qξ ← qξ + SC·(sun_o·NP_η,ξ)·a_retro·C1^αn·Sgrid_η·(C1·C2)/(π·d^2)·A_k·α_k
               qη ← qη + qξ
```

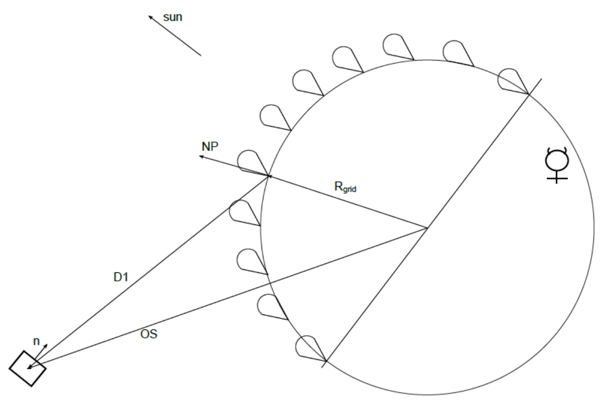

C1	angle between reflection direction and spacecraft position
C2	angle between S/C surface and grid point on the planet's surface

Note: tear drop shapes are dimensionless representations of Albedo directional refection

European Space Agency

Directional reflection

8. ALBEDO RADIATION

8.1 Constants and Planet Environment Parameters

Planet Albedo coefficient: $\mathbf{a} \equiv 0.12$

Directional reflection described by $a_{retro}(\cos(\phi_{retro}))^{\alpha n}$

Enter values for directional reflection:

$a_{retro} := 0.138$

$\alpha n := 0.3$

Calculate hemispherical reflection coefficient from directional reflection:

$$a_h := \frac{a_{retro}}{\pi} \cdot \int_0^{2\pi} \int_0^{\frac{\pi}{2}} \cos(\phi_{retro})^{\alpha n} \cdot \cos(\phi_{retro}) \cdot \sin(\phi_{retro})\, d\phi_{retro}\, d\theta_{retro}$$

$a_h = 0.1200$

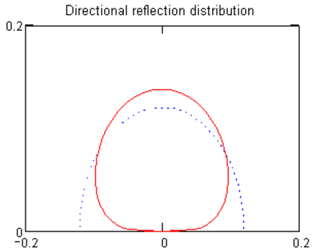

Reminder: Diffusive Albedo:

$$QA_{k,j} = \sum_{\text{grid,sunlit}} SC \cdot a \cdot C3 \cdot S_{\text{grid}} \cdot \alpha_k \cdot A_k \cdot \frac{C1 \cdot C2}{\pi \cdot d^2}$$

$$
\begin{aligned}
QA_{k,j} := \; & q\eta \leftarrow 0 \cdot \text{watt} \\
& C0 \leftarrow \cos\left(\frac{\Delta\eta}{2}\right) \\
& \text{for } \eta \in 1 .. N\eta \\
& \quad q\xi \leftarrow 0 \cdot \text{watt} \\
& \quad \text{for } \xi \in 1 .. N\xi_\eta \\
& \quad\quad D \leftarrow OS_o^{\langle j \rangle} - R_p \cdot C0 \cdot NP_{\eta,\xi} \\
& \quad\quad d \leftarrow |D| \\
& \quad\quad D1 \leftarrow \frac{D}{d} \\
& \quad\quad C1 \leftarrow sun_o \cdot D1 \quad \text{if } (sun_o \cdot D1) > 0 \\
& \quad\quad C1 \leftarrow 0 \quad \text{otherwise} \\
& \quad\quad C2 \leftarrow n_{o_{k,j}} \cdot (-D1) \quad \text{if } \left[n_{o_{k,j}} \cdot (-D1)\right] > 0 \\
& \quad\quad C2 \leftarrow 0 \quad \text{otherwise} \\
& \quad\quad \boxed{q\xi \leftarrow q\xi + SC \cdot (sun_o \cdot NP_{\eta,\xi}) \cdot a_{retro} \cdot C1^{\alpha n} \cdot Sgrid_\eta \cdot \frac{C1 \cdot C2}{\pi \cdot d^2} \cdot A_k \cdot \alpha_k} \\
& \quad q\eta \leftarrow q\eta + q\xi
\end{aligned}
$$

NP Unit vector normal to planet's surface
a_{retro} geometric albedo
αn exponent for directional reflection
Sgrid Area of the planet's surface grid
α solar absorptivity

European Space Agency

Reference Orbit Case

Perihelion case:
diffusive Albedo (as considered so far for BepiColombo analyses)

2.1 Input Orbital Parameters

Altitude of periapsis: $h_p := 400 \cdot 10^3 \cdot m$

Altitude of apoapsis: $h_a := 1508 \cdot 10^3 m$

Orbit inclination: $io := 90 \cdot deg$

Nadir pointing

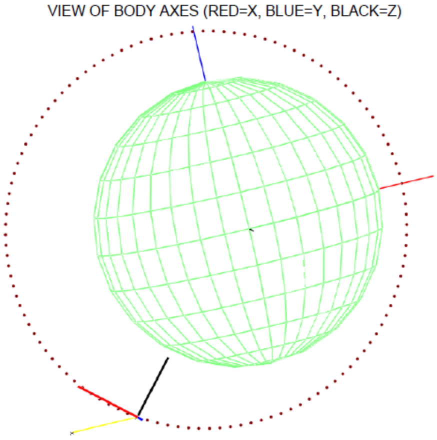

European Space Agency

Albedo heat fluxes comparison (nadir- pointing cube)

- Directional albedo is considered the most realistic approach
- Differences in peak Albedo fluxes can be significant between the different models

A1 – Anti- Velocity
A2 – Normal to Orbit
A3 – Nadir
A4 – Velocity
A5 – Normal to Orbit
A6 – Zenith

Steering profiles provided by ESOC

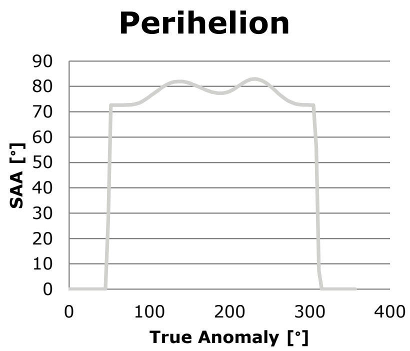

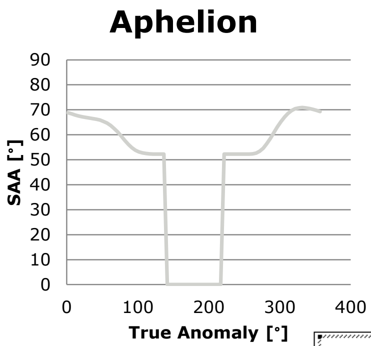

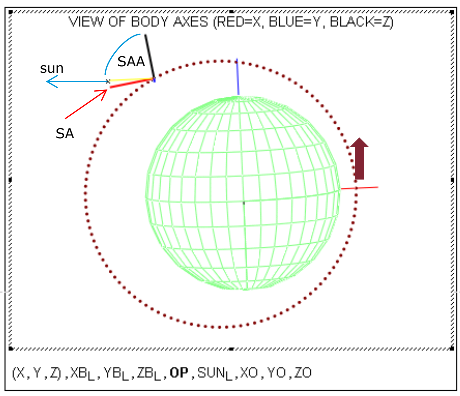

Albedo heat fluxes comparison (Steering profile)

- Directional albedo is considered the most realistic approach
- Differences in peak Albedo fluxes can be significant between the different models

A3 – Front
A6 – Back

diffusive

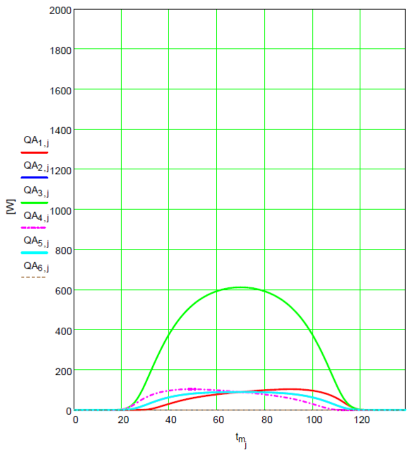

directional

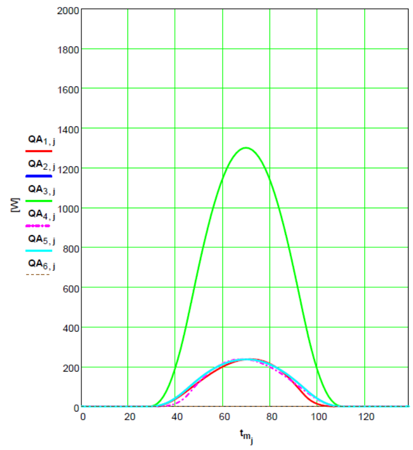

European Space Agency

Solar Panel Thermal Model

1. 2 Nodes: Front and back
2. Front covered with optical solar reflector (OSR)
3. Back is bare CFC or covered with OSR
4. Solar Panel Area = 1322 mm * 2065 mm, thickness = 22.8 mm
5. Consist of CFC Honeycomb between CFC Sheets
6. Thermal inertia is null

Panel	Front Side	Back Side
Outer Panels	a) OSR 47% EOL: $\alpha/\varepsilon = 0.601/0.827$	1) Bare CFC EOL: $\alpha/\varepsilon = 0.92/0.825$
Inner Panel	b) OSR 82% EOL: $\alpha/\varepsilon = 0.372/0.803$	2) OSR 100% EOL: $\alpha/\varepsilon = 0.25/0.79$

NB1: Case a1 represents Cells/OSR ratio of the outermost panels (2 and 3). Case b2 represent inner panel.
NB2: Null thermal inertia considered: only slightly conservative assumption and closer to real operational mode where SA temperatures are kept close to constant values
[See BC-ASO-AN-116068 Is.3 par.5.1.3 and 5.3 (selected values)]

European Space Agency

Thermal Analysis Cases

Analysis cases are combinations of the following points:

1. 3 SA combinations of optical properties (front/back) have been considered (outer panel, inner panel, and worst case optical properties combination): a1, b2, b1.
2. Solar Panel is at constant angle to the Sun: 90°, 78°, and 65°
3. Perihelion and Aphelion orbits
4. 4 different Albedo modelling approaches:
   a. bond albedo 0.119 (fully diffused)
   b. full retro-reflection 0.12
   c. full retro-reflection 0.138
   d. directional albedo
5. 2 realistic steering profiles (perihelion & aphelion) provided by ESOC

Note: ThermXL and Esatan software (part of Esatan-TMS suite) has been used for SA temperatures calculation

European Space Agency

Temperature of inner panel with ESOC SAA profile at Perihelion

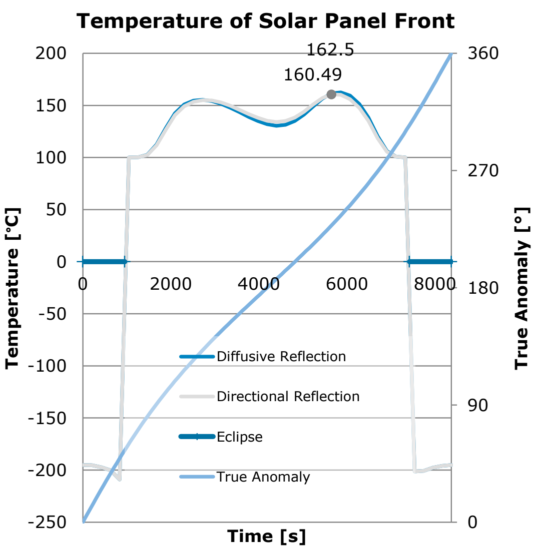

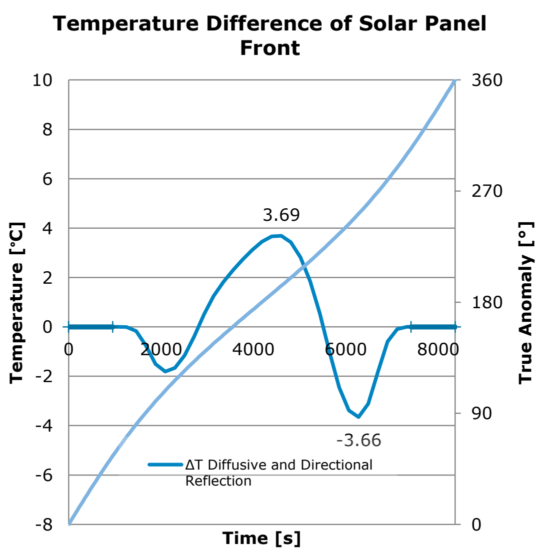

European Space Agency

Temperature of outer panel with ESOC SAA profile at Perihelion

esa

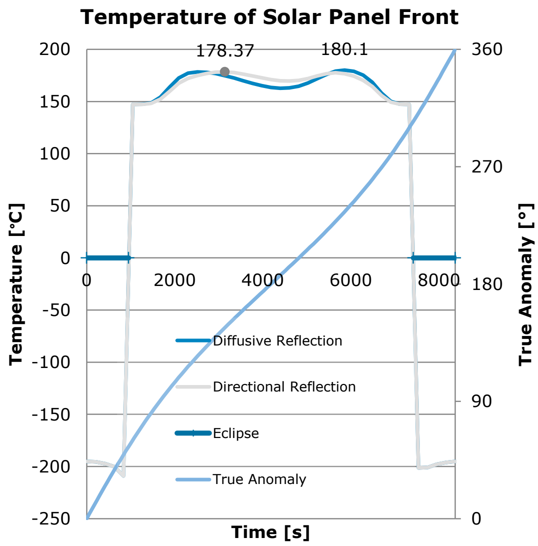

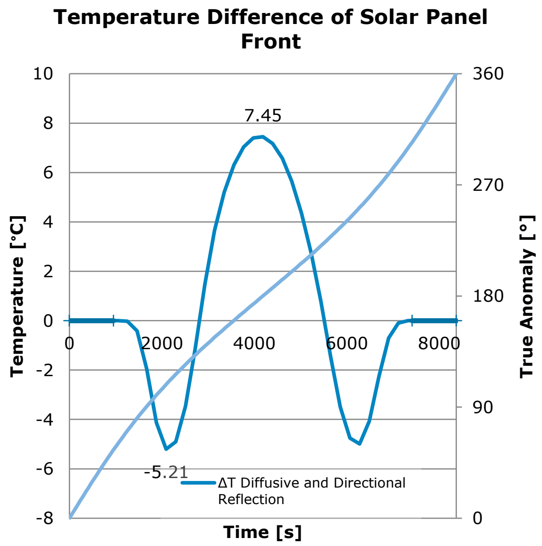

European Space Agency

Temperature of inner panel with ESOC SAA profile at Aphelion

esa

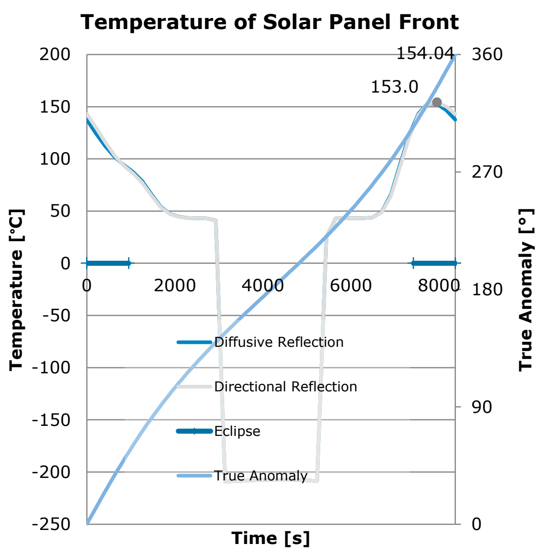

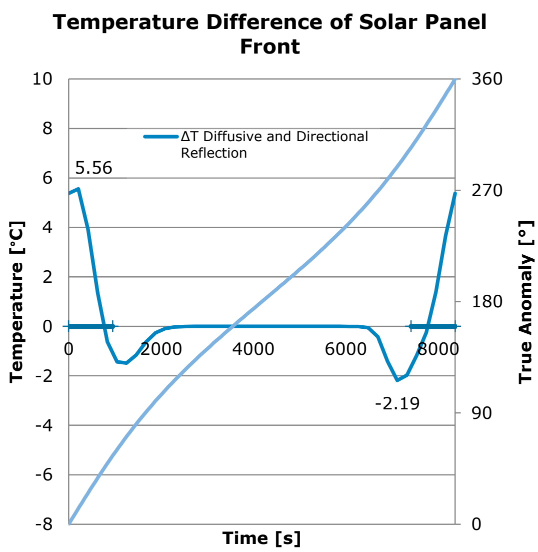

European Space Agency

Temperature of outer panel with ESOC SAA profile at Aphelion

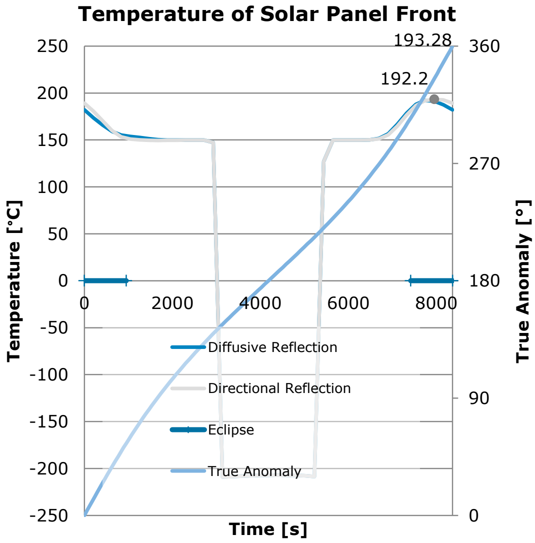

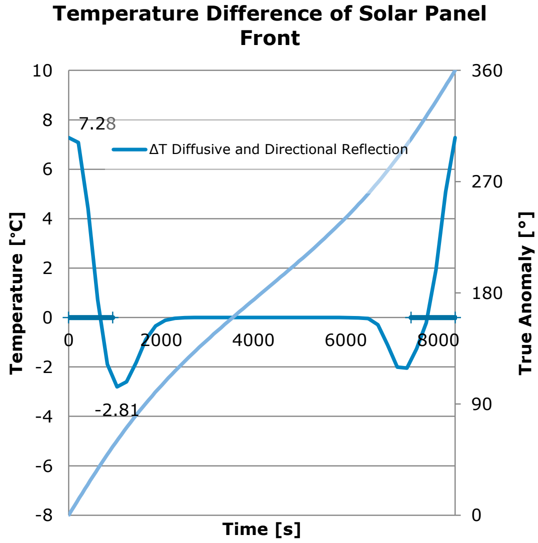

European Space Agency

Summary

1. A simplified model of Mercury Albedo has been built
2. Environmental heat fluxes have been calculated
3. The impact on MPO SA temperatures has been studied for:

- Perihelion and Aphelion orbits
- 4 different Albedo modelling approaches (diffusive vs retro-reflection)
- 3 SA combinations of optical front/back properties
- 3 fixed SAA: 90deg, 78deg and 65deg angles
- 2 realistic steering profiles (perihelion & aphelion) provided by ESOC

Note: The most realistic Albedo modelling approach is considered the one with Albedo directional reflection (i.e. diffused reflection with much higher energy concentration around the direction of retro-reflection).

European Space Agency

Conclusions 1/2

1. Albedo modelling has a no negligible influence on SA temperatures
2. Fixed SA SAA (not realistic case): for the directional retro-reflection (considered the best engineering case), the SA front side worst ΔT (directional minus diffusive albedo) during orbit is ~+14/-10degC for outermost panels and ~+10/-5degC for the innermost panel
3. Variable SAA (realistic steering profile case): for the directional retro-reflection, the SA front side worst ΔT during orbit is less than +8degC/-5degC for outermost panels and less then +4/-4degC for the innermost panel
4. Worst ΔT is a peak (limited time duration), not applicable to the whole orbit: around sub-solar point the directional albedo provides the highest temperatures.

European Space Agency

Conclusions 2/2

5. There are parts of the orbit where the diffusive albedo approach is conservative: in those areas Industry models are conservative (safe in temperature), but SAA steering profile might not be optimized at best (reduced power generation).
6. Results are preliminary estimations based on simplified models of planet and SA (e.g. 2 nodes for SA), averaged optical properties for SCA+OSR, albedo modelling approach for Mercury not consolidated.
7. Worst cases occur in SA panels with bare CFC on the backside (outermost panels) and are usually more pronounced in cases with bigger SAA (as visible within analysis cases with fixed SAA).

European Space Agency

Additional Slides

esa

European Space Agency

General comments 1/2

esa

1. Using thermal models for definition of SA steering profile at Mercury is very challenging and was never done before.
2. In this study is estimated the effect that albedo might have on SA. This effect changes based on real environment to be found at Mercury and on modelling assumptions: an improvement of models themselves might help, but will not solve the problem (thermal models limitations, software limitations in retro-reflection modelling, and limited knowledge of Mercury albedo itself).
3. The albedo predictions can be also influenced by Mercury albedo coefficients variations over the planet surface: this is an additional source of uncertainty, partially covered by the Planet IR compensation (higher albedo → lower IR). The overall effect was considered negligible by Industry but never quantified.

European Space Agency

General comments 2/2

4. The SA steering calibration at beginning of MPO orbit phases (after MOI) shall be carefully planned by taking extra margins: i.e. started with a target T lower than nominal and fine tuned once SA simplified model is considered properly validated with flight data.
5. A predefined table of sensitivity to SAA variations at different orbit positions and seasons might help the calibration itself and it is recommended (e.g. sensitivity to 1deg angle variation along mission). Simplified SA thermal model profiles might be corrected based on flight T measurements and these sensitivity tables.
6. Impact on SA thermal control, power budgets and operations should be discussed

European Space Agency

Temperature Differences between Albedo Models (1/2)

Case	Max/min ΔT Diffusive and Directional Reflection [K]	Max/min ΔT Diffusive and Retro- Reflection 0.12 [K]	Max/min ΔT Diffusive and Retro- Reflection 0.138 [K]
Perihelion a1y 90 deg	+13.9/-10.0	0.00/-12.33	0.00/-12.33
Perihelion a1y 88 deg	+7.6/-5.3	+5.37/-8.34	+6.79/-8.34
Perihelion a1y 75 deg	+5.5/-3.4	+9.99/-6.40	+11.82/-6.40
Perihelion a1y SAA profile	+7.6/-5.2		
Perihelion b1y 90 deg	+12.2/-10.1	+0.02/-12.37	+0.00/-12.37
Perihelion b1y 88 deg	+8.4/-6.3	+8.03/-9.62	+9.74/-9.62
Perihelion b1y 75 deg	+6.9/-4.4	+14.32/-7.92	+16.71/-7.92
Perihelion b1y SAA profile	+8.4/-7.0		
Perihelion b2y 90 deg	+6.8/-5.0	+0.00/-6.67	+0.00/-6.67
Perihelion b2y 88 deg	+3.8/-3.5	+1.20/-4.71	+1.72/-4.71
Perihelion b2y 75 deg	+2.4/-2.6	+3.34/-3.28	+4.08/-3.28
Perihelion b2y SAA profile	+3.7/-3.8		

Agency

Temperature Differences between Albedo Models (2/2)

Case	Max/min ΔT Diffusive and Directional Reflection [K]	Max/min ΔT Diffusive and Retro- Reflection 0.12 [K]	Max/min ΔT Diffusive and Retro- Reflection 0.138 [K]
Aphelion a1y 90 deg	+13.4/-8.6	+0.00/-11.81	+0.00/-11.81
Aphelion a1y 88 deg	+9.0/-4.4	+0.00/-6.51	+0.00/-6.51
Aphelion a1y 75 deg	+6.9/-2.9	+2.50/-4.78	+3.52/-4.78
Aphelion a1y SAA profile	+7.3/-2.8		
Aphelion b1y 90 deg	+11.5/-8.6	+0.00/-11.75	+0.00/-11.75
Aphelion b1y 88 deg	+7.2/-4.4	+0.00/-6.51	+0.00/-6.51
Aphelion b1y 75 deg	+5.0/-2.9	+0.00/-4.08	+0.64/-4.08
Aphelion b1y SAA profile	+5.5/-2.7		
Aphelion b2y 90 deg	+6.4/-4.0	+0.00/-6.05	+0.00/-6.05
Aphelion b2y 88 deg	+5.8/-3.1	+0.68/-5.02	+1.21/-5.02
Aphelion b2y 75 deg	+6.2/-4.5	+4.43/-4.47	+5.42/-4.47
Aphelion b2y SAA profile	+5.6/-2.3		

Results (1/24): perihelion/outer panel/ SAA 90deg

Front Side	Back Side
OSR 47% EOL: α/ε = 0.601/0.827	Bare CFC EOL: α/ε = 0.92/0.825

ΔT logic: ΔT positive means that the retro-reflection approach gives higher T than the diffusive (Lambertian) reflection

Temperature of Solar Panel Front

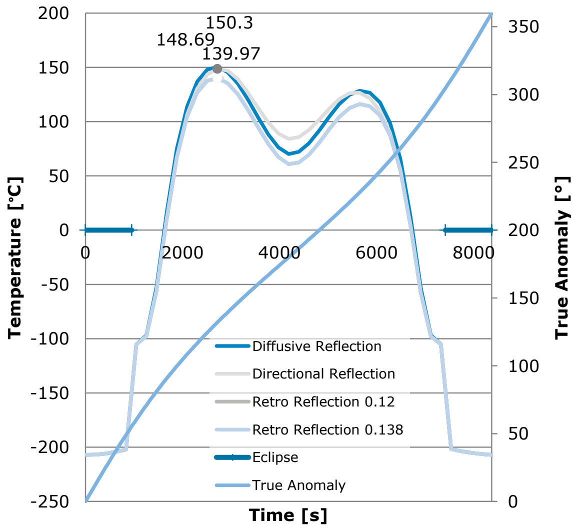

Temperature Difference of Solar Panel Front

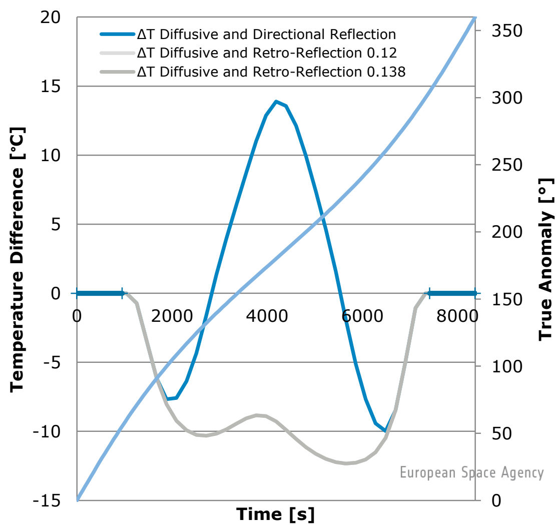

Results (2/24): perihelion/outer panel/ SAA 78deg

Front Side	Back Side
OSR 47% EOL: α/ε = 0.601/0.827	Bare CFC EOL: α/ε = 0.92/0.825

ΔT logic: ΔT positive means that the retro-reflection approach gives higher T than the diffusive (Lambertian) reflection

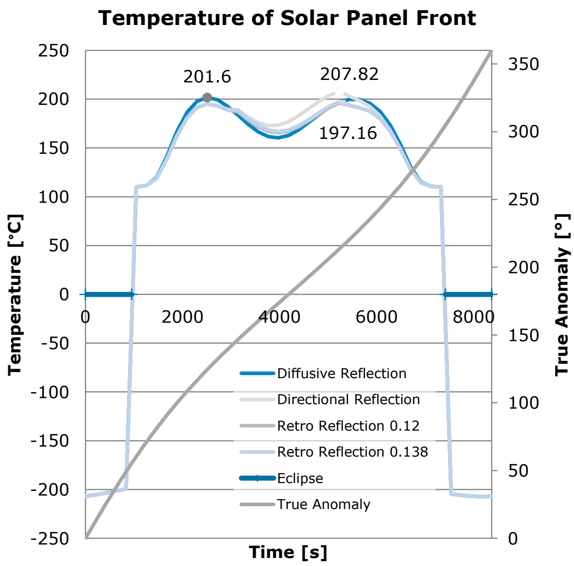

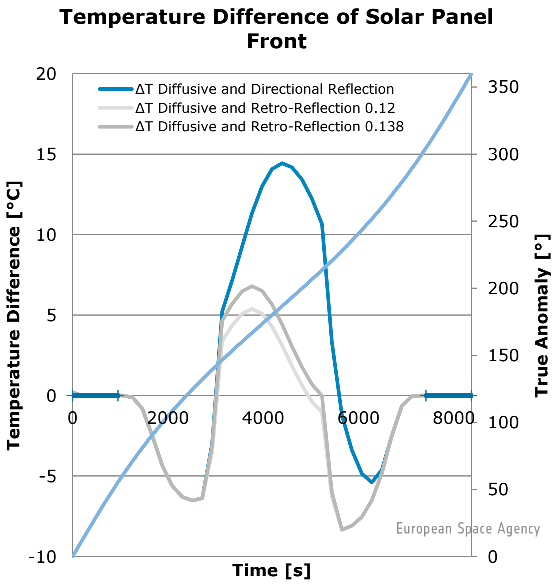

Results (3/24): perihelion/outer panel/ SAA 65deg

Front Side	Back Side
OSR 47% EOL: α/ε = 0.601/0.827	Bare CFC EOL: α/ε = 0.92/0.825

ΔT logic: ΔT positive means that the retro-reflection approach gives higher T than the diffusive (Lambertian) reflection

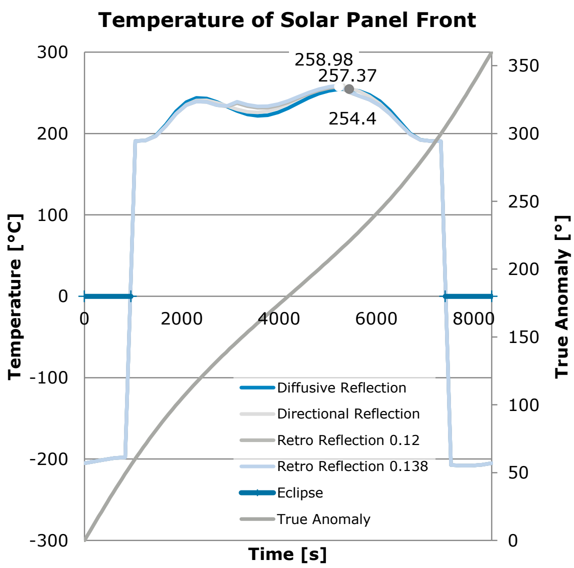

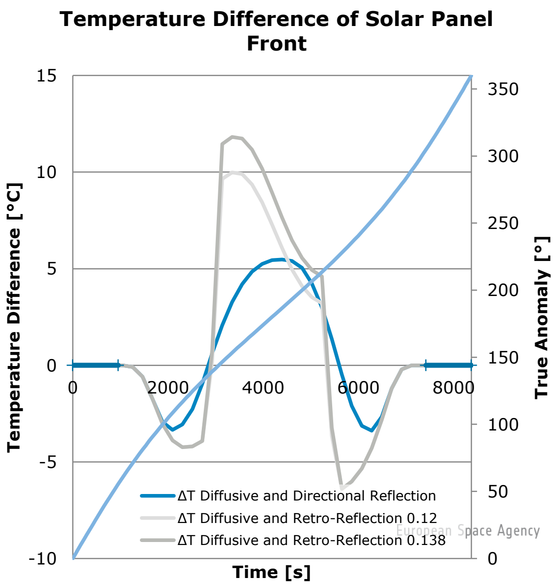

Results (4/24): perihelion/outer panel/ SAA profile

Front Side	Back Side
OSR 47% EOL: α/ε = 0.601/0.827	Bare CFC EOL: α/ε = 0.92/0.825

ΔT logic: ΔT positive means that the retro-reflection approach gives higher T than the diffusive (Lambertian) reflection

Temperature of Solar Panel Front

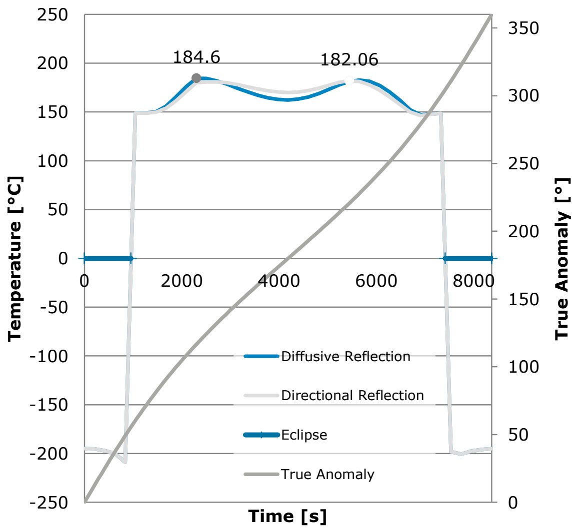

Temperature Difference of Solar Panel Front

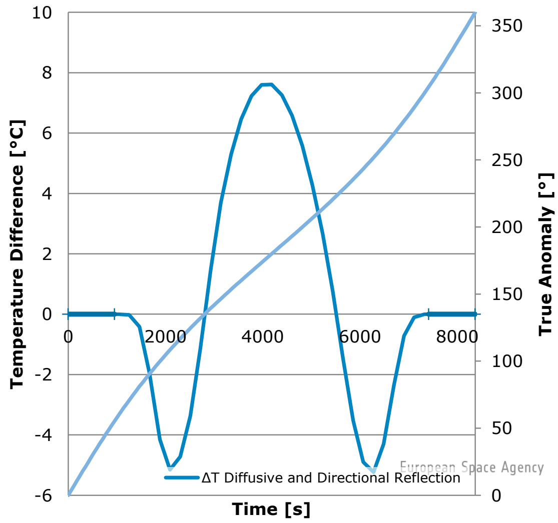

Results (5/24): perihelion/b1/SAA 90deg

Front Side	Back Side
OSR 82% EOL: α/ε = 0.372/0.803	Bare CFC EOL: α/ε = 0.92/0.825

Case a2 is not realistic and not considered. Case b1 might apply to areas of panels 2 and 3 where locally the OSR percentage is higher than the average 47% (TBC if realistic).

ΔT logic: ΔT positive means that the retro-reflection approach gives higher T than the diffusive (Lambertian) reflection

Temperature of Solar Panel Front

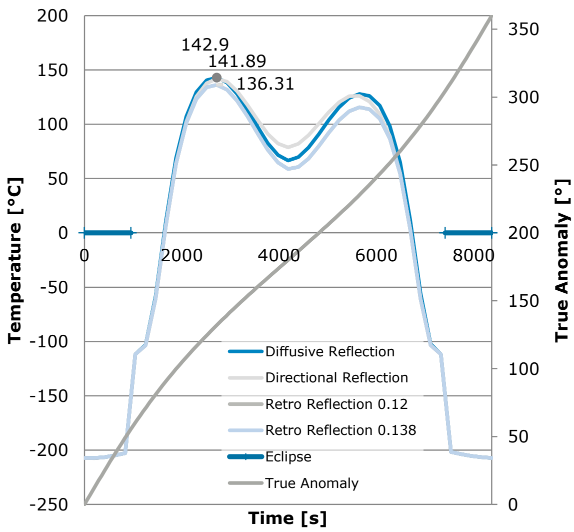

Temperature Difference of Solar Panel Front

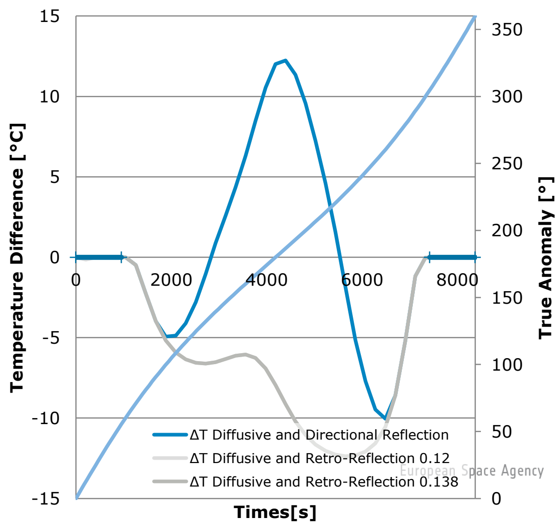

Results (6/24): perihelion/b1/SAA 78deg

Front Side	Back Side
OSR 82% EOL: α/ε = 0.372/0.803	Bare CFC EOL: α/ε = 0.92/0.825

ΔT logic: ΔT positive means that the retro-reflection approach gives higher T than the diffusive (Lambertian) reflection

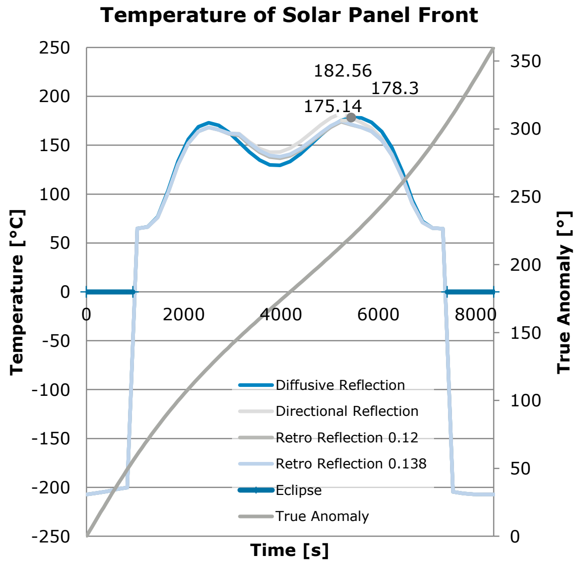

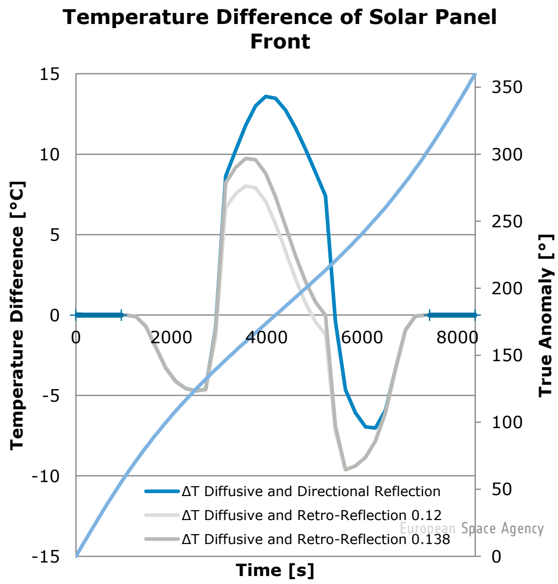

Results (7/24): perihelion/b1/SAA 65deg

Front Side	Back Side
OSR 82% EOL: α/ε = 0.372/0.803	Bare CFC EOL: α/ε = 0.92/0.825

ΔT logic: ΔT positive means that the retro-reflection approach gives higher T than the diffusive (Lambertian) reflection

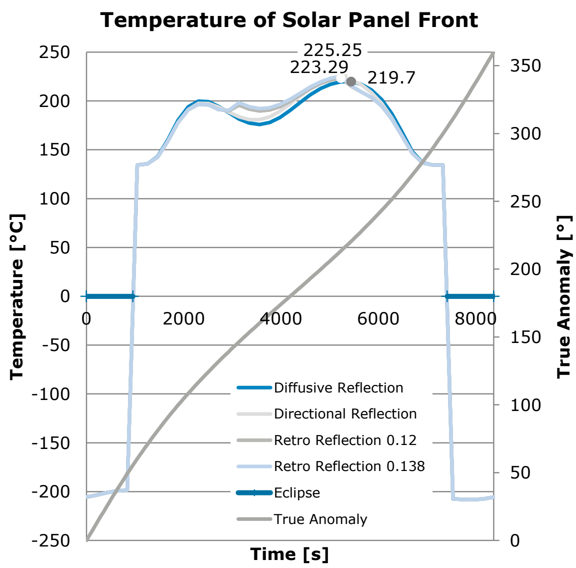

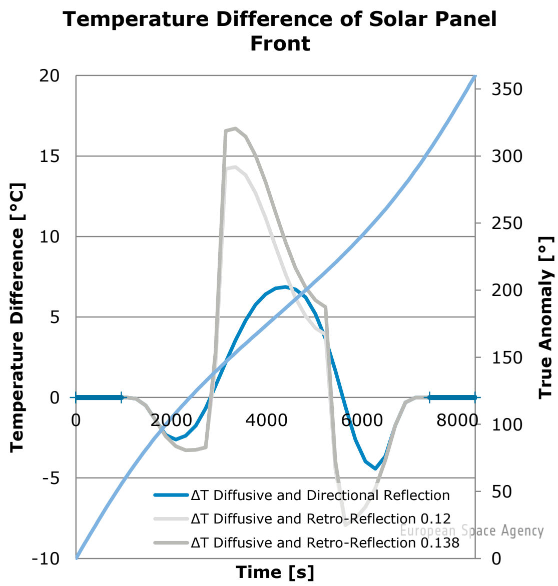

Results (8/24): perihelion/b1/SAA profile

esa

Front Side	Back Side
OSR 82% EOL: α/ε = 0.372/0.803	Bare CFC EOL: α/ε = 0.92/0.825

ΔT logic: ΔT positive means that the retro-reflection approach gives higher T than the diffusive (Lambertian) reflection

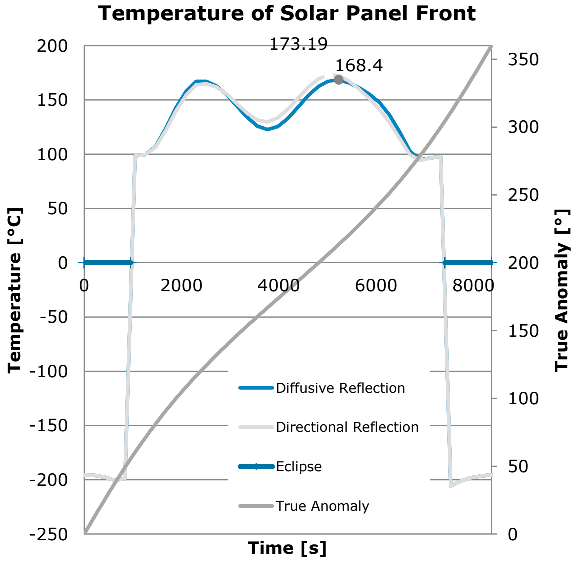

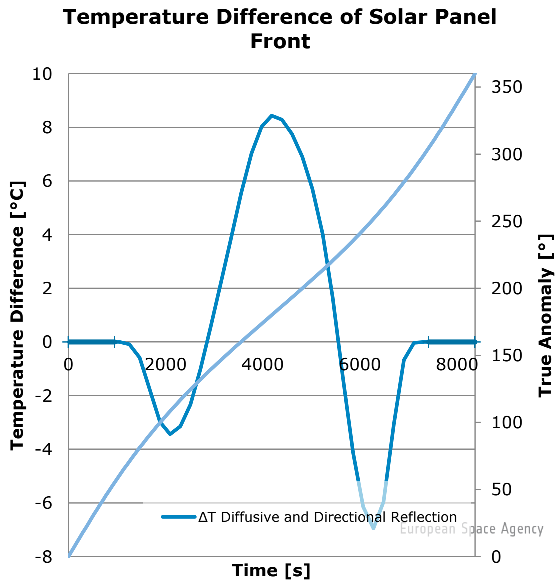

Results (9/24): perihelion/inner panel/ SAA 90deg

esa

Front Side	Back Side
OSR 82% EOL: α/ε = 0.372/0.803	OSR 100% EOL: α/ε = 0.25/0.79

ΔT logic: ΔT positive means that the retro-reflection approach gives higher T than the diffusive (Lambertian) reflection

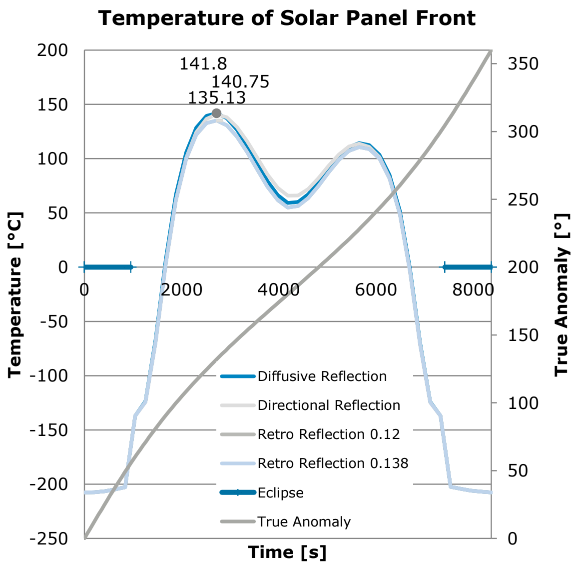

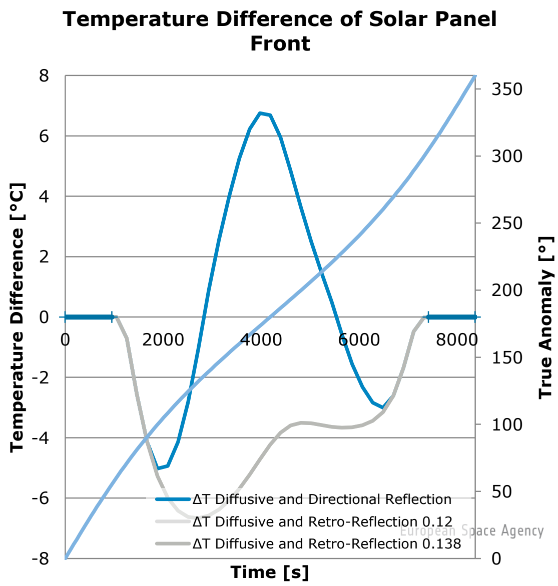

Results (10/24): perihelion/inner panel/ SAA 78deg

Front Side	Back Side
OSR 82% EOL: α/ε = 0.372/0.803	OSR 100% EOL: α/ε = 0.25/0.79

ΔT logic: ΔT positive means that the retro-reflection approach gives higher T than the diffusive (Lambertian) reflection

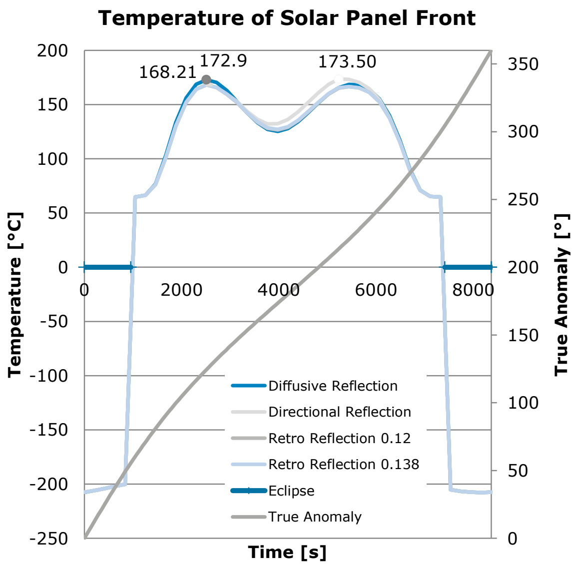

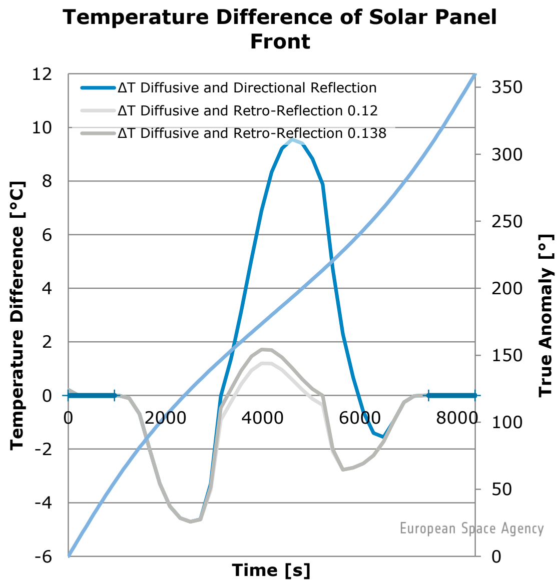

Results (11/24): perihelion/inner panel/ SAA 65deg

Front Side	Back Side
OSR 82% EOL: α/ε = 0.372/0.803	OSR 100% EOL: α/ε = 0.25/0.79

ΔT logic: ΔT positive means that the retro-reflection approach gives higher T than the diffusive (Lambertian) reflection

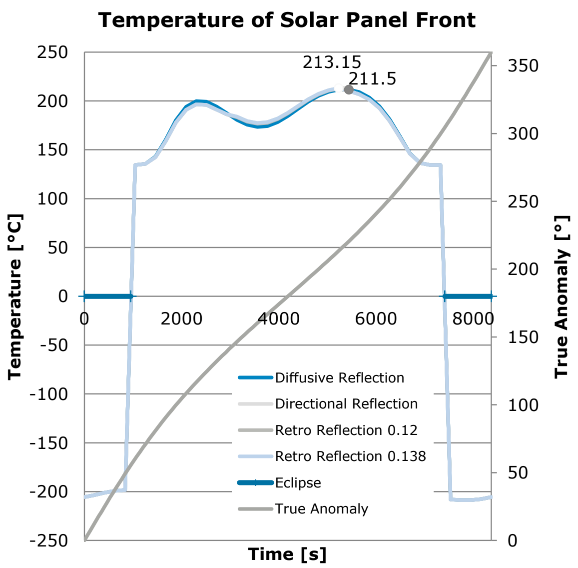

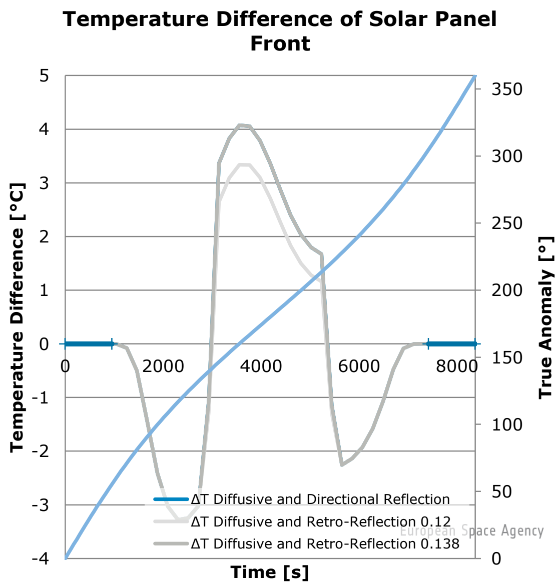

Results (12/24): perihelion/inner panel/ SAA profile

esa

Front Side	Back Side
OSR 82% EOL: α/ε = 0.372/0.803	OSR 100% EOL: α/ε = 0.25/0.79

ΔT logic: ΔT positive means that the retro-reflection approach gives higher T than the diffusive (Lambertian) reflection

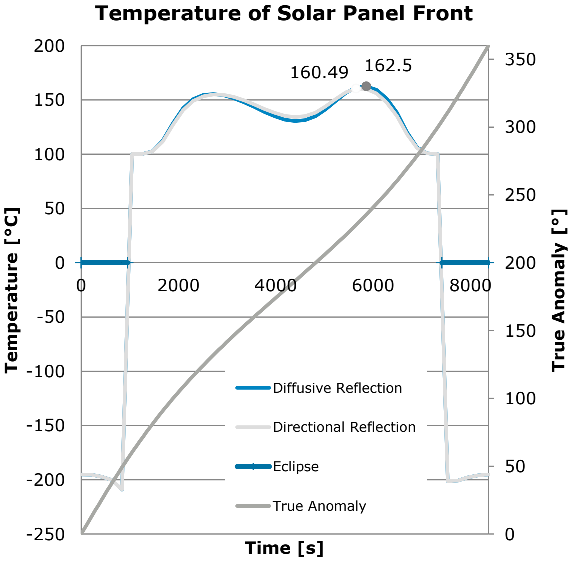

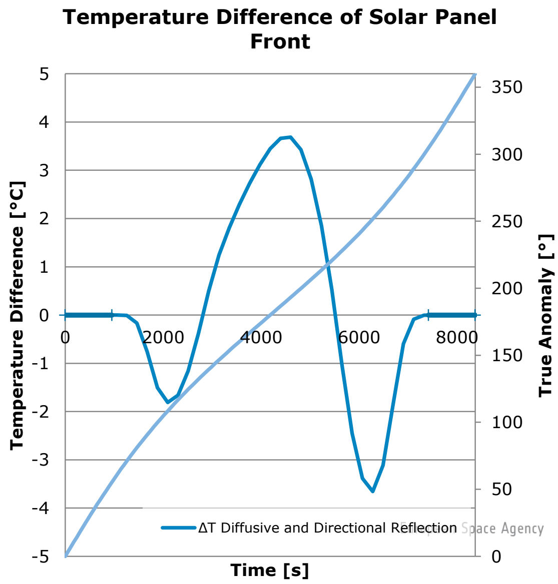

European Space Agency

Results (13/24): aphelion/outer panel/ SAA 90deg

esa

Front Side	Back Side
OSR 47% EOL: α/ε = 0.601/0.827	Bare CFC EOL: α/ε = 0.92/0.825

ΔT logic: ΔT positive means that the retro-reflection approach gives higher T than the diffusive (Lambertian) reflection

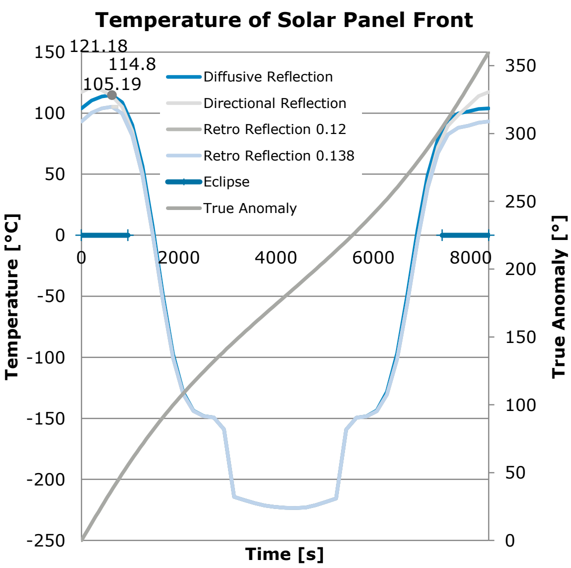

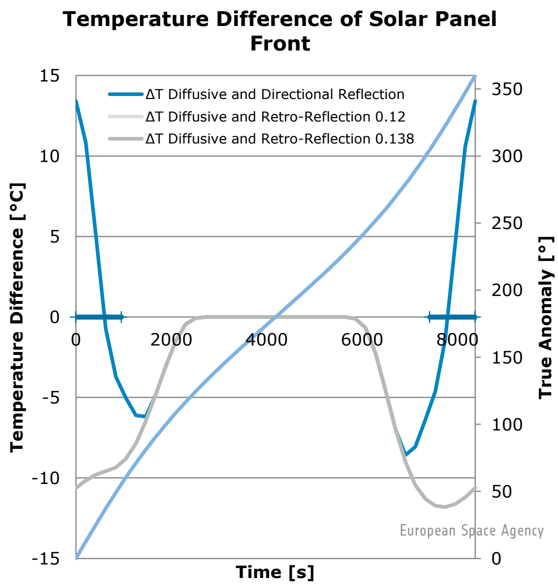

European Space Agency

Results (14/24): aphelion/outer panel/ SAA 78deg

Front Side	Back Side
OSR 47% EOL: α/ε = 0.601/0.827	Bare CFC EOL: α/ε = 0.92/0.825

ΔT logic: ΔT positive means that the retro-reflection approach gives higher T than the diffusive (Lambertian) reflection

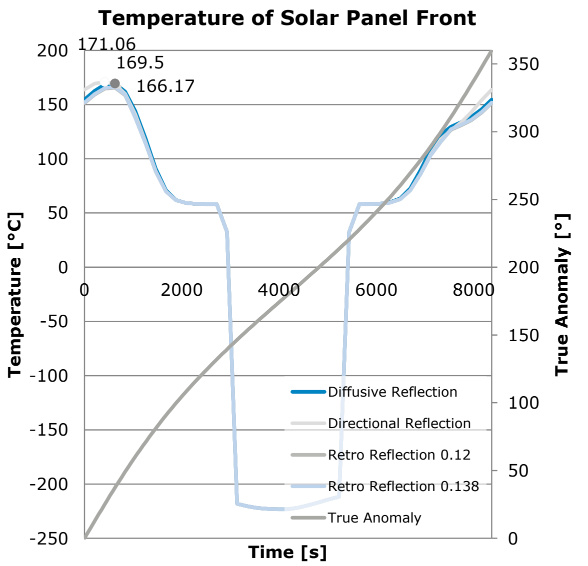

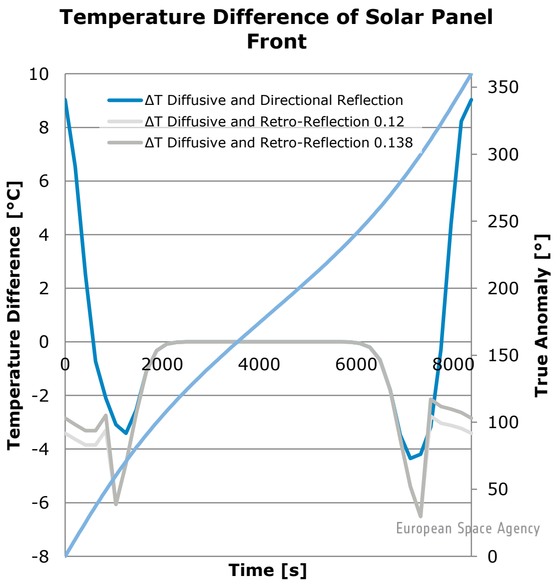

Results (15/24): aphelion/outer panel/ SAA 65deg

Front Side	Back Side
OSR 47% EOL: α/ε = 0.601/0.827	Bare CFC EOL: α/ε = 0.92/0.825

ΔT logic: ΔT positive means that the retro-reflection approach gives higher T than the diffusive (Lambertian) reflection

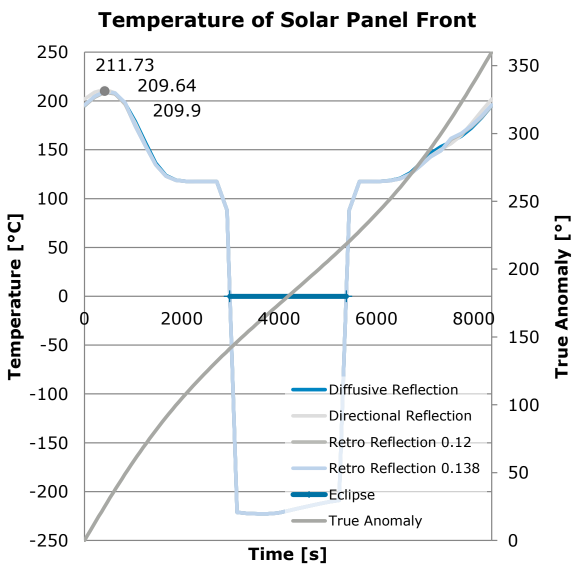

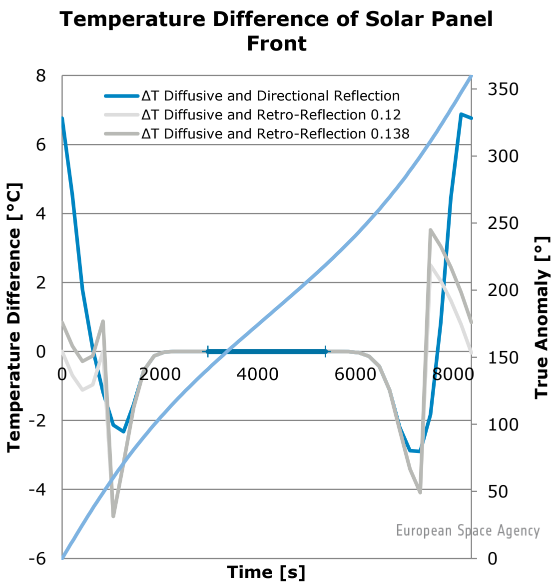

Results (16/24): aphelion/outer panel/ SAA profile

Front Side	Back Side
OSR 47% EOL: α/ε = 0.601/0.827	Bare CFC EOL: α/ε = 0.92/0.825

ΔT logic: ΔT positive means that the retro-reflection approach gives higher T than the diffusive (Lambertian) reflection

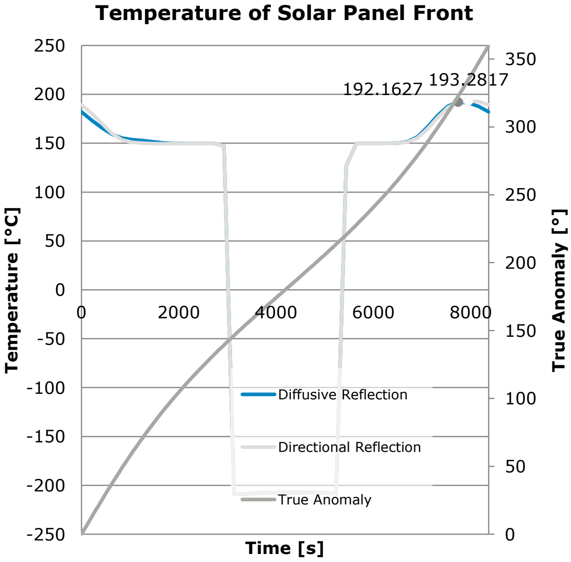

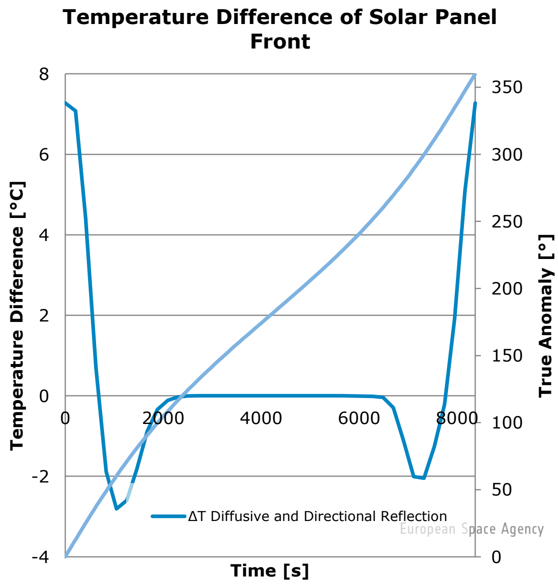

Results (17/24): aphelion/b1/SAA 90deg

Front Side	Back Side
OSR 82% EOL: α/ε = 0.372/0.803	Bare CFC EOL: α/ε = 0.92/0.825

ΔT logic: ΔT positive means that the retro-reflection approach gives higher T than the diffusive (Lambertian) reflection

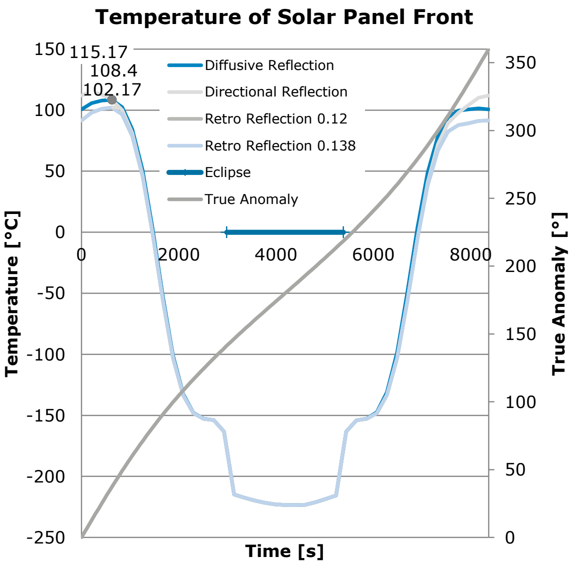

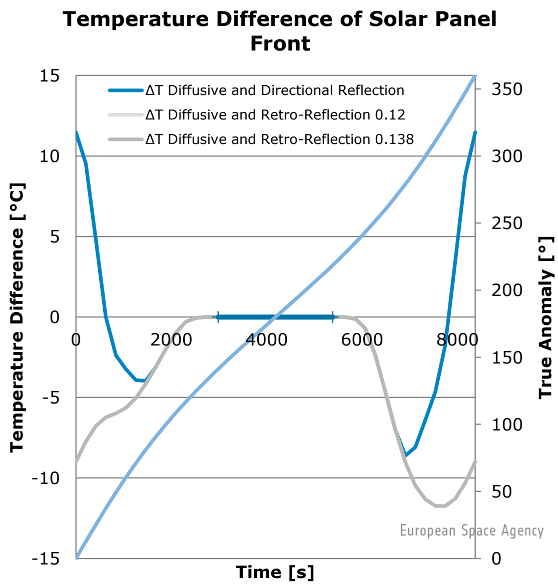

Results (18/24): aphelion/b1/SAA 78deg

Front Side	Back Side
OSR 82% EOL: α/ε = 0.372/0.803	Bare CFC EOL: α/ε = 0.92/0.825

ΔT logic: ΔT positive means that the retro-reflection approach gives higher T than the diffusive (Lambertian) reflection

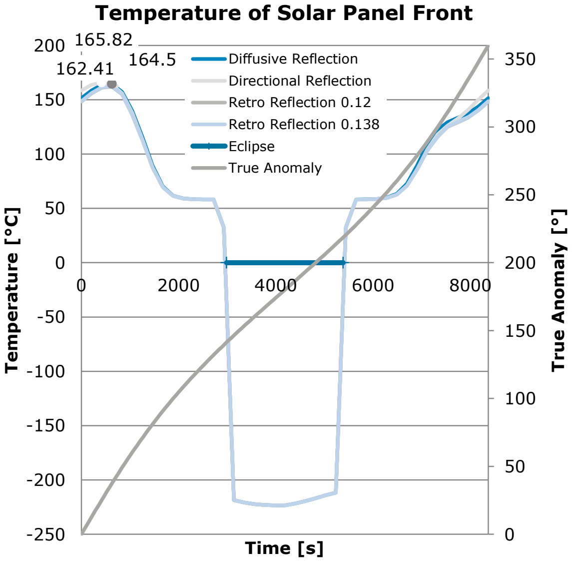

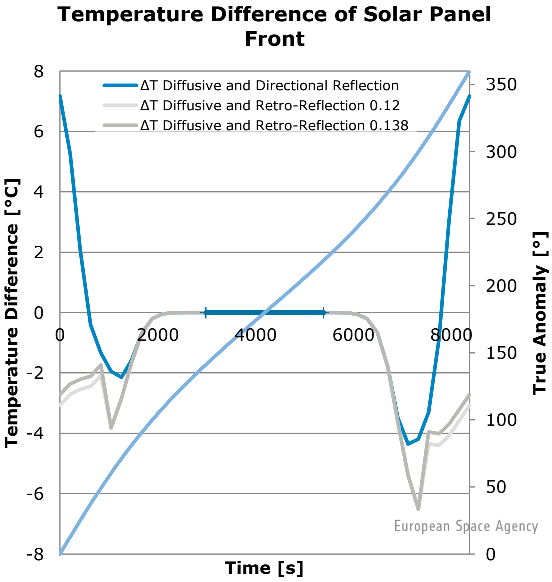

Results (19/24): aphelion/b1/SAA 65deg

Front Side	Back Side
OSR 82% EOL: α/ε = 0.372/0.803	Bare CFC EOL: α/ε = 0.92/0.825

ΔT logic: ΔT positive means that the retro-reflection approach gives higher T than the diffusive (Lambertian) reflection

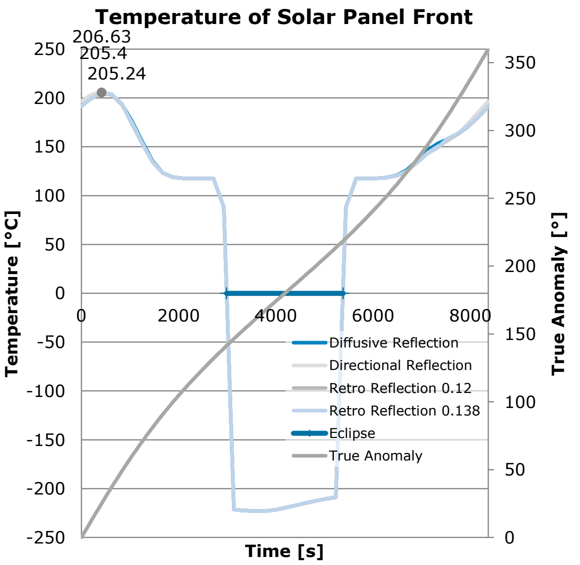

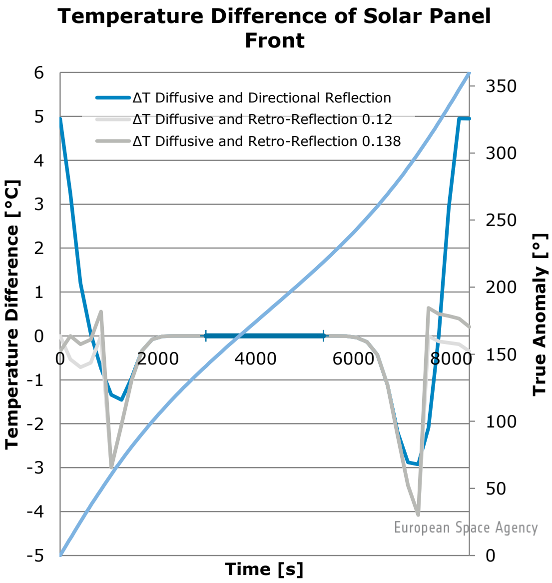

Results (20/24): aphelion/b1/SAA profile

Front Side	Back Side
OSR 82% EOL: α/ε = 0.372/0.803	Bare CFC EOL: α/ε = 0.92/0.825

ΔT logic: ΔT positive means that the retro-reflection approach gives higher T than the diffusive (Lambertian) reflection

Temperature of Solar Panel Front

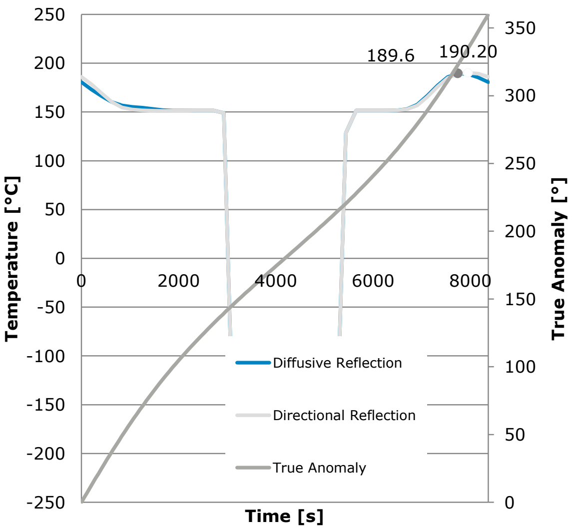

Temperature Difference of Solar Panel Front

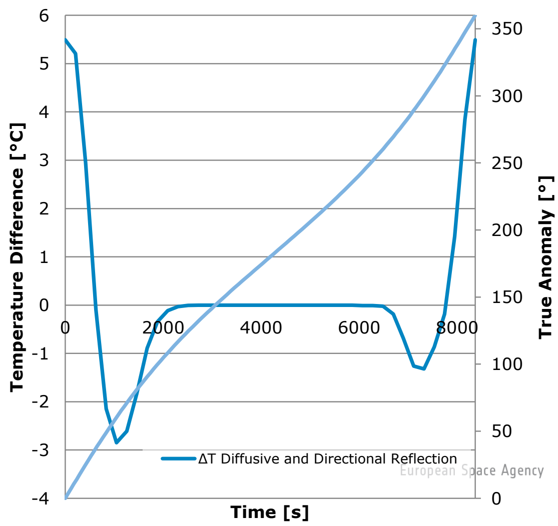

European Space Agency

Results (21/24): aphelion/inner panel/ SAA 90deg

Front Side	Back Side
OSR 82% EOL: α/ε = 0.372/0.803	OSR 100% EOL: α/ε = 0.25/0.79

ΔT logic: ΔT positive means that the retro-reflection approach gives higher T than the diffusive (Lambertian) reflection

Temperature of Solar Panel Front

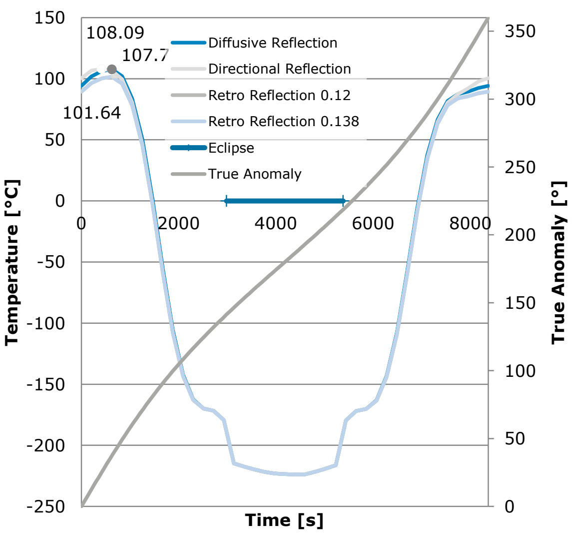

Temperature Difference of Solar Panel Front

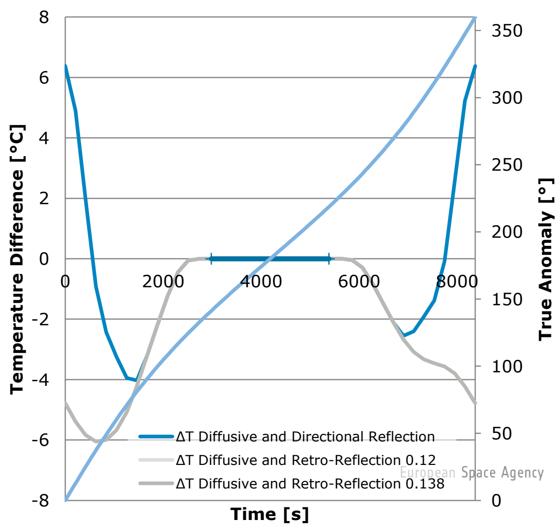

European Space Agency

Results (22/24): aphelion/inner panel/ SAA 78deg

Front Side	Back Side
OSR 82% EOL: α/ε = 0.372/0.803	OSR 100% EOL: α/ε = 0.25/0.79

ΔT logic: ΔT positive means that the retro-reflection approach gives higher T than the diffusive (Lambertian) reflection

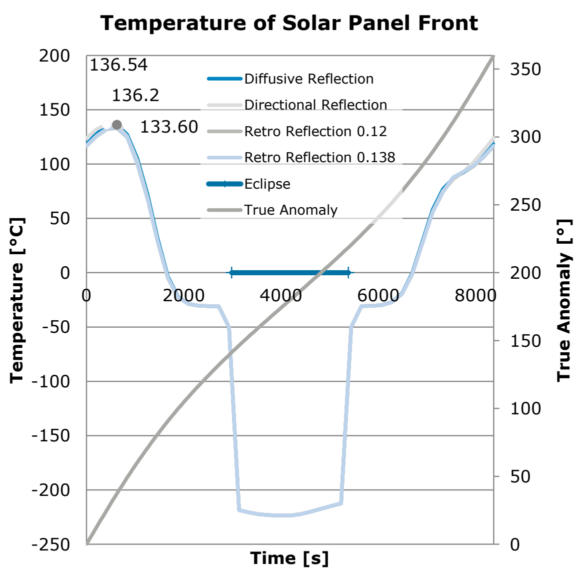

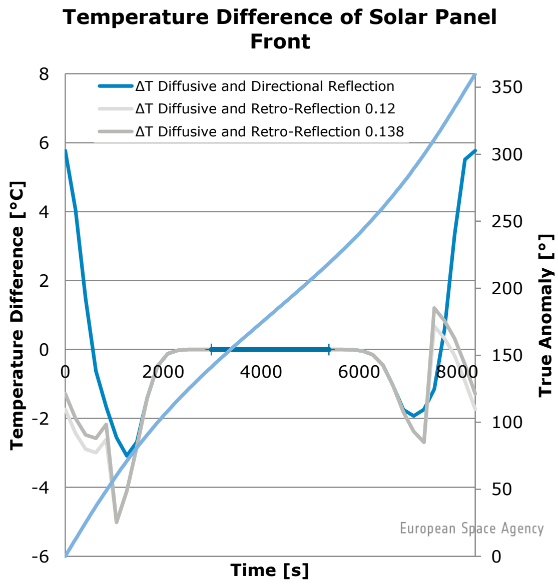

Results (23/24): aphelion/inner panel/ SAA 65deg

Front Side	Back Side
OSR 82% EOL: α/ε = 0.372/0.803	OSR 100% EOL: α/ε = 0.25/0.79

ΔT logic: ΔT positive means that the retro-reflection approach gives higher T than the diffusive (Lambertian) reflection

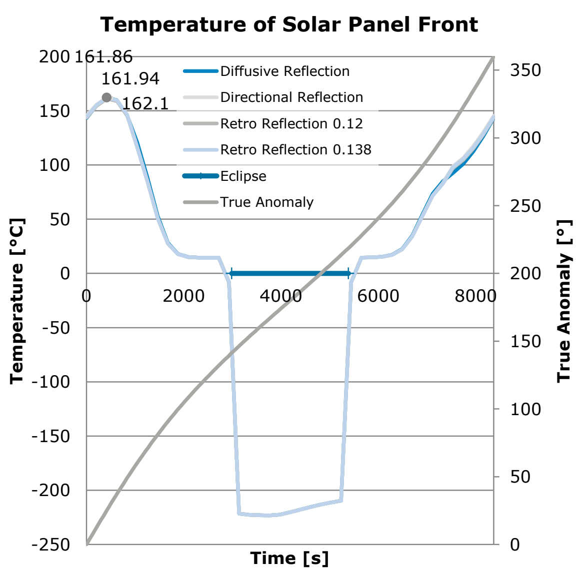

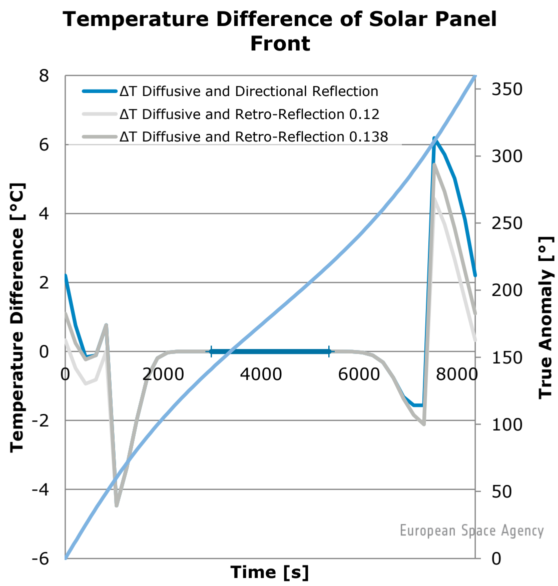

Results (24/24): aphelion/inner panel/ SAA profile

Front Side	Back Side
OSR 82% EOL: α/ε = 0.372/0.803	OSR 100% EOL: α/ε = 0.25/0.79

ΔT logic: ΔT positive means that the retro-reflection approach gives higher T than the diffusive (Lambertian) reflection

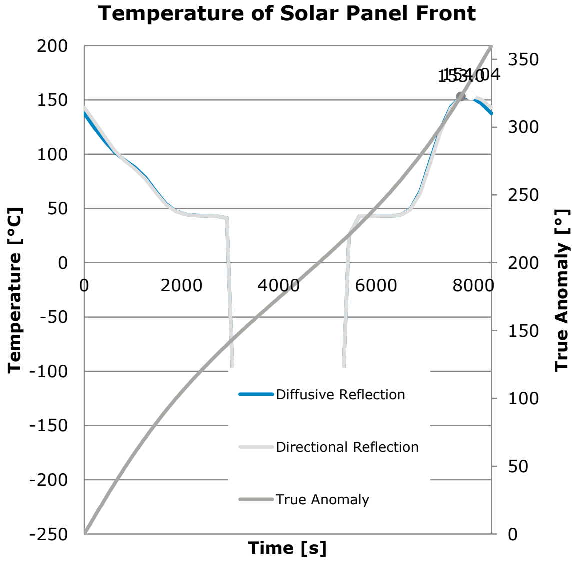

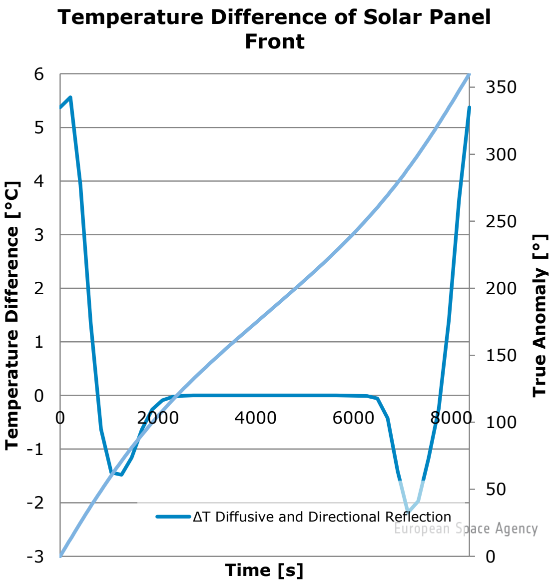

European Space Agency

Only retro-reflection

The orbit is divided in three regions with δ_{retro} as the indicator function:

$$\delta_{retro_j} := \begin{cases} 0 & \text{if } OS_o^{\langle j \rangle} \cdot sun_o < 0 \\ 0 & \text{if } \left| d^{\langle j \rangle} \right| > R_p \\ 1 & \text{otherwise} \end{cases}$$

$$\mathbf{OSS} = (\mathbf{OS} \cdot \mathbf{sun}) \cdot \mathbf{sun}$$
$$\mathbf{d} = \mathbf{OS} - \mathbf{OSS}$$

OS	Position vector
R_p	Planet's mean radius
sun	Solar unit vector (unit vector from the center of the planet pointing to the sun)

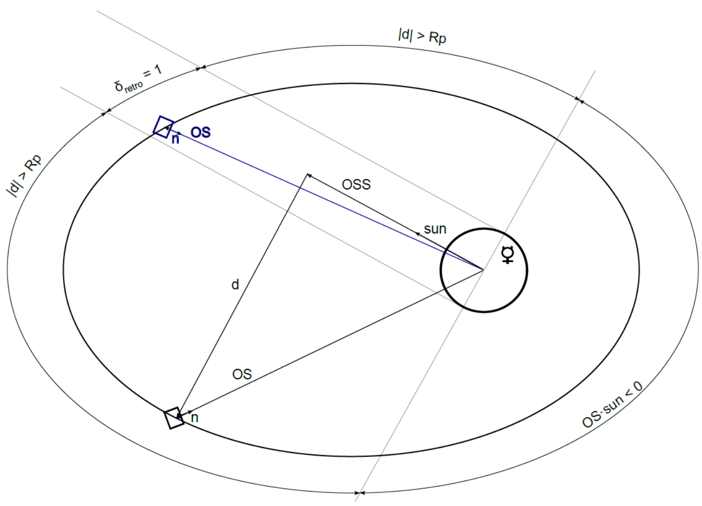

European Space Agency

Only retro-reflection

- The orbit is allocated into a number of points along the orbit (different positions).
- The start and end points of the retro-reflection cylinder are found by counting along the orbit until δ_{retro} becomes 1 and then 0, respectively.
- The respective points represent positions along the orbit and therefore specific times.

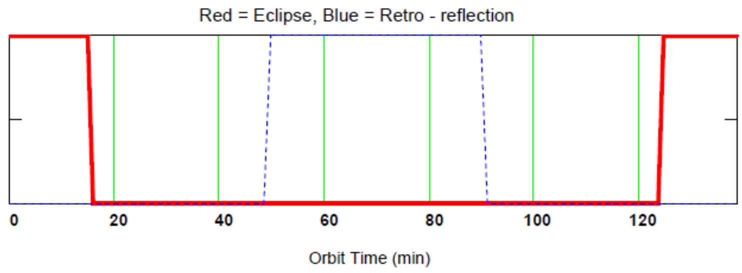

European Space Agency

Only retro-reflection

- Albedo is assumed to be reflected back in the direction of the sun
- Like the eclipse, it is assumed as a cylinder

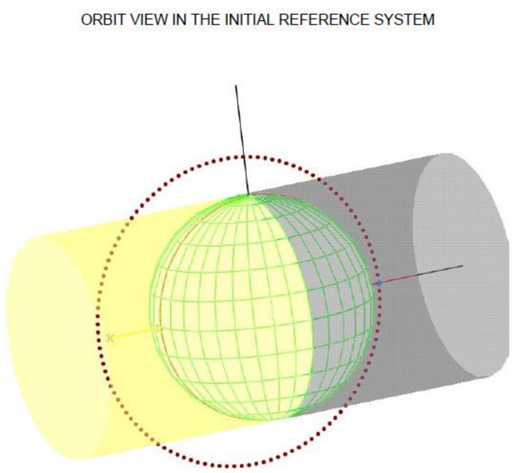

European Space Agency

Only retro-reflection

esa

$$C2_{SA_{k,j}} := \begin{cases} F \leftarrow 0 \ \text{if} \ \left(n_{o_{k,j}} \cdot sun_o\right) > 0 \\ F \leftarrow -\left(n_{o_{k,j}} \cdot sun_o\right) \ \text{otherwise} \end{cases}$$

$$QA_{k,j} := SC \cdot a \cdot \alpha_k \cdot A_k \cdot C2_{SA_{k,j}} \cdot \delta retro_j$$

QA	Absorbed Albedo flux
n	Normal to the surfaces
SC	Solar flux
α	Visible, hemispherical absorptance
A	Area
C2	Aspect angle of the surface
a	Planet Albedo coefficient

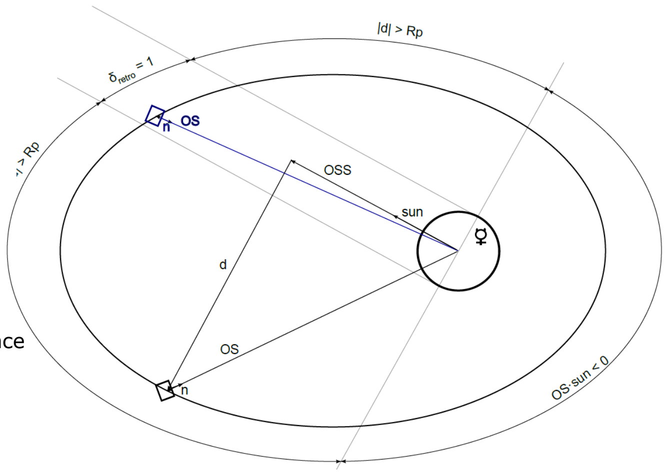

European Space Agency

Only retro-reflection – reference case

esa

A1 – Anti- Velocity
A2 – Normal to Orbit
A3 – Nadir
A4 – Velocity
A5 – Normal to Orbit
A6 – Zenith

a = 0.12

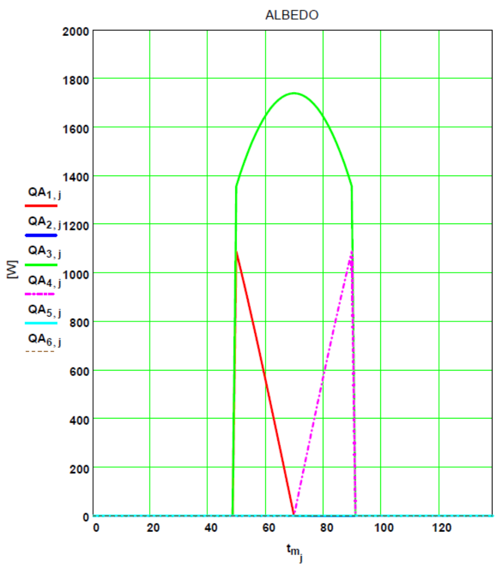

a = 0.138

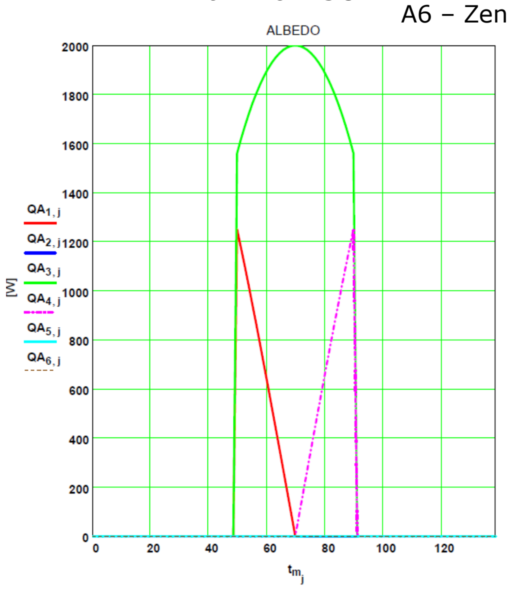

ean Space Agency

Solar Heat Fluxes – reference case

Perihelion case: incident (*) Solar heat fluxes calculated on a nadir pointing orbiting cube of 1m side

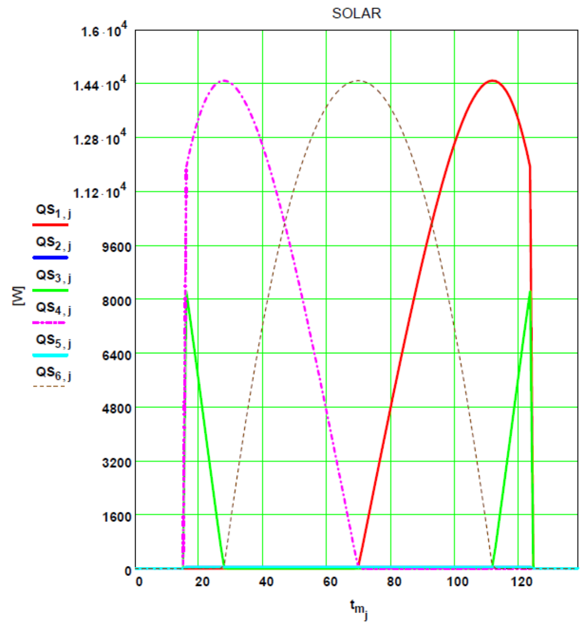

A1 – Anti- Velocity
A2 – Normal to Orbit
A3 – Nadir
A4 – Velocity
A5 – Normal to Orbit
A6 – Zenith

(*) incident → absorbed by 1sqm black body surface

European Space Agency

IR Radiation Heat Fluxes – reference case

Perihelion case: incident (*) IR heat fluxes calculated on a nadir pointing orbiting cube of 1m side

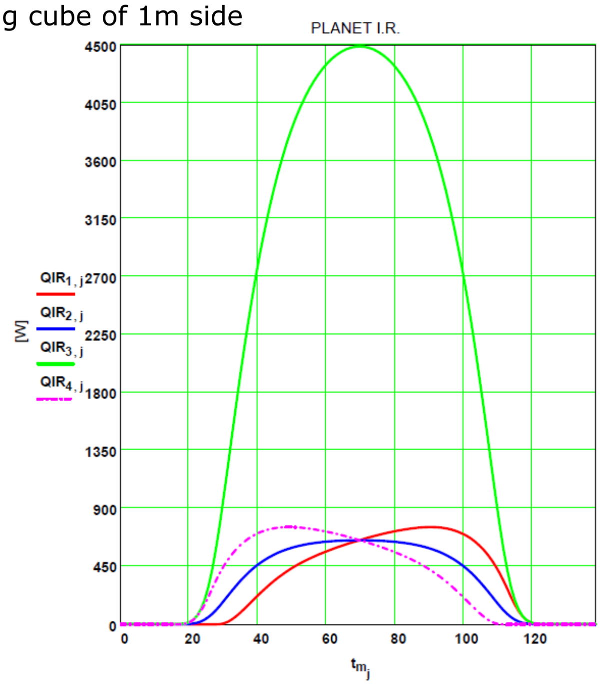

A1 – Anti- Velocity
A2 – Normal to Orbit
A3 – Nadir
A4 – Velocity
A5 – Normal to Orbit
A6 – Zenith

(*) incident → absorbed by 1sqm black body surface

European Space Agency

Albedo Heat Fluxes (diffusive model) – reference case

Perihelion case: incident (*) Albedo heat fluxes calculated on a nadir pointing orbiting cube of 1m side

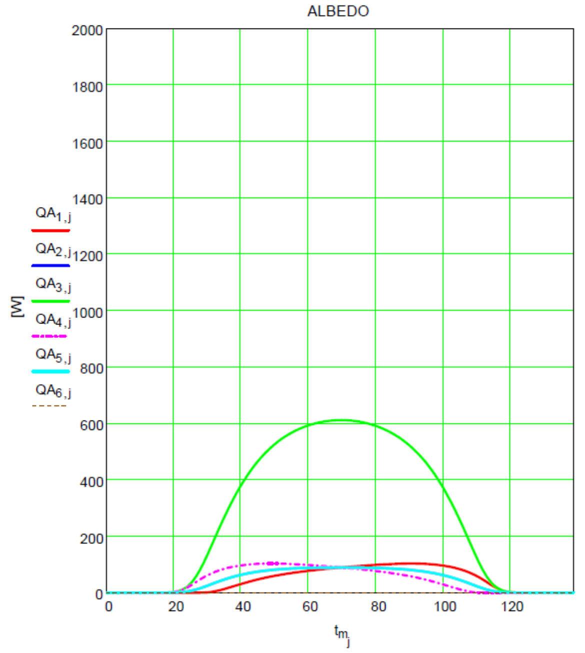

A1 – Anti- Velocity
A2 – Normal to Orbit
A3 – Nadir
A4 – Velocity
A5 – Normal to Orbit
A6 – Zenith

(*) incident → absorbed by 1sqm black body surface

European Space Agency

Solar Panel Attitude

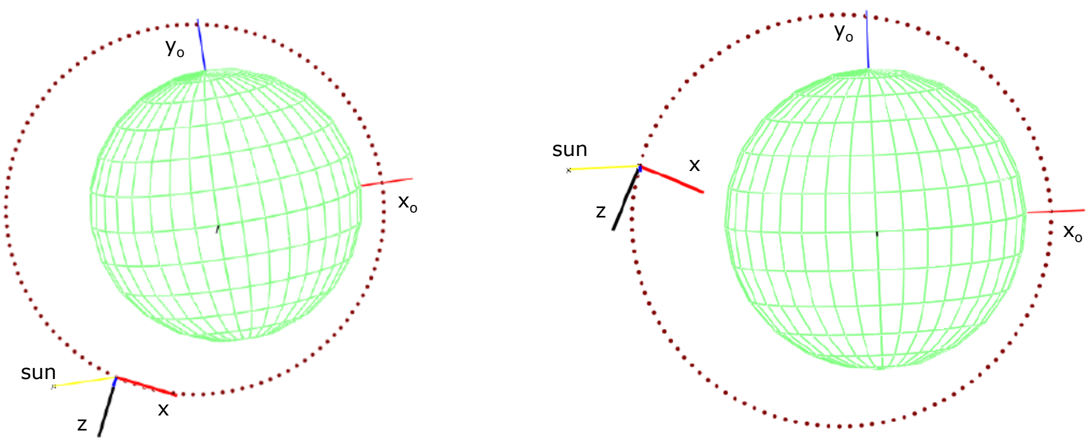

SAA (Sun Aspect Angle): angle between solar panel and sun vector

- Solar array plane is represented by the XZ plane
- SAA=90° means Sun lies within the XZ plane (no energy)

European Space Agency

Solar Flux – SAA = 65°

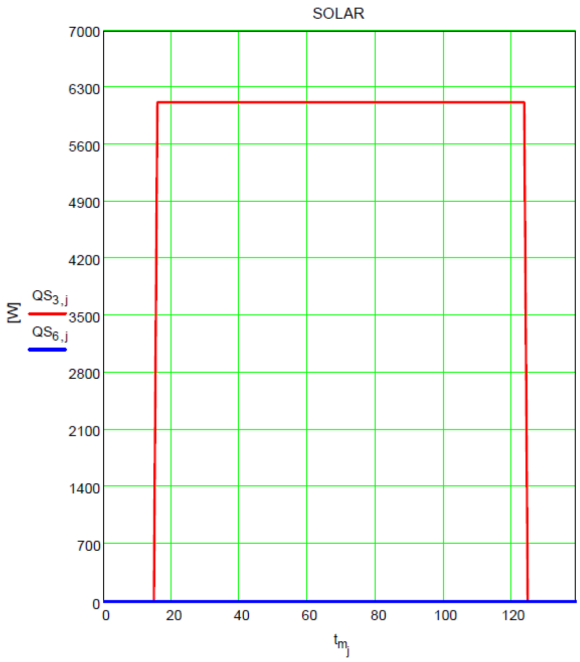

European Space Agency

IR Planetary Radiation – SAA = 65°

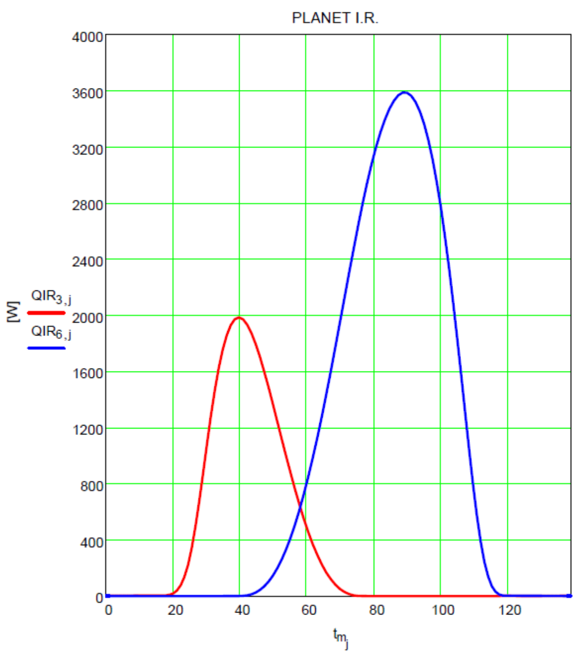

European Space Agency

Albedo heat fluxes comparison (SA with SAA=65°)

- Directional albedo is considered the most realistic approach
- Differences in peak Albedo fluxes can be significant between the different models

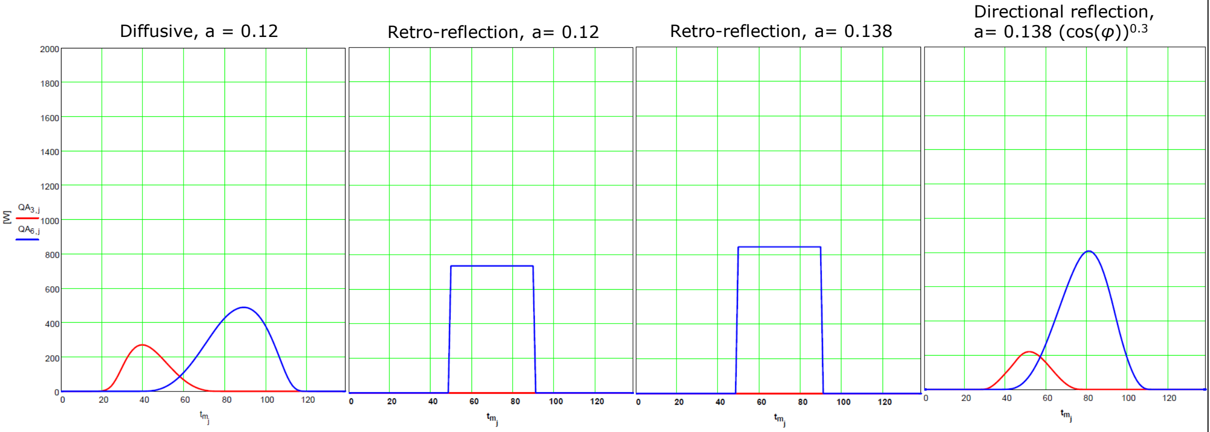

QA6: Albedo flux incident on SA front side
QA3 : Albedo flux incident on SA back side

European Space Agency

Appendix D

On the thermal design and modelling of calibration blackbodies for the FCI and IRS instruments on MTG

Nicole Melzack
(RAL Space, United Kingdom)

Abstract

[1] The Meteosat series of spacecraft are meteorological satellites, providing a range of data that inform weather forecasts across Europe. First generation satellites have flown, second generation (MSG) are currently operational, and the third generation (or MTG) will provide data well into the 2030s. Two instruments going on the MTG satellites will be calibrated using the blackbody targets that are being designed at RAL Space.

The blackbody targets are required to operate at temperatures between 100–370 K. The challenge involved in this includes providing single targets that can physically achieve and operate successfully at both thermal extremes, while also meeting stringent temperature gradient requirements. This presentation will cover the thermal design solution, which involves using helium gas conduction, and how it has been modelled in ESATAN-TMS. The testing of the prototype and the limitations of modelling gas conduction in ESATAN-TMS will also be discussed.

[1] Due to severe weather conditions the author was unable to attend the workshop and present this material.

On the thermal design and modelling of calibration blackbodies for the FCI and IRS instruments on MTG.

Nicole Melzack, RAL Space, STFC


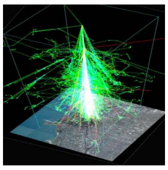

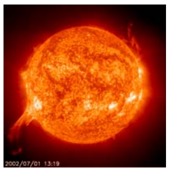

RAL Space

European Space Thermal Analysis Workshop
3-4th November 2015

Science & Technology Facilities Council

RAL Space

Outline

- Meteosat
- Blackbodies
- Thermal challenges and design overview
- Breadboard model

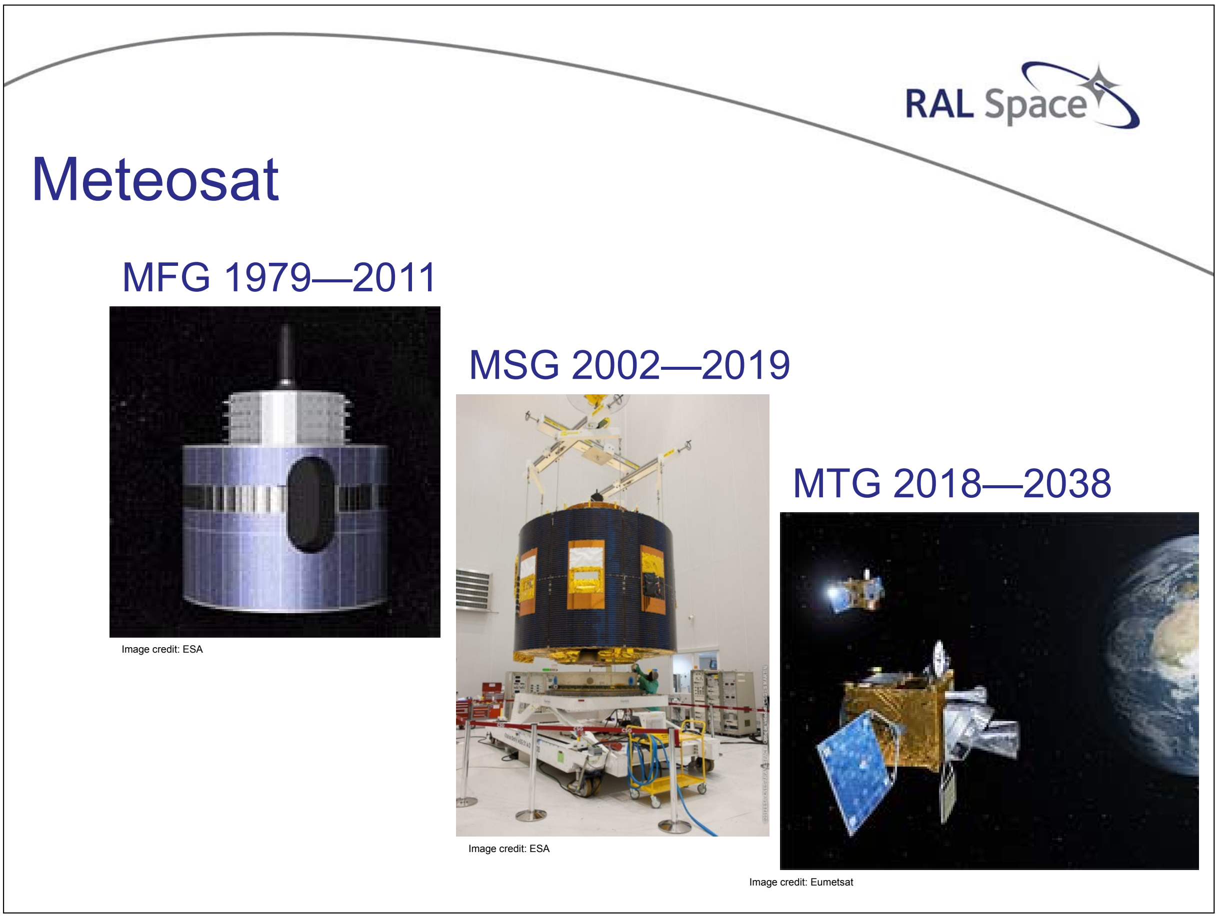

The Meteosat series of spacecraft are meteorological satellites, providing data that inform weather forecasts across Europe. The first generation satellites flew between 1979 and 2011, and the second generation is still operational – and expected to be until 2019.

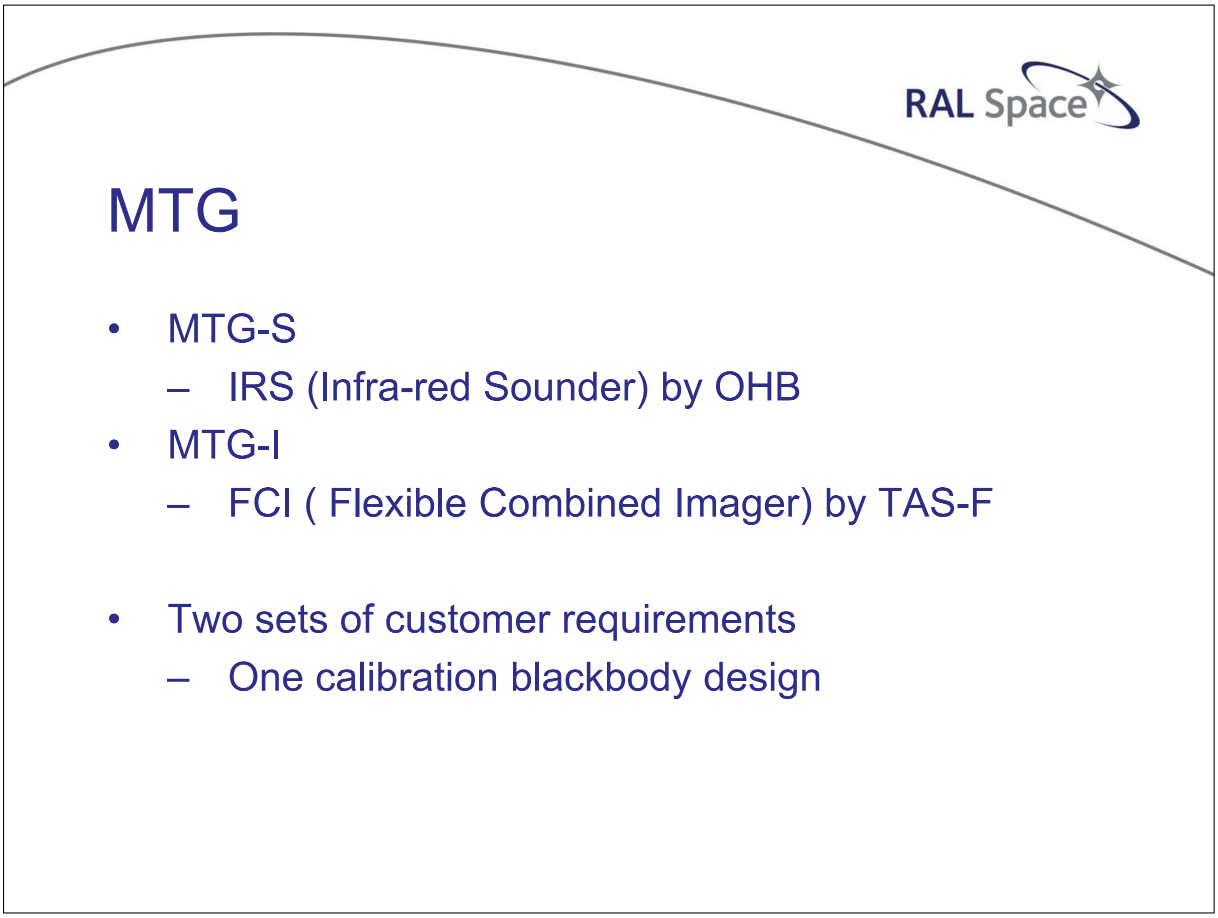

Meteosat third generation, or MTG, will be taking over and the first satellites should be launching in 2018. MTG has two types of spacecraft; Sounding – MTG-S and Imaging – MTG-I. Instruments that will be going on both spacecraft are being designed and produced by OHB in Germany and TAS-F in France.

In order to calibrate their instruments on the ground, both TAS-F and OHB will be using the calibration targets that we're designing at RAL Space. So we are combining two sets of customer requirements in order to deliver a single blackbody design.

RAL Space

Blackbody calibration target

- Target of accurately known temperature and high (~1) emissivity
- Precisely controlled
  - Better than instrument can measure
- Used to calibrate instrument
- Often a baseplate surrounded by a baffle

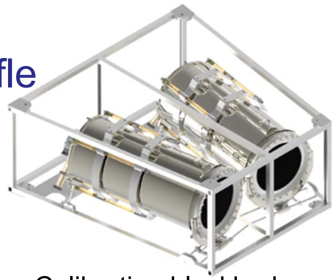

Calibration blackbody

A blackbody calibration target is a target that an instrument views, that is controlled to a very accurate temperature and emissivity (ideally 1). Normally they comprise of a baseplate that the instrument views surrounded by a baffle to protect it from the environment. The calibration target needs to be controlled more precisely than what the instrument can measure, which is how it is used as a calibration source, and so the requirements can be quite stringent.

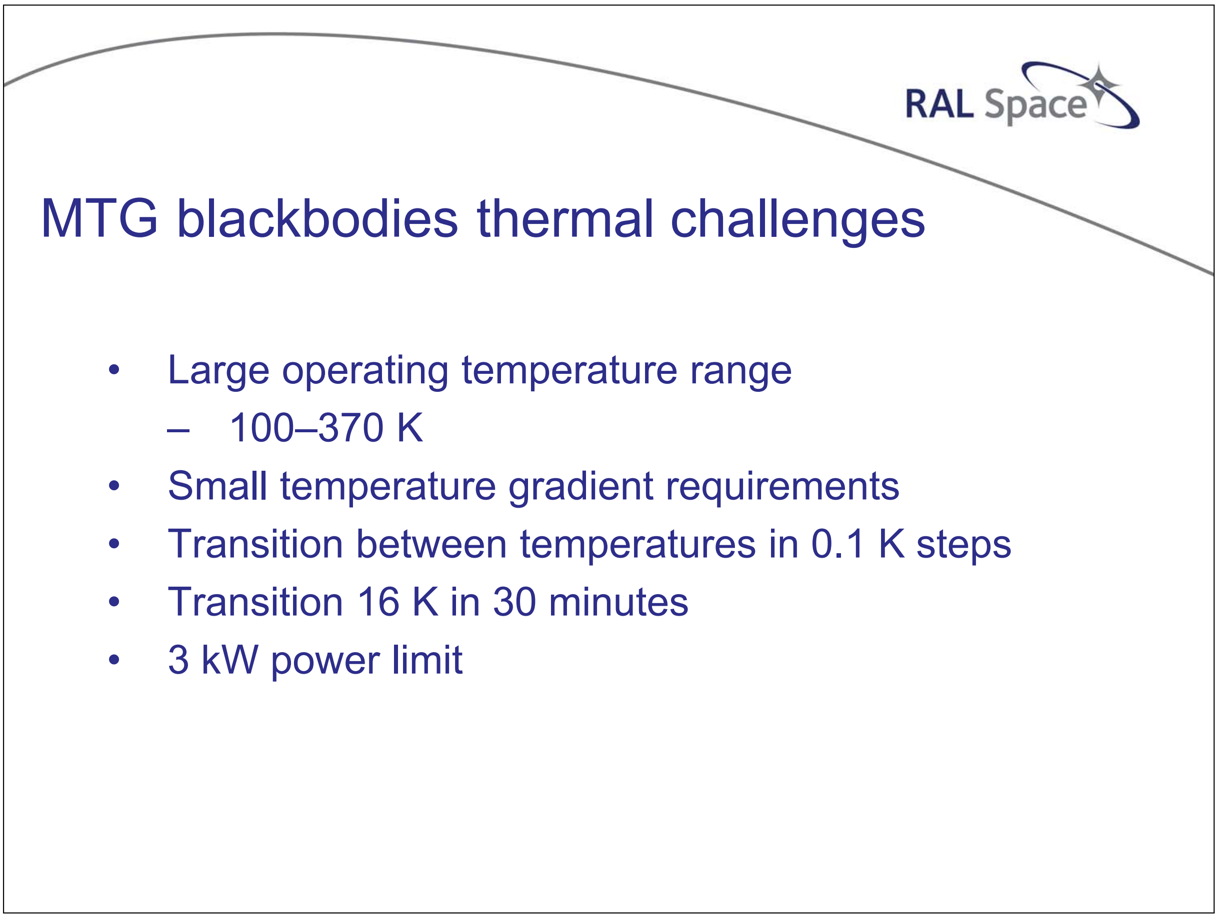

Taking both sets of customer requirements into account, the MTG blackbody design will need to: be able to operate between 100 – 370 K. Thus we need one design that can both physically achieve and operate successfully at this wide range of temperatures. The blackbodies also need to have a uniform temperature – so what instrument sees can't vary by more than 200 mK. Furthermore, the blackbodies need to be able to transition between temperatures relatively accurately and quickly, and with only a 3 kW power limit.

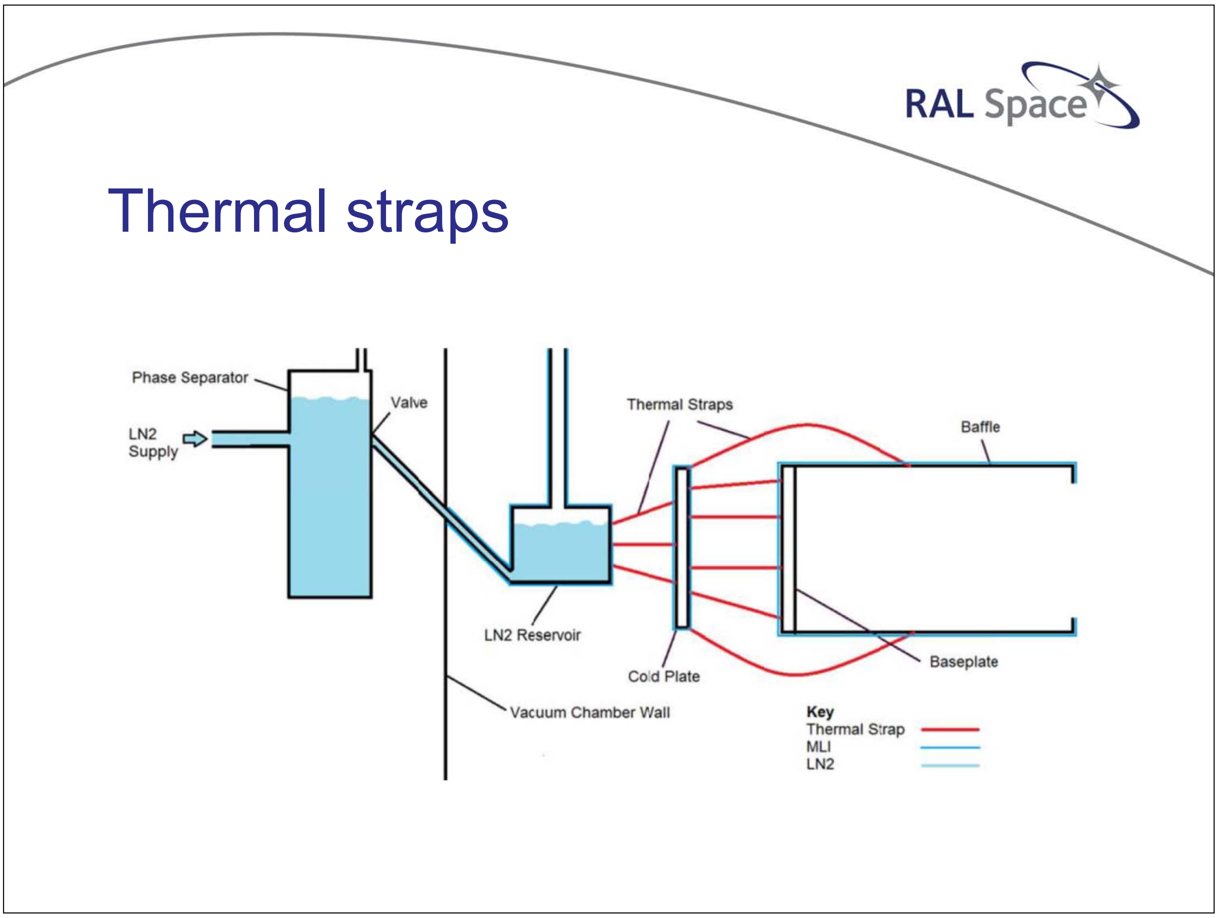

To get down to the colder temperatures, the customer requirements specify that we should use liquid nitrogen. LN2 is about 77 K, so being able to thermally link the blackbody to it will allow us to run the whole thing cold, and still be able to use heaters to control the temperature. The first idea was to have a reservoir of LN2 , connected to a cold plate, which then connected to the cavity with copper thermal straps. This was the proposed solution that won us the work. The cold plate would be used for coarse control and would have heaters on it. The cavity itself would be used for finer temperature control.

However, with this design there was no way to turn off this LN2 link for when the blackbodies needed to be at the hotter temperatures, this would lead to a high demand for heater power, and the potential waste of nitrogen. The boiling LN2 could cause vibration issues – although the flexibility of the thermal straps allow them to dampen this effect. Furthermore, the straps would provide point source cooling, which would make it harder to achieve the required uniformity.

During the proposal stage it was identified that having a variable conductive link to the LN2 would allow us to save on heater power and nitrogen. So the next stage in the design was to investigate this.

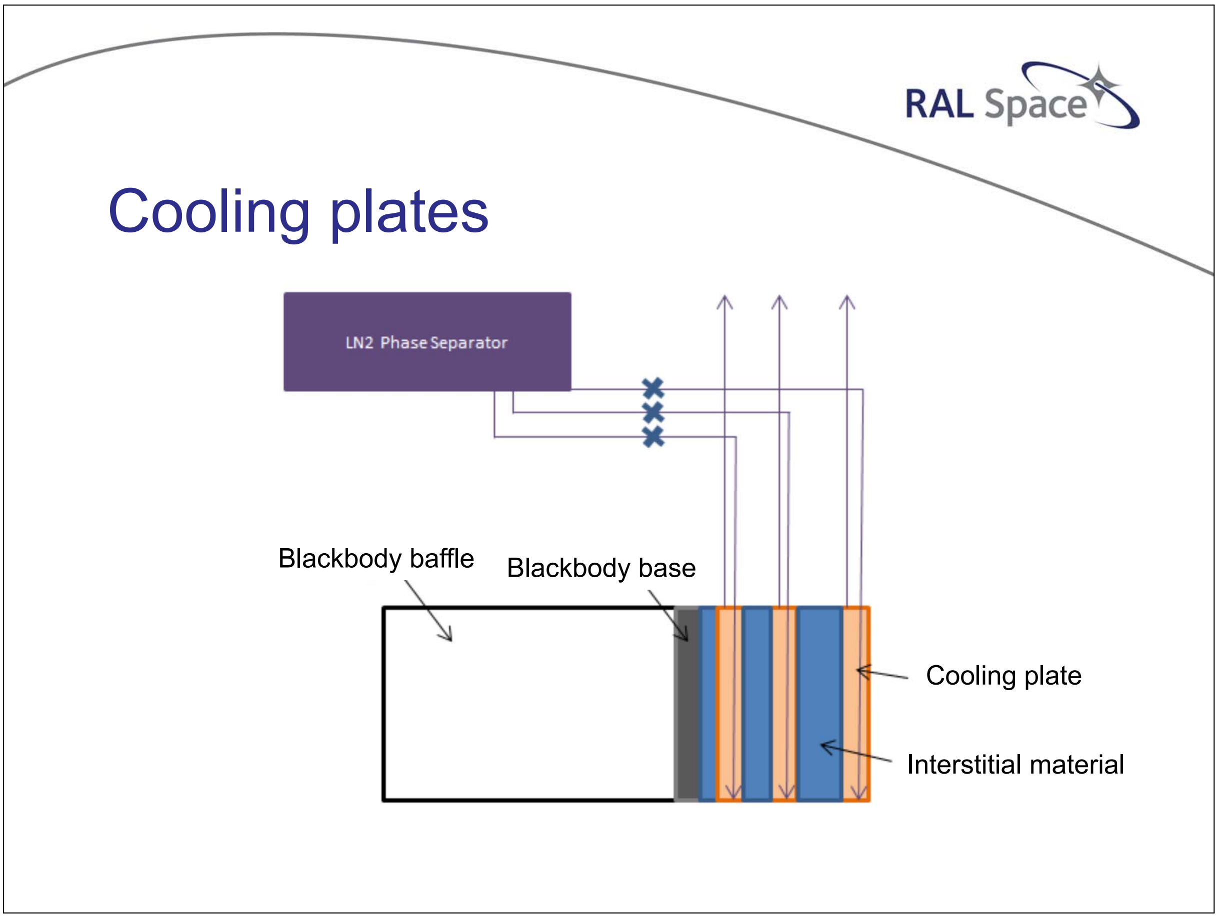

The idea progressed to having three cooling plates (instead of the one cold plate shown previously). The plates would have piping in which could be filled with LN2, and be at different distances from the back of the cavity. Controlling which plates were filled with nitrogen achieved different conductive links to the cold LN2. This design gave the uniformity in temperature required at the base of the blackbody, but didn't address the uniformity of the baffle – which is required for the radiometric design.

We needed a way that we could have a variable conductive link to the LN2 surrounding the entire cavity.

Then we started looking at the HIRDLS blackbody targets, which were developed at Oxford University by Bob Watkins, and Dan Peters who now works at RAL Space.

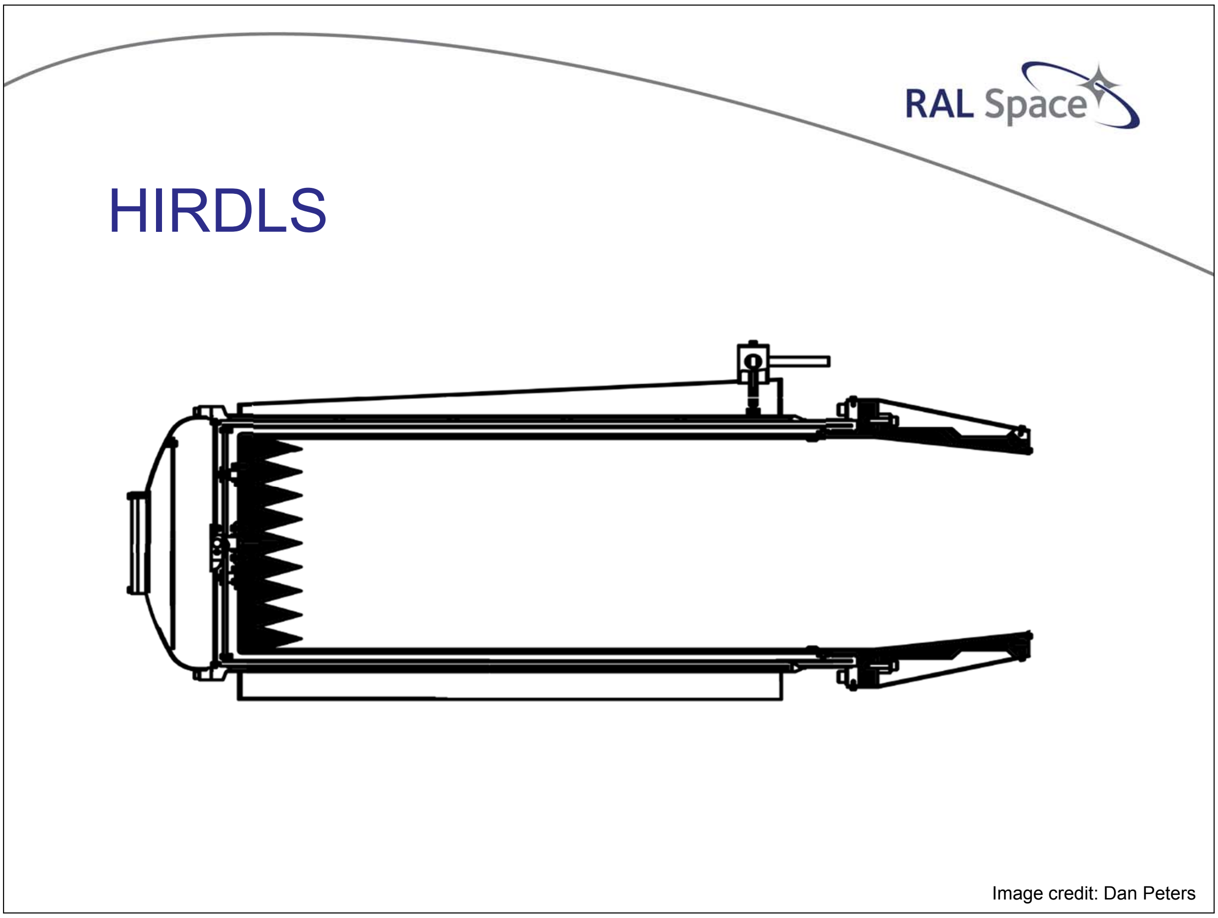

HIRDLS is an instrument that flew on the NASA Aura mission. The ground calibration target for this instrument covered the blackbody in a jacket of LN2, with a He gas gap between it and the cavity, and is the design that we have taken forward for the MTG calibration targets.

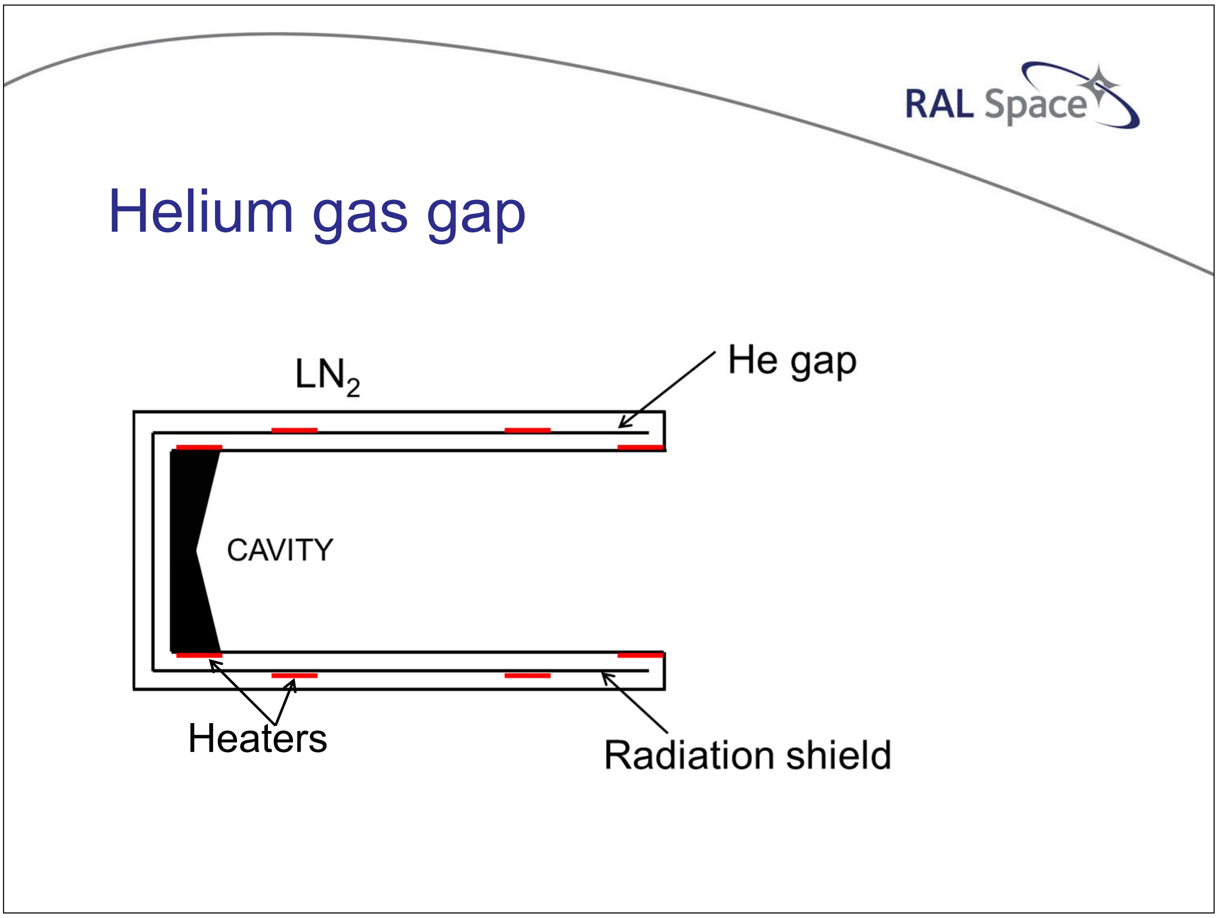

Helium's thermal conductivity changes with pressure, and so with 1 bar of He we get the maximum conductive link, with 0 bar, we get a vacuum and effectively no conductive link through the gas gap. At pressures in between we get varying conductance – hence the idea to operate the gap as a variable conductance gas gap heat switch.

RAL Space

Main thermal control aspects

- Helium conductivity
- Heater control to minimise gradients
- Radiation shield thermo-optical properties

RAL Space

Helium conductivity in a gas gap

Helium thermal conductivity in a helium gas gap

$$k(T) = k_{bulk}(T) \cdot \left(1 + \frac{8}{3} \cdot \frac{k_{bulk}(T) \cdot T}{e \cdot p \cdot \sqrt{3 \cdot R \cdot T}} \cdot \left(\frac{1}{\alpha_1} + \frac{1}{\alpha_2} - 1\right)\right)^{-1}$$

k_{bulk} is the bulk conductivity of He
T is temperature
e is the gap thickness
p is the pressure of the gas
R is the specific gas constant
α is the thermal accommodation factor

Equation from:
'Active-mirror-laser-amplifier thermal management with tuneable helium pressure at cryogenic temperatures', A. Lucianetti et al., Optics Express, Vol 19, Issue 13, pp. 12766 – 12780, 2011.

The thermal conductivity we get from gaseous helium in a gap depends not only on its pressure. The temperature of the helium gas itself is a big contributor. The size of the gap we're using also plays a role – the smaller the gas gap the better the thermal conductivity. We also need to take into account the energy exchange between the solid surface and the gas at either side of the gas gap – which is represented by the thermal accommodation factor.

All of these factors are taken into account in this equation. So this is what I used to calculate the thermal conductivity value, k, and then plugged that into the equation for the conductive link, or GL to use with the ESATAN software.

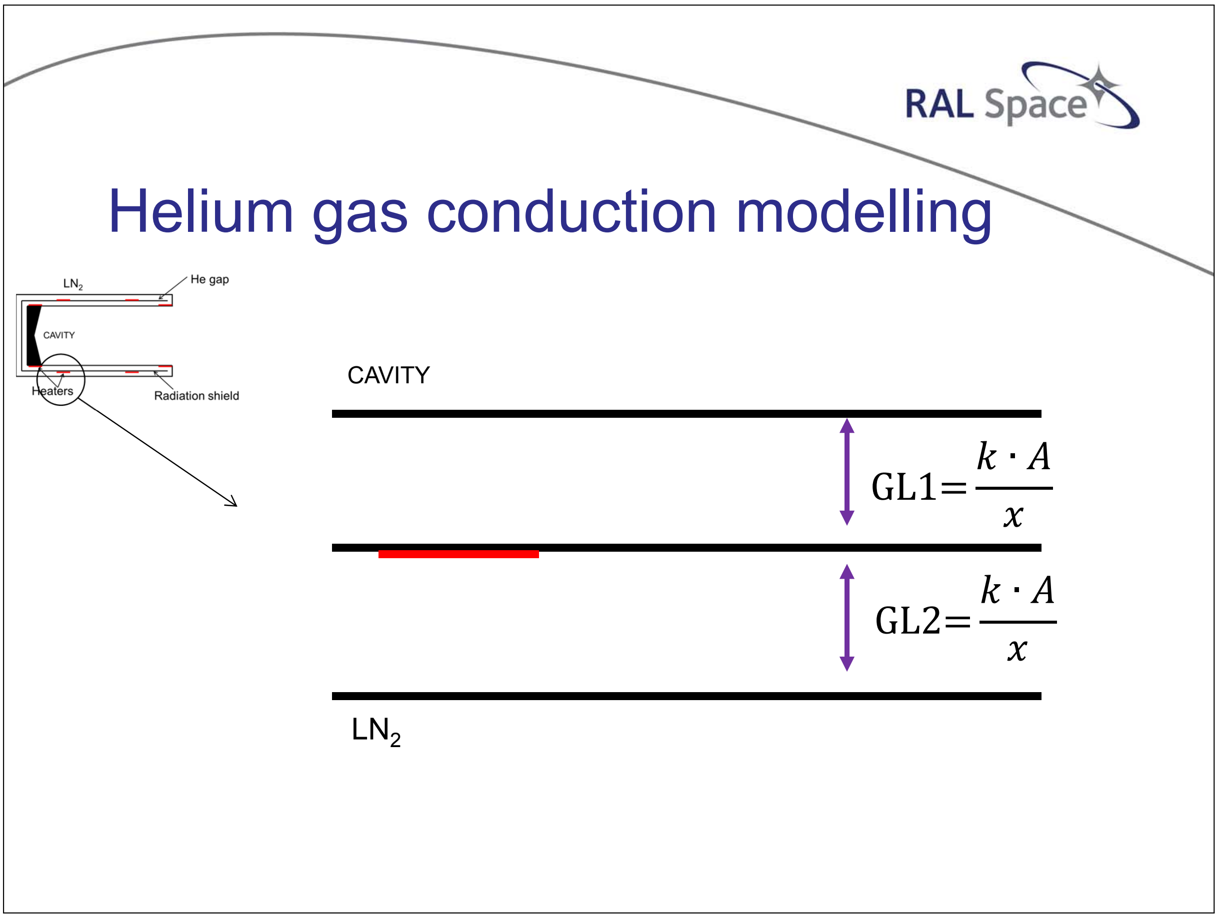

For the other conductive links in the thermal model, such as the bolted interfaces, I used the ESATAN Workbench to define a contact conductance. However, I did not define any geometry to be the helium, and so all the helium conduction modelling was done through the ESATAN file

I treated either side of the radiation shield as its own helium gas gap, and calculated the GLs required for each gap.

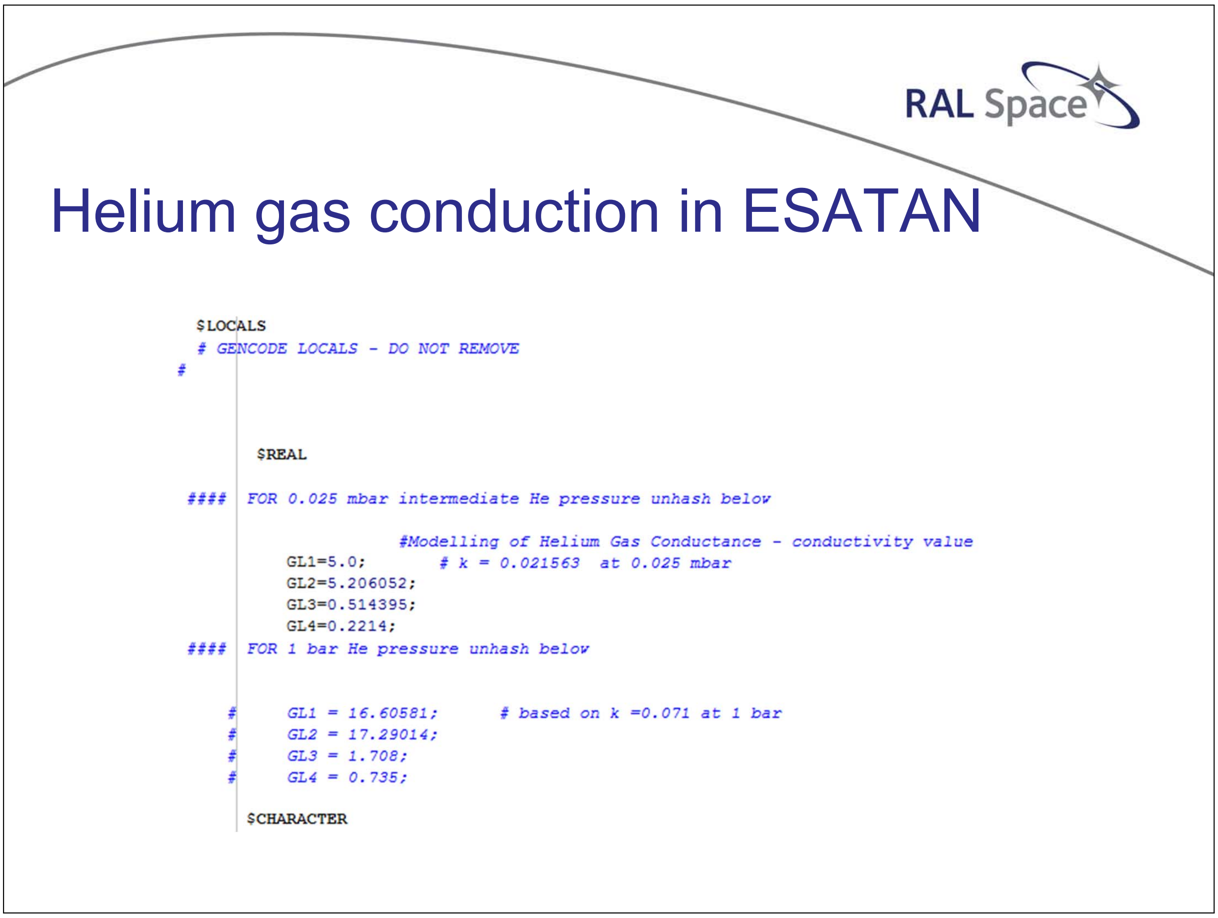

I then used these in the template file, and made node-node GL links between the relevant surfaces in the $CONDUCTORS block.

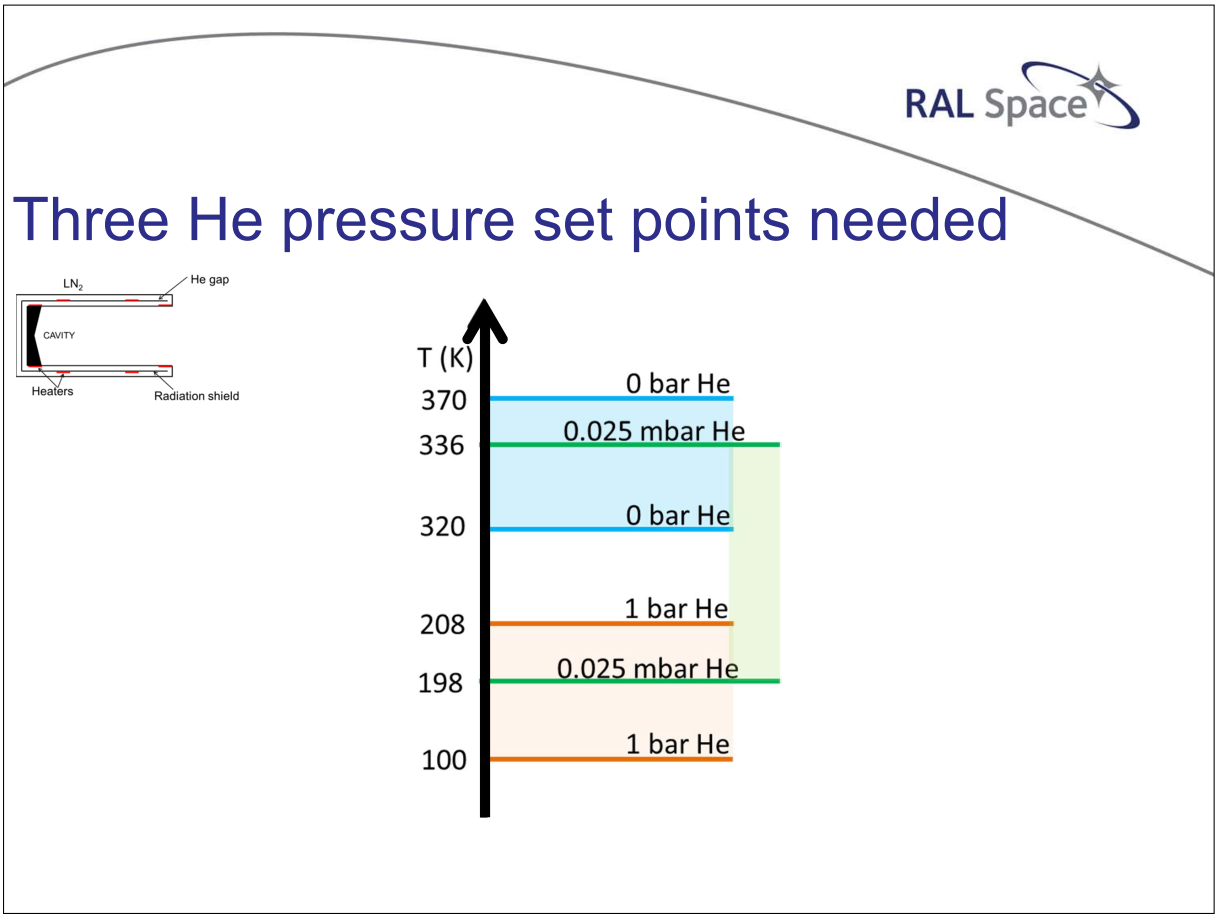

On a practical level it's easier to control the power input into heaters, than it is to control the pressure in a gas gap. So once I'd set up the model, I looked to see the smallest number of helium pressures I could use to control over the entire temperature range – given the 3 kW power limit.

I looked at the two easier options first, 1 bar for the cold cases, and 0 bar for the hot cases. I looked into what the maximum controllable temperature was for each set point (using 'full power') and the minimum controllable temperature (using about 300 W in total). But there was a gap here. And with a bit of trial and error I found a helium pressure that would bridge the gap and allow us to control over the entire range.

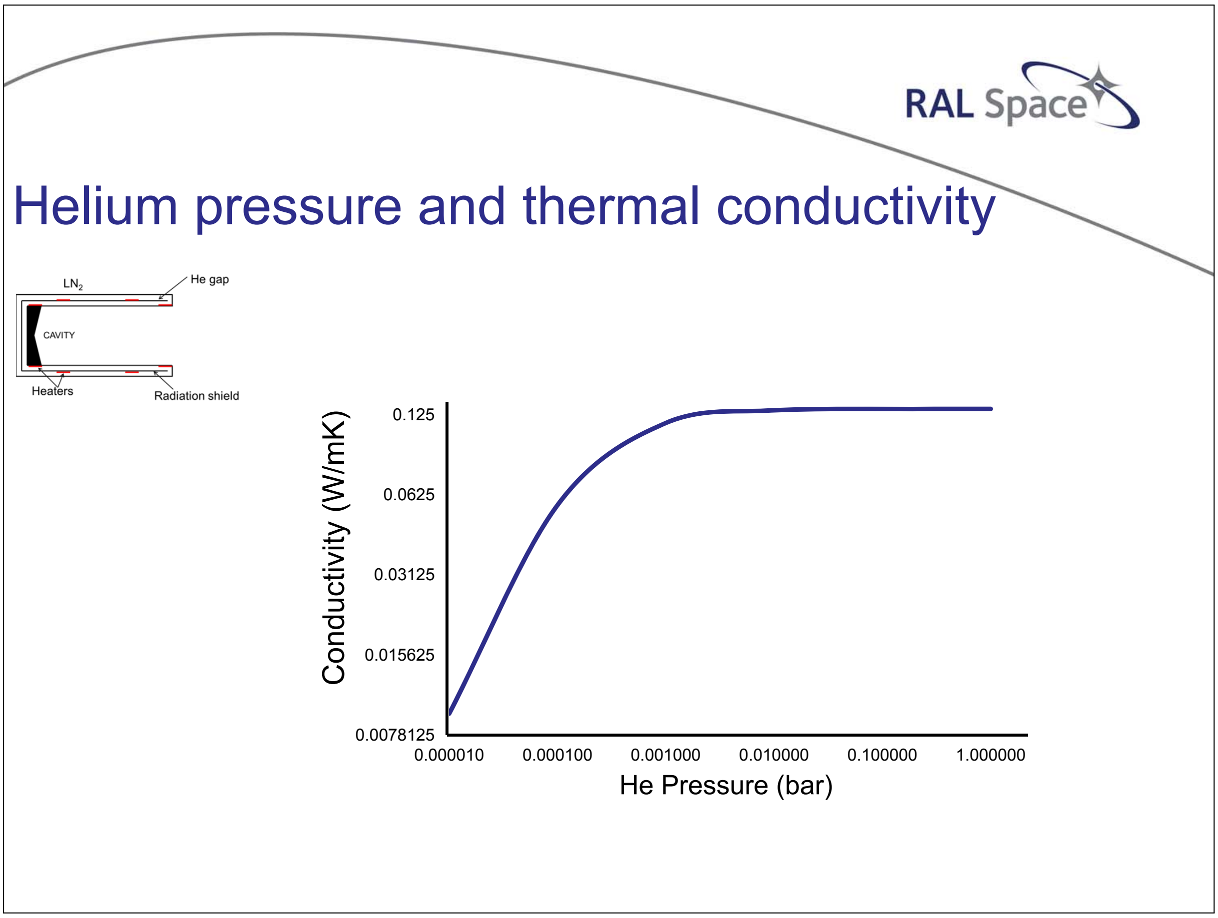

You may notice that 0.025 mbar is a very low pressure to use here, and that's because the relationship between conductivity and pressure is extremely non-linear, this is a log plot of the relationship at 260 K.

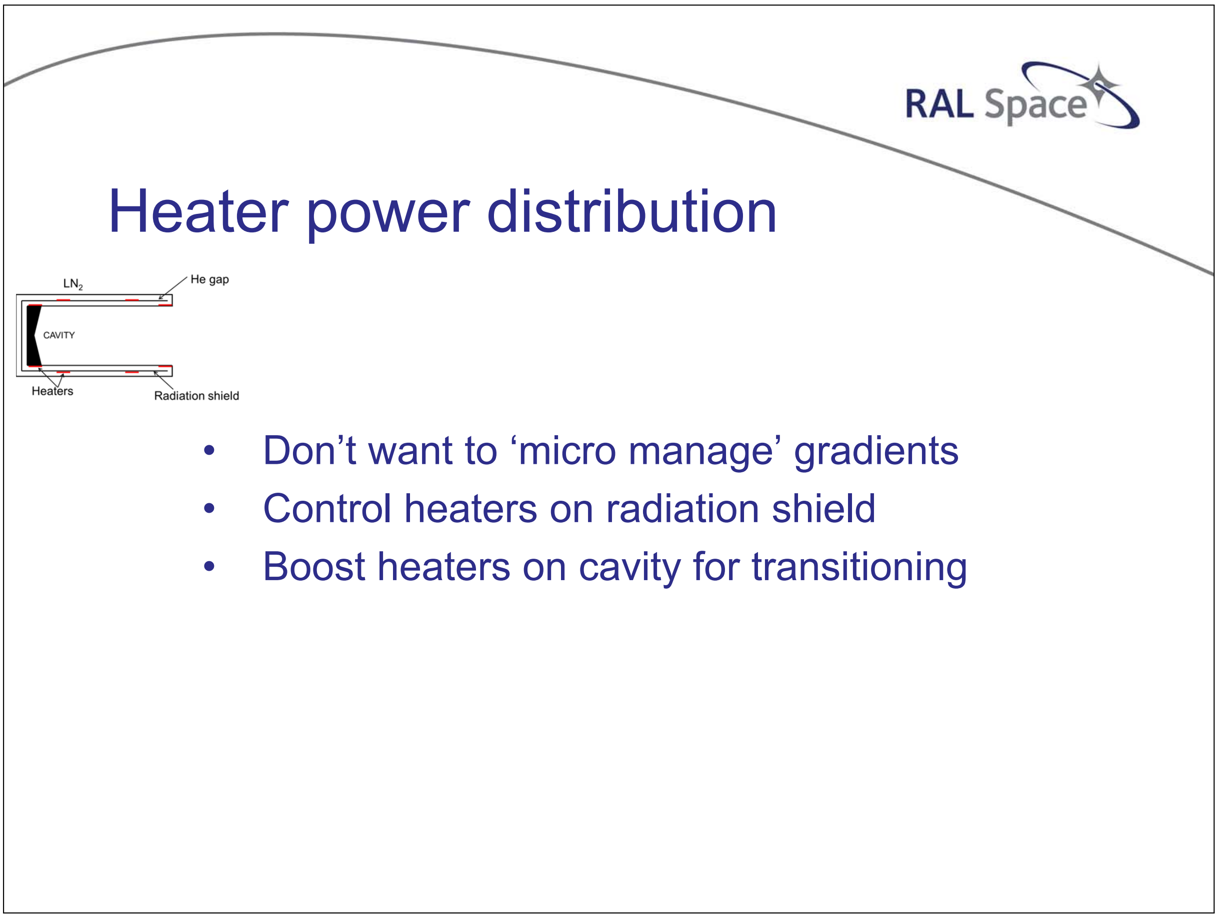

With regards to the heater powers, we needed to be careful that we weren’t micro managing the gradients, we didn’t want to be putting heat inputs into each node, as that makes the system far too reliant on the power input, and ultimately we want something that is inherently uniform.

The solution here was to control the cavity temperature using the radiation shield. The control heaters on here would make the heat reaching the cavity more uniform. Modelling and analysing this in ESATAN again took trial and error. I initially used the workbench to add boundary condition at potential ’heater’ nodes, however I found this took too long and started writing the inputs into the template files myself, I also experimented with parametric cases – running one case after another and just changing the heater location or heat input, which did speed up my analysis.

There is a conflict in the customer requirements. The uniformity requirement lends itself to a high thermal mass, however the fast transition time between temperatures would be easier to meet with less mass.

Meeting the uniformity requirements has meant that there is a need for boost heaters on the cavity, which will only be used when temperature transitions are taking place, to speed up the time taken to go between set-points.

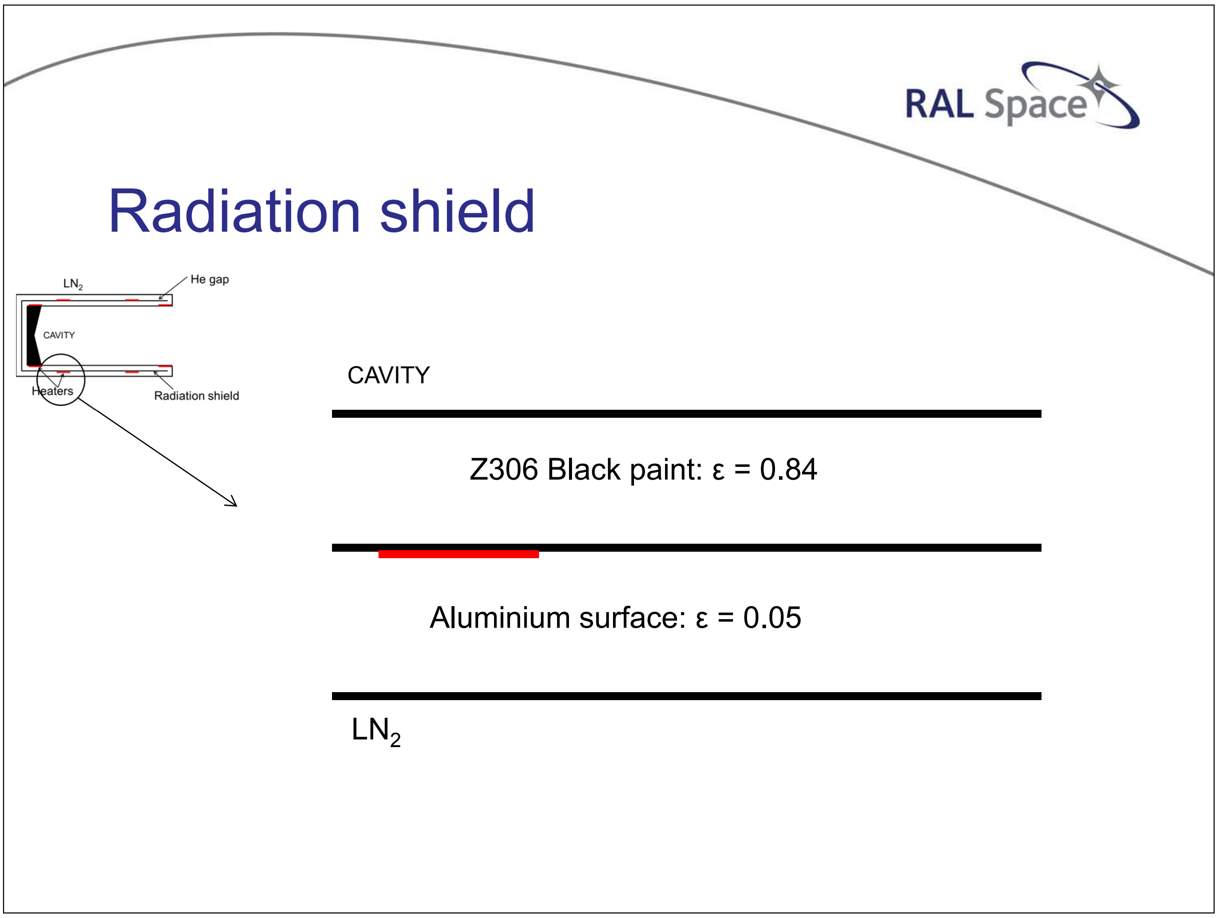

Since the main control heaters are on the radiation shield, we need to ensure that there is always a thermal link between the heated shield and the cavity, even when there is no helium in the gas gap. Conversely, on the other side of the shield, we want the thermal link between the cold liquid nitrogen and the shield to be dominated by the gas conduction.

The solution here was to use surface coatings, so the cavity and shield surfaces which face each other are painted black with a high emissivity and good thermal link at all times. However, low emissivity coatings on the LN2 jacket and shield surfaces which face each other will help save heater power and LN2 when running at hotter temperatures.

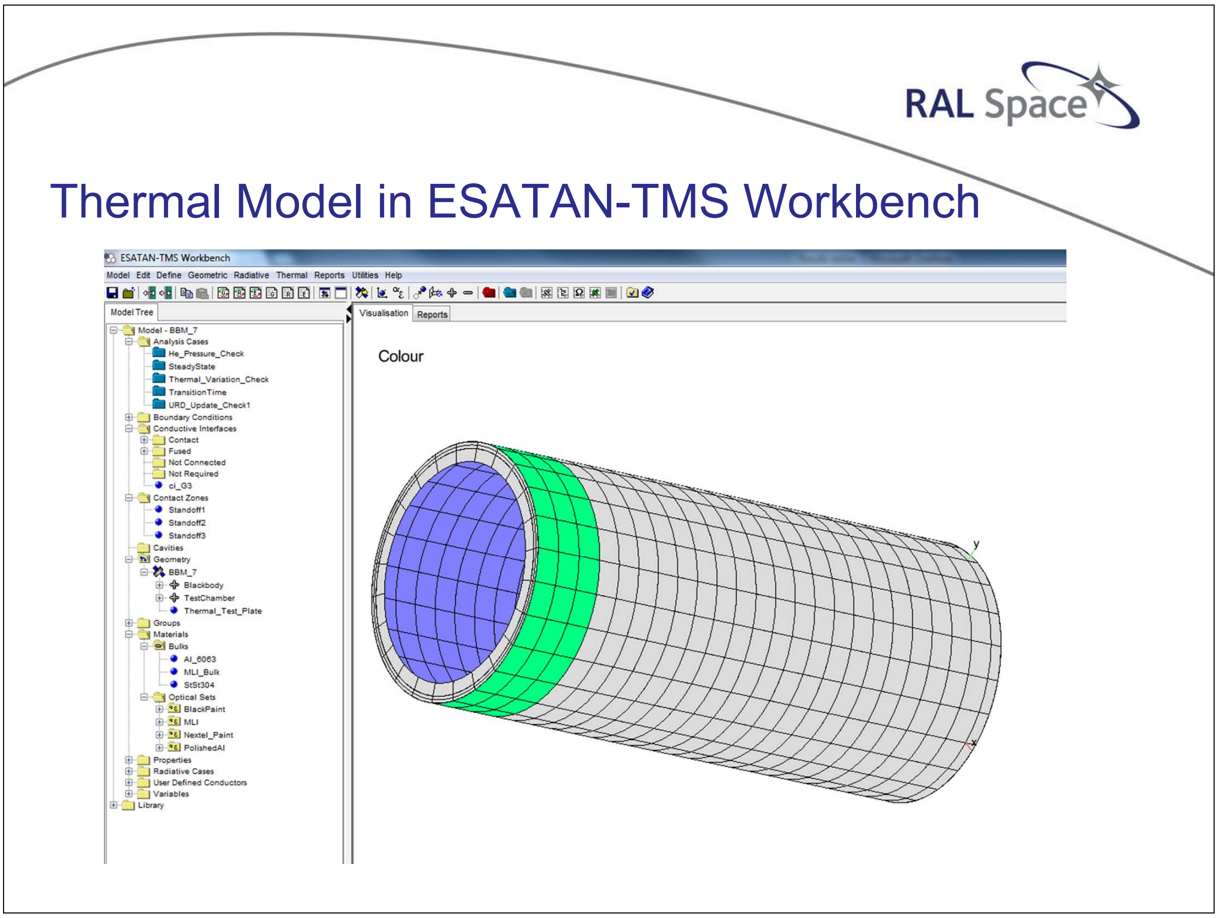

I've used this thermal model for the helium pressures and to optimise the heater distributions, and most recently to create the test predictions for the upcoming breadboard model tests.

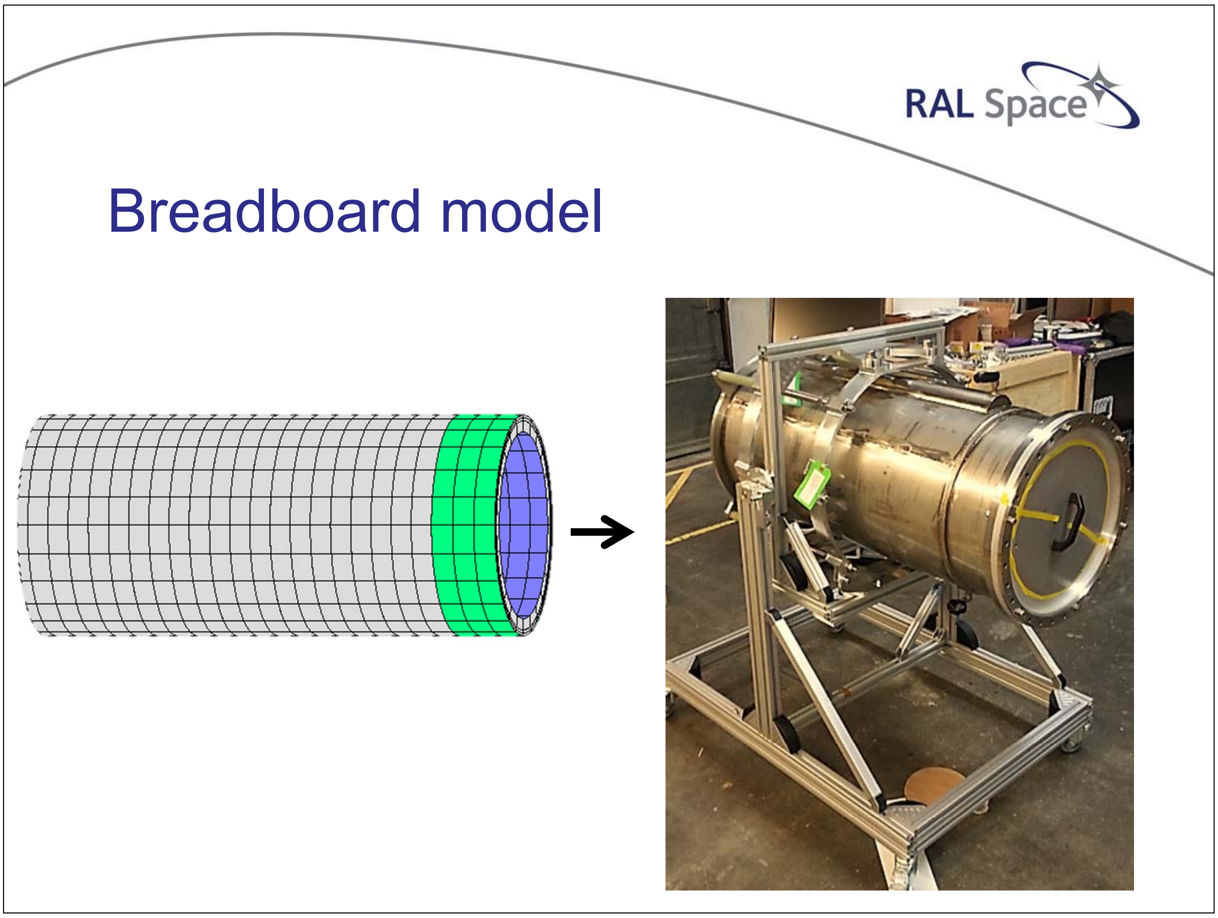

The breadboard model is a prototype of the blackbody that is being used to de-risk the design. It will provide loads of useful data to help me correlate the model and start on the more detailed CDR analysis.

In theory the blackbody will operate at the thermal extremes, but we need to make sure it will be manufactured to withstand those temperatures.

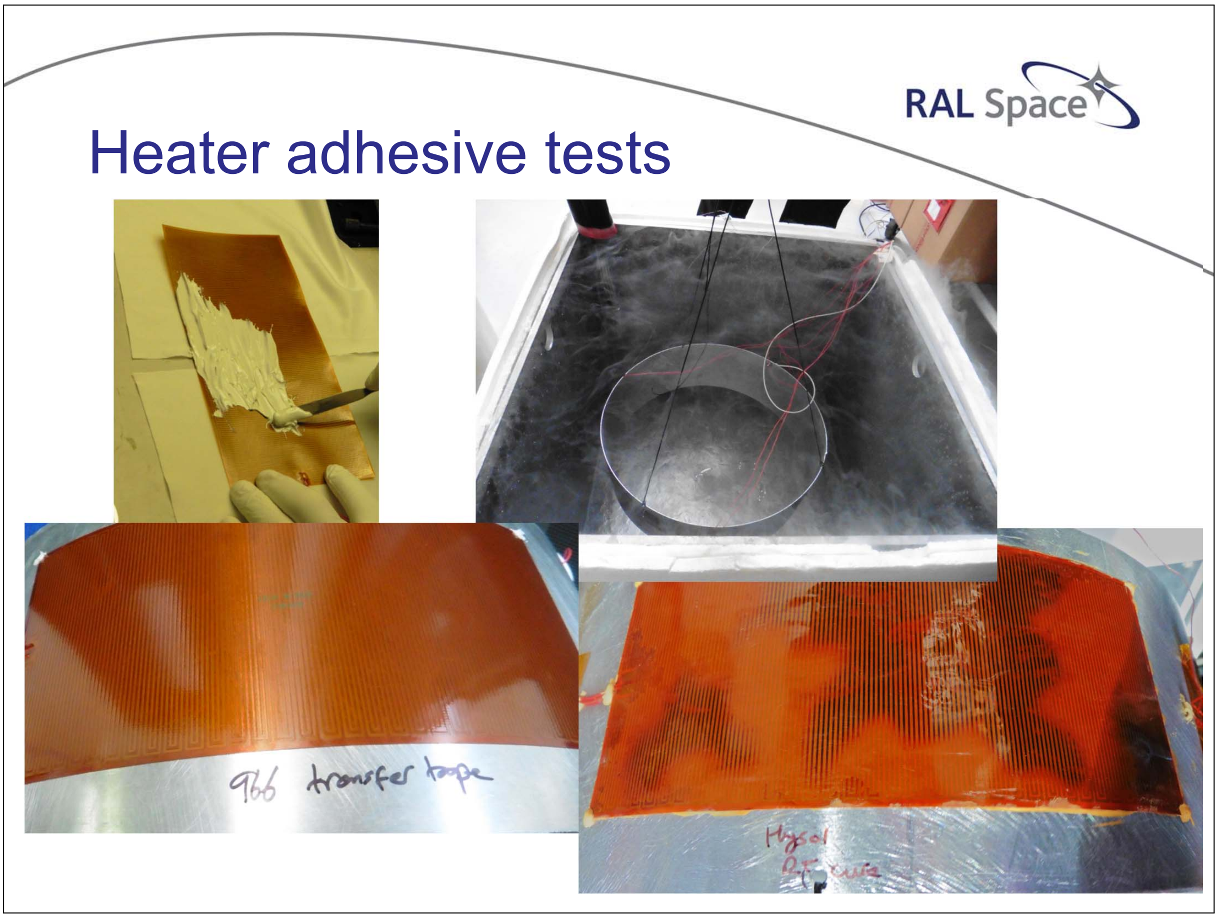

As I said earlier, I've used thermal analysis to size the power requirements and also the locations of the heaters on the blackbody. But in reality, ensuring the heaters maintain a good thermal contact with the structure is down to the adhesive working across the range of operational temperatures.

As a pre-BBM test, four different adhesives were used to attach heaters onto aluminium plates and then curved sections of aluminium. I then helped with the thermal cycling of the samples – using an oven and a bucket of liquid nitrogen to make sure the samples saw the conditions they would in operation. Some of the adhesives failed, we could see blackening on the heaters when we turned them on in the extreme environments. However one of the adhesives, the transfer tape, seemed to survive the best over the course of thermal cycling, and so it has been chosen to attach the heaters to the BBM.

RAL Space

Limitations of model

- Temperature of helium
- Perpendicular conduction modelled only
- No account for possible convection
- Gas gap modelled O(1mm) much larger than conventional gas gaps
- Larger surface area than a conventional gas gap heat switch
- Curved surface

That was one way I've tried to make sure the model and the reality will be as similar as possible. However the main area of uncertainty here will be the helium conduction. There are limitations on the analysis that I have performed, and the equation that I have used to do the initial calculations.

As I'm not modelling the helium gas as nodes in the GMM, I have no way of knowing what the temperature of the gas really is inside the gap. I can make an educated guess on the temperature, and I know that it will be in the range of 77 K and the temperatures reached at the heaters, but I don't know for sure. The temperature will affect the conductivity and I expect this to be a reason for inconsistency with the breadboard model and my predictions at the lower temperatures.

The equation I've used only accounts for the perpendicular conduction across the gap, which is fair enough given that most gas gap heat switches use gaps smaller than a millimetre and don't really need to take anything else into account.

However I've scaled this equation up, and so don't know if the fact that the gap is over a very large and curved surface area will affect its validity. I am optimistic that the breadboard model testing will show that the design works though, as the HIRDLS blackbody targets were successful.

I am looking forward to investigating the results of the tests and correlating my model, not only to progress with the design of these blackbodies, but to further the understanding of how scaled up gas gap heat switches can be used for precise thermal control.


Thank you
Nicole Melzack, RAL Space, STFC
Email: Nicole.Melzack@stfc.ac.uk
Tel: +441235 567147
European Space Thermal Analysis Workshop
3-4th November 2015
RAL Space
Science & Technology Facilities Council

Appendix E

Development of methodologies for Brightness Temperature evaluation for the MetOp-SG MWI radiometer

Alberto Franzoso
(CGS, Italy)

Sylvain Vey
(ESA/ESTEC, The Netherlands)

Abstract

The MicroWave Instrument (MWI) is a conical scanning radiometer, which shall be embarked on MetOp Second Generation satellite. MWI will provide precipitation monitoring as well as sea ice extent information. It is now entering the detailed design phase.

Conical scanning radiometers are characterized by a continuous instrument calibration, with the sensors passing, at every rotation, below two calibration sources: a cold sky reflector providing 3K reference, and an On Board Calibration Target (OBCT) which provides an Hot temperature reference.

The high performance required to the instrument implies that the OBCT temperature is known with high accuracy, and that the gradients along its surface are suppressed. However, gradients are intrinsic to the structure of the OBCT, and driven by the day-night induced temperature cycles of its environment. Gradients can therefore only be minimized through a very extensive use of active control on the OBCT thermal environment.

The development of a Brightness Temperature computation method, i.e. the computation of the temperature sensed by the radiometer in the RadioFrequency (RF) band, was therefore a necessary step for the instrument thermal control optimization. It allowed to assign the limited instrument resources in the most efficient way, and to justify the design solutions.

In this presentation the details of the Brightness Temperature (BT) computation are provided. The OBCT temperature maps are generated by Thermica 4.6.1 using its fast-spin feature and are then post-processed with MatLab, filtering them with the Feed Horns Patterns. This results in the BT profiles along the orbit, with their associated errors. The method is then extended to the *High Frequency* analysis in order to assess the influence of each position of the rotation cycle on the BT. Results are shown, demonstrating that a passive thermal control is suitable to meet the strict performance requirements.

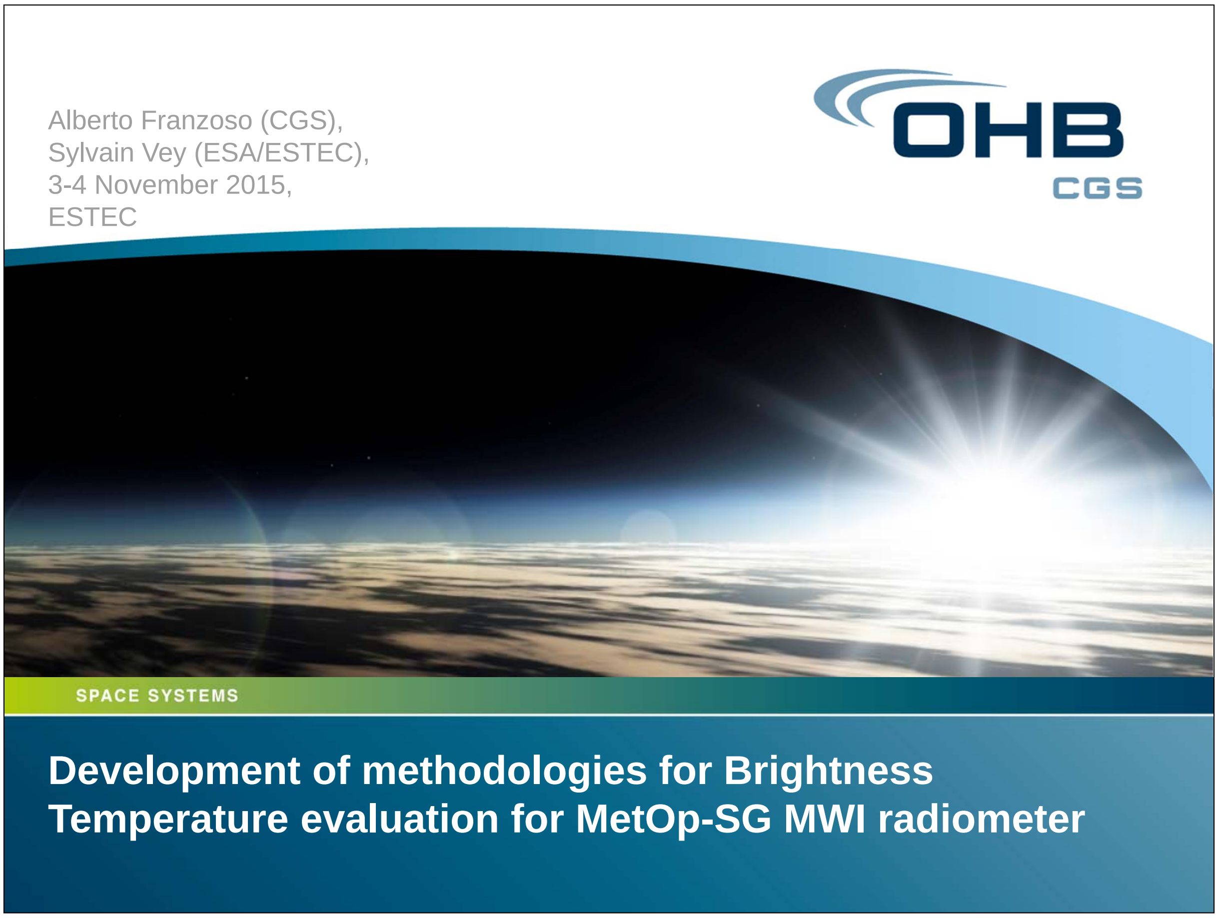
Alberto Franzoso (CGS),
Sylvain Vey (ESA/ESTEC),
3-4 November 2015,
ESTEC
OHB
CGS
SPACE SYSTEMS
Development of methodologies for Brightness Temperature evaluation for MetOp-SG MWI radiometer

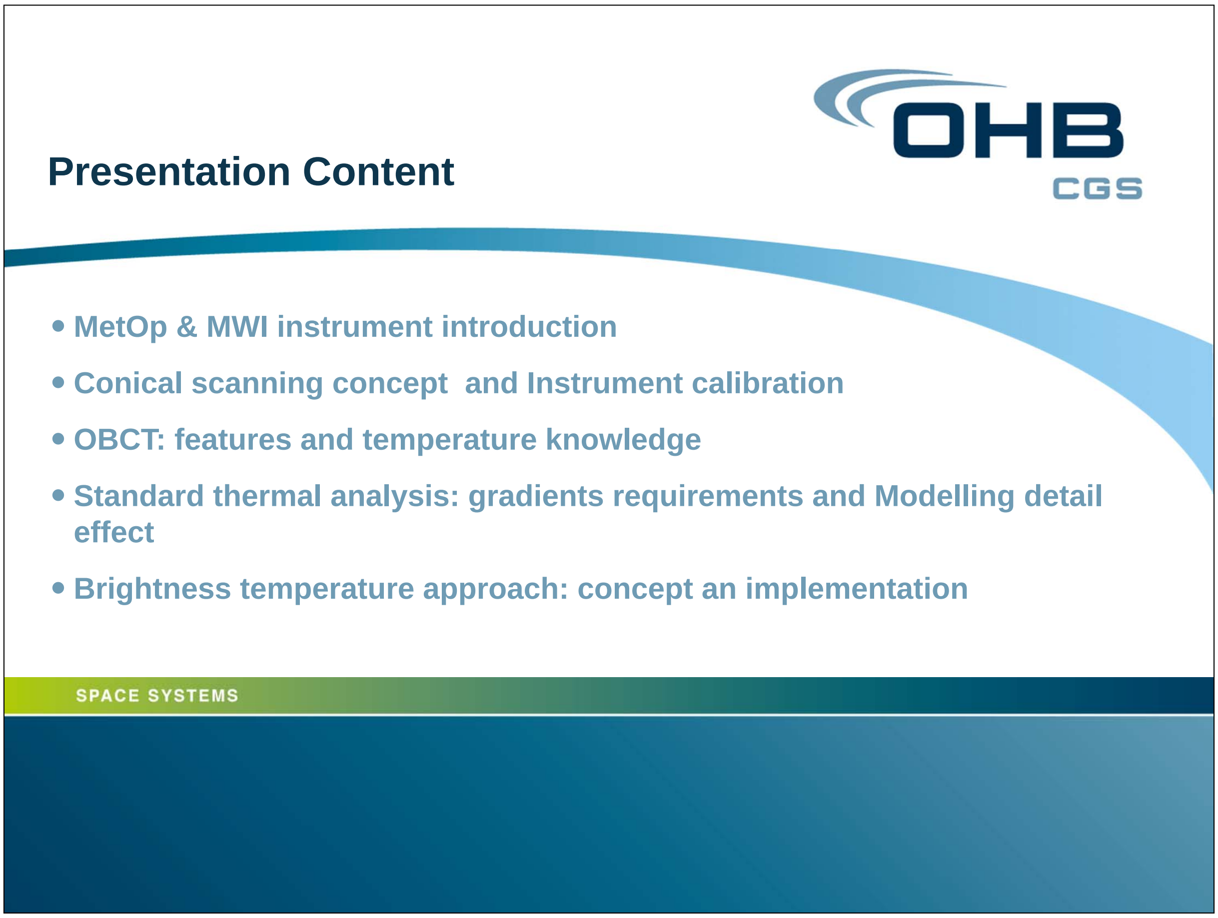
Presentation Content
OHB
CGS
• MetOp & MWI instrument introduction
• Conical scanning concept and Instrument calibration
• OBCT: features and temperature knowledge
• Standard thermal analysis: gradients requirements and Modelling detail effect
• Brightness temperature approach: concept an implementation
SPACE SYSTEMS

MWI instrument introduction

OHB CGS

METOP Second Generation overview

- MetOp-Second Generation: follow-on system to the 1st gen. series of MetOp (**Met**eorological **Op**erational) satellites, which currently provide operational meteorological observations from polar orbit.
- To provide operational observations and measurements from polar orbit for numerical weather prediction and climate monitoring in the early 2020's to mid-2040's timeframe.
- To provide services to atmospheric chemistry, operational oceanography and hydrology.
- With respect to First Generation:
  - To ensure continuity
  - to improve the accuracy / resolution of the measurements;
  - to add new measurements / missions.

CGS S.p.A. / Title of the presentation / Date — Seite 3

OHB CGS

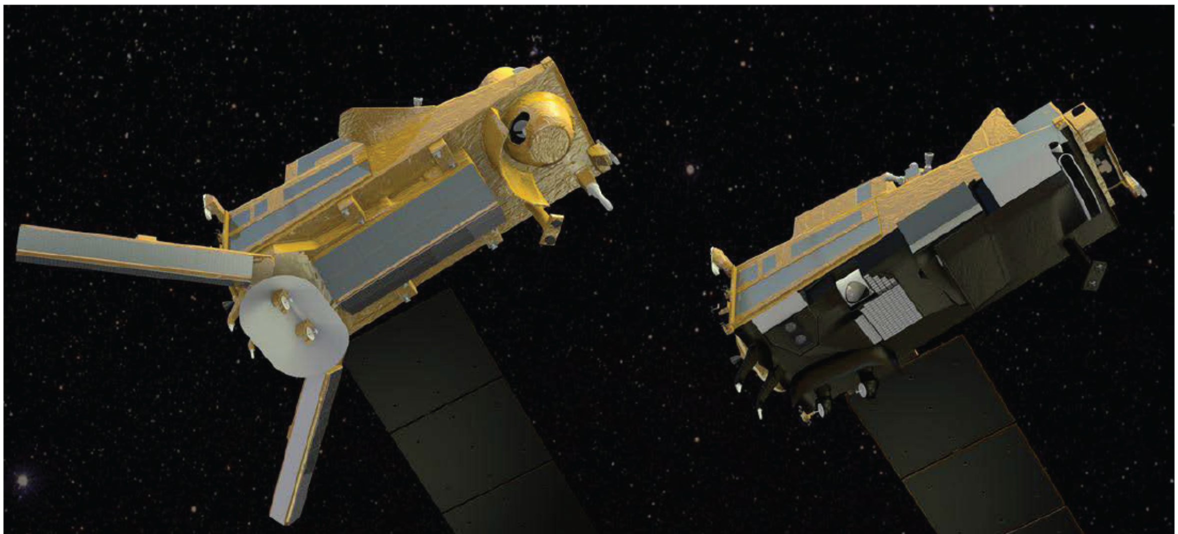

- Launch mass = **3.93** tons
- Mean power consumption in operation = **2.5** kW
- Data rate = day / night / peak
  15 / 15 / 19 Mbps

- Launch mass = 4,22 tons
- Mean power consumption in operation = **3.2** kW
- Data rate = day / night / peak
  64 / **25** / **85** Mbps

- Launcher: Soyuz in Kourou / Falcon 9 / Ariane 5 / **Ariane 6**
- Orbit: MetOp Sun Synchronous Orbit **835 km mean altitude**, 9h30 Local Time at Descending Node
- Controlled re-entry into the South Pacific Ocean Uninhabited Area

CGS S.p.A. / MWI OBCT Brightness Temperature Computation/ November 2015 — Seite 4

OHB CGS

MWI instrument overview

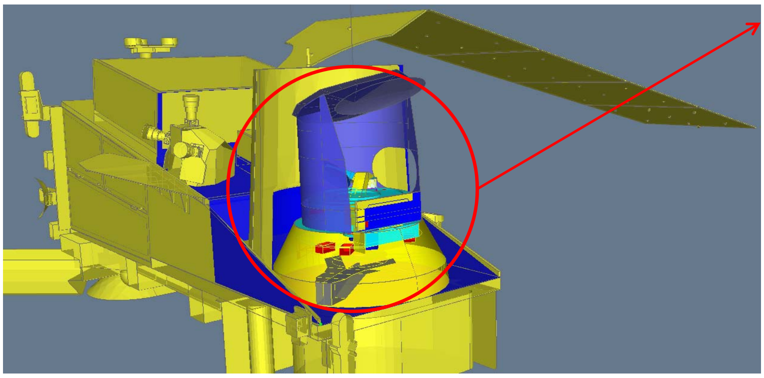

MicroWave Imager:

- Conical scanning radiometer
- Cloud and precipitation, snow and sea-ice, profiles of water vapor and temperatures
- Collects MW radiation from Earth and atmosphere
- Frequency range of 18.7GHz to 183.3GHz
- Constant speed rotation at 45rpm

CGS S.p.A. / MWI OBCT Brightness Temperature Computation/ November 2015 Seite 5

OHB CGS

MWI instrument introduction

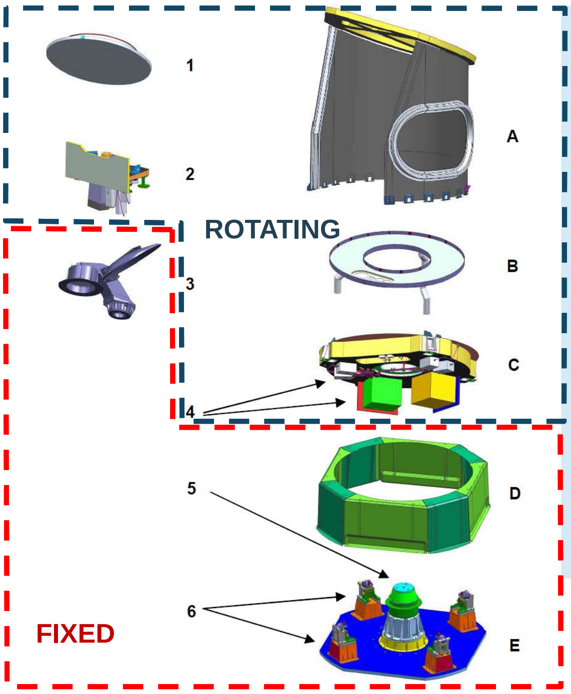

A	Tube Structure (Rotating Part)	
B	Racetrack (Rotating Part)	
C	Rotating Deck (Rotating Part)	
D	Thermal Skirt (Fixed Part)	
E	Baseplate (Fixed Part)	
1	Main Reflector (Rotating Part)	
2	Front End Sub-Assembly (Rotating Part)	
3	Calibration Assembly (Fixed Part)	
4	Low Frequency Equipment, FEE and CDPU (Rotating Part)	
5	Scan Mechanism (Joint between Rotating and Fixed Part)	
6	Launch Locking Devices (Fixed Part)	

CGS S.p.A. / MWI OBCT Brightness Temperature Computation/ November 2015 Seite 6

MWI instrument introduction

Instrument Calibration

- Calibration principle based on linearity of receiver chain.
- Linear interpolation used to calculate the scene brightness temperature from 2 known reference temperatures
  - Cold Sky Target, i.e. calibration reflector @ 3K
  - On Board Calibration Target (OBCT): hot RF source at known temperature
- The antenna rotation (45 RPM) creates observation cycles
- Necessity of accurate knowledge of OBCT temperature

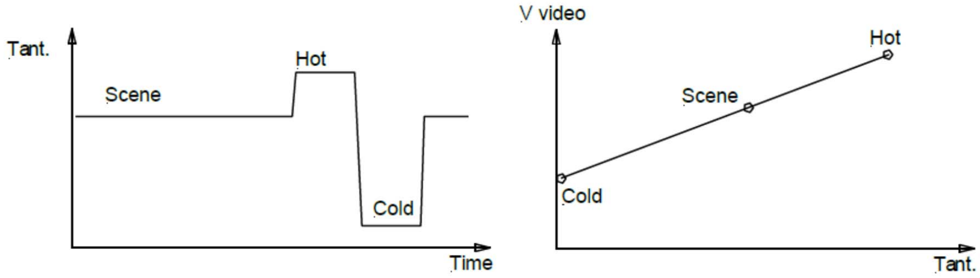

CGS S.p.A. / MWI OBCT Brightness Temperature Computation/ November 2015 Seite 7

OBCT

OBCT structure

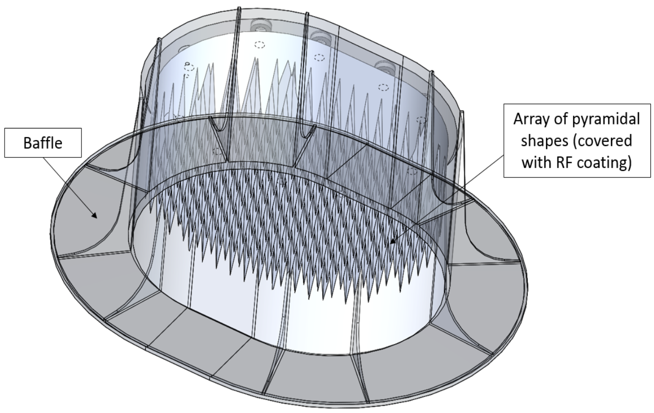

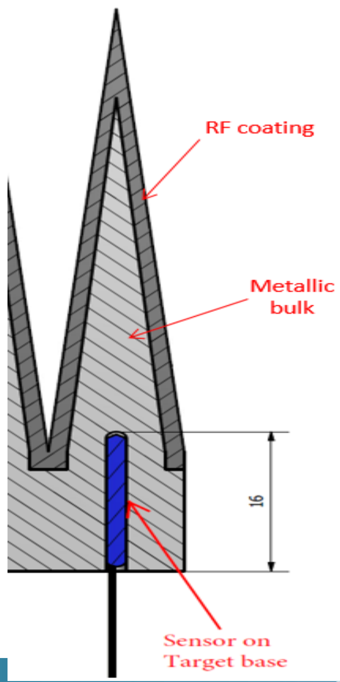

- Regular pyramidal pattern to have a RF perfect absorber (-40dB return loss)
- ECCOSORB RF coating
- Baffling system for protection from environment

CGS S.p.A. / MWI OBCT Brightness Temperature Computation/ November 2015 Seite 8

OHB CGS

OBCT requirements

- First Issue:
  - Derived from initial system level error apportionment
  - Attempt to translate the temperature knowledge accuracy into gradients & stability requirements

OBCT specific requirements (operational cases)		
Quantity	**Required value**	**Notes/remarks**
OP temperature variation over one orbit	< 5°C	
OP temperature variation over lifetime	n.a.	
Surface temperature variation over one orbit	< 0.1°C/s	
Nominal gradient across the surface	< 0.35 °C	
Gradient variation across the surface over one orbit	< 0.25°C	
Gradient variation across the surface over one rotation	< 0.1°C/s	
Surface temperature knowledge	0.15°C	applicable to measurement chain overall accuracy, and considering gradient uncertainty from thermal model

CGS S.p.A. / MWI OBCT Brightness Temperature Computation/ November 2015 Seite 9

OBCT Standard Thermal Analysis

OHB CGS

OBCT environment

- Sun Intrusion: avoid direct and reflected Solar Fluxes on Pyramids (local hot spots)
  - Solutions: “Racetrack” baffling system
- Orbital oscillation of environment
  - Variable sink temperatures
  - Massive base is stable
  - Lighter peaks have wider oscillation
- Result: typical gradient along pyramids, in top-bottom direction

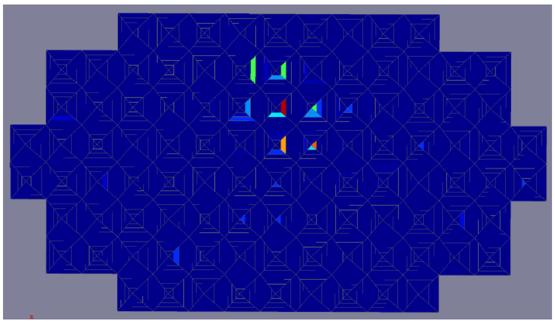

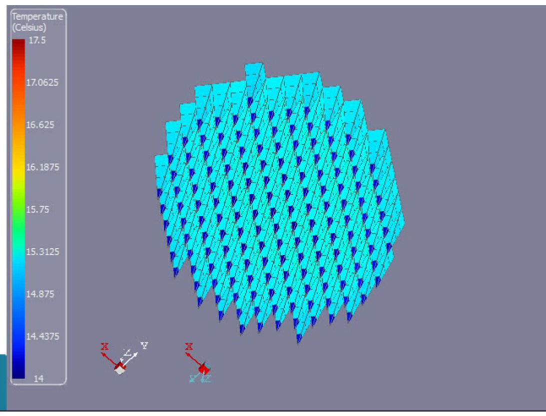

CGS S.p.A. / MWI OBCT Brightness Temperature Computation/ November 2015

Stadard Thermal Analysis

Model detail level and gradients

- Step 0: Initial Phase A model: 4 pyramid layers,
  - 1 node for bulk
  - 1 node for epoxy layer, with mass
- Step 1: Final Phase A model:
  - 1 node for bulk
  - 1 node with Cp for epoxy core
  - 1 node, massless, for epoxy surface
- Step 2: Phase B1 model:
  - 1 node for bulk
  - 4 nodes for each side, with Cp for epoxy core
  - 4 nodes for each side, massless, for epoxy surface
- Gradient estimation: ~0.15-0.3K (COMPLIANT)
- OBCT: for final OBCT ~4000 nodes

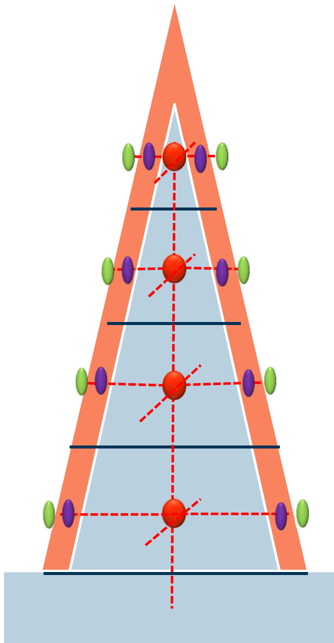

CGS S.p.A. / MWI OBCT Brightness Temperature Computation/ November 2015 Seite 11

- Step 3: Phase B2 model:
  - Tip area with NO aluminum core
  - Base area with discontinuity (epoxy)

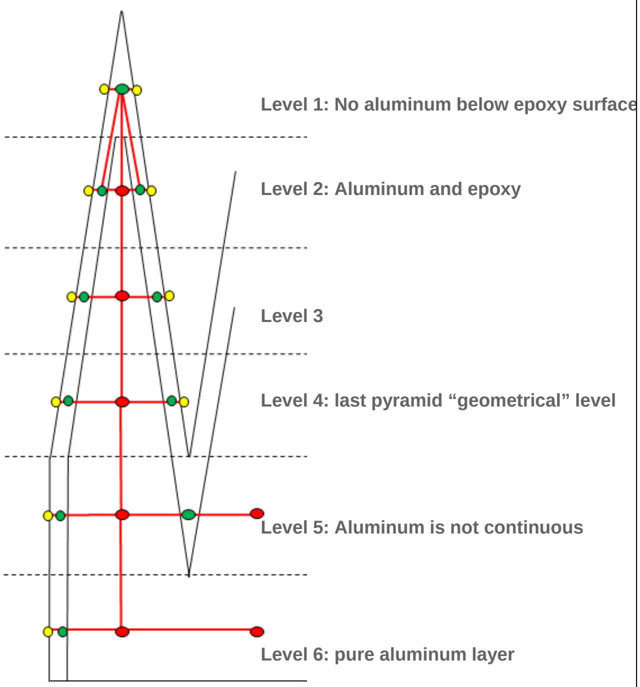

CGS S.p.A. / MWI OBCT Brightness Temperature Computation/ November 2015 Seite 12

- Gradient over OBCT surface,
  - from step 2 (blue)
  - to step 3 (red):

effect of model detail

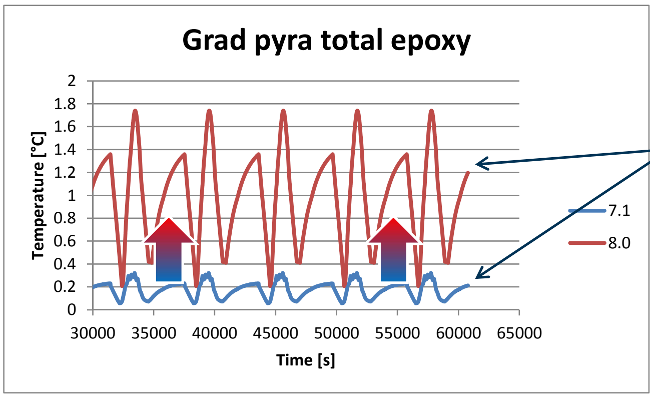

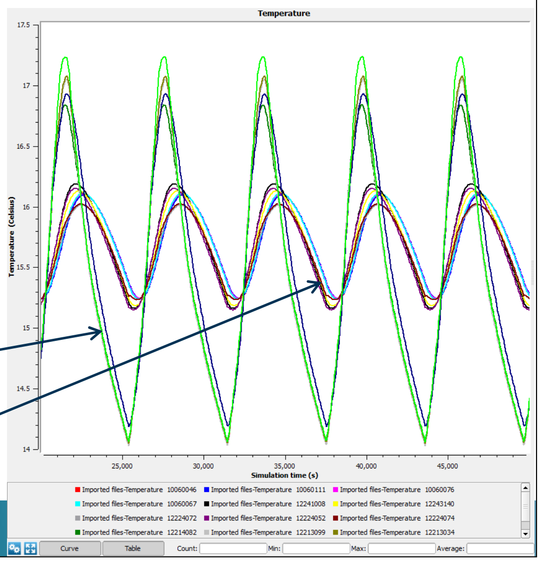

- Temperature orbital oscillations:
  - Level 1 (tips)
  - Levels 2 to 6 (all other nodes)

CGS S.p.A. / MWI OBCT Brightness Temperature Computation/
November 2015

- The tips, once modelled in a more realistic way, amplify the already known «tip-bottom» gradient by about one order of magnitude.
- Gradients have a very regular pattern (no local hot spots), all tips are typically at the same temperature with a dispersion of ~0.5K
- Requirements are far from being respected in the current configuration
- Corrective actions to reduce (but not realistically a by factor 10) the gradients are:
  - […] (long list of unfeasible options for other system constraints)
  - Racetrack **active heater control** to damp its oscillations
    - ROM estimation: ~200W heater (150% of entire instrument budget)
- Alternative: coupled RF&Thermal analysis
  - temperature maps post-processing to verify brightness temperature, the *real* quantity of interest
  - To investigate the effect of the «Shape» of the gradient pattern, not only its max value

OBCT brightness temperature,
detected by each feed horn,
in any operational condition,
shall not deviate from the PRT temperatures
by more than ±0.25K

CGS S.p.A. / MWI OBCT Brightness Temperature Computation/
November 2015

Seite 14

NEW ANALYTICAL APPROACHES

OHB CGS

- At the core of the approach there is the consideration that each feed horn is actually «filtering» the pyramids temperature, combining them in a unique «Brightness Temperature» (BT) reading.
- This is achieved through a kind of weighted average of the physical temperatures
- The real meaningful information, important to assess the performance of the instrument, is not really the gradient along the surface, but the difference between the PRT temperature and the BT acquired by the horns
- In this sense, NOT ALL THE GRADIENTS are equivalent; a periodic gradient is much less harmful than a uniform gradient, because the horn is a low-pass filter.

High level Logic flow:

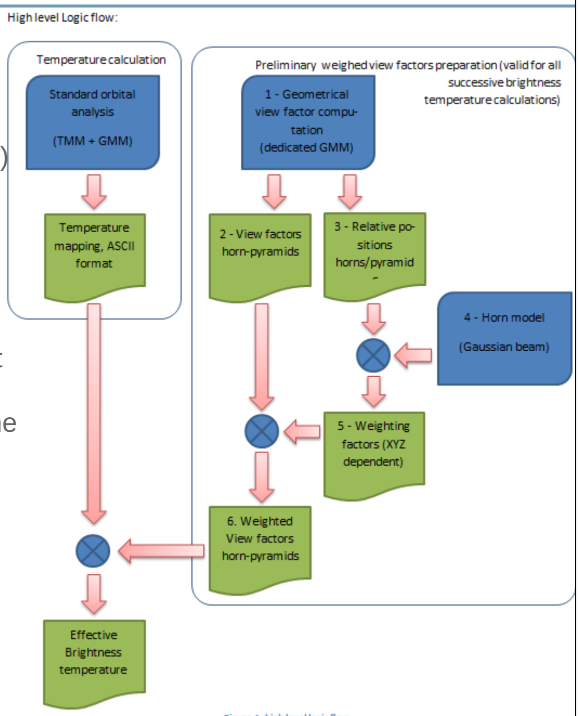

Figure 1: high level logic flow

CGS S.p.A. / MWI OBCT Brightness Temperature Computation/ November 2015

Seite 15

NEW ANALYTICAL APPROACHES

OHB CGS

- A Gaussian horn beam is considered, according to ADS-Tolouse inputs (responsible of Radiofrequency Assembly)
  - Different for each of the 7 horns;
  - Function of r, z
- The beam is the weighting factor for the physical temperatures

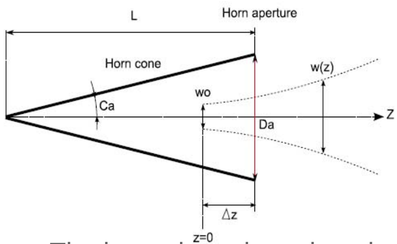

$$E(r) = Eo\exp\left(\frac{r^2}{w(z)^2}\right)$$

$$w(z) = wo\sqrt{1+\left(\frac{z}{zr}\right)^2}$$ With

$$zr = \pi\frac{wo^2}{\lambda} \quad and \quad wo = 0.29\,Da$$

$$\Delta z = \frac{L}{1+\left(\frac{\lambda L}{\pi wo^2}\right)^2}$$

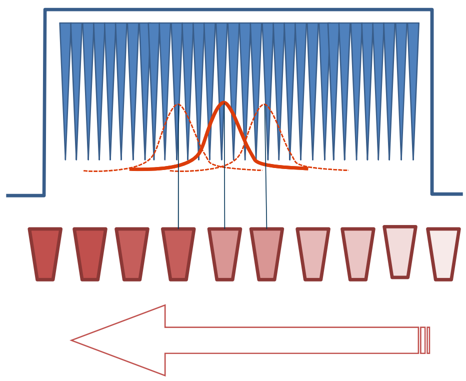

- The beam is projected on the pyramids, at several different instrument rotation angles, weighting it to its view factor to the horn
- Per each rotation angle, each pyramid surface element is weighted in a different way
- Per each angle (and per each horn) the BT is calculated
- The BT is compared to the PRT temperatures
- The difference is the error contribution to the BT evaluation

CGS S.p.A. / MWI OBCT Brightness Temperature Computation/ November 2015

Seite 16

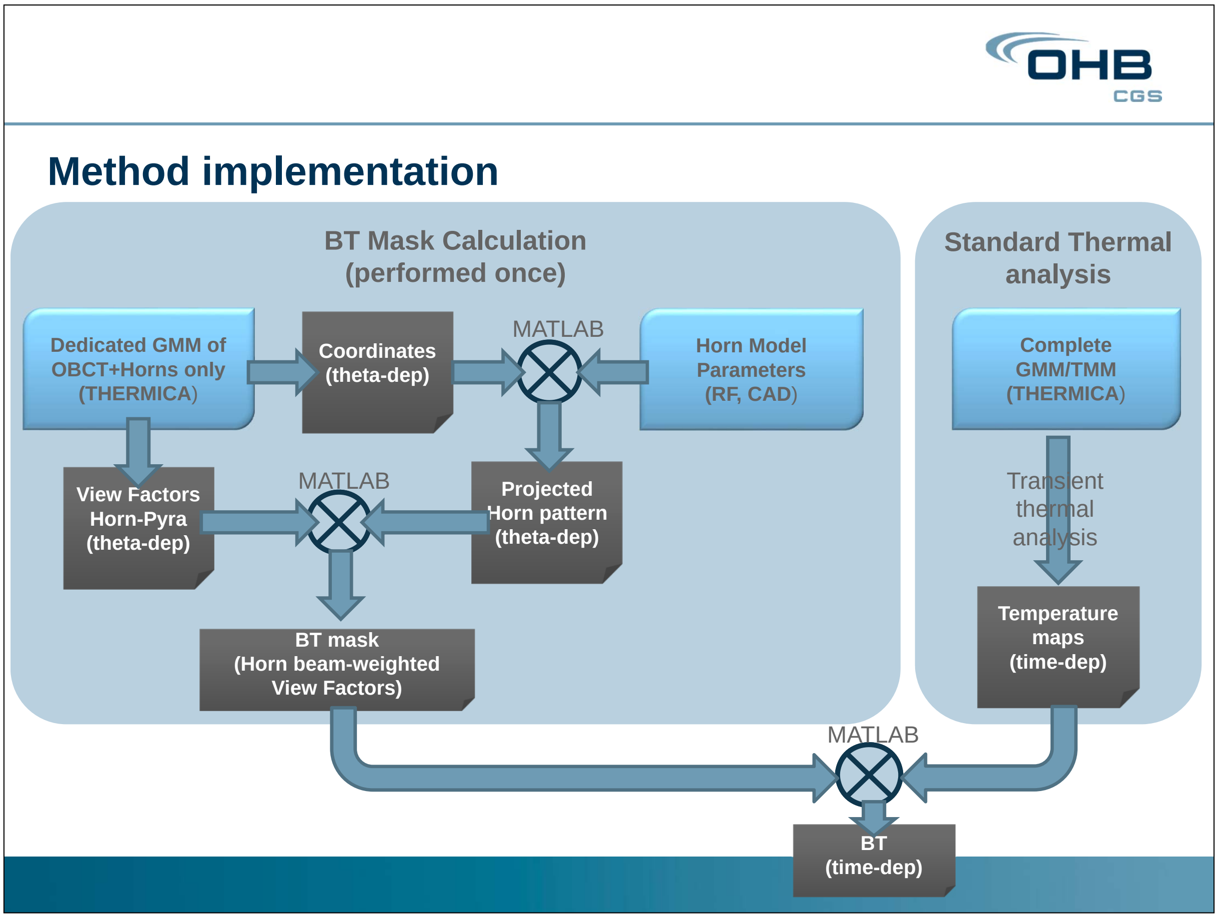
Method implementation
BT Mask Calculation
(performed once)
Standard Thermal analysis
Dedicated GMM of OBCT+Horns only (THERMICA)
Coordinates (theta-dep)
MATLAB
Horn Model Parameters (RF, CAD)
Complete GMM/TMM (THERMICA)
View Factors Horn-Pyra (theta-dep)
MATLAB
Projected Horn pattern (theta-dep)
Transient thermal analysis
Temperature maps (time-dep)
BT mask (Horn beam-weighted View Factors)
MATLAB
BT (time-dep)

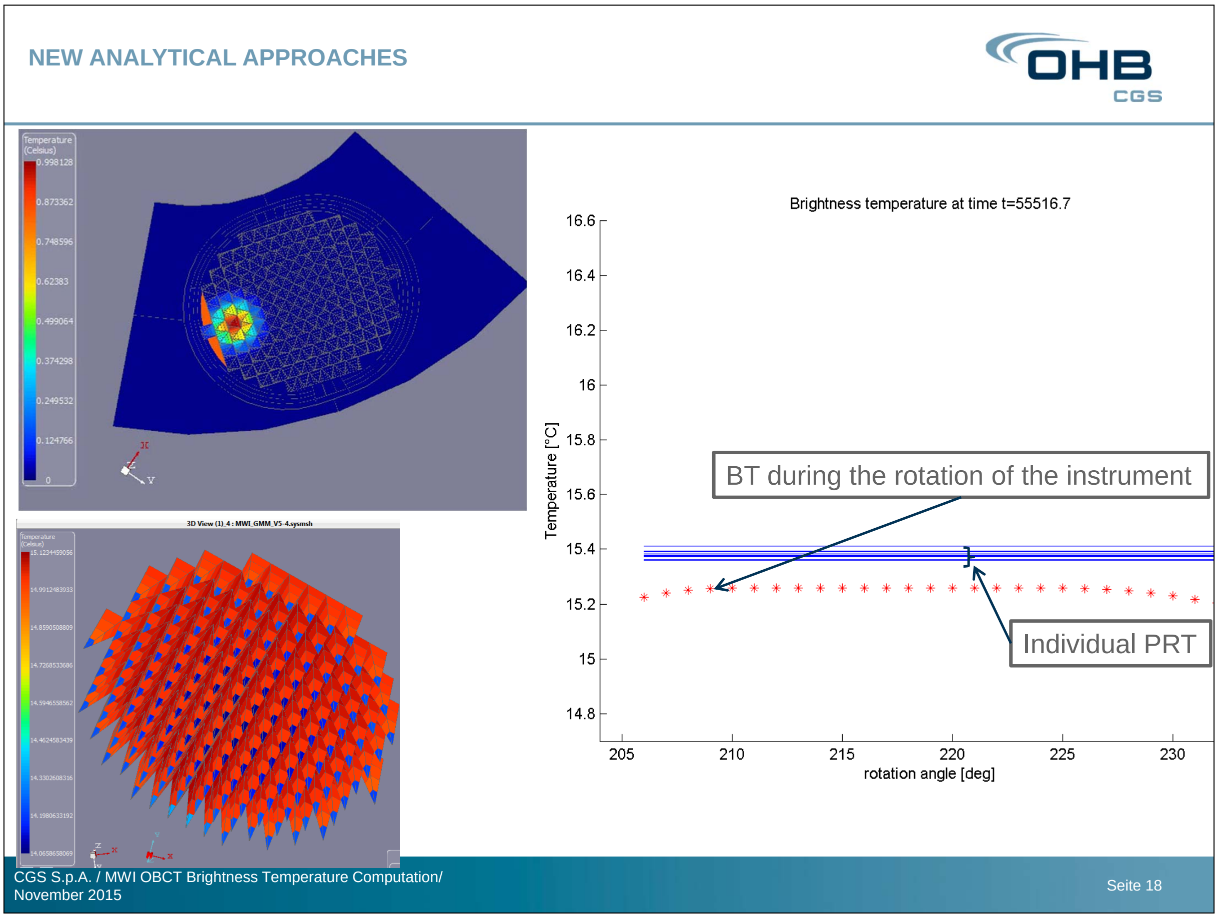
NEW ANALYTICAL APPROACHES
Brightness temperature at time t=55516.7
Temperature [°C]
rotation angle [deg]
BT during the rotation of the instrument
Individual PRT
CGS S.p.A. / MWI OBCT Brightness Temperature Computation/
November 2015
Seite 18

NEW ANALYTICAL APPROACHES

OHB CGS

- The BT evaluation is performed at each orbital position of standard thermal analysis.
- A profile of the ERROR PRT--BT is available in function of orbital time
- The profile is typically presented as the profile of the Average ERROR value + standard deviation band.
  - Average error over the central area of the feed horn path below the OBCT (typically, 5° wide)
  - Standard deviation is the deviation of the error computed all over this 5° wide window (typically, with a step of 1°)

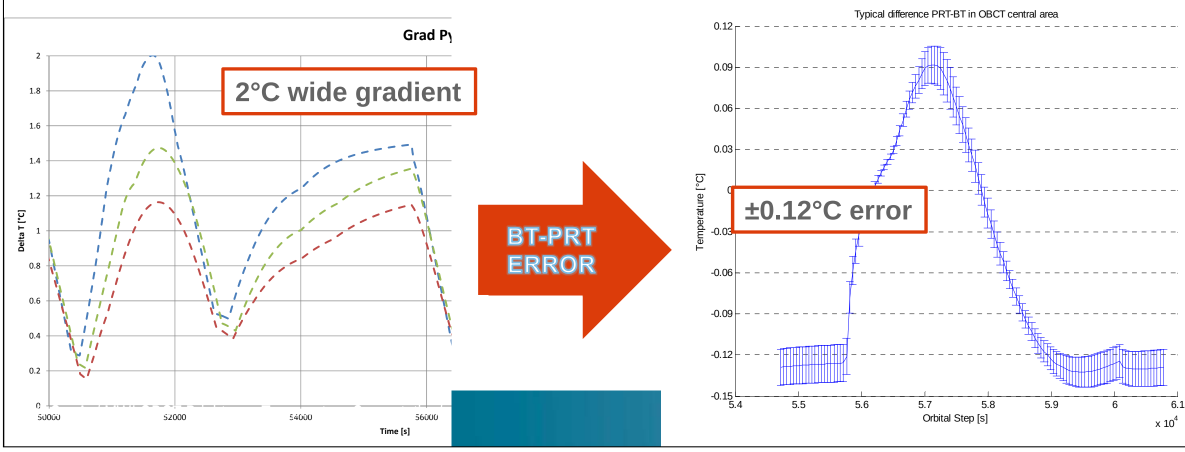

Conclusions

OHB CGS

- Generic Temperature Gradient requirements results are often dependent on Model Detail
- In case of MWI OBCT, gradient requirement could no longer be met, unless a big amount of resources are assigned to thermal control
- A re-discussion of requirements was needed (should be a general good practice)
- A joint RF-thermal analysis was carried, developing routines to compute the Brightness Temperature profiles along the orbit and comparing to the PRT readings
- Analysis allowed to demonstrate that the proposed design was compatible with performance targets
- Method allowed to refine thermal control system and to correctly assign the instrument resources

CGS S.p.A. / MWI OBCT Brightness Temperature Computation/
November 2015

Seite 20

Appendix F

MASCOT thermal design
how to deal with late and critical changes

Luca Celotti   Małgorzata Sołyga
(Active Space Technologies GmbH, Germany)

Volodymyr Baturkin   Kaname Sasaki   Christian Ziach
(DLR, Germany)

Abstract

MASCOT is a lander built by DLR, embarqued on JAXA's Hayabusa-2, a scientific mission to study the asteroid 162173 1999 JU3, launched on the 3rd of December 2014. As part of the project challenges, the short schedule for the whole development of the lander (2.5 years from PDR to launch), the strict and contrasting thermal requirements for different phases of the mission, mass&power/technology/volume limitations put the thermal design at the edge of the state of art technology solutions. As a result, the thermal system development has been on-going until the last phases of the project, on order to cope with late changes and technologies development.

This presentation focusses on the thermal control system evolution during the last months before launch and just after it and the tight schedule available to cope with late system changes. It shows the design modifications and updates, together with thermal modelling changes following intensive testing phases, in particular for the lander battery pack and the heating/pre-heating strategy for different mission phases. Many thermal vacuum campaigns, modelling re-iterations, better understanding of the main S/C thermal behaviour, together with the great team determination helped reaching a succesfull launch followed by an on-flight system verification.


MASCOT thermal design: how to deal with late and critical changes
activespace technologies
Luca Celotti
November, 3-4 2015
ESTEC, Nordwijk - The Netherlands
making space a global endeavour
activespace technologies
Luca Celotti, Małgorzata Sołyga
ActiveSpace Technologies GmbH
DLR
Volodymyr Baturkin, Kaname Sasaki, Christian Ziach
DLR Institut für Raumfahrsysteme
Explorationssysteme RY-ES

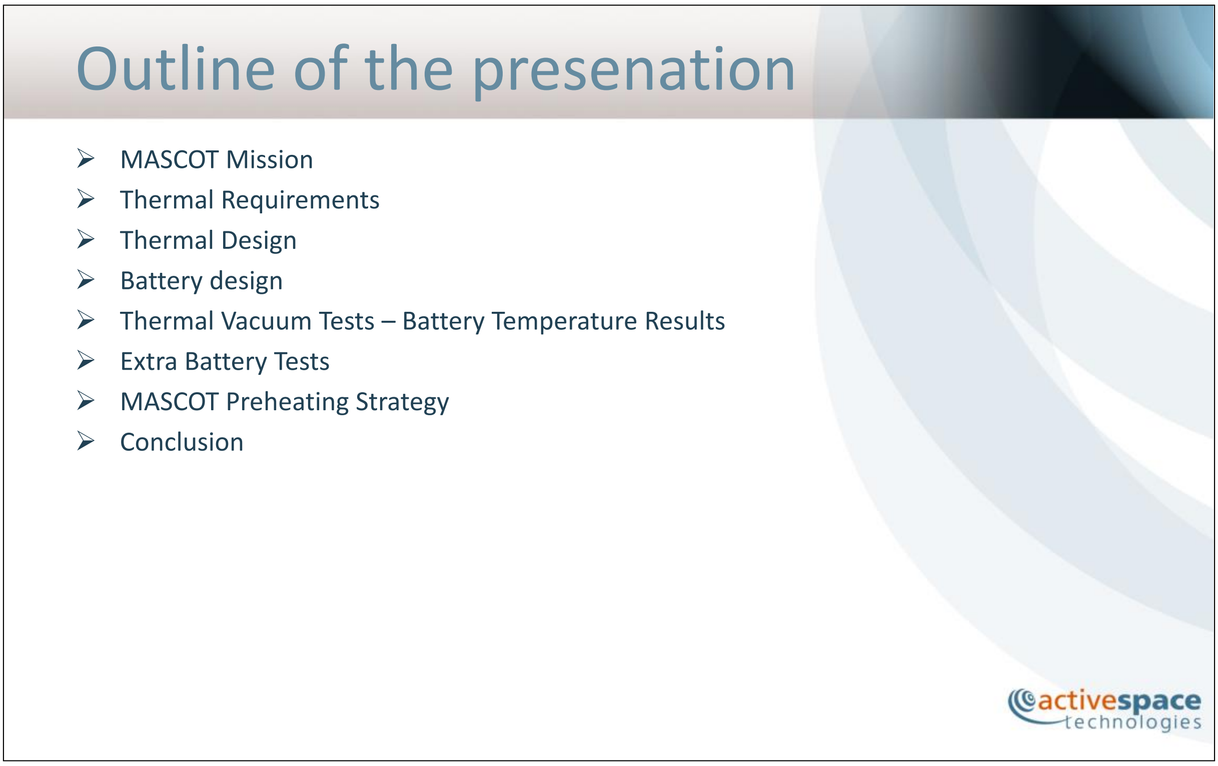
Outline of the presenation
MASCOT Mission
Thermal Requirements
Thermal Design
Battery design
Thermal Vacuum Tests – Battery Temperature Results
Extra Battery Tests
MASCOT Preheating Strategy
Conclusion
activespace technologies

MASCOT Misison

MASCOT (Mobile Asteroid surface SCOuT)

- A lander built by DLR (in collaboration with CNES)
- On-board JAXA's Hayabusa-2 mission, a scientific mission to study the asteroid "Ryugu" (former 162173 1999 JU3)
- Smaller than 300x300x200mm³
- Carries 4 payloads for scientific investigation of the asteroid surface:
  - IR spectrometer (mOmega)
  - Camera
  - Magnetometer
  - Radiometer
- Will be released by the mothership and "fall" on the asteroid surface

Courtesy of DLR

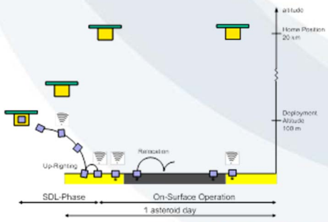

Courtesy of DLR

Thermal requirements

The thermal requirements MASCOT must satisfy and the environment in which it will operate vary significantly, depending on the mission phase:

- Cruise Phase: MASCOT is attached to HY-2 on its way to the asteroid

→ In this phase, the lander should limit as much as possible the heat exchange with the S/C and with the environment

- Near-Asteroid Phase: MASCOT is still attached to HY-2, which is hovering above the asteroid
- On-Asteroid Phase: In this Phase MASCOT is performing its operations on the asteroid surface (after free-fall phase)

→ In those two phases, the lander should reject as much heat as possible in order not to reach maximum operational temperature limits.

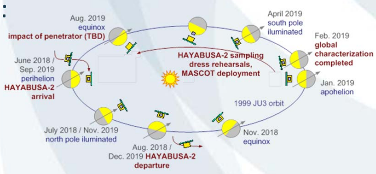

Courtesy of DLR

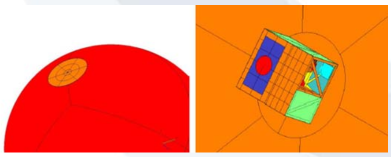

Thermal design

The design should fulfill the contrasting requirements during different mission phases and it should insulate MASCOT from HY-2 as much as possible and be passive (due to the limited power provided by HY-2).

Thus, it was decided to use variable conductance heat transfer technology from the electronic box (the most dissipative element) to the radiator.

Heating power available is going to be distributed to the most critical parts (mOmega, EBOX, battery).

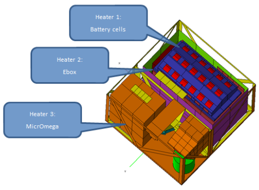

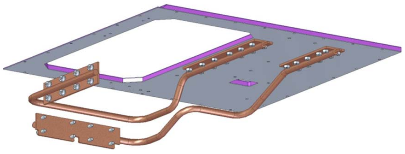

Courtesy of DLR

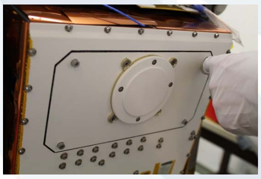

Courtesy of DLR

→ ***The heating strategy for the battery unit and its design has evolved during the whole project, making crucial parts of the thermal subsystem.***

activespace technologies

Battery design

The battery of MASCOT includes 9 cells. In order to keep these cells warm enough to operate (above -40°C), each cell is wrapped with a flexible heater.

The design was then modified and the heaters have been placed in elements between the cells. Before the heaters were wrapping each cell.

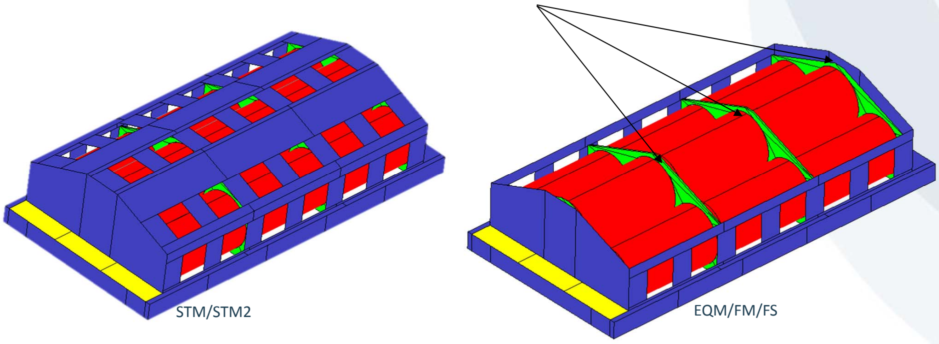

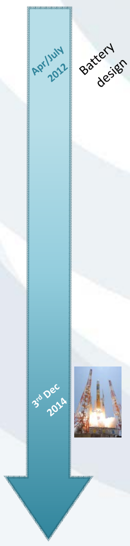

activespace technologies

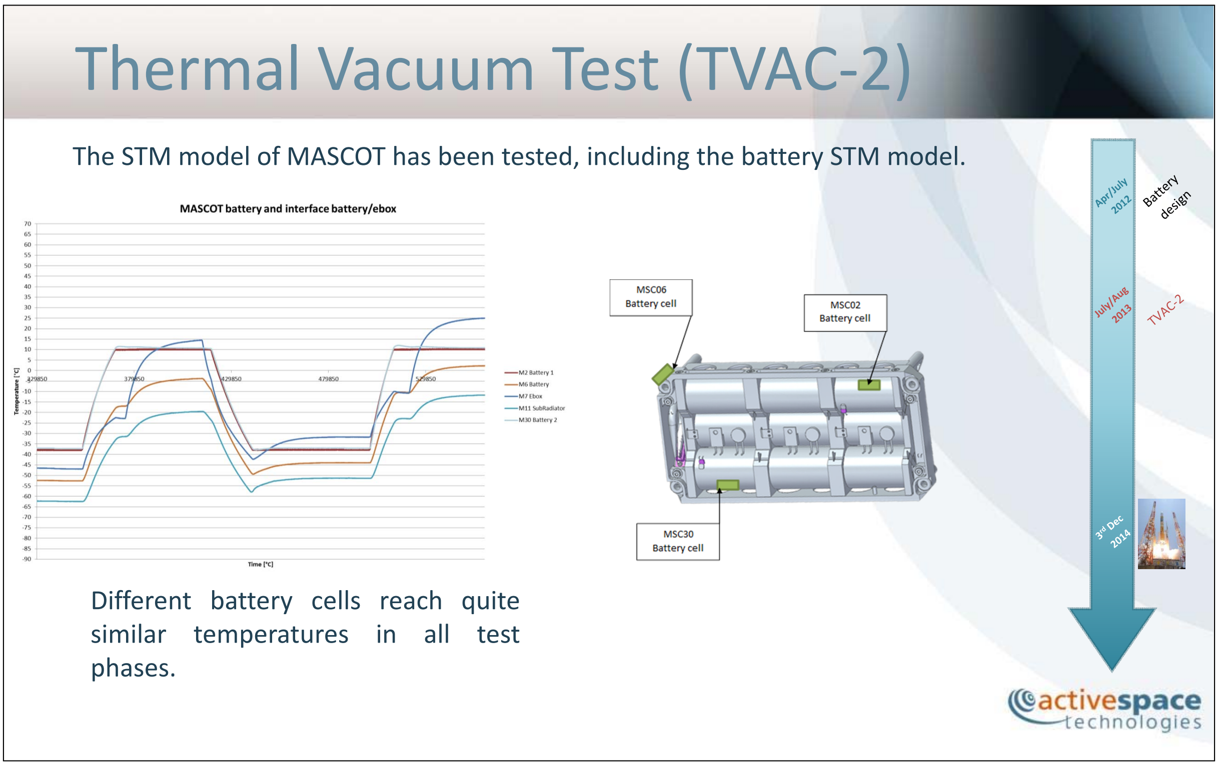
Thermal Vacuum Test (TVAC-2)
The STM model of MASCOT has been tested, including the battery STM model.
MASCOT battery and interface battery/ebox
Temperature [°C]
Time [°C]
M2 Battery 1
M6 Battery
M7 Ebox
M11 SubRadiator
M30 Battery 2
MSC06
Battery cell
MSC02
Battery cell
MSC30
Battery cell
Different battery cells reach quite similar temperatures in all test phases.
Apr/July 2012
Battery design
July/Aug 2013
TVAC-2
3rd Dec 2014
activespace technologies

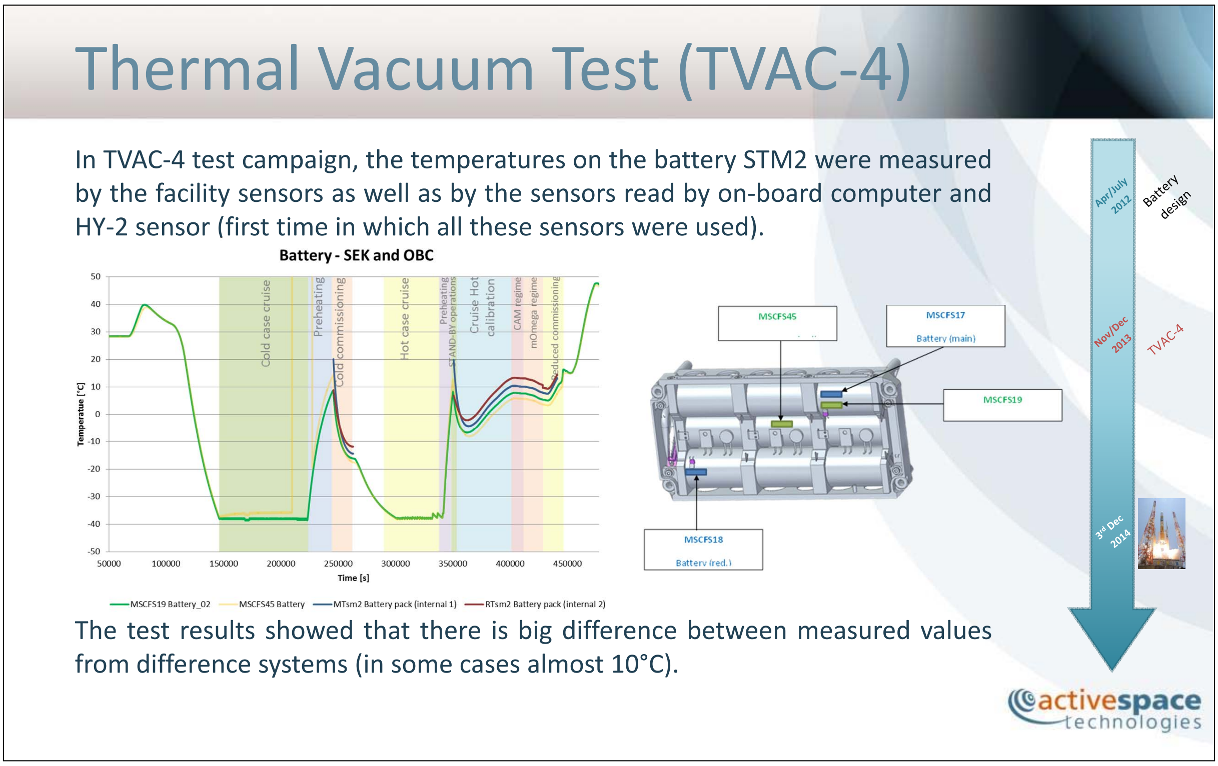
Thermal Vacuum Test (TVAC-4)
In TVAC-4 test campaign, the temperatures on the battery STM2 were measured by the facility sensors as well as by the sensors read by on-board computer and HY-2 sensor (first time in which all these sensors were used).
Battery - SEK and OBC
Temperatue [°C]
Time [s]
Cold case cruise
Preheating
Cold commissioning
Hot case cruise
Preheating
STAND-BY operations
Cruise Hot calibration
CAM regime
mOmega regime
Reduced commissioning
MSCFS19 Battery_02
MSCFS45 Battery
MTsm2 Battery pack (internal 1)
RTsm2 Battery pack (internal 2)
MSCFS45
MSCFS17
Battery (main)
MSCFS19
MSCFS18
Battery (red.)
The test results showed that there is big difference between measured values from difference systems (in some cases almost 10°C).
Apr/July 2012
Battery design
Nov/Dec 2013
TVAC-4
3rd Dec 2014
activespace technologies

Sensors calibration

After the test campaign (TVAC-4) an extra test has been performed by DLR in order to verify the measurements coming from different sensors on the battery STM2.

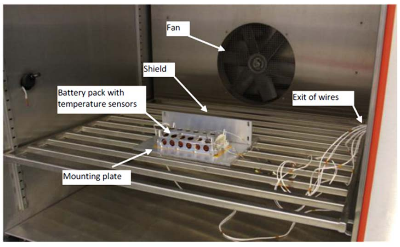

Courtesy of DLR

Temperature [°C]					
Climatic chamber Set up	Main HY PT2000	RET HY PT2000	Main OBC PT1000	RET OBC PT1000	SEK PT100 (average for 4 sensors)
-38.0	-38.50	-38.06	-35.46	-35.75	-38.19
0.0	-0.34	0.16	3.37	3.15	0.05
21.0	20.72	21.26	24.92	24.70	20.93
22.0	21.87	22.52	26.08	25.86	22.12
50.0	49.95	50.54	54.95	54.73	50.20

Temperature sensors (HY-2 and OBC) differences fixed via re-calibration and new temperature/resistance curves.

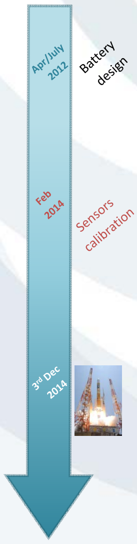

activespace technologies

Flight simulation test in JAXA

First use of battery EQM

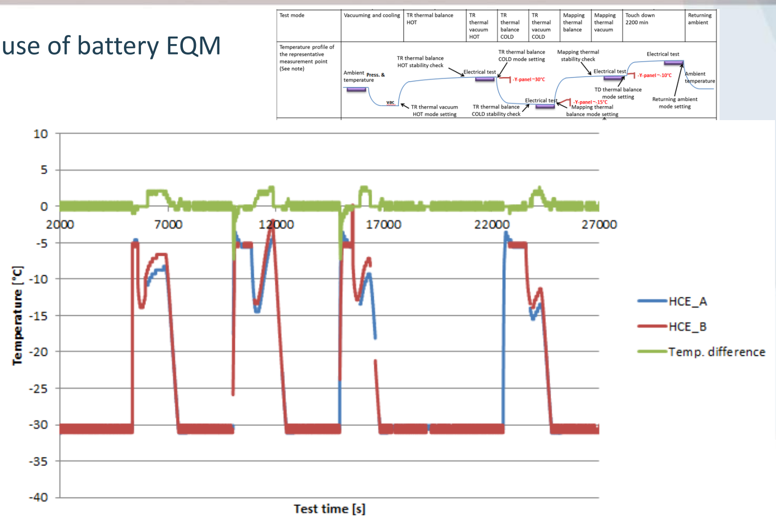

Regardless for the calibration fixed, temperature differences betwee the HY-2 sensors are present, moreover an anomalous long duration of pre-heating phases appeared.

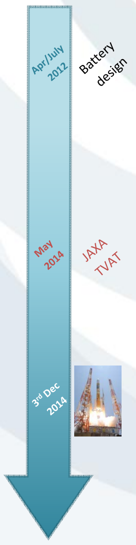

activespace technologies

Thermal Vacuum Test (TVAC-5)

In this test the FM of MASCOT has been tested with the FM model of the battery. During this test the big temperature difference between the cells have been noticed as well as a much longer preheating duration.

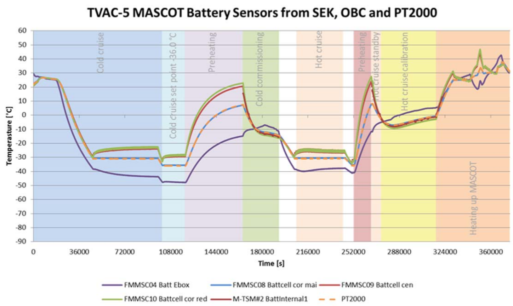

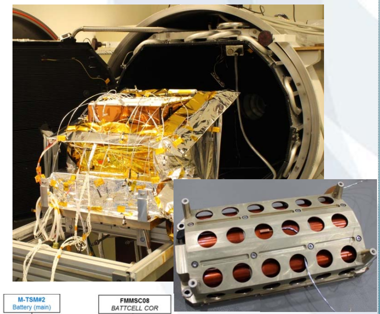

Courtesy of DLR/CNES/SAFT

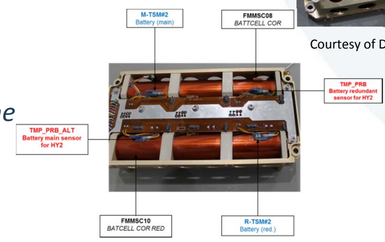

A clear HW issue is present, appearing in the EQM and FM, not present in the STMs.

Further investigations were necessary!

activespace technologies

Extra battery tests – FM IR test

- Deep evaluation of the design changes implemented by the battery supplier
- IR test perfomed on the FM by DLR to evaluate the heaters efficiency

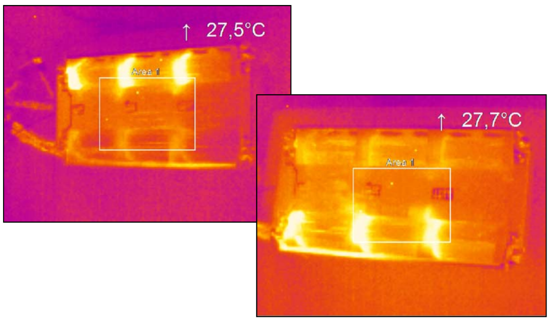

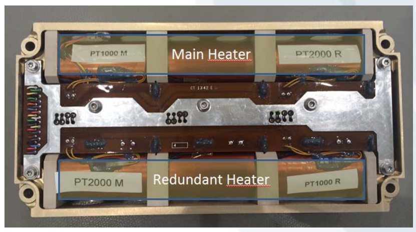

Courtesy of DLR/CNES/SAFT

The heaters and spreaders do not provide enough heating uniformity to the battery pack generating a longitudinal temperature difference.

The position of the temperature sensors controlling the heating lines generates a temperature difference along the cells.

activespace technologies

Extra battery tests – FM/FS test

Comparative heating test for FM and FS model has been performed. Test results showed that the thermal behaviour of both battery models is very similar.

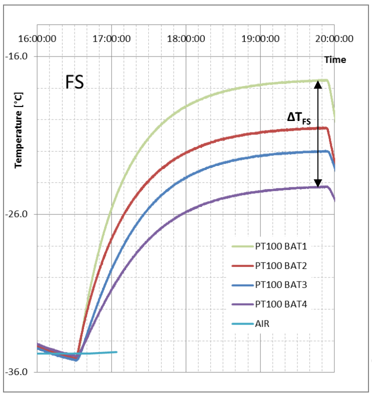

Courtesy of DLR

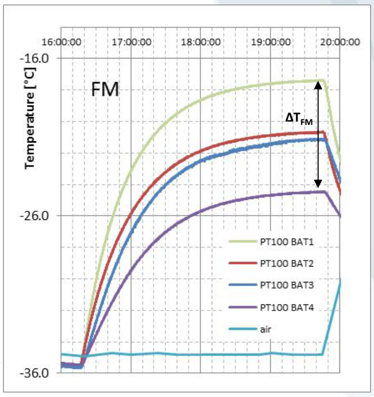

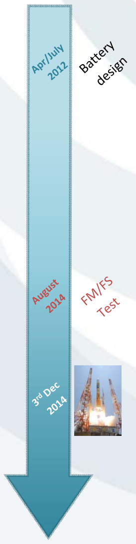

Battery FS is chosen for flight, while the FM unit will be used for testing in order to investigate the thermal behaviour of the current battery design.

EQM heaters positioning is confirmed equal to FM/FS and different from STMs by the supplier.

activespace technologies

Thermal Vacuum Test (TVAC-6)

In TVAC-6 test campaign the FS of MASCOT has been tested with the battery FM. The main objective of this test was better thermal characterisation of the battery (as the idea of a stnad-alone test of the battery was discarded due to difficulties in replicating similar boundary conditions) – due to this fact on the battery almost 30 temperature sensors have been mounted.

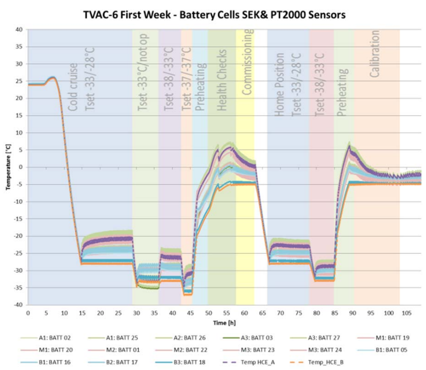

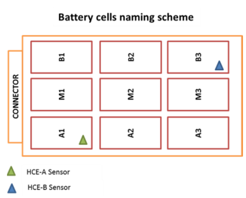

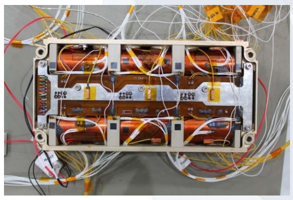

Courtesy of DLR/CNES/SAFT

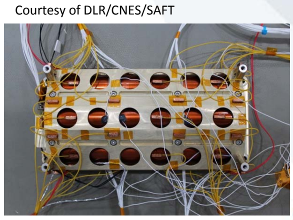

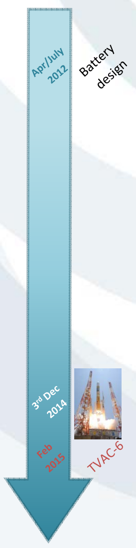

activespace technologies

Thermal Vacuum Test (TVAC-6)

After the test, correlation performed and battery thermal model updated to represent also the real hardware behaviour.

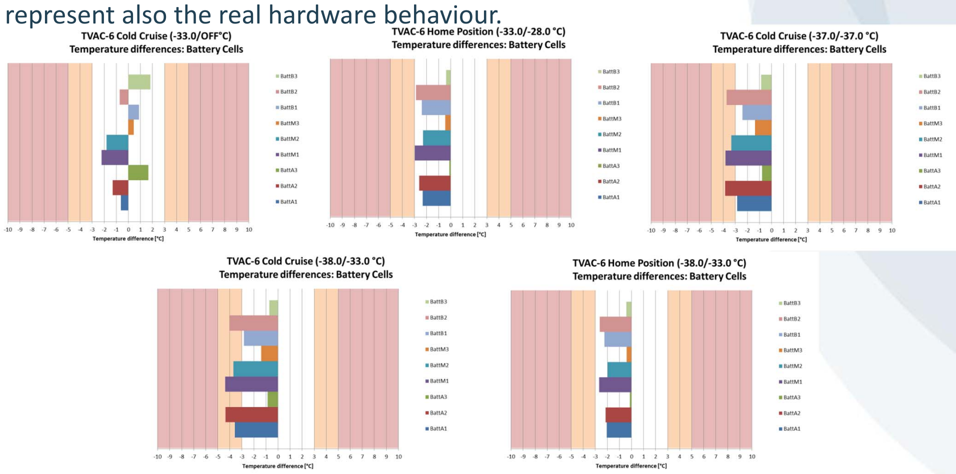

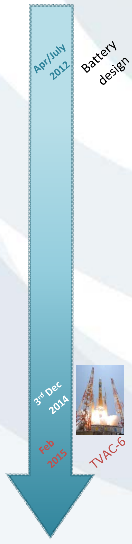

As this vacuum campaign happned after launch, a strategy for the launch and the first health-chack had to be evaluated, together with the pre-heating strategy.

activespace technologies

MASCOT preheating strategy

In order to keep MASCOT within the temperature limits, a heating and pre-heating strategy has been prepared (together with HY-2).

The MASCOT global thermal beahviour is kept within the ranges controlling the temperature of the battery pack (2 sensors) via two <u>independent</u> heating lines (A, B).

For health-checks the temperature of the whole lander has to be raised via raising the temperature set controlling he battery.

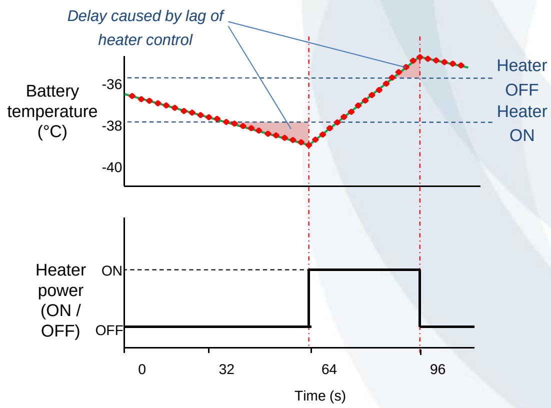

Courtesy of DLR

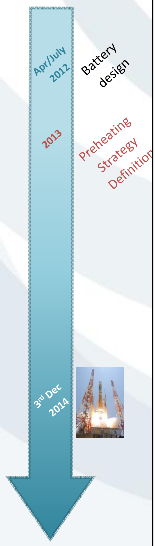

activespace technologies

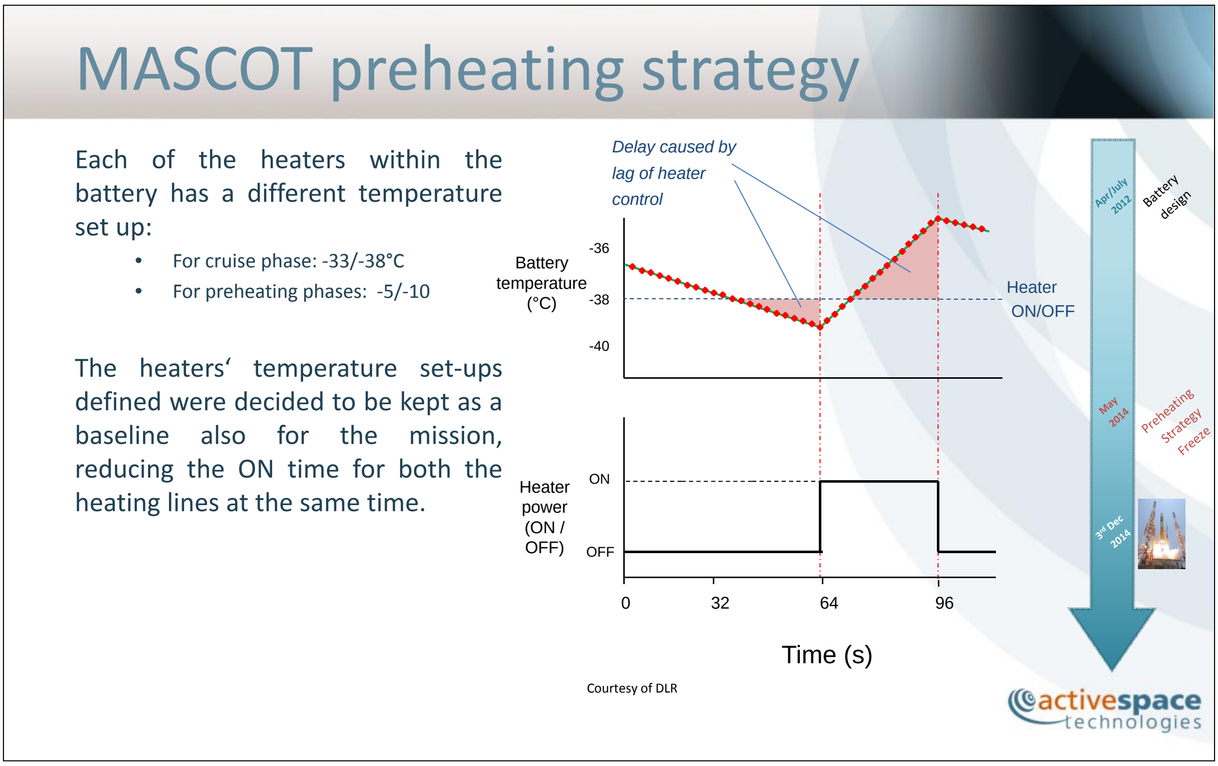
MASCOT preheating strategy
Each of the heaters within the battery has a different temperature set up:
• For cruise phase: -33/-38°C
• For preheating phases: -5/-10
The heaters' temperature set-ups defined were decided to be kept as a baseline also for the mission, reducing the ON time for both the heating lines at the same time.
Delay caused by lag of heater control
Battery temperature (°C)
-36
-38
-40
Heater ON/OFF
Heater power (ON / OFF)
ON
OFF
0
32
64
96
Time (s)
Courtesy of DLR
Apr/July 2012
Battery design
May 2014
Preheating Strategy Freeze
3rd Dec 2014
activespace technologies

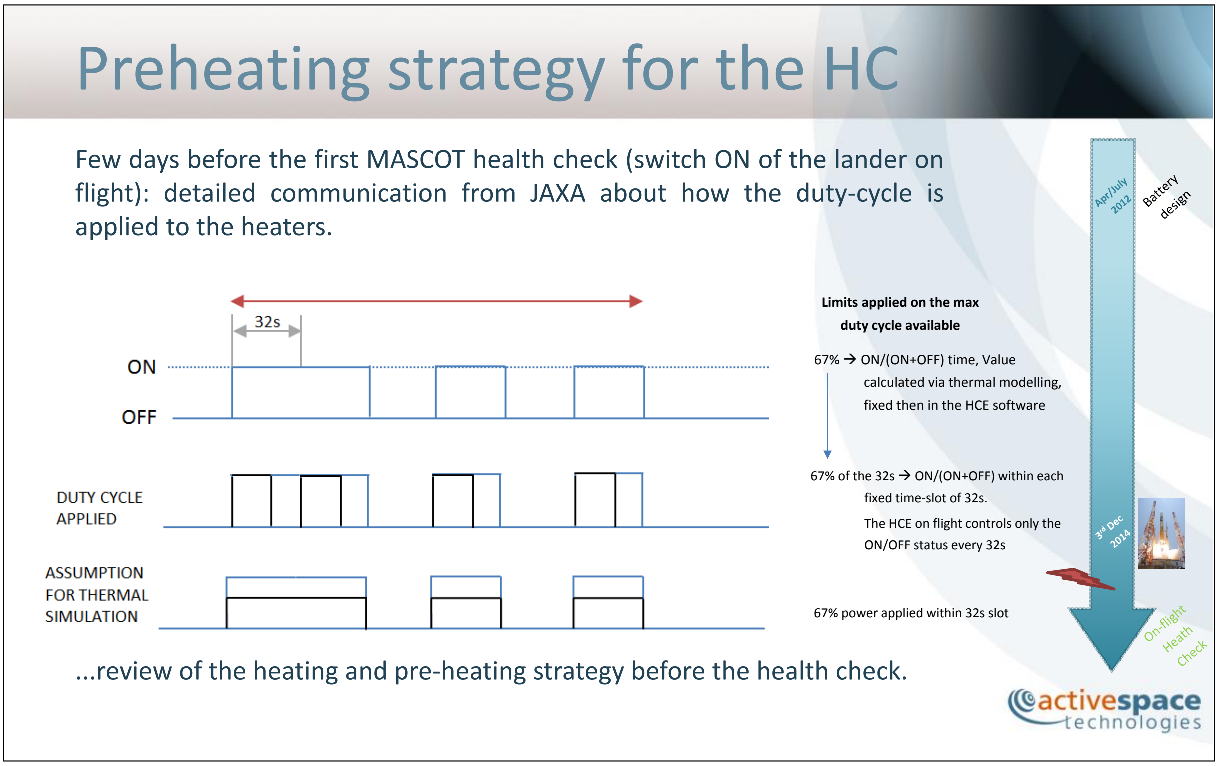
Preheating strategy for the HC
Few days before the first MASCOT health check (switch ON of the lander on flight): detailed communication from JAXA about how the duty-cycle is applied to the heaters.
32s
ON
OFF
DUTY CYCLE APPLIED
ASSUMPTION FOR THERMAL SIMULATION
Limits applied on the max duty cycle available
67% → ON/(ON+OFF) time, Value calculated via thermal modelling, fixed then in the HCE software
67% of the 32s → ON/(ON+OFF) within each fixed time-slot of 32s.
The HCE on flight controls only the ON/OFF status every 32s
67% power applied within 32s slot
...review of the heating and pre-heating strategy before the health check.
Apr/July 2012
Battery design
3rd Dec 2014
On-flight Heath Check
activespace technologies

Preheating strategy for the HC

After the understanding how the HY-2 operates the heaters, different options for health check temperature set-ups have been analysed.

Case	HY-2 voltage	Heater	Status	Tset	Max duty cycle	Power applied [W]
Hot Cruise (Two heaters work)	50 V	HCE-A	Works	-20°C	35.0%	2.70
		HCE-B	Works	-15°C	60.0%	4.63
Hot Preheating (Two heaters work)	50 V	HCE-A	Works	-10°C	35.0%	2.70
		HCE-B	Works	-5°C	60.0%	4.63
Hot Health Check (Two heaters work)	50 V	HCE-A	Works	-10°C	35.0%	2.70
		HCE-B	Works	-5°C	60.0%	4.63
Hot Cruise (One heater works)	50 V	HCE-A	OFF	-	-	-
		HCE-B	Works	-15°C	60.0%	4.63
Hot Preheating (One heater works)	50 V	HCE-A	OFF	-	-	-
		HCE-B	Works	-5°C	60.0%	4.63
Hot Health Check (One heater works)	50 V	HCE-A	OFF	-	-	-
		HCE-B	Works	-5°C	60.0%	4.63
Cold Cruise Two (Two heaters work)	50 V	HCE-A	Works	-20°C	35.0%	2.70
		HCE-B	Works	-15°C	60.0%	4.63
Cold Preheating (Two heaters work)	50 V	HCE-A	Works	-10°C	35.0%	2.70
		HCE-B	Works	-5°C	60.0%	4.63
Cold Health Check (Two heaters work)	50 V	HCE-A	Works	-10°C	35.0%	2.70
		HCE-B	Works	-5°C	60.0%	4.63
Cold Preheating (Two heaters work, **different temp set**)	50 V	HCE-A	Works	-15°C	35.0%	2.70
		HCE-B	Works	-10°C	60.0%	4.63
Health check (Two heaters work, **different temp set**)	50 V	HCE-A	Works	-15°C	35.0%	2.70
		HCE-B	Works	-10°C	60.0%	4.63
Cold Cruise One (One heater works)	50 V	HCE-A	Works	-20°C	35.0%	2.70
		HCE-B	OFF	-	-	-

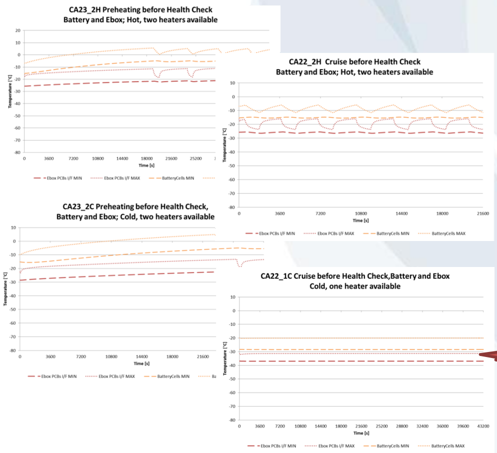

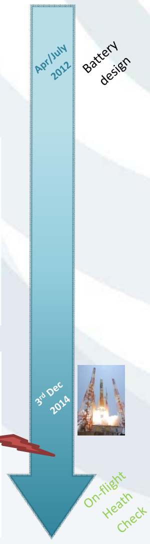

Preheating strategy for the HC

Thermal simulations (includign hte temperature gradient on the battery cells) allowed to prepare the procedures to follow during the first health check of MASCOT.

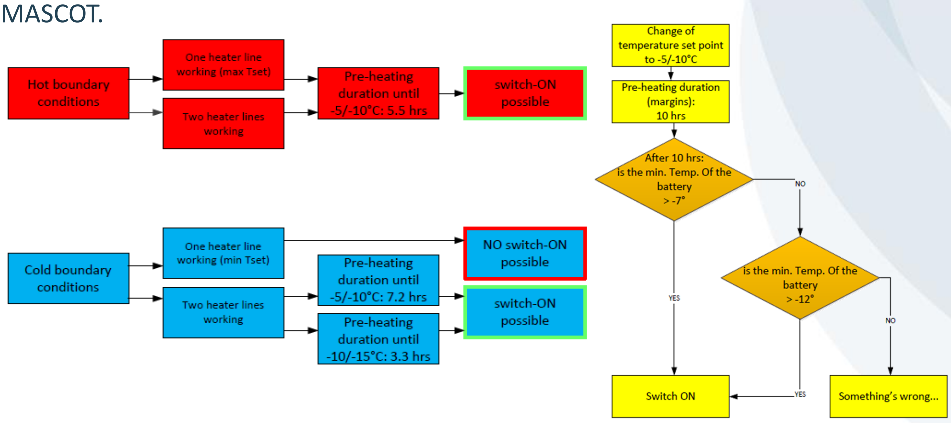

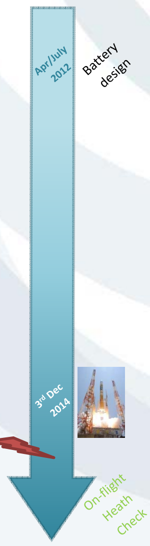

Conclusion

MASCOT is a lander built by DLR, embarqued on JAXA's Hayabusa-2, a scientific mission to study the asteroid "Ryugu" (former 162173 1999 JU3), launched on the 3rd of December 2014. As part of the project challenges, the short schedule for the whole development of the lander (2.5 years from PDR to launch), the strict and contrasting thermal requirements for different phases of the mission, mass&power/technology/volume limitations put the thermal design at the edge of the state of art technology solutions. As a result, the thermal system development has been on-going until the last phases of the project, on order to cope with late changes and technologies development.

This presentation focusses on the thermal control system evolution during the last months before launch and even just after it. Thermal vacuum campaigns, modelling re-iterations, better understanding of the main S/C thermal behaviour, together with the great team determination helped reaching a succesfull launch followed by an on-flight system verification.

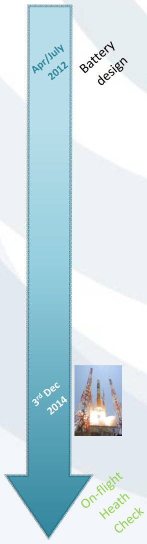

http://www.lizard-tail.com/isana/hayabusa2/ (Update from 10/2015)

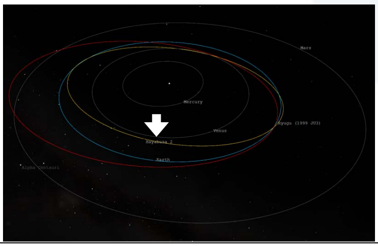

activespace technologies

Contacts

Thank you for the attention!

For further information

Luca Celotti
luca.celotti@activespacetech.eu

Tel: +49 (0) 30 6392 6090
Fax: +49 (0) 30 201 632 829

Carl-Scheele Str. 14
12489 Berlin
Germany

activespace technologies

Appendix G

Solar Orbiter SPICE
Thermal Design, Analysis and Testing

Samuel Tustain
(RAL Space, United Kingdom)

Abstract

[1] The Spectral Imaging of the Coronal Environment (SPICE) is one of ten instruments comprising the ESA Solar Orbiter payload. The instrument, currently being built at the STFC Rutherford Appleton Laboratory, is a high resolution imaging spectrometer operating at extreme ultraviolet wavelengths. We are currently in the build phase, with thermal testing of the flight model instrument due to commence shortly.

At an orbital perihelion of just 0.28 AU, there are numerous key design challenges that must be overcome for the instrument to survive the harsh thermal environment that it will be subjected to. In the last 18 months, the instrument has already undergone considerable thermal testing to qualify the design. The results of the tests completed thus far have provided essential inputs into the existing detailed thermal model, which is constructed using ESATAN-TMS. This presentation will discuss how the thermal analysis and testing have complemented each other for this project, while also providing impressions of ESATAN-TMS from the perspective of a relatively early user.

[1] Due to severe weather conditions the author was unable to attend the workshop and present this material.

Solar Orbiter SPICE

Thermal Design, Analysis and Testing

Samuel Tustain
Thermal Engineer, STFC Rutherford Appleton Laboratory

29th European Space Thermal Analysis Workshop, 3rd-4th November 2015

Science & Technology Facilities Council

RAL Space

RAL Space

Solar Orbiter - Overview

- Scheduled to launch in 2018
- Science goals are to address how the Sun creates and controls the heliosphere
  - Achieved by observing polar regions of the Sun from as close as 0.28 AU
- Payload comprised of ten instruments:
  - Six remote sensing, including the Spectral Imaging of the Coronal Environment (SPICE) instrument
  - Four in-situ instruments
- Heatshield provides main defence against solar load
  - Contains feedthroughs for remote-sensing payload

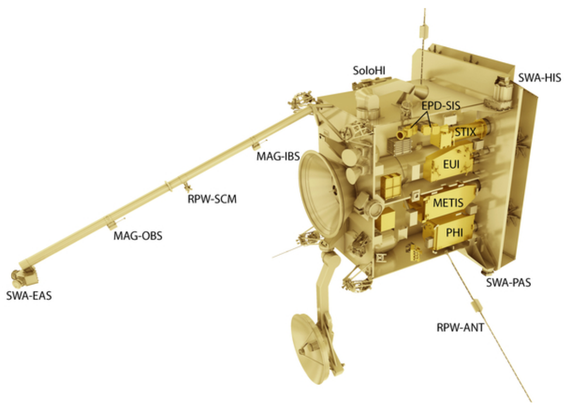

Image credit: ESA

SPICE – Overview

- High resolution imaging spectrometer operating at EUV wavelengths (70.2-105 nm)
- Objective is to provide data on the plasma composition of the Sun
  - Investigate links between the solar surface, corona and inner heliosphere
- Precise optics reflect light beam to detector assembly
- Currently in build phase of project
- Instrument mechanisms being provided by collaborating organisations

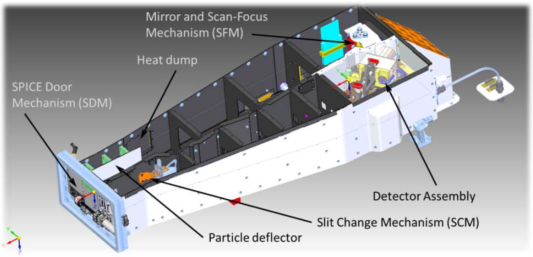

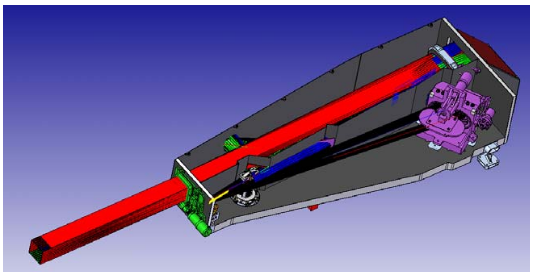

SPICE – Thermal Design

- Solar load is roughly 13 times greater than on Earth orbit
- Spacecraft heatshield blocks most incoming radiation
- Primary mirror has a 10 nm boron carbide (B_4C) coating
  - Reflective to UV radiation, but mostly transparent to visible and IR
- Secondary mirror (HRM) rejects this unnecessary load to deep space
- Only a small fraction of reflected UV load required, so pre-slit mirrors and heat dump radiator used to further reject heat
- Cold element interface maintains detectors at -20 ºC

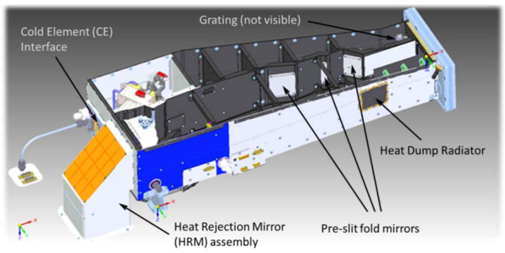

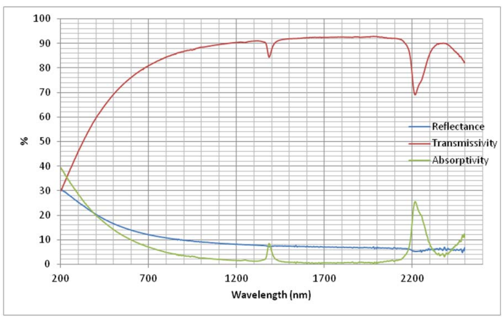

Boron carbide wavelength dependent thermo-optical properties, data obtained by MPS

SPICE – Thermal Design

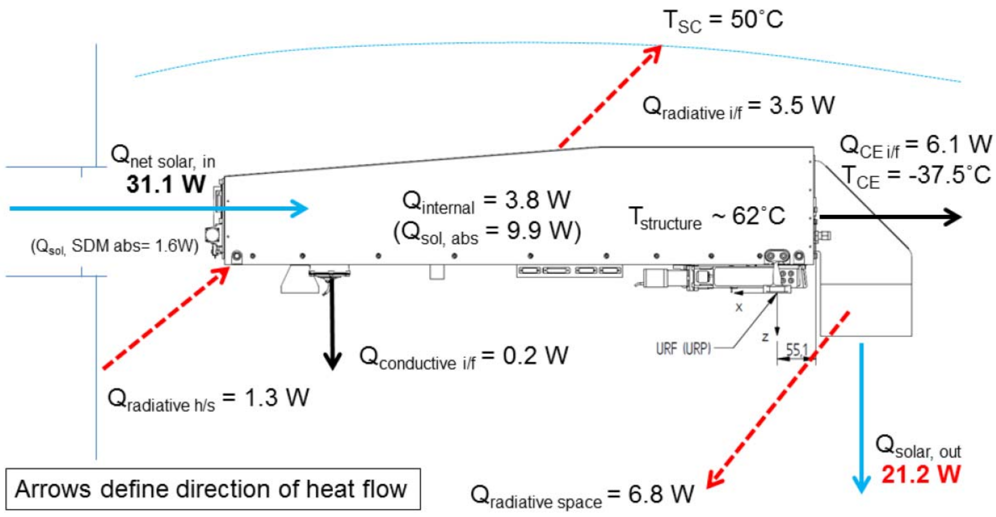

Detailed Thermal Model

- Constructed using ESATAN-TMS r7sp2
- Sub-models used for each subsystem
- Numerous configurations:
  - BOL/EOL
  - Door open/closed
  - Operational/Non-operational
- Three primary radiative cases:
  - Hot operational (0.28 AU)
  - Cold operational (0.91 AU)
  - Cold non-operational (1.5 AU)

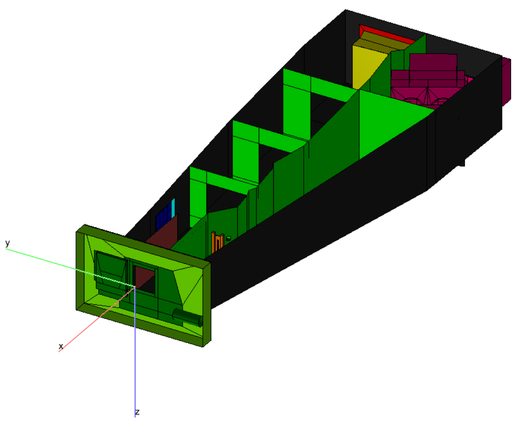

RAL Space

Test Objectives and Plan

- To verify the thermal design, specifically:
  - Management of solar load
  - Key internal thermal interfaces (e.g. across mirror mounts)
  - External thermal interfaces
  - Minimum and maximum temperatures
- Key tests to achieve this:
  - STM
    - High Flux Mirror Test
    - Thermal Balance Test
  - FM
    - Detector Assembly Thermal Balance Test (in progress)
    - Thermal Balance Test (to be completed)
- Thermal Vacuum Test on STM and FM to qualify the thermal design over predicted temperature range

RAL Space

High Flux Mirror Test

- Designed to simulate the primary mirror in the worst case hot environment
- Objectives:
  - To experimentally determine thermo-optical properties of mirror
  - Observe impact on mirror temperatures
- High intensity lamp used as the test source to provide solar-like flux
  - Intensity roughly 20% of flight load
- Heat dump positioned behind mirror
  - Heat load absorbed from the lamp is deduced by replicating temperatures using heaters
- Test completed both with and without mirror
  - Difference in values indicates transmitted heat load

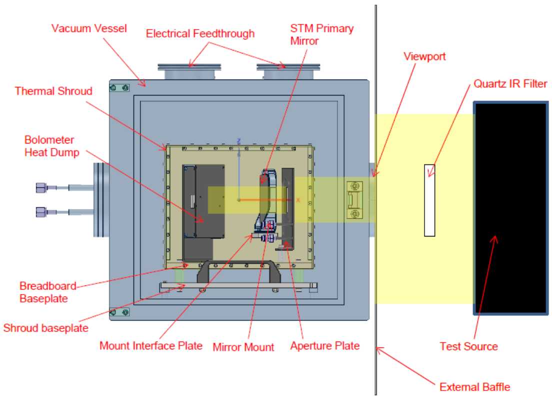

RAL Space

High Flux Mirror Test

- Results showed that ~80% of the incoming beam was transmitted
- Analysis of the incident spectrum show that this closely matched the expected transmission from the MPS data

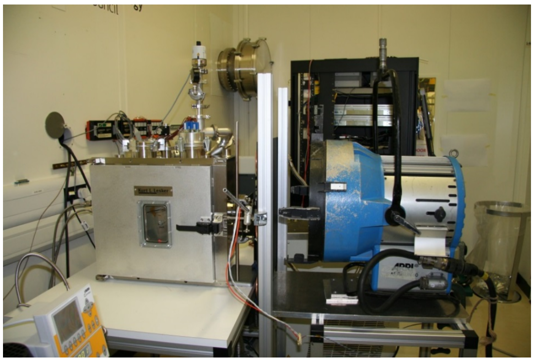

RAL Space

SPICE – Test Rig

- Specialised test rig built for thermal testing of SPICE, to simulate spacecraft cavity
- Fluid pipes around shroud allow interface temperatures to be simulated
- Heaters simulate heat flows from instrument to spacecraft
- Shroud is wrapped in multi-layer insulation (MLI) to minimise heat flow from vacuum chamber
- Test rig successfully completed commissioning tests prior to instrument testing

RAL Space

STM Thermal Balance Test

- Eight test cases in total
  - Two involving mercury lamp (less intensity than previous lamp, but more flight-representative UV spectrum)
  - Six use test heaters to simulate absorbed loads
- 'Beam dump' maintained at 100 K by cryocooler to simulate deep space view from heat rejection mirror
- STM thermal model built to provide test predictions and inform test inputs

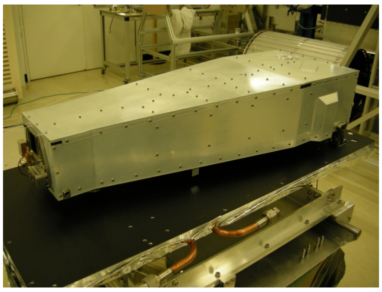

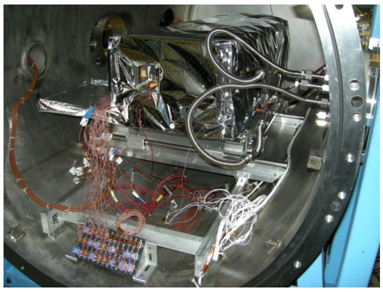

RAL Space

Detector Assembly Thermal Test

- Thermal vacuum and thermal balance testing on GSFC produced Detector Assembly (DA)
  - Verify thermal design (particularly cold element interface) and functional performance
  - Correlate DA submodel (not included in STM)
- DA has its own separate test rig
- Submodel extracted from flight model to generate test predictions
- Test is ongoing

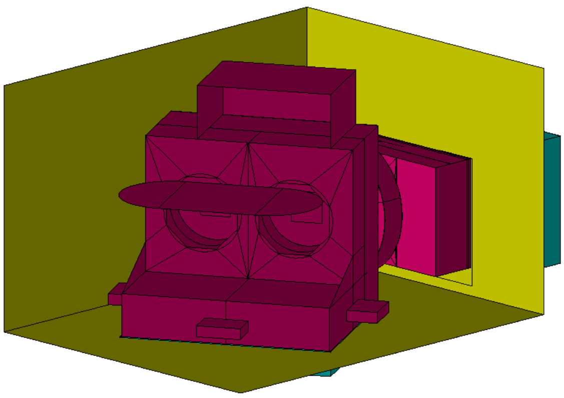

RAL Space

Correlation

- ECSS standard used:
  - Temperature deviation < 5 ºC
  - Mean deviation of temperature difference within ±2 ºC
  - Standard deviation of temperature difference < 3 ºC
- Particularly essential for this instrument because a realistic solar load cannot be easily replicated during testing
- Submodel structure has proven useful

RAL Space

Future Tests

- Upcoming tests on flight instrument
  - Thermal balance and thermal vacuum
  - First test with instrument and DA together
- No test heaters available for instrument structure
- Mercury lamp to be used once more for hot operational test cases

ESATAN-TMS Impressions

- Generally good!
- Workbench is relatively user friendly
- Library system should be reviewed
  - Store data in text format? Easier to modify
  - Update process between ESATAN-TMS versions is not well documented
- Performing cutting operations can sometimes be frustrating
- Undo button!

Conclusion

- SPICE must withstand extreme thermal environment
- Tests carried out:
  - High Flux Mirror Test
  - Thermal Rig Commissioning Test
  - STM Thermal Balance Test
- Future tests:
  - FM Detector Assembly Thermal Test
  - FM Thermal Balance Test

Contact Details

Samuel Tustain
Thermal Engineering Group
Email: samuel.tustain@stfc.ac.uk
www.ralspace.stfc.ac.uk

Appendix H

Spatial Temperature Extrapolation Case Study
Gaia in-flight

Matthew Vaughan
(ESA/ESTEC, The Netherlands, Airbus Defence and Space, France)

Abstract

The project IAMITT (Innovative Analysis Methods for Improved Thermal Testing) was defined by ESA to address the issues of thermal test quality, cost and schedule reduction. One aspect of this project concerns the application of the techniques of spatial extrapolation with the aim to provide a full thermal map of a spacecraft given input temperature sensor data. This information is of particular interest during spacecraft thermal testing where a temperature may be recovered in the case of a sensor malfunction. It could also be useful in the prediction of temperatures for areas of the spacecraft that are normally difficult to instrument or to give the thermal engineer a more informed choice on the positioning of sensors.

A novel case study was proposed using the Gaia spacecraft to perform an extrapolation using the thermal model and in-flight telemetry. Firstly the thermal environment of Gaia's orbit at L2 is considered together with the requirements for an extrapolation. The algorithms behind the extrapolation are then highlighted together with the techniques used to combine in-flight telemetry with a correlated thermal model. The procedure of synchronising the time in the model with the flight data is then discussed including the assumptions made with respect to solar fluxes and internal dissipations.

The results are then presented comparing the differences between the model predicted and in-flight extrapolated temperatures. A heat balance on the boundary nodes is also used as an additional method to check the method against predicted values. Finally the extrapolated temperatures are visualised on the thermal model and possible benefits to the thermal engineer are reviewed.

This work has been carried out under the *Young Graduate Trainee in Industry* scheme of ESA in cooperation with Airbus Defence and Space, Toulouse, France.

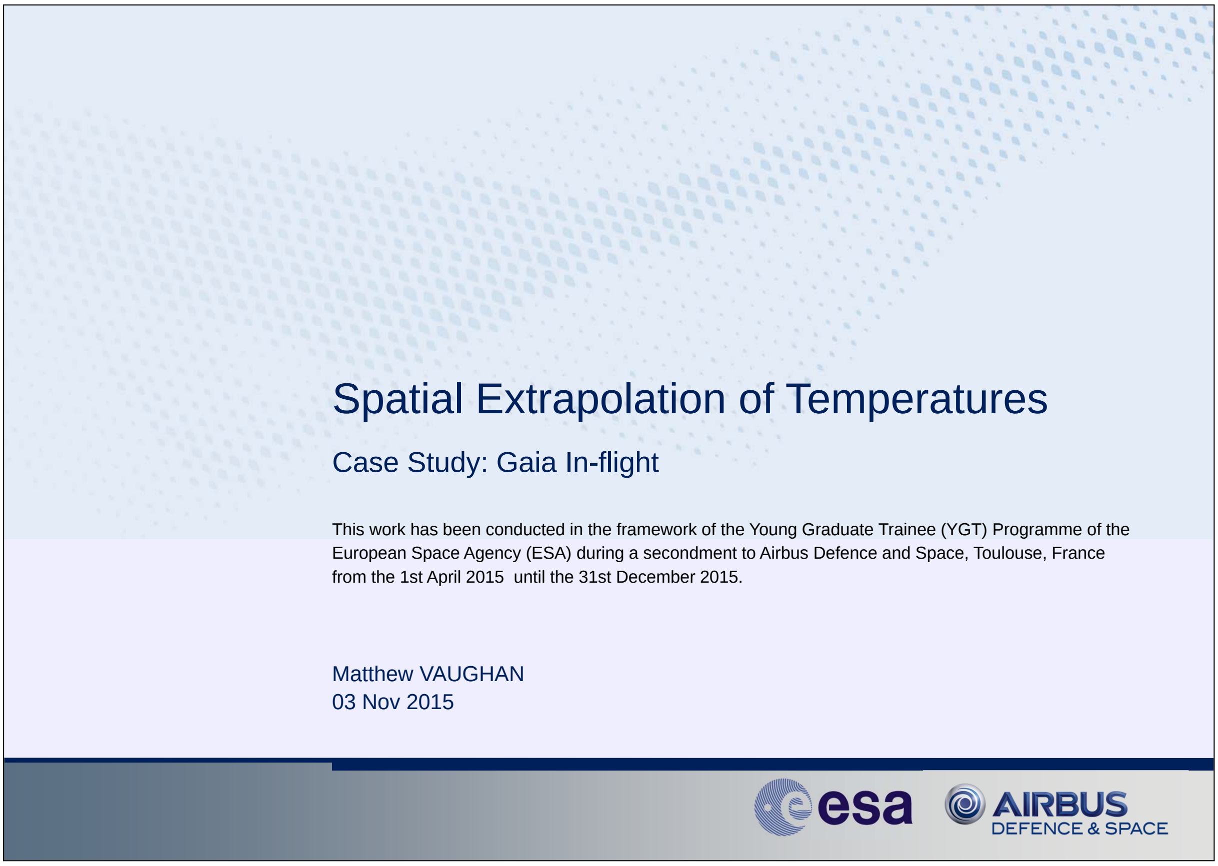

Title and introduction slide

- Work carried out during the Young Graduate Trainee scheme at ESTEC, ESA
- There are about 80 positions available each year for recent graduates in all areas of space
- Worked within the ESTEC Thermal analysis and verification department
- Seconded to industry in cooperation with Airbus Defence and Space, Toulouse, France, in the mechanical and thermal department.
- The work carried out consisted of mainly R&D projects and new techniques to aide thermal testing

Spatial Extrapolation of Temperature. Case Study: Gaia In-Flight

Innovative Analysis Methods for Improved Thermal Testing (IAMITT)

Module	Objective	Interest
Thermal Test Database (TTD)	Complete and centralised database (all data, real-time)	Support to other modules
3D display (3D)	Real time 3D visualization of all data (Temperatures, Dissipations) Thermal model based displays	Better understanding and monitoring, quality enhancement and risk mitigation.
Spatial extrapolation (SE)	Complete map of temperatures (all nodes of thermal model).	Quality enhancement, risk mitigation, sensor reduction (for recurrent models of satellites).
Temporal extrapolation (TE)	Equilibrium temperature prediction Estimation of TB end of phase date.	Time and cost savings.
Thermal model updating Tool (TMUT)	Near real time thermal model test conditions and parameters updating.	Time and cost savings, quality enhancement

IAMMIT - 26th European Space Thermal Analysis Workshop - Melanie Doolaeghe & Andre Capitaine (Astrium Satellites, France)

3 November 2015 2

IAMITT Slide

- So how does the spatial extrapolation of temperature module fit into the bigger picture?
- Under umbrella of the bigger project called IAMITT (Innovative Analysis Methods for Improved Thermal Testing)
- Techniques developed to improve test quality, cost, schedule reduction and to provide more information for the thermal engineer
- Some are connected for example viewing live results of an extrapolation on 3D model during test
- The spatial extrapolation project started 10 years ago with a internship project at Airbus Defence and Space, Toulouse, France
- It has been continually developed and over the last 8 months applied to case studies.
- For more information see the presentation on IAMMIT during the 26th European Space Thermal Analysis Workshop: https://exchange.esa.int/thermal-workshop/attachments/workshop2012/index.htm

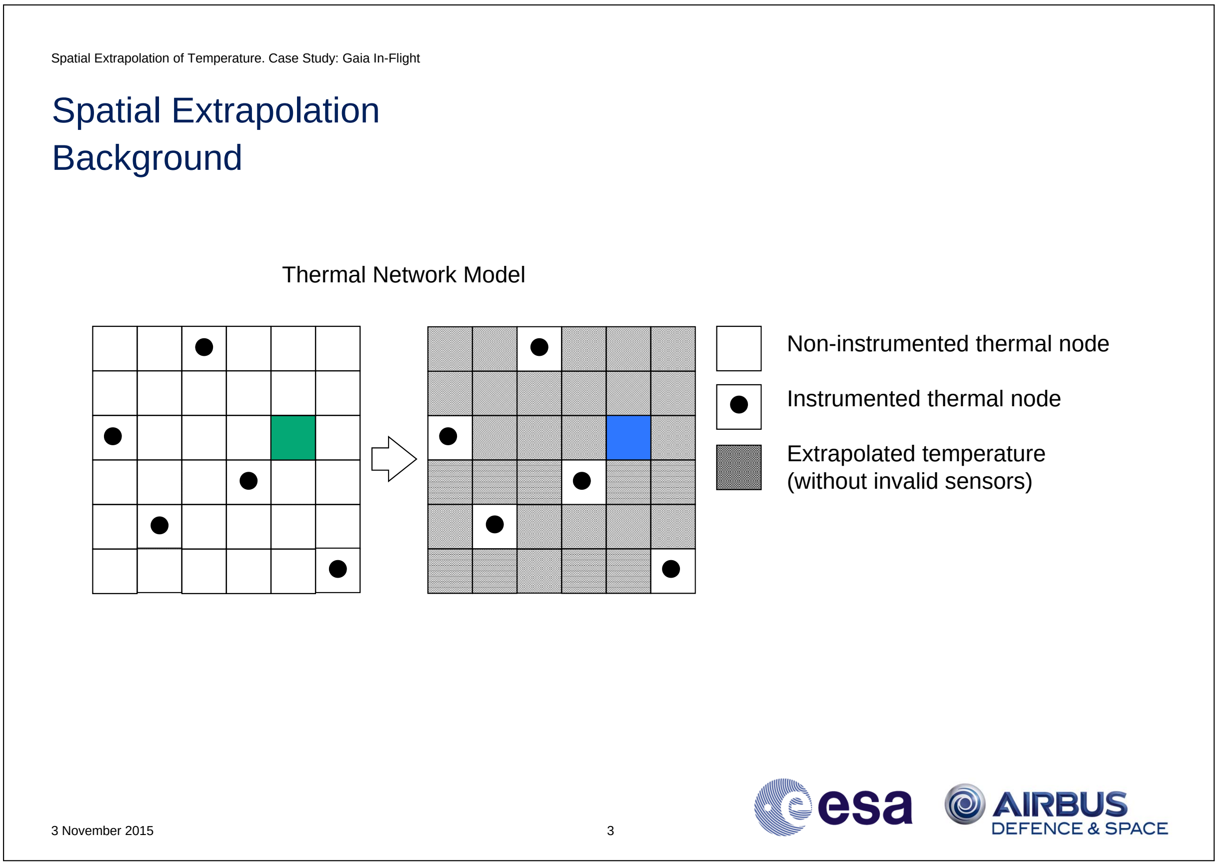

Background Slide
Using the thermal network model with a sensor to node mapping we can extrapolate to find the remaining temperatures.
How are these techniques useful?

- Information on areas of the spacecraft that are difficult to instrument
- Recover the temperature of malfunctioning thermocouples
- Improve the positioning of sensors on recurrent designs of satellites

Example: Telecoms satellite during transient TVAC:

- Extrapolation performed with 100% of available thermocouples
- Extrapolation then recomputed with only 50%
- Results: On average 90% of the removed sensor temperatures are extrapolated to within 5 degrees of the measured

To understand this firstly we need to take a look at the algorithm.

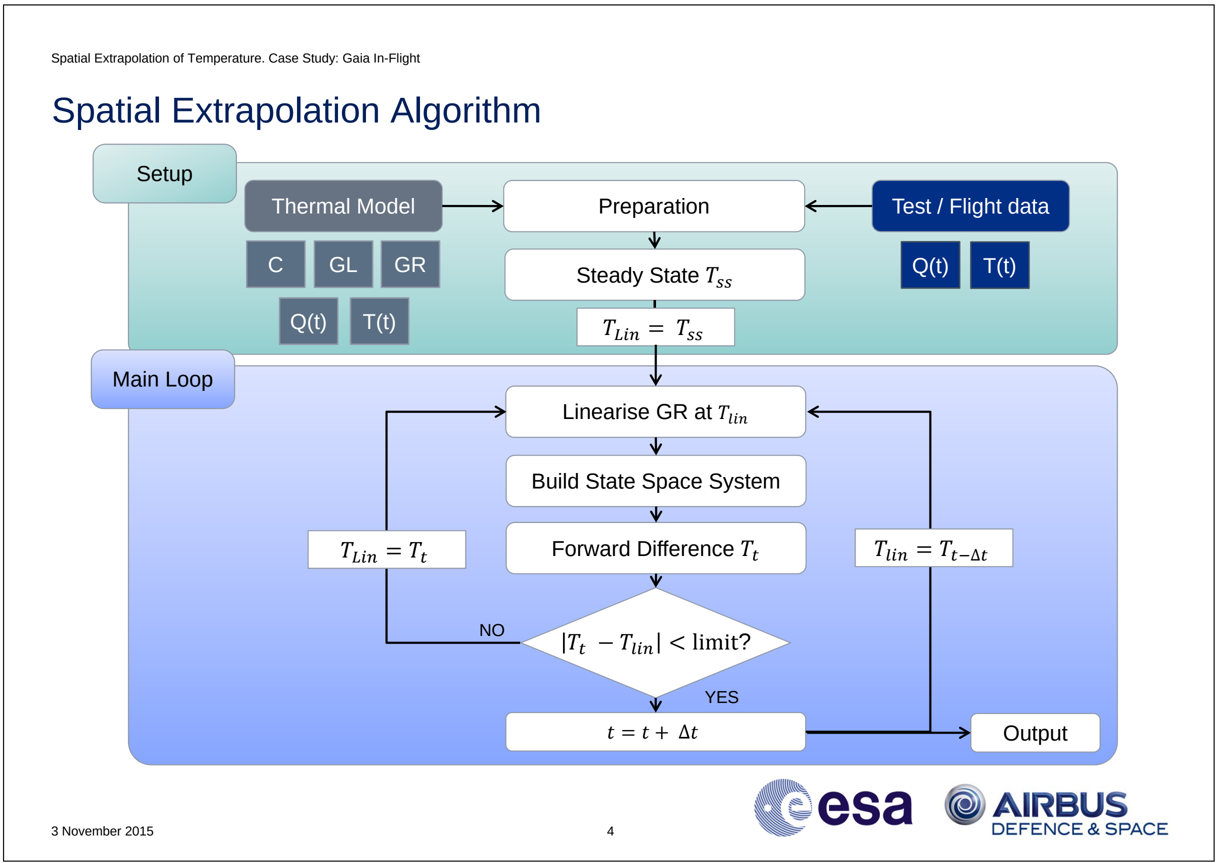

Algorithm
Q: How can we fuse the two data sources (Thermal Mathematical Model and Test/Flight data)?
A: Using a state space representation of our thermal model driven by the sensor readings.
Setup:

- Left: CSV dumped matrices from a thermal solver describing the thermal network
- Right: Test or flight data with temperature and heat readings
- Prepare system - removal inactive nodes - locate arithmetic nodes - sample sensors using mapping to nodes.
- The data acts as a transient boundary condition in the model.
- Steady State, average of current sensor T

Main loop (transient):

- Linearisation non linear conductors (T to the 4th power term)
- Build state space system and perform a forward difference to obtain the next T
- Check convergence on linearisation temperature
- Output timestep

The extrapolated temperatures are evaluated using the model driven by the inputs, which are heat sources and sensor temperatures.

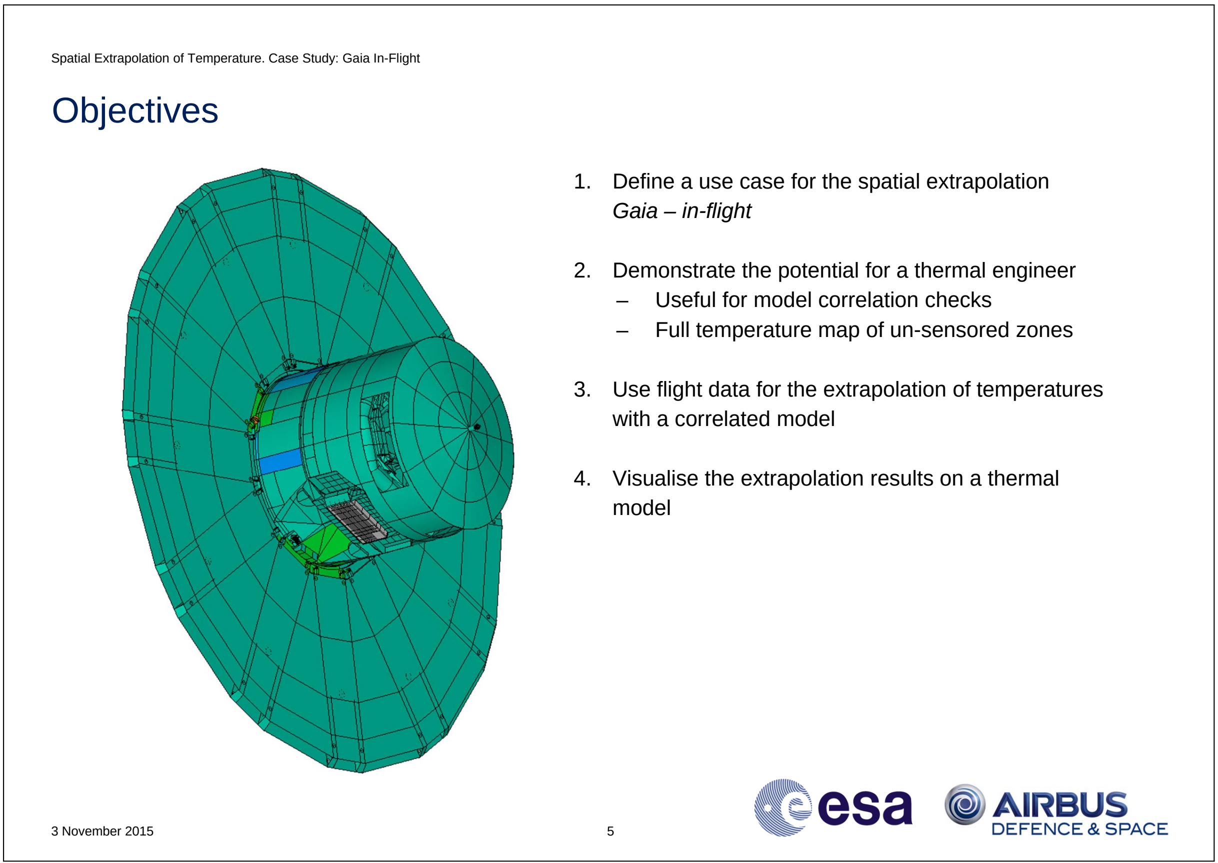

Objectives

- Understanding of the prediction quality of the extrapolation
- Map of a spacecraft already in-flight
- Possibly provide information to help other disciplines
- Extrapolation only using flight telemetries (several hundred in comparison to a thermal balance test of several thousand)
- Perform heat balances on the extrapolation as a check
- Display results back onto the thermal model

Spatial Extrapolation of Temperature. Case Study: Gaia In-Flight

Gaia Background

3D dynamic map of the Milky Way

Launched December 2013

Lissajous orbit around L2
(1.5 X10^{6}km from the COE)

Spin period 6 hours around central axis
45° to sun-earth line

Stable thermal environment
Albedo and IR fluxes negligible

Solar constant at L2 :
1293 – 1388 W/m^2

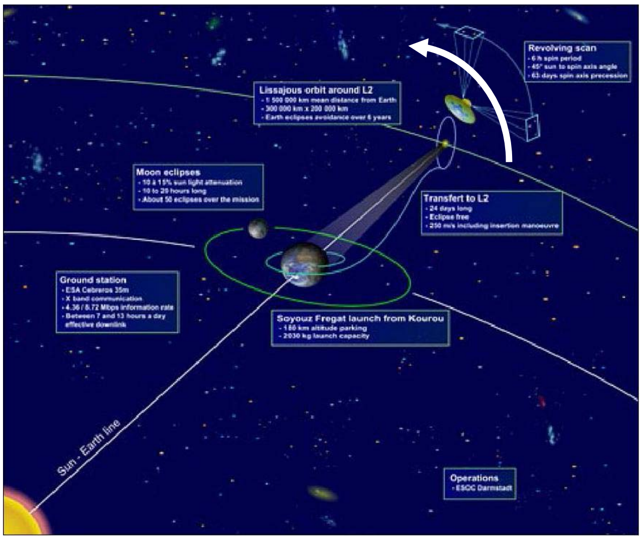

Image Ref: ESA, https://directory.eoportal.org/web/eoportal/satellite-missions/g/gaia, accessed 15/10/2015

3 November 2015 6

Background on Gaia

- Positioned in a stable thermal environment
- Solar constant is a function of distance from the sun and position within orbit - slightly weaker than at earth
- For the extrapolation data, 6 hour rotations around the spacecraft central axis are taken into account
- The position in the Lissajous orbit over several rotations is considered to have a negligible impact

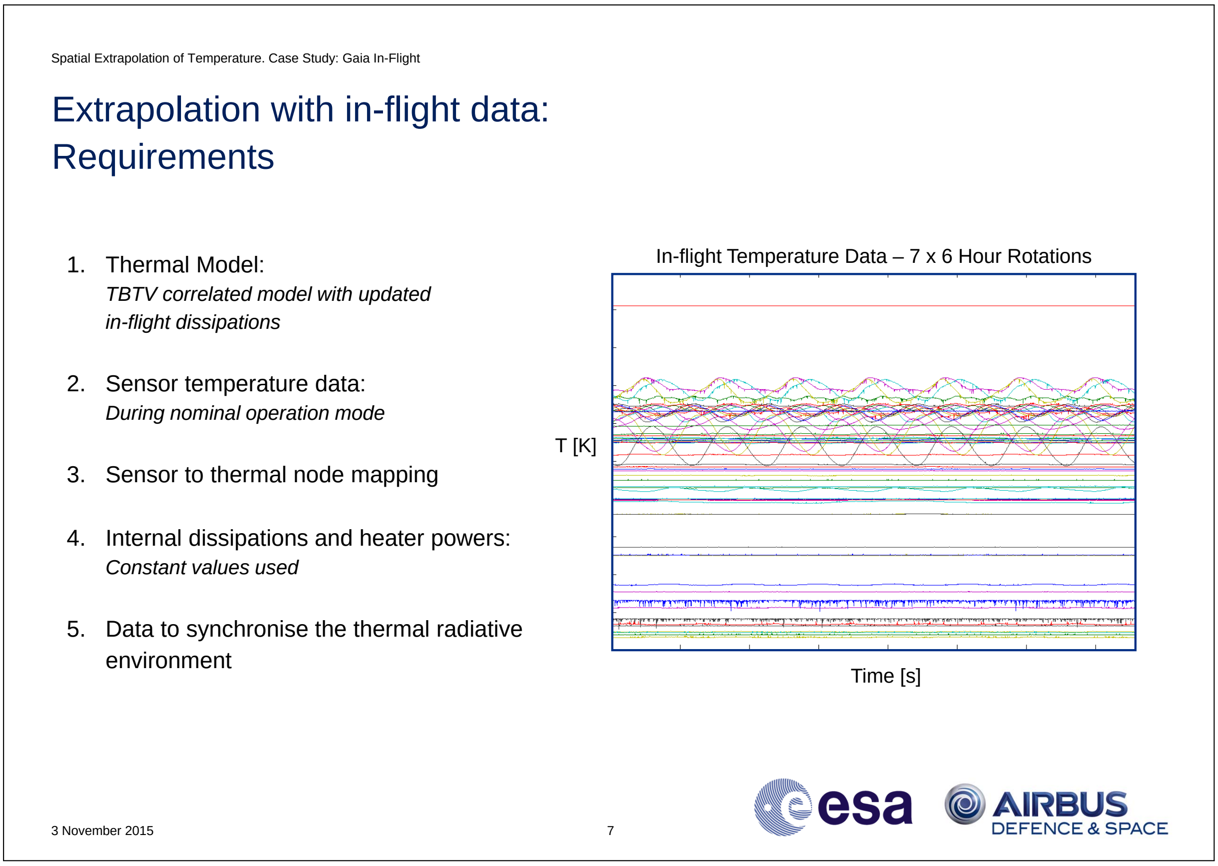

Requirements

- TBTV correlated model with updated in-flight dissipations
- During nominal operation mode there are small standard deviations in the dissipations, in June 2014
- 7 x 6 hour rotations of telemetry considered with 147 temperature sensors
- Mapping file, multiple telemetries to thermal nodes
- Spacecraft ancillary data to synchronise the orbit in the model and in flight

How do we process the sensor data?

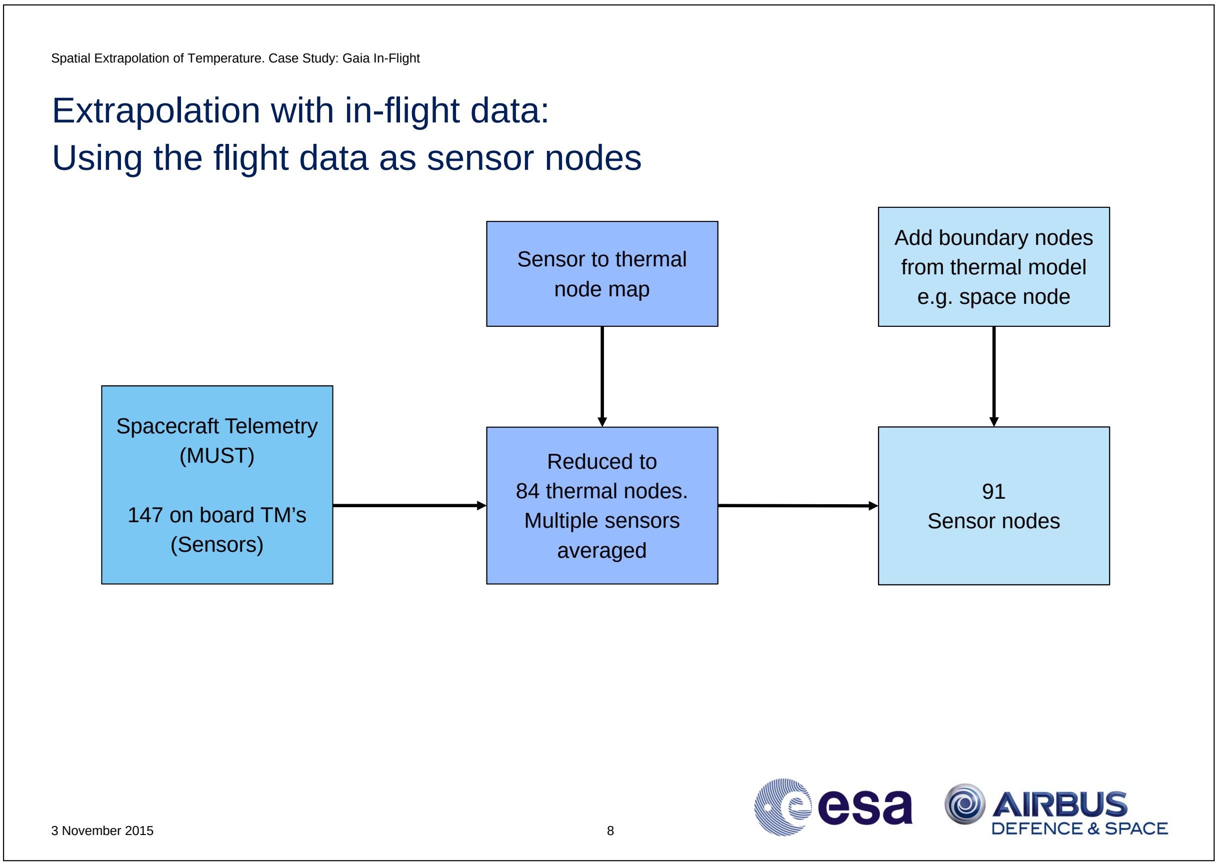

Processing the flight data

- Start with 147 on board telemetries
- These are reduced to only 84 thermal nodes in the model by averaging multiple sensors to nodes
- Important to note that some of the nodes have a dissipation set in the model
- Finally any boundaries not instrumented must be included from the model for example the space environment node.
- Sampled approximately every 30 seconds for 42 hours
- Almost ready to extrapolate, we just need to syncronise the solar fluxes on the model

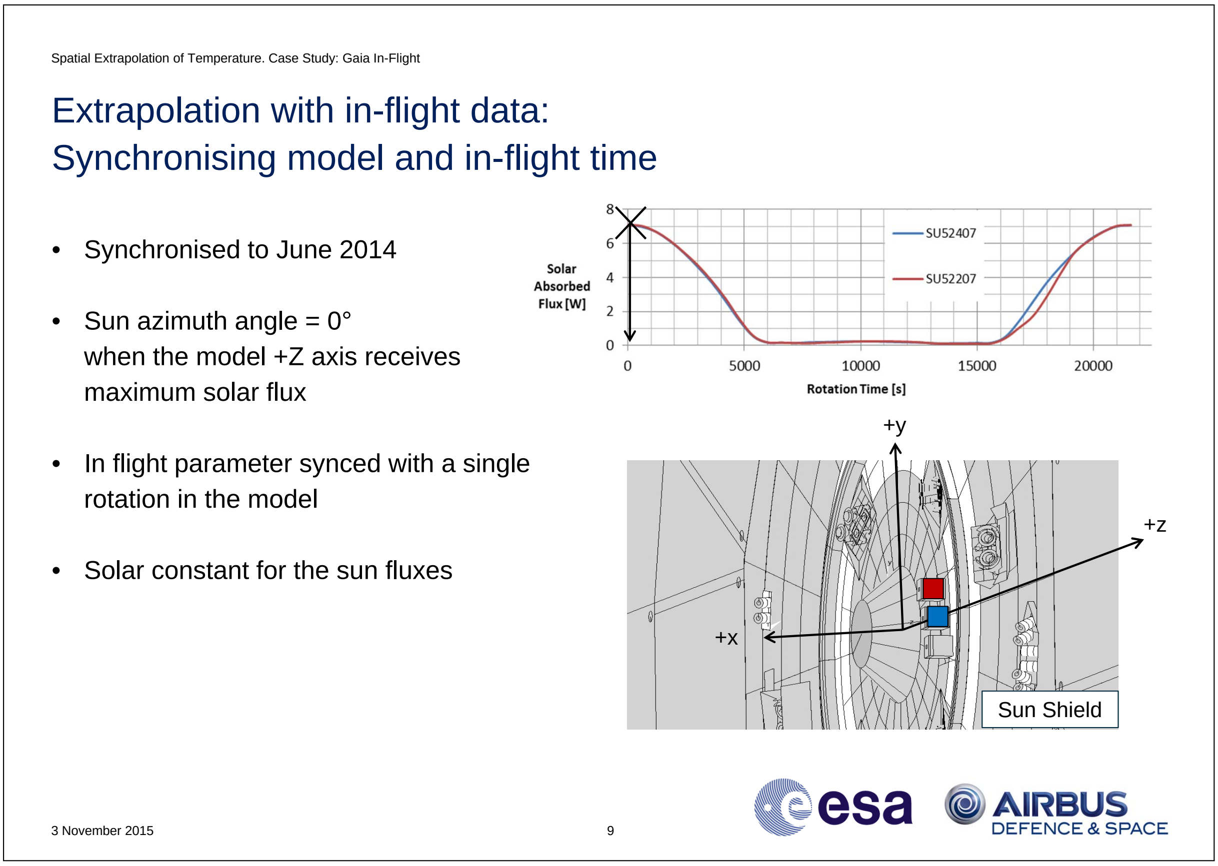

Synchronising the model and in-flight time

- Synchronised to June 2014
- We have the ancillary parameter, sun azimuth angle which is equal to zero when the Z-axis of the spacecraft is pointing towards the sun.
- Therefore we can plot the flux on these surfaces and conclude that the maximum flux corresponds to an angle of 0 degrees.
- The solar fluxes are then synchronised with the in-flight time
- Finally the solar constant requires scaling for the day of the year and position within the orbit
- IR and albedo fluxes are considered negligible.

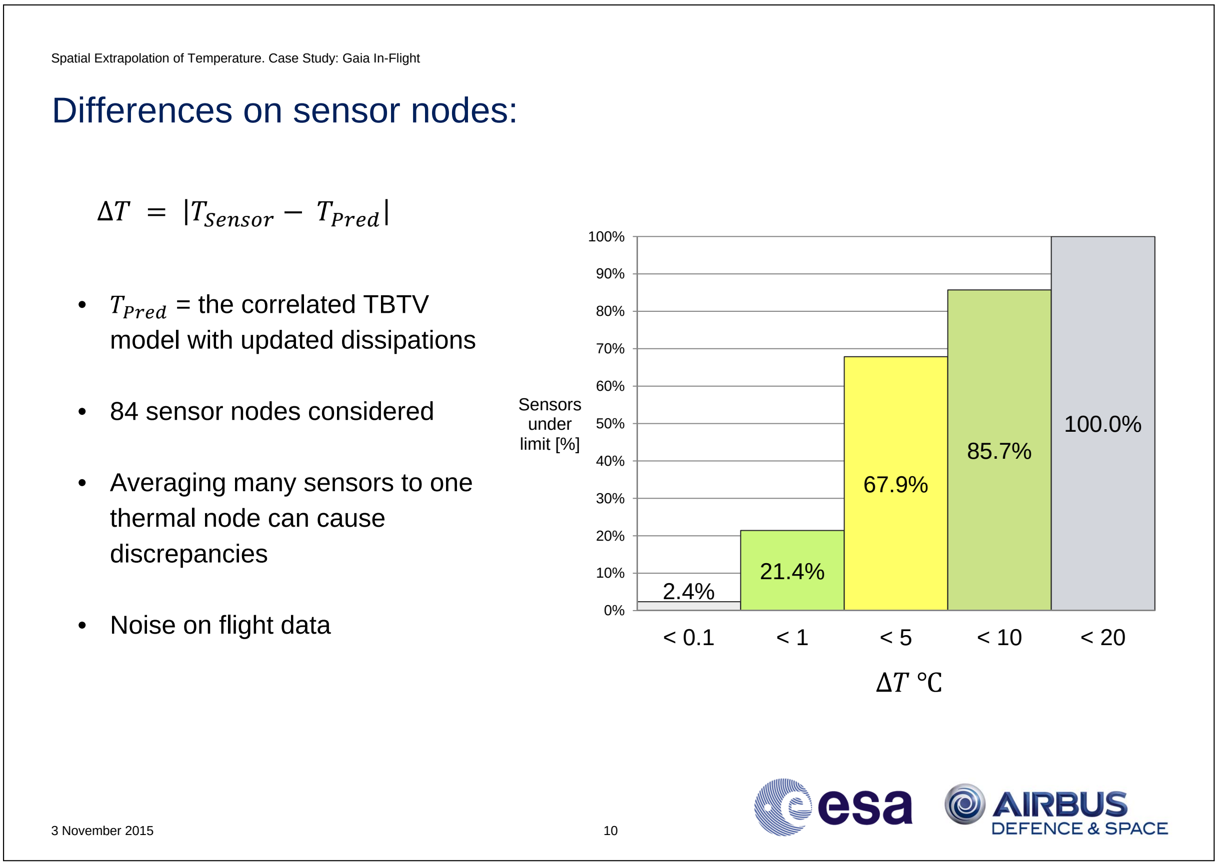

Comparison of sensor nodes

- Which checks can we provide to the thermal engineer?
- 84 Sensor nodes difference to measured averaged over 7 rotations
- Absolute difference sensor and predicted

Cause of discrepancies:

- Averaging many sensor nodes to one thermal node
- Dissipations not exactly constant and can cause large discrepancies with small nodal capacities
- Comparing two types of thermal node: boundary and diffusion
- Sensor nodes with a heat flux present
- Poor representation of zones with distributed heat flux

Now we move onto the rest of the temperatures, the extrapolated ones:

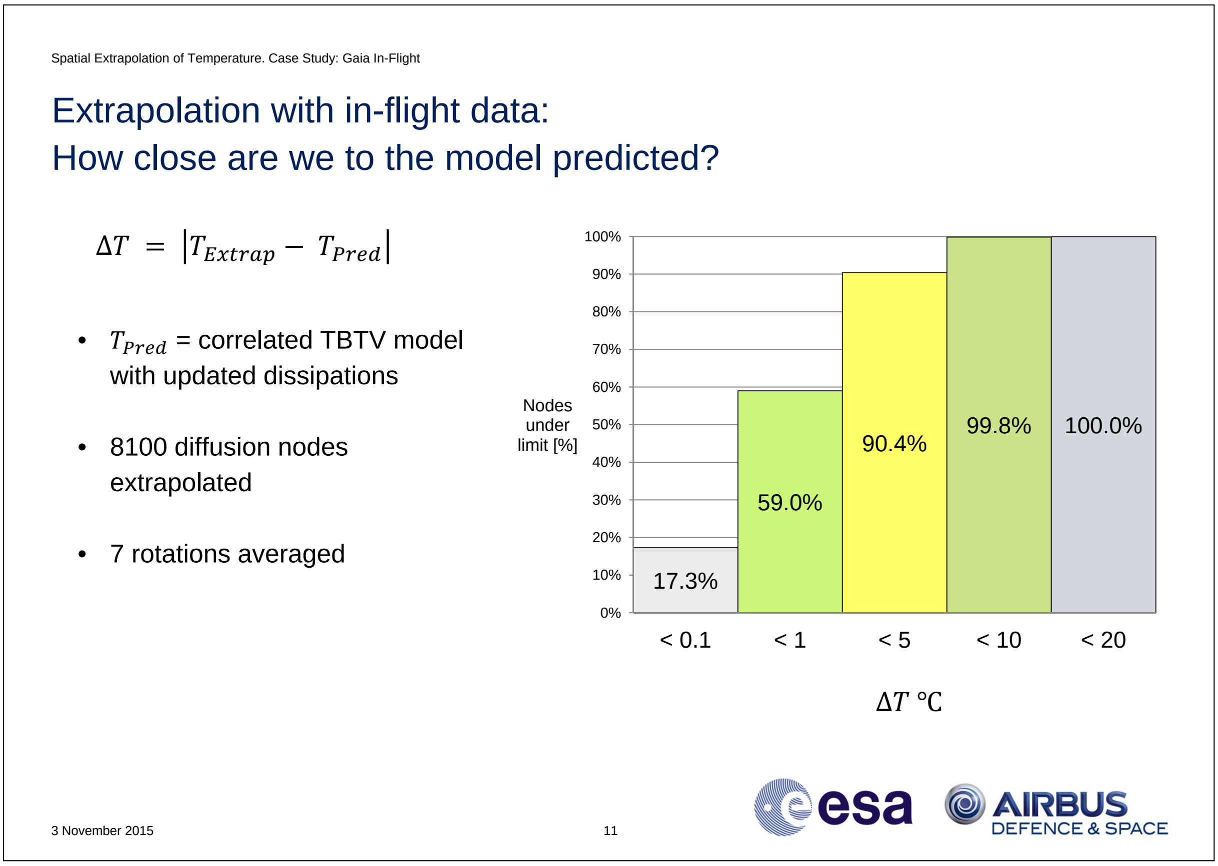

Comparison of extrapolated nodes

- Difference between extrapolated and correlated TBTV model on 8100 nodes
- 90% of the nodes under 5 degrees
- On the one hand maybe many of the nodes are not impacted by small changes in temperature seen on the sensors
- But it shows a good level of accuracy around sensor zones, useful if we lose a telemetry during flight / thermocouple during test.

So what is the effect of adding many more boundary/sensor nodes to the thermal model?

Spatial Extrapolation of Temperature. Case Study: Gaia In-Flight

Extrapolation with in-flight data: Heat Balances

Net heat flow into boundary nodes
Averaged over 7 rotations

Method	No. of boundary nodes
Extrapolation	91
ESATAN	7

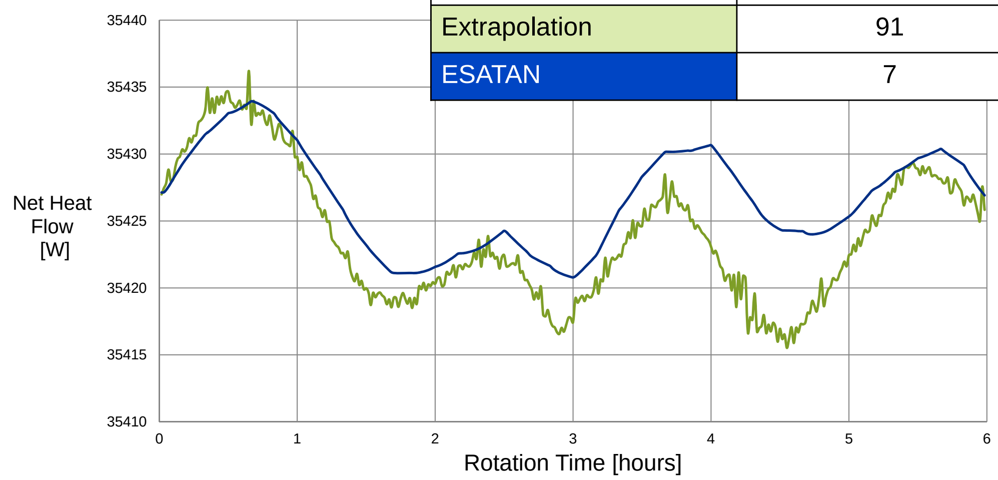

3 November 2015 12

Heat Balances on boundary nodes

- Plot shows the net heat flux into the boundary nodes averaged over 7 rotations for one rotation
- Most of the heat flux is attributed to the space node, sun flux immediately lost to environment.
- Correlations are very close, the scale on the right shows around a 7 or 8 W max difference on the rotation.
- The boundary nodes are pushing and pulling the model, adding heat where it is needed and removing where it's in excess
- There is an effect from distributed heat loads with one sensor node poorly representing a fraction of this heat load.

We have provided a few checks for the engineer and now we would like to view our results back on the original model:

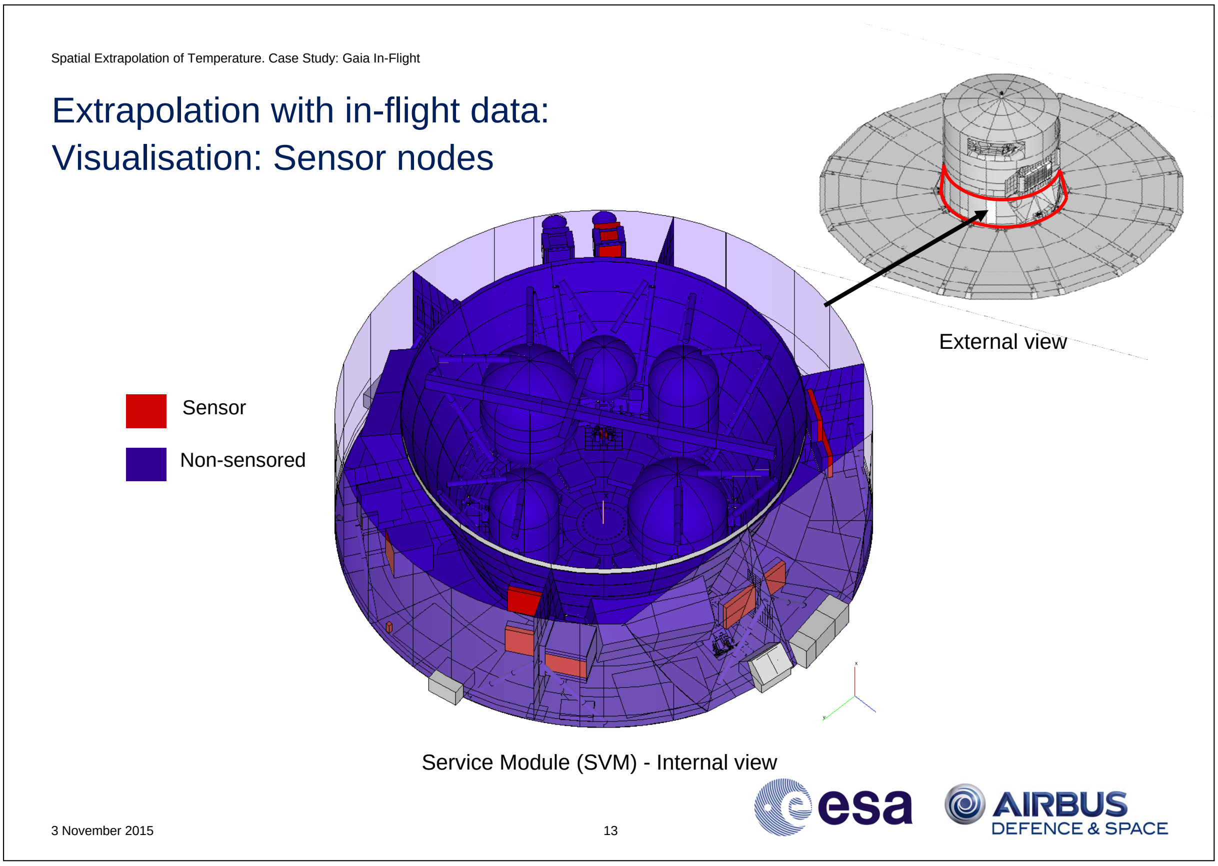

Visualisation - sensor positions

- Interested mainly in the service module where most of the electronics and units are housed.
- Red is a sensored node (note that some are internal and do not have a visualisation available)
- Able to see the zones which are well sensored and therefore can be more confident of the prediction around these zones
- Structure and areas around the tanks are not sensored

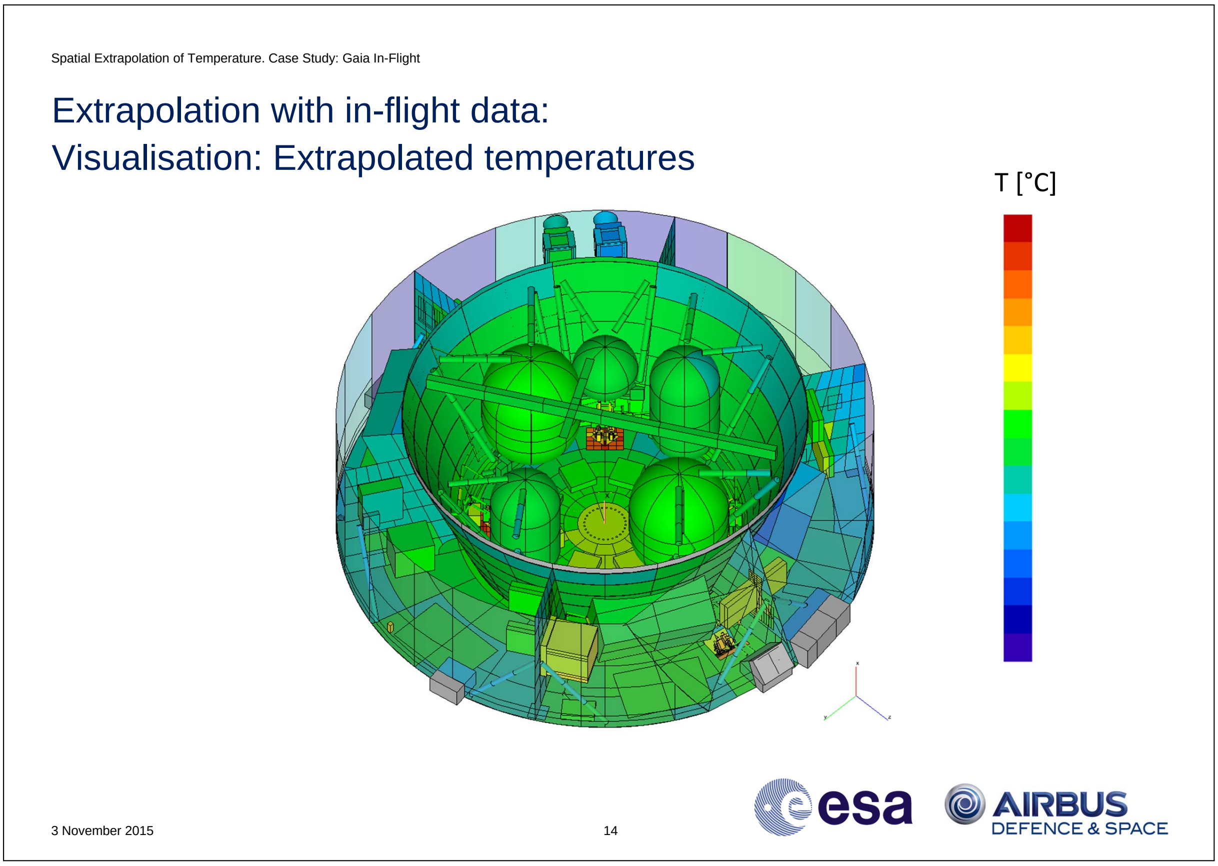

Visualisation - Extrapolated temperature

- Plotted are the extrapolated results along with the sensor temperatures
- It is possible to plot other information for example variation of temperature over one rotation
- The software can currently provide a live solution when each set of sensor readings are available, test or flight
- Typically only a few fast iterations are required when the data has been processed.

One final interesting visualisation is the difference between the predicted and extrapolated

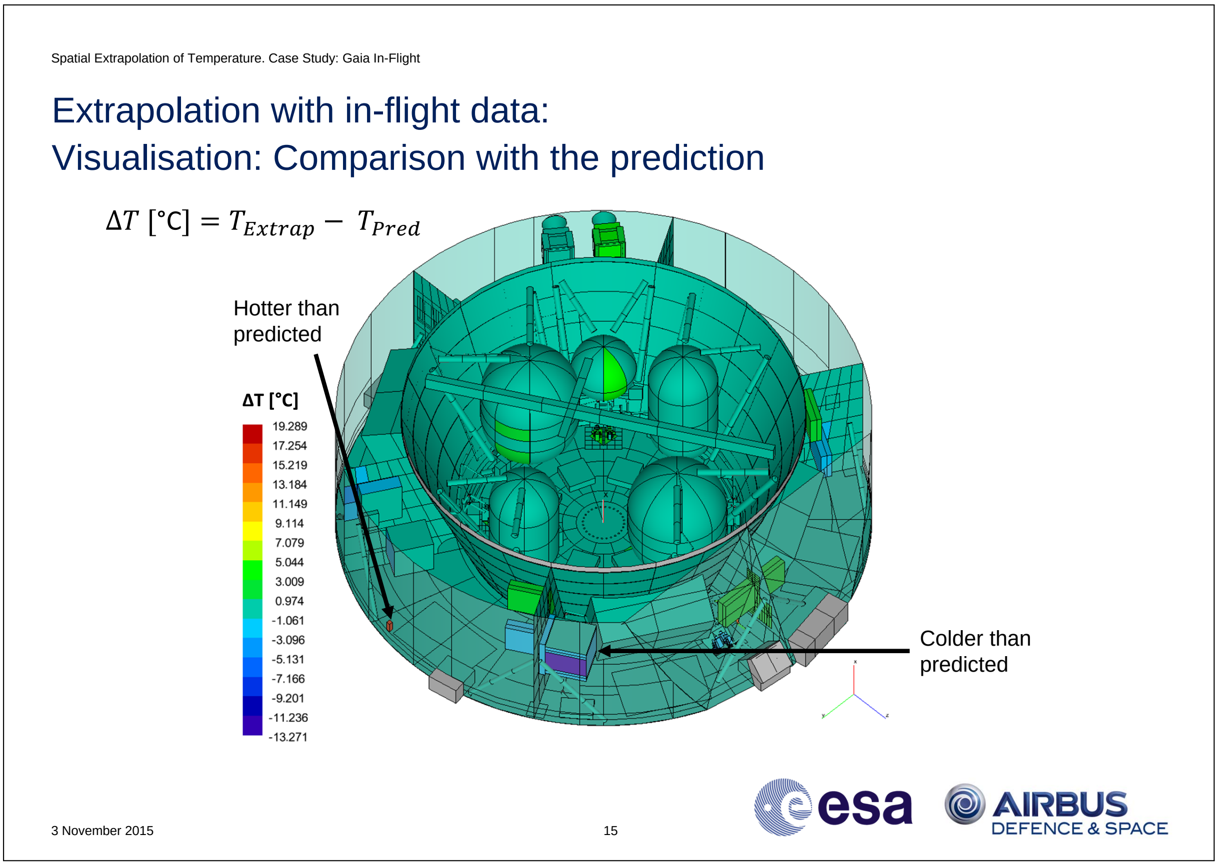

Visualisation - Differences

- So the turquoise / green colour shows a small near zero difference
- It can be seen that there is a uniform distribution across the satellite
- Some units are seen to be hotter and colder than predicted
- The thermal engineer can then revisit the dissipations or modelling assumptions
- Gives the engineer a fast check during a correlation to view localised effects.

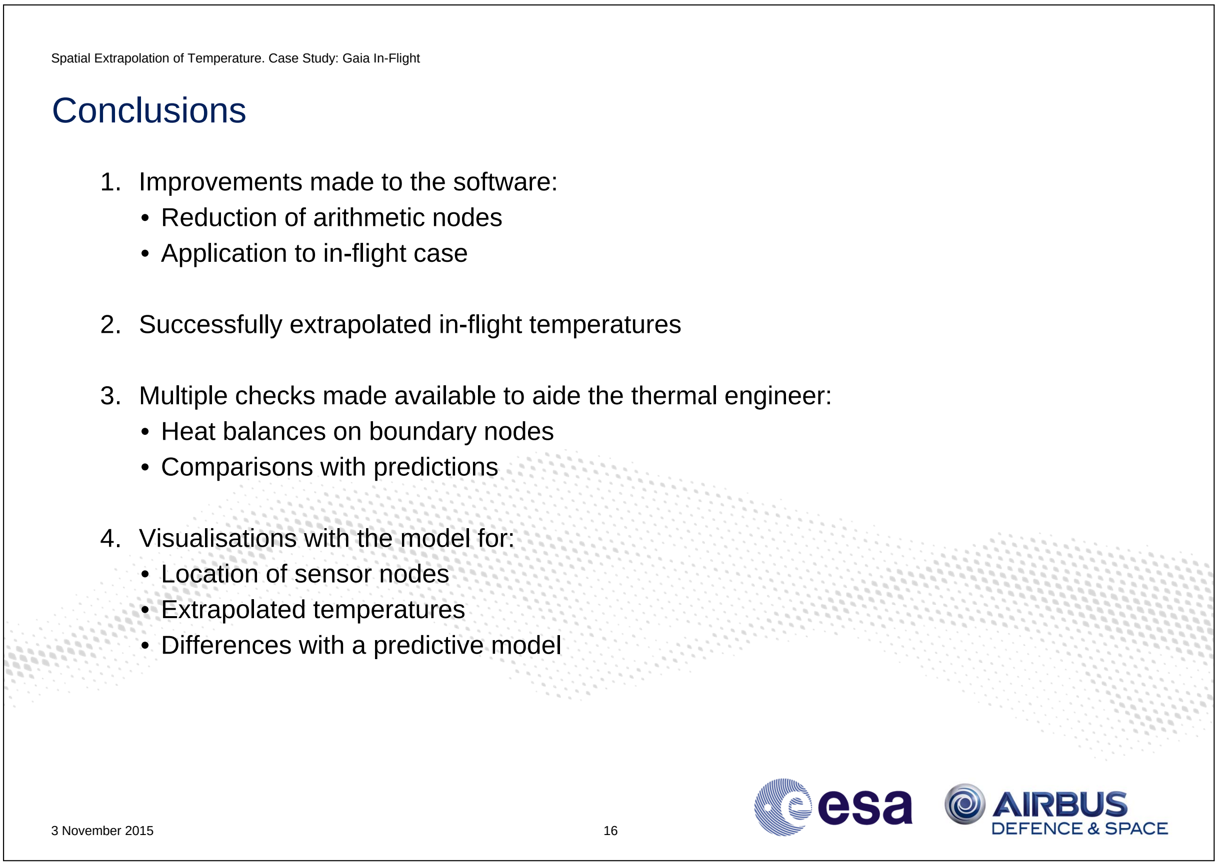

Conclusions

- We generated a full flight map of temperatures as an aide for the thermal engineer.
- This could help in the correlation process to identify temperatures of units with malfunctioning sensors
- We note that in the case of flight where fewer temperature sensors are available, the overall temperatures are not greatly impacted by the change seen on the sensor nodes. However it could be useful for localised checks in the vicinity of units.
- We have been able to reproduce a live thermal view of an in-flight spacecraft with software that can be run live as telemetry is downloaded.

Questions received during the workshop

Q: Have you performed any tests on a unit level to verify the results?

A: We have not performed tests on a unit level but instead on a spacecraft level during thermal balance testing. The techniques have shown good results on a variety of telecommunications and earth observation spacecraft. During these case studies we typically have more thermocouples available and therefore able to produce a better quality map of temperatures.

Q: How can you be sure that the temperatures you calculate are 'real'?

A: This comes down to the equations used in the algorithm. The algorithm is based on solving a system of differential equations representing a collection of nodal heat balances similar to a thermal solver. The physics of the extrapolation are captured inside of the thermal model using the sensor data as transient boundary conditions.

Appendix I

Accelerating ESATAN-TMS Thermal Convergence for Strongly Coupled Problems

Christian Wendt Sébastien Girard
(Airbus Defence and Space, Germany)

Abstract

ESATAN-TMS Thermal solves the heat conductance differential equation (DE) for the lumped parameter thermal network node temperatures considering heat sources as well as linear (also one way) and quartic (radiative) heat exchanges between the nodes. Extensions to this modeling are available for fluid loops and ablation, namely FHTS and ABLAT. However, embedding other relevant thermodynamic phenomena, as e.g. ice sublimation during ascent of a launcher or pressurization/depressurization of a vessel, may provoke other strongly coupled heat sources and additional, segregated DE, which may impact the accuracy of the result. Even then one will usually succeed in reaching the required accuracy by choosing sufficient small time-steps, but at the cost of significantly increased CPU time. An innovative method based on a predictor-corrector-method (PCM), representing a workaround for accelerating the convergence, has been implemented and will be explained here. This method uses standard ESATAN entities only, i.e. auxiliary nodes, heat sources and one way linear conductors. For the example of ice sublimation during launcher's ascent this method is explained in detail and the benefit is demonstrated in conjunction with a specific solver option provided by ESATAN-TMS Thermal software developers in the frame of this work. Using this innovative method the time-step can be increased by nearly a factor of 100 for the given example.

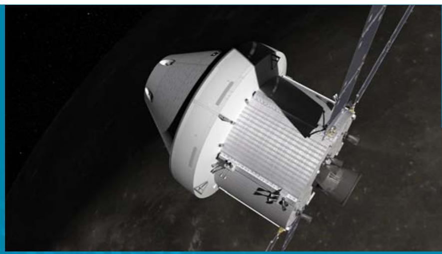

Accelerating ESATAN's Convergence for Strongly Coupled Problems

Christian Wendt, Sébastien Girard,
Airbus DS
03.11.2015

AIRBUS DEFENCE & SPACE

Accelerating ESATAN's Convergence for Strongly Coupled Problems

TEB 1 VEHICLE ENGINEERING

Agenda

- Introduction
- Proposed Predictor-Corrector Method (PCM)
- Demonstration case: Ice sublimation
- Improvement for ice sublimation induced by the method
- Conclusion and next steps

17 November 2015 2

AIRBUS DEFENCE & SPACE

TEB 1 VEHICLE ENGINEERING

Introduction

- Problem
  - Strongly coupled heat sources and additional, segregated Differential Equations (DE) within ESATAN (which solely solves for the heat conductance DE) may impact the accuracy of the results
  - Usually, sufficient small time-steps succeed in reaching the required accuracy, BUT at the cost of CPU time
  - Thus, ways have been studied to accelerate ESATAN's convergence for a required time-step
  - Example outlined here is for ice sublimation during launcher's ascent (strong coupling comes from huge amount of latent heat of ice sublimation of about 3 MJ/kg)

- Methods studied
  - Enabling SLCRNC, benefit from control-constant METHOD has been systematically studied:
    - METHOD=0 (default): $VARIABLES1 is called once for the forward step and twice for the backward step
    - METHOD=2: $VARIABLES1 is called at every iteration, BUT at the cost of CPU time
  - Workaround to accelerate convergence by linear approximation (predictor-corrector-method PCM) is based on ESATAN basic features:

$$Y = Y|_{T^{old}} + \left.\frac{\partial Y}{\partial T}\right|_{T^{old}} \delta T$$

$$\text{where } \delta T = T - T^{old} \text{ is the difference of temperature } T^{old} \text{ at } \$VARIABLES1 \text{ access}$$
$$\text{and the current temperature } T \text{ of the iteration}$$

AIRBUS DEFENCE & SPACE

Accelerating ESATAN's Convergence for Strongly Coupled Problems

TEB 1 VEHICLE ENGINEERING

Proposed PCM

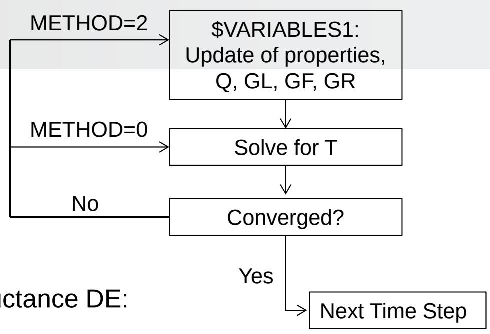

Recall of the general Lumped Parameter heat conductance DE:

$$C_i \frac{dT_i}{dt} = Q_i + \sum_{j \neq i} GL(T_j, T_i)(T_j - T_i) + \sum_{j \neq i} GF(T_j, T_i)(T_j - T_i) + \sum_{j \neq i} GR(T_j, T_i)(Tj^4 - Ti^4)$$

PCM for an affected temperature node:

$$C \frac{dT}{dt} = Q + GF(T^{old}, T)(T^{old} - T)$$

where:

T^{old}	temperature at \$VARIABLES1 access
T	current temperature of the iteration
$Q = f(..., T^{old})$	heat source
$GF(T^{old}, T) = -\frac{\partial f}{\partial T}$	

AIRBUS DEFENCE & SPACE

TEB 1 VEHICLE ENGINEERING

Proposed PCM, cont'd

PCM for an affected auxiliary variable node with C=0 (arithmetic node):

$0 = Q + GF(0, X)(0 - X) + GF(\delta T/2, X)(\delta T/2 - X)$ $\Rightarrow X = X^{old} + \frac{\partial X}{\partial T}\delta T$

where:
X *auxillary variable*

$\delta T/2 = (T^{old} - T)/2$
derived from an arithmetic node containing $\delta T/2$*:*
$0 = GF(T, \delta T/2)(T - \delta T/2) + GF(T^{old}, \delta T/2)(T^{old} - \delta T/2)$
with $GF(T, \delta T/2) = GF(T^{old}, \delta T/2) = 1$

$$Q = X^{old}\left(1 + \left(\frac{1}{2\frac{\partial X}{\partial T}} - 1\right)^{-1}\right)$$

$GF(0, X) = 1$

$$GF(\delta T/2, X) = \left(\frac{1}{2\frac{\partial X}{\partial T}} - 1\right)^{-1}$$

AIRBUS DEFENCE & SPACE

Accelerating ESATAN's Convergence for Strongly Coupled Problems

TEB 1 VEHICLE ENGINEERING

Proposed PCM: Explanation of $\delta T/2$ Calculation-Scheme

D1 : T1	*current ice surface temperature of the iteration*
$B2: T2 = -T^{old}$	*at $VARIABLES1 access*
D3 : T3	*half of temperature difference, C3=0*

0=GF(1,3) (T1-T3) + GF(2,3) (T2-T3)
with
GF(1,3) = 1
GF(2,3) = 1

$\Rightarrow$ *T3=(T1+T2)/2*
$\widehat{=}$ $T3 = (T - T^{old})/2$

$\Rightarrow$ T3= δT/2

AIRBUS DEFENCE & SPACE

Accelerating ESATAN's Convergence for Strongly Coupled Problems

Proposed PCM: Explanation of X Calculation-Scheme

D1: T1=X *auxiliary variable, C1=0*
B2: T2=0
D3: T3=δT/2 *half of temperature difference, C3=0*

0=Q1 +GF(2,1) (T2-T1) + GF(3,1) (T3-T1)
with

$$Q1 = X^{old}\left(1+\left(\frac{1}{2\frac{\partial X}{\partial T}}-1\right)^{-1}\right) \quad \textit{at \$VARIABLES1 access}$$

GF(2,1) = 1

$$GF(3,1) = \left(\frac{1}{2\frac{\partial X}{\partial T}}-1\right)^{-1}$$

$$\Rightarrow 0 = X^{old}\left(1+\left(\frac{1}{2\frac{\partial X}{\partial T}}-1\right)^{-1}\right) - T1 + \left(\frac{1}{2\frac{\partial X}{\partial T}}-1\right)^{-1}(T3-T1)$$

$$\Leftrightarrow T1\left(1+\left(\frac{1}{2\frac{\partial X}{\partial T}}-1\right)^{-1}\right) = X^{old}\left(1+\left(\frac{1}{2\frac{\partial X}{\partial T}}-1\right)^{-1}\right) + \left(\frac{1}{2\frac{\partial X}{\partial T}}-1\right)^{-1} T3$$

$$\Leftrightarrow T1 = X^{old} + \left(\frac{1}{2\frac{\partial X}{\partial T}}-1\right)^{-1} \Big/ \left(1+\left(\frac{1}{2\frac{\partial X}{\partial T}}-1\right)^{-1}\right) T3$$

$$\Rightarrow T1 = X^{old} + \frac{\partial X}{\partial T}\delta T$$

17 November 2015 7

Accelerating ESATAN's Convergence for Strongly Coupled Problems

Ice Sublimation during Ascent: Description

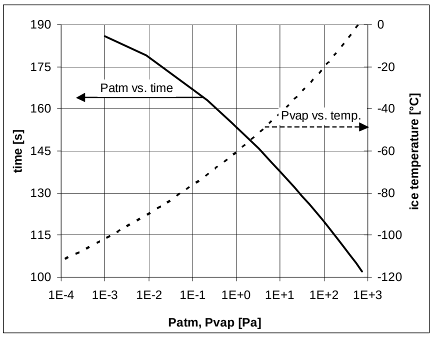

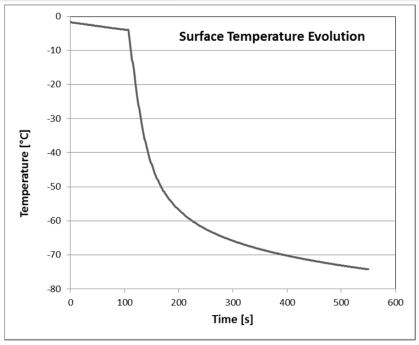

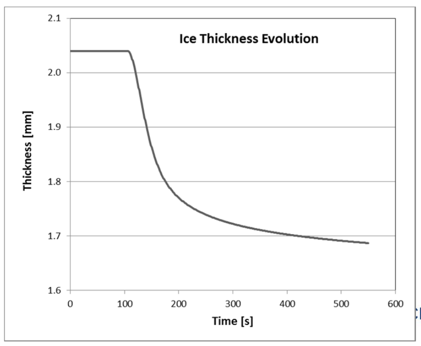

$$\dot{m} = \frac{\gamma \cdot \left(p_{vap} - p_{amb}\right)}{\sqrt{\frac{2 \cdot \pi \cdot \Re \cdot T}{M_{H_2O}}}}$$ Ice sublimation flow rate (Hertz-Knudsen) [kg/s/m²]

$$Q = A \cdot \dot{m} \cdot H$$ Ice cooling rate [W]

$$\dot{\tau} = \frac{\dot{m}}{\rho}$$ Ice thickness reduction rate [m/s] (additional, segregated DE)

17 November 2015 8

Ice Sublimation during Ascent: Implementation of PCM

Ice surface temperature T-PCM:

$$C\frac{dT}{dt} = Q + GF(T^{old}, T)(T^{old} - T)$$

where:

$$Q = A\ \dot{m}^{old} H$$

$$GF(T^{old}, T) = -H\frac{\partial \dot{m}}{\partial T}$$

Ice sublimation rate M-PCM:

$$0 = Q + GF(0, \dot{m})(0 - \dot{m}) + GF(\delta T/2, \dot{m})(\delta T/2 - \dot{m})$$

$$\Rightarrow \dot{m} = \dot{m}^{old} + \frac{\partial \dot{m}}{\partial T}\delta T$$

where:

$$GF(0, \dot{m}) = 1$$

$$Q = \dot{m}^{old}\left(1 + \left(\frac{1}{2\frac{\partial \dot{m}}{\partial T}} - 1\right)^{-1}\right)$$

$$GF(\delta T/2, \dot{m}) = \left(\frac{1}{2\frac{\partial \dot{m}}{\partial T}} - 1\right)^{-1}$$

Ice vapor pressure P-PCM:

$$0 = Q + GF(0, p)(0 - p) + GF(\delta T/2, p)(\delta T/2 - p)$$

$$\Rightarrow p = p^{old} + \frac{\partial p}{\partial T}\delta T$$

where:

$$GF(0, p) = 1$$

$$Q = p^{old}\left(1 + \left(\frac{1}{2\frac{\partial p}{\partial T}} - 1\right)^{-1}\right)$$

$$GF(\delta T/2, p) = \left(\frac{1}{2\frac{\partial p}{\partial T}} - 1\right)^{-1}$$

Ice Sublimation during Ascent: Network

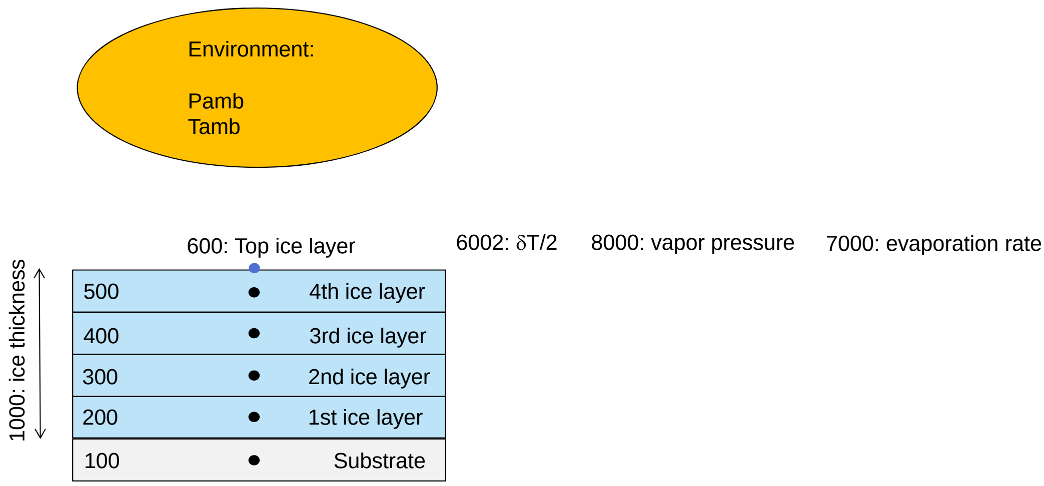

Accelerating ESATAN's Convergence for Strongly Coupled Problems

Ice Sublimation during Ascent: Cases

Duration: 0 … 550s
Required time resolution: 1s

Time steps: 0.0001s (reference)
0.01s
0.1s
0.5s
1s

SLCRNC	Convergence Acceleration		
METHOD=0	NOMINAL (w/o PCM)	T-PCM	TMP-PCM
METHOD=2	NOMINAL (w/o PCM)	T-PCM	TMP-PCM

AIRBUS DEFENCE & SPACE

17 November 2015 11

Accelerating ESATAN's Convergence for Strongly Coupled Problems

Ice Sublimation during Ascent: Max Deviations for METHOD=0

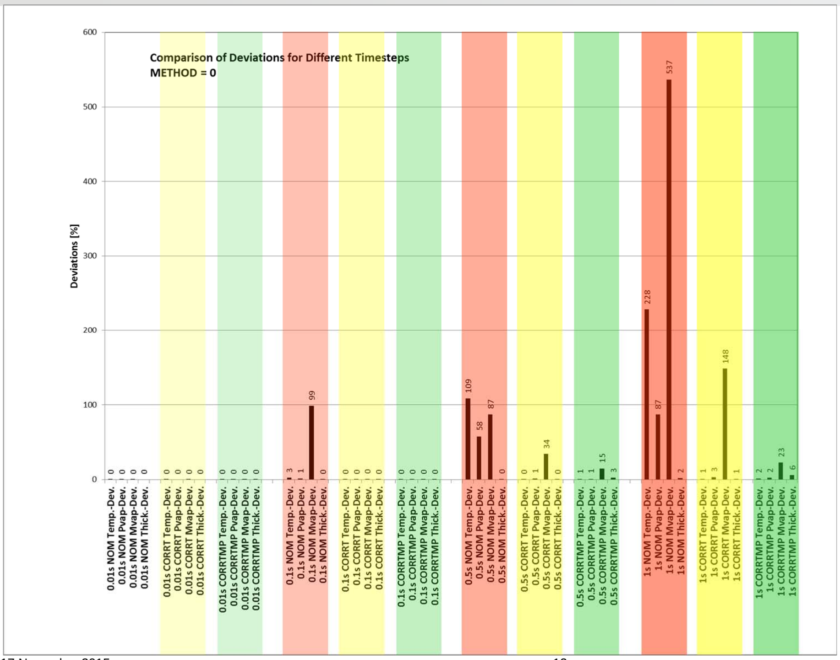

AIRBUS DEFENCE & SPACE

17 November 2015 12

Accelerating ESATAN's Convergence for Strongly Coupled Problems

Ice Sublimation during Ascent: Max Deviations for METHOD=2

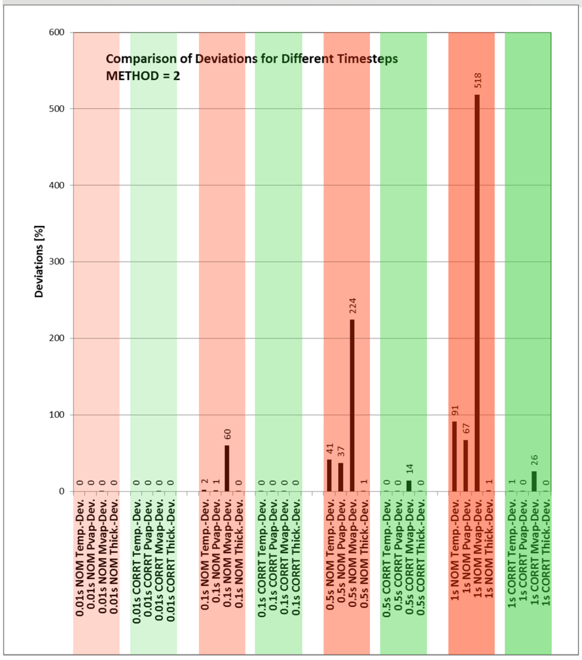

No significant benefit from *M-PCM* und *P-PCM* *correction*

17 November 2015 13

AIRBUS DEFENCE & SPACE

Accelerating ESATAN's Convergence for Strongly Coupled Problems

Conclusion

- PCM workaround for strongly coupled and additional DE generally explained:
  - PCM for temperature node
  - PCM for auxillary variable node (airthmetic)

- Example given concerning ice sublimation during ascent:
  - SLCRNC with METHOD=0 and METHOD=2 studied
  - Ice surface temperature correction: T-PCM
  - Ice sublimation rate correction: M-PCM (arithmetic)
  - Ice vapor pressure correction: P-PCM (arithmetic)
  - Ice thickness reduction DE

  ➢ Exact results are obtained without PCM with a time-step of 0.01s
  ➢ With a time-step of 1s correct results have been achieved
    ➢ For METHOD=0 with TMP-PCM
    ➢ For METHOD=2 with T-PCM (M-PCM and P-PCM in addition give no significant improvement)

➢ Need for dedicated System Elements and a general way to couple more thermodynamic equations to ESATAN‘s heat conductance DE,
as e.g. ice sublimation, pressurization / depressurization of a vessel, …

17 November 2015 14

AIRBUS DEFENCE & SPACE

Appendix J

OHB System
Thermal Result Viewer

Markus Czupalla S. Rockstein C. Scharl M. Matz
(OHB System, Germany)

Abstract

Driven by mission demands for improved performance, more precise prediction etc. a trend is observed to bigger thermal models simulated with a high transient resolution. The built-in post- processing capabilities of commercial software codes often cannot cope with the model and result file sizes. Further the necessary post-processing is split over multiple tools which are often not easy to handle.
Over the last couple of years an integral thermal post-processing tool has been developed at OHB Munich, which combined the necessary capabilities and offers a convenient and fast user I/F. The Thermal Result Viewer (TRV) has among others the following main features:

- Import of result files in different formats:
  - *.TMD
  - *.out
  - *.csv
- Import of the model structure from different sources:
  - GMM model (*.erg)
  - TMM result file (*.TMD)
  - Excel list (*.xlsx)
  - Manual setting in the program
- Simultaneous visualization of 3-D and 2-D temperature and heat flux maps and plots for selected groups
- Transient group based visualization of the internal hat fluxes in a model (conductive and radiative) – without the necessity to program it into the TMM beforehand.
- Easy and intuitive graphical user Interface (GUI)

A Demonstration of the TRV functionality will be presented and discussed in the presentation.

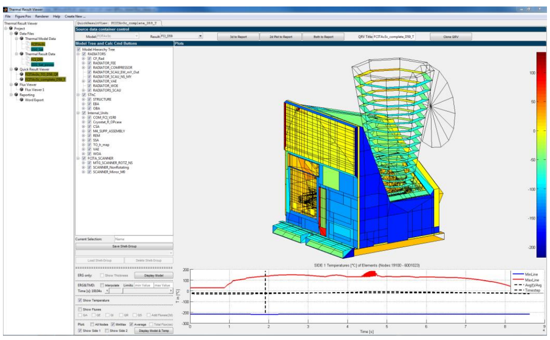

Figure J.1: Example Temperatures Visualization in TRV

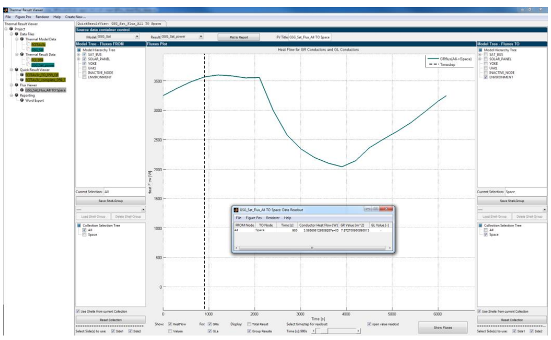

Figure J.2: Example Heat Flux Visualization in TRV

OHB System AG
Markus Czupalla
03.11.2015

SPACE SYSTEMS

OHB System – Thermal Result Viewer

We. Create. Space.

Table of Contents

Seite 2 OHB System AG

Thermal Result Viewer - Rationale

- Need to quickly and efficiently post-process and visualize:
  - Temperatures:
    - transient evolutions
    - 3-D maps
  - Fluxes:
    - Environmental (QS, QA, QE, etc.)
    - Heat flows between parts (conductive, radiative) → establish heat flux budgets in post-processing
- Be able to work with or without GMM
- Allow easy grouping
  - re-using of available model structure
  - customized groups from excel
  - Manual group setup in GUI
- All is also possible with other tools (in ESATAN-TMS, Excel, Therm-NV etc.) but with significant effort.

→ **Efficiency increase and ease of use were and are the main targets for the TRV**

Seite 3 OHB System AG

Thermal Result Viewer – Modules

- TRV is setup in a modular object oriented fashion
- Development is centralized on a server accessible to all OHB colleagues
- The TRV modules are:
  - **Data files** → import of data and sorting (optional)

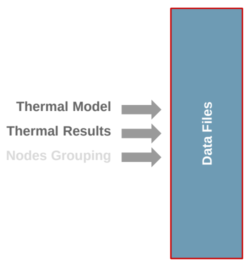

Seite 4 OHB System AG

Thermal Result Viewer – Modules

- TRV is setup in a modular object oriented fashion
- Development is centralized on a server accessible to all OHB colleagues
- The TRV modules are:
  - **Data files** → import of data and sorting (optional)
  - **Quick Result Viewer** → temperature and environmental fluxes visualization

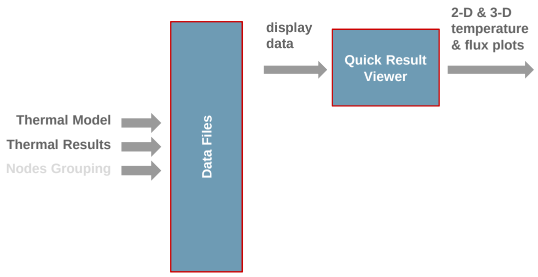

Seite 5 OHB System AG

Thermal Result Viewer – Modules

- TRV is setup in a modular object oriented fashion
- Development is centralized on a server accessible to all OHB colleagues
- The TRV modules are:
  - **Data files** → import of data and sorting (optional)
  - **Quick Result Viewer** → temperature and environmental fluxes visualization
  - **Flux viewer** → heat flow visualization

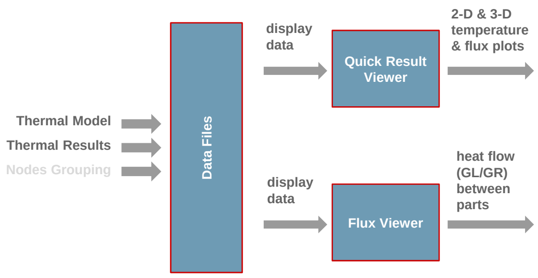

Seite 6 OHB System AG

Thermal Result Viewer – Modules

- TRV is setup in a modular object oriented fashion
- Development is centralized on a server accessible to all OHB colleagues
- The TRV modules are:
  - **Data files** → import of data and sorting (optional)
  - **Quick Result Viewer** → temperature and environmental fluxes visualization
  - **Flux viewer** → heat flow visualization
  - **Reporting** → fine post-processing of figures and export

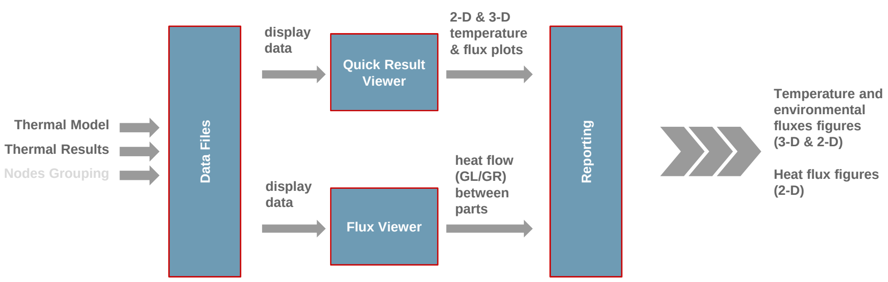

Seite 7 OHB System AG

Thermal Result Viewer – Modules

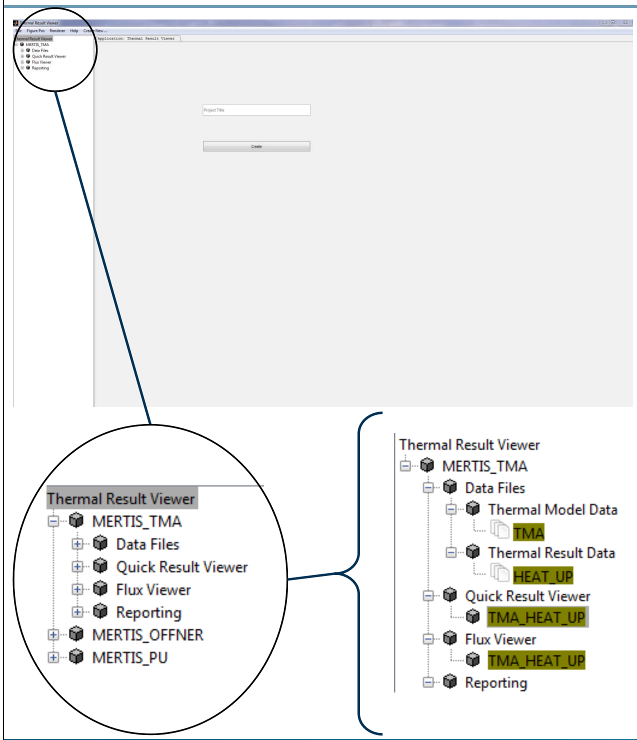

- To start a project/session name is requested
- Multiple projects/sessions can be started in parallel
- Each project/session contains the following modules
  - Date Files
  - Quick Result Viewer
  - Flux Viewer
  - Reporting

Seite 8 OHB System AG

Thermal Result Viewer – Data Files

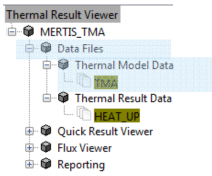

- **Thermal Model Data:**
  - Loading of GMMs in *.erg format
  - Multiple GMMs can be loaded simultaneously
  - GMMs can be named

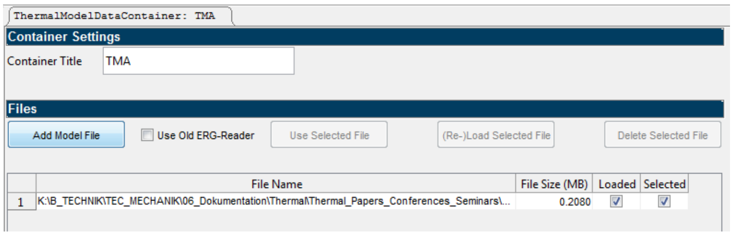

Seite 9 OHB System AG

Thermal Result Viewer – Data Files

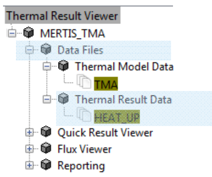

- **Thermal Result Data:**
  - Loading of temperature and flux results in *.TMD format
  - Loading of custom node hierarchies
  - Multiple results can be loaded simultaneously
  - Results can be named

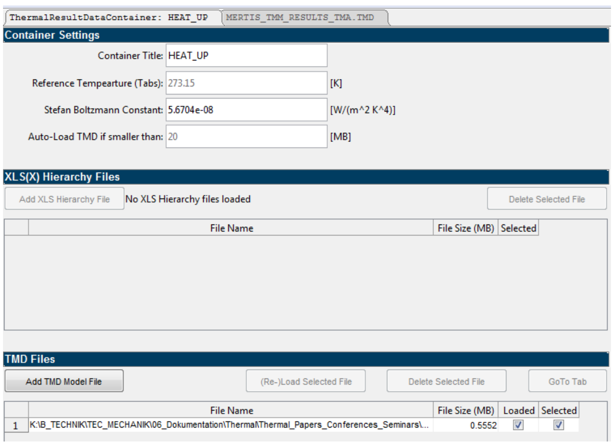

Seite 10 OHB System AG

Thermal Result Viewer – Data Files

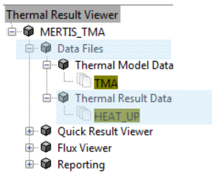

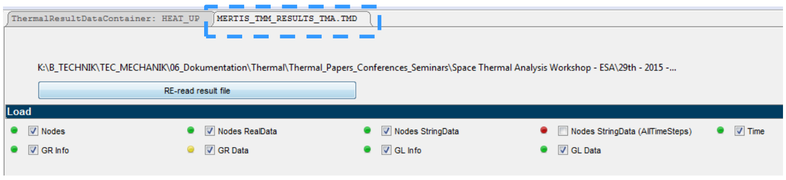

- **Thermal Result Data:**
  - Loading of TMDs in *.erg format
  - Loading of custom node hierarchies
  - Multiple results can be loaded simultaneously
  - Results can be named
  - Parts of results to be loaded and used can be selected (important for big files sizes)
  - Check is possible if needed data is available

Seite 11 OHB System AG

Thermal Result Viewer – Quick Result Viewer

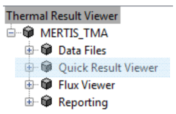

- Used model and used result file must be selected
- Views can be named and multiple can be created

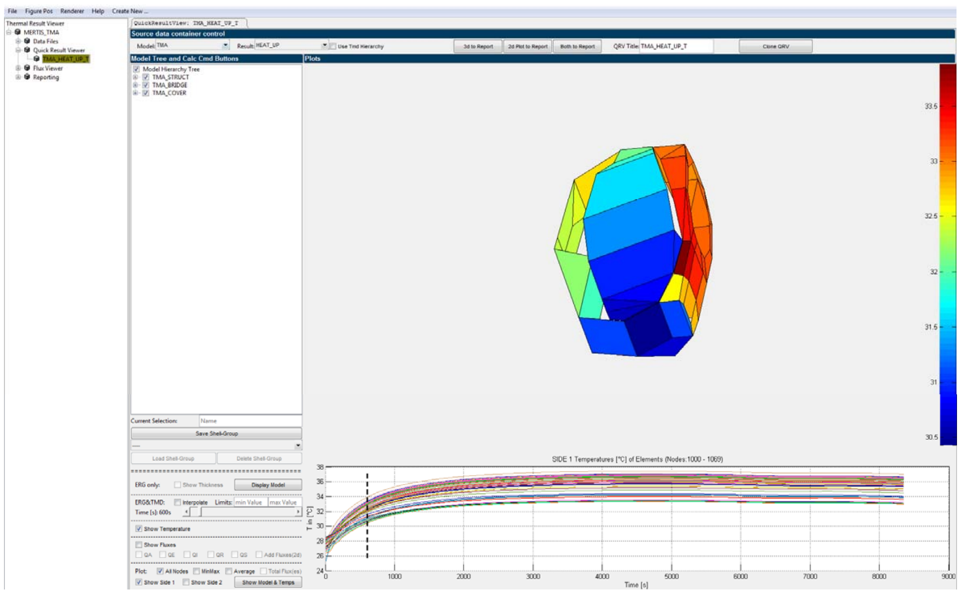

Seite 12 OHB System AG

Thermal Result Viewer – Quick Result Viewer

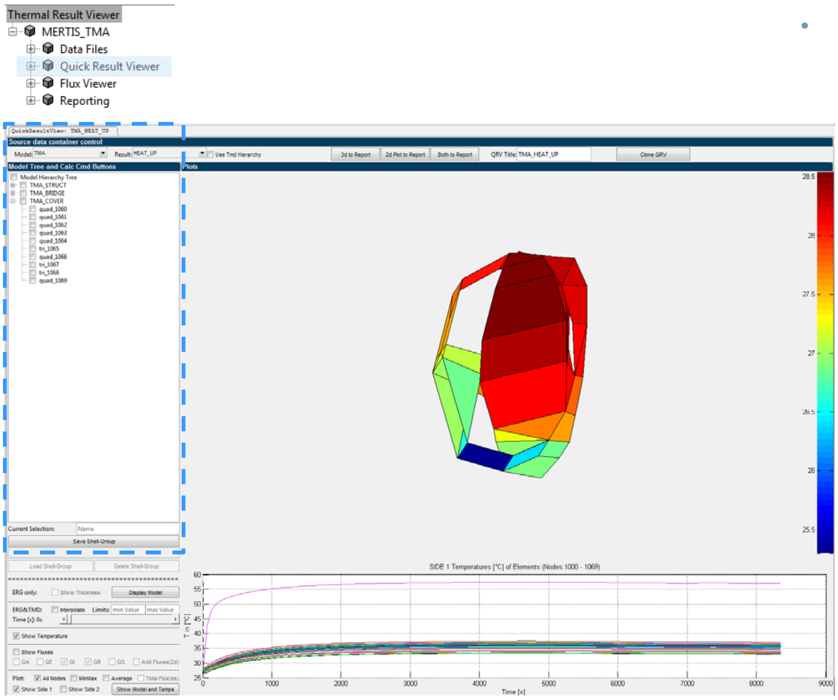

- **Model hierarchy:**
  - Imported from GMM or TMD or customized external files
  - Displayed as foldable tree
  - Shells with no temperatures are greyed out
  - Temperatures with no shells are combined in an "from_TMD" nodes group

Seite 13 OHB System AG

Thermal Result Viewer – Quick Result Viewer

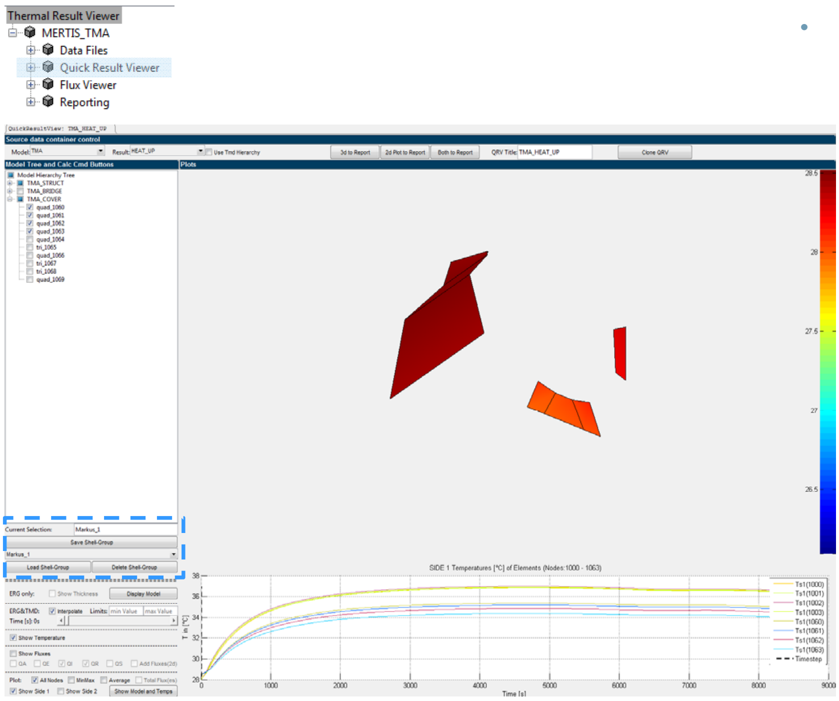

- **Model hierarchy:**
  - Imported from GMM or TMD or customized external files
  - Displayed as foldable tree
  - Shells with no temperatures are greyed out
  - Temperatures with no shells are combined in an "unassigned nodes" group
  - Shells/nodes can be grouped manually an become selectable
  - The manual section is detached from the loaded and valid model structure

    → the model itself cannot be re-structured

Seite 14 OHB System AG

Thermal Result Viewer – Quick Result Viewer

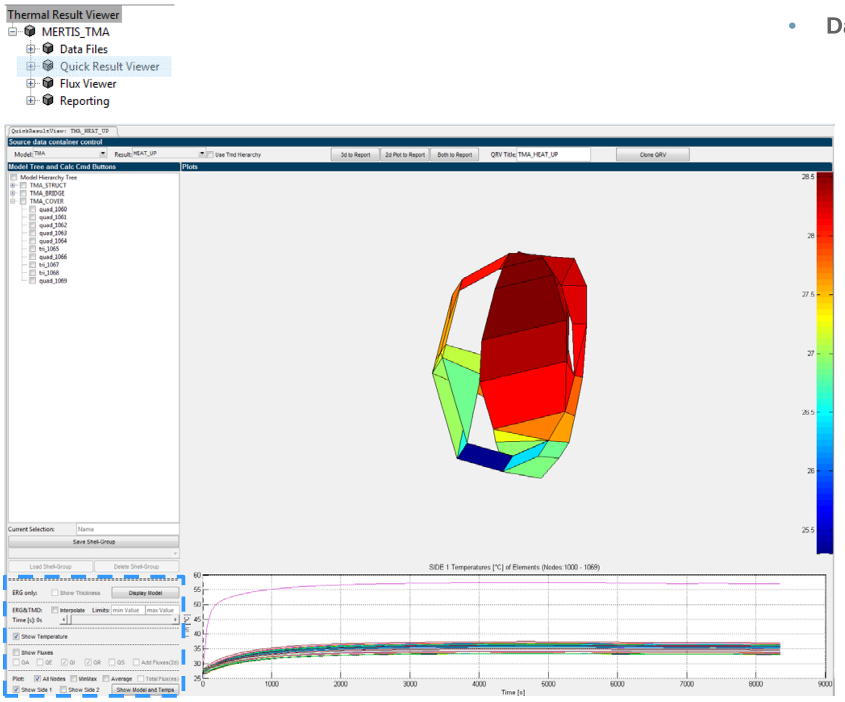

- **Data selection:**
  - Allows selection of items/data to be displayed
  - Model can be displayed stand-alone to visualize the shell thicknesses
  - Color map can be "flat" or "interpolated"

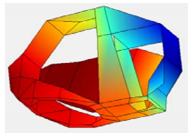

  - Shown time point for 3-D color map can be selected
  - Type of results can be selected (Temperatures, Fluxes)
  - min/max values and/or average values can be displayed
  - Sides of GMM are selectable (e.g. to show MLI)

Seite 15 OHB System AG

Thermal Result Viewer – Quick Result Viewer

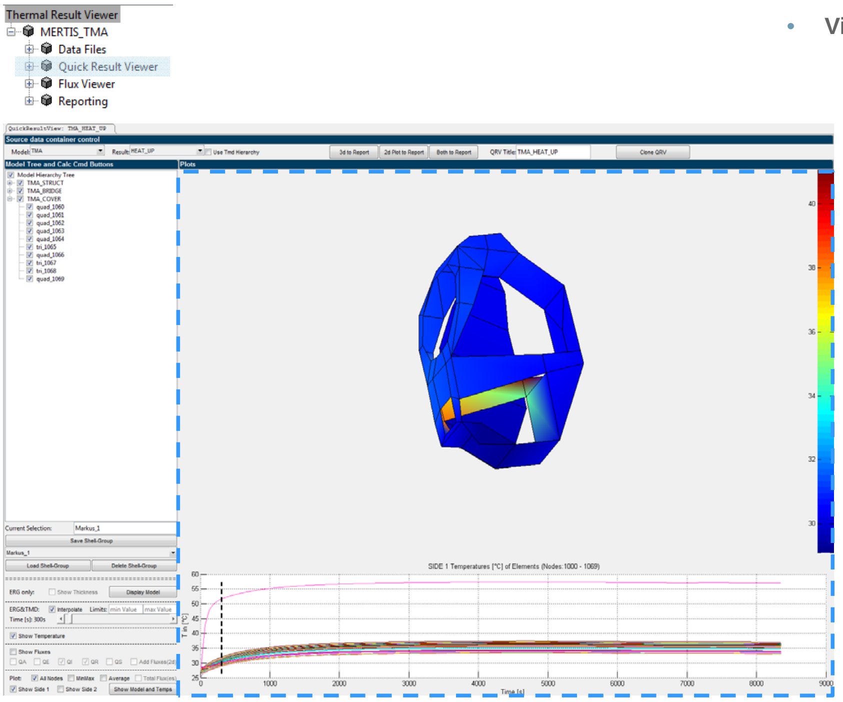

- **Views 3-D/2-D:**
  - 3-D color map and 2-D are displayed simultaneously
  - Shown time point for 3-D color map can be selected and is indicated in the 2-D plot
  - 3-D view can be rotated, zoomed, and paned

Seite 16 OHB System AG

Thermal Result Viewer – Quick Result Viewer

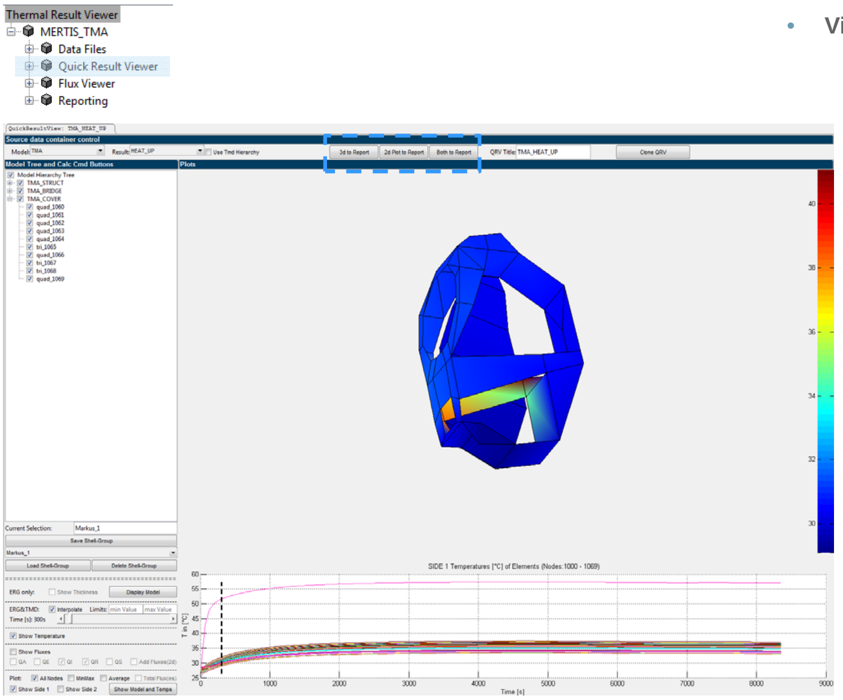

- **Views 3-D/2-D:**
  - 3-D color map and 2-D are displayed simultaneously
  - Shown time point for 3-D color map can be selected and is indicated in the 2-D plot
  - 3-D view can be rotated, zoomed, and paned
  - Plots can be "sent" to the report where thy can be further post processed

Seite 17 OHB System AG

Thermal Result Viewer – Quick Result Viewer

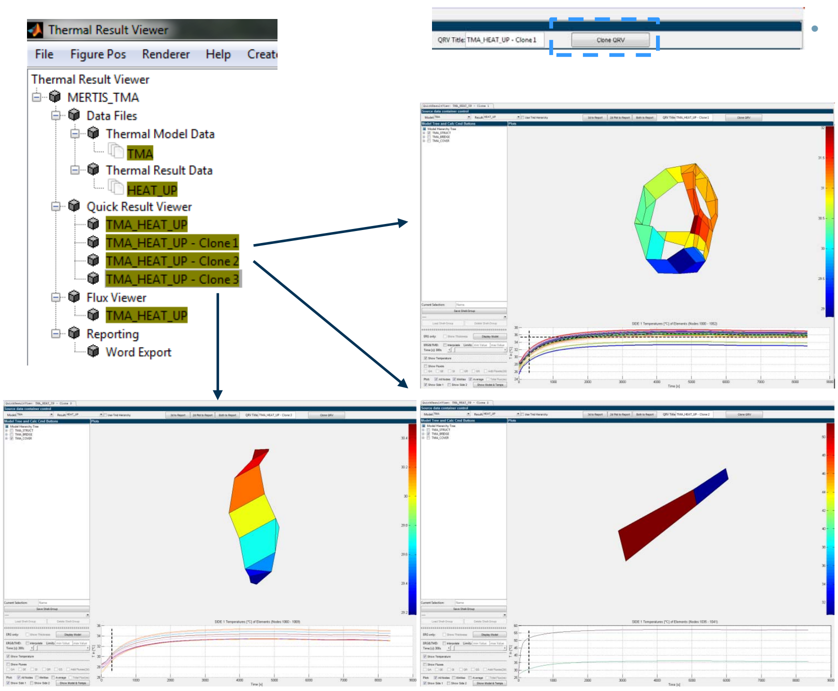

- **Views 3-D/2-D:**
  - 3-D color map and 2-D are displayed simultaneously
  - Shown time point for 3-D color map can be selected and is indicated in the 2-D plot
  - 3-D view can be rotated, zoomed, and paned
  - Plots can be "sent" to the report where thy can be further post processed
  - QRV can be "cloned" to generate multiple views of the same
  - Each view is fully independent of the others
  - Each view can be accessed from the data selection tree

Seite 18 OHB System AG

Thermal Result Viewer – Flux Viewer

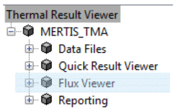

- Allows to visualize the exchanged **heat flows between model parts in the POST-PROCESSING** without the need to program it into the solver a priori
- Used model and used result file must be selected
- Based on Temperatures, GLs and GRs from TMD

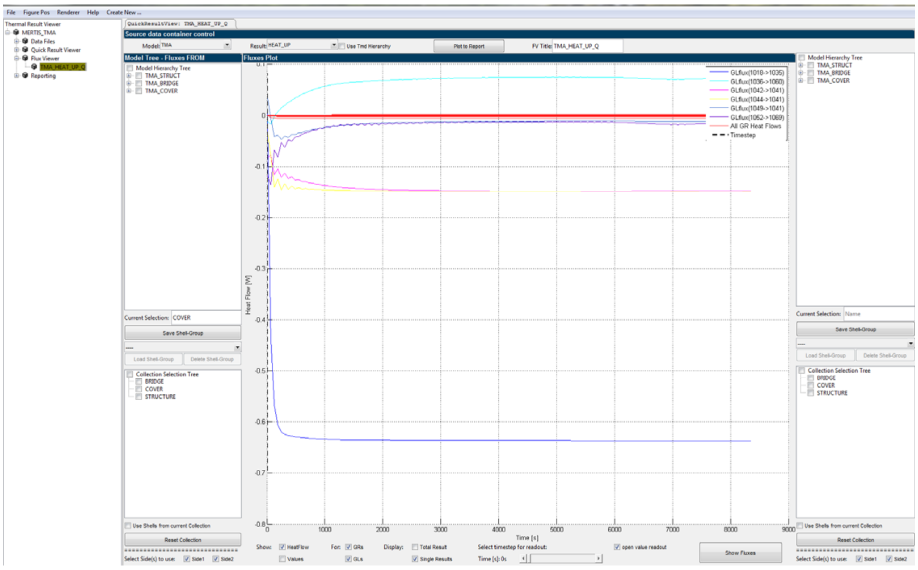

Seite 19 OHB System AG

Thermal Result Viewer – Flux Viewer

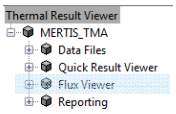

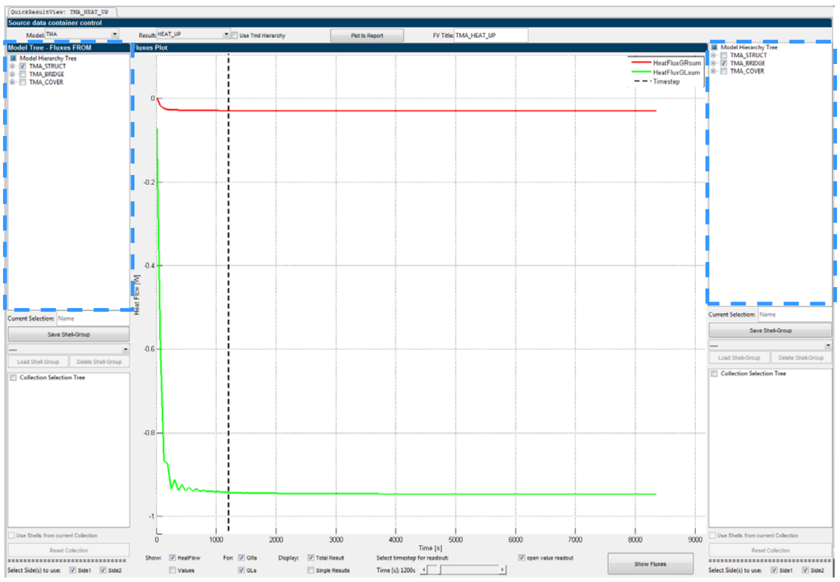

- **Model Hierarchy:**
  - Imported from GMM or TMD
  - Displayed as foldable trees **ON BOTH SIDES**
  - Allows easy selection of flux groups
    - Fluxes FROM → TO

Seite 20 OHB System AG

Thermal Result Viewer – Flux Viewer

OHB

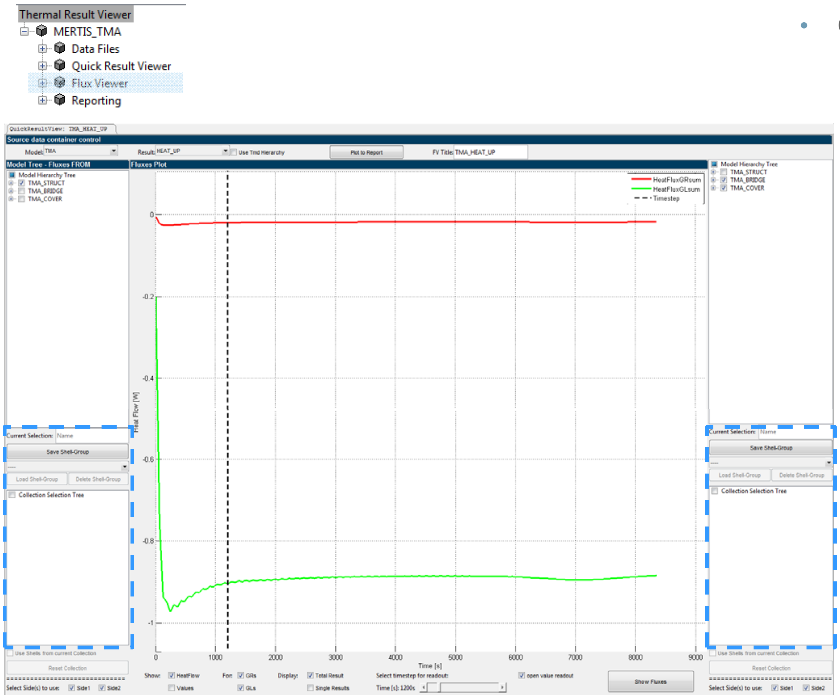

- **Collectors:**
  - Custom node groups can be set up
  - Displayed in separate selection boxes
  - Allows to plot fluxes from one group to multiple groups in one plot
    - The top tree gives either a sum of **all fluxes** or single fluxes from all nodes

Seite 21 OHB System AG

Thermal Result Viewer – Flux Viewer

OHB

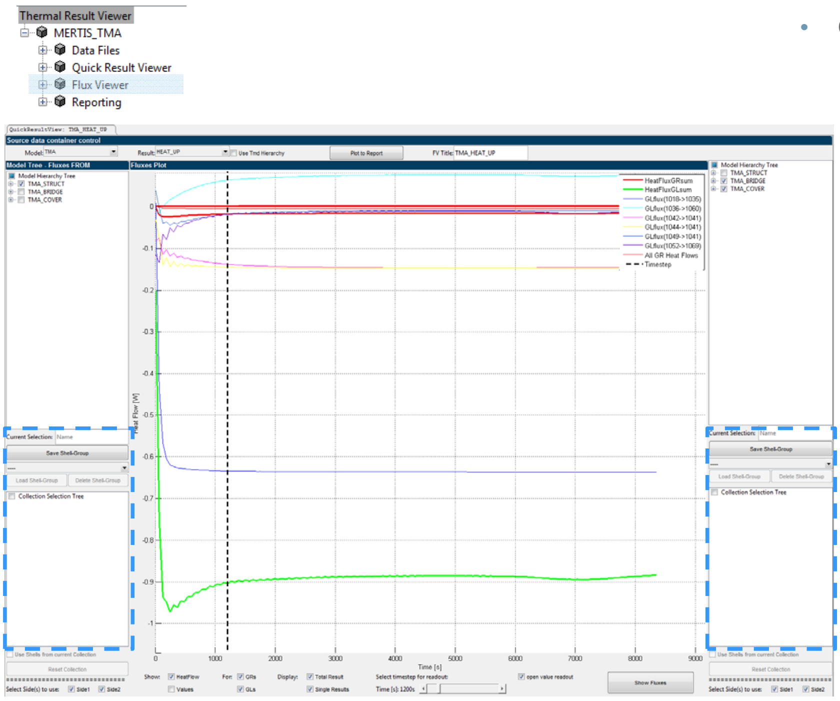

- **Collectors:**
  - Custom node groups can be set up
  - Displayed in separate selection boxes
  - Allows to plot fluxes from one group to multiple groups in one plot
    - The top tree gives either a sum of all fluxes or **single fluxes** from all nodes

Seite 22 OHB System AG

Thermal Result Viewer – Flux Viewer

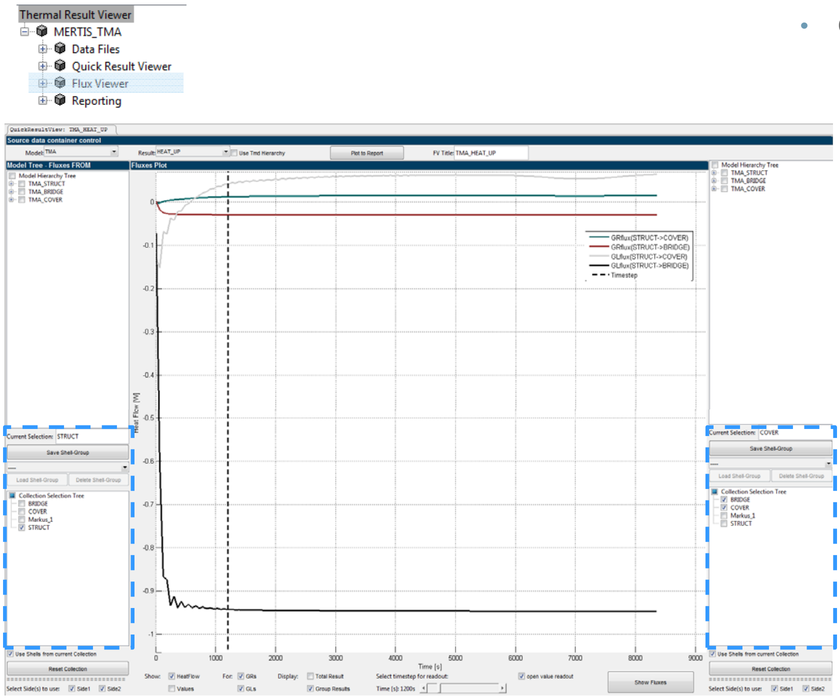

- **Collectors:**
  - Custom node groups can be set up
  - Displayed in separate selection boxes
  - Allows to plot fluxes from one group to multiple groups in one plot
    - The top tree gives either a sum of all fluxes or **single fluxes** from all nodes
    - Sub-groups are needed to allow visualization of partial flux totals

Seite 23 OHB System AG

Thermal Result Viewer – Flux Viewer

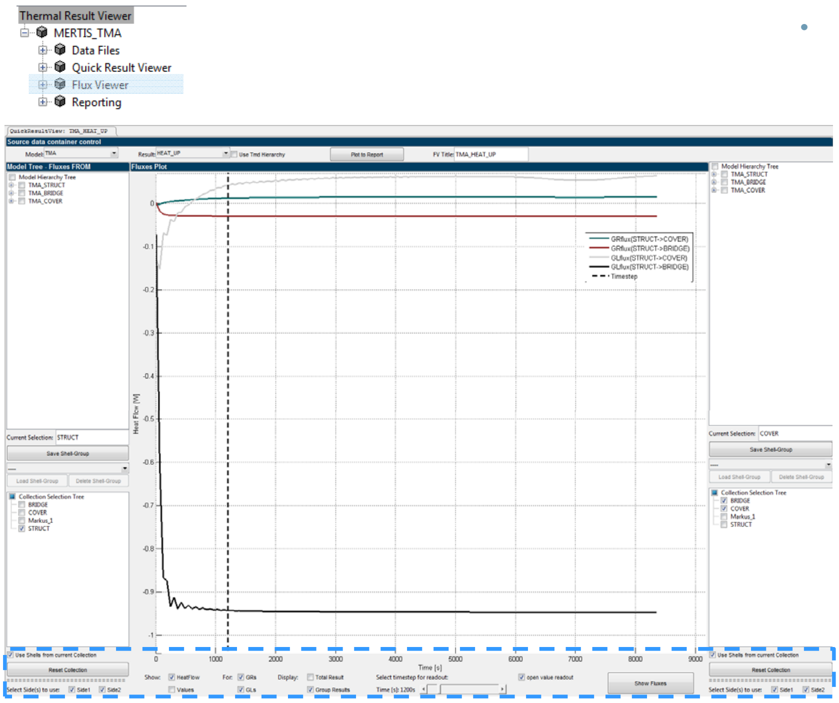

- **Data selection:**
  - Allows selection of items/data to be displayed
  - Heat flows or GL/GR values between groups can be displayed
  - GL and/or GR values/fluxes
  - Total and/or single results can be displayed
  - Shown time point can be selected

Seite 24 OHB System AG

Thermal Result Viewer – Flux Viewer

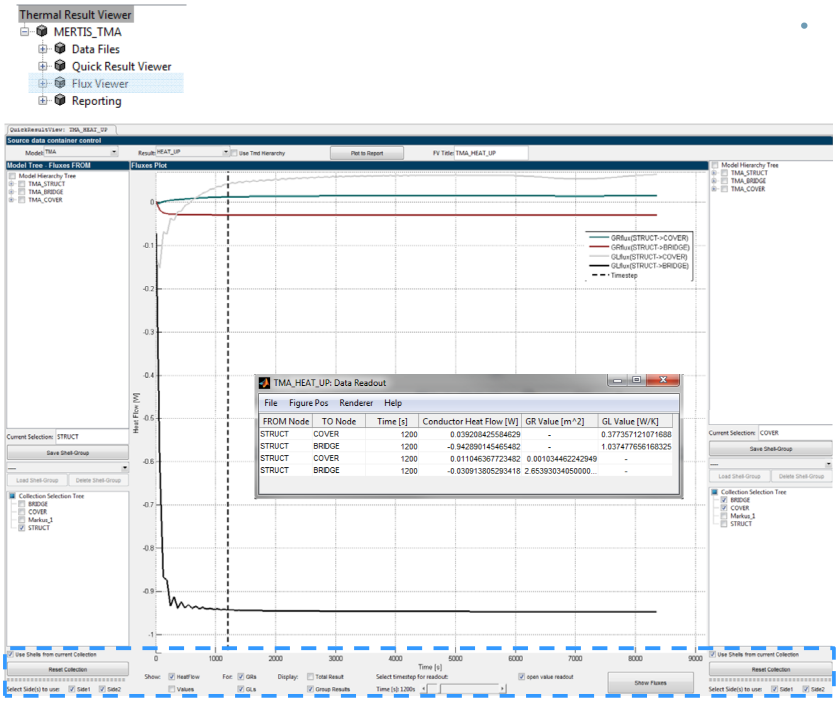

- **Data selection:**
  - Allows selection of items/data to be displayed
  - Heat flows or GL/GR values between groups can be displayed
  - GL and/or GR values/fluxes
  - Total and/or single results can be displayed
  - Shown time point can be selected
  - Precise values for selected time point are displayed as a pop-up table
  - Side 1 and/or side 2 of shells can be selected

Seite 25 OHB System AG

Thermal Result Viewer – Reporting

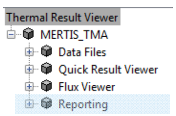

- Allows fine-tuning of selected figures (e.g. annotations)
- Allows export to figures
- Allows export to word (under development)

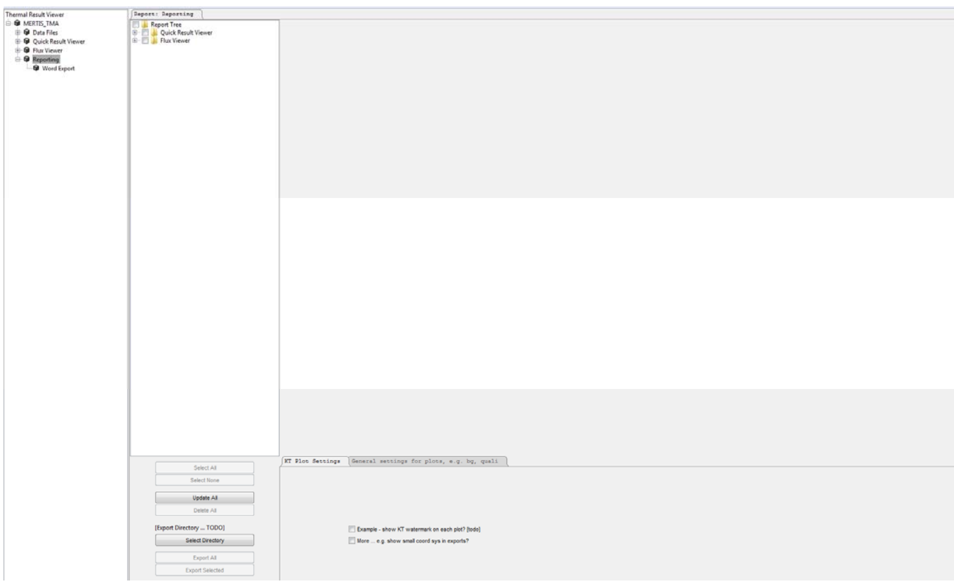

Seite 26 OHB System AG

Thermal Result Viewer – Reporting

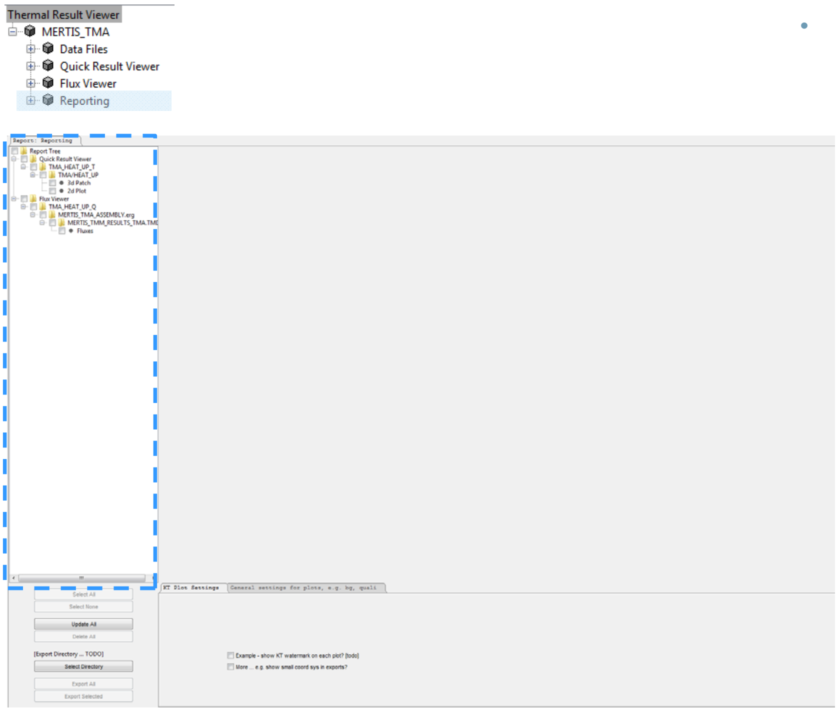

- **Selection Tree:**
  - Allows selection of plots which were sent to the report from quick result viewer or flux viewer
  - Each view can be accessed separately (2-D or 3-D)
  - Each view can be post treated with MATLAB functionalities (e.g. add legend, change axis, annotate, etc.)

Seite 27 OHB System AG

Thermal Result Viewer – Reporting

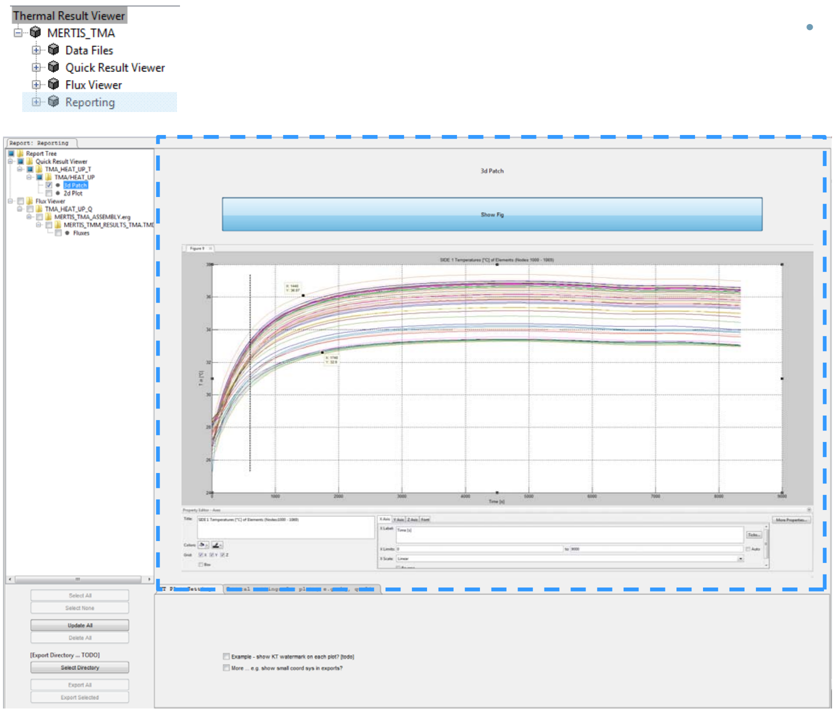

- **Work area:**
  - Each view can be post treated with MATLAB functionalities (e.g. add legend, change axis, annotate, etc.)

Seite 28 OHB System AG

Thermal Result Viewer – Reporting

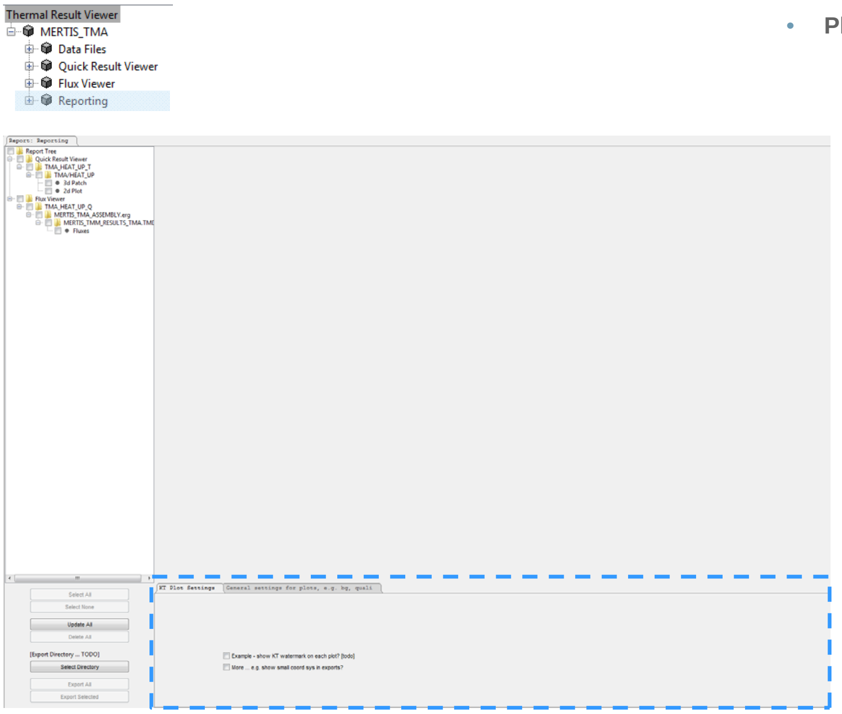

- **Plot settings:**
  - Allows to add watermark
  - Allows to set quality of plots
  - Allows to change font size globally

Seite 29 OHB System AG

Thermal Result Viewer – Reporting

- **Export section:**
  - allows export to picture file formats into dedicated folders

Seite 30 OHB System AG

Thermal Result Viewer – Future Work

- **Batch mode:**
  - Re-use of post-processing templates for:
    - other cases
    - model versions
  - Enable an a priori creation of post-processing templates outside of GUI:
    - Pre-set which parameters of which nodes are to be displayed together in a figure
    - Import setting
    - Export figures
- **Automated Reporting:**
  - Auto export all crated figures
- **Movies:**
  - Enable TRV to show movies of the temperature evolution
- **Model Comparison:**
  - Side by side views of different models or model versions
- **Miscellaneous:**
  - Allow node identification in the plots
    - 3-D → shell picking → highlight node in tree and curve in 2-D
    - 2-D → curve picking → highlight node in tree and in 3-D

Seite 31 OHB System AG

Thermal Result Viewer – summary

- A **T**hermal **R**esult **V**iewer has been developed at OHB
- **It allows:**
  - Quick review of thermal models and thermal results in an integrated environment
    - temperatures → 3-D and 2-D
    - environmental Fluxes → 3-D and 2-D
  - Quick and efficient review of heat flows between parts in a thermal model
    - purely in POST-PROCESSING
    - easy selection and collection options
    - conductive and radiative fluxes can be visualized
  - Automated export of plots into picture files

→ the efficiency of thermal result post-processing has been significantly increased compared to standard state-of the tool combinations

Seite 32 OHB System AG

Appendix K

Overview of ECSS Activities for Space Thermal Analysis

James Etchells
(ESA/ESTEC, The Netherlands)

Abstract

This presentation will provide an overview of the two ongoing ECSS activities in the field of space thermal analysis, in particular:

- ECSS-E-HB-31-03: Thermal analysis handbook
- ECSS-E-ST-3104: Exchange of Thermal Model Data for Space Applications

The thermal analysis handbook will soon be sent out for public review and this workshop therefore provides an opportunity to make the community aware of it.
Concerning the standard on thermal model exchange, this is the formalisation under ECSS of the STEP-TAS protocol. The aims and objectives of the working group will be presented along with some discussion about the expected form of the final standard.

Overview of ECSS Activities for Space Thermal Analysis

James Etchells
James.Etchells@esa.int

02/11/2015

Issue/Revision: 0.0
Reference:
Status: For Information Only
ESA UNCLASSIFIED - For Official Use

European Space Agency

What is ECSS

- ECSS = **E**uropean **C**ooperation for **S**pace **S**tandardization
  - Organization started in 1993
  - task is to develop a common set of **consistent** standards for hardware, software, information and activities to be applied in space projects

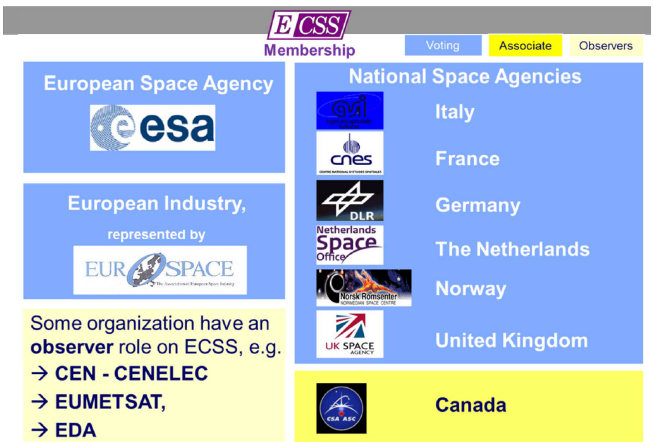

James Etchells | ESTEC | 02/11/2015 | Slide 2
ESA UNCLASSIFIED - For Official Use

European Space Agency

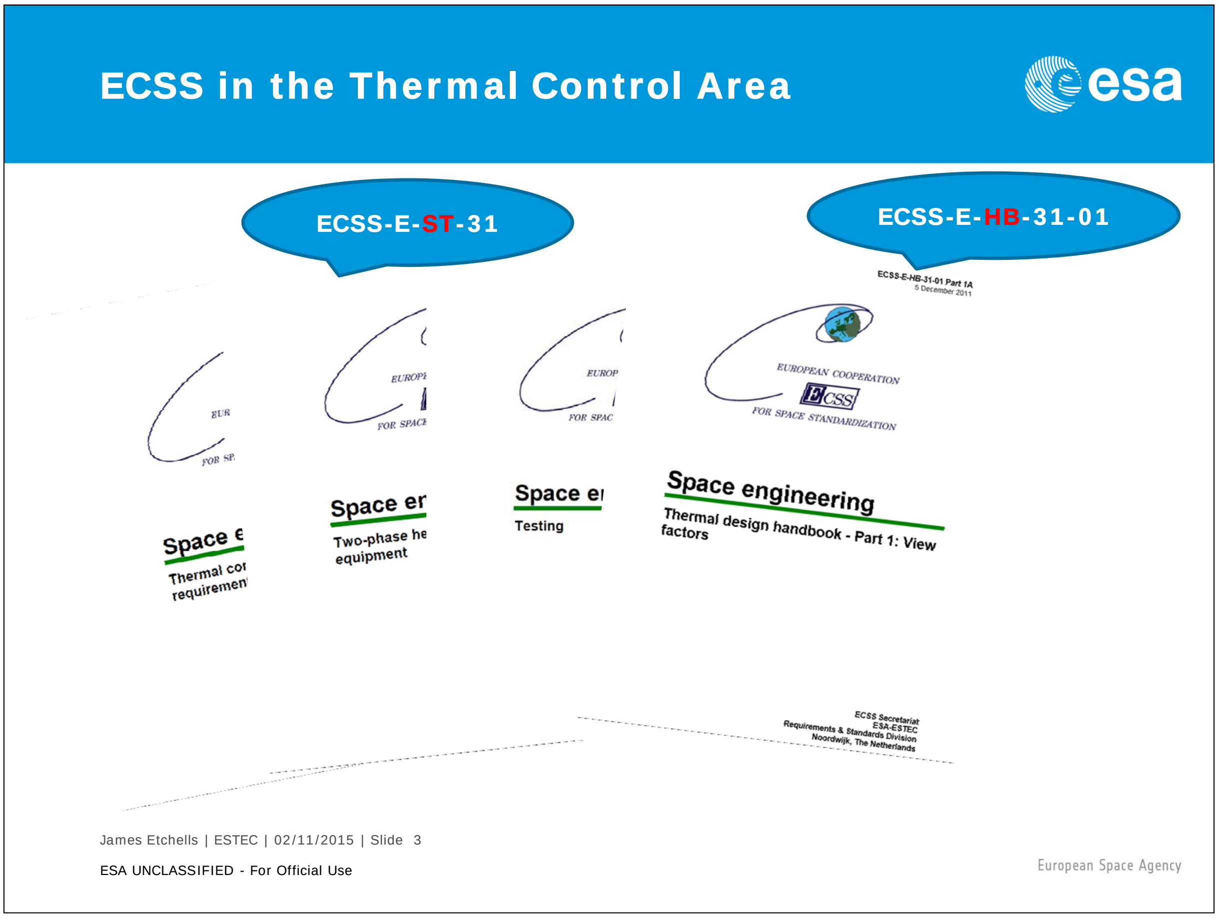
ECSS in the Thermal Control Area
esa
ECSS-E-ST-31
ECSS-E-HB-31-01
ECSS-E-HB-31-01 Part 1A
5 December 2011
EUROPEAN COOPERATION
ECSS
FOR SPACE STANDARDIZATION
Space engineering
Thermal design handbook - Part 1: View factors
Space e
Thermal co
requiremen
Space er
Two-phase he
equipment
Space e
Testing
ECSS Secretariat
ESA-ESTEC
Requirements & Standards Division
Noordwijk, The Netherlands
James Etchells | ESTEC | 02/11/2015 | Slide 3
ESA UNCLASSIFIED - For Official Use
European Space Agency

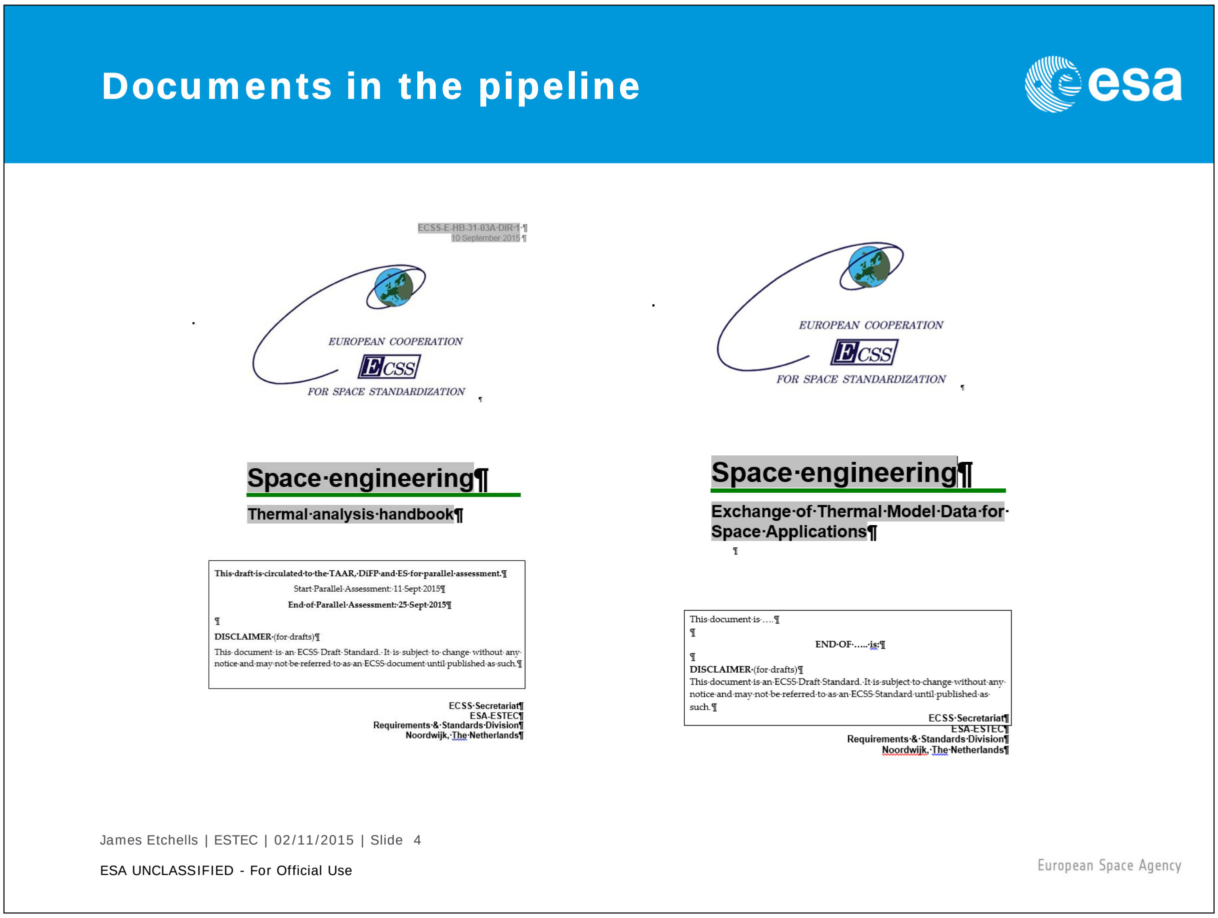
Documents in the pipeline
esa
ECSS-E-HB-31-03A-DIR-1
10 September 2015
EUROPEAN COOPERATION
ECSS
FOR SPACE STANDARDIZATION
Space engineering
Thermal analysis handbook
This draft is circulated to the TAAR, DiFP and ES for parallel assessment.
Start Parallel Assessment: 11 Sept 2015
End of Parallel Assessment: 25 Sept 2015
DISCLAIMER (for drafts)
This document is an ECSS Draft Standard. It is subject to change without any notice and may not be referred to as an ECSS document until published as such.
ECSS Secretariat
ESA-ESTEC
Requirements & Standards Division
Noordwijk, The Netherlands
EUROPEAN COOPERATION
ECSS
FOR SPACE STANDARDIZATION
Space engineering
Exchange of Thermal Model Data for Space Applications
This document is ....
END-OF-.....is
DISCLAIMER (for drafts)
This document is an ECSS Draft Standard. It is subject to change without any notice and may not be referred to as an ECSS Standard until published as such.
ECSS Secretariat
ESA-ESTEC
Requirements & Standards Division
Noordwijk, The Netherlands
James Etchells | ESTEC | 02/11/2015 | Slide 4
ESA UNCLASSIFIED - For Official Use
European Space Agency

esa

ECSS-E-HB-31-03
THERMAL ANALYSIS HANDBOOK

James Etchells | ESTEC | 02/11/2015 | Slide 5

ESA UNCLASSIFIED - For Official Use

European Space Agency

History of the handbook

esa

Proposal at NESTA:
- Handbook on Thermal Model *Validation*

Conclusions:
- General agreement with idea
- Checklist would be useful
- Not a standard (not applicable doc)
- Don't be too prescriptive
- Old ECSS standard content
- Observation that is a big undertaking
- Action on ESA to make 1st draft

ESA UNCLASSIFIED – For Official Use

esa
estec

DOCUMENT

Guidelines for Space Thermal Modelling and Analysis

In the context of computational analysis:
- Verification "did we solve the equations correctly?"
- Validation "did we solve the correct equations?"

ECSS
FOR SPACE STANDARDIZATION

Space·engineering¶

Thermal·analysis·handbook¶

S. De Palo (TAS-I)
G. Jahn (Airbus DS)
P. Lardet (SODERN) *
P. Oger (Airbus DS)
J. Vallega (CRISA)
* Left WG due to new roles

James Etchells | ESTEC | 02/11/2015 | Slide 6

ESA UNCLASSIFIED - For Official Use

European Space Agency

Thermal Analysis Handbook: Table of Contents

Current Status

- Draft reviewed by Working Group (Internal Assessment)
- Draft reviewed by TAAR (Parallel Assessment)
  - Comments/suggestions have been included
- Next step is **Public Review**, options :
  1. Limit review to NESTA members
  2. Full public review

esa

ECSS-E-ST-31-04
EXCHANGE OF THERMAL MODEL DATA

aka STEP-TAS

James Etchells | ESTEC | 02/11/2015 | Slide 9

ESA UNCLASSIFIED - For Official Use

European Space Agency

Why STEP-TAS?

esa

SET-ATS (1991)

- CNES Initiative "Standard d'Exchange et Transfert – Application Thermique Spatiale"
- Based on French SET Z68-300 European aircraft industry

ICE-TAS (1994)

- ESA study to find common data models for exchanging thermal data between tools
- Identified "STEP" standard as most promising technology of the day

STEP-TAS (1998-2008)

- 1st prototype in Europe and US in 1998
- Simplification and rigourisation of STEP-TAS internally at ESTEC
- Development of TASverter to *facilitate* exchange + *validate* protocol

IITAS (2009)

- Industrial Implementation of STEP-TAS (Conformance Class 1 or 3)
- Interfaces in ESATAN-TMS, eTherm, Thermica, TMG, Thermal Desktop

James Etchells | ESTEC | 02/11/2015 | Slide 10

ESA UNCLASSIFIED - For Official Use

European Space Agency

What is STEP-TAS?

- **STEP** = Standard for the Exchange of Product Model Data, ISO 10303
  - There are a number of STEP standards - Application Protocols (APs)
  - Best known is AP203/214 for CAD
  - Uses a formal data model definition language called EXPRESS (ISO10303-11)
  - STEP protocol provides structure, but also algorithmic rules to ensure integrity of datasets
- **TAS** = Thermal Analysis for Space
  - Specific AP for space thermal analysis with 4 modules:
    - NRF : Network Results Format [TMM / Test data]
    - MGM : Meshed Geometric Module [GMM - static]
    - SKM : Space Kinematic Module [GMM - moving]
    - SMA : Space Mission Analysis [GMM - trajectory]
  - Protocol very generic, can be applied to other disciplines e.g. space environment (STEP-SPE)
  - Thermal specific information introduced via run-time dictionary specifying, e.g. what thermal nodes is, what a thermo-optical property is, etc.

James Etchells | ESTEC | 02/11/2015 | Slide 11

ESA UNCLASSIFIED - For Official Use

European Space Agency

Formalisation under ECSS

- Original plan was to formalise STEP-TAS standard under ISO
  - STEP-TAS is a fully conforming ISO 10303 application protocol
- Eventually ECSS was preferred over ISO
  - Lighter process, quicker to update if needed, more relevant to space domain
- Working Group starting in 2015:

H. Brouquet (ITP Engines)	P. Hugonnot (TAS-F)
K. Duffy (MAYA HTT)	R. Muenstermann (Airbus DS (D))
J. Etchells (ESA)	T. Soriano (Airbus DS (F))
A. Fagot (DOREA)	T van Eekelen (Samtech / Siemens)
D. Gibson (ESA)	

- *But*, no precedent in ECSS for this kind of standard … how to deal with it?

James Etchells | ESTEC | 02/11/2015 | Slide 12

ESA UNCLASSIFIED - For Official Use

European Space Agency

Formalisation under ECSS

```
ENTITY mgm_rectangle
  SUBTYPE OF(mgm_primitive_bounded_surface);
  p1 : mgm_3d_cartesian_point;
  p2 : mgm_3d_cartesian_point;
  p3 : mgm_3d_cartesian_point;
WHERE
  wr1: mgm_verify_points_use_context_length_quantity_type(
    [p1, p2, p3], geometric_item.containing_model);
  wr2: mgm_verify_points_span_orthogonal_system(p1, p2, p3,
    mgm_get_context_uncertainty_value(
      geometric_item.containing_model, 'point_coincidence_length'));
END_ENTITY;
```

Data structure

Rules

Difficult to reconcile these two styles

a. Inspection of the spacecraft (including structure and cable harnesses) shall be performed to verify that there are no ungrounded metal components.

b. Resistance testing shall be carried out on grounded metal components to ensure that their grounding meet the requirements in 9.2.2.

James Etchells | ESTEC | 02/11/2015 | Slide 13

ESA UNCLASSIFIED - For Official Use

European Space Agency

Expected Outputs

- Short set of ECSS style requirements targeted at tool developers
  - Focus on: validation, conformance, diagnostics
- STEP-TAS Protocol captured as a *normative* annex
  - Normative Annex must be a DRD description
- Change request to thermal standard

Formal ECSS

Where do you come in (as an end-user)?

- Use the STEP-TAS Interfaces
  - They work pretty well (last slide)
- Report any problems to tool developers and ESA
  - **step-tas@thermal.esa.int**

James Etchells | ESTEC | 02/11/2015 | Slide 14

ESA UNCLASSIFIED - For Official Use

European Space Agency

Future perspectives

- Make TASverter for TMM available soon
  - First issue supports SINDA <-> ESATAN
- Updates to STEP-TAS SDK
  - full validation
  - Improve diagnostics emitted by STEP-TAS SDK
- Web portal for STEP-TAS with forum, FAQ, recipes, downloads etc
- STEP-TAS viewer and validation
  - To replace BagheraView

James Etchells | ESTEC | 02/11/2015 | Slide 15

ESA UNCLASSIFIED - For Official Use

European Space Agency

Current Status

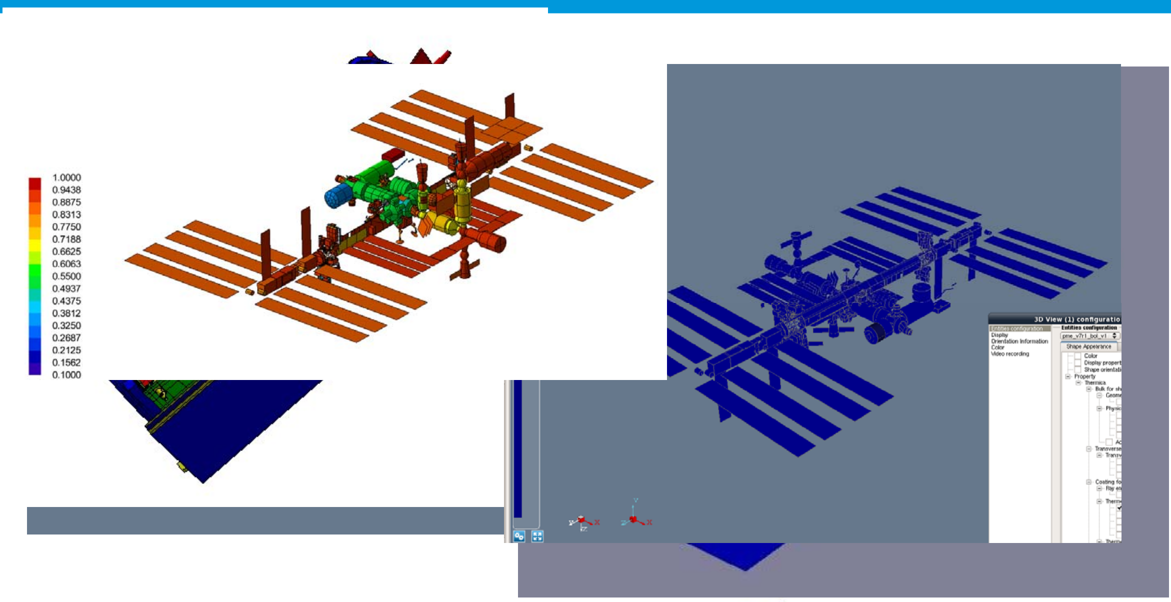

James Etchells | ESTEC | 02/11/2015 | Slide 16

ESA UNCLASSIFIED - For Official Use

European Space Agency

END

James Etchells | ESTEC | 02/11/2015 | Slide 17

ESA UNCLASSIFIED - For Official Use

European Space Agency

Appendix L

Improve thermal analysis process with Systema V4 and Python

Alexandre Darrau
(Airbus Defence and Space, France)

Abstract

When performing analyses, thermal engineers follow a methodology to ensure results quality and traceability. However, some checking or/and post-processing operations are still manually done or are performed later in the analysis process, leading to error and time wasting.
The purpose of this presentation is to introduce how the Airbus Defence & Space Thermal Engineering department in Toulouse is working to overcome these difficulties using new Systema V4 functions and Python technology. An example for each thermal analysis stage is going to be presented to illustrate.

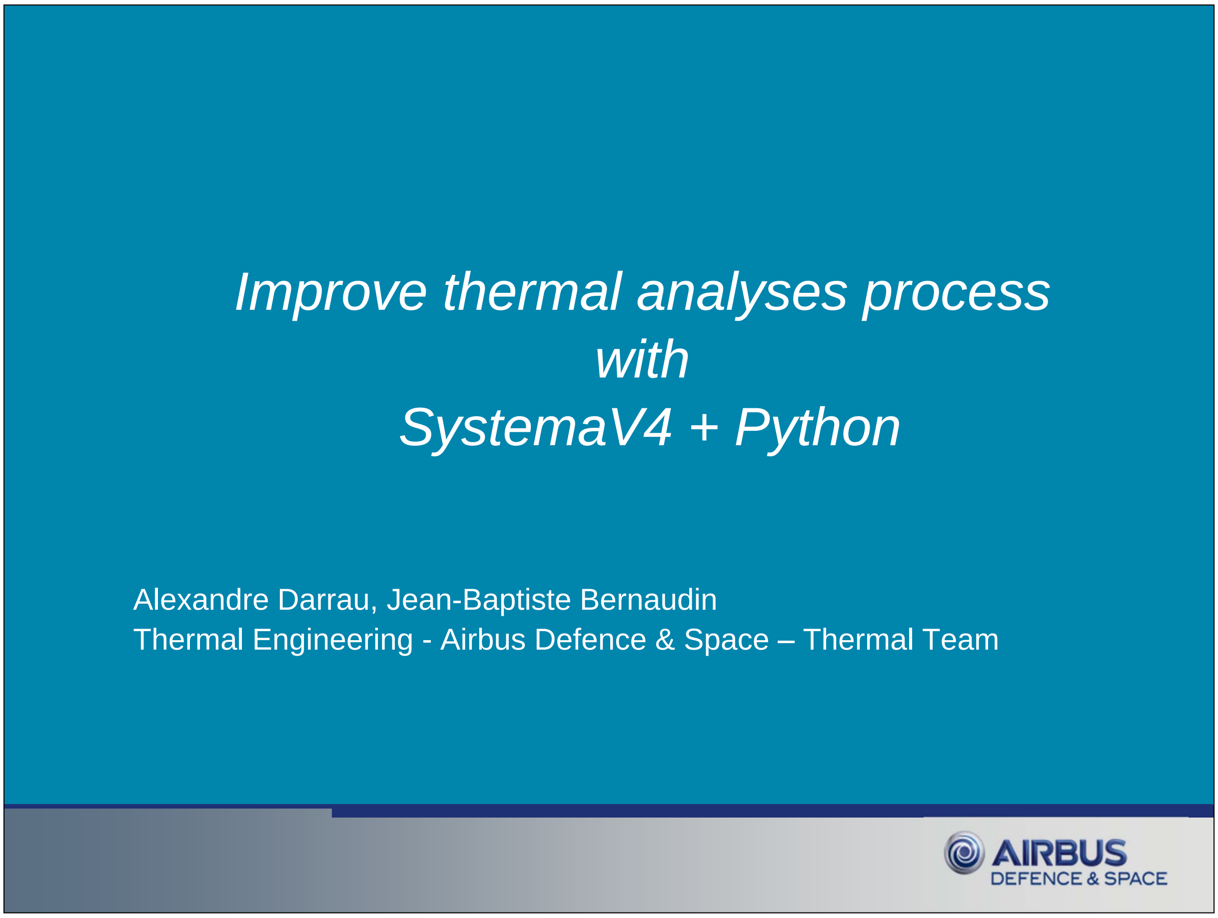
Improve thermal analyses process
with
SystemaV4 + Python
Alexandre Darrau, Jean-Baptiste Bernaudin
Thermal Engineering - Airbus Defence & Space – Thermal Team
AIRBUS
DEFENCE & SPACE

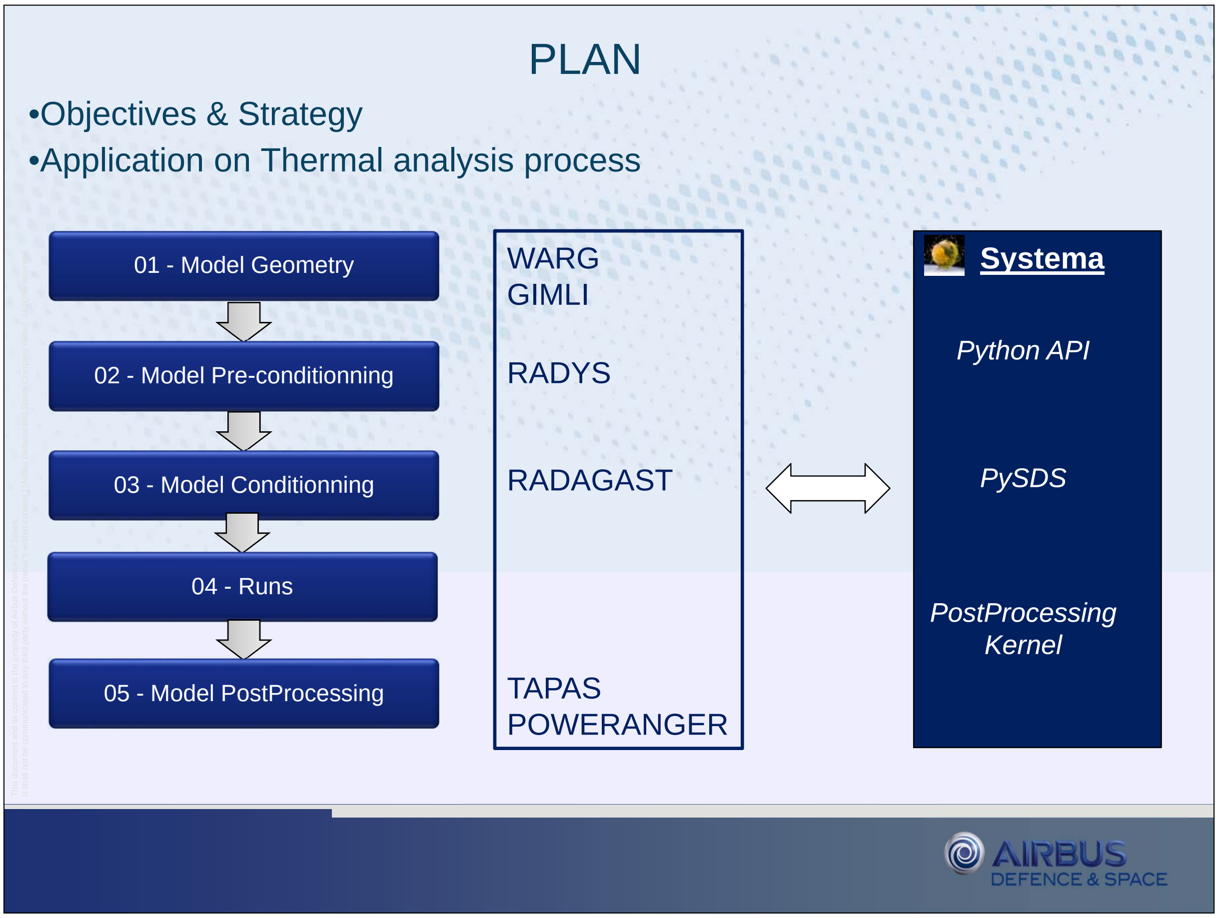
PLAN
•Objectives & Strategy
•Application on Thermal analysis process
01 - Model Geometry
02 - Model Pre-conditionning
03 - Model Conditionning
04 - Runs
05 - Model PostProcessing
WARG
GIMLI
RADYS
RADAGAST
TAPAS
POWERANGER
Systema
Python API
PySDS
PostProcessing Kernel
AIRBUS
DEFENCE & SPACE

Objectives & Strategy (1/2)

Objectives: Support thermal engineer !

- **Prevent** time wasting + manual operations ➔ **Automatisation (helper tools…)**
- **Ensure** thermal analysis quality ➔ **Check at each analysis stage**
- **Remove** industrials softwares borders ➔ **Object-Oriented + Modular approach**
- **Standardize** data presentations.

Automatic tools will **never** replace engineer thermal but **only optimize** its time !

11/03/2015

AIRBUS DEFENCE & SPACE

Objectives & Strategy (2/2)

Strategy:

- Set global methodology to pinpoint thermal engineer needs
- For each need, define a method to apply.
- When a tool is needed:
  - Use object oriented approach
  - Split data treatment from format
  - Category: modelling helper tool, checker, analysis tool

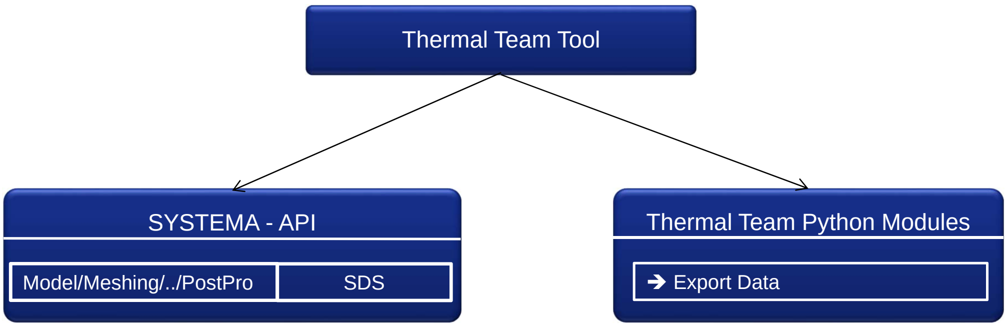

11/03/2015

AIRBUS DEFENCE & SPACE

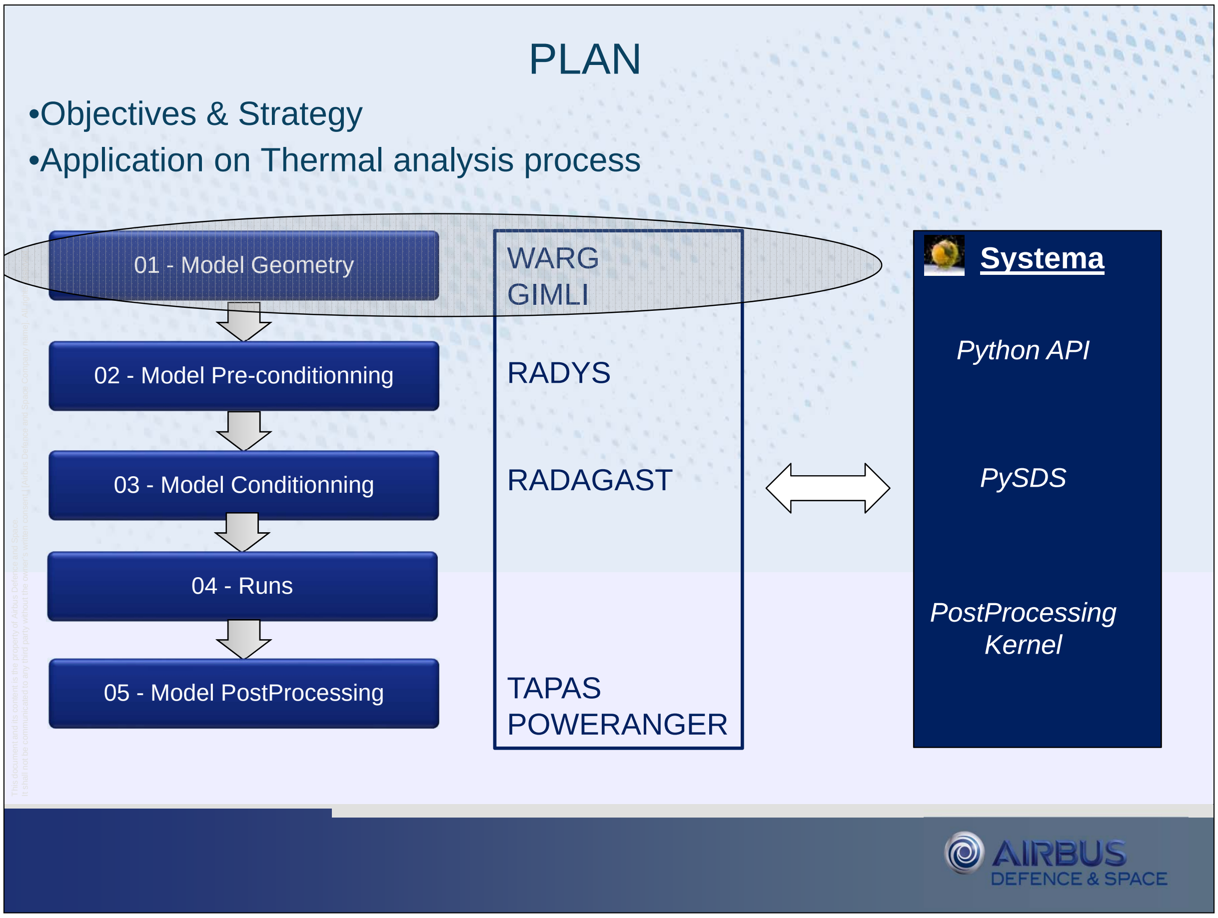
PLAN
•Objectives & Strategy
•Application on Thermal analysis process
01 - Model Geometry
02 - Model Pre-conditionning
03 - Model Conditionning
04 - Runs
05 - Model PostProcessing
WARG
GIMLI
RADYS
RADAGAST
TAPAS
POWERANGER
Systema
Python API
PySDS
PostProcessing Kernel
AIRBUS
DEFENCE & SPACE

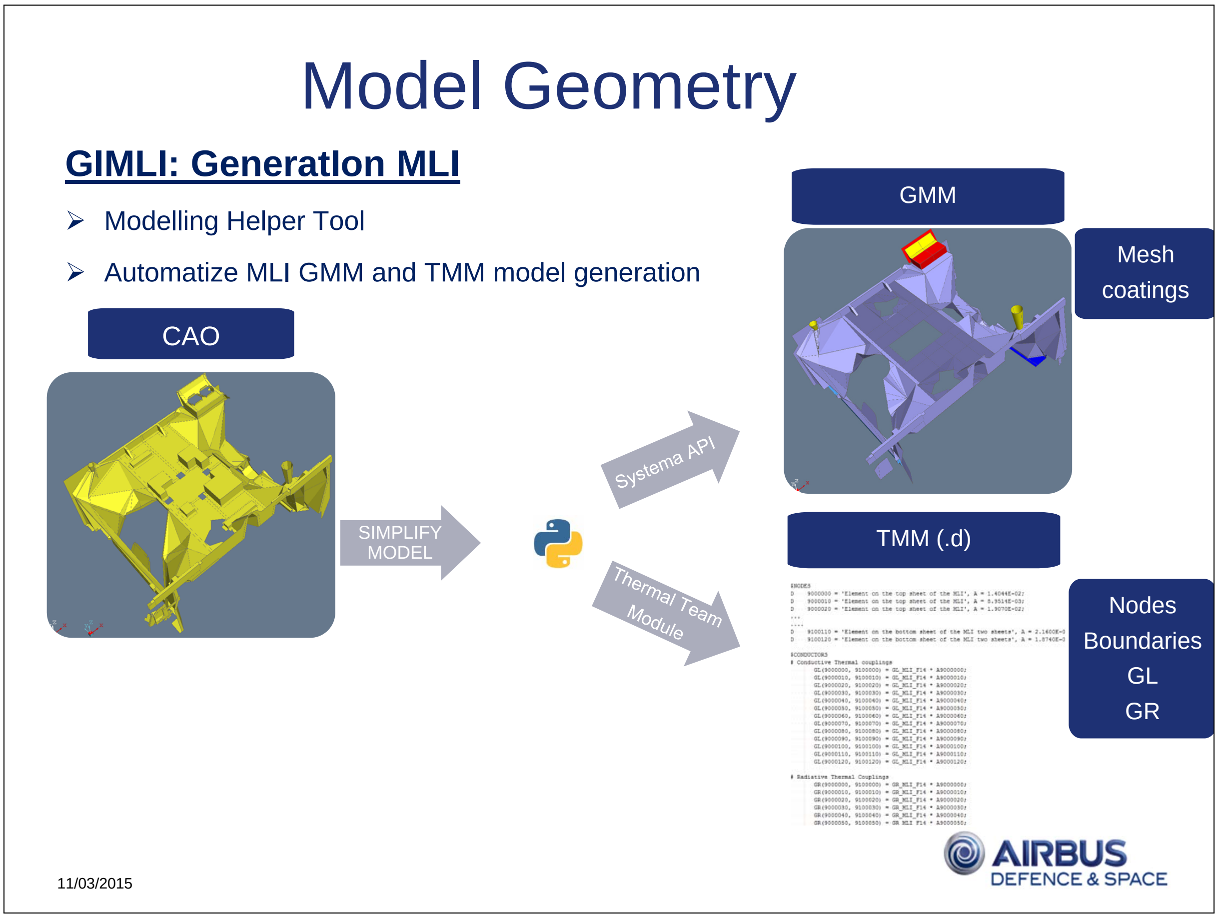
Model Geometry
GIMLI: GeneratIon MLI
Modelling Helper Tool
Automatize MLI GMM and TMM model generation
CAO
SIMPLIFY MODEL
Systema API
Thermal Team Module
GMM
Mesh coatings
TMM (.d)
Nodes
Boundaries
GL
GR
11/03/2015
AIRBUS
DEFENCE & SPACE

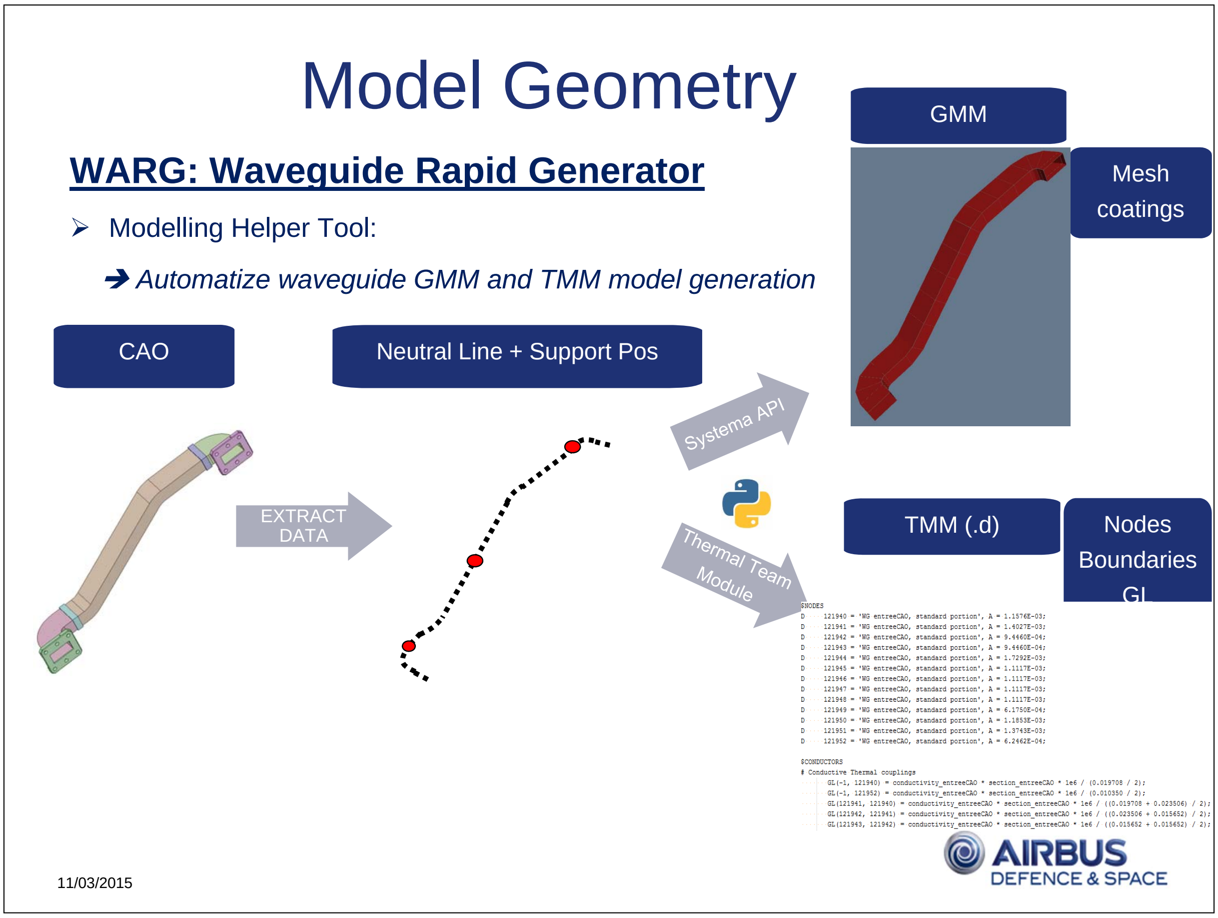
Model Geometry
WARG: Waveguide Rapid Generator
Modelling Helper Tool:
Automatize waveguide GMM and TMM model generation
CAO
Neutral Line + Support Pos
EXTRACT DATA
Systema API
Thermal Team Module
GMM
Mesh coatings
TMM (.d)
Nodes Boundaries GL
AIRBUS DEFENCE & SPACE
11/03/2015

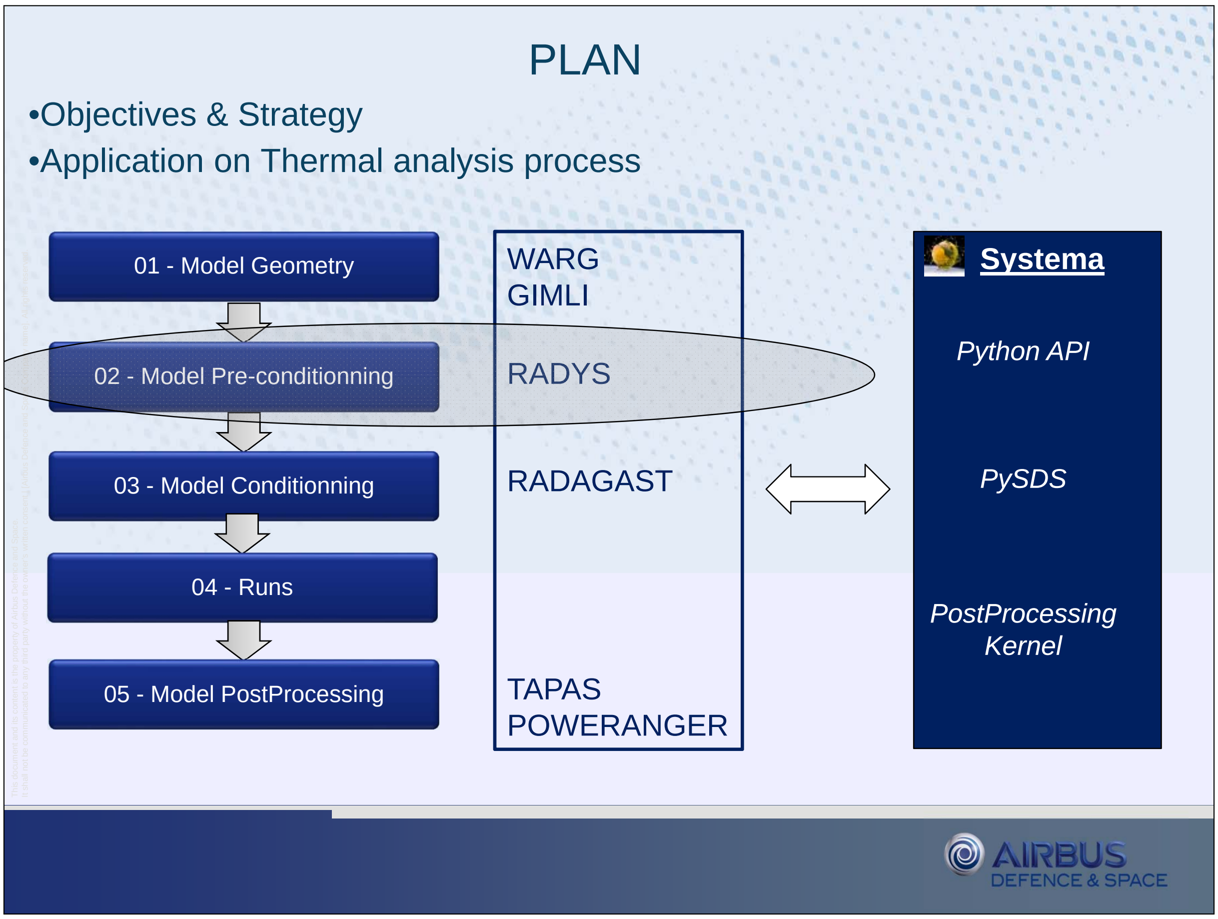
PLAN
•Objectives & Strategy
•Application on Thermal analysis process
01 - Model Geometry
02 - Model Pre-conditionning
03 - Model Conditionning
04 - Runs
05 - Model PostProcessing
WARG
GIMLI
RADYS
RADAGAST
TAPAS
POWERANGER
Systema
Python API
PySDS
PostProcessing Kernel
AIRBUS DEFENCE & SPACE

Model Preconditionning

RADYS: Radiative synthesis

- Checker tool : *Check radiative cases data and generate report before run!*

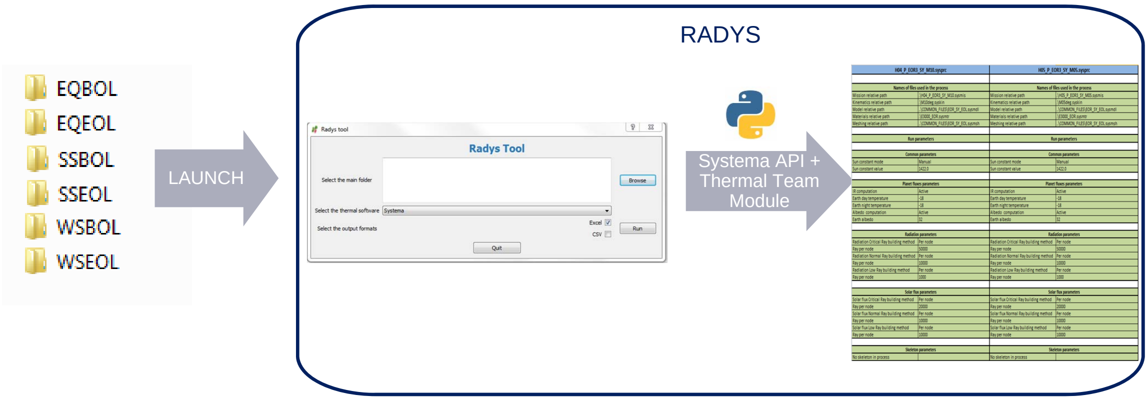

11/03/2015

Model Preconditionning

RADYS: Radiative synthesis

- Checker tool : *Check radiative cases data and generate report before run!*

Names of files used in the process		Names of files used in the process	
Mission relative path	.\H04_P_EOR3_SY_M10.sysmis	Mission relative path	.\H05_P_EOR3_SY_M05.sysmis
Kinematics relative path	.\M10deg.syskin	Kinematics relative path	.\M05deg.syskin
Model relative path	..\COMMON_FILES\EOR_SY_EOL.sysmdl	Model relative path	..\COMMON_FILES\EOR_SY_EOL.sysmdl
Materials relative path	.\E3000_EOR.sysmtr	Materials relative path	.\E3000_EOR.sysmtr
Meshing relative path	..\COMMON_FILES\EOR_SY_EOL.sysmsh	Meshing relative path	..\COMMON_FILES\EOR_SY_EOL.sysmsh
Run parameters		**Run parameters**	
Common parameters		**Common parameters**	
Sun constant mode	Manual	Sun constant mode	Manual
Sun constant value	1422.0	Sun constant value	1422.0
Planet fluxes parameters		**Planet fluxes parameters**	
IR computation	Active	IR computation	Active
Earth day temperature	-18	Earth day temperature	-18
Earth night temperature	-18	Earth night temperature	-18
Albedo computation	Active	Albedo computation	Active
Earth albedo	32	Earth albedo	32
Radiation parameters		**Radiation parameters**	
Radiation Critical Ray building method	Per node	Radiation Critical Ray building method	Per node
Ray per node	50000	Ray per node	50000
Radiation Normal Ray building method	Per node	Radiation Normal Ray building method	Per node
Ray per node	10000	Ray per node	10000
Radiation Low Ray building method	Per node	Radiation Low Ray building method	Per node
Ray per node	1000	Ray per node	1000
Solar flux parameters		**Solar flux parameters**	
Solar flux Critical Ray building method	Per node	Solar flux Critical Ray building method	Per node
Ray per node	20000	Ray per node	20000
Solar flux Normal Ray building method	Per node	Solar flux Normal Ray building method	Per node
Ray per node	10000	Ray per node	10000
Solar flux Low Ray building method	Per node	Solar flux Low Ray building method	Per node
Ray per node	10000	Ray per node	10000
Skeleton parameters		**Skeleton parameters**	
No skeleton in process		No skeleton in process	

11/03/2015

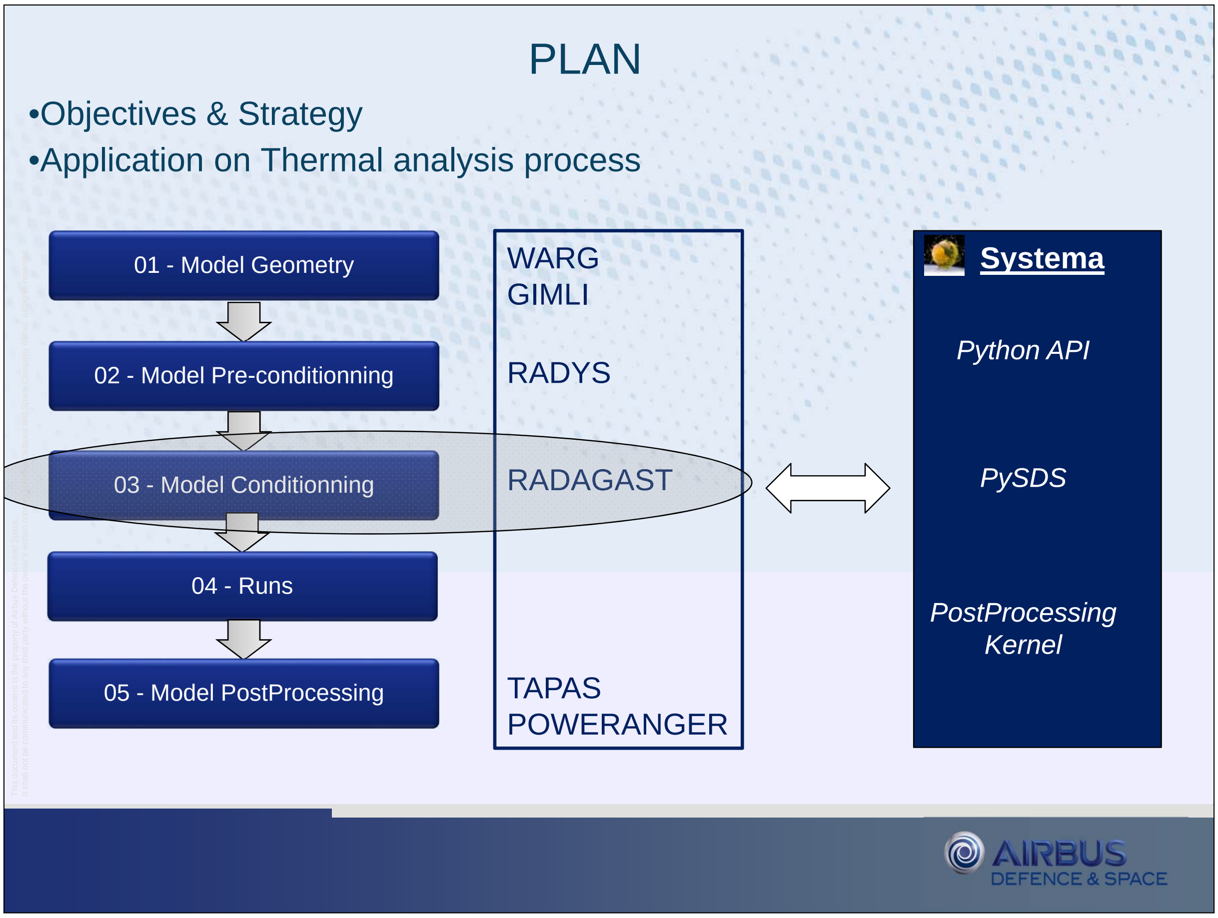
PLAN
•Objectives & Strategy
•Application on Thermal analysis process
01 - Model Geometry
02 - Model Pre-conditionning
03 - Model Conditionning
04 - Runs
05 - Model PostProcessing
WARG
GIMLI
RADYS
RADAGAST
TAPAS
POWERANGER
Systema
Python API
PySDS
PostProcessing Kernel
AIRBUS
DEFENCE & SPACE

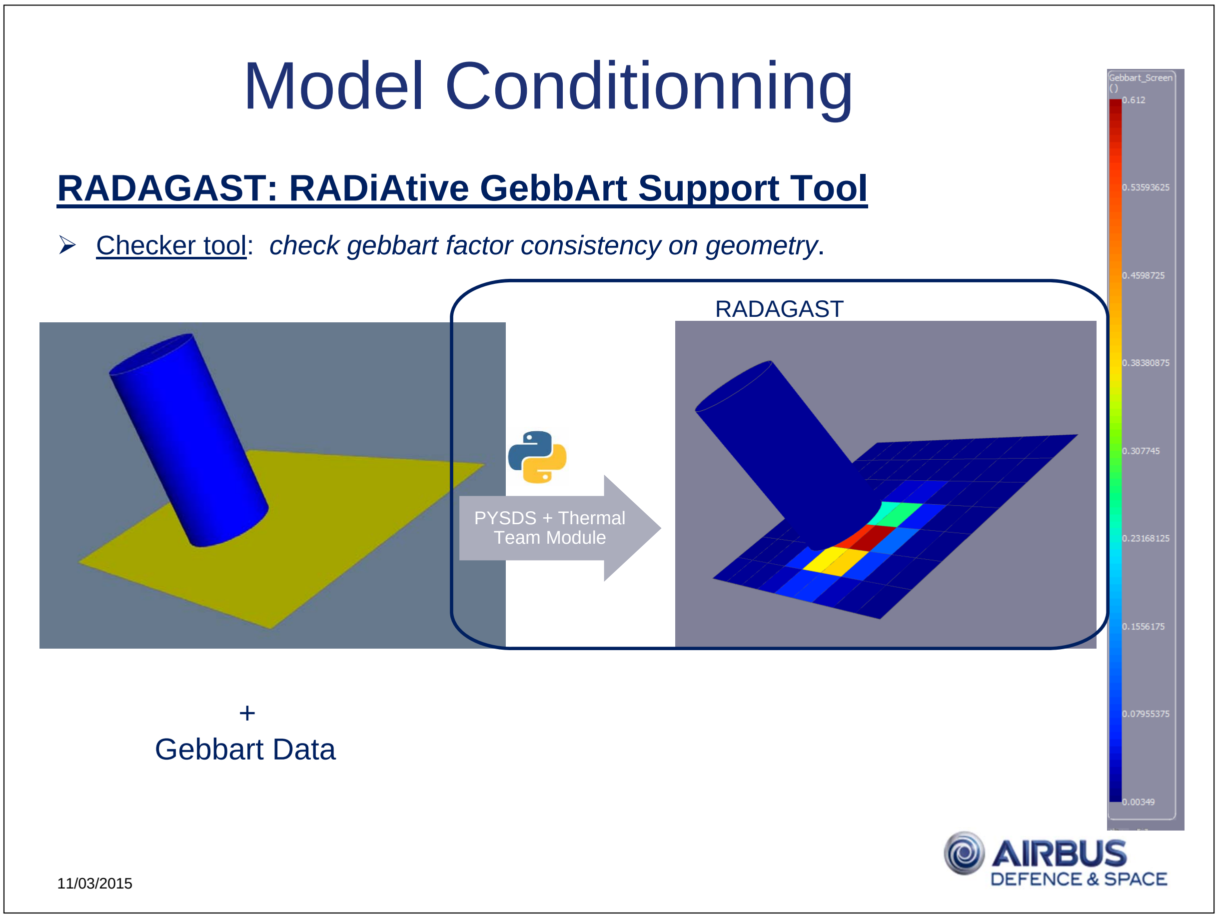
Model Conditionning
RADAGAST: RADiAtive GebbArt Support Tool
➢ Checker tool: check gebbart factor consistency on geometry.
RADAGAST
PYSDS + Thermal Team Module
+
Gebbart Data
11/03/2015
AIRBUS
DEFENCE & SPACE

Model Conditionning

RADAGAST: RADiAtive GebbArt Support Tool

➢ Check gebbart factor consistency on geometry.

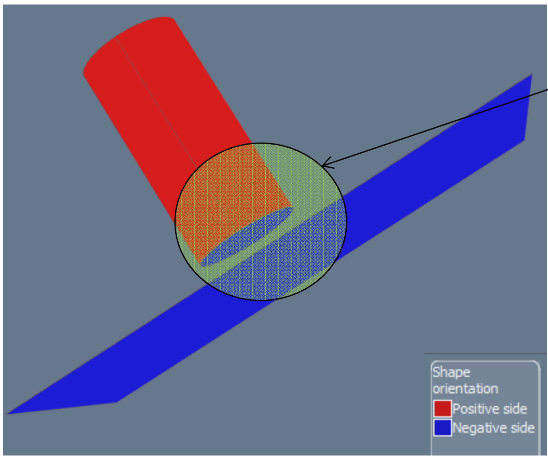

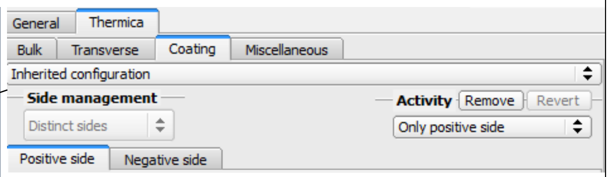

Face active see inactive one !

11/03/2015

AIRBUS DEFENCE & SPACE

PLAN

- Objectives & Strategy
- Application on Thermal analysis process

01 - Model Geometry
02 - Model Pre-conditionning
03 - Model Conditionning
04 - Runs
05 - Model PostProcessing

WARG
GIMLI
RADYS
RADAGAST
TAPAS
POWERANGER

Systema

Python API

PySDS

PostProcessing Kernel

AIRBUS DEFENCE & SPACE

Model PostProcessing

POWERANGER: POWEr Range GEneratoR

- Tool for thermal analysis
  - *Perform power budget on groups **after** thermisol runs.*
  - *Steady-State and Transient cases on selected times.*
  - *Taking into account GL,GR variations and Edges elements.*
  - *Having graphical views of power* exchanges and table synthesis.

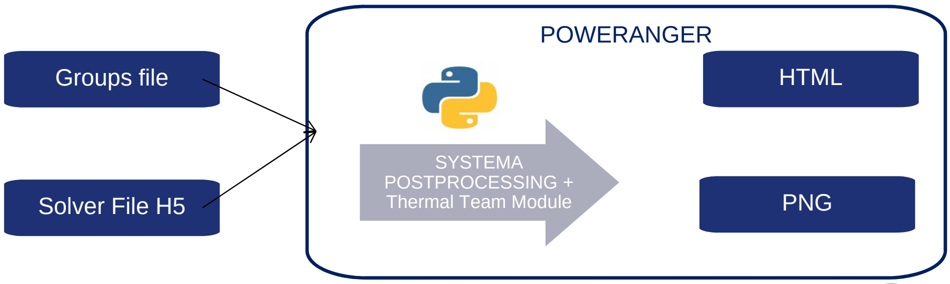

11/03/2015

AIRBUS DEFENCE & SPACE

Model PostProcessing

POWERANGER: POWEr Range GEneratoR

- Tool for thermal analysis

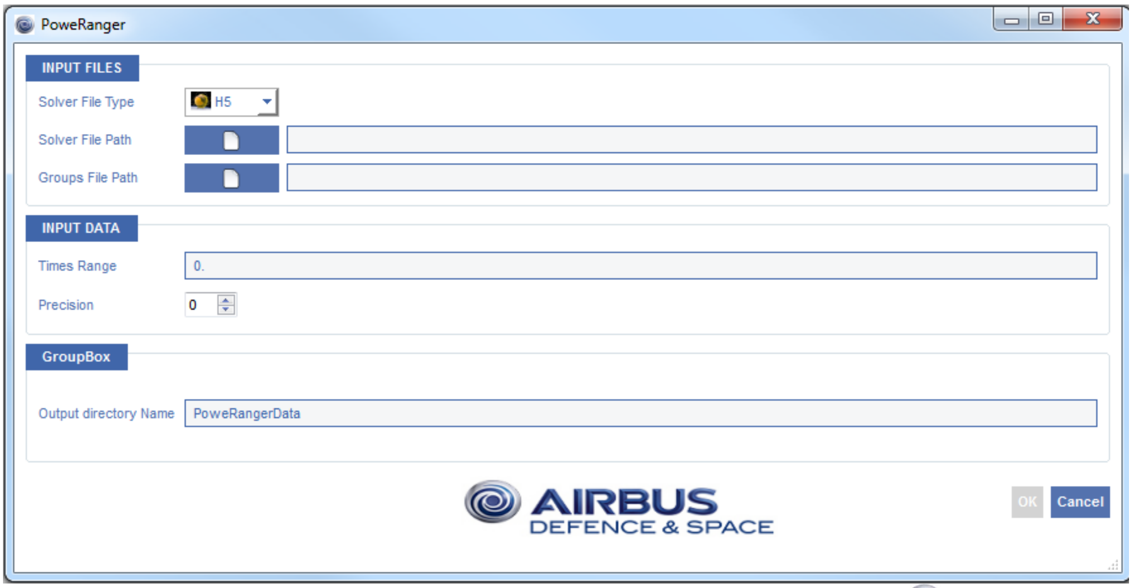

11/03/2015

AIRBUS DEFENCE & SPACE

Model PostProcessing

POWERANGER: POWEr Range GEneratoR

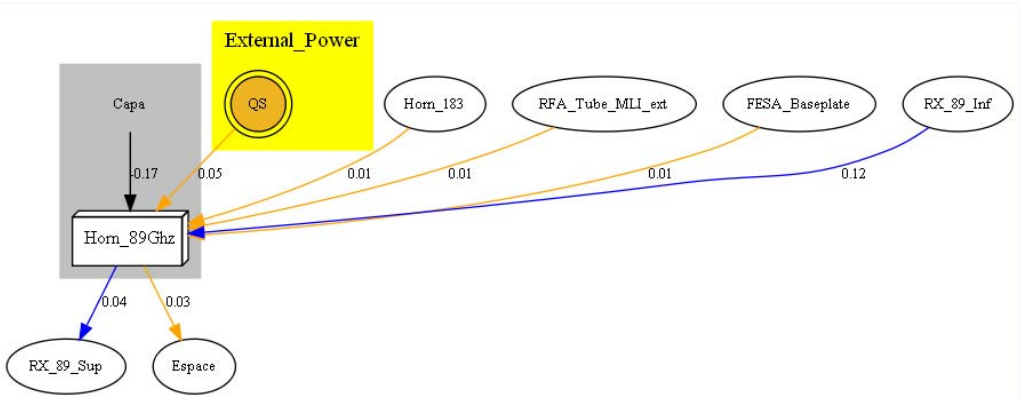

11/03/2015

Model PostProcessing

TAPAS: Thermal Analysis PostProcessing Airbus Satellite

- Compute Tmin/max/ave/Gradients on groups **AFTER** runs
- Compute QI/QR/QS/QA/QE on groups **AFTER** runs
- Compute Mass Balance **AFTER** runs + Manage Equipement status
- Generate automatically charts (2d and horizontal bars), 3dviews
- Generate automatically Excel + HTML thermal reports

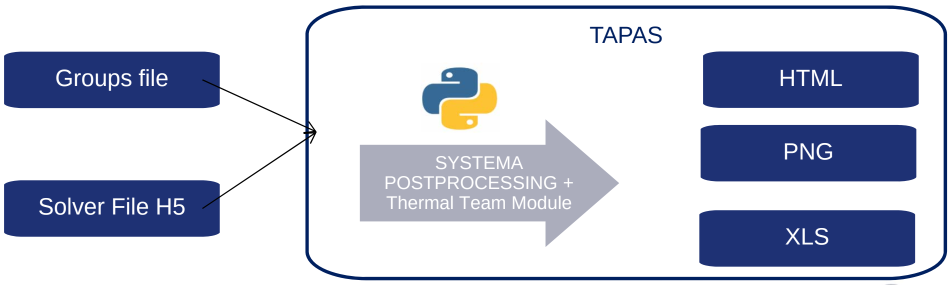

11/03/2015

Model PostProcessing

TAPAS:

TA-PAS

AIRBUS DEFENCE & SPACE

TA-PAS

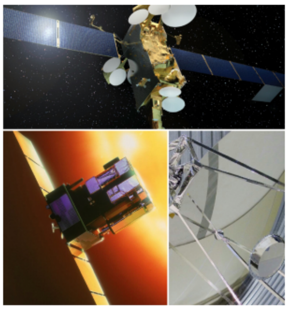

contact: alexandre.darrau@airbus.com

Help SAVE < Back Next > Cancel

11/03/2015

AIRBUS DEFENCE & SPACE

Model PostProcessing

TAPAS:

TA-PAS

ENTITIES INFORMATION

Entities Definition

Entities | Equipment Status | Mass Budget Data

Groups	Temperature	QI	QR	QS	QA	QP	Mass
PX_Bypass	☑	☑	☐	☐	☐	☑	☑
PX_Cables	☑	☑	☑	☐	☐	☐	☑
Shunt	☑	☑	☑	☐	☐	☐	☐
PX_MainPanel	☑	☐	☑	☐	☐	☐	☐
PX_Pack	☑	☐	☐	☑	☑	☐	☐
PX_ModulesTRP	☑	☐	☐	☑	☑	☐	☐
PX_ModulesT...	☑	☐	☐	☑	☐	☐	☐
PX_ModulesT...	☑	☐	☐	☐	☐	☐	☐
PX_IntraModul...	☑	☐	☐	☐	☐	☐	☐
PX_Radiateur	☑	☐	☐	☐	☐	☐	☐
PX_Total_Hea...	☑	☐	☐	☐	☐	☐	☐
PX_HeatingL1	☑	☐	☐	☐	☐	☐	☐

Help SAVE < Back Next > Cancel

11/03/2015

AIRBUS DEFENCE & SPACE

Model PostProcessing

TAPAS:

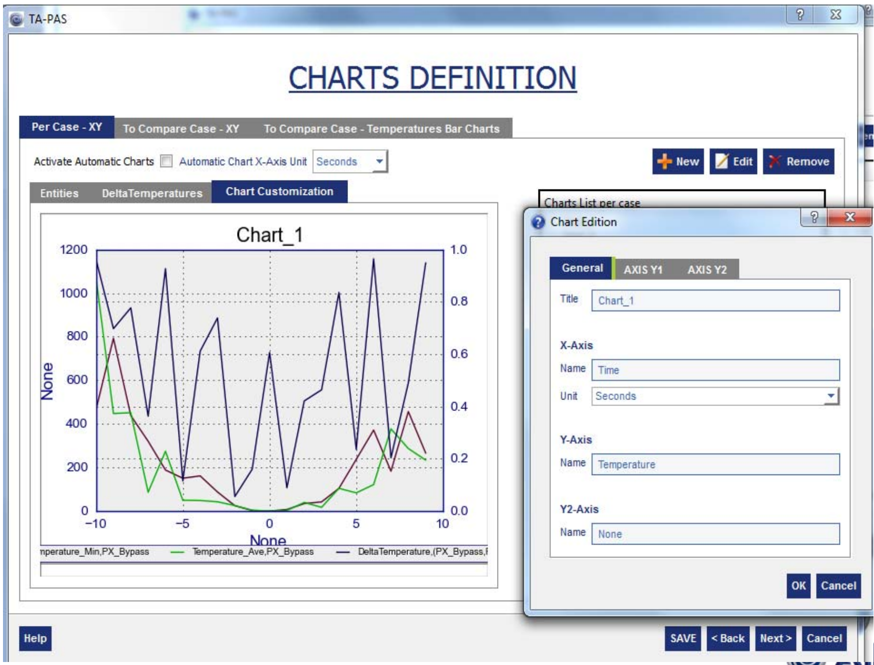

11/03/2015

Model PostProcessing

TAPAS:

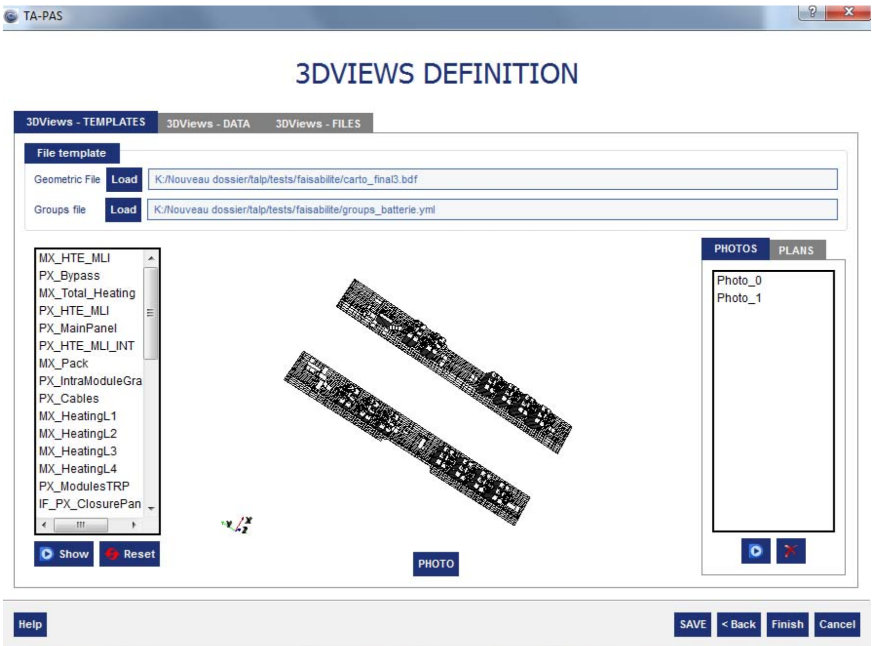

11/03/2015

TA-PAS

HTML

AIRBUS DEFENCE & SPACE

PROJECT NAME

CASE 1

AUTO_CHARTS CHARTS 3DVIEWS

THERMAL CASES
- ALL_CASES
- CASE 1
- CASE 2

PREDICTION TEMPERATURES

EQEOL	UNITS STATUS	COLD LIMITS		PREDICTED	CALCULATED	CALCULATED	PREDICTED	HOT LIMITS		MARGINS	
		NO-OPERATING [C]	DESIGN [C]	TMIN [C]	TMIN [C]	TMAX [C]	TMAX [C]	DESIGN [C]	NO-OPERATING [C]	COLD [C]	HOT [C]
HeatPipes											
PX_HP20600		-100.0	-5.0(*)	11.5	12.5	27.7	28.7	5.0	100.0	111.5	23.7
PX_HP20700		-100.0	-5.0	11.1	12.1	26.9	27.9	5.0	100.0	111.1	22.9
PX_HP20800		-100.0	-5.0	11.5	12.5	27.8	28.8	5.0	100.0	111.5	23.8
MLI											
MX_HTE_MLI		-100.0	-5.0	-168.7	-167.7	450.0	451.0	5.0	100.0	-68.7	446.0
MX_HTE_MLI_INT		-100.0	-5.0	11.0	12.0	60.9	61.9	5.0	100.0	111.0	56.9
PX_HTE_MLI		-100.0	-5.0	-180.0	-179.0	450.0	451.0	5.0	100.0	-80.0	446.0
PX_HTE_MLI_INT		-100.0	-5.0	10.8	11.8	43.9	44.9	5.0	100.0	110.8	39.9
Others											
Bass		-100.0	-5.0	-14.6	-13.6	37.7	38.7	5.0	100.0	85.4	33.7
Structure											
PX_MainPanel		-100.0	-5.0	5.3	6.3	33.8	34.8	5.0	100.0	105.3	29.8
PX_Radiateur		-100.0	-5.0	-11.9	-10.9	27.2	28.2	5.0	100.0	88.1	23.2

11/03/2015

AIRBUS DEFENCE & SPACE

TA-PAS

	A	B	C	D	E	F	G	N	O	P	Q	R
1–2	EQEOL	CERTAINT		UNITS STATUS	COLD LIMITS		PREDICTED	PREDICTED	HOT LIMITS		MARGINS	
3		Operating			No-Operating [C]	Design [C]	TMIN [C]	TMAX [C]	Design [C]	No-Operating [C]	Cold [C]	Hot [C]
4		MIN	MAX									
5	HeatPipes											
6	PX_HP20600	-1	1		-100	-5	11,5	28,7	5	100	111,5	23,7
7	PX_HP20700	-1	1		-100	-5	11,1	27,9	5	100	111,1	22,9
8	PX_HP20800	-1	1		-100	-5	11,5	28,8	5	100	111,5	23,8
9	MLI											
10	MX_HTE_MLI	-1	1		-100	-5	-168,7	451	5	100	-68,7	446
11	MX_HTE_MLI_INT	-1	1		-100	-5	11	61,9	5	100	111	56,9
12	PX_HTE_MLI	-1	1		-100	-5	-180	451	5	100	-80	446
13	PX_HTE_MLI_INT	-1	1		-100	-5	10,8	44,9	5	100	110,8	39,9
14	Others											
15	Bass	-1	1		-100	-5	-14,6	38,7	5	100	85,4	33,7
16	Structure											
17	PX_MainPanel	-1	1		-100	-5	5,3	34,8	5	100	105,3	29,8
18	PX_Radiateur	-1	1		-100	-5	-11,9	28,2	5	100	88,1	23,2
19	Structure_MX											
20	MX_MainPanel	-1	1		-100	-5	10,7	32,6	5	100	110,7	27,6
21	MX_Radiateur	-1	1		-100	-5	-8	27,5	5	100	92	22,5
22	Units											
23	Interpack	-1	1		-100	-5	-0,4	3,7	5	100	99,6	-1,3
24	MX_Bypass	-1	1		-100	-5	12,4	43,7	5	100	112,4	38,7
25	MX_Cables	-1	1	ON-Forced	-100	-5	12,6	74,8	5	100	17,6	69,8
26	MX_ModulesTRP	-1	1		-100	-5	13	30,6	5	100	113	25,6
27	MX_Pack	-1	1	ON	-100	-5	12,4	74,8	5	100	17,4	69,8
28	PX_Bypass	-1	1	ON	-100	-5	12,4	45,4	5	100	17,4	40,4
29	PX_Cables	-1	1	ON	-100	-5	11,9	59,7	5	100	16,9	54,7
30	PX_IntraModuleGradient	-1	1		-100	-5	-0,8	2,1	5	100	99,2	-2,9
31	PX_ModulesTRP	-1	1		-100	-5	12,9	30,8	5	100	112,9	25,8
32	PX_ModulesTRP_1CMF	-1	1		-100	-5	12,9	30,8	5	100	112,9	25,8
33	PX_ModulesTRP_2CMF	-1	1		-100	-5	12,9	30,8	5	100	112,9	25,8
34	PX_Pack	-1	1	ON	-100	-5	11,6	98,7	5	100	16,6	93,7
35	Shunt	-1	1	ON	-100	-5	12,5	98,7	5	100	17,5	93,7

11/03/2015

AIRBUS DEFENCE & SPACE

TA-PAS

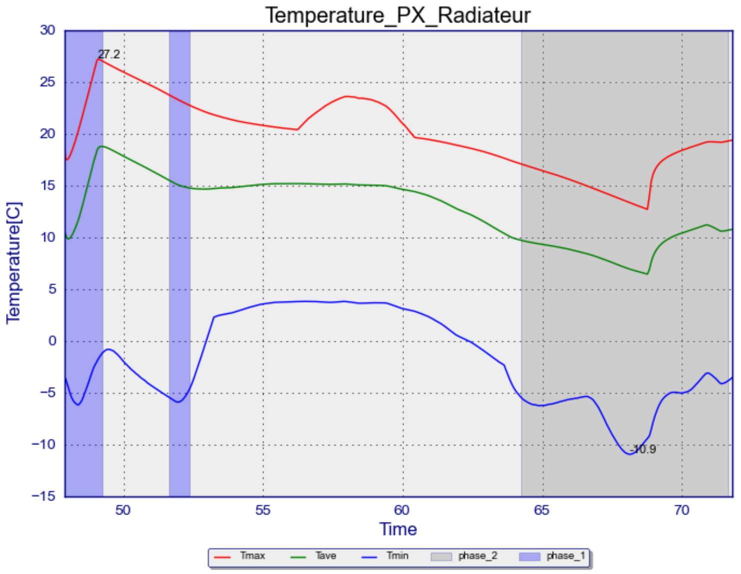

11/03/2015

AIRBUS DEFENCE & SPACE

TA-PAS

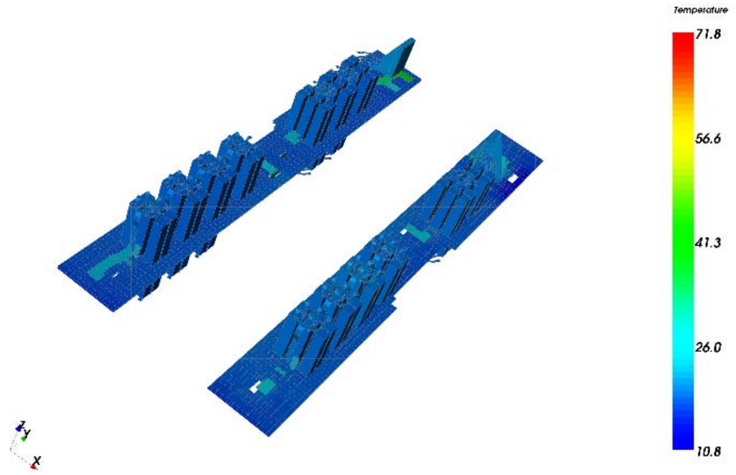

11/03/2015

AIRBUS DEFENCE & SPACE

TA-PAS

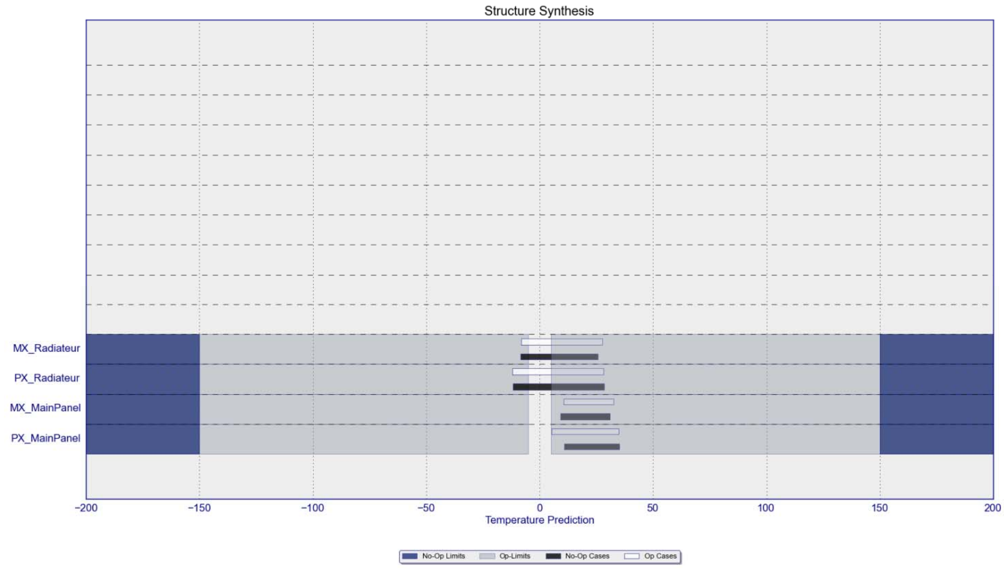

11/03/2015

AIRBUS DEFENCE & SPACE

CONCLUSIONS

- Thanks to SYSTEMA API, it is possible to:
  - *Optimize time model/meshing creations*
  - *Easily check thermal model.*
  - *Plotting user data on mesh.*
- Thanks to Python, it is possible to :
  - *Create simple tools without deep software engineering knowledege.*
  - *Wrap Systema API*
  - *Design tools with oriented object approach.*
  - *Create user friendly tools thanks to existing packages.*
- Collaboration with Systema Team to improve existing functions and create new ones:
  - *Materials data to be integrated in API*
  - *Implementing new box in postprocessing library*
  - *….*

11/03/2015

AIRBUS DEFENCE & SPACE

QUESTIONS ?

11/03/2015

Appendix M

Finite element model reduction for spacecraft thermal analysis

Lionel Jacques Luc Masset Gaetan Kerschen
(Space Structures and Systems Laboratory, University of Liège, Belgium)

Abstract

The finite element method (FEM) is widely used in mechanical engineering, especially for space structure design. However, FEM is not yet often used for thermal engineering of space structures where the lumped parameter method (LPM) is still dominant.
Both methods offer advantages and disadvantages and the proposed global approach tries to combine both methods:

- The LPM conductive links are error-prone and still too often computed by hand. This is incompatible with the increasing accuracy required by the thermal control systems (TCS) and associated thermal models. Besides offering the automatic and accurate computation of the conductive links, the FEM also provides easy interaction between mechanical and thermal models, allowing better thermo-mechanical analyses.

- On another hand, due to the large number of elements composing a FE model, the computation of the radiative exchange factors (REFs) is prohibitively expensive. New methods to accelerate the REFs computation by ray-tracing are necessary. Ray-tracing enhancement methods were presented in the previous editions, providing at least a 50% reduction of the number of rays required for a given accuracy. Another way to speed up the REF computation consists in grouping the FE external facets into super-faces. Surfaces in FEM are approximated where primitives are used in the LPM. In parallel to super-faces, quadric surface fitting of selected regions in the FE mesh is therefore performed where high surface accuracy is required for the computation of the radiative links and environmental heat loads.

Last year's presentation focused solely on the first point. Developments of super-face ray-tracing with quadrics fitting will be presented. In addition to REFs, orbital heat loads computation is also implemented with significant improvement. The presentation will also address the global process involving first the detailed FE model conductive reduction, then the super-faces generation with selective quadric fitting for the computation of REFs and orbital heat loads and finally the computation of the reduced model temperatures. Detailed FE model temperature field can then be computed back from the reduced ones and the reduction matrices for potential thermo-mechanical analyses.

Université de Liège

FINITE ELEMENT MODEL REDUCTION FOR SPACECRAFT THERMAL ANALYSIS

Lionel Jacques[1,2], Luc Masset[1], Gaetan Kerschen[1]

[1] Space Structures and Systems Laboratory, University of Liège
[2] Centre Spatial de Liège

29th Space Thermal Analysis Workshop, ESTEC, Nov. 3rd, 2015

Finite Element vs. Lumped Parameter

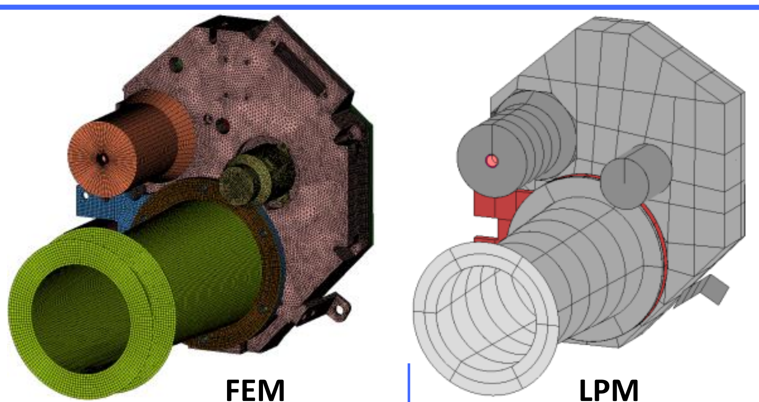

	FEM	LPM
# nodes	10^4 - 10^6	10^1 - 10^3
Conductive links computation	✓ Automatic	✗ Manual, error-prone
Radiative links computation	✗ Prohibitive	✓ Affordable
Surface accuracy for ray-tracing	✗ FE facets	✓ Primitives
User-defined components	✗ Difficult	✓ Easy
Thermo-mech. analysis	✓ Same mesh	✗ Mesh extrapolation

2

Reconciliation through a global approach

Radiative links computation

- Reduce # of rays: quasi-Monte Carlo method (isocell, Halton)
- Reduce # of facets: super-face concept (mesh clustering)
- Parallelization: GPUs

Surface accuracy for ray-tracing

- Quadrics fitting

Conductive links, thermo-mech. analysis and user-defined compts.

- Reduce detailed FE mesh (keep conductive info. of the detailed geometry)
- Able to recover detailed T° from reduced
- Transform reduced FE model to LP model to enable user-defined comp.

3

Outline

Ray-tracing enhancement

FEM clustering & conductive reduction

Super-face ray-tracing

Integrating the developments

Conclusions & perspectives

4

Outline

Ray-tracing enhancement

FEM clustering & conductive reduction

Super-face ray-tracing

Integrating the developments

Conclusions & perspectives

5

Ray-tracing: origin + direction sampling

$$F_{ij}(B_{ij}) = \frac{\text{Number of rays emitted by facet i, directly (finally) hitting j}}{\text{total number of rays emitted by facet i}}$$

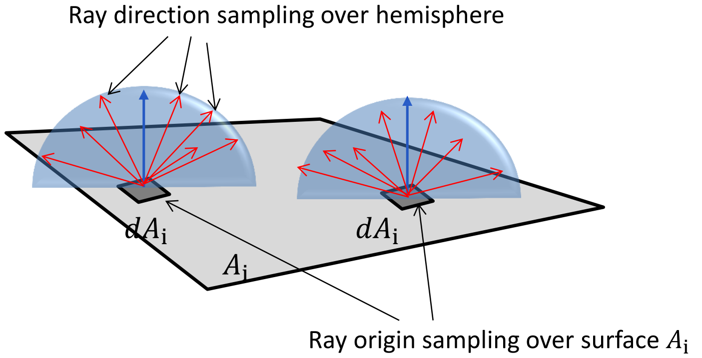

Reference solution: ESATAN-TMS

→ crude Monte Carlo: random direction & origin sampling, 1 ray / origin

$$error \propto \frac{1}{\sqrt{N_{rays}}}$$

6

4-D QUASI-MC SAMPLING: 2 QUADRANGLES

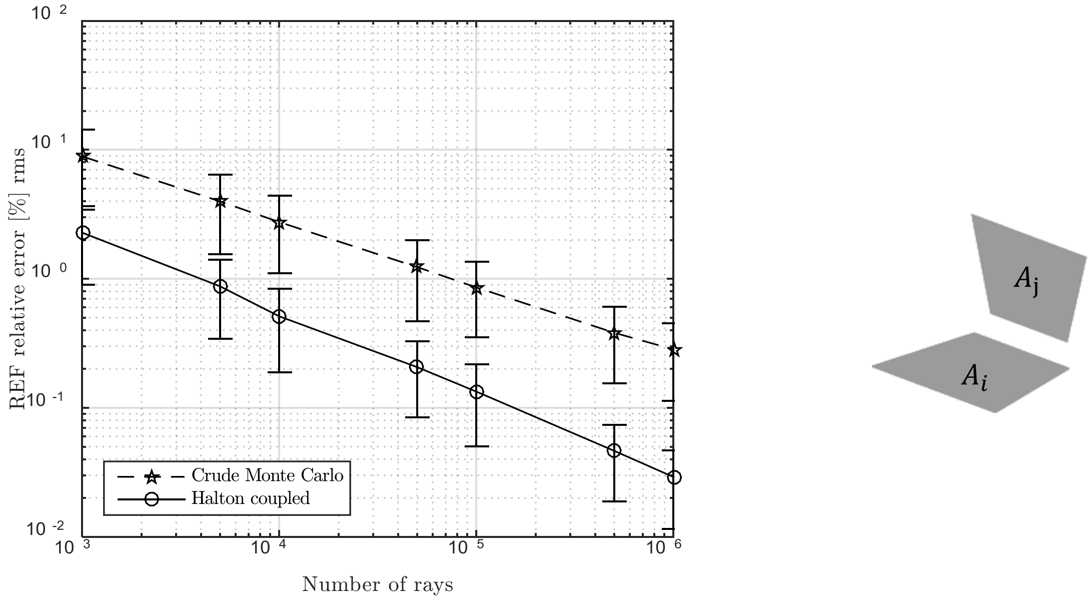

7

4-D QUASI-MC SAMPLING

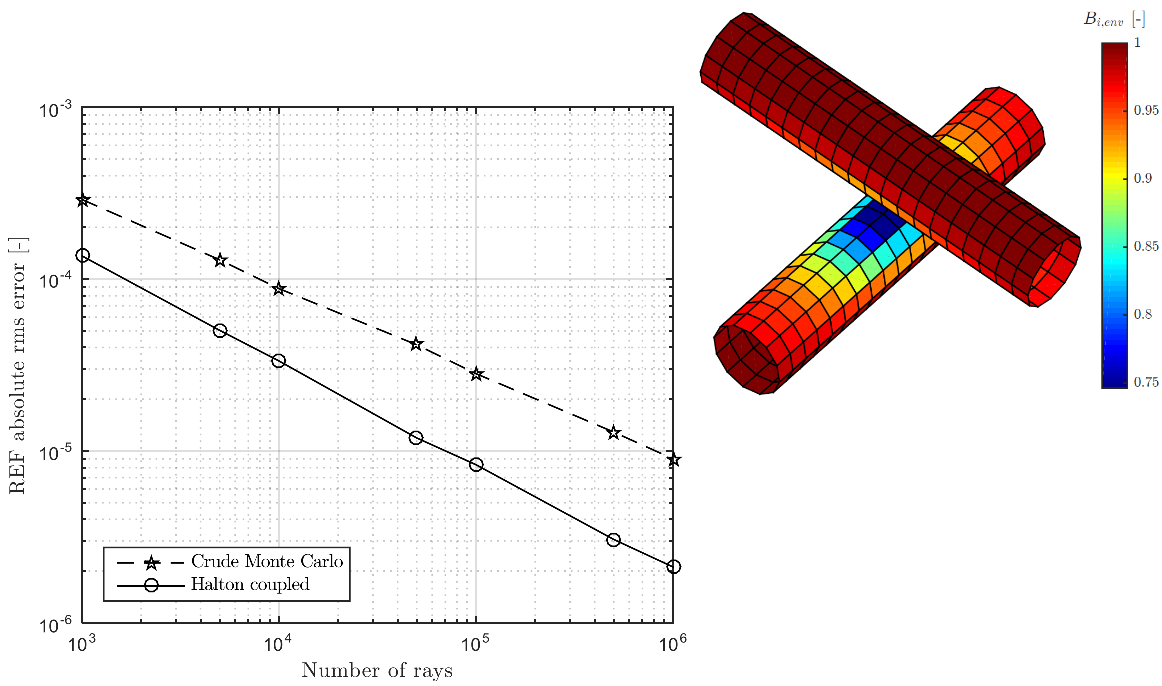

8

Outline

Ray-tracing enhancement

FEM clustering & conductive reduction

Super-face ray-tracing

Integrating the developments

Conclusions & perspectives

9

Mesh clustering: 3 steps

K-mean clustering initialization (user input # cluster) → cluster center

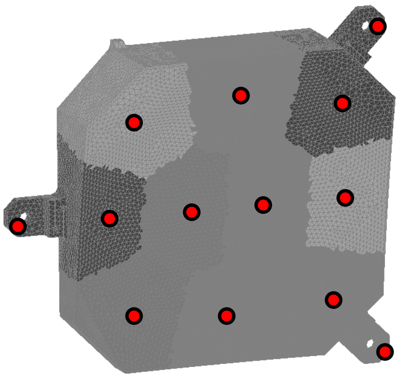

10

Mesh clustering: 3 steps

K-mean clustering initialization (user input # cluster) → cluster center

Greedy region growing

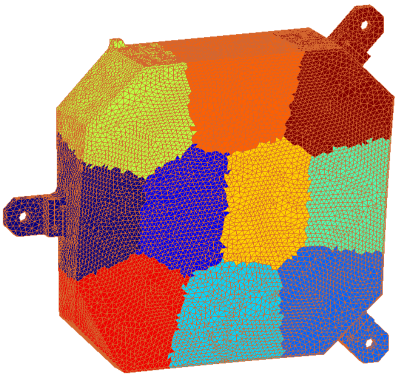

11

Mesh clustering: 3 steps

K-mean clustering initialization (user input # cluster) → cluster center

Greedy region growing

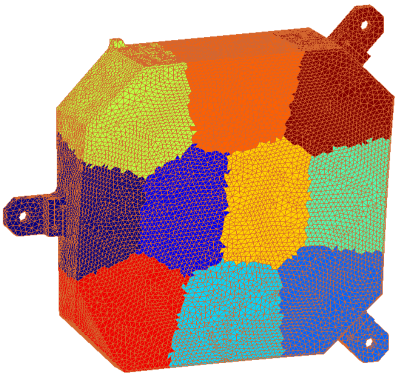

Boundary smoothing

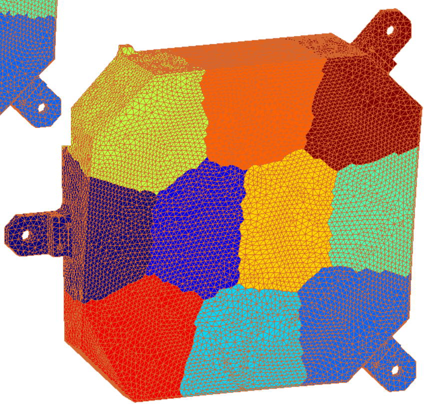

12

Mesh clustering: 3 steps

Heterogeneous mesh

Material constraints

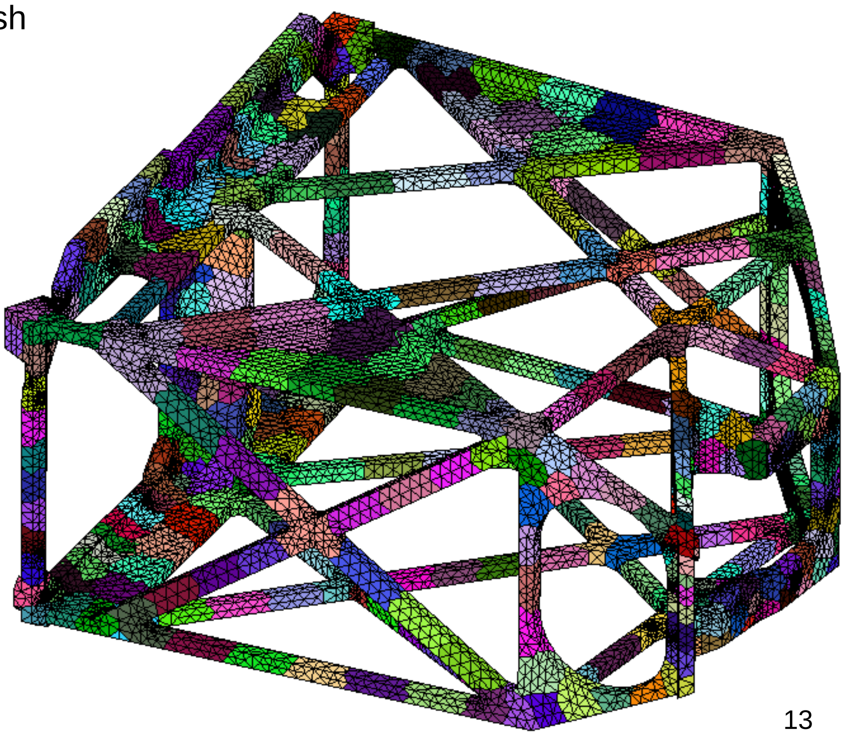

13

Problem of Guyan condensation

Cannot use cluster center as retained node

No (or known) heat load on condensed nodes

Heat load on selected node ≠ heat load on cluster

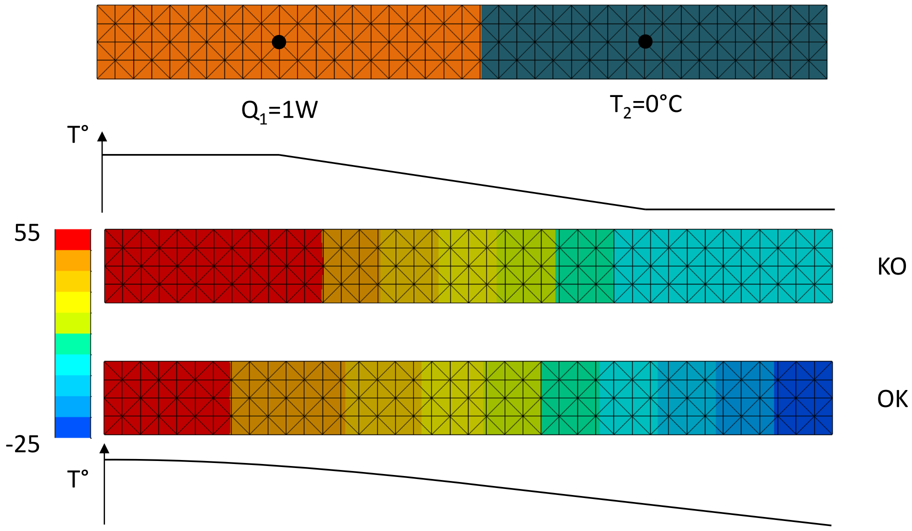

14

Create new “super-nodes”

Not picking a representative node of the cluster but creating new nodes

A super-node = weighted (area, volume) average each node cluster

$$\mathbf{T_{SN}} = \mathbf{AT}$$

$$T_{SN_i} = \sum_{j=1}^{N} A_{ij} T_j \qquad \sum_{j=1}^{N} A_{ij} = 1$$

15

More than 10% error

	Detailed	ESATAN	Reduced
ΔT [K]	22.5	27.4	22.5
# nodes	35k	422	397
# links	>200000	473	78600

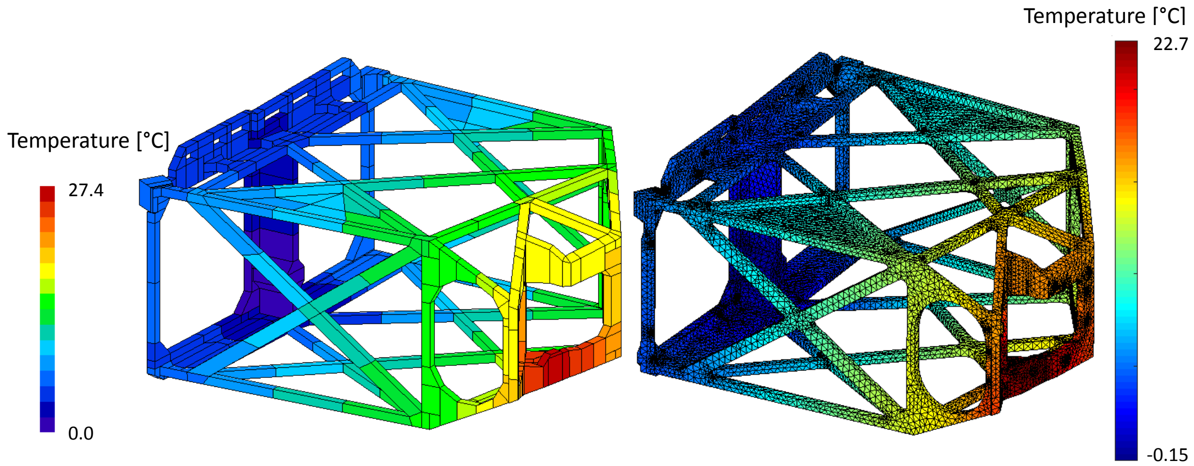

16

Outline

Ray-tracing enhancement

FEM clustering & conductive reduction

Super-face ray-tracing

Integrating the developments

Conclusions & perspectives

17

Selective quadric fitting

Automatic quadric mesh fitting of user selected regions (e.g. optics)

$$f(\mathbf{x}) = \mathbf{C}^{\mathrm{T}}\mathbf{F} \qquad \mathbf{F}(\mathbf{x}) = [1, x, y, z, xy, xz, yz, x^2, y^2, z^2]^{\mathrm{T}}$$

$$\mathbf{C} = [c_0, \dots, c_9]^{\mathrm{T}}$$

$$error \approx \sum_{S_i \in R} \int_{S_i} \frac{f(\mathbf{x})^2}{|\nabla f(\mathbf{x})|^2} d\sigma \approx \frac{\mathbf{C}_0^{\mathrm{T}} M \mathbf{C}_0^{\mathrm{T}}}{\mathbf{C}_0^{\mathrm{T}} N \mathbf{C}_0^{\mathrm{T}}}$$

With $\mathbf{M} = \frac{1}{n}\sum_{\substack{i=1,\\ \mathbf{x}_i \in R}}^{n} \mathbf{F}(\mathbf{x}_i)\mathbf{F}(\mathbf{x}_i)^{\mathrm{T}}$ $\qquad$ $\mathbf{N} = \frac{1}{n}\sum_{\substack{i=1,\\ \mathbf{x}_i \in R}}^{n} \nabla\mathbf{F}(\mathbf{x}_i)\nabla\mathbf{F}(\mathbf{x}_i)^{\mathrm{T}}$

$\mathbf{C}$ is the eigen vector associated with minimum eigen value of

$$\mathbf{M} - \lambda\mathbf{N}$$

18

Selective quadric fitting

Entrance baffle of EUI instrument onboard Solar Orbiter

Cone recognition

Shape error ~1nm

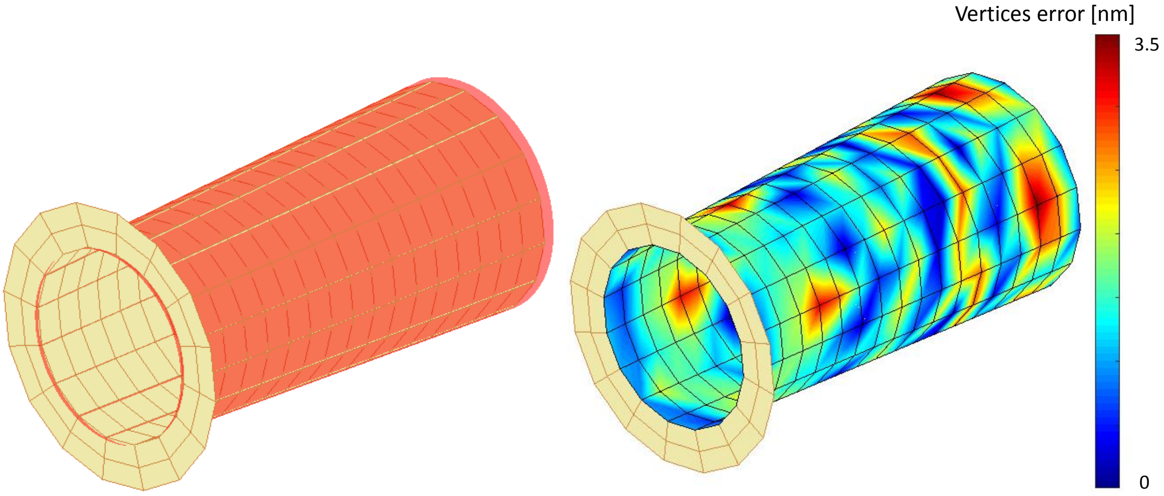

19

Ray-tracing with quadrics

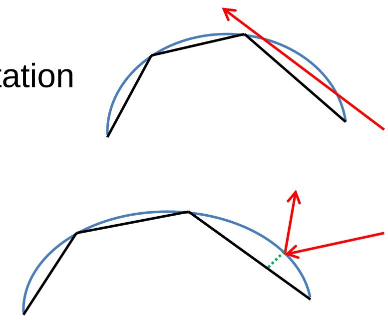

Use directly the quadric for the intersection computation

→ avoid lost grazing rays

→ better shadow

Project normally to the quadric to determine which super-face

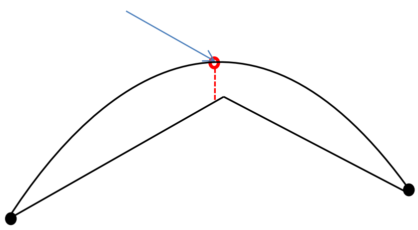

20

Fitted cylinder vs. ESARAD cylinder

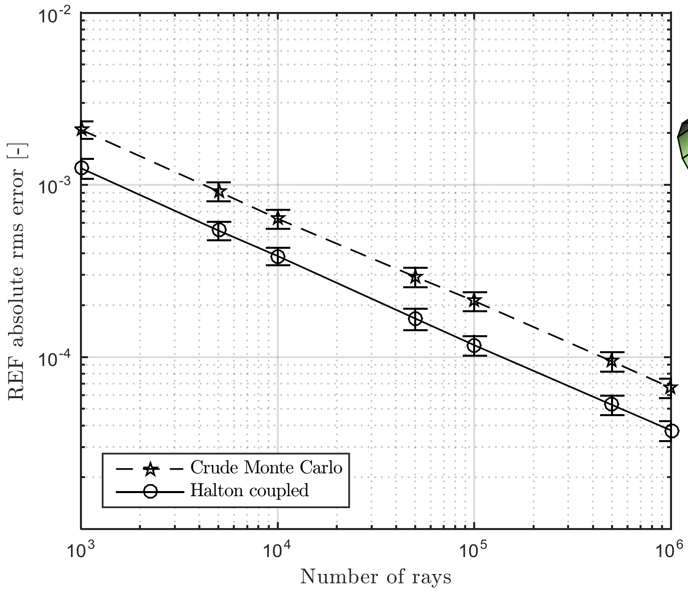

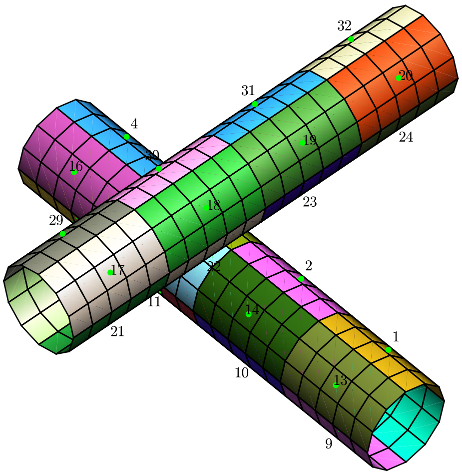

21

Outline

Ray-tracing enhancement

FEM clustering & conductive reduction

Super-face ray-tracing

Integrating the developments

Conclusions & perspectives

22

Conduction + radiation

	Detailed	ESATAN	Reduced
T_{IF} [°C]	-11.9	-10.8	-12.4
T_{min} [°C]	-20.2	-21.8	-20.6
# nodes	35k	422	397
# cond. links	>200k	473	78.6k
# rad. links	1500k	41k	55k

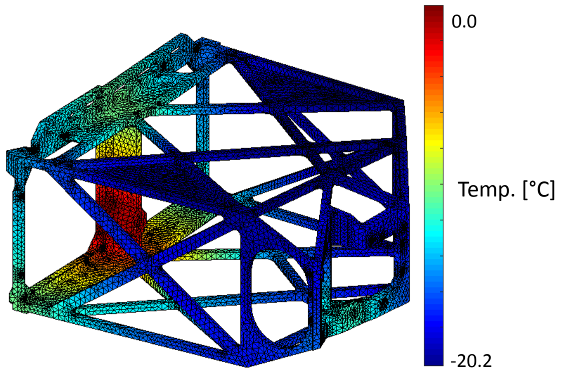

Detailed

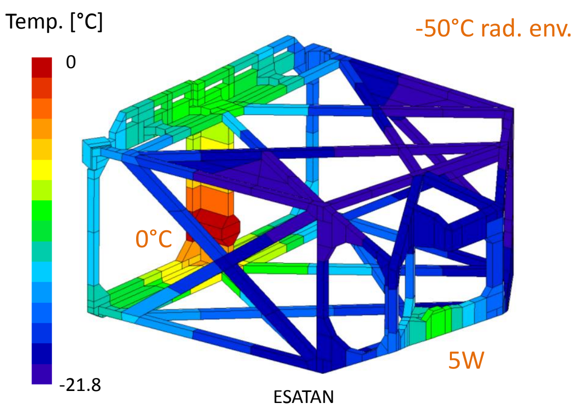

ESATAN

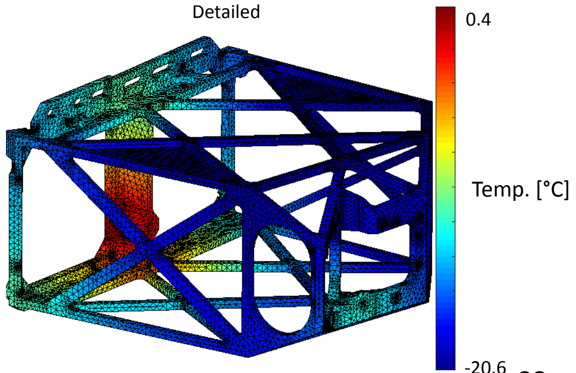

Reduced

23

Putting the building blocks together

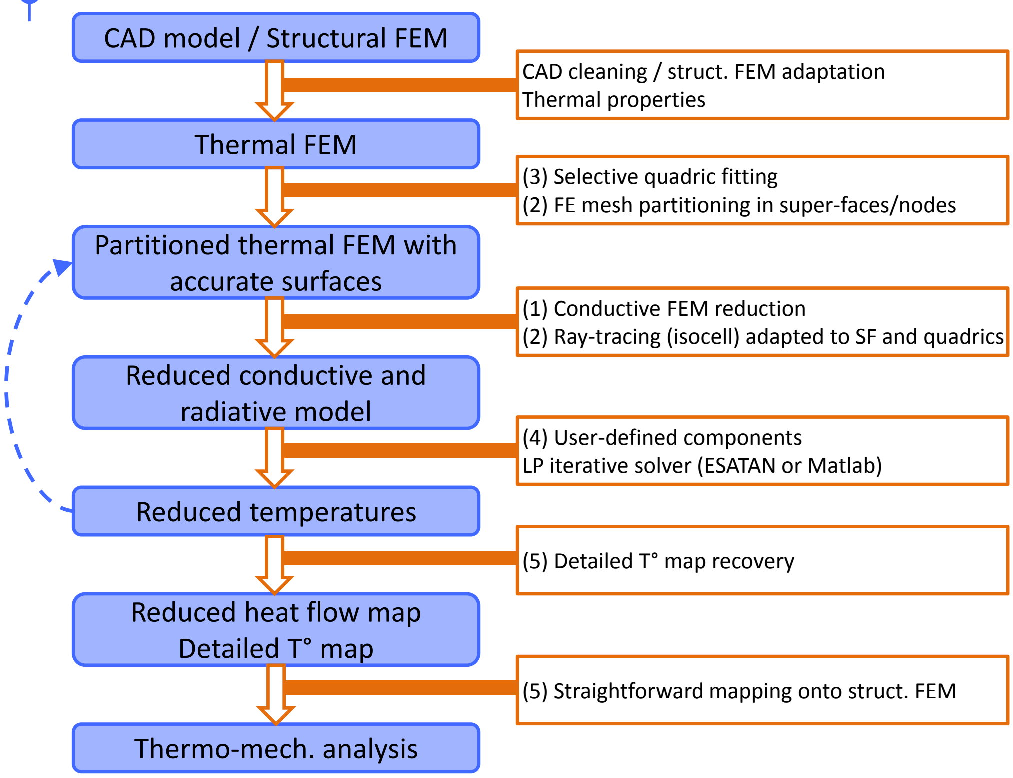

24

Global tool development

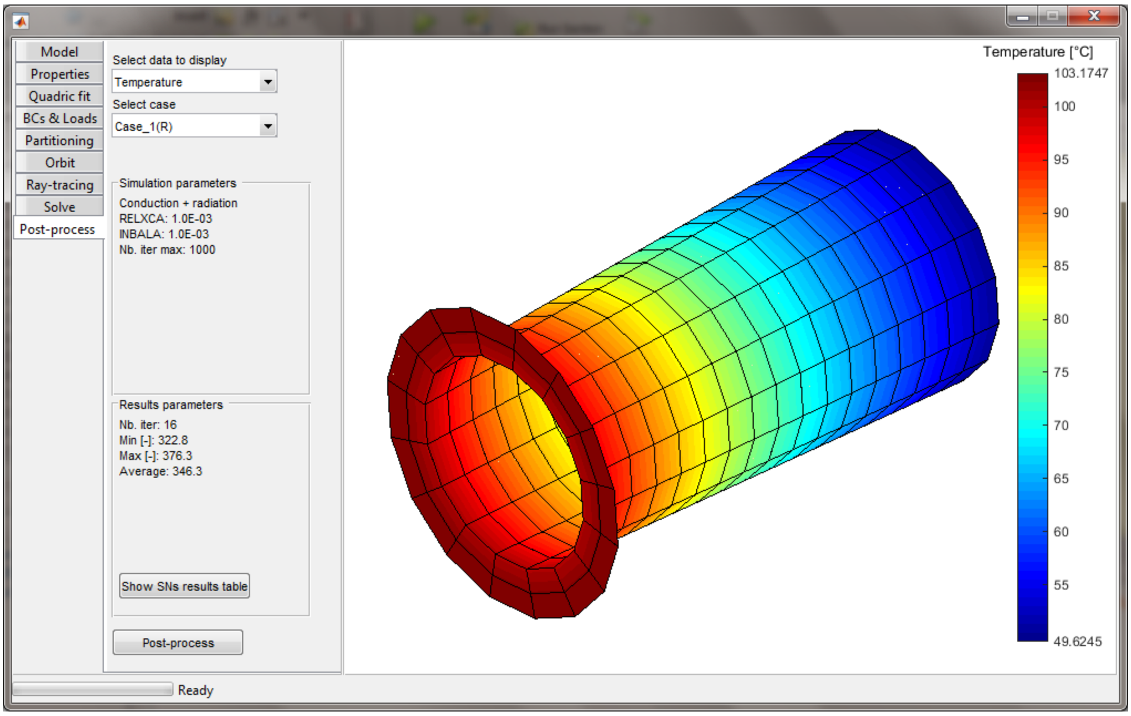

25

CONCLUSIONS & PERSPECTIVES

Global approach for conduction and radiation

Takes advantages of both lumped parameter and finite element methods:

- More accurate conductive links
- Accurate shape recognition used for ray-tracing
- Reduce the gap between thermal and structural analyses

Perspectives:

- Iterative process with automatic refinement in high ΔT regions
- GPUs with Matlab parallel computing toolbox® and CUDA®
- Quadric fitting → opto-thermo-structural analyses

26

Thank you for your attention…

Any question?

27

CONTACT

Lionel Jacques, ljacques@ulg.ac.be
Thermal Engineer & PhD student

- University of Liège
  Space Structures and Systems Lab
  1, Chemin des Chevreuils (B52/3)
  Liege, B-4000, Belgium
  http://www.ltas-s3l.ulg.ac.be/

- Centre Spatial de Liège
  Liège Science Park
  Avenue Pré-Aily
  B-4031 Angleur Belgium
  http://www.csl.ulg.ac.be

28

Appendix N

The Thermal Design of the KONTUR-2 Force Feedback Joystick

Ralph Bayer
(DLR, Germany)

Abstract

The KONTUR-2 Mission is a cooperation between the German Aerospace Center (DLR), ROSKOSMOS, RSC Energia and the Russian State Scientific Center for Robotics and Technical Cybernetics (RTC). Its purpose is to study the feasibility of using teleoperation to control robots for tasks such as remote planetary explorations. The operating human would be stationed in orbit around the celestial body in a spacecraft. For KONTUR-2, the earth is utilized as the celestial body, and the ISS as the spacecraft with the ISS crewmember as the operator. The main goals of this mission are the development of a space-qualified 2 degrees of freedom (DoF) force feedback joystick as the human machine interface (HMI), the study and implementation of underlying technologies to enable telepresence in space, and the analysis of telemanipulation performance of robotic systems. The DLR KONTUR force feedback joystick was upmassed and installed in the Russian Service Module of the ISS in August 2015. The first of a series of experiments to be completed by December 2016, were carried out successfully.

Meeting the thermal requirements of the joystick is one of the key challenges in the KONTUR-2 Mission. This presentation focuses on the thermal design for the force feedback joystick to cope with the unique conditions in a manned spacecraft. In order to reduce complexity, and further improve safety aspects for the integration on board the Russian segment of the ISS, active cooling has been eliminated in the force feedback joystick. Furthermore, as a safety measure, a temperature control system (TCS) has been developed and implemented able to respond to all unforeseen disturbances.

This presentation outlines DLR's approach to handle the unpredictable thermal output of the mechatronic system, resulted from a complex combination of the specific task, and the operating handling of the Cosmonaut. This in turn directly influenced the design to meet the mission's requirements, which includes the physical human-joystick interaction, storage on board the ISS, electronic components, operation time, and system performance.

The Thermal Design of the KONTUR-2 Force Feedback Joystick

Ralph Bayer

German Aerospace Center (DLR)
Robotic and Mechatronic Centrum (RMC)
Institute of Robotics and Mechatronics

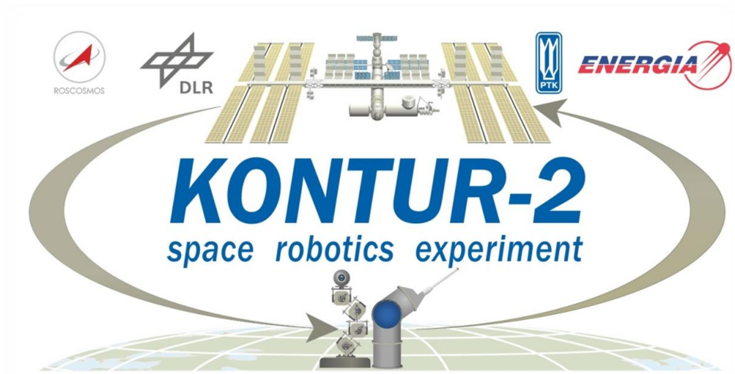

Outline

- KONTUR-2 mission overview
- Thermal requirements
- Thermal design
- Analysis cases and results
- Temperature Control System (TCS)
- Thermal test and results
- Conclusion and Outlook

KONTUR-2 mission overview

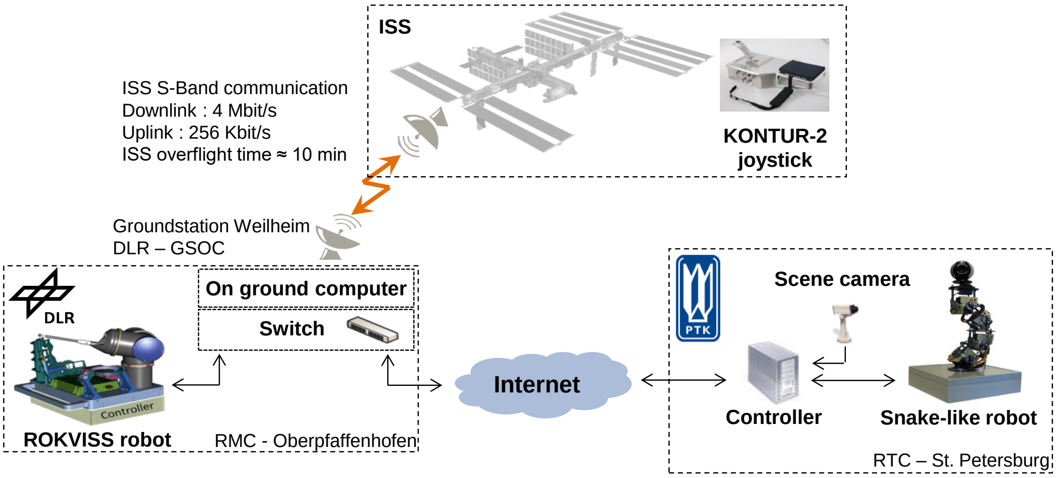

Feasibility study

Telepresence for remote planetary exploration

Experiment scenario

Teleoperating robot on the planetary surface from orbit

DLR

KONTUR-2 mission overview

Goals

- Development of a space-qualified force feedback joystick as the human machine interface (HMI)
- Development of telepresence technologies
- Study of ergonomics and human factors of the force feedback in microgravity

Joystick specifications

- Maximum force on joystick handle: 15 N
- Workspace: +/- 20°
- 2 Degrees of freedom

History: ROKVISS experiment

- Verification of robotic components in space

KONTUR-2 Joystick in Operation Mode

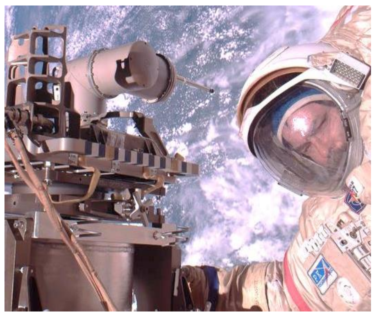

ROKVISS robot on board the ISS

DLR

KONTUR-2 challenges

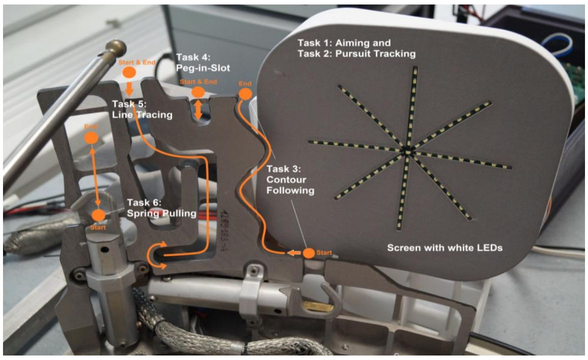

KONTUR-2 task board of the ROKVISS robot


Cosmonaut O. Kononenko performs a task on ISS

Difficult thermal conditions

Unpredictable motor load, which is a complex combination of

- Different tasks
- Operating behavior of the cosmonaut
- Side effects e.g. telepresence performance, friction modeling

Thermal requirements

Requirements

- Joystick housing maximum allowable temperature: 40°C
- Operational temperature range of on-board electronics and motors
- No active cooling system
- Continuous operating time: 30 minutes

Environmental qualification tests

- Humidity cycles
- Temperature cycles
- Offgassing (toxicity)

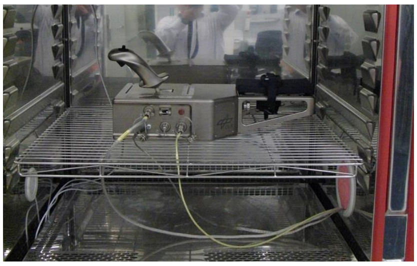

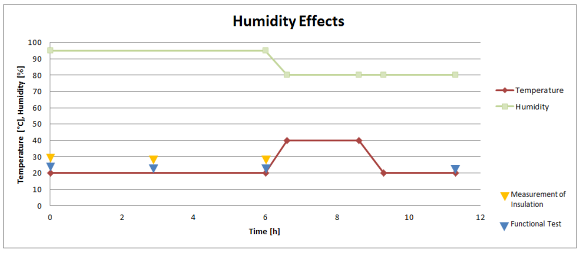

DLR.de • Chart 7 > 29th European Space Thermal Analysis Workshop > Ralph Bayer • 03+04.11.15

Thermal design - model

- FEM analysis (ANSYS 14.0)
- No printed circuit boards (PCBs)

General boundary conditions

- ISS ambient temperature condition ≤ 28°C
- Complete insulation between joystick and ISS structure
- Heat flows with +10% margin

Conductive boundary conditions

- Air inside the joystick appeals thermoconductive (neglected)
- Ideal thermal contact between mechanical parts
- Electronic components attached to the mechanical parts through interface materials (gap pads)

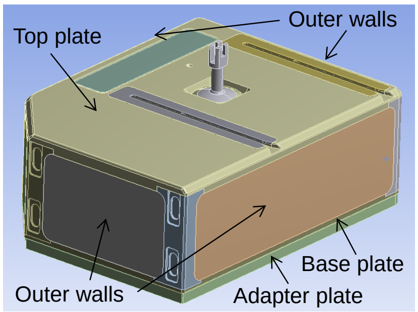

Joystick housing FEM model (ANSYS)

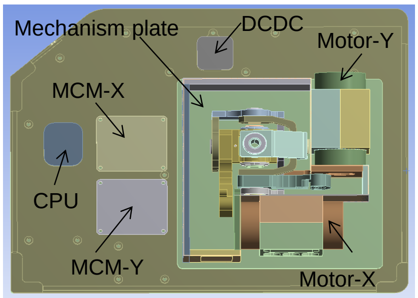

Joystick components inside

DLR.de • Chart 8 > 29th European Space Thermal Analysis Workshop > Ralph Bayer • 03+04.11.15

Thermal design - model

Radiative boundary conditions

- Heat radiation exchange in the environment
  → Joystick housing with electroplated chromium coating: ε=0.1
  → Adapter plate with black anodized aluminium: ε=0.82
- Heat radiation exchange inside the joystick

Convective boundary conditions

- Airflow (0,05 m/s) of the ISS air supply near the joystick
  → Similitude model of a plane plate in a longitudinal flow for specific plates and walls (worst case)

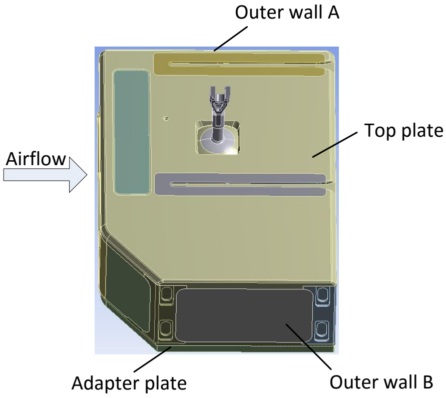

ISS supply airflow direction with respected plates and walls

Thermal design – analysis cases

Analysis cases based on states

Standby

- Initial state after switching on and booting
- Passive mode – only communication possible
- Intended as pause mode

Electric Components	States		
	Standby	Idle	Operation
Motors	None	None	Load-depending
Motor Control Module (MCM)	None	≈ 3.5 W	Load-depending
DCDC-Converter	≈ 1.9 W	≈ 1.9 W	≈ 1.9 W
Microcontroller Module (CPU)	≈ 5.0 W	≈ 5.0 W	≈ 5.0 W

Heat dissipation for basic states of the joystick

Idle

- Joystick is calibrated
- Motor Control Modules (MCM) are active but no torque is commanded
- Intermediate state between standby and operation

Operation

- All hard- and software components are active including force feedback control

Thermal design – analysis cases

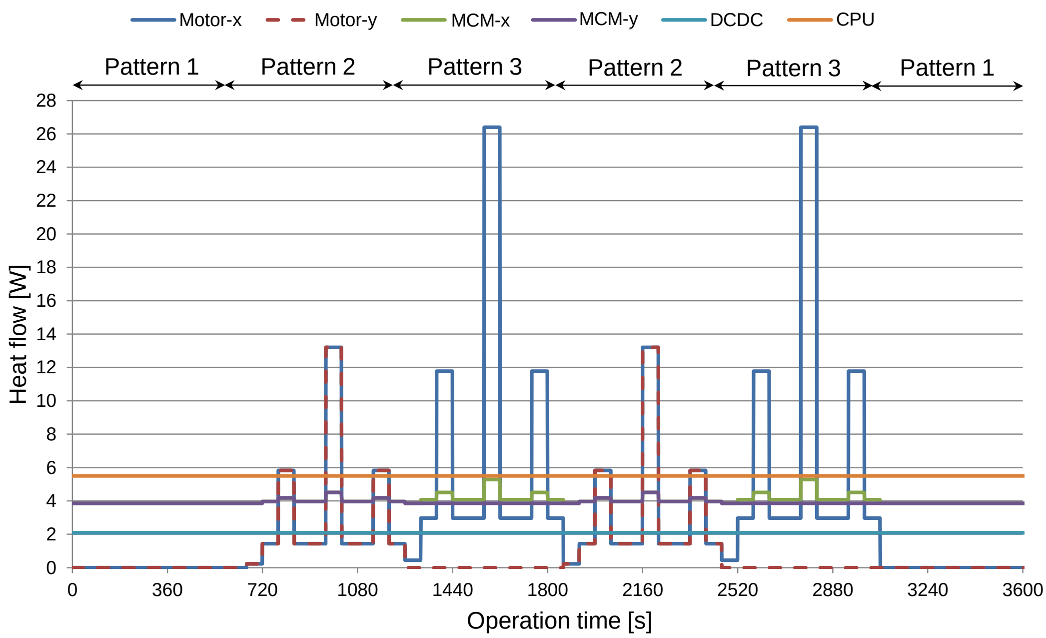

DLR.de • Chart 11 > 29th European Space Thermal Analysis Workshop > Ralph Bayer • 03+04.11.15

Analysis results

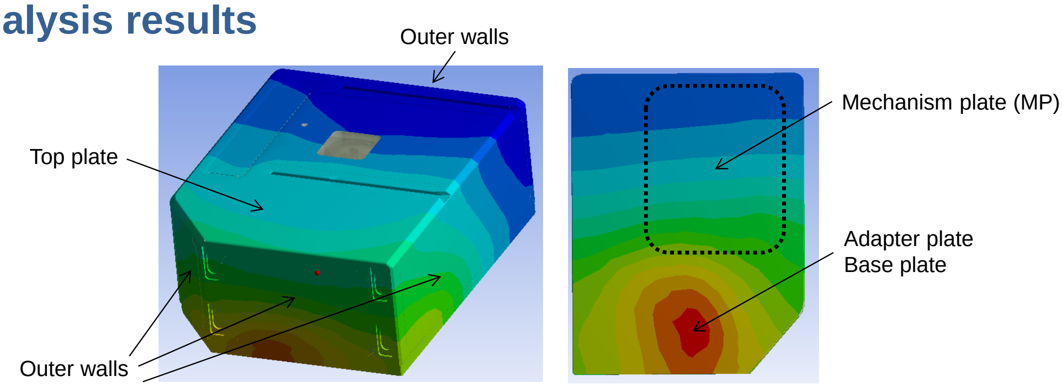

Characteristic joystick temperature distribution from the front side

Characteristic hotspot from bottom side

Housing location	Standby	Idle	Operation		
	Steady state > 5 h	Steady state > 2 h	30 min	60 min	30 min (without adapter plate)
	°C	°C	°C	°C	°C
Base plate	37.70	46.38	34.60	38.64	40.00
Adapter plate	37.64	46.32	34.55	38.58	–
Outer walls	37.49	46.03	34.27	38.65	38.66
Mechanism plate	36.83	45.29	33.53	37.48	37.17
Top plate	36.68	44.72	33.10	37.00	36.10

DLR

DLR.de • Chart 12 > 29th European Space Thermal Analysis Workshop > Ralph Bayer • 03+04.11.15

Temperature Control System (TCS)

Objectives

1. Observance of the temperature limits for the electronic components
2. Observance of max. housing temperature

   → Even when the joystick is operated incorrectly

- 9 temperature sensors are monitored every 1 sec.

Temperature sensor of one motor housing

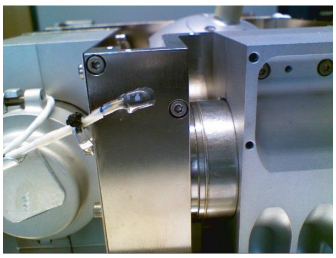

Temperature sensor T_Case near the top plate of the the joystick housing

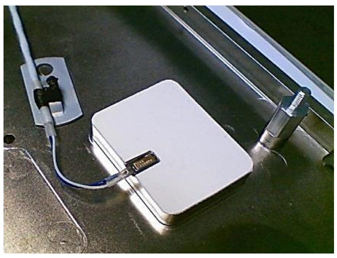

Temperature sensor near the CPU

DLR

DLR.de • Chart 13 > 29th European Space Thermal Analysis Workshop > Ralph Bayer • 03+04.11.15

Temperature Control System (TCS)

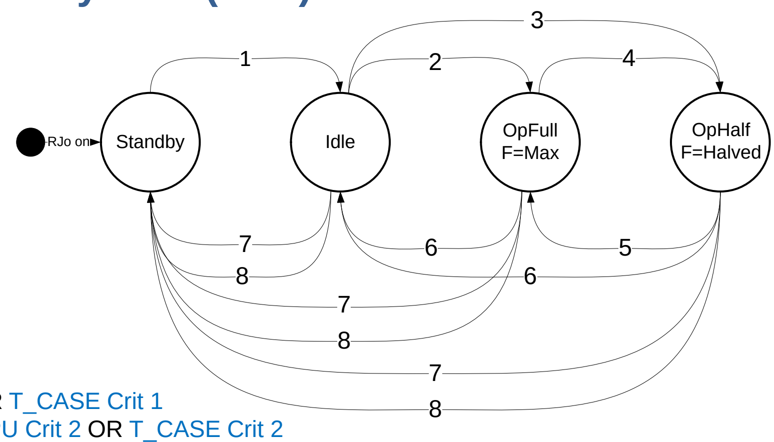

→ Additional state: OpHalf

Statemachine conditions

1: Calibrate AND T_CPU Crit 1 OR T_CASE Crit 1
2: Application activated AND T_CPU Crit 2 OR T_CASE Crit 2
3: Application activated AND T_CPU Crit 3 OR T_CASE Crit 3
4: T_CPU Crit 4 OR T_CASE Crit 4
5: T_CPU Crit 5 OR T_CASE Crit 5
6: Application deactivated
7: Standby
8: T_CPU Crit 8 OR T_CASE Crit 8

If T_CPU is invalid use T_DCDC
If T_CASE is invalid use T_MotorX OR T_MotorY

DLR

DLR.de • Chart 14 > 29th European Space Thermal Analysis Workshop > Ralph Bayer • 03+04.11.15

Thermal test

Test cases

1. Standby state until steady state
2. Idle state until TCS switches to standby state
3. Operational state (stirring) with elastic band
   a. $F_H = 5$ N
   b. $F_H = 10$ N
   c. $F_H = 15$ N (max. force)
   → Higher load than normal usage!

- Joystick in thermal chamber
- No adapter plate
- Worst case ambient temperature is 28°C
- Housing isolated with polystyrene, foam and bubble wrap to reduce convectional heat transfer

Isolated joystick

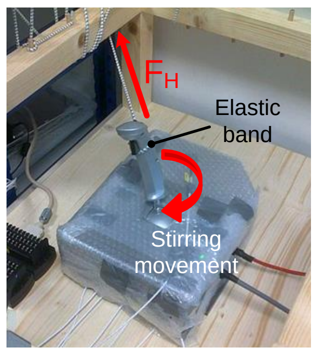

Stirring demo

DLR

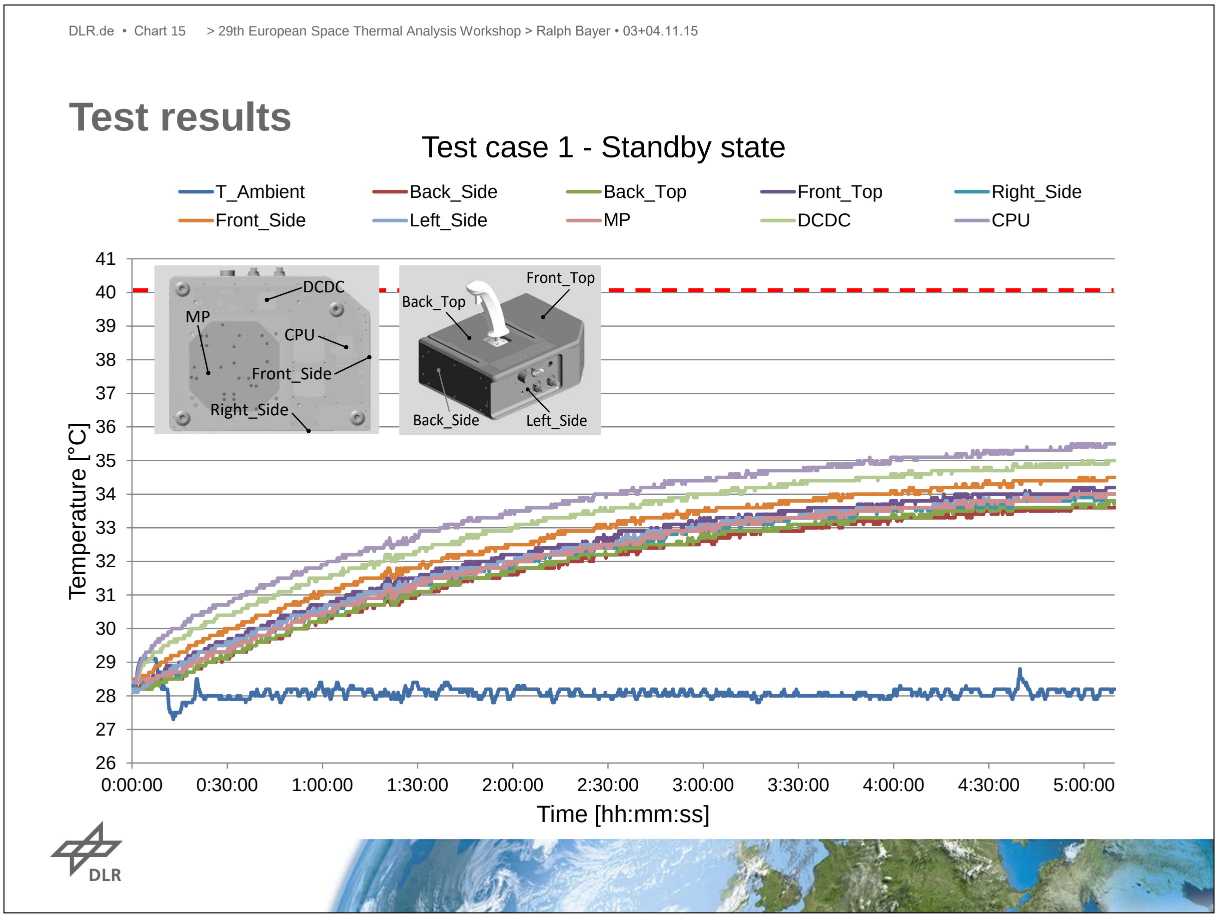
DLR.de • Chart 15 > 29th European Space Thermal Analysis Workshop > Ralph Bayer • 03+04.11.15
Test results
Test case 1 - Standby state
T_Ambient
Back_Side
Back_Top
Front_Top
Right_Side
Front_Side
Left_Side
MP
DCDC
CPU
DCDC
MP
CPU
Front_Side
Right_Side
Front_Top
Back_Top
Back_Side
Left_Side
Temperature [°C]
41
40
39
38
37
36
35
34
33
32
31
30
29
28
27
26
0:00:00
0:30:00
1:00:00
1:30:00
2:00:00
2:30:00
3:00:00
3:30:00
4:00:00
4:30:00
5:00:00
Time [hh:mm:ss]
DLR

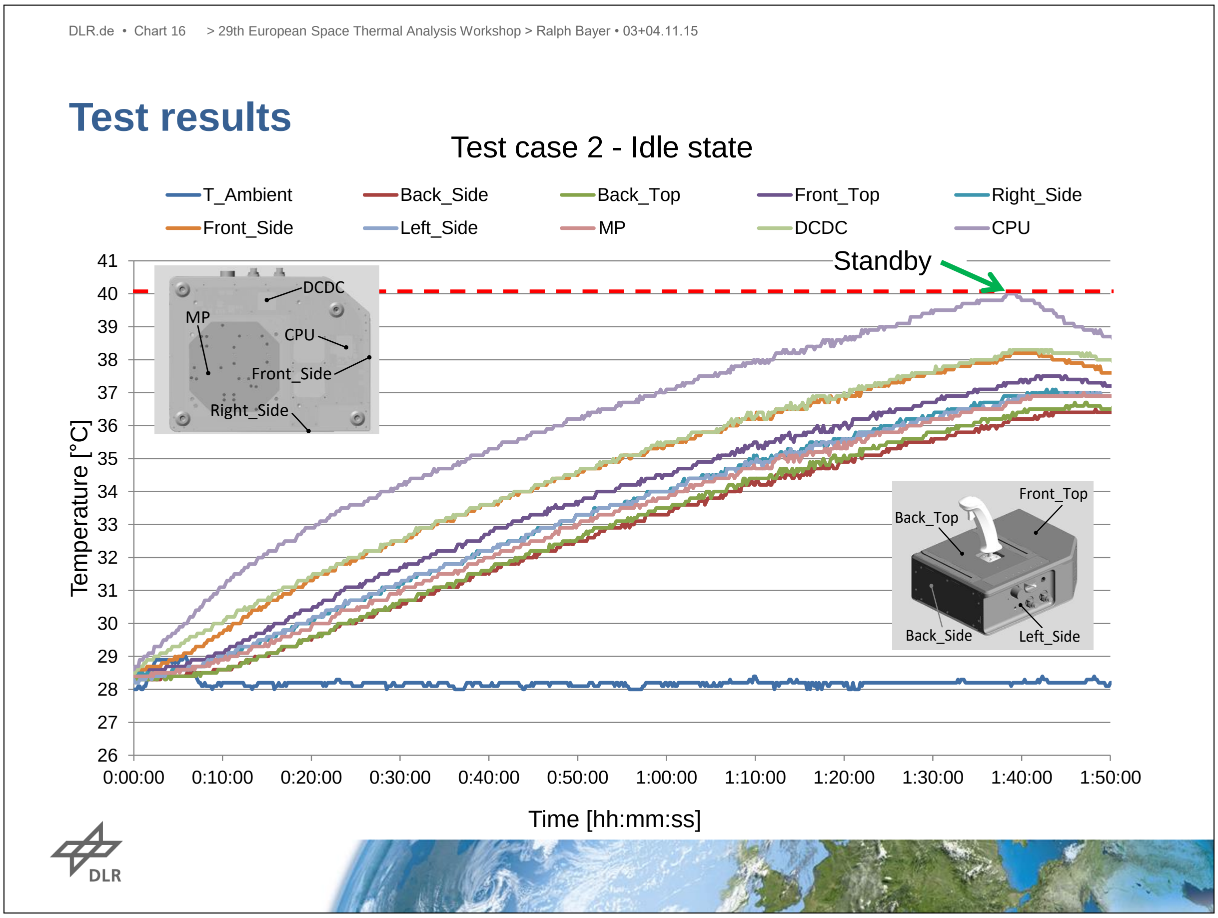
DLR.de • Chart 16 > 29th European Space Thermal Analysis Workshop > Ralph Bayer • 03+04.11.15
Test results
Test case 2 - Idle state
T_Ambient
Back_Side
Back_Top
Front_Top
Right_Side
Front_Side
Left_Side
MP
DCDC
CPU
Standby
DCDC
MP
CPU
Front_Side
Right_Side
Front_Top
Back_Top
Back_Side
Left_Side
Temperature [°C]
41
40
39
38
37
36
35
34
33
32
31
30
29
28
27
26
0:00:00
0:10:00
0:20:00
0:30:00
0:40:00
0:50:00
1:00:00
1:10:00
1:20:00
1:30:00
1:40:00
1:50:00
Time [hh:mm:ss]
DLR

DLR.de • Chart 17 > 29th European Space Thermal Analysis Workshop > Ralph Bayer • 03+04.11.15

Test results

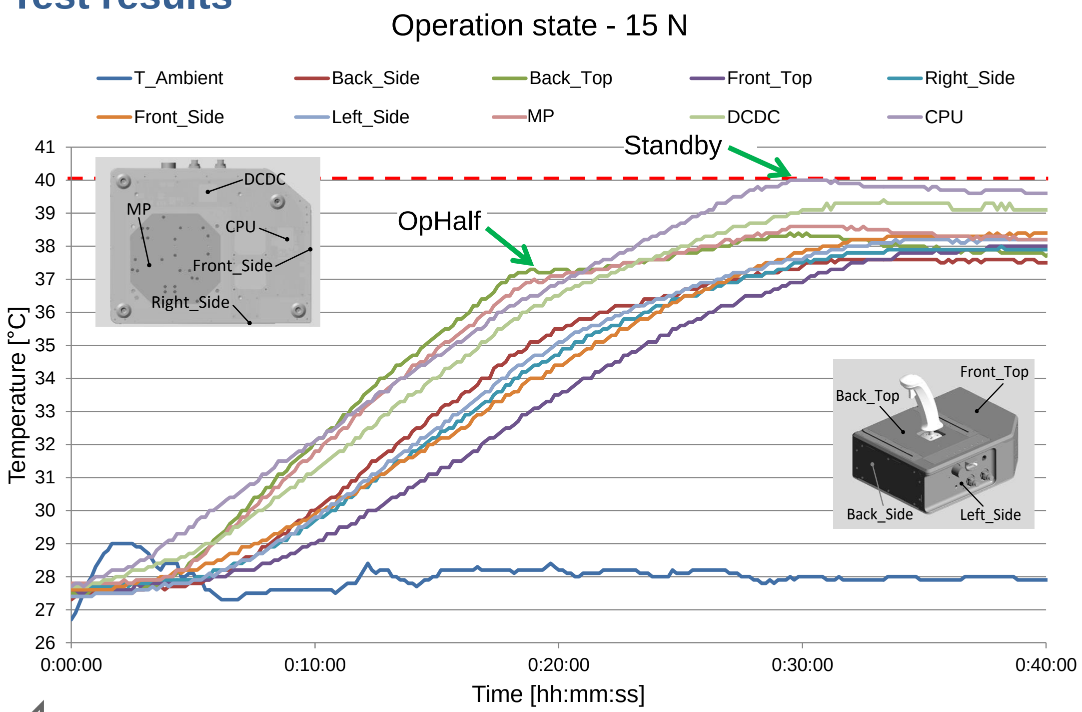

DLR

DLR.de • Chart 18 > 29th European Space Thermal Analysis Workshop > Ralph Bayer • 03+04.11.15

Conclusion

Thermal design

- The thermal analysis model has been verified by thermal tests
- Thermal test have clearly proven that the joystick fulfills all thermal requirements under the assumed boundary conditions.
- The TCS has successfully been developed, implemented and tested.
- All environmental qualification and acceptance tests have been passed

KONTUR-2 mission

- The force feedback joystick was installed in the Russian service module in August 2015
- First experiments were conducted successfully

DLR

DLR.de • Chart 19 > 29th European Space Thermal Analysis Workshop > Ralph Bayer • 03+04.11.15

Outlook

- KONTUR-2 joystick shall operate until December 2015 on board the ISS
- During ongoing experiments all performance data will be recorded for each session
  → Ergonomic study for using force feedback in microgravital environment
  → Study of space related telepresence control performance
  → Evaluation of TCS-Concept for other robots
  → Further verification of thermal FEM-model

Haptics experiment with telepresence from space:

Handshake between cosmonaut on board the ISS and earth representative planned in December 2015

Cosmonaut handshake training with the KONTUR-2 joystick engineering model and the DLR humanoid robot Justin between the cosmonauts G. Padalka and O. Kononenko

DLR

DLR.de • Chart 20 > 29th European Space Thermal Analysis Workshop > Ralph Bayer • 03+04.11.15

Thank you for your attention!

For further information, visit our website

http://www.dlr.de/rmc/rm/en

Ralph Bayer

German Aerospace Center (DLR)
Robotic and Mechatronic Centrum (RMC)
Institute of Robotics and Mechatronics

Münchener Strasse 20
Oberpfaffenhofen
82234 Wessling
Germany

Tel.: +49 8153 28-3548
Fax: +49 8153 28-1134

http://rmc.dlr.de/rm/en/staff/ralph.bayer/
Ralph.Bayer@dlr.de

DLR

Appendix O

ESATAN Thermal Modelling Suite
Product Developments and Demonstration

Chris Kirtley Nicolas Bures
(ITP Engines UK Ltd, United Kingdom)

Abstract

Product Developments

ESATAN-TMS r7 was released at the end of 2014 and focused on improvements throughout the thermal modelling process, taking into account feedback received through our customer survey. The work has continued at a high-level, with a significant number of developments being finalised which centre on improving both the effectiveness of the interface and the *look and feel* of the product. Through close discussions with customers, the next release will also see a series of developments, either extending existing functionality or providing exciting new modelling features.
This presentation outlines the developments to be included within the next release of ESATAN-TMS.

Product Demonstration

A demonstration of the development version of ESATAN-TMS shall be provided, focusing on the new features of the product.


ESATAN-TMS
thermal modelling suite
ESATAN-TMS
Product Overview
Chris Kirtley,
Henri Brouquet
29th European Thermal & ECLS Software Workshop
3 – 4 November 2015, ESA/Estec, Noordwijk, The Netherlands

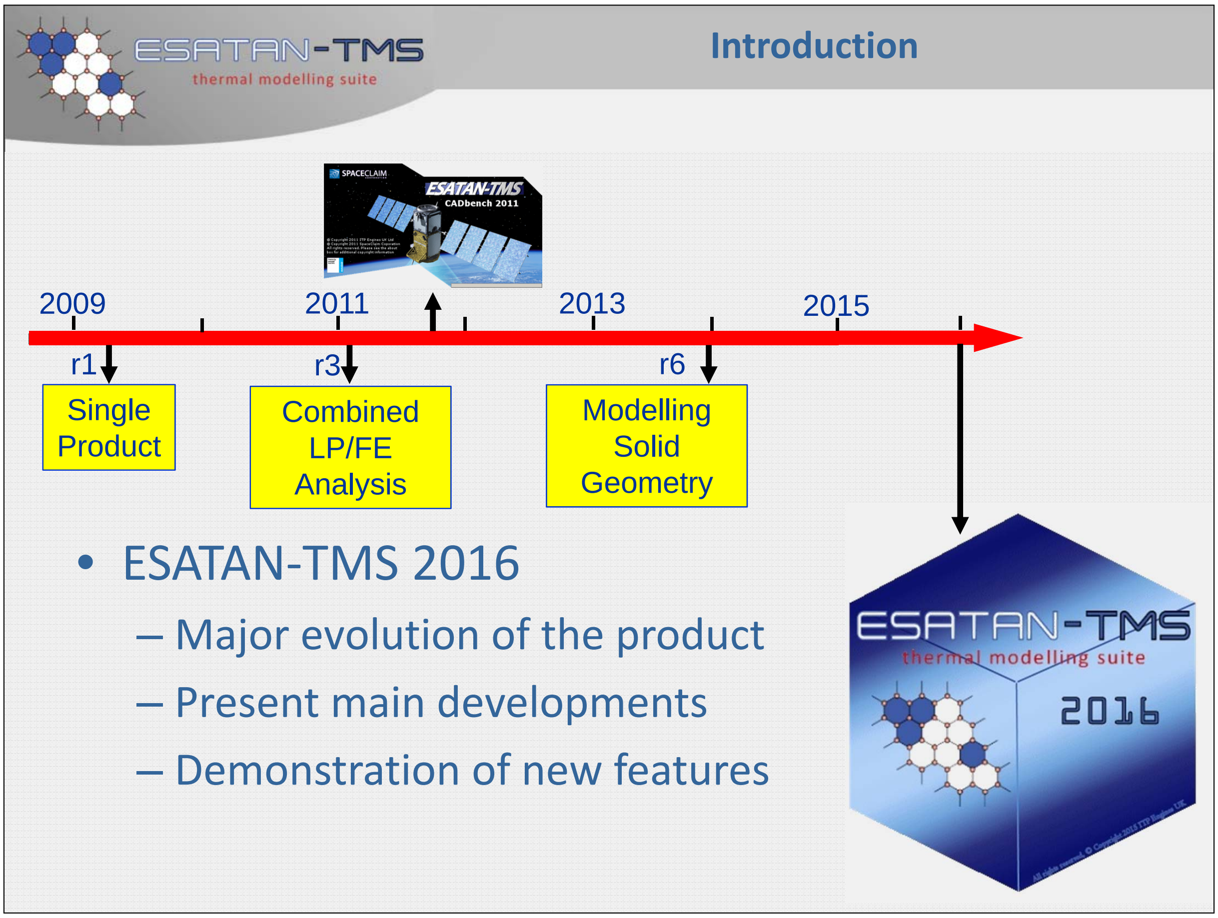
ESATAN-TMS
thermal modelling suite
Introduction
ESATAN-TMS
CADbench 2011
2009
2011
2013
2015
r1
r3
r6
Single Product
Combined LP/FE Analysis
Modelling Solid Geometry
• ESATAN-TMS 2016
– Major evolution of the product
– Present main developments
– Demonstration of new features
ESATAN-TMS
thermal modelling suite
2016

Presentation Contents

- ESATAN-TMS 2016 Developments
  - Improved Geometry Modelling
  - Bulk Material Definition
  - Radiative Analysis
  - Linear Conduction
  - Thermal Boundary Conditions
  - Thermal Analysis
  - Post-processing

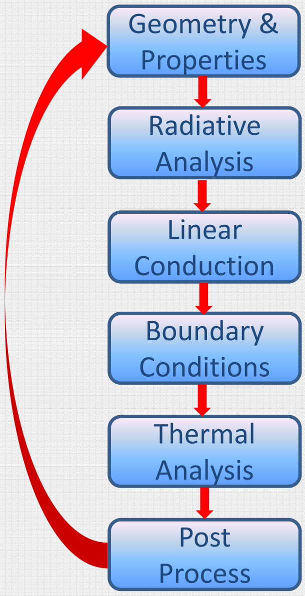

Presentation Contents

- ESATAN-TMS 2016 Developments
  - New ESATAN-TMS Workbench
  - Improved Geometry Modelling
  - Bulk Material Definition
  - Radiative Analysis
  - Linear Conduction
  - Thermal Boundary Conditions
  - Thermal Analysis
  - Post-processing

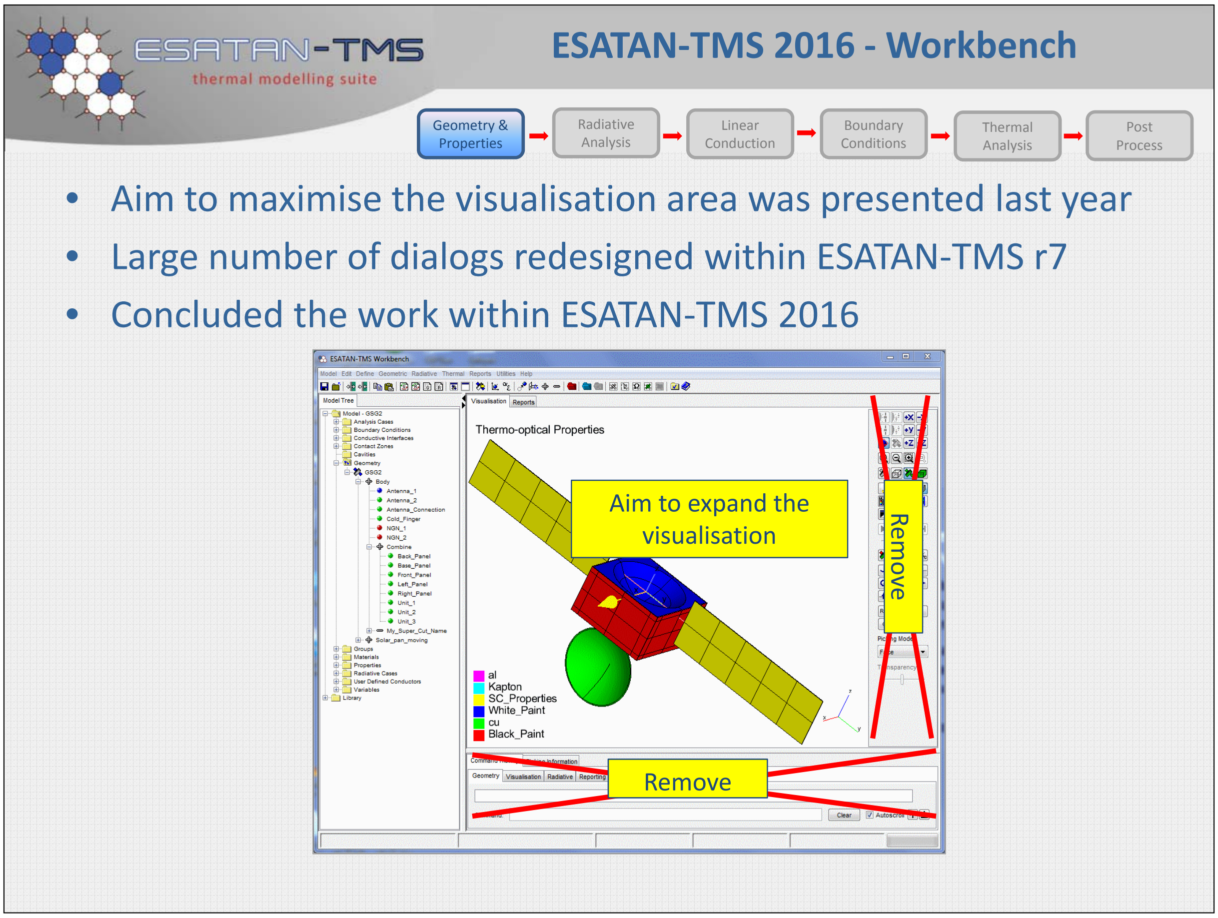
ESATAN-TMS
thermal modelling suite
ESATAN-TMS 2016 - Workbench
Geometry & Properties
Radiative Analysis
Linear Conduction
Boundary Conditions
Thermal Analysis
Post Process
• Aim to maximise the visualisation area was presented last year
• Large number of dialogs redesigned within ESATAN-TMS r7
• Concluded the work within ESATAN-TMS 2016
Thermo-optical Properties
Aim to expand the visualisation
Remove
Remove
al
Kapton
SC_Properties
White_Paint
cu
Black_Paint

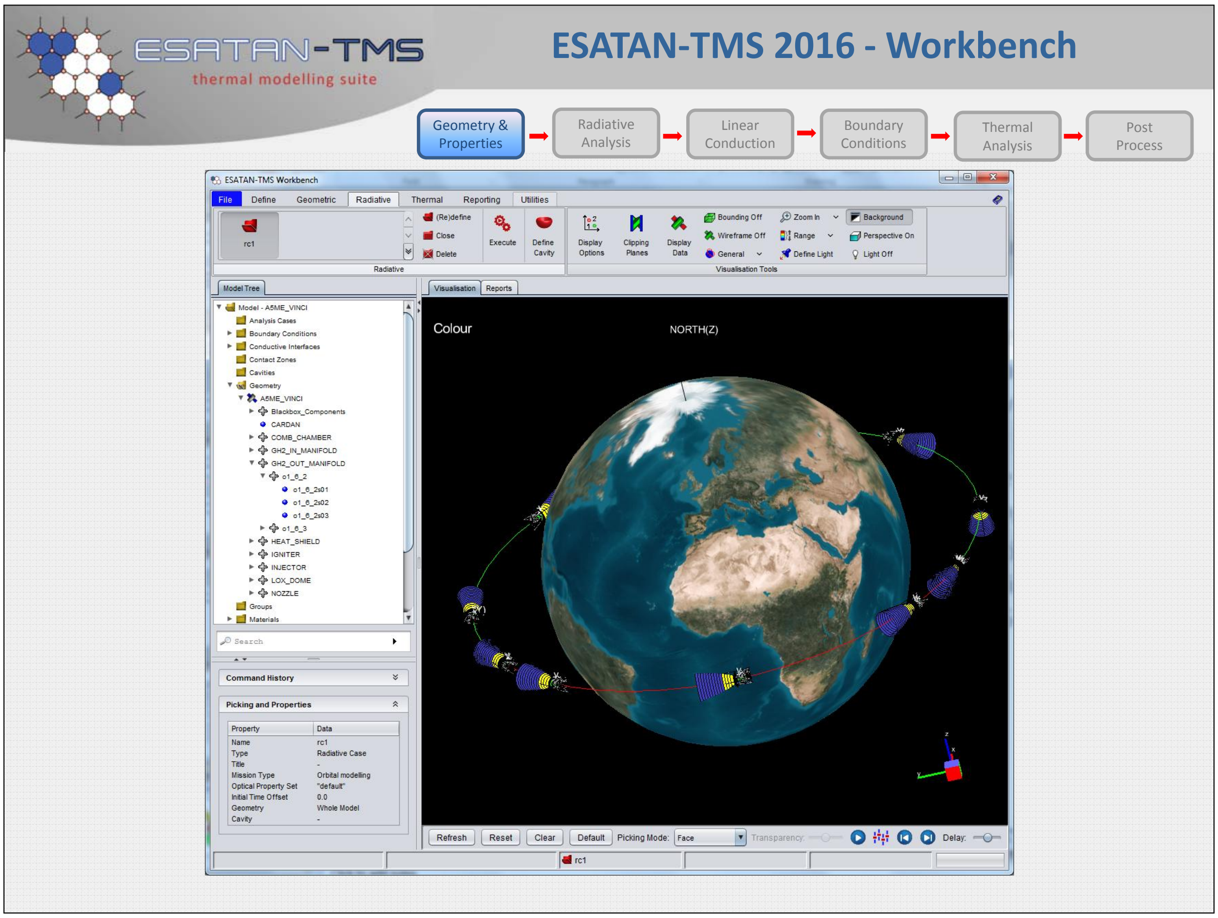
ESATAN-TMS
thermal modelling suite
ESATAN-TMS 2016 - Workbench
Geometry & Properties
Radiative Analysis
Linear Conduction
Boundary Conditions
Thermal Analysis
Post Process
ESATAN-TMS Workbench
Colour
NORTH(Z)

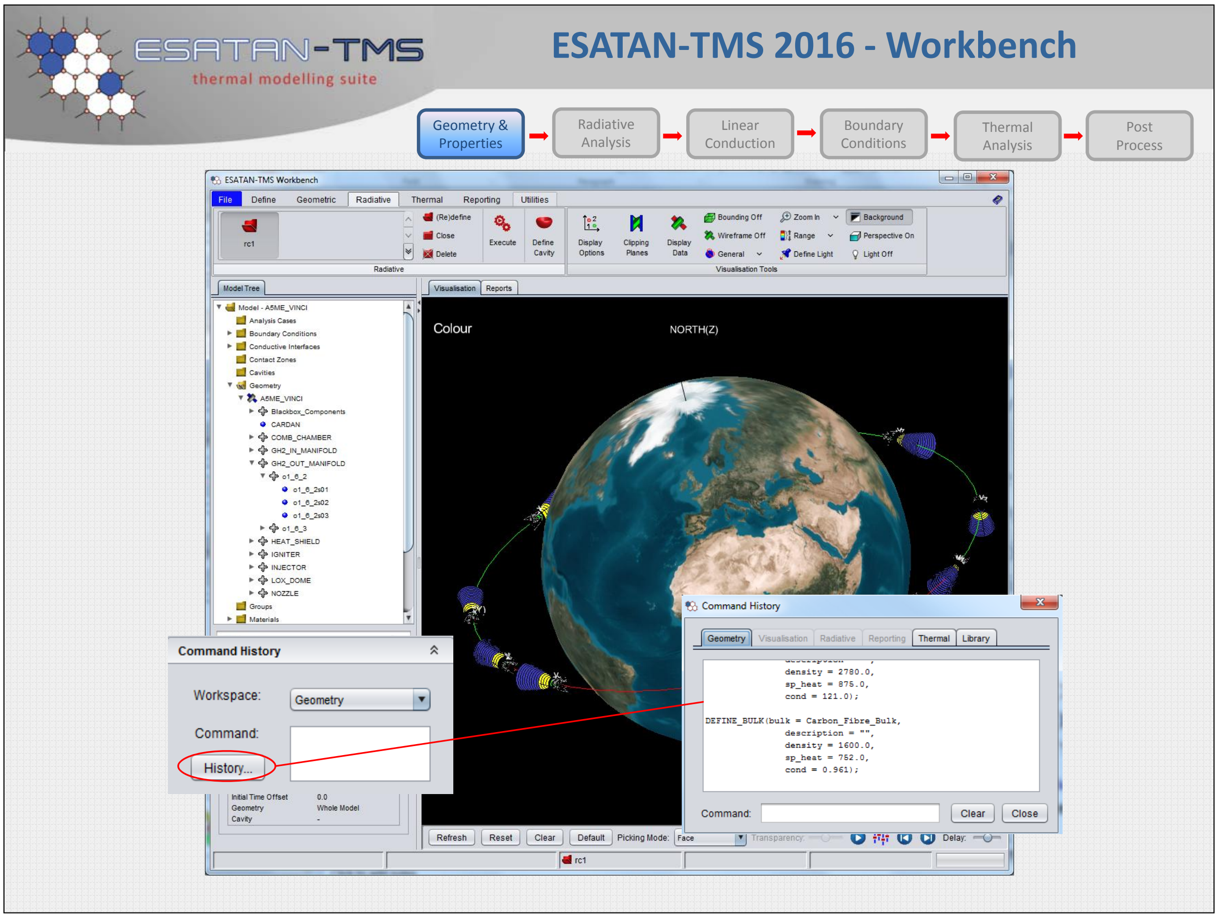
ESATAN-TMS
thermal modelling suite
ESATAN-TMS 2016 - Workbench
Geometry & Properties
Radiative Analysis
Linear Conduction
Boundary Conditions
Thermal Analysis
Post Process
Command History
Workspace:
Geometry
Command:
History...
Command History
Geometry
Visualisation
Radiative
Reporting
Thermal
Library
density = 2780.0,
sp_heat = 875.0,
cond = 121.0);
DEFINE_BULK(bulk = Carbon_Fibre_Bulk,
description = "",
density = 1600.0,
sp_heat = 752.0,
cond = 0.961);
Command:
Clear
Close
Colour
NORTH(Z)

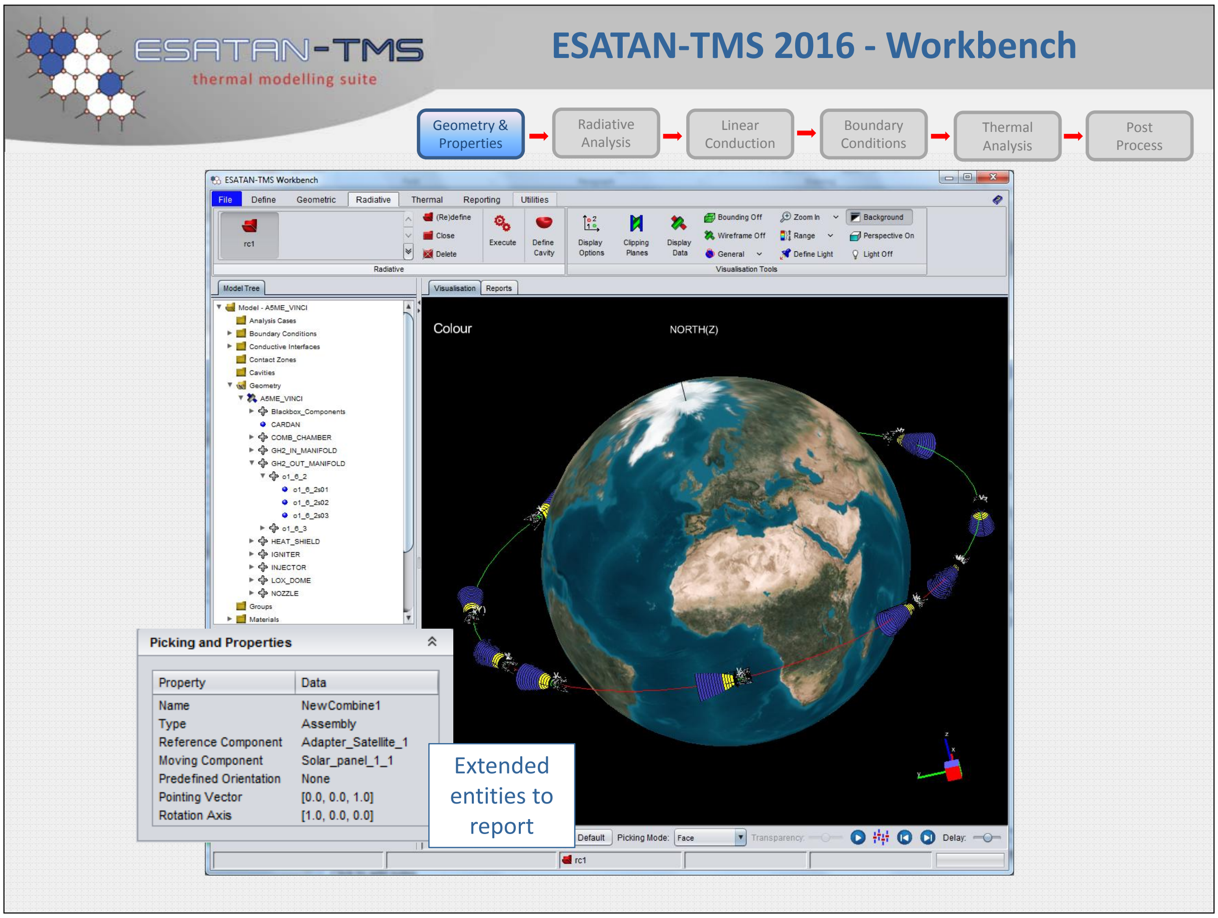
ESATAN-TMS
thermal modelling suite
ESATAN-TMS 2016 - Workbench
Geometry & Properties
Radiative Analysis
Linear Conduction
Boundary Conditions
Thermal Analysis
Post Process
Picking and Properties
Property
Data
Name
NewCombine1
Type
Assembly
Reference Component
Adapter_Satellite_1
Moving Component
Solar_panel_1_1
Predefined Orientation
None
Pointing Vector
[0.0, 0.0, 1.0]
Rotation Axis
[1.0, 0.0, 0.0]
Extended entities to report
Colour
NORTH(Z)

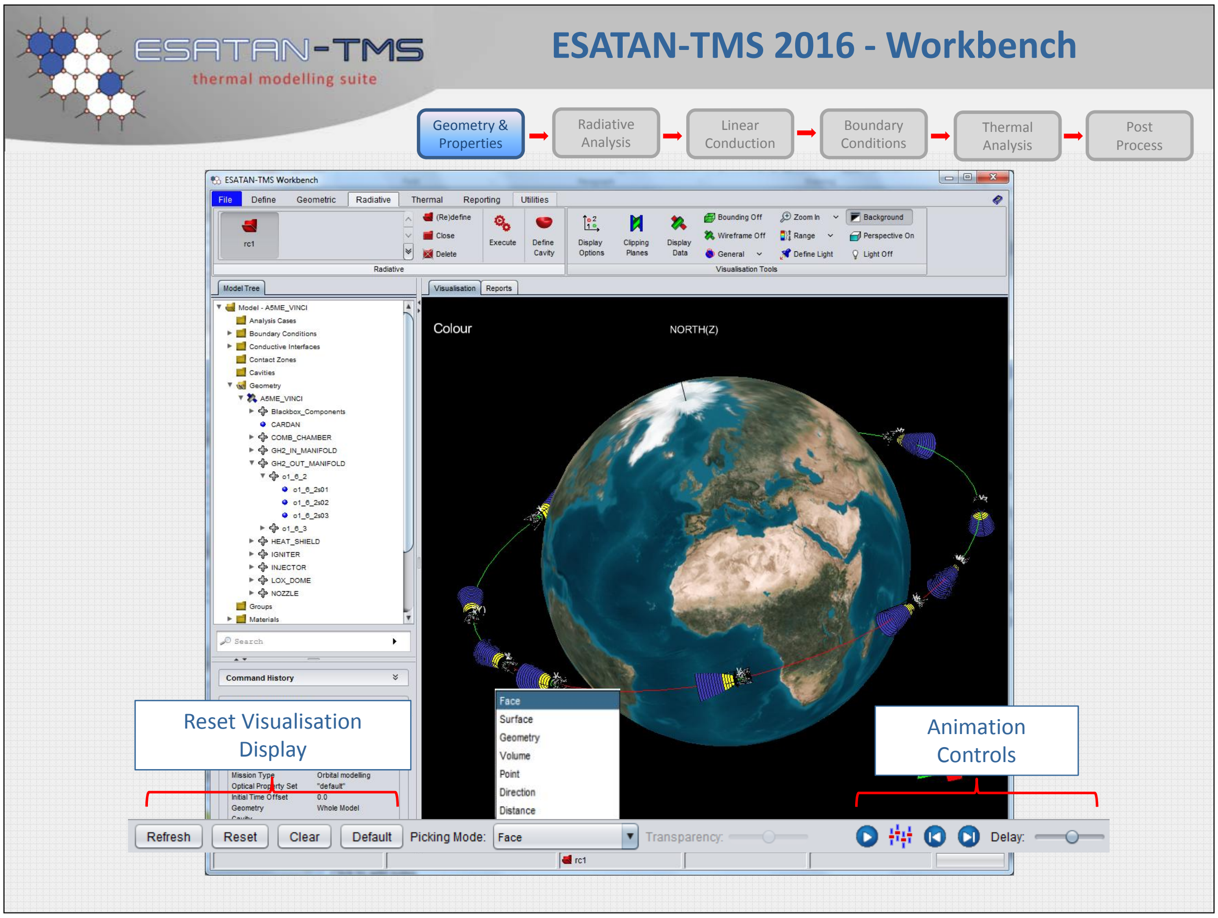
ESATAN-TMS
thermal modelling suite
ESATAN-TMS 2016 - Workbench
Geometry & Properties
Radiative Analysis
Linear Conduction
Boundary Conditions
Thermal Analysis
Post Process
Reset Visualisation Display
Animation Controls
Refresh
Reset
Clear
Default
Picking Mode:
Face
Transparency:
Delay:
Colour
NORTH(Z)
Face
Surface
Geometry
Volume
Point
Direction
Distance

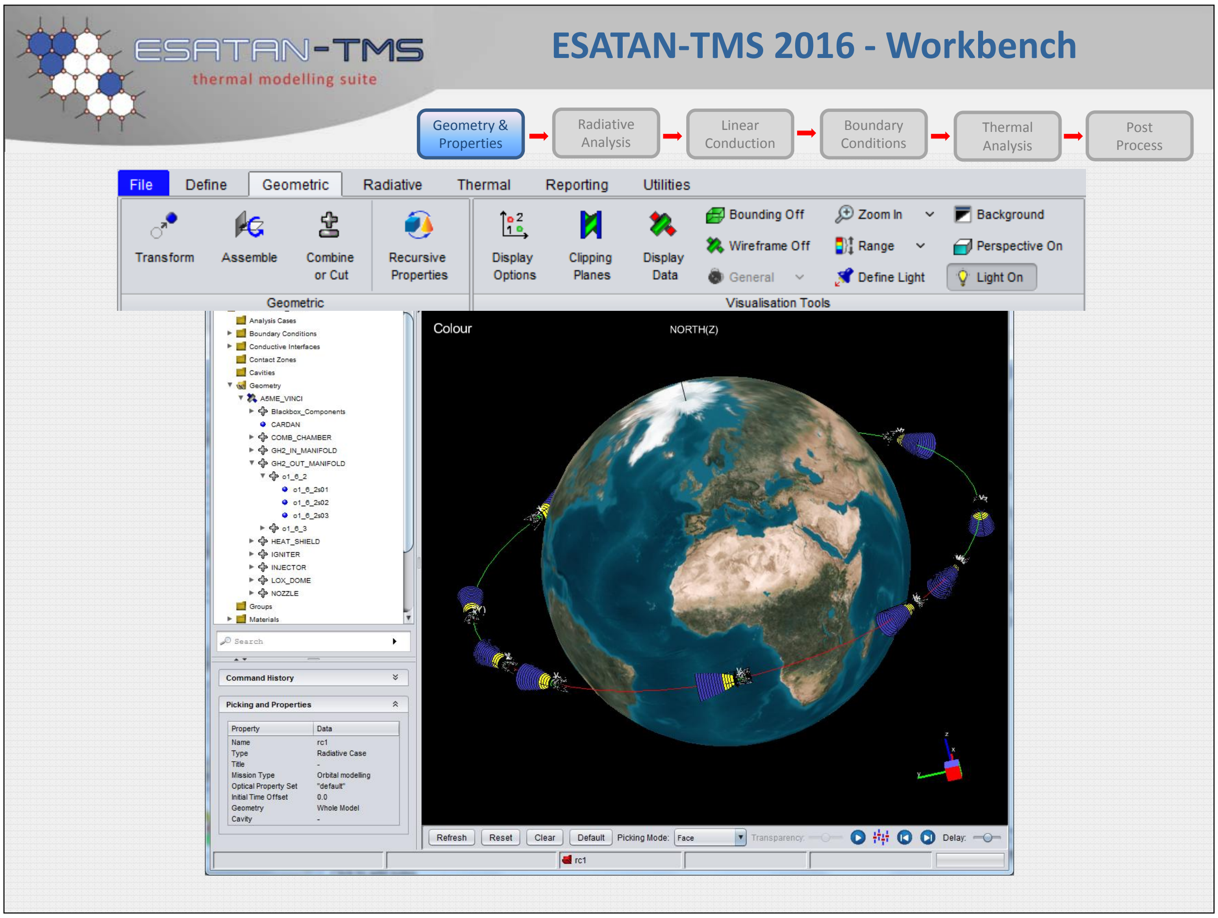
ESATAN-TMS
thermal modelling suite
ESATAN-TMS 2016 - Workbench
Geometry & Properties
Radiative Analysis
Linear Conduction
Boundary Conditions
Thermal Analysis
Post Process
File
Define
Geometric
Radiative
Thermal
Reporting
Utilities
Transform
Assemble
Combine or Cut
Recursive Properties
Display Options
Clipping Planes
Display Data
Bounding Off
Wireframe Off
General
Zoom In
Range
Define Light
Background
Perspective On
Light On
Geometric
Visualisation Tools
Colour
NORTH(Z)

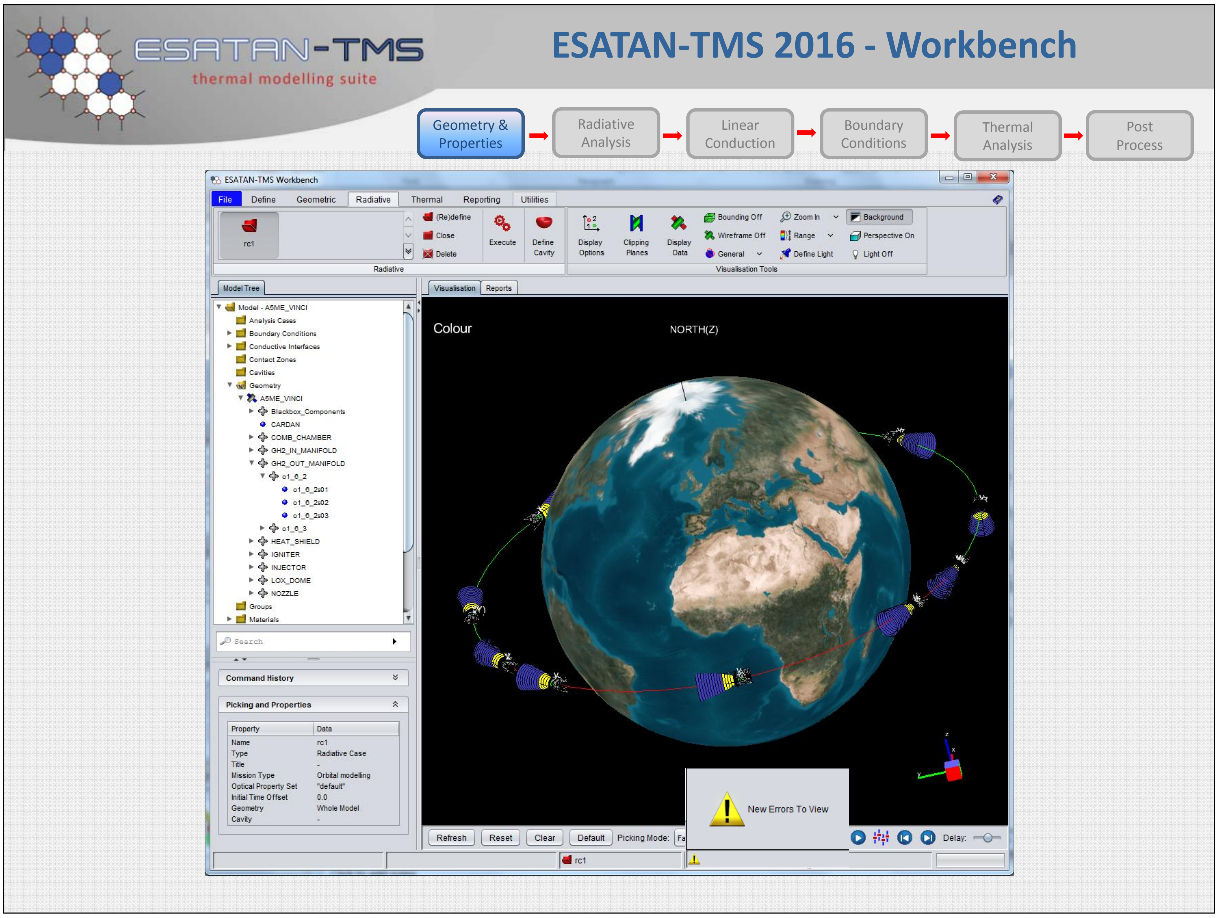
ESATAN-TMS
thermal modelling suite
ESATAN-TMS 2016 - Workbench
Geometry & Properties
Radiative Analysis
Linear Conduction
Boundary Conditions
Thermal Analysis
Post Process
ESATAN-TMS Workbench
Colour
NORTH(Z)
New Errors To View
Refresh
Reset
Clear
Default
Picking Mode:

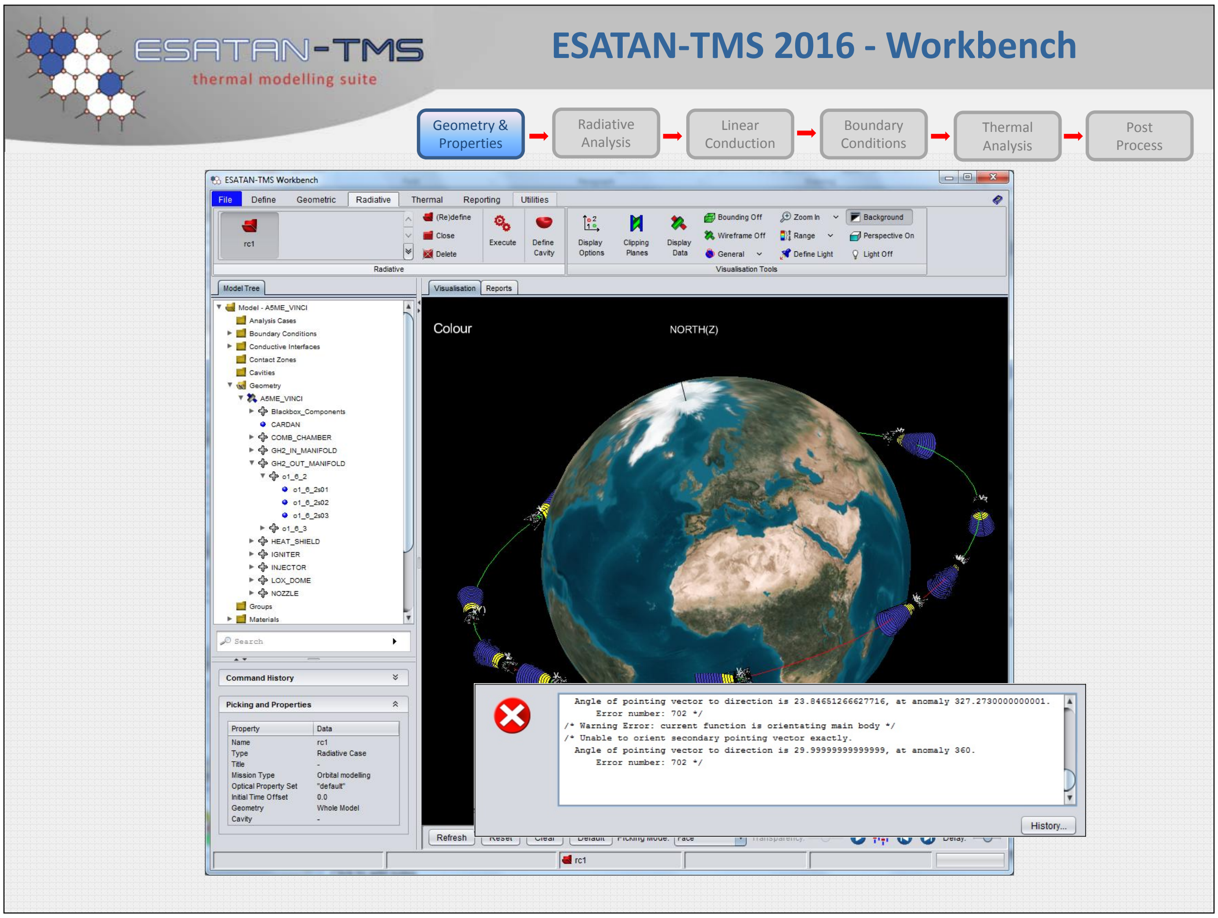
ESATAN-TMS
thermal modelling suite
ESATAN-TMS 2016 - Workbench
Geometry & Properties
Radiative Analysis
Linear Conduction
Boundary Conditions
Thermal Analysis
Post Process
ESATAN-TMS Workbench
Colour
NORTH(Z)
Angle of pointing vector to direction is 23.84651266627716, at anomaly 327.2730000000001.
Error number: 702 */
/* Warning Error: current function is orientating main body */
/* Unable to orient secondary pointing vector exactly.
Angle of pointing vector to direction is 29.99999999999999, at anomaly 360.
Error number: 702 */
History...

ESATAN-TMS thermal modelling suite

ESATAN-TMS 2016 - Workbench

Geometry & Properties → Radiative Analysis → Linear Conduction → Boundary Conditions → Thermal Analysis → Post Process

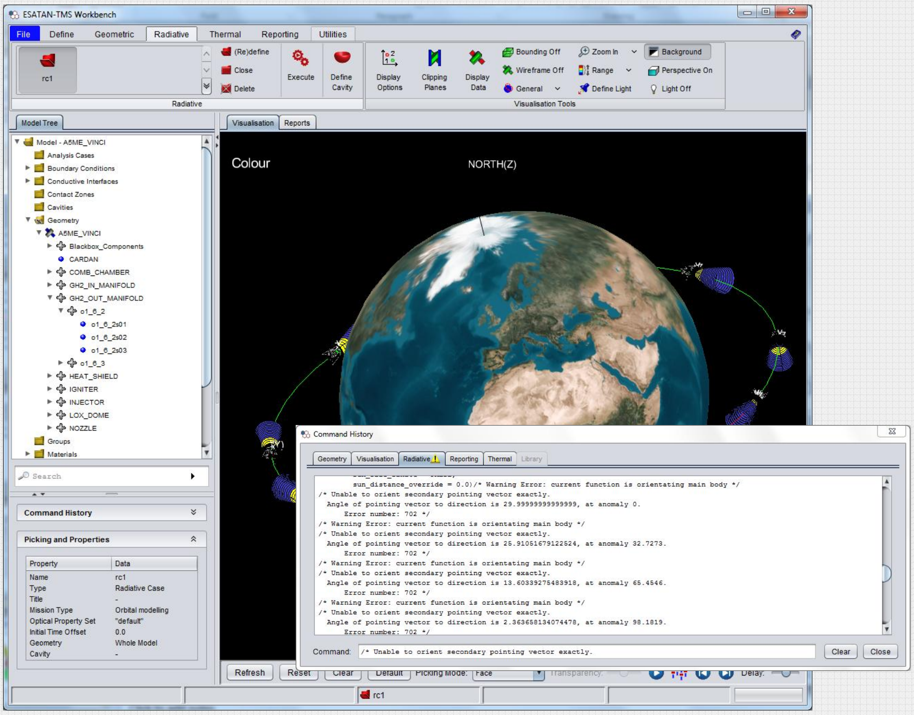

ESATAN-TMS thermal modelling suite

Presentation Contents

- ESATAN-TMS 2016 Developments
  - New ESATAN-TMS Workbench
  - Improved Geometry Modelling
  - Bulk Material Definition
  - Radiative Analysis
  - Linear Conduction
  - Thermal Boundary Conditions
  - Thermal Analysis
  - Post-processing

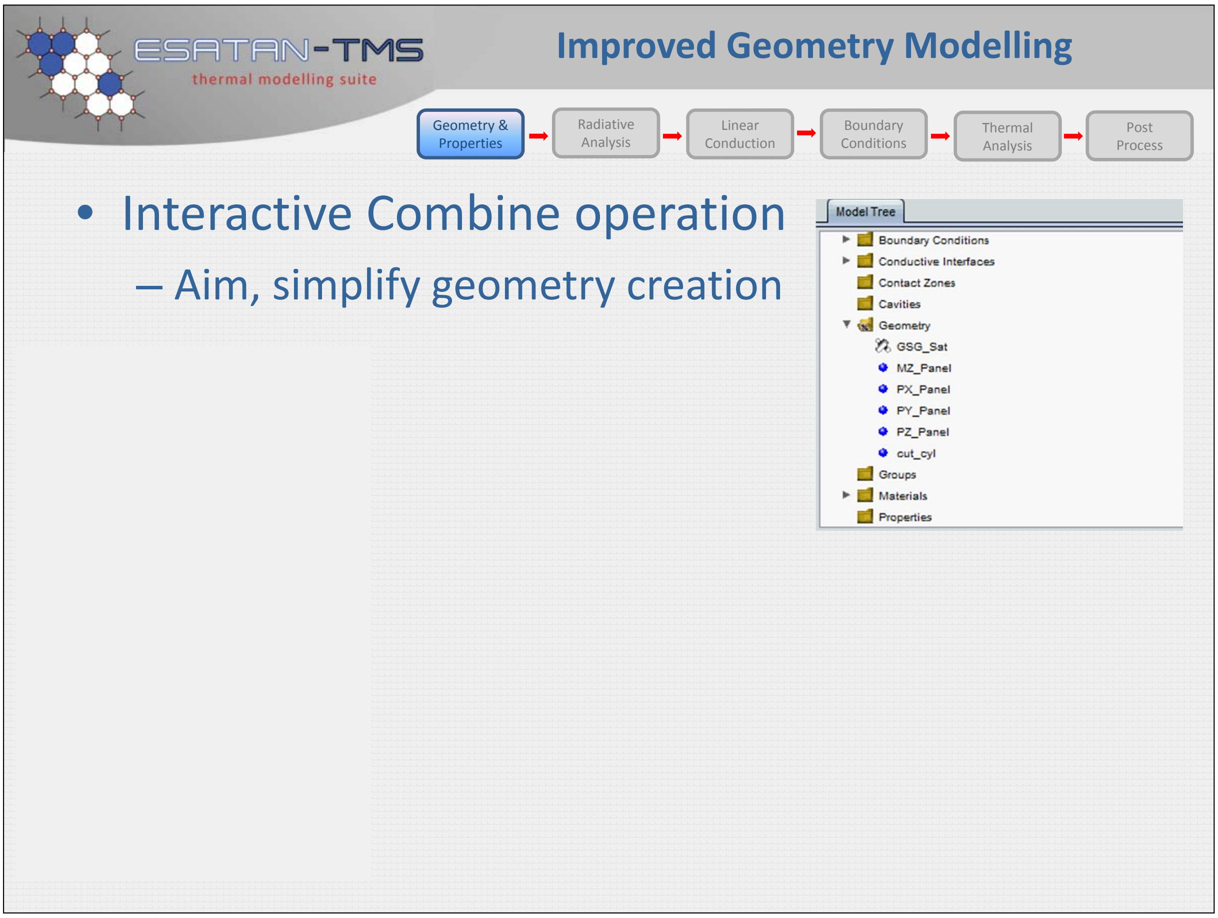

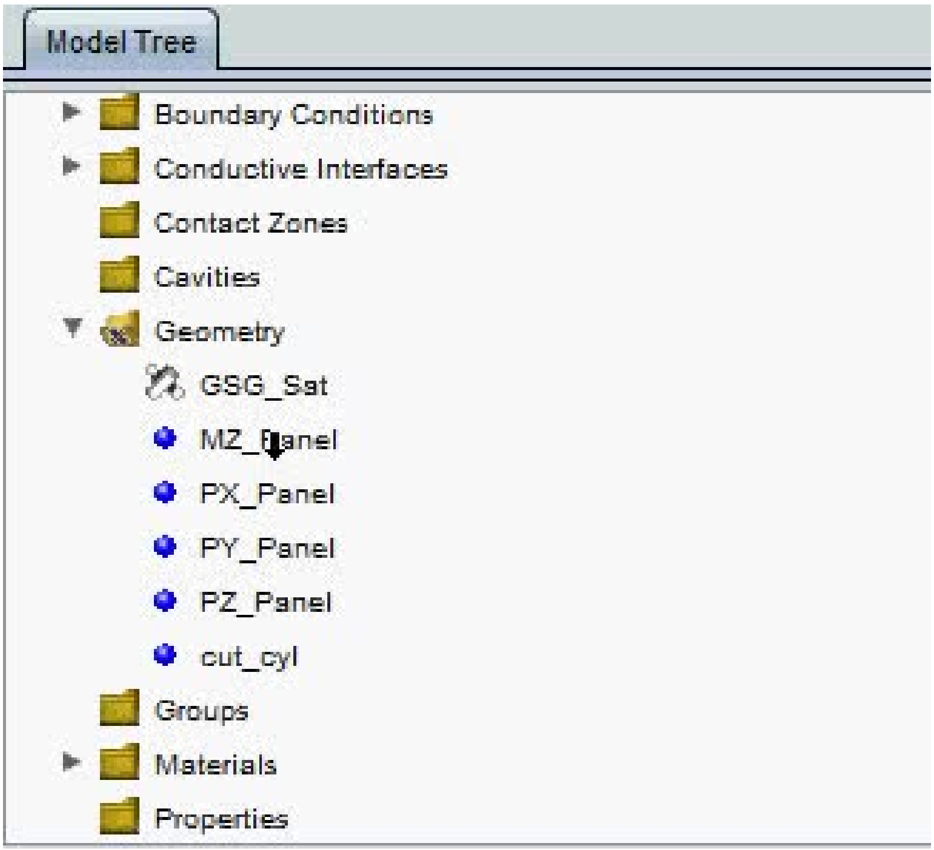

Save the attachment to disk or (double) click on the picture to run the movie.

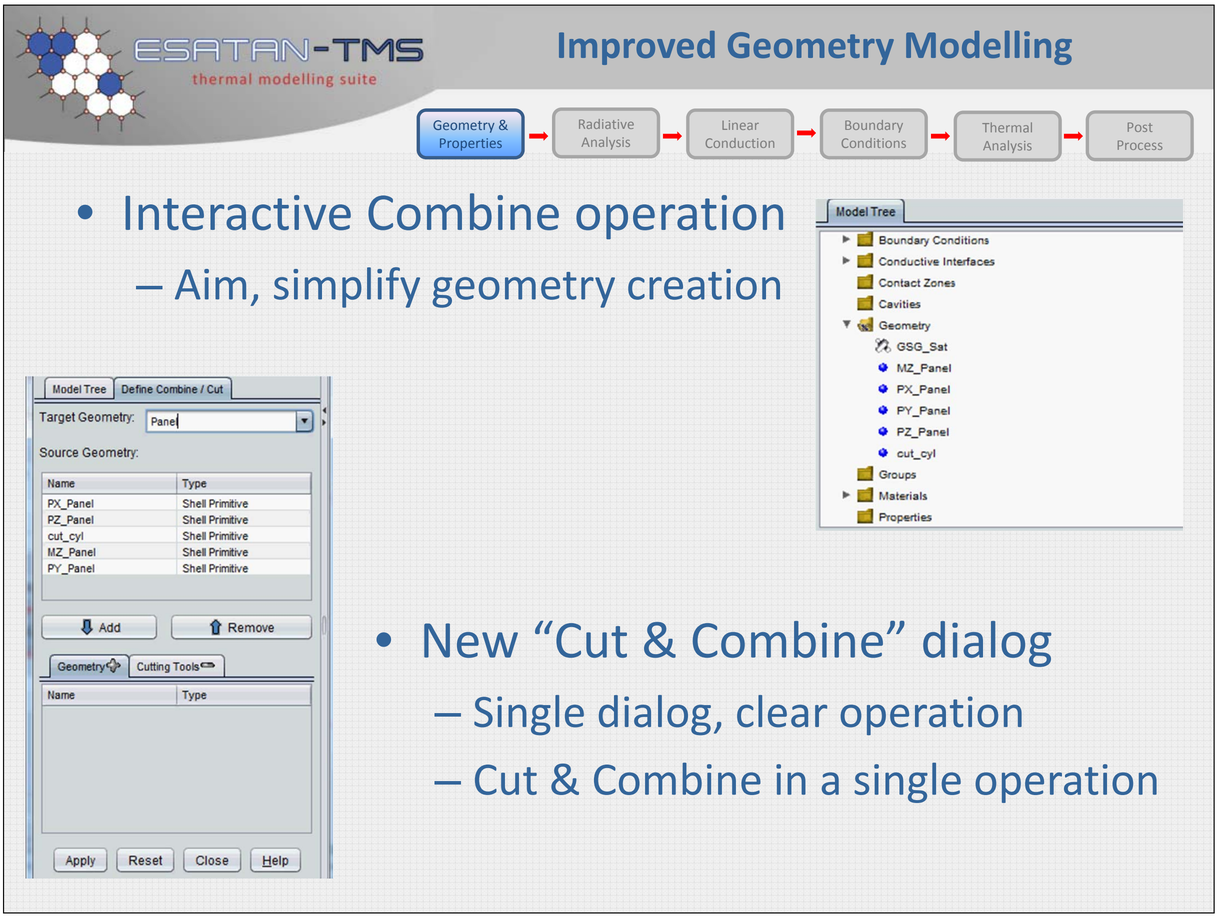

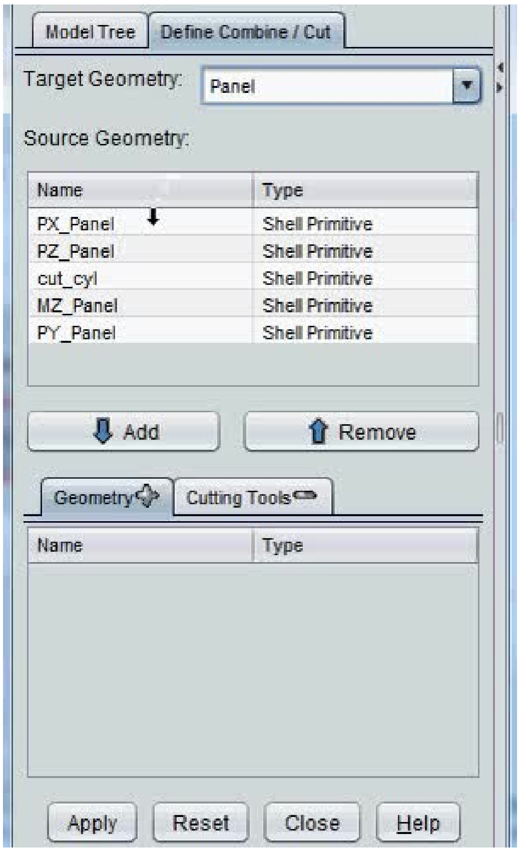

Save the attachment to disk or (double) click on the picture to run the movie.

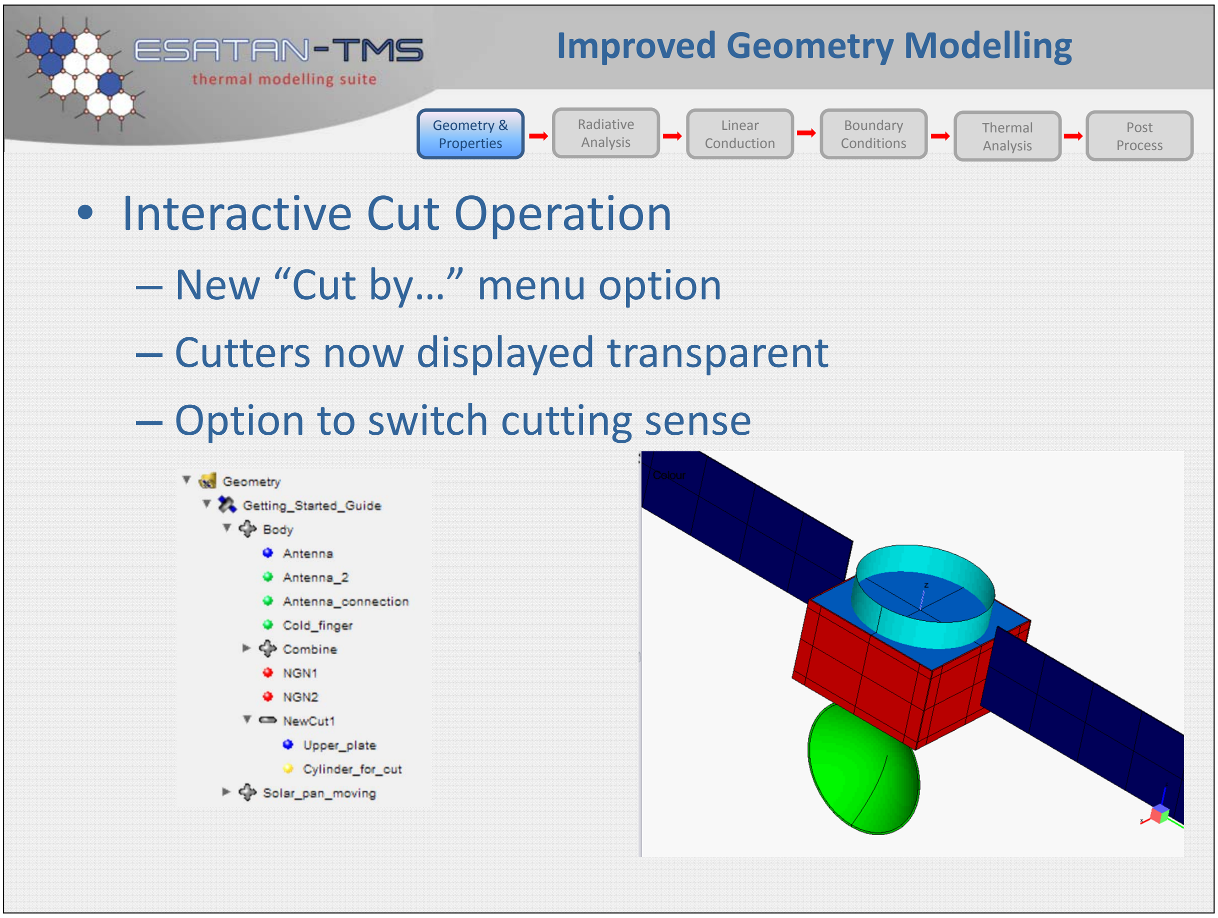

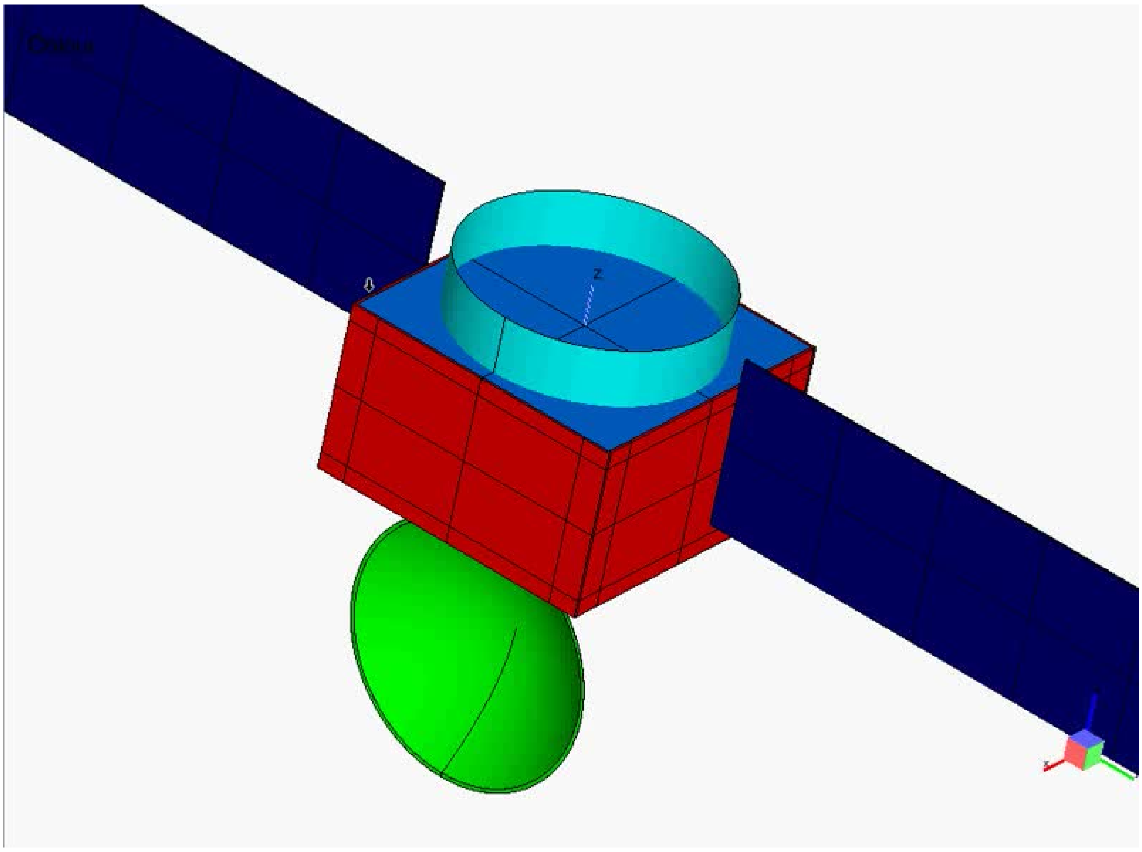

Save the attachment to disk or (double) click on the picture to run the movie.

ESATAN-TMS
thermal modelling suite

Improved Geometry Modelling

Geometry & Properties → Radiative Analysis → Linear Conduction → Boundary Conditions → Thermal Analysis → Post Process

- Increased control of node numbering
  - Request from customers
  - Improved flexibility using Recursive Properties
    - Node range across multiple geometry
  - Extension for LP & FE geometry

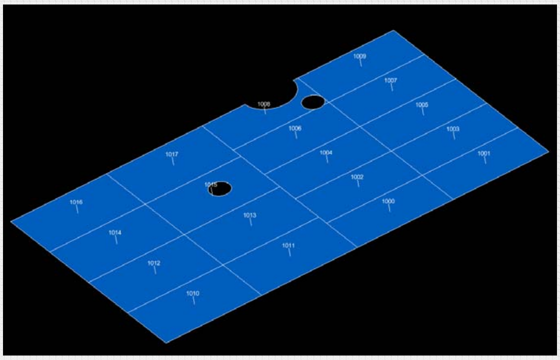

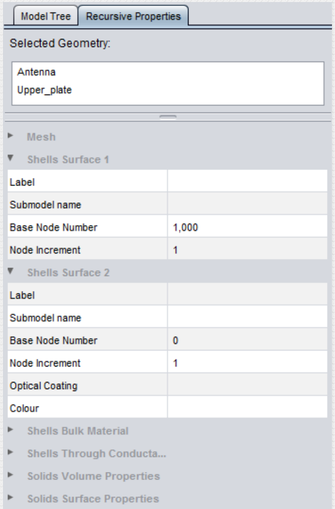

ESATAN-TMS
thermal modelling suite

Presentation Contents

- ESATAN-TMS 2016 Developments
  - Redesign of ESATAN-TMS Workbench
  - Improved Geometry Modelling
  - Bulk Material Definition
  - Radiative Analysis
  - Linear Conduction
  - Thermal Boundary Conditions
  - Thermal Analysis
  - Post-processing

ESATAN-TMS
thermal modelling suite

Bulk Material Definition

Geometry & Properties → Radiative Analysis → Linear Conduction → Boundary Conditions → Thermal Analysis → Post Process

- Support for orthotropic material conductivity
  - Model composite materials, such as honeycomb
  - For orthotropic conductivity k1, k2 & k3 defined
  - Display “Material Orientation”, to validate application of material

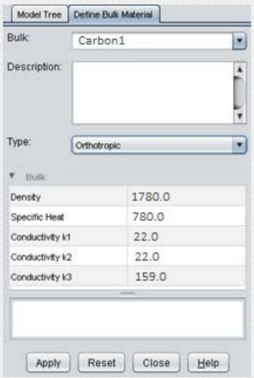

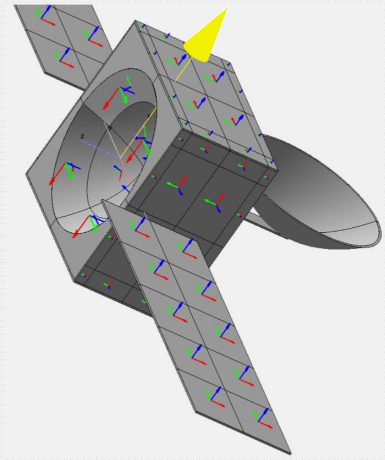

ESATAN-TMS
thermal modelling suite

Presentation Contents

- ESATAN-TMS 2016 Developments
  - New ESATAN-TMS Workbench
  - Improved Geometry Modelling
  - Bulk Material Definition
  - Radiative Analysis
  - Linear Conduction
  - Thermal Boundary Conditions
  - Thermal Analysis
  - Post-processing

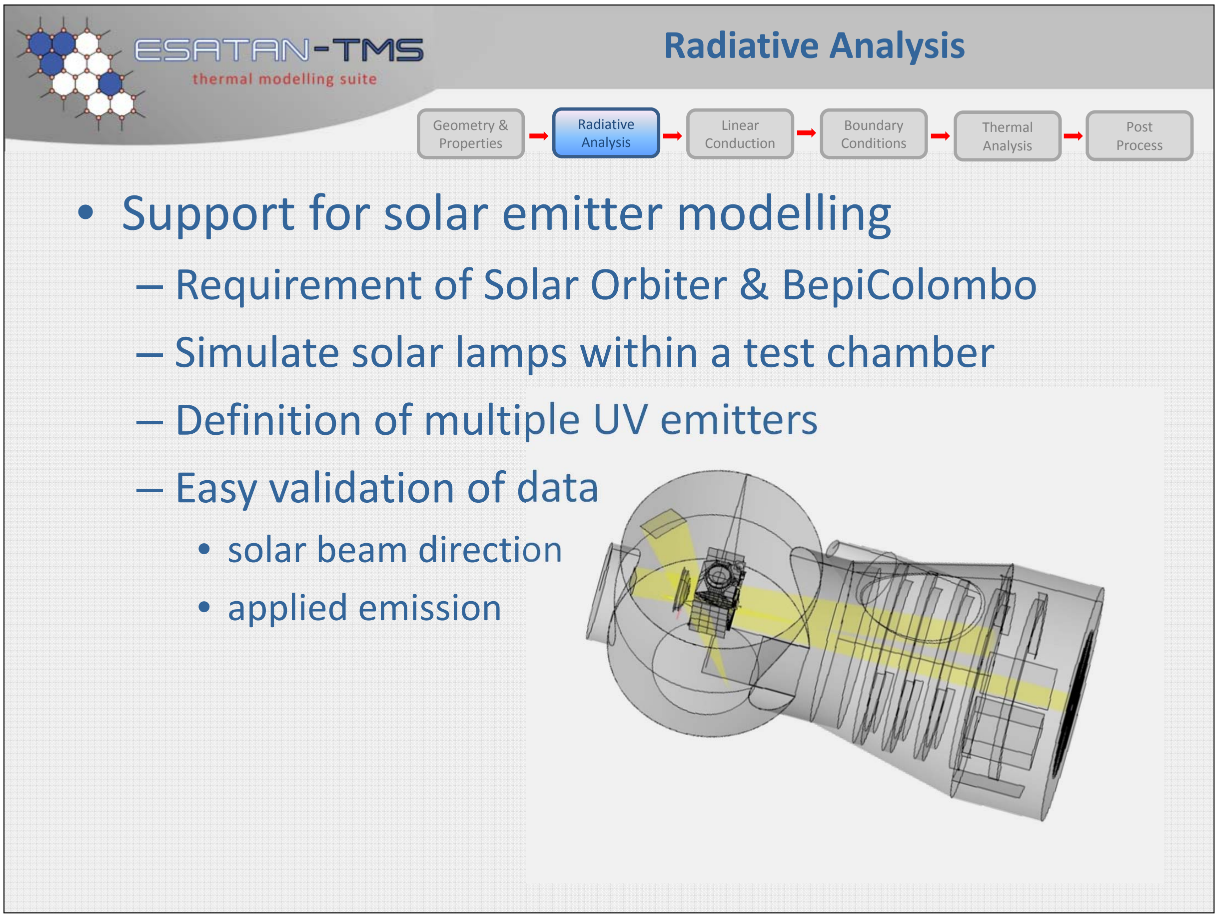
ESATAN-TMS
thermal modelling suite
Radiative Analysis
Geometry & Properties
Radiative Analysis
Linear Conduction
Boundary Conditions
Thermal Analysis
Post Process
• Support for solar emitter modelling
– Requirement of Solar Orbiter & BepiColombo
– Simulate solar lamps within a test chamber
– Definition of multiple UV emitters
– Easy validation of data
• solar beam direction
• applied emission

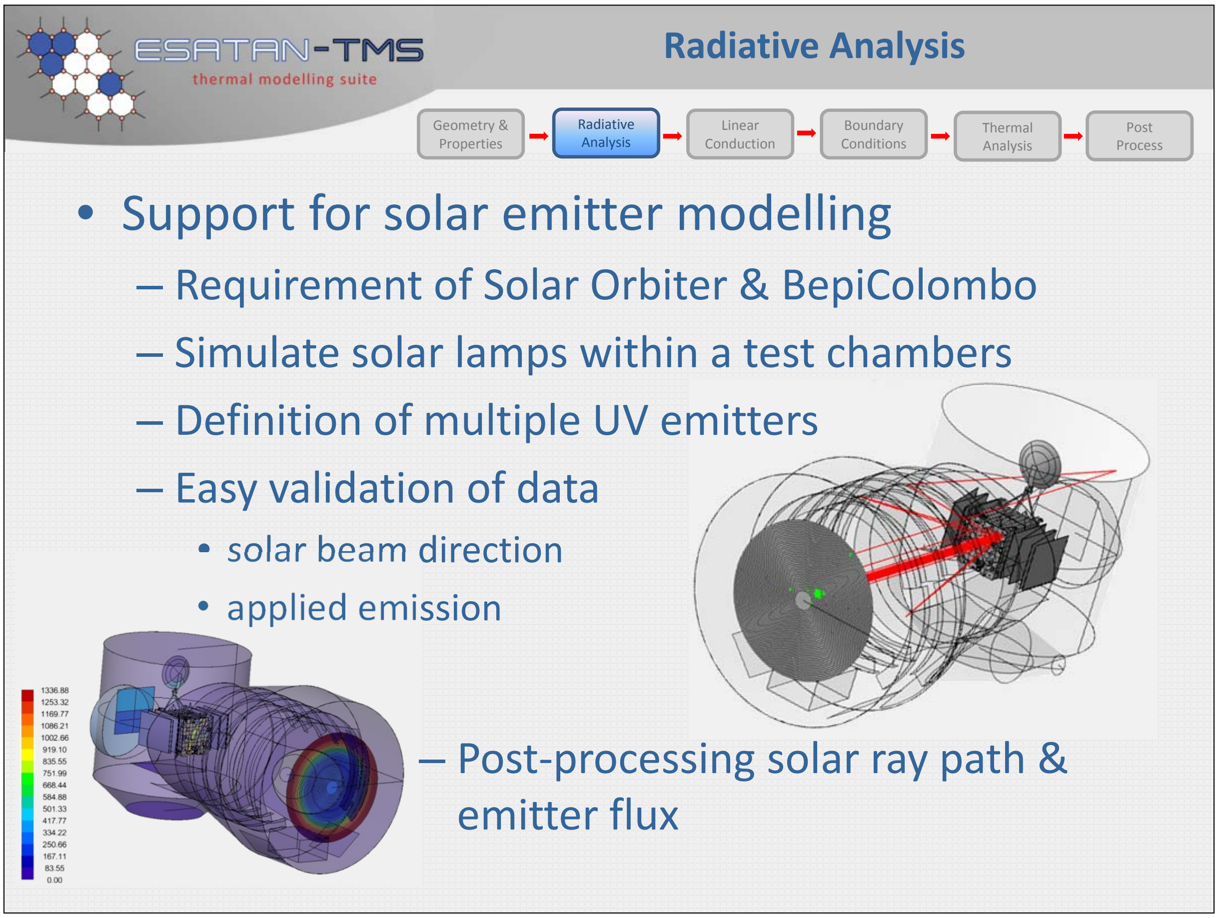
ESATAN-TMS
thermal modelling suite
Radiative Analysis
Geometry & Properties
Radiative Analysis
Linear Conduction
Boundary Conditions
Thermal Analysis
Post Process
• Support for solar emitter modelling
– Requirement of Solar Orbiter & BepiColombo
– Simulate solar lamps within a test chambers
– Definition of multiple UV emitters
– Easy validation of data
• solar beam direction
• applied emission
– Post-processing solar ray path & emitter flux

ESATAN-TMS thermal modelling suite

Radiative Analysis

Geometry & Properties → Radiative Analysis → Linear Conduction → Boundary Conditions → Thermal Analysis → Post Process

- Extended environment & mission definition
  - Time-dependent spacecraft orientation & assembly pointing
    - Request to support step change between positions
    - General extension, can be applied to temperature & heat load Boundary Conditions

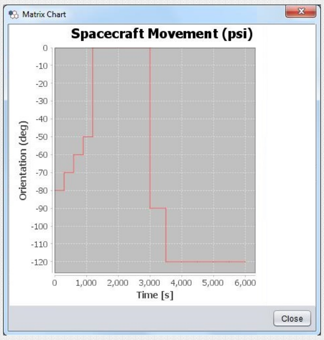

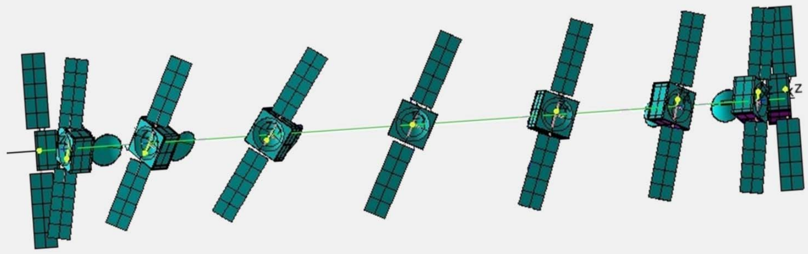

ESATAN-TMS thermal modelling suite

Radiative Analysis

Geometry & Properties → Radiative Analysis → Linear Conduction → Boundary Conditions → Thermal Analysis → Post Process

- Extended environment & mission definition
  - Support for default planet data
  - Orbit definition by semi-major axis & eccentricity
  - Definition of mission for more than one orbit
  - Orbit positions defined by times
  - Support for planet image

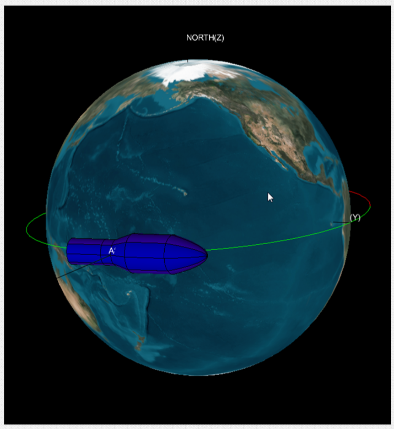

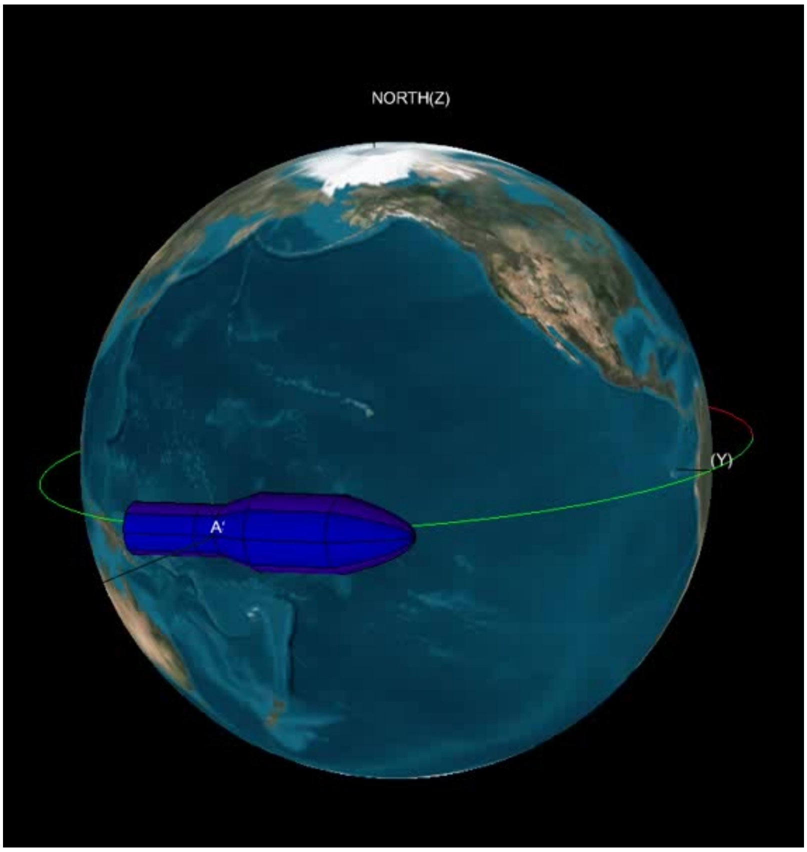

Save the attachment to disk or (double) click on the picture to run the movie.

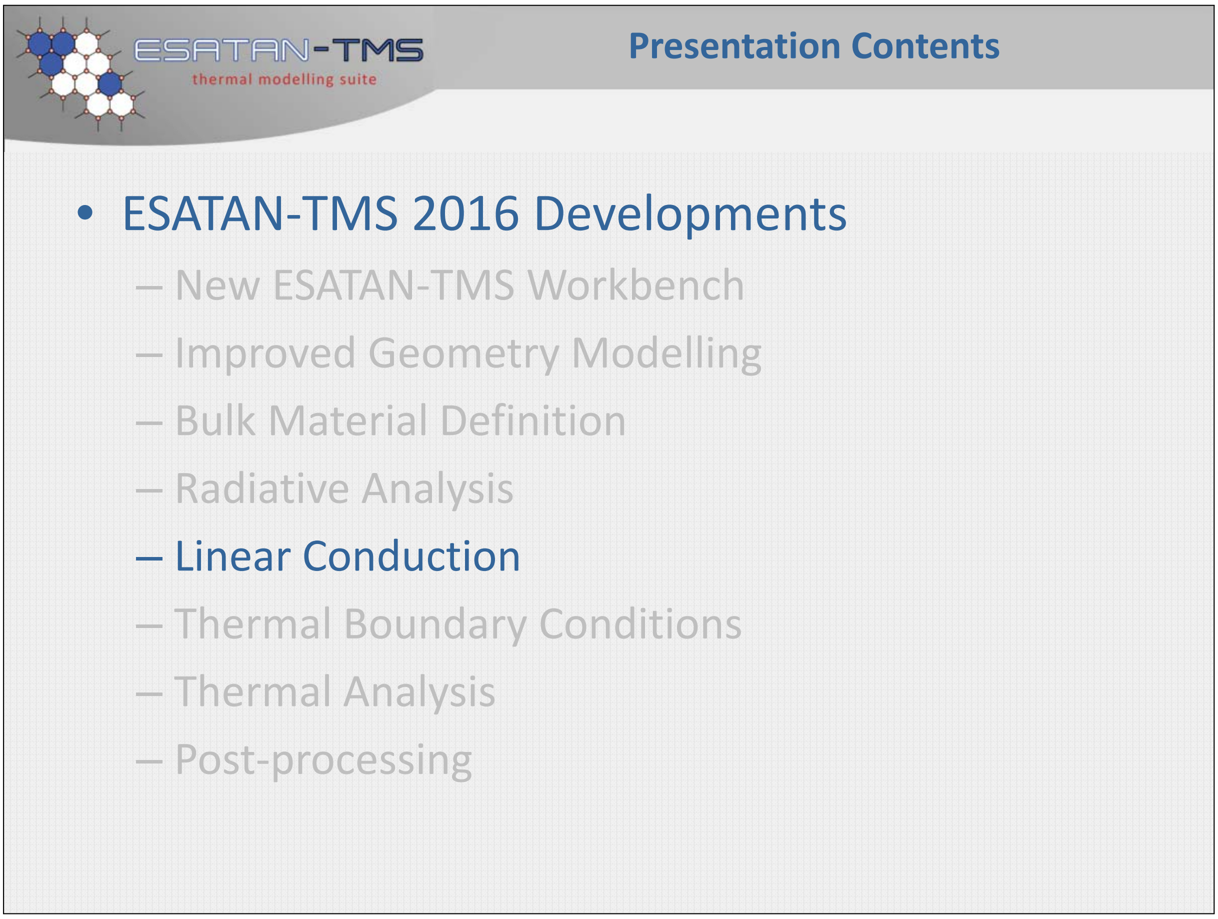

ESATAN-TMS thermal modelling suite

Linear Conduction

Geometry & Properties → Radiative Analysis → Linear Conduction → Boundary Conditions → Thermal Analysis → Post Process

- Extension of Conductor Interfaces identification
  - Identification of interfaces for displayed geometry
    - Increased flexibility to generate Conductive Interfaces between components
  - Interfaces now automatically identified on **cut** geometry

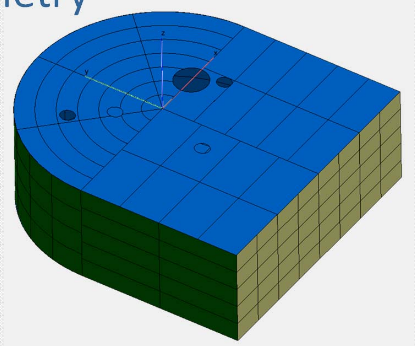

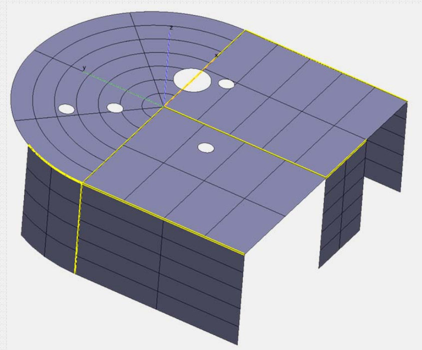

ESATAN-TMS thermal modelling suite

Linear Conduction

Geometry & Properties → Radiative Analysis → Linear Conduction → Boundary Conditions → Thermal Analysis → Post Process

- Non-linear convective User-Defined Conductor
  - Request from AIRBUS D & S
  - Support for linear or non-linear convection

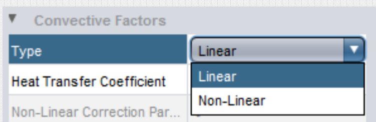

$$Q_{conv} = kS\left(T_{fluid} - T_{wall}\right)^{(1+\alpha)}$$

K = non-linear convective coefficient

S = convective surface area

α = correction coefficient

ESATAN-TMS thermal modelling suite

Presentation Contents

- ESATAN-TMS 2016 Developments
  - New ESATAN-TMS Workbench
  - Improved Geometry Modelling
  - Bulk Material Definition
  - Radiative Analysis
  - Linear Conduction
  - Thermal Boundary Conditions
  - Thermal Analysis
  - Post-processing

ESATAN-TMS thermal modelling suite

Thermal Boundary Conditions

Geometry & Properties → Radiative Analysis → Linear Conduction → Boundary Conditions → Thermal Analysis → Post Process

- Support for thermostat from Workbench
  - Heat load can now be controlled by a thermostat
  - Ability to control the thermostat based on Min, Max or Mean temp

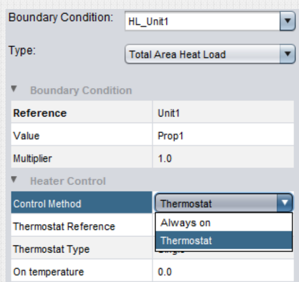

Thermal Boundary Conditions

ESATAN-TMS thermal modelling suite

Geometry & Properties → Radiative Analysis → Linear Conduction → Boundary Conditions → Thermal Analysis → Post Process

- Support for thermostat from Workbench
  - Heat load can now be controlled by a thermostat
  - Ability to control the thermostat based on Min, Max or Mean temp

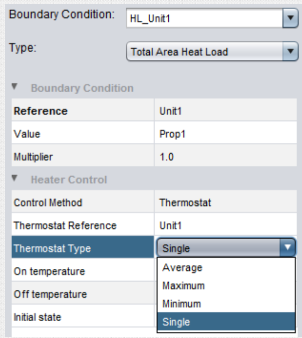

Thermal Boundary Conditions

ESATAN-TMS thermal modelling suite

Geometry & Properties → Radiative Analysis → Linear Conduction → Boundary Conditions → Thermal Analysis → Post Process

- Support for thermostat from Workbench
  - Heat load can now be controlled by a thermostat
  - Ability to control the thermostat based on Min, Max or Mean temp

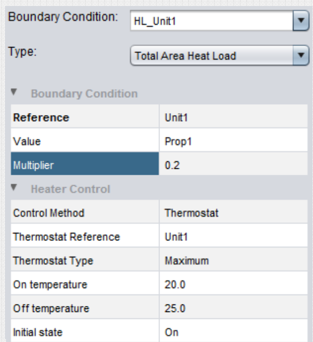

- Heat load multiplier can be defined
  - Request from customers
  - Apply the same heat load to multiple Boundary Conditions, with different scaling factors

Presentation Contents

- ESATAN-TMS 2016 Developments
  - New ESATAN-TMS Workbench
  - Improved Geometry Modelling
  - Bulk Material Definition
  - Radiative Analysis
  - Linear Conduction
  - Thermal Boundary Conditions
  - Thermal Analysis
  - Post-processing

Thermal Analysis

Geometry & Properties → Radiative Analysis → Linear Conduction → Boundary Conditions → Thermal Analysis → Post Process

- Simplified interface for defining the thermal analysis
  - Maintain template file
  - Single tab design
    - Select Boundary Conditions
    - Define thermal solution
    - Define thermal solution output
    - Select to Run Analysis...

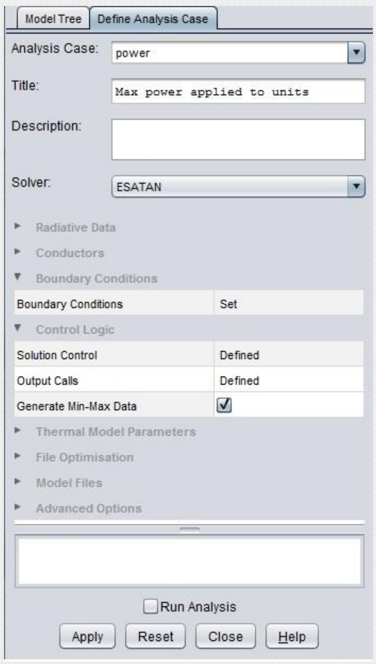

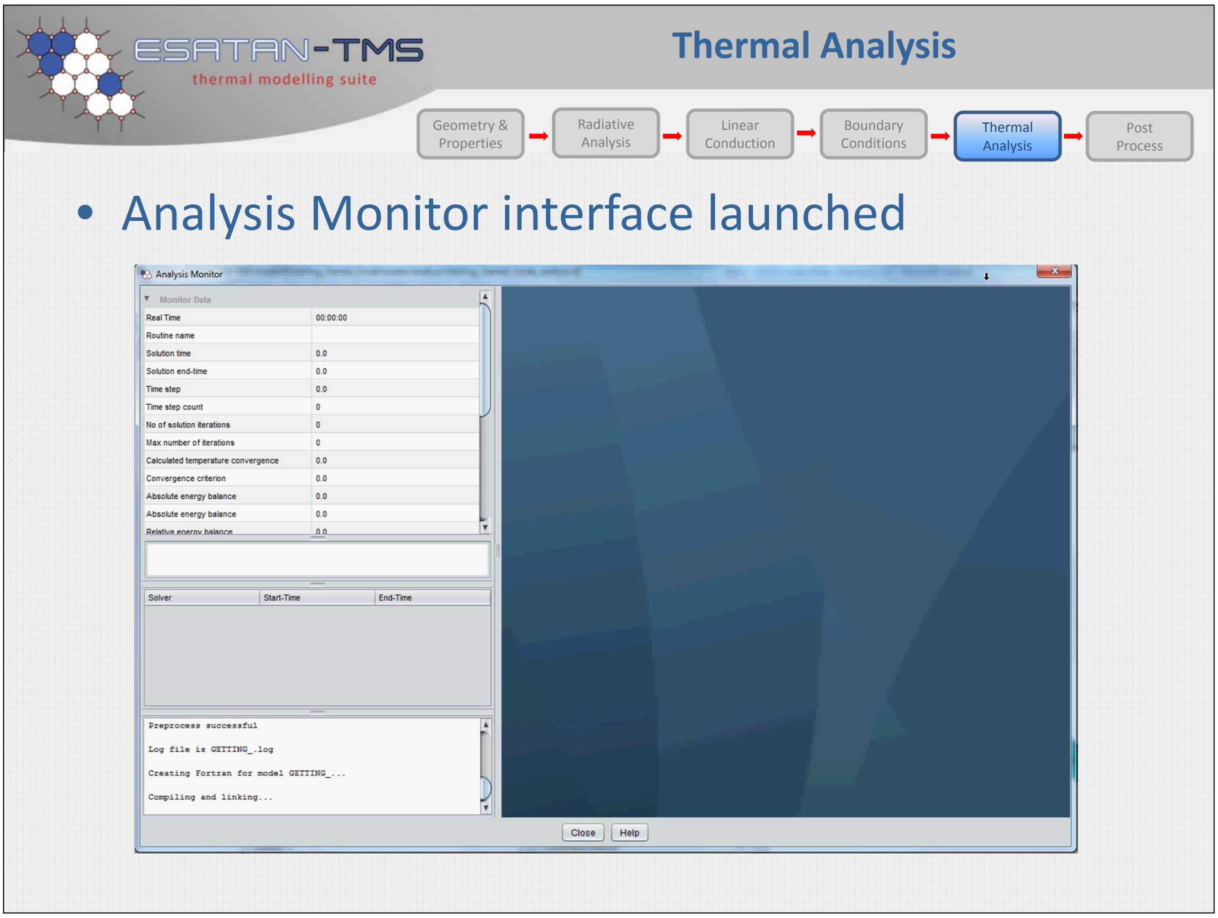

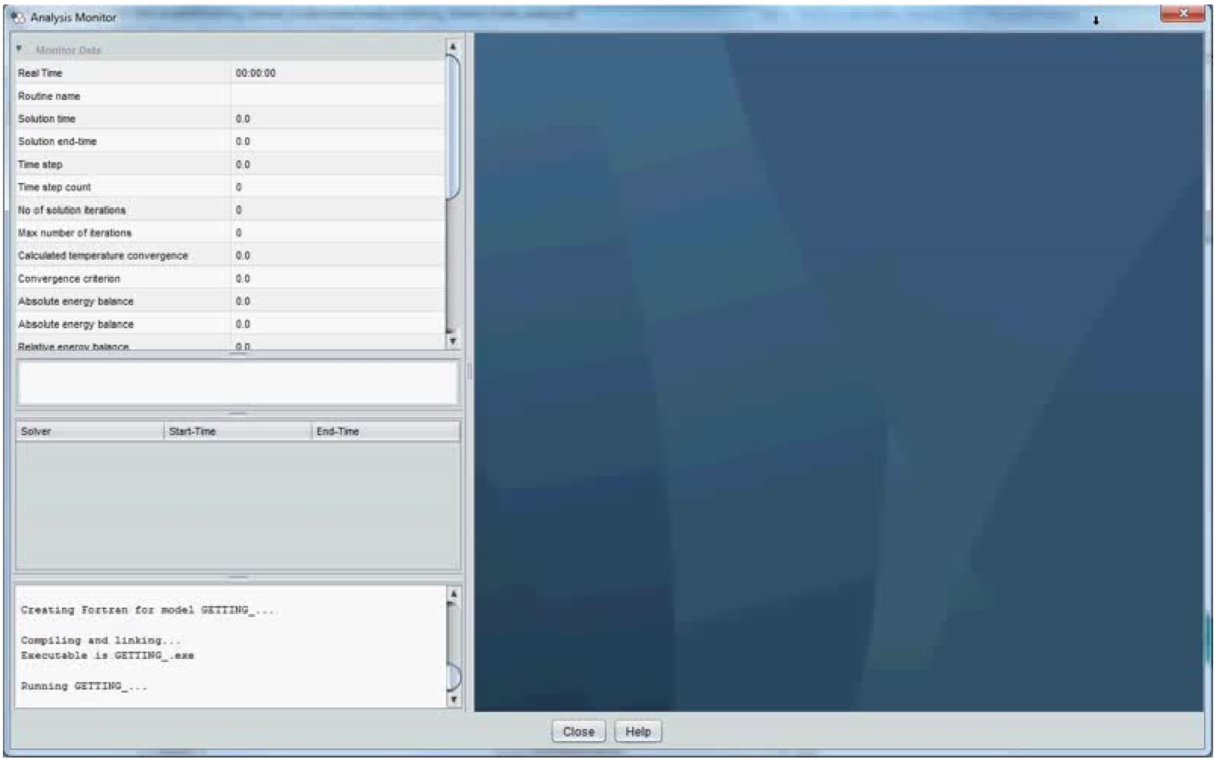

Save the attachment to disk or (double) click on the picture to run the movie.

ESATAN-TMS thermal modelling suite

Presentation Contents

- ESATAN-TMS 2016 Developments
  - New ESATAN-TMS Workbench
  - Improved Geometry Modelling
  - Bulk Material Definition
  - Radiative Analysis
  - Linear Conduction
  - Thermal Boundary Conditions
  - Thermal Analysis
  - Post-processing

ESATAN-TMS thermal modelling suite

Post-Processing

Geometry & Properties → Radiative Analysis → Linear Conduction → Boundary Conditions → Thermal Analysis → Post Process

- Improved mechanism of displaying data
  - Right-click from model tree
    - Immediate display of data

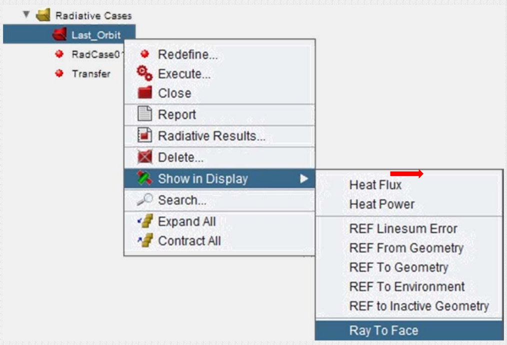

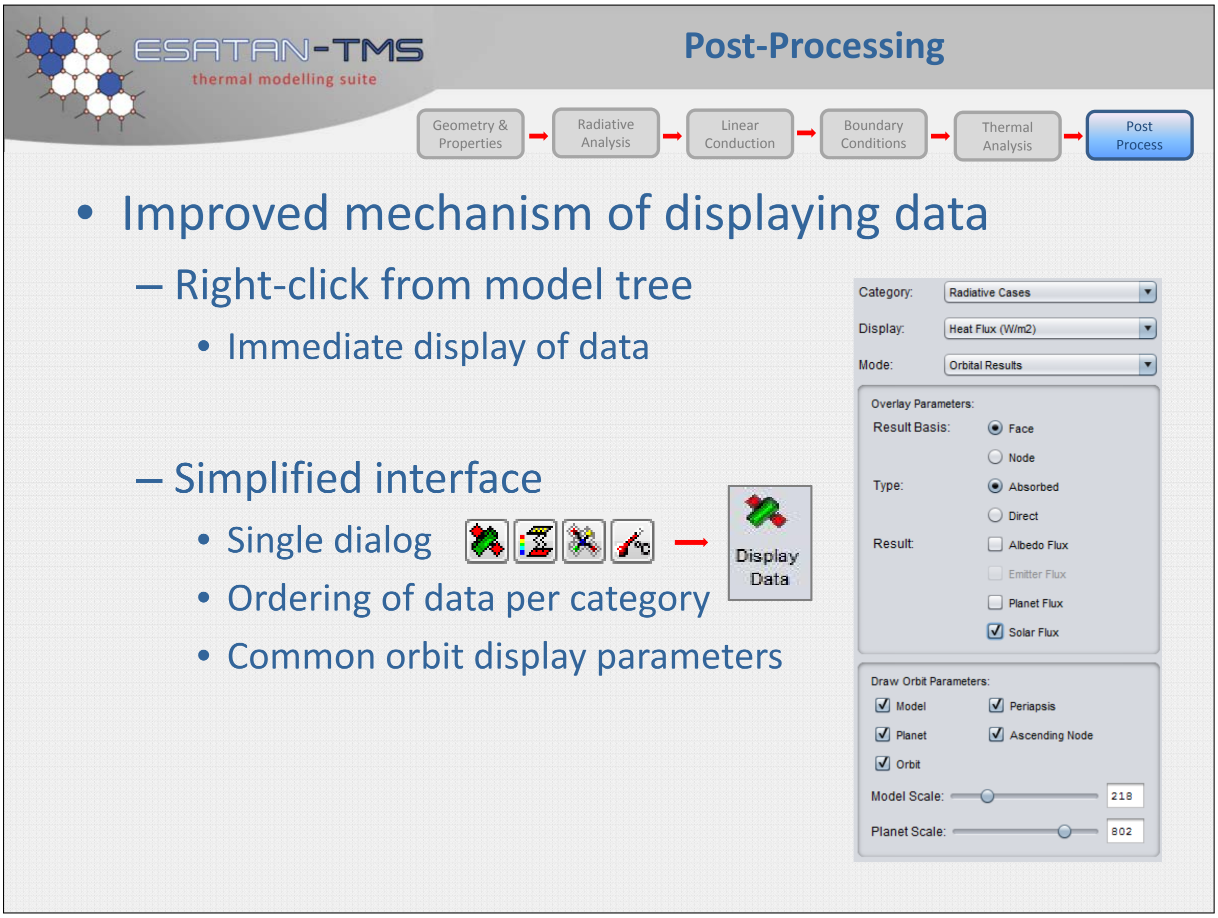
ESATAN-TMS
thermal modelling suite
Post-Processing
Geometry & Properties
Radiative Analysis
Linear Conduction
Boundary Conditions
Thermal Analysis
Post Process
• Improved mechanism of displaying data
– Right-click from model tree
• Immediate display of data
– Simplified interface
• Single dialog
• Ordering of data per category
• Common orbit display parameters
Display Data
Category: Radiative Cases
Display: Heat Flux (W/m2)
Mode: Orbital Results
Overlay Parameters:
Result Basis: Face
Node
Type: Absorbed
Direct
Result: Albedo Flux
Emitter Flux
Planet Flux
Solar Flux
Draw Orbit Parameters:
Model
Periapsis
Planet
Ascending Node
Orbit
Model Scale: 218
Planet Scale: 802

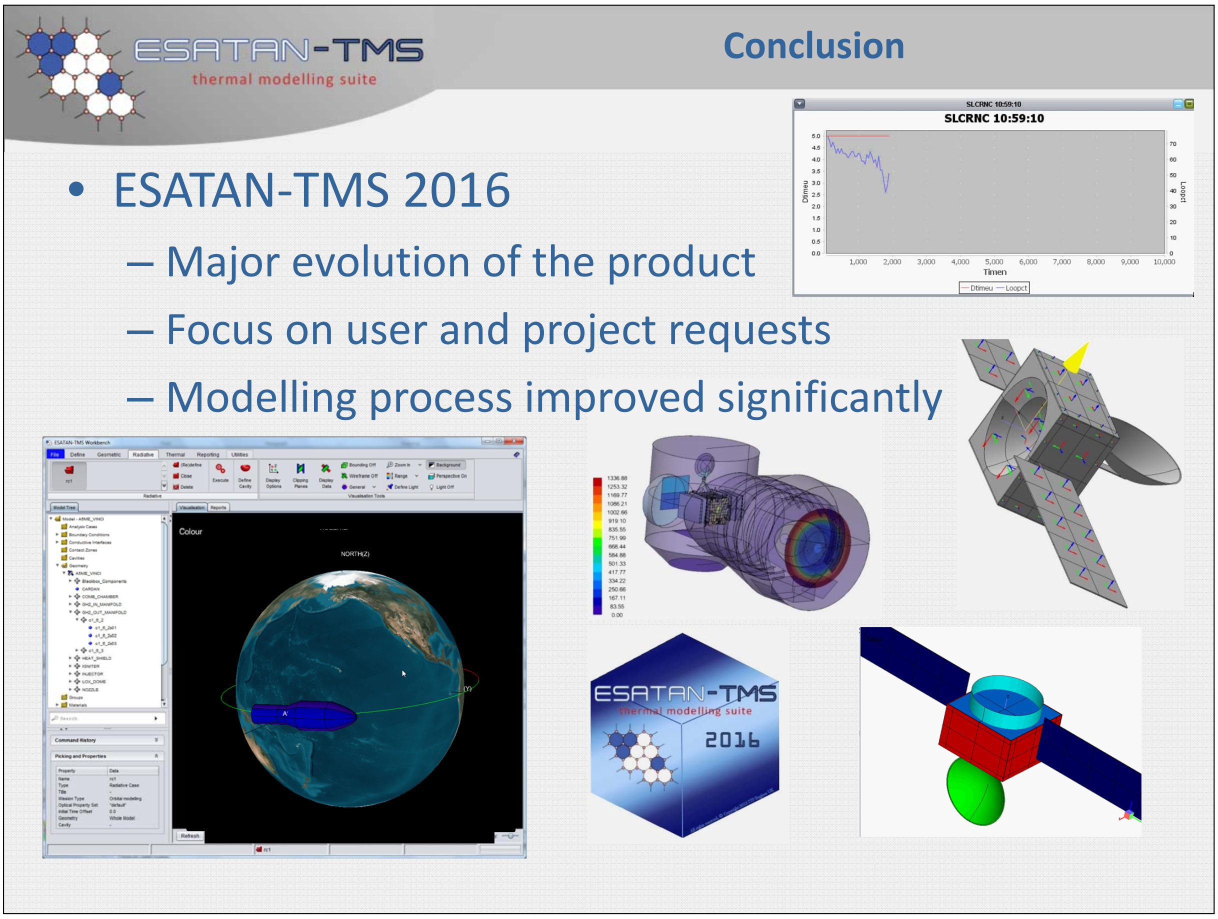
ESATAN-TMS
thermal modelling suite
Conclusion
• ESATAN-TMS 2016
– Major evolution of the product
– Focus on user and project requests
– Modelling process improved significantly
SLCRNC 10:59:10
ESATAN-TMS
thermal modelling suite
2016

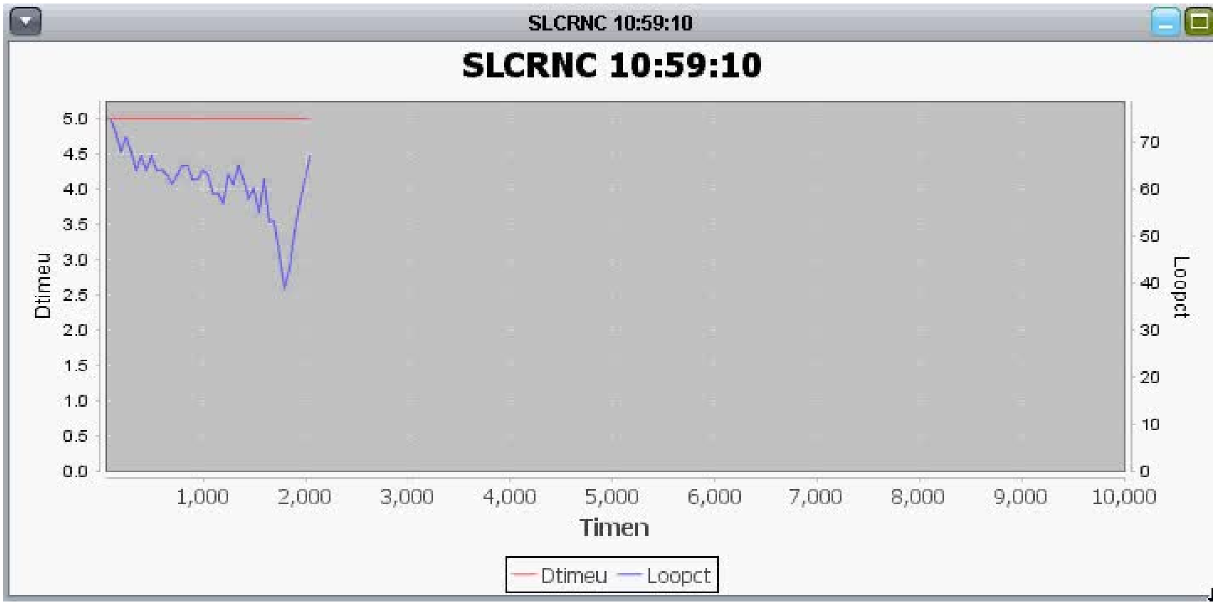

Save the attachment to disk or (double) click on the picture to run the movie.

Appendix P

SYSTEMA — THERMICA

Timothée Soriano Rose Nerriere
(Airbus Defense and Space SAS, France)

Abstract

SYSTEMA, currently in version 4.7.1, is a framework for space physics applications including THERMICA, a package dedicated to thermal simulations.
The next version will be the 4.8.0 and will include a new schematic module which will allow the definition of power systems and will ease the thermo-electrical simulation process.
Besides, SYSTEMA has the ability to manage the solar system including different moons, like Ganymede, Europa and others for which orbits are approximated by Keplerian laws around a particular date of interest. A trajectory defined around a moon like Ganymede will lead to simulate fluxes both from the moon itself but also from other planets, like Jupiter in this example.
Finally, a new applicative module within Systema, called Mapping, offers the possibility to transfer data from one model to another one: fluxes from a Plume analysis to a thermal model, temperatures to an outgassing model or to mechanical mesh. For the temperature mapping, a new method based on a "backward RCN" has been set-up. This method is capable of interpolating temperatures within a re-built quadratic profile onto the thermal mesh and offers then a very accurate mapping consistent with the hypothesis of the thermal simulation.

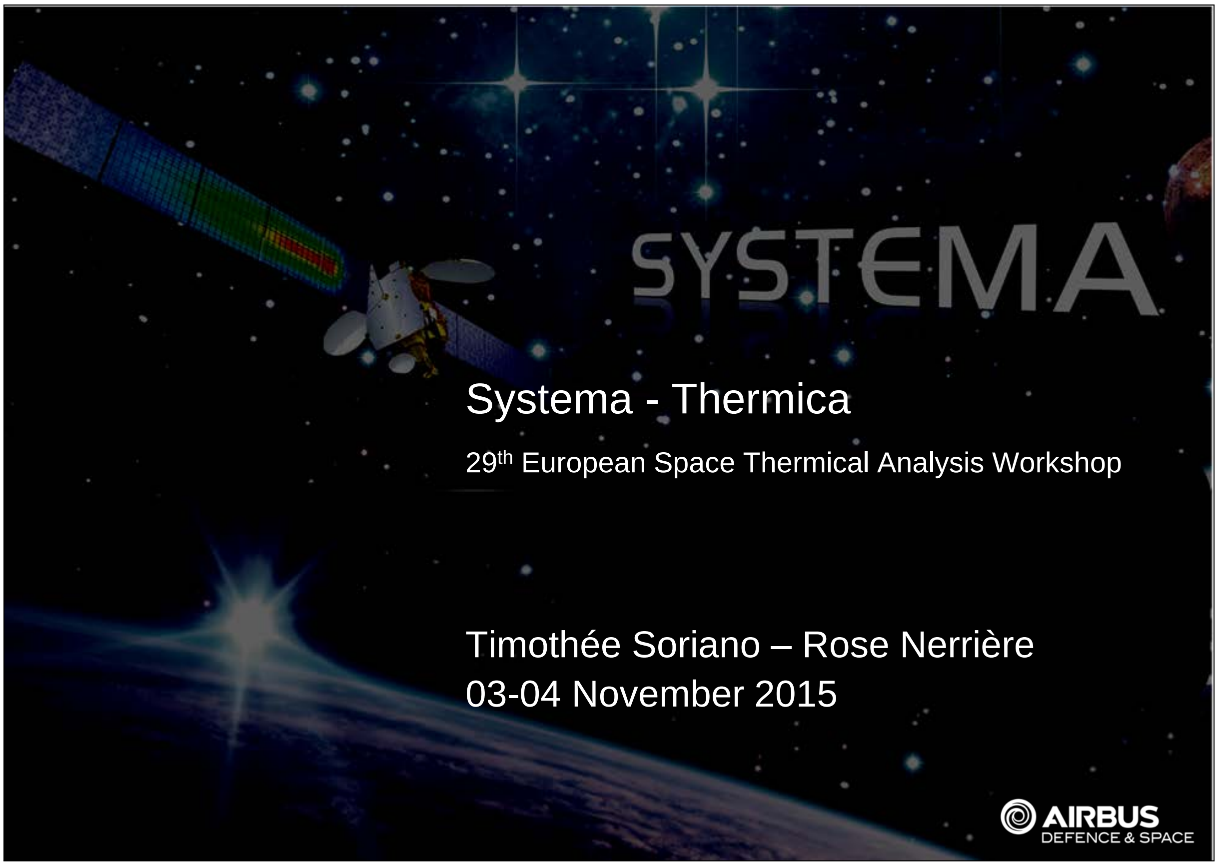
SYSTEMA
Systema - Thermica
29th European Space Thermical Analysis Workshop
Timothée Soriano – Rose Nerrière
03-04 November 2015
AIRBUS
DEFENCE & SPACE

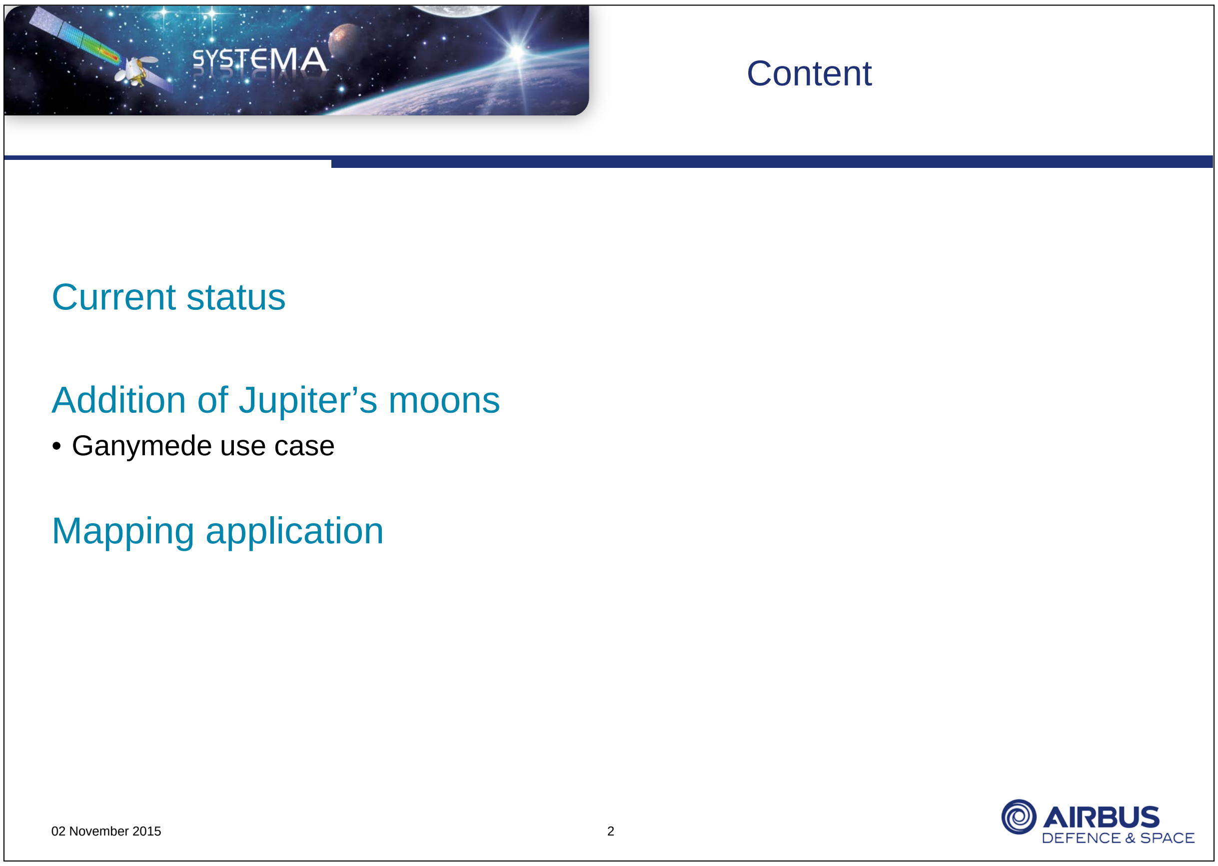
SYSTEMA
Content
Current status
Addition of Jupiter's moons
• Ganymede use case
Mapping application
02 November 2015
2
AIRBUS
DEFENCE & SPACE

Current status

Long Term Support current version: v4.5.3 (08/2013)

02 November 2015 3

AIRBUS DEFENCE & SPACE

Current status

Latest Release: v4.7.1 (06/2015)

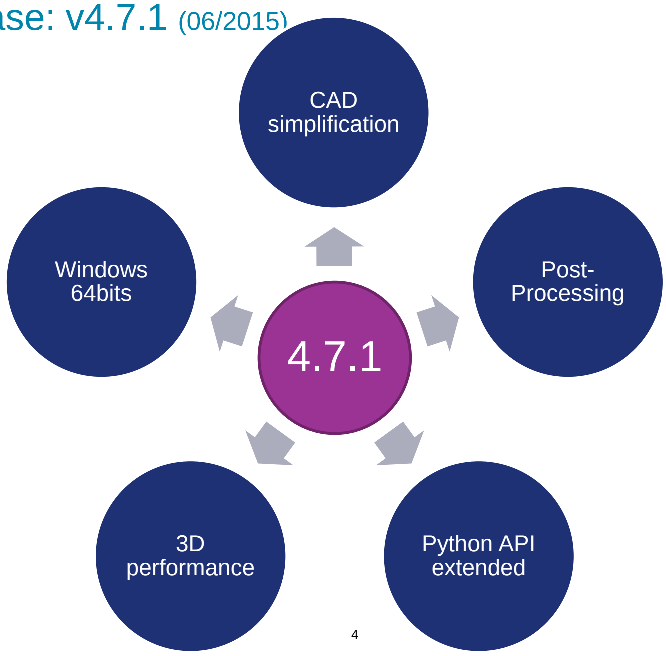

02 November 2015 4

AIRBUS DEFENCE & SPACE

SYSTEMA

Current status

v4.7.1

Search tool

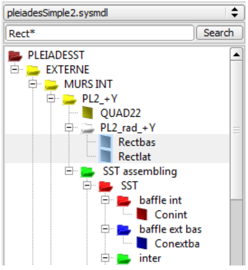

Multi-edition on Meshing

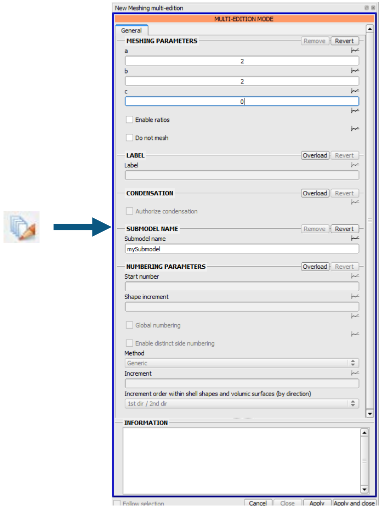

Integrated User Manual

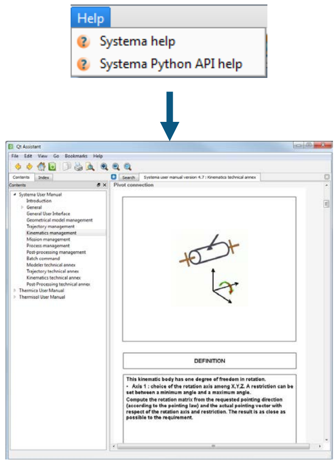

02 November 2015 5

AIRBUS DEFENCE & SPACE

SYSTEMA

Current status

v4.7.1

- Import/Export of ASCII Ephemeris files
- Follow the CIC exchange protocol: restriction of ESA standard CCSDS
- Trajectory Time-Position-Velocity

Cartesian position and velocity in planet inertial reference Gamma50
Cartesian position and velocity in planet inertial reference J2000
East longitude, latitude and altitude (spherical coordinates) in planet rotational reference
Cartesian position and velocity in a planet inertial reference (frozen planet rotational reference)
Stk ephemeride file (.e)
CNES CIC based OEM ephemeride file (.txt)

– Import of Trajectory :
  – OEM files (Orbit Ephemeris Message) → x, y, z positions

02 November 2015 6

AIRBUS DEFENCE & SPACE

Current status

v4.7.1

- Kinematics law “Transformation defined in a file”:

Transformation matrix
Rotations in transformed axis - Z-Y'-X"
Rotations in transformed axis - X-Y'-Z"
Rotations in fixed axis - Z-Y-X
Rotations in fixed axis - X-Y-Z
STK attitude file (*.a)
CNES CIC based AEM spacecraft attitude file (*.txt)
CNES CIC based MEM moving body attitude file (*.txt)

  – Import of Kinematics :
    – AEM files for satellite attitude (Attitude Ephemeris Message) → quaternions
    – MEM files for moving bodies attitude (Mission Ephemeris Message) → rotation angle

- Export of HDF5 results :
  – MEM files (Mission Ephemeris Message) → thermal results

02 November 2015 7 AIRBUS DEFENCE & SPACE

Current status

Next Release: v4.8.0 (S1 2016)

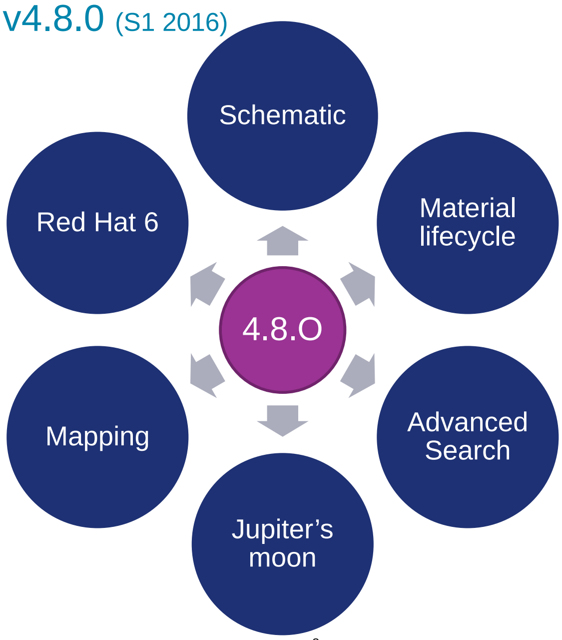

02 November 2015 8 AIRBUS DEFENCE & SPACE

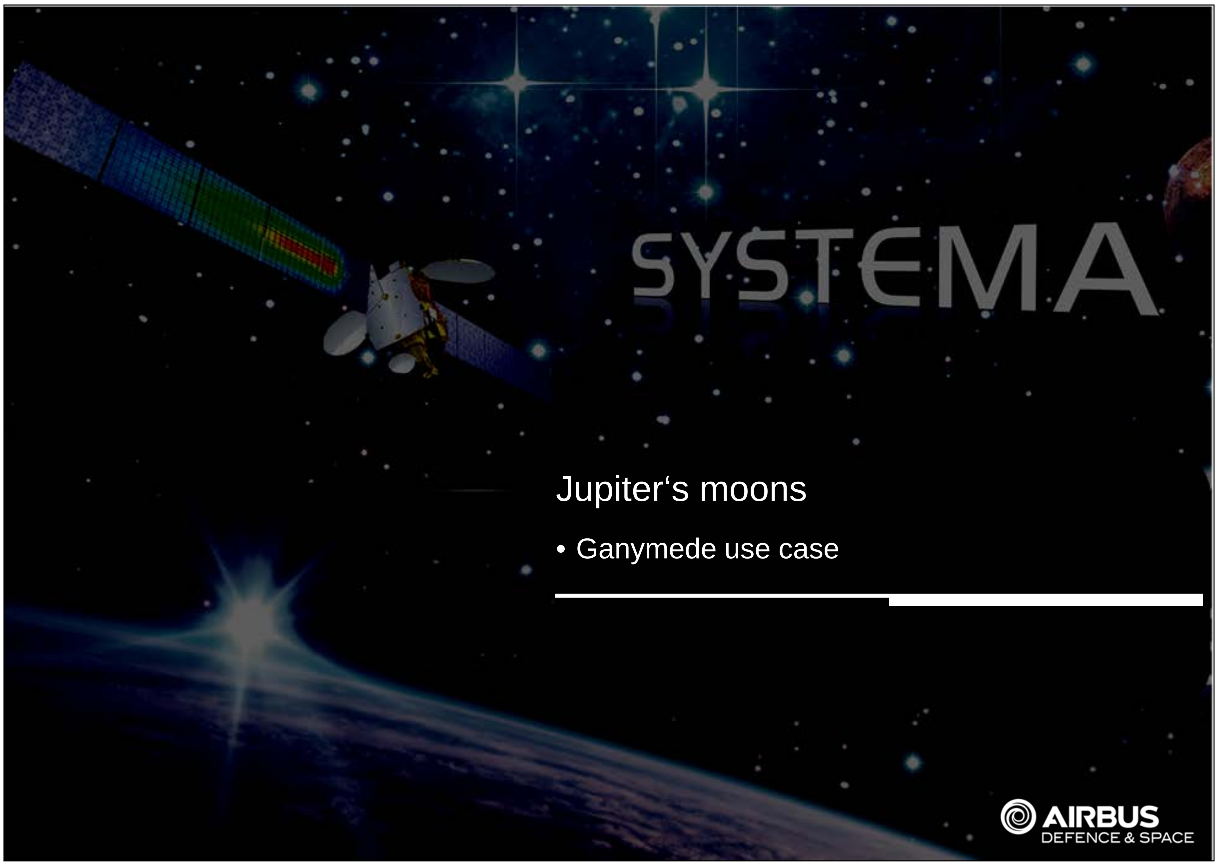

Jupiter's moons

Implementation of moons in Systema
- Texture of the moon
- Ephemeris information

→ Orbits approximated by Keplerian laws from a fixed date

Make mission and analyses around moons with Systema

JUICE mission
- Launch in 2022 and start of the mission in 2030
- Callisto and Europa flybys
- Orbit around Ganymede

02 November 2015 10 AIRBUS DEFENCE & SPACE

Jupiter's moons

Ganymede
- Available since version 4.7

Europa / Callisto
- Available in 4.8.0

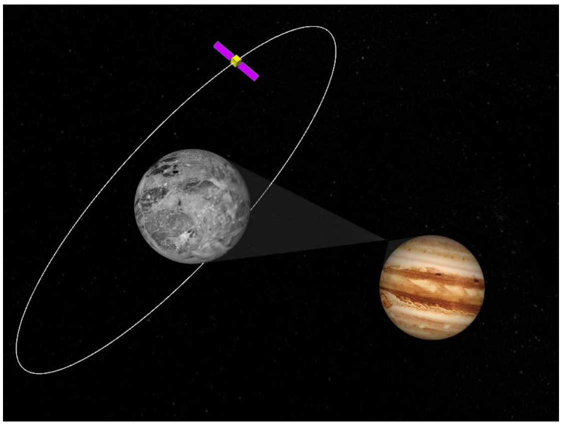

02 November 2015 11

AIRBUS DEFENCE & SPACE

Jupiter's moons

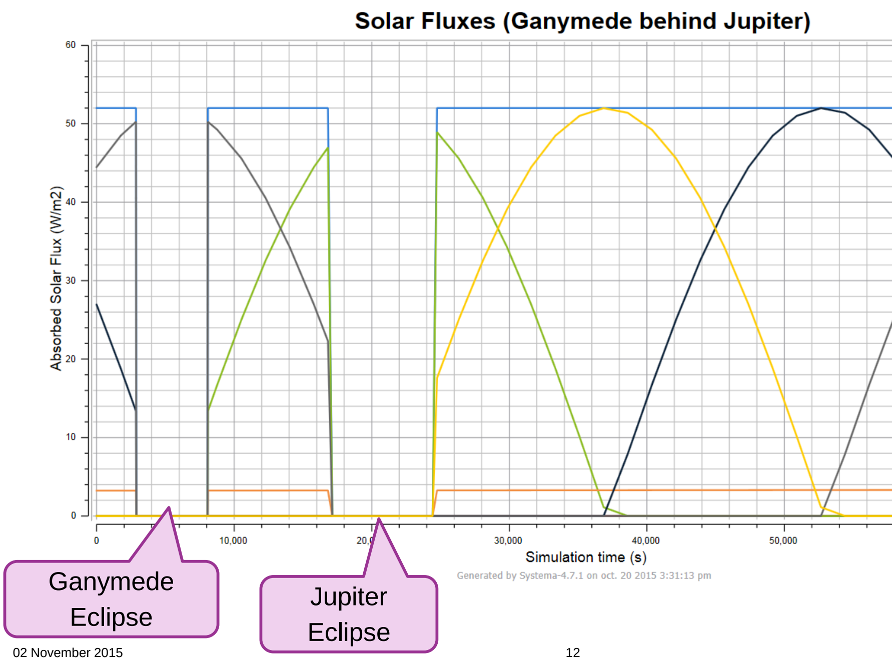

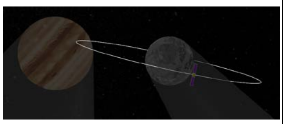

02 November 2015 12

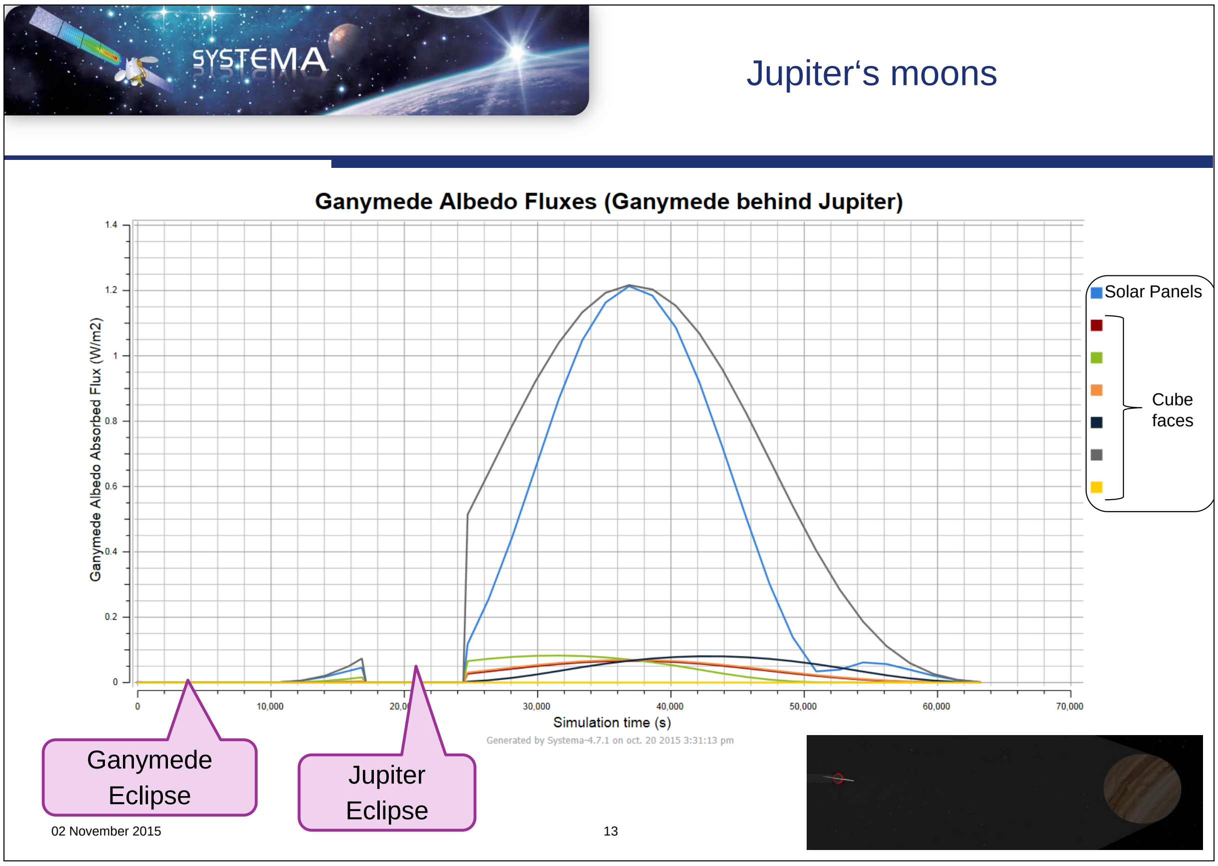
SYSTEMA
Jupiter's moons
Ganymede Albedo Fluxes (Ganymede behind Jupiter)
Ganymede Albedo Absorbed Flux (W/m2)
Simulation time (s)
Solar Panels
Cube faces
Ganymede Eclipse
Jupiter Eclipse
02 November 2015
13

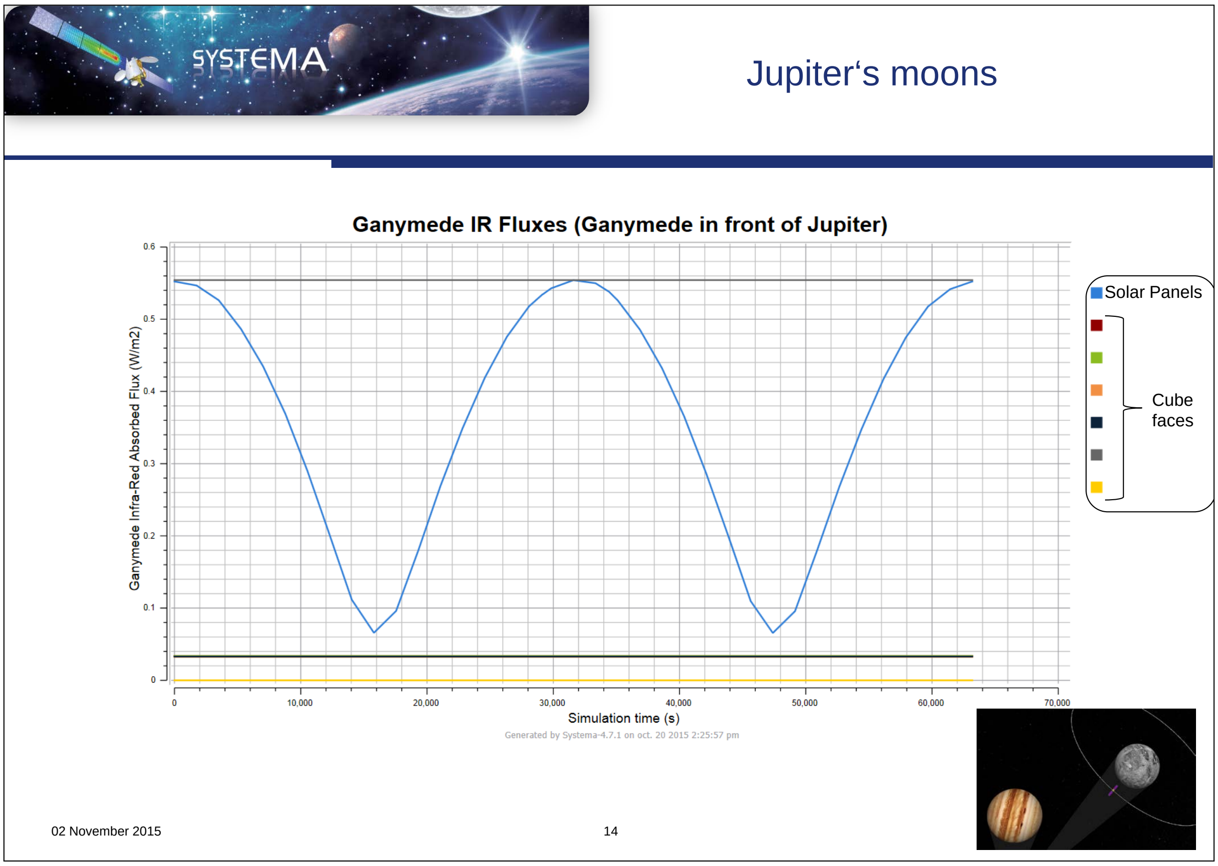
SYSTEMA
Jupiter's moons
Ganymede IR Fluxes (Ganymede in front of Jupiter)
Ganymede Infra-Red Absorbed Flux (W/m2)
Simulation time (s)
Solar Panels
Cube faces
02 November 2015
14

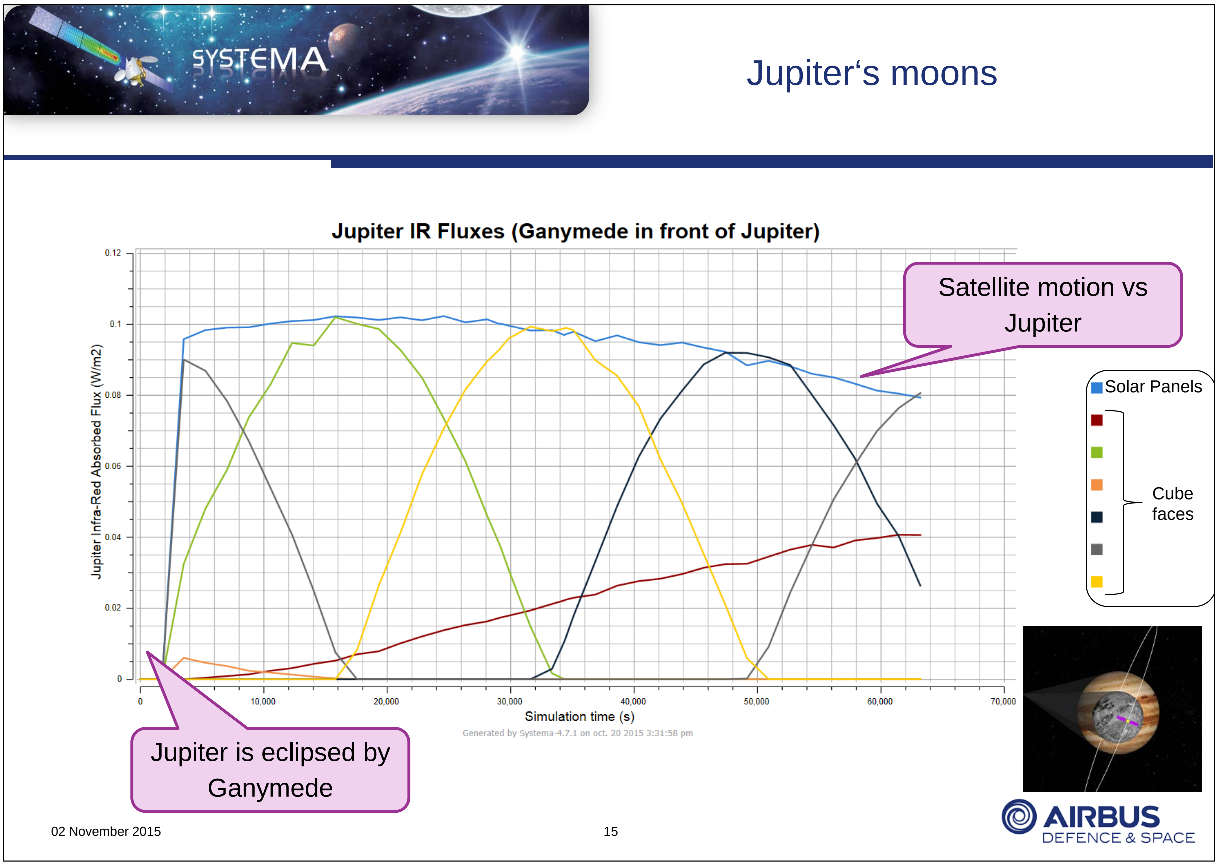
SYSTEMA
Jupiter‘s moons
Jupiter IR Fluxes (Ganymede in front of Jupiter)
Jupiter Infra-Red Absorbed Flux (W/m2)
0.12
0.1
0.08
0.06
0.04
0.02
0
0
10,000
20,000
30,000
40,000
50,000
60,000
70,000
Simulation time (s)
Generated by Systema-4.7.1 on oct. 20 2015 3:31:58 pm
Satellite motion vs Jupiter
Solar Panels
Cube faces
Jupiter is eclipsed by Ganymede
02 November 2015
15
AIRBUS
DEFENCE & SPACE

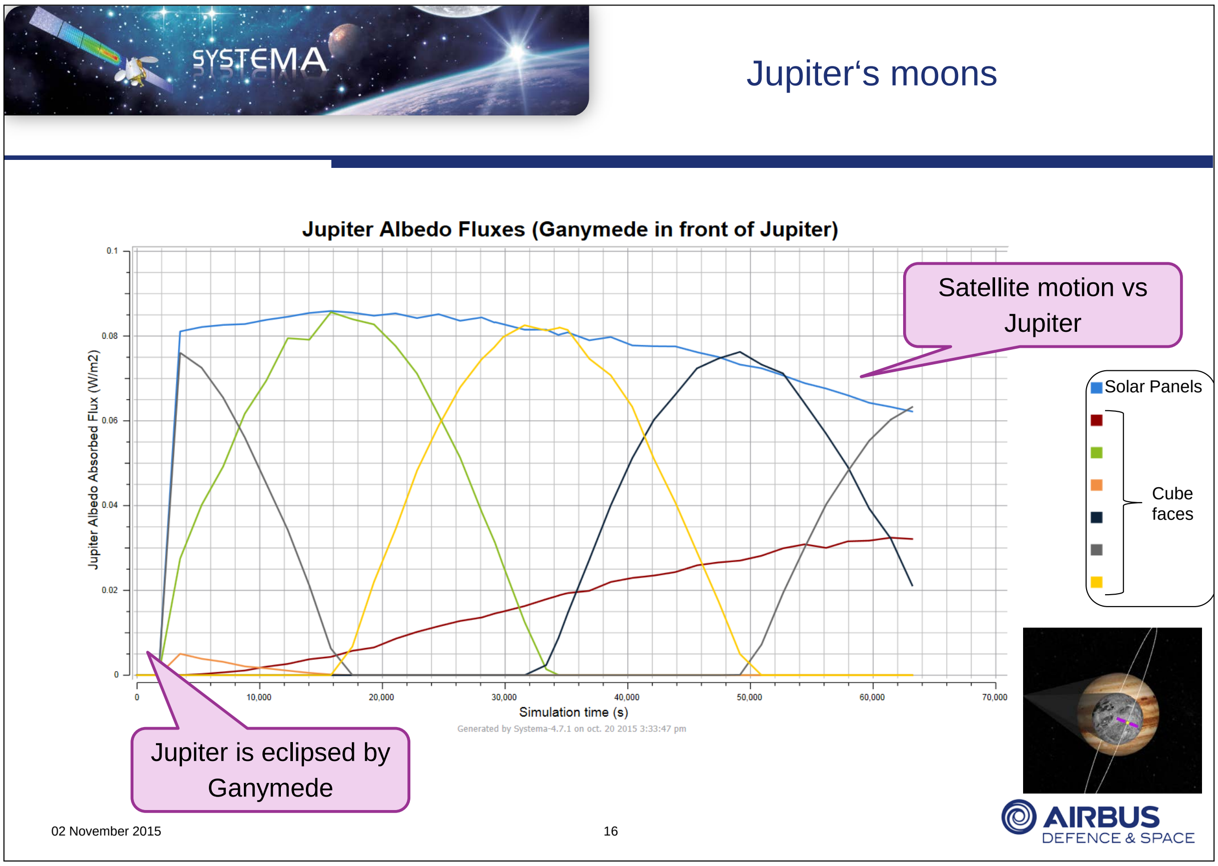
SYSTEMA
Jupiter‘s moons
Jupiter Albedo Fluxes (Ganymede in front of Jupiter)
Jupiter Albedo Absorbed Flux (W/m2)
0.1
0.08
0.06
0.04
0.02
0
0
10,000
20,000
30,000
40,000
50,000
60,000
70,000
Simulation time (s)
Generated by Systema-4.7.1 on oct. 20 2015 3:33:47 pm
Satellite motion vs Jupiter
Solar Panels
Cube faces
Jupiter is eclipsed by Ganymede
02 November 2015
16
AIRBUS
DEFENCE & SPACE

Jupiter‘s moons

Conclusions

- Relative positions of planet / moon / sun
- Sun eclipses from both Ganymede and Jupiter
- Jupiter eclipse from Ganymede
- Ganymede and Jupiter fluxes simulated

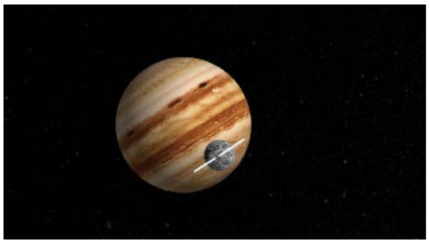

Realistic simulations around any moons are possible

In the future

- update existing moon’s properties
- add new moons

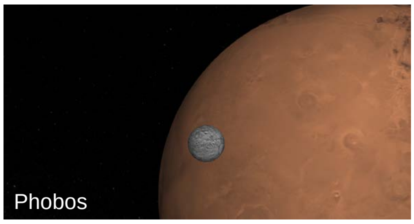

02 November 2015 17

AIRBUS DEFENCE & SPACE

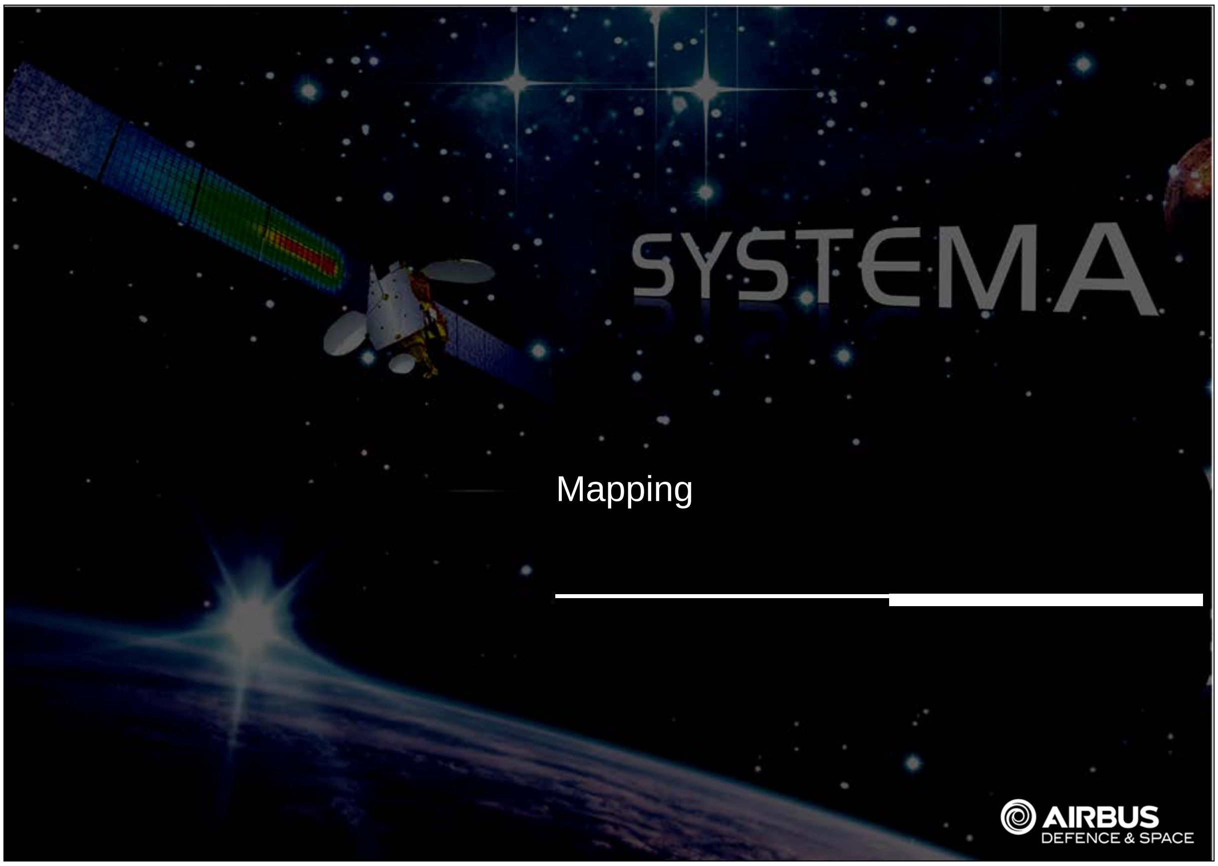

SYSTEMA

Mapping

Context: Multi-physics analysis

- **Need to transfer data**
  - Temperatures from *Thermal analysis* to *Mechanical mesh*
  - Fluxes from *Plume analysis* to *Thermal model*
  - Temperatures from *Thermal analysis* to *Outgassing model*

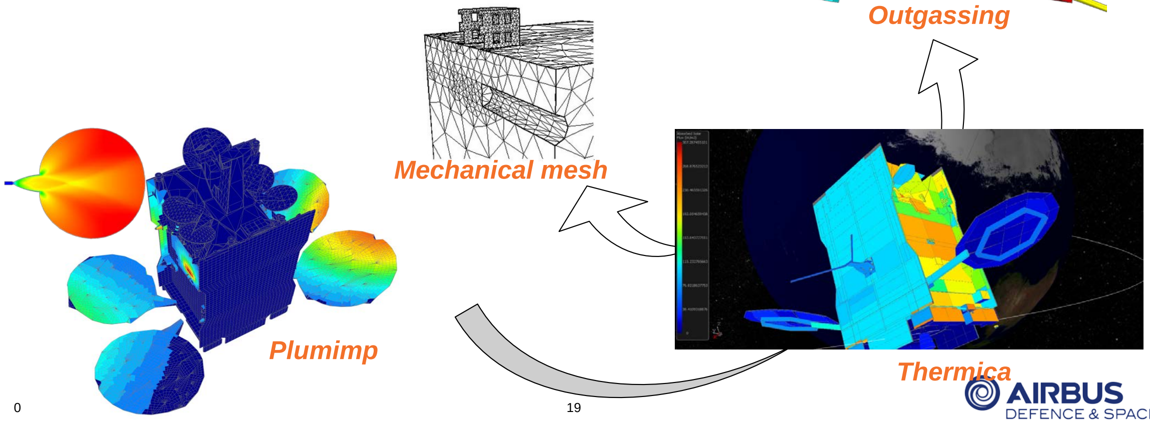

0 19

AIRBUS DEFENCE & SPACE

SYSTEMA

Mapping

Geometrical associations

- **By projection from detailed to coarse model**
  - Detailed elements are projected to the nearest geometry of the coarse model (by ray-tracing)
  - The projection is normal to the coarse geometry
  - Correspondences between mesh are generated
  - Including parametric coordinates of projected points

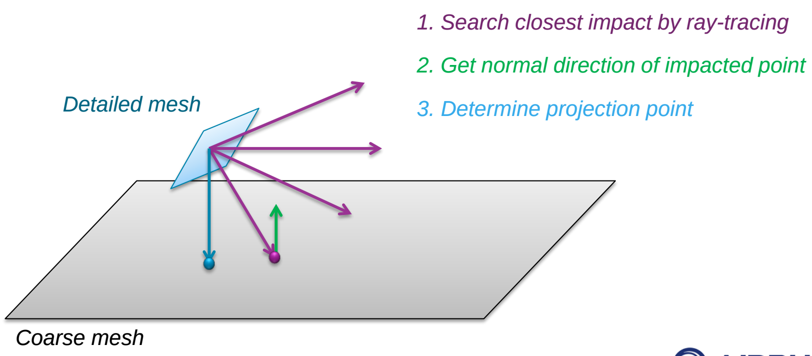

02 November 2015 20

AIRBUS DEFENCE & SPACE

Mapping

Mapping of fluxes

- **According to cross-section of projection**

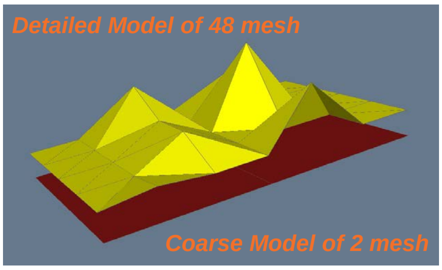

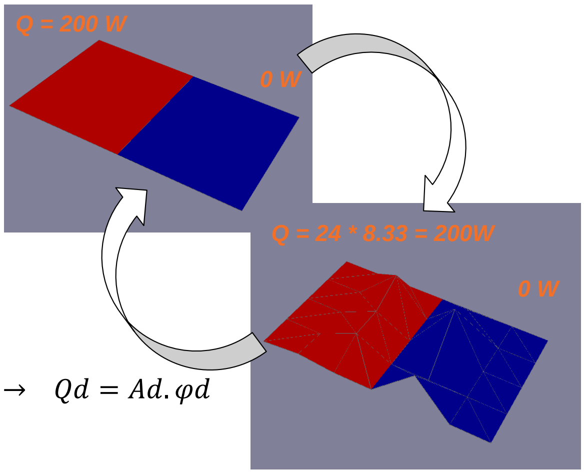

$$Qc \rightarrow \varphi c = \frac{Qc}{Ac} \Longrightarrow \varphi d = \varphi c.\cos\theta \rightarrow Qd = Ad.\varphi d$$

02 November 2015 21

AIRBUS DEFENCE & SPACE

Mapping

Mapping of temperatures

- **By a backward RCN method**

  – The RCN method (Reduced Conductive Network) is an innovative algorithm that deals with the conduction in accordance with radiative and external fluxes ray-tracing methods. It is based on a finite volume integration of conductive fluxes computed through a model reduction of a detailed sub-mesh model.

  – The model reduction used by the RCN algorithm may also export “backward matrices” allowing to recover a detailed temperature profile from temperatures computed on the thermal model.

  – Using the RCN method for the conduction allows then to rebuild an accurate and detailed temperature profile and so to perform a temperature mapping of a very good quality

02 November 2015 22

AIRBUS DEFENCE & SPACE

SYSTEMA

Mapping

Mapping of temperatures

- **Process**
  - – Import a Nastran file into Systema and save it as Systema native format
  - – Create a process with the two models and the mapping module

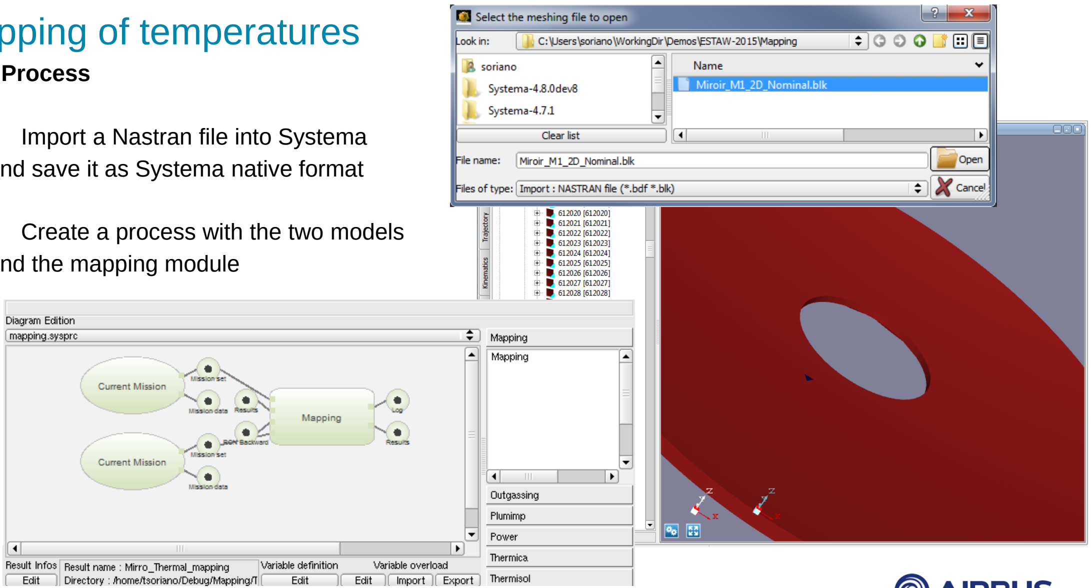

02 November 2015 23

AIRBUS DEFENCE & SPACE

SYSTEMA

Mapping

The backward RCN method

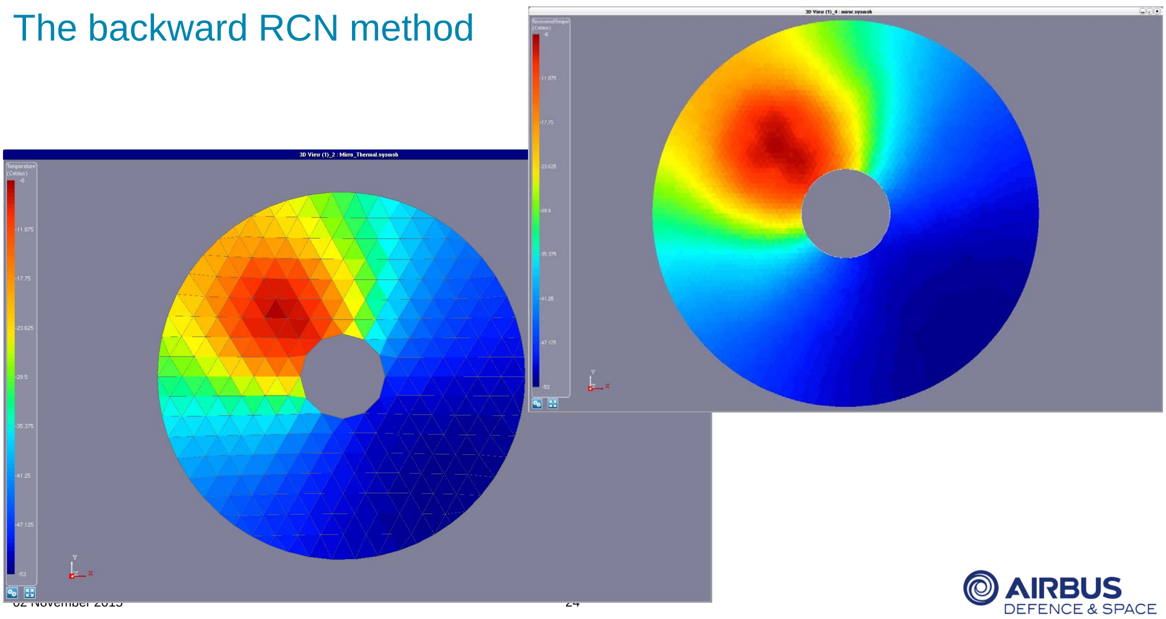

AIRBUS DEFENCE & SPACE

Mapping

The backward RCN method

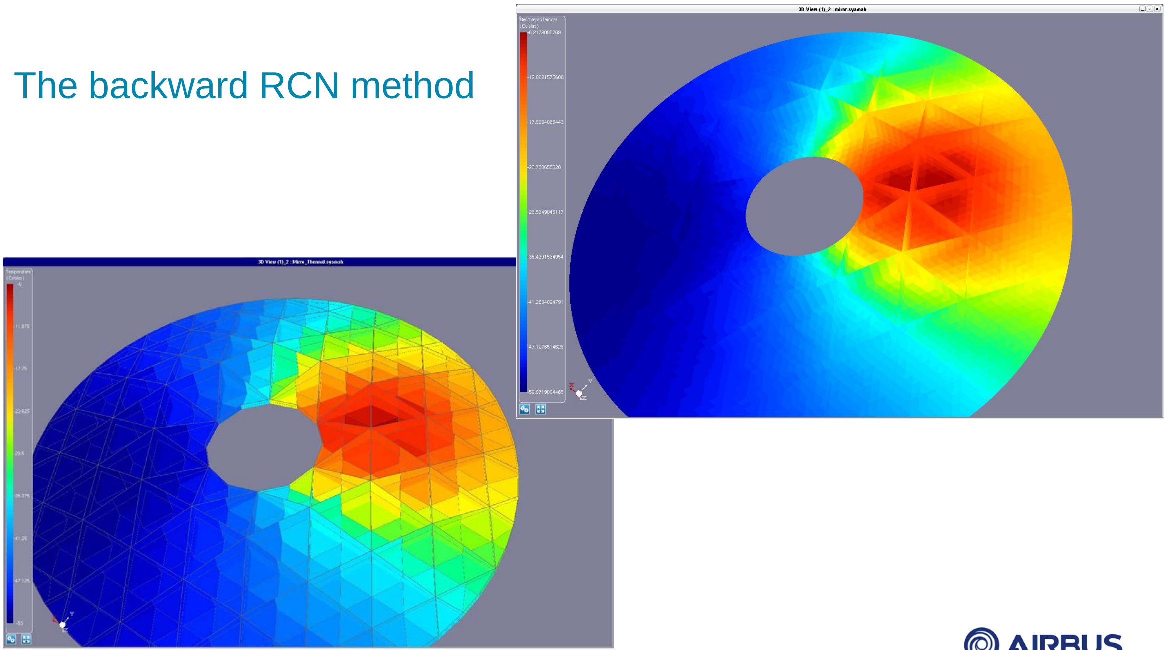

02 November 2015 25

AIRBUS DEFENCE & SPACE

Mapping

Consistency of the RCN Conduction and RCN backward Mapping

- **Coarse model**

Boundary @ 0°C

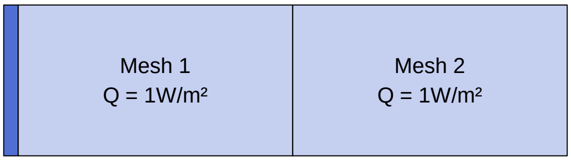

  – Computed average temperatures with the RCN conduction: T1 = 34.66 °C T2 = 74.66 °C

- **Detailed model**

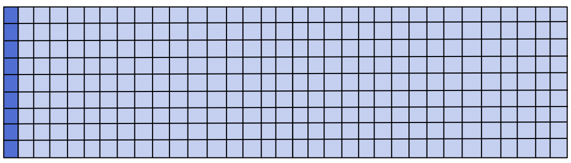

02 November 2015 26

AIRBUS DEFENCE & SPACE

SYSTEMA

Mapping

Consistency of the RCN Conduction and RCN backward Mapping

- **Detailed model: Results**

Identical results between:

- Detailed simulation (RCN)
- Coarse simulation mapped to detailed model

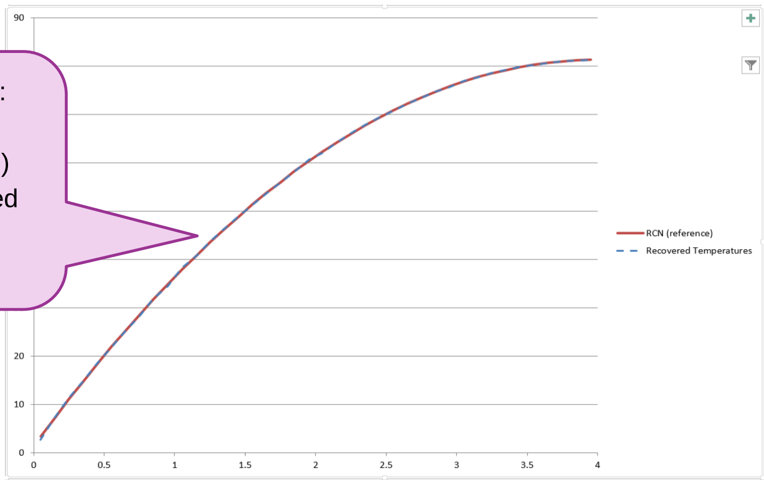

02 November 2015 27

AIRBUS DEFENCE & SPACE

SYSTEMA

Mapping

Consistency of the RCN Conduction and RCN backward Mapping

- **Coarse model: Results**

The simplified RCN (classical lambda.S/l formulae) leads to a convergence of the temperatures with the mesh discretization

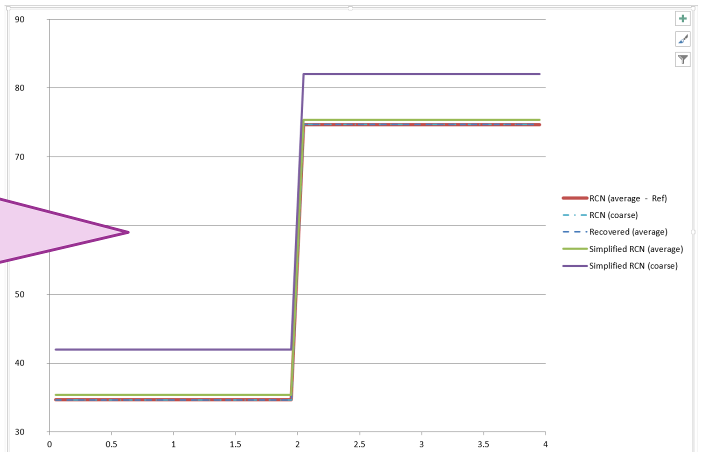

02 November 2015 28

AIRBUS DEFENCE & SPACE

SYSTEMA

Mapping

Conclusion

- **The new Mapping module allows to transfer data (temperatures, fluxes…) between different models**
  - Projected areas may be used to be conservative on the powers
  - Backward RCN brings a complete solution and do not involve any extrapolation of temperatures (the temperature profile obtained is such as the really considered at temperature integration level)

02 November 2015 29

AIRBUS DEFENCE & SPACE

SYSTEMA

SYSTEMA
THERMICA
THERMISOL

Visit our web site :

www.systema.airbusdefenceandspace.com

Contact:
timothee.soriano@airbus.com
rose.nerriere@airbus.com

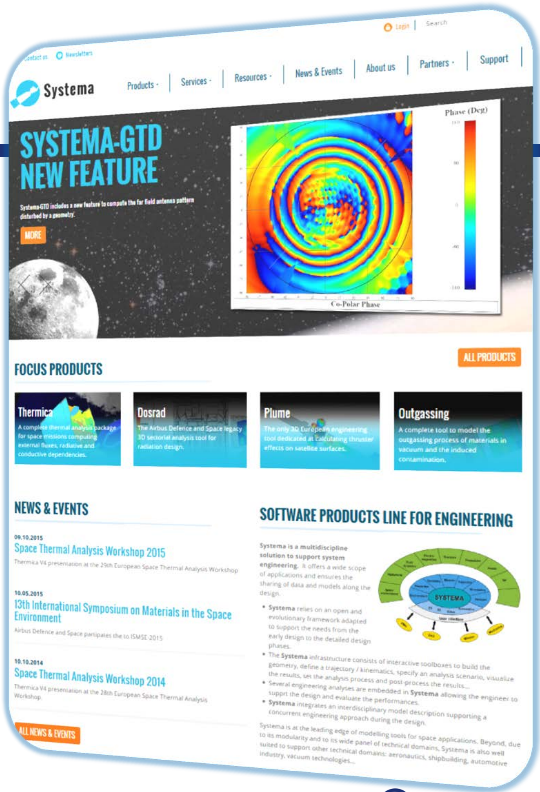

02 November 2015 30

AIRBUS DEFENCE & SPACE

Appendix Q

Thermal Spacecraft Simulator Based on TMM Nodal Model
Return of Experience

Sandrine Leroy François Brunetti
(DOREA, France)

Abstract

Many advantages have been depicted to use the same thermal mathematical model from early design phases to operational phases of the satellite : higher reliability of the thermal model, cost reduction by reusing the model and adaptations work load minimisation.
The dynamic spacecraft system simulator is used to validate the spacecraft control center, but also to train operators. This last user case implies the simulator to react to not predicable events, unplanned scenarios while respecting the physics of the environment.
The thermal analysis model is used to validate the satellite design by predicting temperature ranges for embedded units by calculating temperatures of thermal control elements for given configurations of the environment. Because it is also important to simulate the logic of the flight software (such as thermal regulation), an implementation of the transient state based on simulated time cannot be avoided.
The implementation of a satellite simulator connected to the real flight software using the same thermal nodal model faces many challenges such as the recalculation "on the fly" of the view factors, solar, albedo and earth fluxes impacts on the external CAD model. Another challenge is to make the loop flight software - power dissipation generator - thermal calculator not hanging. For this reason, the thermal simulator regulation must be switched off in order to let the flight software drive the thermostats and thermal temperatures time response should also be adjusted in order to fit the physics time .
Thales Alenia Space Cannes asked DOREA to implement the thermal real-time simulator based on the thermal mathematical model (TMM) provided by thermal analysis team. Thanks to the very good time performances of the e-Therm thermal core calculator (external fluxes, view factors and temperatures calculations), a real time module with parallelism features have been implemented to fit the challenge.
After the success of the O3B Networks and Alphasat dynamic spacecraft simulators in 2013, Thales Alenia Space asked DOREA to implement all the following thermal simulators such as Iridium Next, TKM, SGDC and in the future T3S, K5 and KA7.

Dorea
http://www.dorea.fr

Headquarter
Rés. de l'Olivet, Bat F
06110 Le Cannet
Tel : +33 4 93 69 07 48

Technical Center
« Les Alisiers »
Zone 3 moulins
06600 Sophia Antipolis
Tel : +33 4 92 90 08 29

DOREA TECHNOLOGY

Thermal Spacecraft Simulator Based on TMM Nodal Model Return of Experience.

sandrine.leroy@dorea.fr
francois.brunetti@dorea.fr

DOREA TECHNOLOGY

Presentation (1)

- **Purpose**
  - A Dynamic Spacecraft System Simulator (DSSS) is a dedicated software tool that simulates the full satellite for operational phases.
- **Use Cases**
  - Used to train operators while handling the Spacecraft Control Center (SCC).
  - It is also used to validate the development of the SCC.
  - Used to validate the Check Out Equipment (OCOE) center.

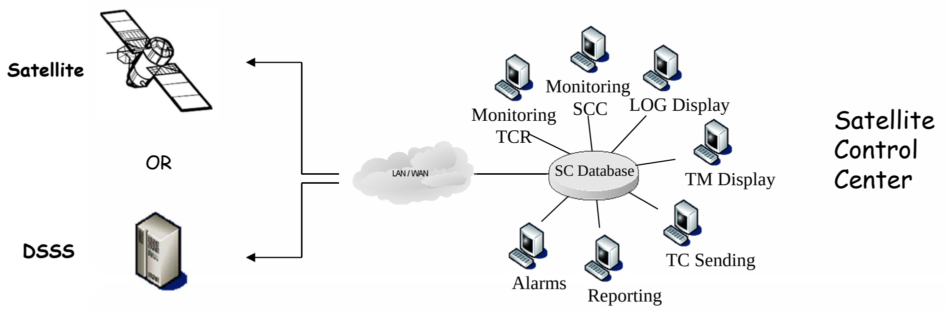

Réf: DOR/PRE/2015/005 - 2

DOREA TECHNOLOGY

Presentation (2)

- **DSSS Components:**
  - Real OnBoard flight Software (OBS).
  - Payload / PLIU and TTC modeling,
  - AOCS models,
  - Power "dissipator" module,
  - Thermal TMM Model (TCS).
- **DSSS Characteristics :**
  - It is a real time application,
  - It should simulate the environment and physics as much as possible,
  - Thermal is the subsystem that needs the simulation of physics. A processor is dedicated to the thermal simulator.
- **Advantages**
  - The scope is to reduce the development cost of the DSSS.
  - Using the TMM provided at CDR or PSR has an enormous advantage to fit with the qualifications.

Réf: DOR/PRE/2015/005 - 3

DOREA TECHNOLOGY

Architecture of SCSIM-TCS

- **Thermal Simulator module (TCS):**
  - DOREA implemented for Thales Alenia Space (TAS) a thermal simulator (SCSIM-TCS) part of the DSSS (SCSIM). The calculator is based on e-Therm CORE module.
  - As it is CPU consuming, a dedicated processor is allocated to the thermal simulator.
  - The architecture is using a co-simulation between the SCSIM (scheduler including the flight software) and the thermal simulator (SCSIM-TCS). The used protocol layer is TCP-IP with a native protocol interface (exchanging binary data values).

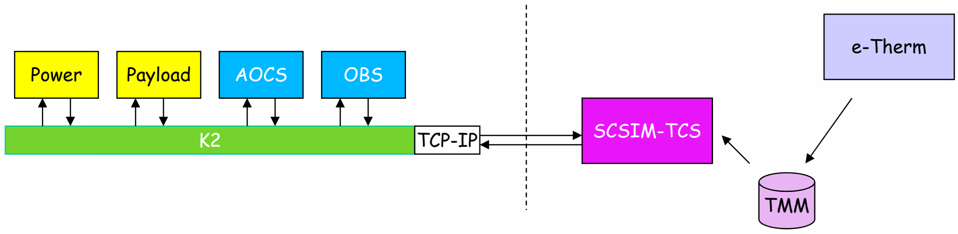

Réf: DOR/PRE/2015/005 - 4

DOREA TECHNOLOGY

SCSIM-TCS Characteristics

- **Thermal Simulator module (TCS):**
  - SCSIM-TCS performs offline conductive and radiative couplings with a storage in a database of couplings according to the kinematics of the spacecraft.
  - SCSIM-TCS performs a online solar, albedo and earth flux calculation "on the fly".
  - Temperature calculation is calculated in a separate process in parallel of the external fluxes calculation.
  - Temperature regulation is performed by the control loop flight software <=> TCS.
- **Customisation:**
  - The time constant of the thermal simulator is deduced from the thermal analysis (around 1s) and the meeting time with the flight software is not less than 32s (speed x1).
  - External fluxes calculation is performed with a threshold based on the Sun/Sat/Earth angles.

Réf: DOR/PRE/2015/005 - 5

DOREA TECHNOLOGY

Validation

- **Successful deployment:**
  - The SCSIM-TCS thermal simulator has been validated in operational conditions for the satellites Alphasat (CNES/ESA/ADS/TAS) and O3B Networks, TKM, Iridium Next satellites (TAS Cannes).
  - It is currently running for SGDC and T3S, K7 and K5A are in preparation.
  - Requirements on T° : delta < 5°C on TM (telemetry = thermistances)
- **Validation approach:**
  - DOREA implemented an automated validation process able to compare given scenarii results provided by e-Therm (decided at KoM) with SCSIM-TCS with automated report generation.
  - DOREA provided a recorder mode enable to store all the flight software inputs in order to reproduce the orbital and powers dissipation "off line".

Réf: DOR/PRE/2015/005 - 6

Issues

- **Main Issue:**
  - SCSIM-TCS does know nothing about the future of the scenario.
  - SCSIM- TCS has to calculate on the fly the moving of the sun and earth (for instance positioning to SAM). At thermal analysis level, the calculator knows at the start all the different modes.

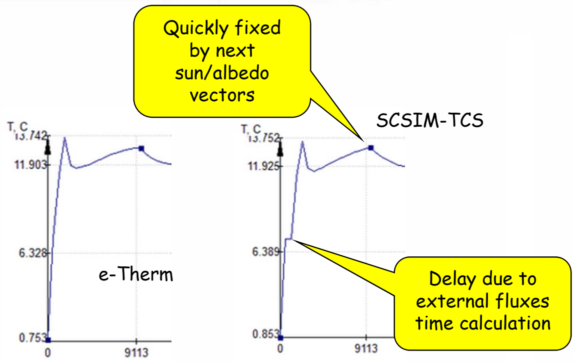

- **Solutions:**
  - Both calculators (external fluxes and temperatures) are running in parallel.
  - Discretisation of the external geometry is tuned to reach a good compromise speed / fluxes error.
  - GMM is reduced in order to not decrease TH precision.
  - A CPU time of 20s is reached to a full external fluxes recalculation.

Réf: DOR/PRE/2015/005 - 7

Model Adaptation

- **Adaptation of GMM**
  - If the model comes from other tools such as ESATAN TMS or SYSTEMA, models are converted thanks to STEP-TAS.
  - From the model provided at CDR or PSR, a GMM reduction should be performed to avoid previous issue (up to 1200 faces).

- **Adaptation of TMM**
  - If the model comes from other tools such as ESATAN TMS or SYSTEMA, models are converted thanks to TMRT.
  - A simplified tubing model and a simplified reccurent part of the geometry will be inserted.
  - If needed (up to 6000 nodes) the TMM should be reduced thanks to TMRT.
  - Missing TH (thermistances) should be added.

Réf: DOR/PRE/2015/005 - 8

DOREA TECHNOLOGY

Conclusions

- **e-Therm improvements**
  - The SCSIM-TCS, part of the SCSIM spacecraft simulator DSSS inherits of all e-Therm improvements (CORE) requiring a small cost of maintenance for DSSS.
  - The DSSS global development costs have been reduced, and in particular the thermal simulator cost is reduced to the CDR/PSR model adaptation, the software itself is not impacted too much.
- **Models improvements**
  - New features to facilitate the GMM reduction are in process. e-Therm radiative session will provide a feature customised to the GMM reduction need for DSSS purpose.
- **Experimental**
  - Experimental solutions for automated GMM reduction based on the GMM but also TMM topology are studied at DOREA.

Réf: DOR/PRE/2015/005 - 9

Appendix R

Correlation of two thermal models

Marije Bakker Roel van Benthem
(NLR, The Netherlands)

Abstract

Reduced thermal models are often required in the design phase of projects. Reduced models have the advantage that they provide a reasonable level of accuracy while maintaining short calculation times. It is common to first build a detailed model, which is then reduced in the same software package. Grouping of nodes and thermal properties requires a lot of physical insight and can be a tedious job.
This presentation will offer a different approach with the same advantages, but without the tedious node grouping in the reduction step. An analytical model for the thermal analysis of wiring is correlated with a more accurate numerical model. By this correlation, the level of accuracy of the analytical model is increased, while maintaining short calculation times. The model has been developed for aircraft applications, but can be used for aerospace applications as well. After a short introduction in the model and its applications, the presentation will mainly focus on the different steps in the correlation process.

Correlation of two thermal models

Marije Bakker, marije.bakker@nlr.nl
Roel van Benthem, roel.van.benthem@nlr.nl

FOKKER ELMO

Dedicated to innovation in aerospace

open engineering

Outline of the presentation

- Common way of model reduction
- Description of the models
- Correlation of the two models
- Using RMS as measure
- Fine-tuning of correlation using test results
- Conclusions and recommendations

Common way of model reduction

- Select approach, e.g. nodal model
- Build detailed model in ESATAN
  - If detailed FEM model is available, FEM model can be converted to ESATAN model
  - Depending on application the number of nodes can vary from a couple of dozens to over 1,000 nodes
  - For each node, the thermal properties have to be added
- Group nodes
  - Limited number of nodes allowed
  - Select nodes with similar properties and group them (TEDIOUS!)
  - Combine the thermal properties of all nodes in a group

Common way of model reduction

Objective:
Use as much of the information from the detailed model as possible in the reduced model without increasing the calculation time of the reduced model

Reduced model is often used integrated in a larger model

Advantages reduced model:
- Fast results
- Decent level of accuracy despite limited level of detail

These advantages can also be obtained by correlation of two models
- Model 1: analytical model ('reduced' model)
- Model 2: numerical model ('detailed' model)

Description of the models

Application:
Thermal analysis of wiring bundle designs (of aircraft, but the model can also be used for (aero)space applications)

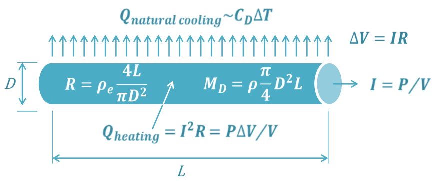

Objective:
Investigate weight reductions and improved safety

Description of the models

TDM – 'reduced' model

- Low level of detail
- Java model using a matrix solver (steady state)
- Network model
- Heat transfer calculated using analytical functions
- Typical calculation time per case: ~ 1 sec.

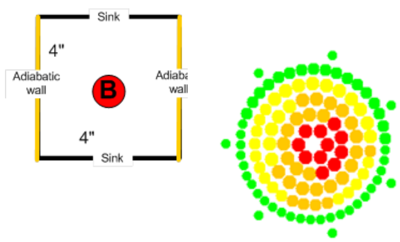

OOFELIE::Multiphysics numerical model
(Open Engineering)

- High level of detail
- Fine grid
- 3D model
- Complex, detailed calculations for heat transfer
- Typical calculation time per case: ~ 1 hour

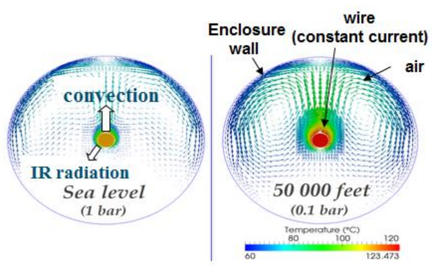

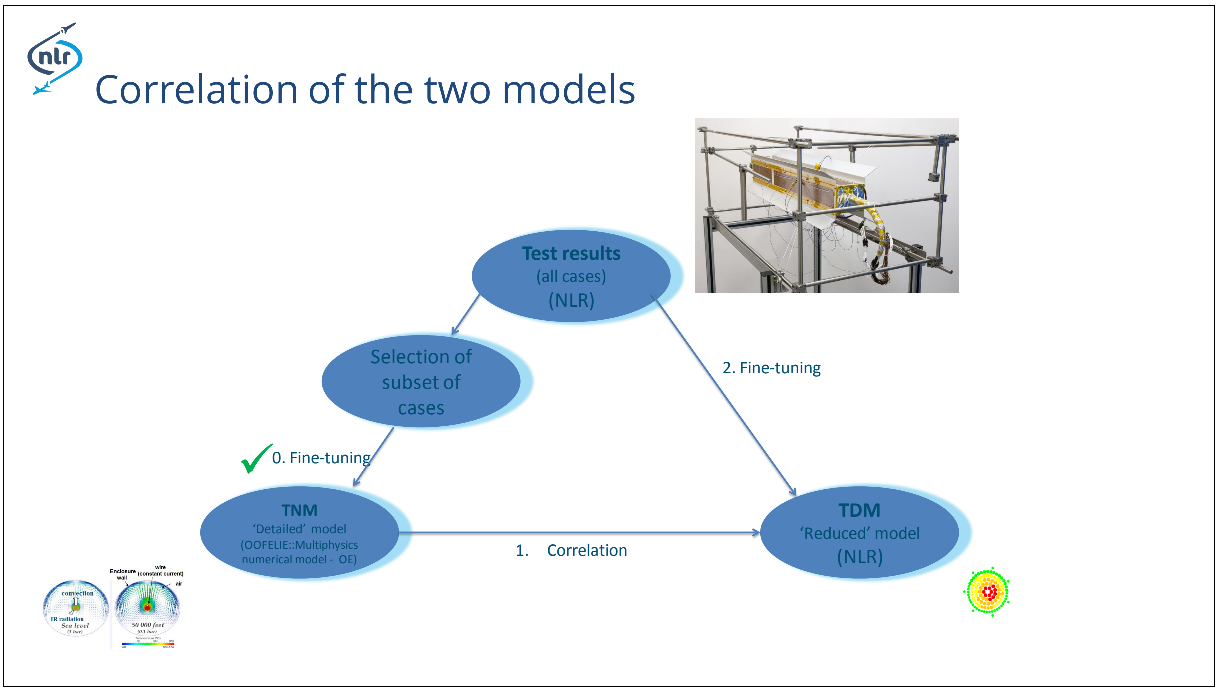
Correlation of the two models
Test results
(all cases)
(NLR)
Selection of subset of cases
2. Fine-tuning
0. Fine-tuning
TNM
'Detailed' model
(OOFELIE::Multiphysics numerical model - OE)
1. Correlation
TDM
'Reduced' model
(NLR)

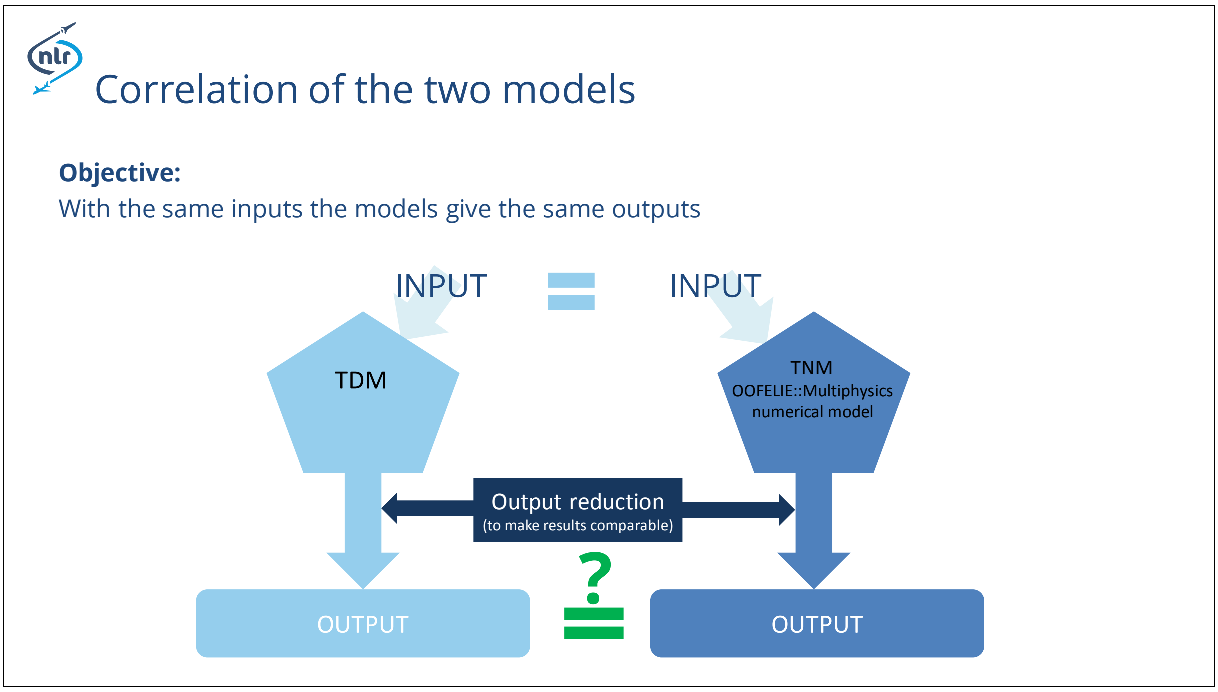
Correlation of the two models
Objective:
With the same inputs the models give the same outputs
INPUT
INPUT
TDM
TNM
OOFELIE::Multiphysics numerical model
Output reduction
(to make results comparable)
?
OUTPUT
OUTPUT

Correlation of the two models

Assumption:
For the same set of inputs both models give the same output if each coupling C (conductive, radiative and convective) from *i* to *j* is the same ∀ *i,j*

Approach:
Find function *f(x)* such that $f(x)*C_{ij\_TDM} = C_{ij\_TNM}$

Conditions:
- Function *f(x)* is different for conductive, radiative and convective couplings and for different combinations of *i* and *j*
- Only one dependency is allowed in the function *f(x)*, i.e., *x* can be e.g. pressure or power

Correlation of the two models

Question: How can C_{ij_TDM} and C_{ij_TNM} be found?

Answer:
Sensitivity analysis

Example: 3 nodes, only conduction

$$P_i = C_{ij} * (T_i - T_j) + C_{ik} * (T_i - T_k)$$

$$T_i = \frac{1}{C_{ij}+C_{ik}} P_i + \frac{C_{ij}}{C_{ij}+C_{ik}} T_j + \frac{C_{ik}}{C_{ij}+C_{ik}} T_k$$

$$C_{ij} = \frac{\cancel{C_{ij}+C_{ik}}}{1} * \frac{C_{ij}}{\cancel{C_{ij}+C_{ik}}} = \left(\frac{\partial T_i}{\partial P_i}\right)^{-1} \left(\frac{\partial T_i}{\partial T_j}\right)$$

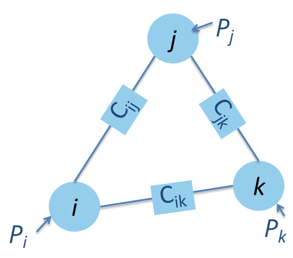

Sensitivity analysis: $\frac{\partial T_i}{\partial T_j} \cong \frac{T_i(T_j=T_0+\Delta T) - T_i(T_j=T_0)}{\Delta T}$

Correlation of the two models

$f(x)*C_{ij\_TDM} = C_{ij\_TNM}$

Use the sensitivity to find all C_{ij_TDM} and C_{ij_TNM}

Assess what *x* in *f(x)* could be:

General:	Power [W]	Pressure [bar]	T1 [°C]	T2 [°C]	T3 [°C]	T4 [°C]
Specific to this model:	Power [W]	Pressure [bar]	T_air [°C]	T_bndl [°C]	T_sink [°C]	T_wall [°C]
C(i,j) (convective)	y	y	y	n	n	n
C(i,k) (convective)	y	y	y	n	n	n
C(i,j) (radiative)	y	n	n	n	y	n
C(i,k) (radiative)	y	n	n	n	y	n
C(i,j) (conductive)	y	n	n	y	n	n
C(i,k) (conductive)	y	n	n	y	n	n
C(m,j) (convective)	y	y	y	n	n	n
C(m,k) (convective)	y	y	y	n	n	n
C(m,j) (radiative)	y	n	n	n	n	y
C(m,k) (radiative)	y	n	n	n	n	y

Correlation of the two models

To find the function *f(x)* such that $f(x)*C_{ij\_TDM} = C_{ij\_TNM}$ a comparison of the couplings is needed

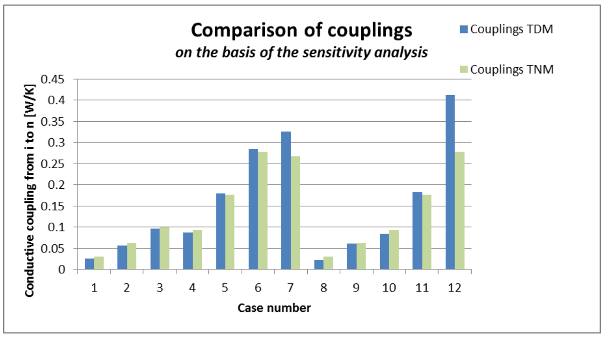

Correlation of the two models

	Power [W]	Pressure [bar]	T_air [degC]	T_bndl [degC]	_sink degC]	T_wall [degC]
C(i,j) (conductive)	y	n	n	y		n

If $f(x) * C_{ij\_TDM} = C_{ij\_TNM}$, then $f(x) = C_{ij\_TNM} / C_{ij\_TDM}$

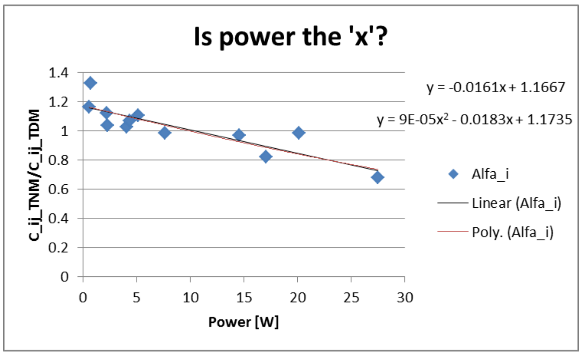

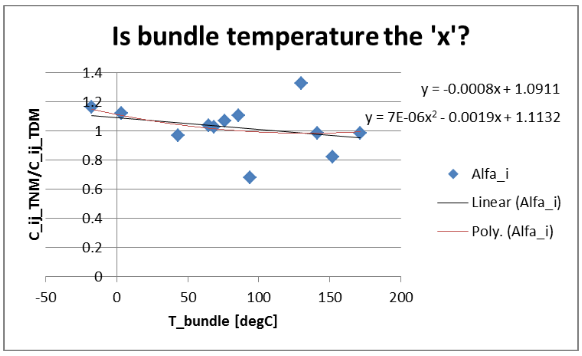

Using RMS as a measure

- Implement all correlation functions (one for each coupling) in the TDM
- The root mean square can be used as a measure for how much the TDM has improved:

$$RMS = \sqrt{\frac{\sum_{i=1}^{N}(T_{TDM\_i} - T_{TNM_i})^2}{N}}$$

- Calculate RMS using the complete subset of cases
- Result:

Correlation step	RMS value
Uncorrelated TDM	10.51
Correlated TDM	16.38
Fine-tuned, correlated TDM	7.69

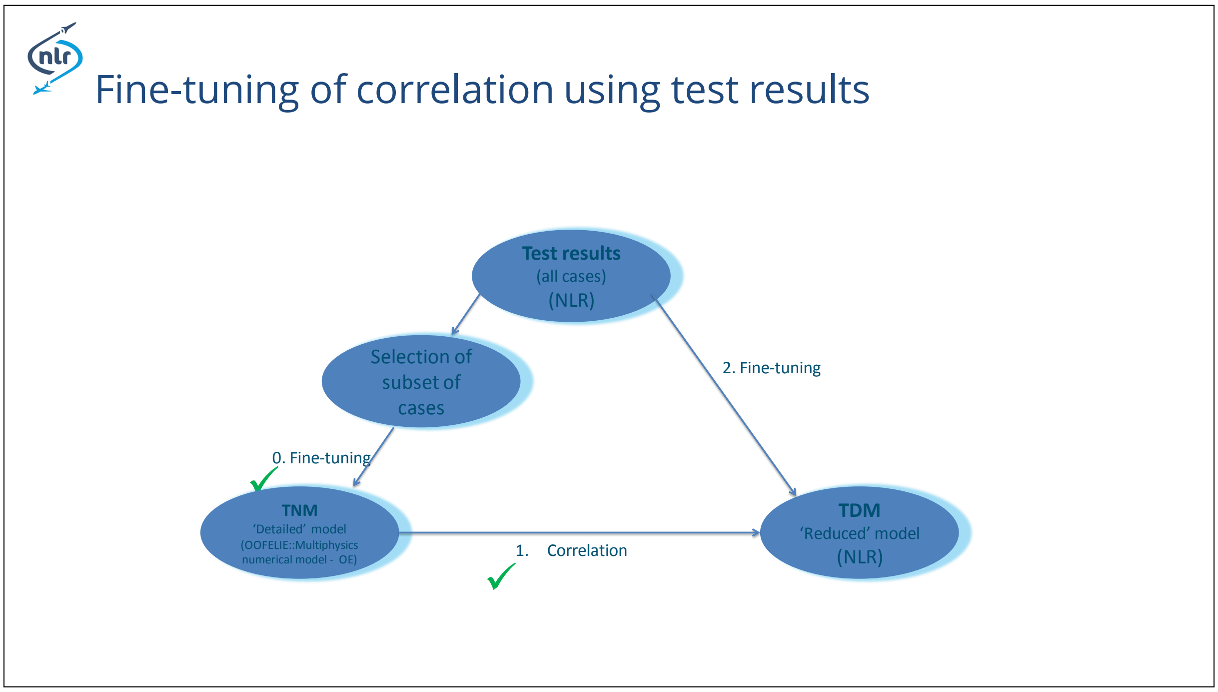
Fine-tuning of correlation using test results
Test results
(all cases)
(NLR)
Selection of
subset of
cases
2. Fine-tuning
0. Fine-tuning
TNM
'Detailed' model
(OOFELIE::Multiphysics
numerical model - OE)
TDM
'Reduced' model
(NLR)
1. Correlation

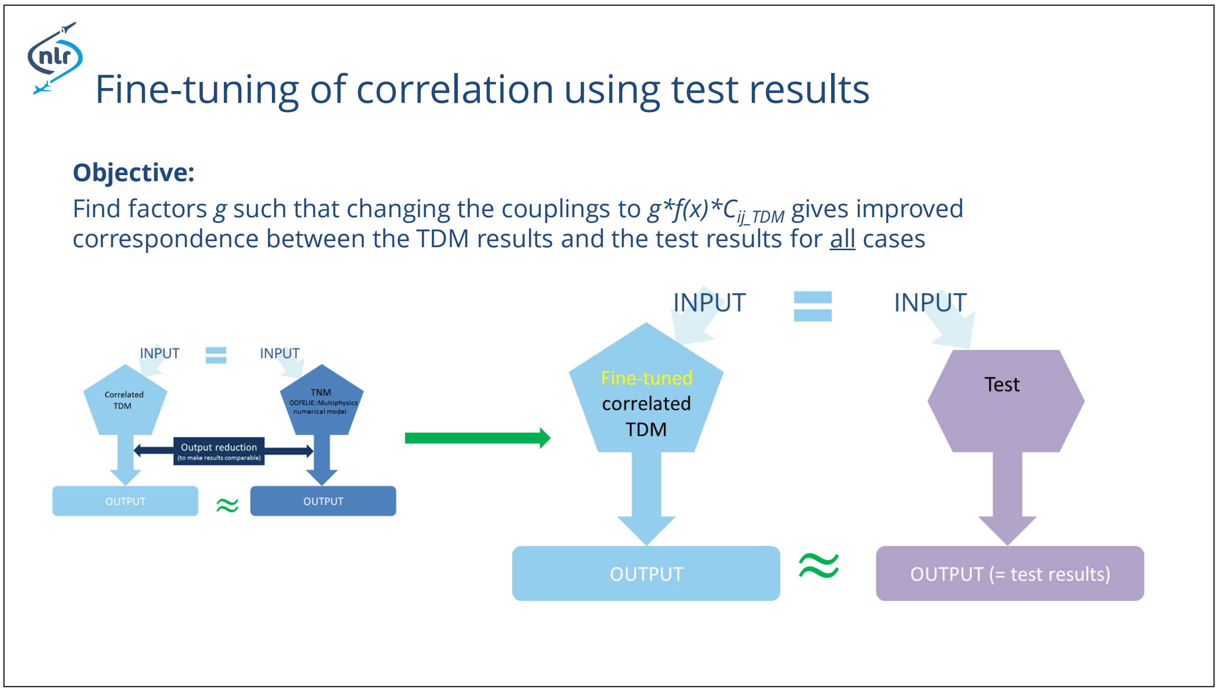
Fine-tuning of correlation using test results
Objective:
Find factors g such that changing the couplings to $g*f(x)*C_{ij\_TDM}$ gives improved correspondence between the TDM results and the test results for all cases
INPUT
INPUT
Correlated TDM
TNM OOFELIE::Multiphysics numerical model
Output reduction (to make results comparable)
OUTPUT
≈
OUTPUT
INPUT
=
INPUT
Fine-tuned correlated TDM
Test
OUTPUT
≈
OUTPUT (= test results)

Fine-tuning of correlation using test results

Measure to determine improvement of correlation:

Correlation Number

$$RMS = \sqrt{\frac{\sum_{i=1}^{N}(T_{TDM\_i} - T_{test\_i})^2}{N}}$$

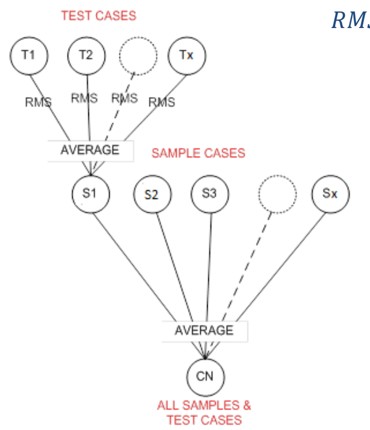

Fine-tuning of correlation using test results

Results:

Fine-tuning step	CN value	Fine-tuning improvements
At start (after finishing TNM correlation)	13.67	
After ~50 iterations	5.89	• Fine-tuning inputs • Slightly scale some correlation functions • Apply some additional minor changes

Conclusions

- **Correlation of two models could be an alternative approach for model reduction, while tedious grouping and reducing step can be avoided**
- **Sensitivity analyses are used to estimate heat transfer couplings**
- **The number of investigated correlation functions has been reduced by a priori assessment of physical dependencies**
- **Use of the sensitivity analysis leads to optimal correlation functions between the models. However, manual fine-tuning is still required.**
- **Correlated TDM gives results that are much better (±10°C) in line with the test results than previous TDM (±15°C)**

Recommendations

- **More research is required to generalize the methodology used**
- **Automation of sensitivity analysis and calculation of correlation functions could be a valuable tool for model comparison without a priori physical understanding of the system**

Appendix S

Experience of Co-simulation for Space Thermal Analysis

François Brunetti
(DOREA, France)

Abstract

Thermal models for space analysis are more and more complex and the idea of having one homogenous model covering different physics such as heat transfer, fluid-dynamics, thermo-dynamics and thermo-elastic is difficult to support. One solution is to open the code to others tools dedicated to bring a complementary physics. The co-simulation is a good candidate to solve the exchange of heterogeneous calculation results but many different techniques and options should be considered at software design level. According to the performances and architecture of the simulators, a co-simulation can be generic or hybrid and impact of the choice of this option may be very expensive. Depending on the physics context, the developer should determine which code would be the master or slave, depending of physics time constants involved in both codes. More depending on computer constraints, an important choice is to specify the communication protocol (such as shared memory or TCP-IP). Some standards such as FMI (Functional Mock Up Interface) are pointing and seam to be pretty candidates, but most of tools provide their own interfaces.

In this presentation we would discuss about DOREA experience and chosen strategy while mixing both CAE simulators : e-Therm (thermal analysis software) bringing the satellite system nodal model and LMS Siemens AMEsim (CFD), especially the dedicated AMErun module with the co-simulation option, to solve the fluids and thermo-dynamics (dysphasic fluxes of a fluid loop) for transient but also steady state calculations.

Dorea
http://www.dorea.fr

Headquarter
Rés. de l'Olivet, Bat F
06110 Le Cannet
Tel : +33 4 93 69 07 48

Technical Center
« Les Alisiers »
Zone 3 moulins
06600 Sophia Antipolis
Tel : +33 4 92 90 08 29

DOREA TECHNOLOGY

Experience of Co-simulation for Space Thermal Analysis

francois.brunetti@dorea.fr

Objectives

- **What it is ?**
  - Simulate a full system with mixed physics or mixed modeling techniques at subsystems level.
- **For what?**
  - Need to mix two heterogeneous subsystems for multiphysics purpose (Ex : nodal mathematical model with finite elements or finite volumes models).
  - Need to run two homogeneous subsystems in parallel.
- **Issues ?**
  - Parallel simulations or embedded simulation (generic or hybrid) ?
  - Different subsystems time constants.
  - Defining a master/slave to schedule meetings.
  - How to model and what type for the interface nodes ?
  - Which communication protocol ?
  - What about the steady state calculation ?
  - What about initialisation ?

Réf: DOR/PRE/2015/004 - 2

DOREA TECHNOLOGY

DOREA experience

- **In the frame of a CNES project:**
  - For thermal analysis purpose, development of MPL dysphasic fluid loop simulation within the full spacecraft global system.
  - e-Therm (TAS thermal analysis software) should interface with Siemens LMS AMEsim (AMErun).
- **Actors:**
  - Thales Alenia Space implements the integration of MPL within the next generation of platforms.
  - Airbus Defence and Space improves its thermal analysis suite of tools : Systema (Thermisol).
  - DOREA develops the integration of MPL simulation within e-Therm.
- **State of the art:**
  - DOREA succeeded in connecting with LMS AMErun via generic co-simulation module, exchanging results between both tools by shared memory.

Réf: DOR/PRE/2015/004 - 3

DOREA TECHNOLOGY

Co-simulation architectures

- **Generic co-simulation:**
  - deploys the both simulators (2 executables) in parallel, with a dedicated communication protocol on a given protocol layer.

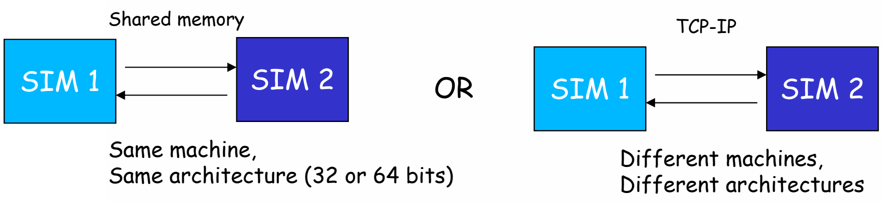

- **Hybrid co-simulation:**
  - links the both simulations into one executable. Simulators exchanges thanks to an API (Application Programming Interface).

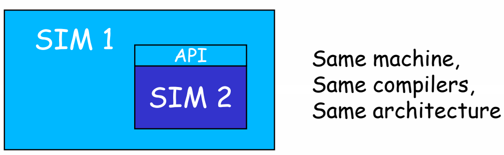

Réf: DOR/PRE/2015/004 - 4

DOREA TECHNOLOGY

Co-simulation architectures

Generic vs Hybrid co-simulations

	Generic	Hybrid
Advantages	•CPU simulation times are done in parallel by several cores (faster). •Both tools are safe to connect or reconnect without interferences.	•Only 1 executable to deploy.
Drawbacks	•TCP-IP may be unsafe and may increase simulation elapsed times	•Compilers, OS and architecture shoud be the same for both tools.

Réf: DOR/PRE/2015/004 - 5

DOREA TECHNOLOGY

Dynamics of communication

- **Sequential approach:**
  - Simulator 1 is waiting results of Simulator 2 before calculating owns.

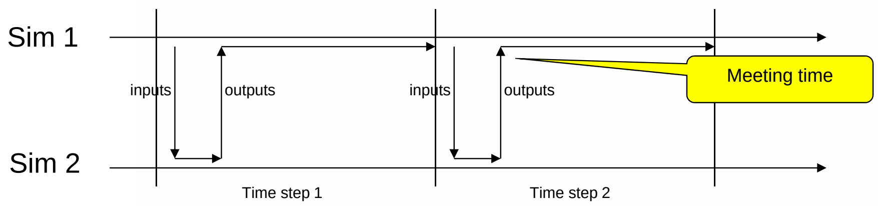

- **Parallel approach:**
  - Simulator 1 performs calculation with Simulator 2 previous time step results.

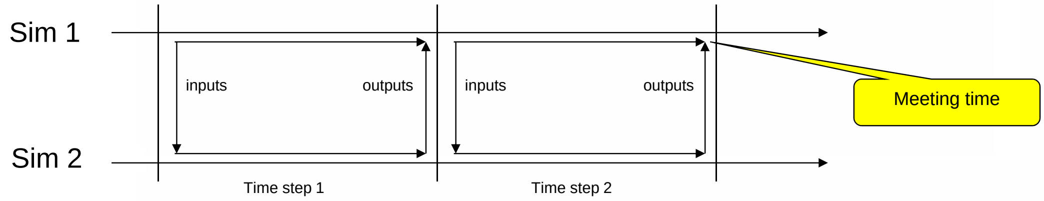

Réf: DOR/PRE/2015/004 - 6

DOREA TECHNOLOGY

Master or Slave ?

- **To share works, we need to define who is giving orders. Recall of the co-simulation protocol:**
  - **The master:**
    - *« Take my inputs, perform your calculation, we will meet at this time. »*
  - **The slave:**
    - *« I finished my calculation. It is time to meet. Take my outputs. »*

- **Who should be the master:**
  - **If one of the both simulators drives the full system, it is clear that this one should be the master.**
  - **If one of the both systems has a biggest time constant, this one should be the master.**
  - **If all subsystems are identical, it does not care who is master.**

Réf: DOR/PRE/2015/004 - 7

DOREA TECHNOLOGY

Nodes « interface »

- **To connect the physics with a nodal model (here thermal analysis mathematical model), we need to define nodes as « interfaces ».**
  - **These nodes are shared by the both models.**
  - **For the subsystem that is not « nodal », it is considered as a constant characteristic of the model (here temperature or exchanged power).**
  - **If both subsystems are nodal models, we can consider conductive or radiative couplings to this node.**
  - **For the subsystem that is « nodal », we need to define if the node is boundary or diffusive.**
- **In our example (thermal analysis for space):**
  - **The « interface » nodes are considered as an input characteristics at AMEsim level and diffusive into e-Therm.**
  - **The temperature is given by e-Therm and the exchange power is returned by AMEsim.**
  - **In our case (heat transfer), the exchange power of interface nodes are considered as internal powers within the equation.**

Réf: DOR/PRE/2015/004 - 8

Protocols and Layers

- **Generic co-simulation protocol layers**
  - **The both executables may communicate thanks to shared memory. They should run on the same cluster node.**
  - **The both executables may also communicate via TCP-IP. Don't care about machines OS, memory or architecture (64 or 32 bits).**

Note : It is obvious that if the meeting time span is short (around the second), TCP-IP is not recommended because of network instabilities.

- **Hybrid co-simulation protocols**
  - **No need of a dedicated protocol, the master calls routines from the API provided by the slave simulator. Warning : time CPU of simulation computation can be added (sequential).**
- **Existing protocols**
  - **The most common protocol is FMI (Functional Mock Up Interface), but native protocols (AMEsim, Simulink, ...) are also provided by developers.**

Réf: DOR/PRE/2015/004 - 9

Convergence (here with AMEsim)

- **Transient State:**
  - **Based on the convergence of the slave simulation, results are taken into account for the calculation of the next time step.**
- **Steady State:**

AMEsim does not provide a steady state calculation, a transient with a stop condition has to be considered.

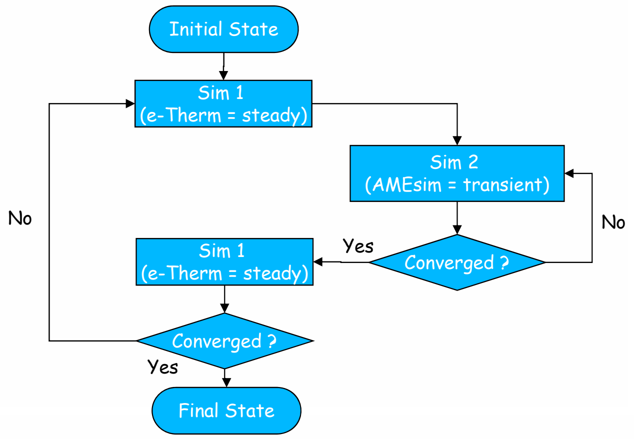

Réf: DOR/PRE/2015/004 - 10

DOREA TECHNOLOGY

Conclusion

- **Experience with AMEsim:**
  - **Siemens LMS AMEsim has a co-simulation module, but more often used to co-simulate 2 AME models from AMEsim.**
  - **Using a tierce application is not fully documented at AMEsim level.**
- **Challenge from DOREA is to make the global system simulator working in steady and transient state.**
  - **For e-Therm / AMEsim co-simulation, a generic co-simulation has been selected because of time responses (time constant for the global system is about 1s)**
  - **e-Therm has been selected as master because it handles all the system model.**
  - **For time performances reasons, a SHM (shared memory) protocol layer has been chosen.**
  - **Regarding to the simplicity of the AMEsim protocol (3 routines are needed), the AMEsim native protocol has been selected.**

Réf: DOR/PRE/2015/004 - 11

Appendix T

GENETIK+
Introducing genetic algorithm into thermal control development process

Guillaume Mas
(CNES, France)

Abstract

In 2014, GENETIK+, a tool that couples CNES genetic algorithm with SYSTEMA Software has been developed, showing great potential to help thermal engineers in their work.
In 2015, new functionnalities have been implemented to GENETIK+ to help analyzing physically the results of the optimization process such as visualization of the response surface and sensitivity analyses.
Thanks to these updates, GENETIK+ has been used on real application cases to show the interest of using optimization algorithm in each steps of thermal control development process.
From worst case analyses to in-flight model correlation, the results obtained with GENETIK+ open new possibilities for thermal engineers.
The objectives of the presentation are to:

- Present GENETIK+ functionalities
- Show the potential of introducing optimization algorithms into thermal control development process

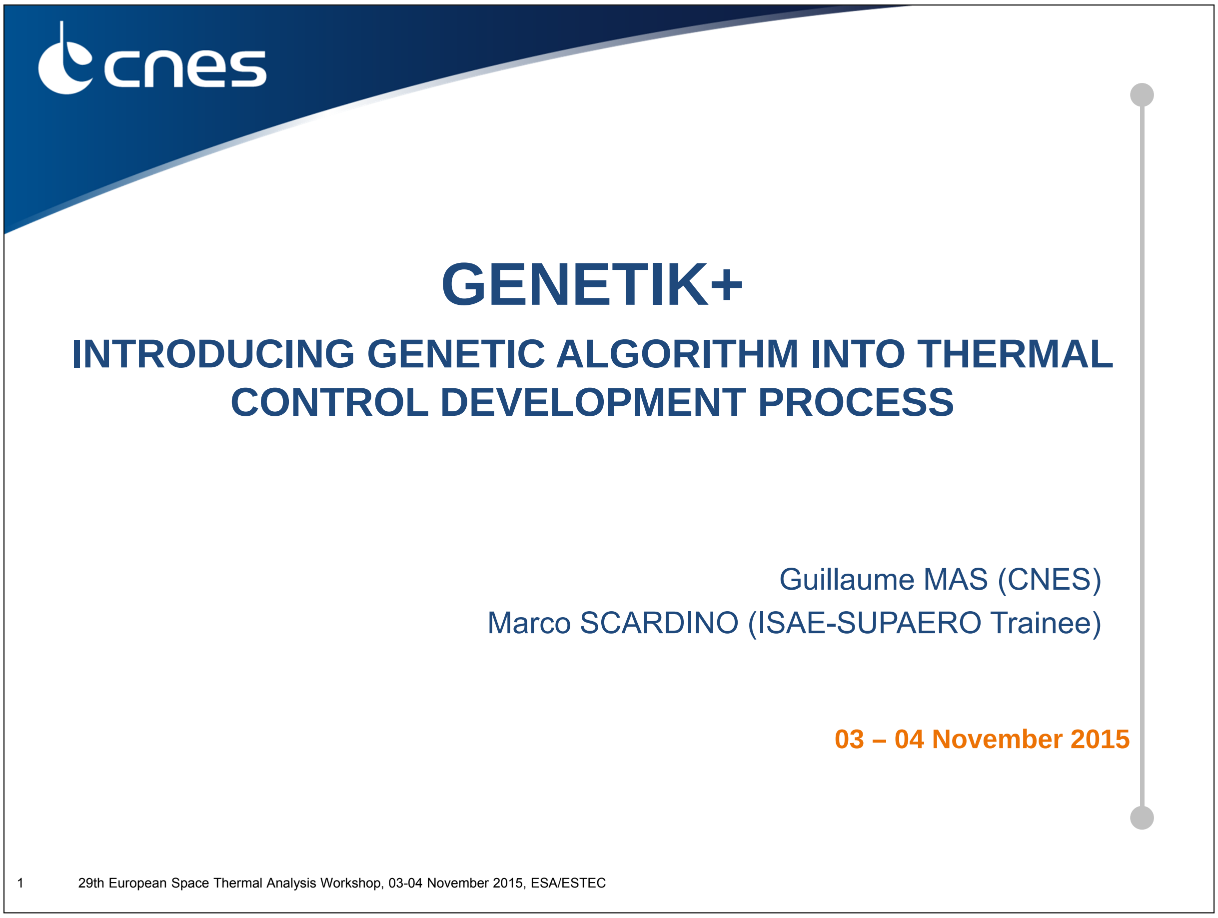
cnes
GENETIK+
INTRODUCING GENETIC ALGORITHM INTO THERMAL CONTROL DEVELOPMENT PROCESS
Guillaume MAS (CNES)
Marco SCARDINO (ISAE-SUPAERO Trainee)
03 – 04 November 2015
1
29th European Space Thermal Analysis Workshop, 03-04 November 2015, ESA/ESTEC

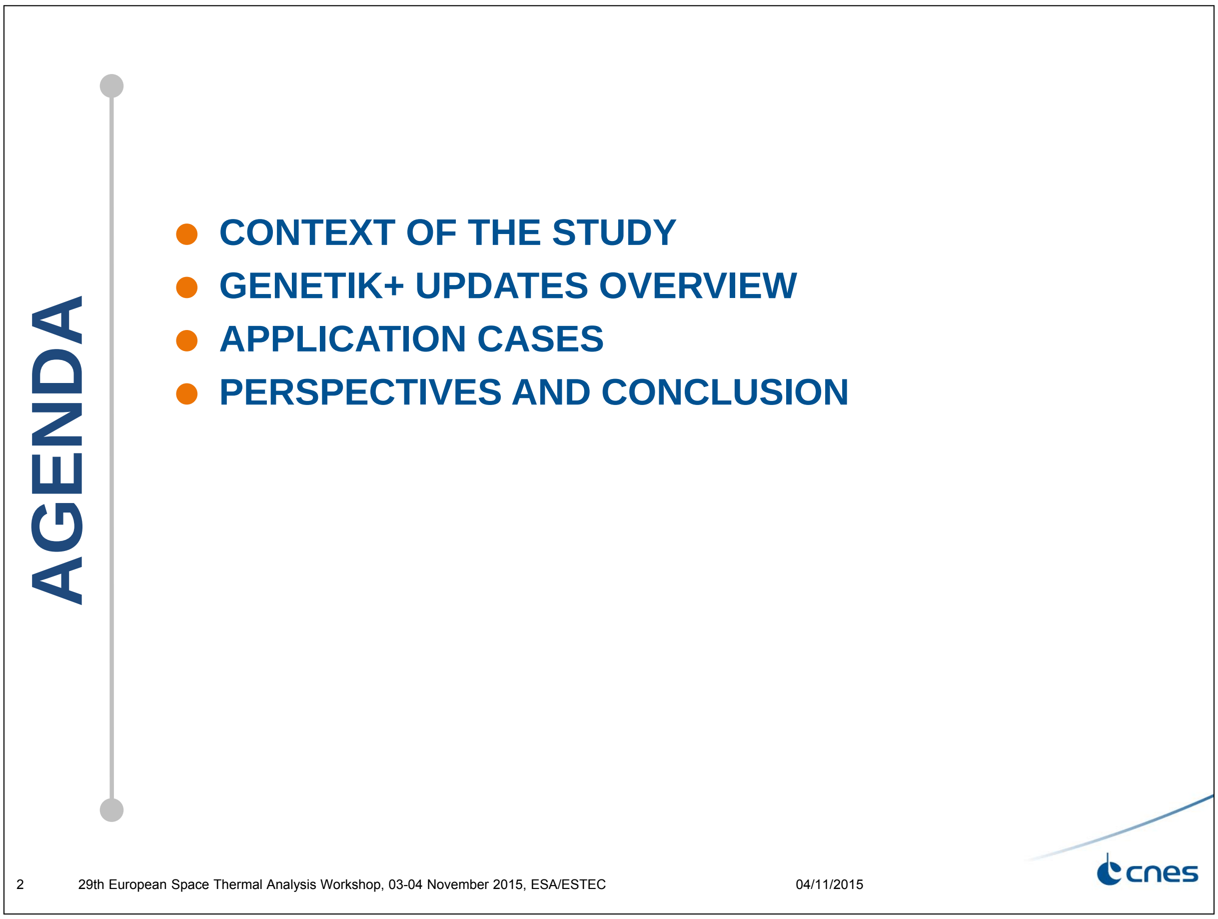
AGENDA
CONTEXT OF THE STUDY
GENETIK+ UPDATES OVERVIEW
APPLICATION CASES
PERSPECTIVES AND CONCLUSION
2
29th European Space Thermal Analysis Workshop, 03-04 November 2015, ESA/ESTEC
04/11/2015
cnes

AGENDA

- **CONTEXT OF THE STUDY**
- GENETIK+ UPDATES OVERVIEW
- APPLICATION CASES
- PERSPECTIVES AND CONCLUSION

3 29th European Space Thermal Analysis Workshop, 03-04 November 2015, ESA/ESTEC 04/11/2015

CONTEXT OF THE STUDY

2014 creation of GENETIK+:

- GENETIK+ allows coupling between SYSTEMA and CNES algorithm GENETIK
- First tests on application cases show great possibilities
- 2014 work conclusions :
  - Full potential to investigate (model correlation, reduction, …)
  - Possibility to use GENETIK+ to explore the space of solution
  - Need post processing tool to understand optimisation process results

4 29th European Space Thermal Analysis Workshop, 03-04 November 2015, ESA/ESTEC 04/11/2015

AGENDA

- CONTEXT OF THE STUDY
- **GENETIK+ UPDATES OVERVIEW**
- APPLICATION CASES
- PERSPECTIVES AND CONCLUSION

GENETIK+ UPDATES OVERVIEW

2015 – Improvement of GENETIK+:

- Increase of GENETIK+ possibilities:
  - Integration of Multi-cases optimization ➔ $Fitness_{TOT} = \sum_{i=1}^{N} \alpha_i Fitness_i$
    - model correlation on several cases (cold and hot configurations,…)
    - Research of optimum design for several orbital configurations
  - New user interface ➔ User friendly
    - GENETIK+ can be used by non experts in optimisation process
  - Increase of source code robustness and validation ➔ GENETIK+ able to be used in a real project context

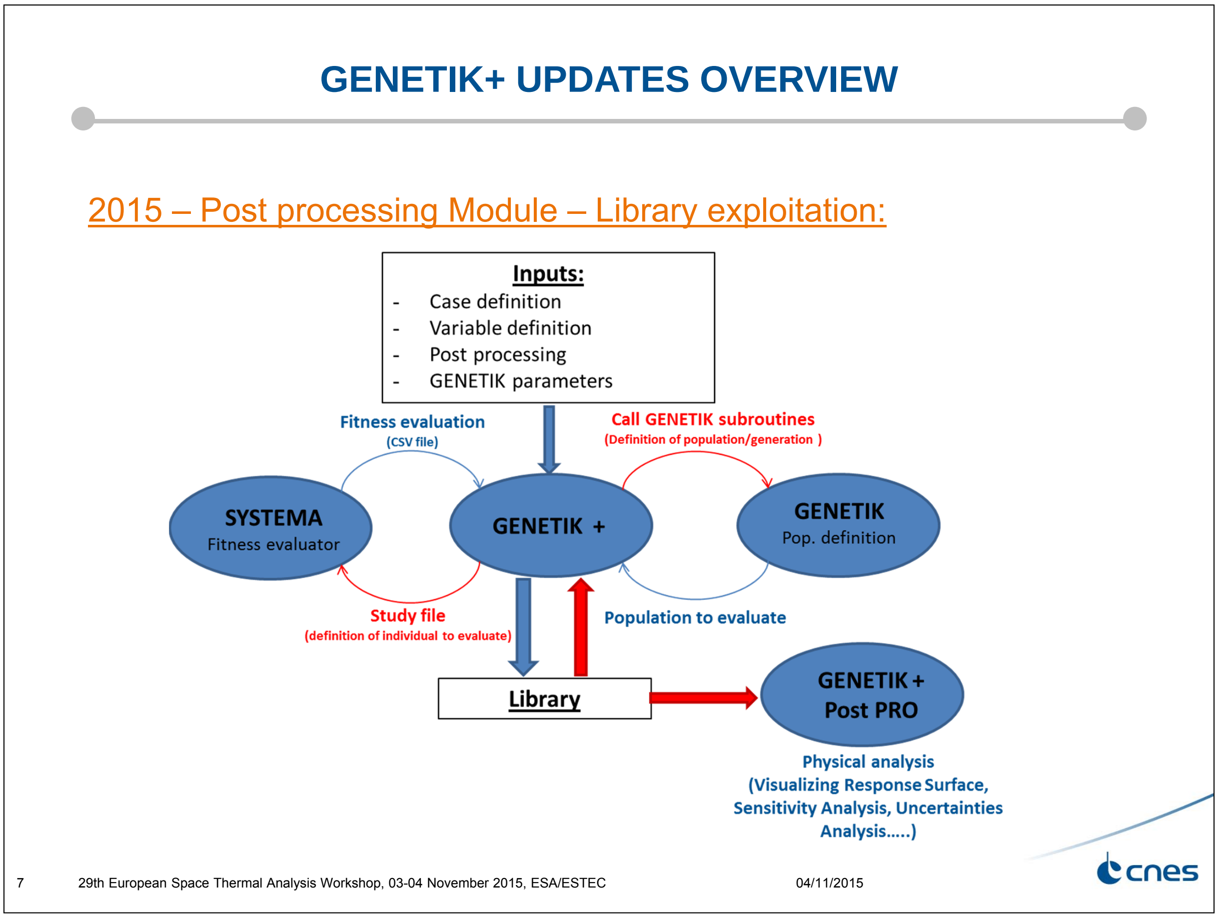
GENETIK+ UPDATES OVERVIEW
2015 – Post processing Module – Library exploitation:
Inputs:
- Case definition
- Variable definition
- Post processing
- GENETIK parameters
Fitness evaluation
(CSV file)
Call GENETIK subroutines
(Definition of population/generation)
SYSTEMA
Fitness evaluator
GENETIK +
GENETIK
Pop. definition
Study file
(definition of individual to evaluate)
Population to evaluate
Library
GENETIK +
Post PRO
Physical analysis
(Visualizing Response Surface,
Sensitivity Analysis, Uncertainties
Analysis.....)
7
29th European Space Thermal Analysis Workshop, 03-04 November 2015, ESA/ESTEC
04/11/2015
cnes

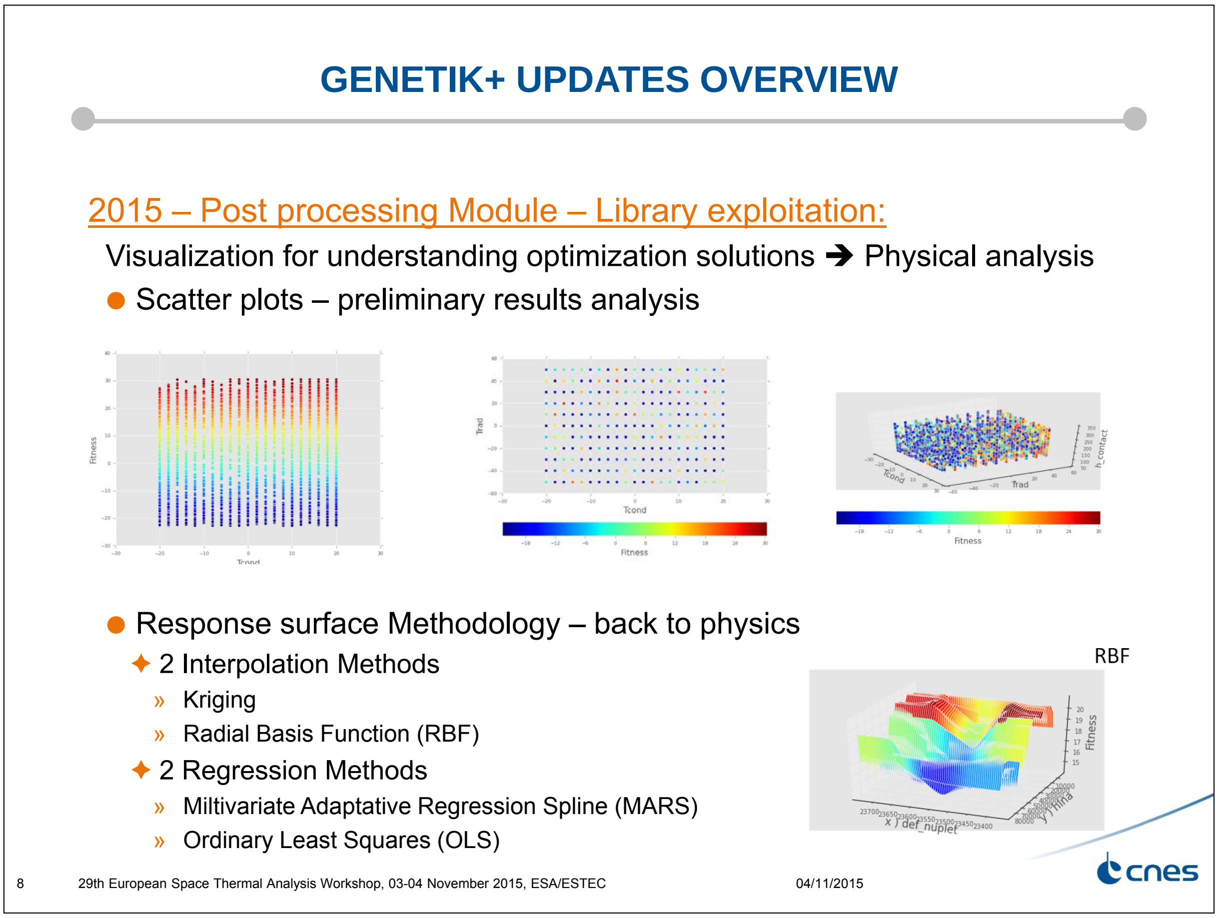
GENETIK+ UPDATES OVERVIEW
2015 – Post processing Module – Library exploitation:
Visualization for understanding optimization solutions ➔ Physical analysis
Scatter plots – preliminary results analysis
Fitness
Tcond
Trad
Tcond
Fitness
h_contact
Tcond
Trad
Fitness
Response surface Methodology – back to physics
2 Interpolation Methods
» Kriging
» Radial Basis Function (RBF)
2 Regression Methods
» Miltivariate Adaptative Regression Spline (MARS)
» Ordinary Least Squares (OLS)
RBF
Fitness
x_i def_nuplet
8
29th European Space Thermal Analysis Workshop, 03-04 November 2015, ESA/ESTEC
04/11/2015
cnes

GENETIK+ UPDATES OVERVIEW

2015 – Post processing Module – Library exploitation:

- Sensitivity analyses on parameters
  - Integration of SOBOL Index method → Global sensitivity analysis on parameters
    - First order impact of each parameters on thermal model behaviour
    - Coupled impact of parameters on thermal model behaviour

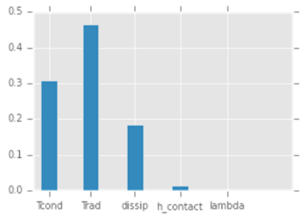

- Parameters uncertainty analysis
  - Find the ΔT max. to cover all the parameters uncertainties
  - Link with parameters distribution law to determine ΔT for a given probability

cnes

AGENDA

- CONTEXT OF THE STUDY
- GENETIK+ UPDATES OVERVIEW
- **APPLICATION CASES**
- PERSPECTIVES AND CONCLUSION

cnes

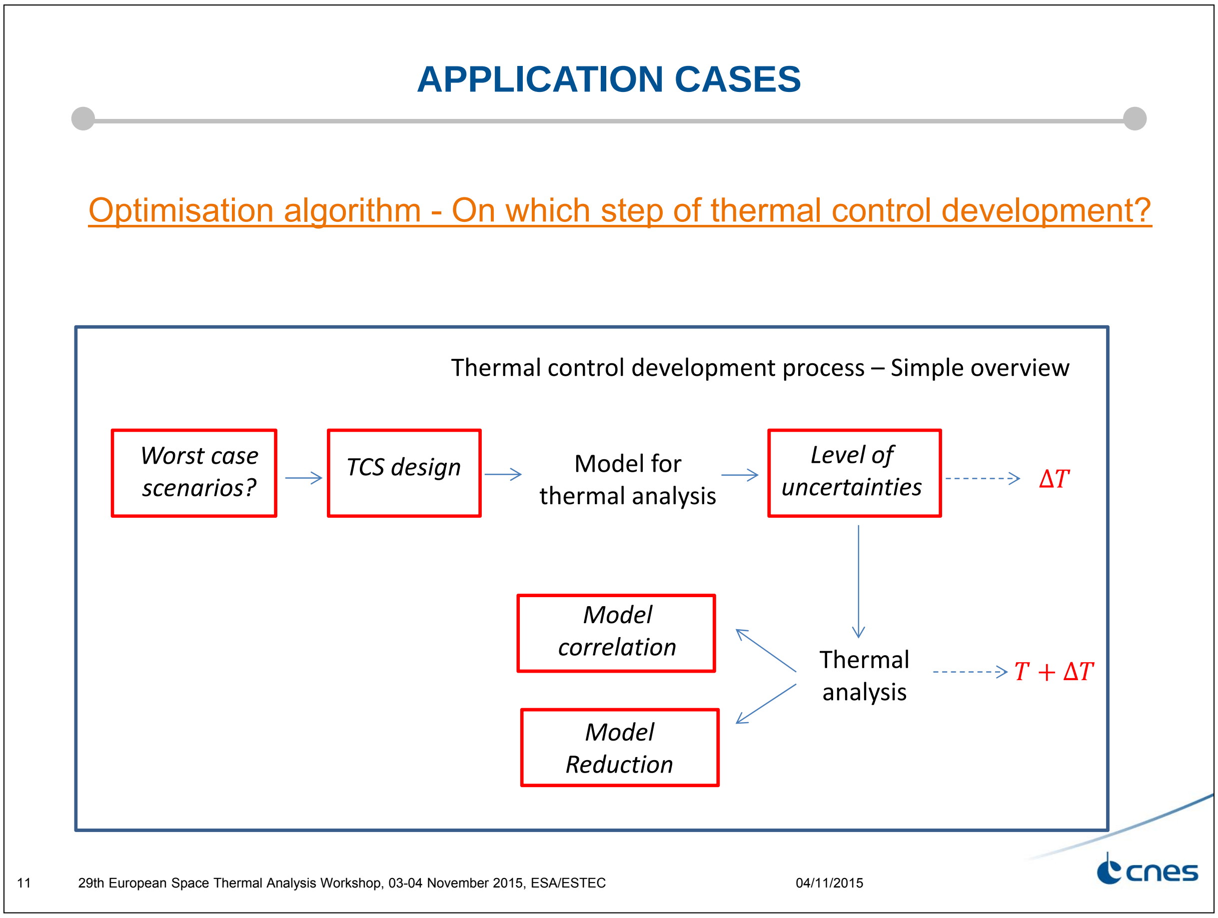
APPLICATION CASES
Optimisation algorithm - On which step of thermal control development?
Thermal control development process – Simple overview
Worst case scenarios?
TCS design
Model for thermal analysis
Level of uncertainties
ΔT
Model correlation
Thermal analysis
$T + \Delta T$
Model Reduction
11
29th European Space Thermal Analysis Workshop, 03-04 November 2015, ESA/ESTEC
04/11/2015
cnes

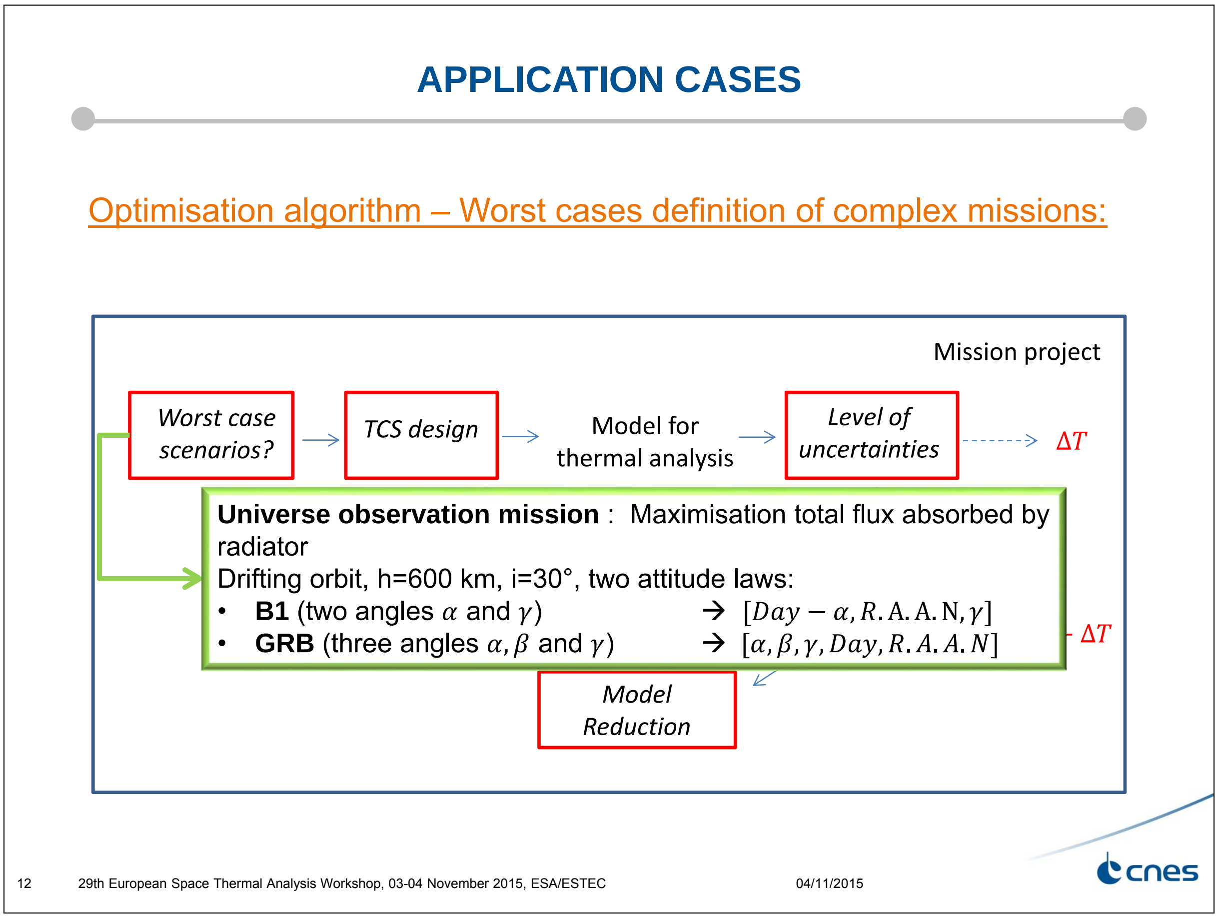
APPLICATION CASES
Optimisation algorithm – Worst cases definition of complex missions:
Mission project
Worst case scenarios?
TCS design
Model for thermal analysis
Level of uncertainties
ΔT
Universe observation mission : Maximisation total flux absorbed by radiator
Drifting orbit, h=600 km, i=30°, two attitude laws:
• **B1** (two angles α and γ) → $[Day - \alpha, R.A.A.N, \gamma]$
• **GRB** (three angles α, β and γ) → $[\alpha, \beta, \gamma, Day, R.A.A.N]$
ΔT
Model Reduction
12
29th European Space Thermal Analysis Workshop, 03-04 November 2015, ESA/ESTEC
04/11/2015
cnes

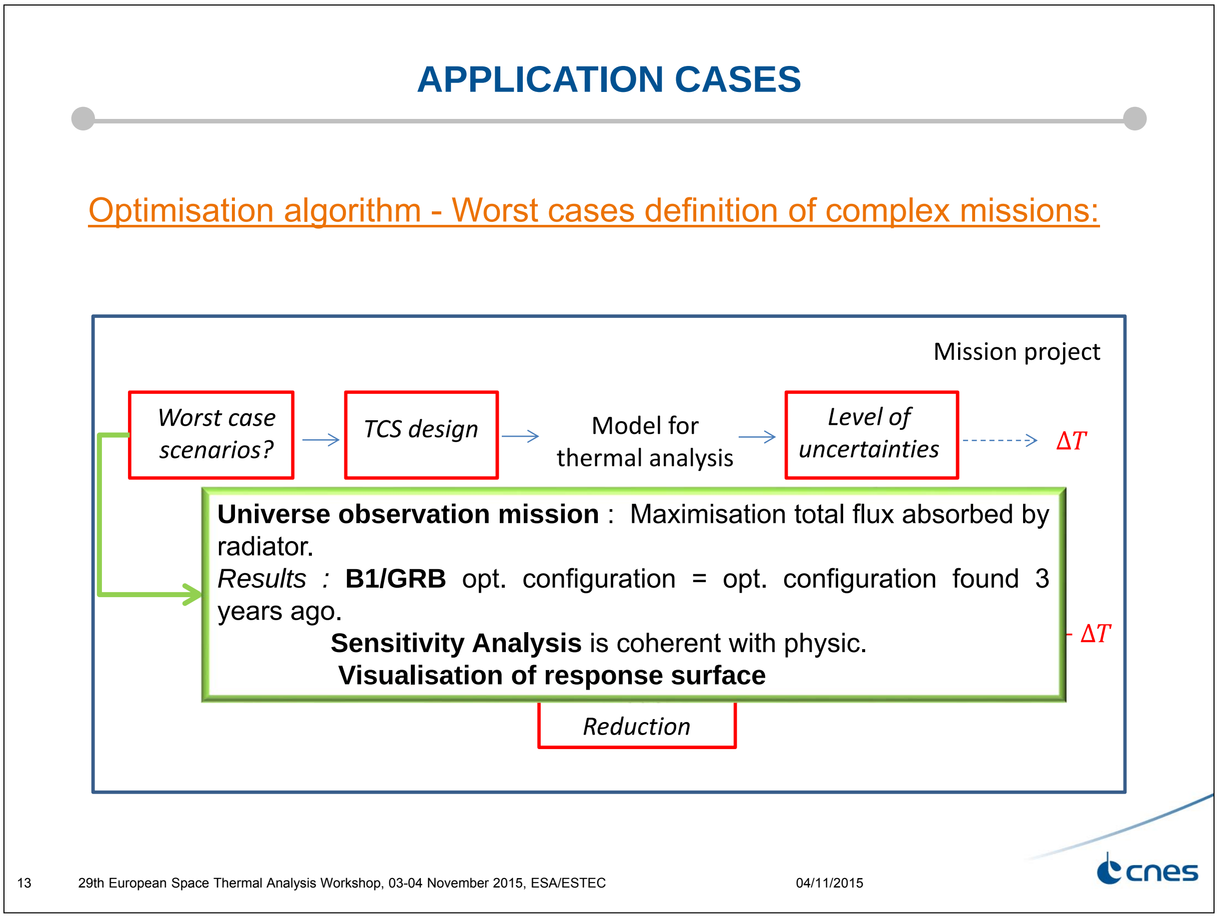
APPLICATION CASES
Optimisation algorithm - Worst cases definition of complex missions:
Mission project
Worst case scenarios?
TCS design
Model for thermal analysis
Level of uncertainties
ΔT
Universe observation mission : Maximisation total flux absorbed by radiator.
Results : B1/GRB opt. configuration = opt. configuration found 3 years ago.
Sensitivity Analysis is coherent with physic.
Visualisation of response surface
ΔT
Reduction
13
29th European Space Thermal Analysis Workshop, 03-04 November 2015, ESA/ESTEC
04/11/2015
cnes

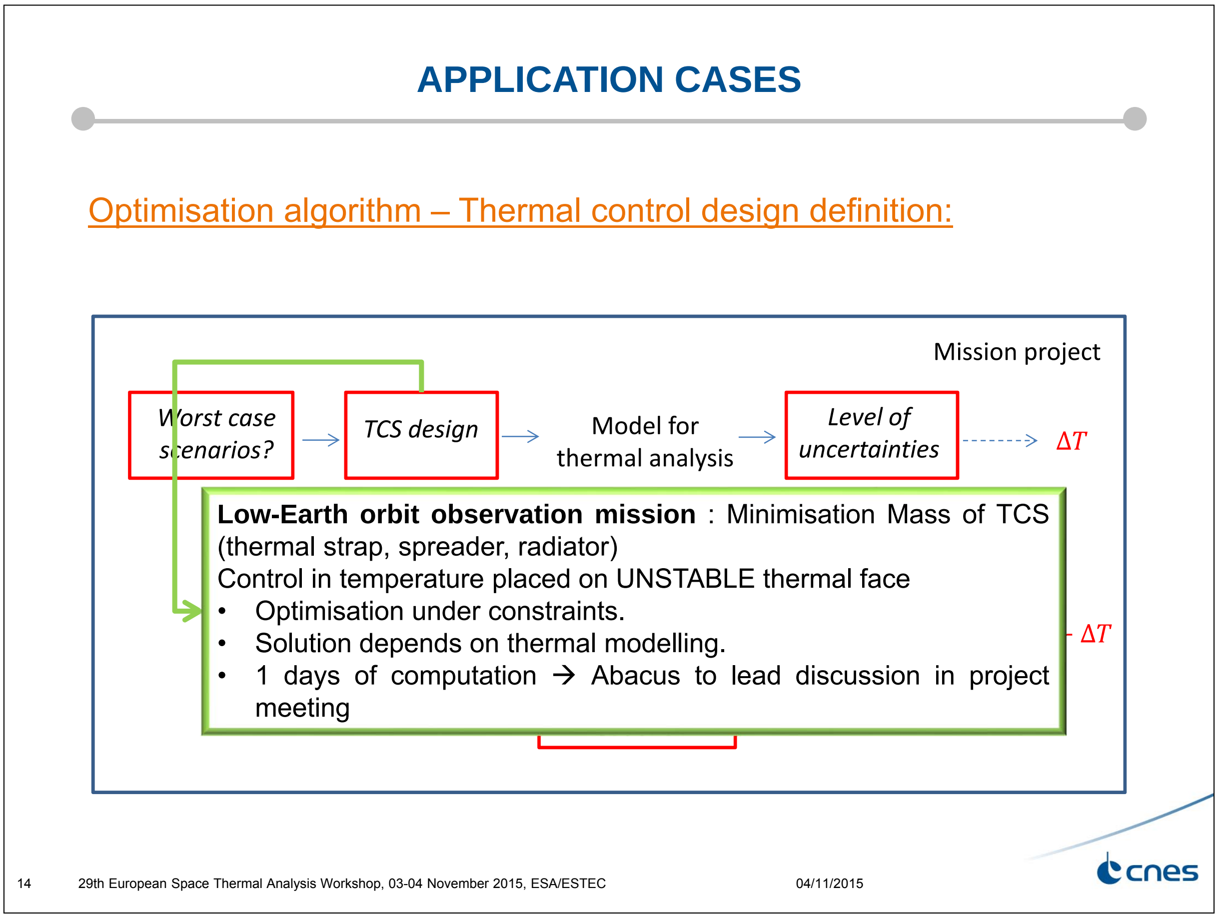
APPLICATION CASES
Optimisation algorithm – Thermal control design definition:
Mission project
Worst case scenarios?
TCS design
Model for thermal analysis
Level of uncertainties
ΔT
Low-Earth orbit observation mission : Minimisation Mass of TCS (thermal strap, spreader, radiator)
Control in temperature placed on UNSTABLE thermal face
• Optimisation under constraints.
• Solution depends on thermal modelling.
• 1 days of computation → Abacus to lead discussion in project meeting
ΔT
14
29th European Space Thermal Analysis Workshop, 03-04 November 2015, ESA/ESTEC
04/11/2015
cnes

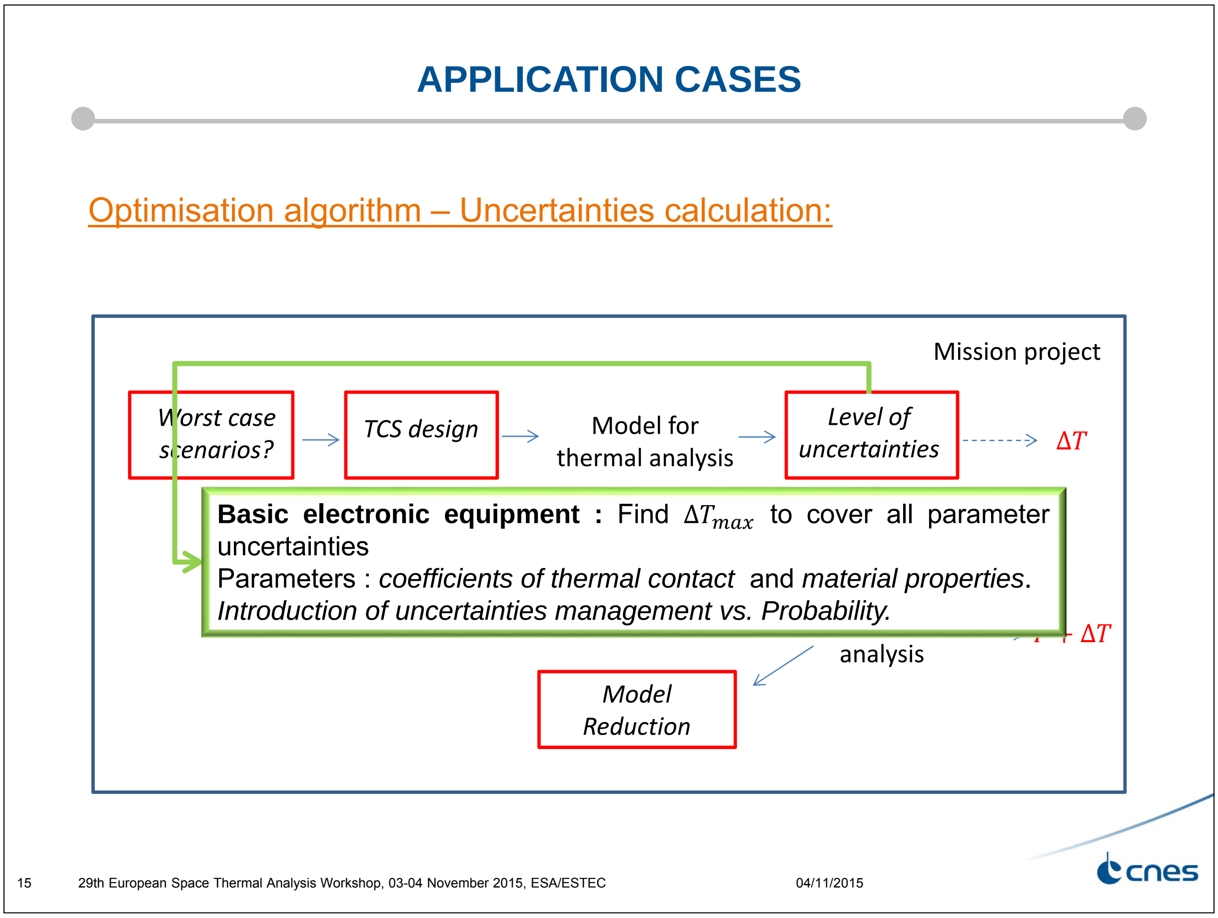
APPLICATION CASES
Optimisation algorithm – Uncertainties calculation:
Mission project
Worst case scenarios?
TCS design
Model for thermal analysis
Level of uncertainties
ΔT
Basic electronic equipment : Find ΔT_{max} to cover all parameter uncertainties
Parameters : coefficients of thermal contact and material properties.
Introduction of uncertainties management vs. Probability.
analysis
ΔT
Model Reduction
15
29th European Space Thermal Analysis Workshop, 03-04 November 2015, ESA/ESTEC
04/11/2015
cnes

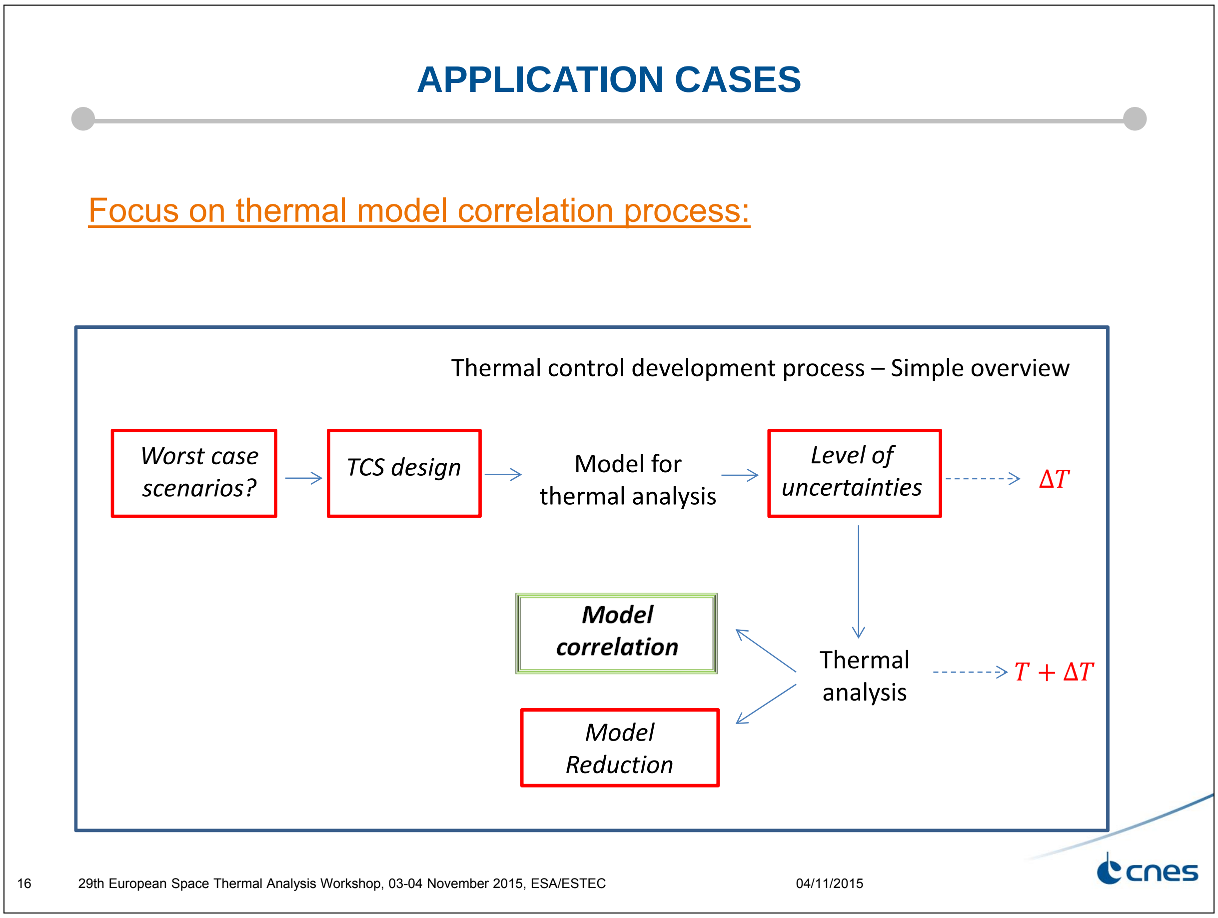
APPLICATION CASES
Focus on thermal model correlation process:
Thermal control development process – Simple overview
Worst case scenarios?
TCS design
Model for thermal analysis
Level of uncertainties
ΔT
Model correlation
Thermal analysis
$T + \Delta T$
Model Reduction
16
29th European Space Thermal Analysis Workshop, 03-04 November 2015, ESA/ESTEC
04/11/2015
cnes

APPLICATION CASES

THERME Experiment - Thermal Model Correlation on flight data:

- Characterise ageing of spatial coating
  - From maximal temperature reached in orbit, find α of coating → radiative equilibrium:

$$\phi_{sol}(\alpha, C_s, \beta) + \phi_{alb}(\alpha, C_s, C_a) + \phi_{Earth}(\varepsilon, C_t) - \phi_{IR}(\varepsilon, T) = 0$$

  - On SDS-4, offset compared to previous in-flight data → Samples not isolated from spacecraft

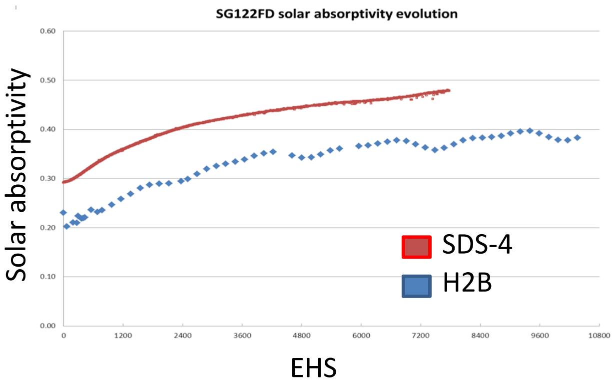

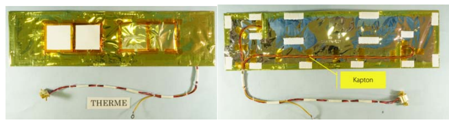

	On ground	In Orbit (first value)
PSBN	0,16	0,3
SG122FD	0,21	0,29

17 29th European Space Thermal Analysis Workshop, 03-04 November 2015, ESA/ESTEC 04/11/2015 cnes

APPLICATION CASES

THERME Experiment - Thermal Model Correlation on flight data:

- "Realistic" samples modelling
  - Thermal leaks: harness-samples (via simple contact and via adhesive tape), MLI-samples (adhesive tape), samples-temperature sensor and harness-SC panel.

    → **5 contact coefficients as parameters**.

  - Correlation process:
    - First approach: Begin of Life (BOL) and End of Life (EOL).
      - BOL properties known / EOL properties unknown
    - Second approach: Begin of Life (BOL).

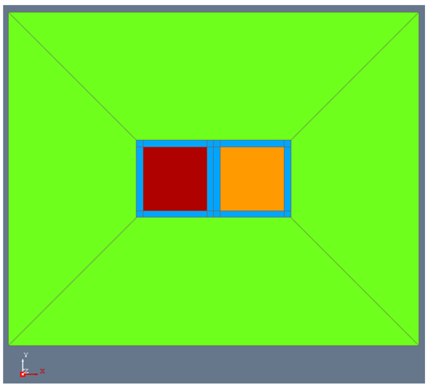

First approach	Second approach
$BOL\ \Delta T_{max} \approx 1.76°C$	$BOL\ \Delta T_{max} \approx 0.0095°C$
$EOL\ \Delta T_{max} \approx 4.96°C$ ($\Delta\alpha_{max} \approx 0.02$)	–

18 29th European Space Thermal Analysis Workshop, 03-04 November 2015, ESA/ESTEC 04/11/2015 cnes

APPLICATION CASES

THERME Experiment - Thermal Model Correlation on flight data:

- Sensor temperature evolution – comparison of the 2 approaches
  - ✦ BOL/EOL approach able to represent whole thermal model behaviour
  - ✦ BOL approach perfect representation in early mission phase

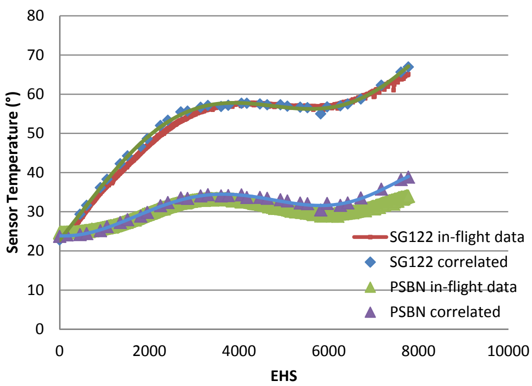

BOL - EOL

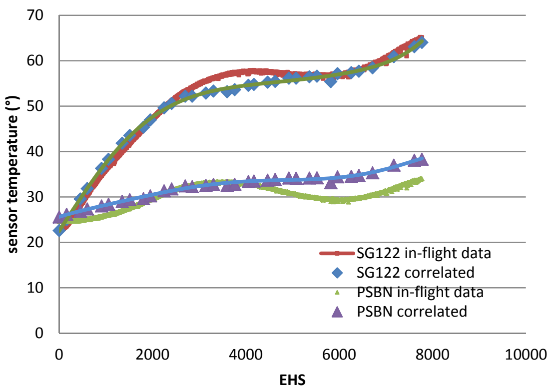

BOL

19 29th European Space Thermal Analysis Workshop, 03-04 November 2015, ESA/ESTEC 04/11/2015 cnes

APPLICATION CASES

THERME Experiment - Thermal Model Correlation on flight data:

- Sensitivity Analysis – Improve THERME design ?
  - ✦ Parameters play different roles on two samples, due to their **different thermal conductivity**.
    - » PSBN (conductive substrate) most influential parameters: *MLI-sample* and *sample-harness via tape*
    - » SG122 (Kapton substrate) most influential parameters: *harness-wall* and *sample-harness*

PBSN

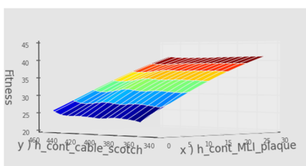

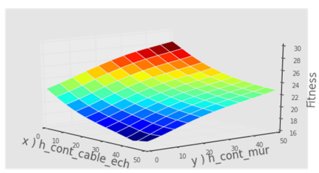

SG122

- New analytic formula for telemetry exploitation
  - ✦ Use of GENETIK+ to explore space of solution $\alpha=f(T_{wall},\phi_{sol},\phi_{Earth})$
  - ✦ Use of Post processing module to extract Response surface and its equation

20 29th European Space Thermal Analysis Workshop, 03-04 November 2015, ESA/ESTEC 04/11/2015 cnes

APPLICATION CASES

Focus on thermal model reduction processes

Thermal control development process – Simple overview

Worst case scenarios? → *TCS design* → Model for thermal analysis → *Level of uncertainties* ⇢ ΔT

Level of uncertainties → Thermal analysis ⇢ $T + \Delta T$

Thermal analysis → *Model correlation*

Thermal analysis → ***Model Reduction***

21 29th European Space Thermal Analysis Workshop, 03-04 November 2015, ESA/ESTEC 04/11/2015

cnes

APPLICATION CASES

Thermal model reduction – Electronic equipment example:

- Classical electronic unit :
  - Composed by: *Printed Circuit Board, internal structure, external structure and harnesses*
  - Two sinks : 2 conductive sink (panel and *external harness*) and radiative sink

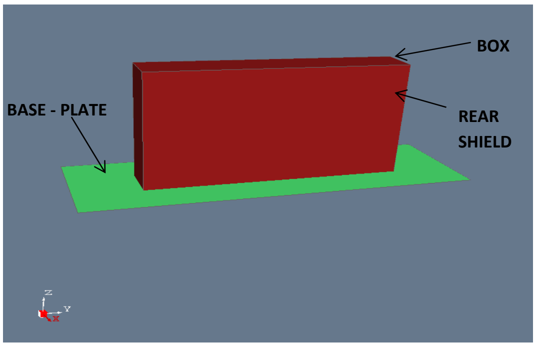

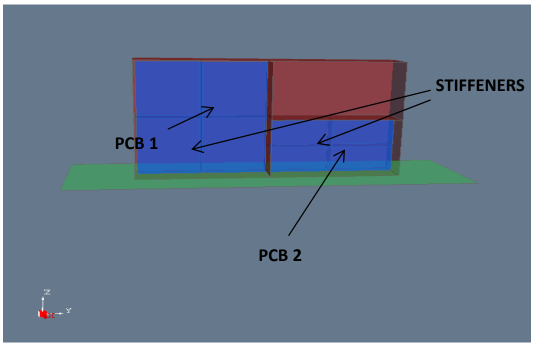

$\approx$ 500 Thermal nodes

22 29th European Space Thermal Analysis Workshop, 03-04 November 2015, ESA/ESTEC 04/11/2015

cnes

APPLICATION CASES

Thermal model reduction – Electronic equipment example:

- 3 working modes: *ON*, *OFF* and *Stand-by.*

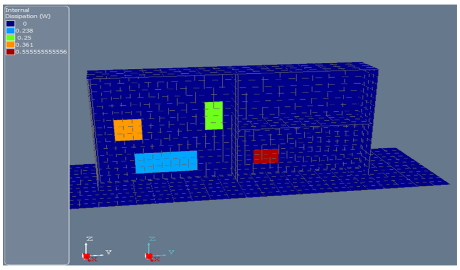

Mode	PCB1 (W)	PCB2 (W)
ON	10,25	5
OFF	0	0
Stand-by	0	5

- 2 configurations: both conductive sinks have the same temperature

Case	T conductive (°)	T radiative (°)	Mode
Hot	50	50	ON
Cold	-10	0	OFF

APPLICATION CASES

Thermal model reduction – Electronic equipment example:

- Two reduction methods:
  1. **<u>"Classical" method</u> : 9 thermal nodes (against ≈ 500 of detailed model)**

  ✦ Objective of GENETIK+: find *conductive couplings* among thermal nodes for the *two configurations* ➔ **22 parameters** (= 22 conductive couplings)

ΔT → Hot case : $\Delta T_{max} = 3{,}63°$ Cold case: $\Delta T_{max} = 0{,}59°$ $\Delta T < 5°$

Interface heat flows →

Case	Heat flow	Reduced (W)	Detailed (W)	Δ (W)
Hot	Rad.	-2,829	1,994	-0,834
	Cond.	-12,421	-13,225	0,834
Cold	Rad.	3,212	3,243	0,031
	Cond.	-3,212	-3,243	-0,031

$\Delta\Phi < 1W$

✦ Conclusions:

» Optimisation with high number of variables

» GENETIK+ allows to reduce thermal model (calculation time 24h)

APPLICATION CASES

Thermal model reduction – Electronic equipment example:

- Two reduction methods:
  2. **Analytical reduction: Find an analytical formula of thermal model Temperature**

- ✦ Steps of the analytical reduction method:
  - » Select *TRPs* (nodal description of reduced model)
  - » Build *Response Surface* with OLS in *Steady-State*, using GENETIK+ data points
    $\rightarrow T_{TRP} = f(External\ cond, mode)$
  - » Find *transient response*

- ✦ Application case – Electronic equipment:
  - » Steady-State Results: 3 TRPs, OLS second degree
  - » Transient Response:
    Hyp: Evolution on time as linear first-order system, *system MISO (Multi Inputs – Single Output)*

$$TRP(t) = \sum_i TRP(t-1)_i + (TRP(\infty)_i - TRP(t-1)_i) \cdot (1 - e^{-t/\tau_i})$$

with $i \in [T\_cond, T\_rad, mode]$

25 29th European Space Thermal Analysis Workshop, 03-04 November 2015, ESA/ESTEC 04/11/2015

APPLICATION CASES

Thermal model reduction – Electronic equipment example:

- Results analysis:
  - ✦ Transient Response: $\mathbf{2°/\,min\ \ T\_cond\ ,\ 10°/\,min\ \ T\_rad}$ and **ON after convergence**

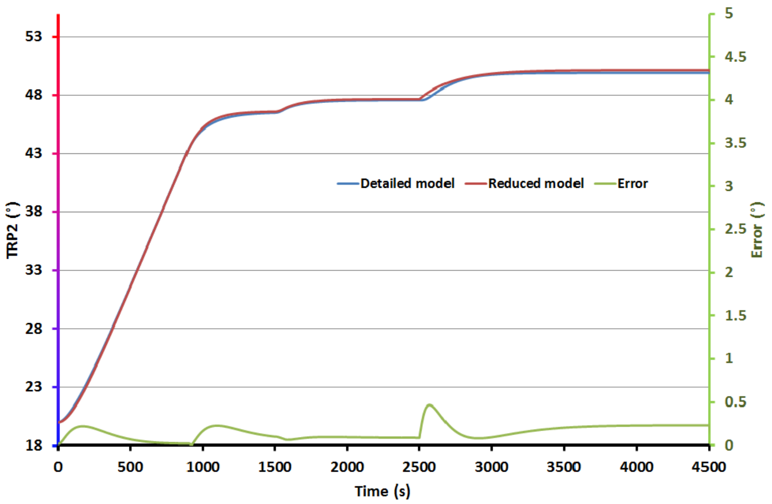

26 29th European Space Thermal Analysis Workshop, 03-04 November 2015, ESA/ESTEC 04/11/2015

AGENDA

- CONTEXT OF THE STUDY
- GENETIK+ UPDATES OVERVIEW
- APPLICATION CASES
- **PERSPECTIVES AND CONCLUSION**

27 29th European Space Thermal Analysis Workshop, 03-04 November 2015, ESA/ESTEC 04/11/2015

PERSPECTIVES AND CONCLUSION

Conclusions:

- The new GENETIK+ version:
  - Optimisation on all steps of TCS definition process.
  - High performance with high number of parameters.
- GENETIK+ Post PRO.
  - *Response Surface* allows visualization of results and introduction of a new reduction method.
  - *Sensitivity Analysis* is physical coherent → Most influential and non influential parameters.
- Principal actor is still Thermal engineer.
- Time reduction for model correlation, model reduction,…….

Future works:

- Parallel coding → reduce calculation time
- Near Real Time model correlation → Extend analytical reduction approach
- Optimisation MultiCriteria

28 29th European Space Thermal Analysis Workshop, 03-04 November 2015, ESA/ESTEC 04/11/2015

Appendix U

List of Participants

Arabaci, Selin
TURKISH AEROSPACE INDUSTRIES INC.-TAI
Turkey
☎ +90 53 3343 6671
✉ sarabaci@tai.com.tr

Bakker, Marije
NLR
Netherlands
✉ marije.bakker@nlr.nl

Banaszkiewicz, Marek
Polish Space Agency
Poland
☎ +48 6 9806 8230
✉ anna.krupa@kprm.gov.pl

Baraggia Au Yeung, Saypen
Argotec
Italy
☎ +39 0 34 5451 8694
✉ saypen.baraggia@argotec.it

Barbagallo, Guido
ESA/ESTEC
Netherlands
✉ guido.barbagallo@esa.int

Bayer, Ralph
German Aerospace Center
Germany
☎ +49 17 5350 7820
✉ Ralph.Bayer@dlr.de

Benthem Van, Roel
Netherlands Aerospace Centre, NLR
Netherlands
☎ +31 6 5169 0565
✉ roel.van.benthem@nlr.nl

Bernaudin, Jean-baptiste
Airbus Defence and Space
France
☎ +33 6 7500 7085
✉ jean-baptiste.bernaudin@airbus.com

Bodendieck, Frank
OHB System AG
Germany
✉ frank.bodendieck@ohb.de

Bouvard, Clémence
AKKA Technologies
France
☎ +33 6 6716 7367
✉ clemence.bouvard@akka.eu

Brouquet, Henri
ITP Engines UK Ltd.
United Kingdom
✉ henri.brouquet@itp-engines.co.uk

Brunetti, Francois
DOREA
France
☎ +33 6 6480 0128
✉ francois.brunetti@dorea.fr

Bugnon, Patrick
AIRBUS DEFENCE & SPACE
France
☎ +33 5 5657 3055
✉ patrick.bugnon@astrium.eads.net

Bures, Nicolas
ITP Engines UK Ltd.
United Kingdom
✉ nicolas.bures@itp-engines.co.uk

Celotti, Luca
Active Space Technologies GmbH
Germany
✉ luca.celotti@activespacetech.eu

Checa, Elena
ESA/ESTEC
Netherlands
✉ Elena.Checa@esa.int

Colizzi, Ettore
ESA/ESTEC
Netherlands
✉ Ettore.Colizzi@esa.int

Cozzoni, Barbara
DLR - Deutsches Zentrum für Luft- und Raumfahrt
Germany
✉ barbara.cozzoni@dlr.de

Czupalla, Markus
OHB System AG
Germany
✉ markus.czupalla@ohb.de

Darrau, Alexandre
Airbus Defence & Space
France
✉ alexandre.darrau@airbus.com

De Palo, Savino
ThalesAlenia Space - Italia
Italy
☎ +39 0 34 9602 3235
✉ savino.depalo@thalesaleniaspace.com

Etchells, James
ESA/ESTEC
Netherlands
✉ James.Etchells@esa.int

Fagot, Alain
DOREA
France
☎ +33 6 7924 1088
✉ alain.fagot@dorea.fr

Fernandez Rico, German
Max-Planck-Institut für Sonnensystemforschung
Germany
☎ +49 551 3 8497 9407
✉ fernandez@mps.mpg.de

Fischer, Jens-oliver
Airbus DS
Germany
✉ jens-oliver.fischer@airbus.com

Fishwick, Nicholas
Airbus Defence & Space
United Kingdom
☎ +44 78 0962 1498
✉ nicholas.fishwick@airbus.com

Franzoso, Alberto
CGS SpA
Italy
✉ afranzoso@cgspace.it

Frey, Anja
ESA/ESTEC
Netherlands
☎ +31 71 565 5068
✉ anja.frey@esa.int

Friso, Enrico
FRS Consulting srl
Italy
✉ enrico.friso@frsconsulting.it

Gabarain, David
None
Netherlands
✉ David.Gabarain@Gmail.com

Gibson, Duncan
Telespazio VEGA UK
United Kingdom
✉ duncan.gibson@esa.int

Girard, Sebastien
Airbus Defence and Space
Germany
☎ +49 151 6524 4855
✉ sebastiendr.girard@airbus.com

Giunta, Domenico
ESA/ESTEC
Netherlands
☎ +31 71 565 3863
✉ Domenico.Giunta@esa.int

Gomez Hernandez, Cesar
ATG Europe
Netherlands
✉ cesar.gomez-hernandez@atg-europe.com

Green, Alex
University College London
United Kingdom
✉ alex.green.09@ucl.ac.uk

Guindi, Joseph
Altran GmbH
Germany
☎ +49 176 8143 9821
✉ joseph.guindi@altran.com

Holzwarth, Matthias
Airbus DS GmbH
Germany
☎ +49 421 539 4328
✉ Matthias.Holzwarth@Airbus.com

Hugonnot, Patrick
Thales Alenia Space
France
☎ +33 6 7356 4110
✉ patrick.hugonnot@thalesaleniaspace.com

Hulier, Jean-pierre
AIRBUS SAFRAN LAUNCHERS
France
☎ +33 6 3836 0259
✉ jean-pierre.hulier@astrium.eads.net

Iorizzo, Filomena
Argotec
Italy
✉ filomena.iorizzo@argotec.it

Ivanov, Dmitri
ESA/ESTEC
Netherlands
☎ +31 6 1932 5331
✉ dimitri.ivanov@esa.int

Jacques, Lionel
Centre Spatial de Liège - University of Liège
Belgium
✉ ljacques@ulg.ac.be

Jeong, Hyeonju
Satrec Initiative
South Korea
☎ +82 10 2250 5738
✉ hjjeong@satreci.com

Kasper, Stefan
Jena-Optronik GmbH
Germany
✉ stefan.kasper@jena-optronik.de

Kirtley, Chris
ITP Engines UK Ltd.
United Kingdom
✉ chris.kirtley@itp-engines.co.uk

Kohut, Peter
RCMT, CTU in Prague
Czech Republic
✉ p.kohut@rcmt.cvut.cz

Kosmrlj, Samo
ESA/ESTEC
Netherlands
☎ +386 3 167 7388
✉ samo.kosmrlj@esa.int

Kuhlmann, Stephan-andré
OHB System AG
Germany
✉ stephan-andre.kuhlmann@ohb.de

Laine, Benoit
ESA/ESTEC
Netherlands
✉ Benoit.Laine@esa.int

Lapensee, Stephane
ESA/ESTEC
Netherlands
✉ Stephane.Lapensee@esa.int

Latha Balakumar, Vishal
Delft University of Technology
Netherlands
☎ +31 6 1731 3082
✉ lbvishal@hotmail.com

Leroy, Sandrine
DOREA
France
☎ +33 6 3305 2546
✉ sandrine.leroy@dorea.fr

Lommatsch, Valentina
German Aerospace Center (DLR)
Germany
✉ valentina.lommatsch@dlr.de

Maibaum, Michael
DLR
Germany
✉ michael.maibaum@dlr.de

Martinez Bueno, Patricia
ATG Europe
Netherlands
✉ patricia.martinez@atg-europe.com

Mas, Guillaume
CNES
France
☎ +33 6 1385 6003
✉ guillaume.mas@cnes.fr

Mecsaci, Ahmad
OHB System AG
Germany
✉ ahmad.mecsaci@ohb.de

Muenstermann, Rolf
AIRBUS Defence&Space
Germany
✉ rolf.muenstermann@airbus.com

Nada, Tarek
National Authority for Remote Sensing and Space Sciences
Egypt
☎ +20 10 6888 9594
✉ tnada@narss.sci.eg

Nerriere, Rose
Airbus Defence and Space
France
✉ rose.nerriere@airbus.com

Orgaz, David
Private
Netherlands
☎ +31 6 8215 7171
✉ david.orgaz.diaz@gmail.com

Pasqualetto Cassinis, Lorenzo
TU Delft
Netherlands
☎ +31 3934 0743 3190
✉ lorenzopasqualetto@gmail.com

Paul, Markus
Astro- und Feinwerktechnik Adlershof GmbH
Germany
✉ m.paul@astrofein.com

Persson, Jan
ESA/ESTEC
Netherlands
✉ jan.persson@esa.int

Peyrou-lauga, Romain
ESA/ESTEC
Netherlands
✉ romain.peyrou-lauga@esa.int

Pin, Olivier
ESA/ESTEC
Netherlands
✉ olivier.pin@esa.int

Poinas, Philippe
ESA/ESTEC
Netherlands
🖂 Philippe.Poinas@esa.int

Preville, Pierre
AKKA
France
🖂 pierre.preville@akka.eu

Puech, François
AIRBUS DEFENCE & SPACE
France
☎ +33 1 3906 2758
🖂 francois.puech@astrium.eads.net

Rana, Hannah
ESA/ESTEC
Netherlands
🖂 hannah.rana@esa.int

Ritter, Heiko
ESA/ESTEC
Netherlands
🖂 Heiko.Ritter@esa.int

Rooijackers, Harrie
ESA/ESTEC
Netherlands
☎ +31 71 565 3453
🖂 Harrie.Rooijackers@esa.int

Scardino, Marco
Isae-Supaero
France
☎ +33 7 7034 2420
🖂 marco.scardino1@gmail.com

Siarov, Stefan
TU Delft
Netherlands
☎ +31 6 3090 1995
🖂

Solyga, Malgorzata
Active Space Technologies GmbH
Germany
🖂 malgorzata.solyga@activespacetech.eu

Soriano, Timothée
Airbus DS
France
🖂 timothee.soriano@airbus.com

Soto, Isabel
SENER Ingenieria y Sistemas
Spain
☎ +34 944 81 7810
🖂 isabel.soto@sener.es

Stroom, Charles
Stremen
Netherlands
🖂 charles@stremen.xs4all.nl

Supper, Wolfgang
ESA/ESTEC
Netherlands
☎ +31 71 565 4735
🖂 wolfgang.supper@esa.int

Terhes, Claudia
ESA/ESTEC
Netherlands
☎ +31 6 5241 6219
🖂 claudia.terhes@esa.int

Theroude, Christophe
Airbus Defence and Space
France
☎ +33 6 7262 0195
✉ christophe.theroude@airbus.com

Tonellotto, Giulio
ESA/ESTEC
Netherlands
✉ giulio.tonellotto@esa.int

Torralbo, Ignacio
IDR/UPM
Spain
☎ +34 6 5194 9800
✉ ignacio.torralbo@upm.es

Tosetto, Andrea
BLUE Engineering
Italy
✉ a.tosetto@blue-group.it

Tunarli, Ediz
Turkish Aerospace Industries
Turkey
☎ +90 53 8353 6346
✉ etunarli@tai.com.tr

Van De Poel, Mathijs
TU Delft
Netherlands
☎ +31 324 7988 6414
✉ mathijs.vandepoel@gmail.com

Van Es, Johannes
NLR
Netherlands
☎ +31 6 1329 0426
✉ johannes.van.es@nlr.nl

Vaughan, Matthew
ESA/ESTEC
France
✉ matthew.vaughan@airbus.com

Verdonck, Julo
Airbus Defence & Space Netherlands
Netherlands
✉ J.verdonck@airbusds.nl

Vivijs, Bart
QinetiQ Space
Belgium
✉ bart.vivijs@qinetiq.be

Vullings, Michiel
ATG Europe
Netherlands
☎ +31 71 579 5561
✉ michiel.vullings@atg-europe.com

Vyas, Shubham
TU Delft
Netherlands
☎ +31 6 1562 3613
✉ shubham143@gmail.com

Winter, Daniel
ESA/ESTEC
Netherlands
☎ +31 4917 3439 1501
✉ daniel.winter@esa.int

Zabalza, Leire
Lidax
Spain
☎ +34 6 6992 9193
✉ leire.zabalza@lidax.com

Zamboni, Andrea
Selex ES
Spain
✉ andrea.zamboni@selex-es.com

Zevenbergen, Paul
Airbus Defence & Space Netherlands
Netherlands
✉ p.zevenbergen@airbusds.nl